

University of Warwick institutional repository: <http://go.warwick.ac.uk/wrap>

A Thesis Submitted for the Degree of PhD at the University of Warwick

<http://go.warwick.ac.uk/wrap/4118>

This thesis is made available online and is protected by original copyright.

Please scroll down to view the document itself.

Please refer to the repository record for this item for information to help you to cite it. Our policy information is available from the repository home page.

Interference Analysis of Broadband Space and Terrestrial Fixed Radio Communications Systems in the Frequency Range 12 to 30 GHz

By

Selçuk KIRTAY BSc MSc AMIEE

A thesis submitted for the degree of Doctor of Philosophy

Department of Engineering

University of Warwick

August 2001

BEST COPY

AVAILABLE

Variable print quality

Contents

List of Figures

List of Tables

Declaration

Acknowledgement

List of Abbreviations

Abstract

Publications

1	Introduction	1
1.1	Frequency Spectrum Management	1
1.2	Fixed Satellite Service (FSS) Systems	7
1.2.1	General Overview of FSS Systems	7
1.2.1.1	Transponders	8
1.2.1.2	High Power Amplifiers	10
1.2.1.3	Earth Stations	11
1.2.1.4	Satellite Orbits	13
1.2.2	Geostationary (GSO) FSS Systems	17
1.2.2.1	Ku Band System Characteristics	17
1.2.2.2	Ka Band System Characteristics	20
1.2.2.3	System Applications	26
1.2.3	Nongeostationary (NGSO) FSS Systems	27
1.2.3.1	System Characteristics	28
1.2.3.2	Network Configurations	34

1.2.3.3	System Applications	36
1.2.3.4	NGSO FSS Interference	37
1.3	Terrestrial Radio Systems Operating in Fixed Service	38
1.3.1	Point-to-Point Radio Links	41
1.3.2	Fixed Wireless Access Networks	42
1.3.2.1	Point-to-Multipoint Architecture	43
1.3.2.2	Mesh Architecture	44
1.3.2.3	Standardisation and Applications	45
1.4	Thesis Structure	46
2	Propagation Characteristics	48
2.1	Atmospheric Gaseous Attenuation	49
2.1.1	International Telecommunications Union- Radiocommunications Recommendation 676 (ITU-R Rec.676)	49
2.1.1.1	Slant Path Attenuation	51
2.1.1.2	Terrestrial Path Attenuation	55
2.1.2	ITU-R Rec.1395	56
2.1.3	Discussion	57
2.2	Terrestrial Path Propagation	59
2.2.1	Wanted Path Propagation Effects	60
2.2.1.1	Multipath Fading	61
2.2.1.2	Rain Fading	66
2.2.1.3	Combined Effects of Multipath and Rain Fading	68
2.2.2	Interference Path Propagation Effects	69

2.2.2.1	Long-term Interference Propagation Mechanisms	70
2.2.2.2	Short-term Interference Propagation Mechanisms	73
2.2.2.3	Combined Effects of Individual Interference Propagation Mechanisms	79
2.2.3	Discussion	82
2.3	Space Path Propagation	83
2.3.1	Wanted Path Propagation Effects	84
2.3.1.1	Rain Fading	84
2.3.2	Interference Path Propagation Effects	89
2.3.3	Discussion	90
2.4	Conclusions	91
3	Review of Issues Related to Interference From NGSO FSS Systems into GSO FSS Systems	94
3.1	Current Regulations	95
3.1.1	Brief History	95
3.1.2	ITU-R Radio Regulations Article S.22	96
3.1.3	ITU-R Recommendation 1323	101
3.2	Previous Work	103
3.2.1	Epfd and Apfd Definitions	104
3.2.2	NGSO/GSO Interference Mitigation Techniques	107
3.2.3	Article S.22 Limits	108
3.2.4	GSO FSS Antenna Reference Radiation Patterns	110
3.2.5	Co-existence of Multiple NGSO FSS Systems	111
3.2.6	Cumulative Effect of Multiple NGSO FSS Systems	112

3.2.7	Interference into Large GSO FSS Earth Stations	113
3.2.8	Synchronisation Loss	114
3.3	Representative GSO/NGSO FSS System Characteristics	115
3.3.1	GSO FSS System Characteristics	116
3.3.2	NGSO FSS System Characteristics	119
3.4	Conclusions	129
4	Sharing Analysis Between GSO and NGSO FSS Systems	130
4.1	Implications of NGSO FSS Mitigation Techniques	131
4.1.1	GSO Arc Avoidance	133
4.1.1.1	Simulation Model Description	133
4.1.1.2	Uplink Simulation Analysis	135
4.1.1.3	Downlink Simulation Analysis	140
4.1.1.4	Discussion	147
4.1.2	Latitude Avoidance	148
4.1.2.1	Simulation Model Description	148
4.1.2.2	Uplink Simulation Analysis	149
4.1.2.3	Downlink Simulation Analysis	153
4.1.2.4	Discussion	155
4.1.3	High Performance NGSO FSS Satellite Antennas	156
4.1.3.1	Simulation Model Description	157
4.1.3.2	Simulation Results	157
4.1.3.3	Discussion	158
4.2	Revision of epfd Limits	158
4.2.1	Conversion from Interference to epfd	160

4.2.2 Multiple NGSO FSS System Interference	162
4.2.2.1 Uplink epfd	162
4.2.2.2 Downlink epfd	165
4.2.3 Conversion from Aggregate-to-Single Entry epfd	167
4.2.4 Continuous epfd versus Staircase epfd	172
4.2.5 Derivation of Limits for Antenna Diameters not Included in Radio Regulations	173
4.2.6 Discussion on Simulation Analysis	175
4.2.7 Implementation of Methodology A'	176
4.2.8 Discussion on Analytic Approach	188
4.3 Impact of GSO FSS Earth Station Reference Antenna Patterns	190
4.3.1 Reference Radiation Patterns	191
4.3.2 Monte Carlo Simulator Design	195
4.3.3 Monte Carlo Simulation Analysis	200
4.3.4 Discussion	203
4.4 Impact of NGSO FSS Interference Peaks	204
4.4.1 Calculation Method	204
4.4.2 Implementation of the Calculation Method	205
4.4.3 Discussion	208
4.5 Conclusions	208
5 Review of Issues Related to Interference From NGSO FSS Systems into FS Systems	212
5.1 Current Regulations	213
5.1.1 Brief History	213

5.1.2	ITU-R Radio Regulations Article S.21	214
5.1.3	ITU-R Recommendations for Analogue/Digital FS System Performance and Availability Objectives	216
5.1.4	ITU-R Recommendations for Fixed Service System Protection	220
5.1.4.1	ITU-R Rec. F.758	220
5.1.4.2	ITU-R Recs. SF.357 and SF.615	221
5.1.4.3	ITU-R Recs. F.1241 and F.1398	222
5.1.4.4	ITU-R Recs. IS.847, IS.849 and P.620	223
5.1.4.5	ITU-R Recs. F.1494 and F.1495	227
5.2	Previous Work	229
5.2.1	Space-to-Earth Interference Paths	230
5.2.2	Terrestrial Interference Paths	232
5.3	Discussion	236
5.3.1	Space-to-Earth Interference Paths	236
5.3.2	Terrestrial Interference Paths	238
5.4	Conclusions	239
6	Sharing Analysis Between FS and NGSO FSS Systems	242
6.1	Interference from NGSO FSS Satellites into Terrestrial Radio Systems Operating within FS	243
6.1.1	Interference Analysis Approach	244
6.1.2	Interference Analysis	245
6.1.2.1	Representative FS Link	245
6.1.2.2	FS Link Interference Criteria	248
6.1.2.3	NGSO FSS System Parameters	252

6.1.2.4	Single Entry Interference Levels	252
6.1.2.5	Interference Scenario	255
6.1.2.6	Simulation Results	256
6.1.2.7	FS Fading Statistics	258
6.1.2.8	Convolution Results	262
6.1.3	Discussion	264
6.2	Interference from NGSO FSS Earth Stations into Terrestrial Radio Systems Operating within FS	266
6.2.1	Analysis Approach	266
6.2.1.1	Single Entry Interference Analysis Method	266
6.2.1.2	Aggregate Interference Analysis Method	268
6.2.2	System Characteristics	270
6.2.2.1	Representative FS Receiver Characteristics	270
6.2.2.2	Representative NGSO FSS Earth Station Transmitter Characteristics	272
6.2.3	Single Entry Interference Analysis	272
6.2.3.1	NGSO FSS Earth Station Operating Within FS Receiver Azimuth Plane	273
6.2.3.2	FS Base Station Receiver Operating Within NGSO FSS Antenna Boresight	280
6.2.4	Aggregate Interference Analysis	284
6.2.5	Discussion	291
6.3	Conclusions	293
7	Conclusions	295
7.1	Chapter 1	295

Contents	viii
7.2 Chapter 2	297
7.3 Chapter 3	300
7.4 Chapter 4	301
7.5 Chapter 5	309
7.6 Chapter 6	311
7.7 Further Work	316
References	318

List of Figures

1.1	ITU Regions	6
1.2	Transparent and Regenerative Configurations	10
1.3	Forces Determining Satellite Trajectory	13
1.4	FSS System Orbits	15
1.5	Example Multibeam Satellite Downlink Coverage	18
1.6	VSAT Network Topologies	19
1.7	Illustrative Spot Beam Downlink Coverage	23
1.8	Four-cell Frequency Re-use Pattern	23
1.9	Ka Band Configurations	25
1.10	Skybridge and Teledesic Constellations	29
1.11	Spot Beam Steering	30
1.12	Fixed Beam Pattern	30
1.13	Links Supported by Typical Transparent NGSO FSS System	34
1.14	Regenerative NGSO FSS System Configuration	36
1.15	Point-to-Multipoint and Mesh System Configurations	41
2.1	Specific Attenuation	50
2.2	Total Slant Path Atmospheric Attenuation (Line Summation)	52
2.3	Total Slant Path Atmospheric Attenuation (Line Summation, Low Elevation Angles)	53
2.4	Total Slant Path Atmospheric Attenuation (Simplified Model, Low Elevation Angles)	54
2.5	Comparison of Total Slant Path Atmospheric Attenuation (Line Summation and Simplified Model, Low Elevation Angles)	55

2.6	Comparison of Total Slant Path Atmospheric Attenuation (Line Summation (Rec.676-4) and Simplified Model (Rec.1395), Low Elevation Angles)	57
2.7	Assumptions For Multipath Fading Modelling	65
2.8	Multipath Fading Statistics	65
2.9	Rain Fading Statistics	67
2.10	Ku Band Rain and Multipath Fading Statistics	68
2.11	Ka Band Rain and Multipath Fading Statistics	69
2.12	Assumptions For Ducting and Layer Reflection Modelling	75
2.13	Comparison of Ducting and Layer Reflection Interference Path Loss Statistics	76
2.14	Rain Scattering Path Loss Statistics	78
2.15	Line-of-sight Path Loss Statistics	81
2.16	Trans-Horizon Path Loss Statistics	81
2.17	Slant Path Geometry	85
2.18	Comparison of 10^0 Elevation Space Path Rain Attenuation	88
2.19	Implications of Elevation Angle	89
3.1	NGSO FSS Interference Paths into GSO FSS Links in Ku and Ka Band	94
3.2	Ku Band epfd Limits (Radio Regulations'98)	99
3.3	Lower Ka Band epfd Limits (Radio Regulations'98)	99
3.4	Upper Ka Band epfd Limits (Radio Regulations'98)	100
3.5	Ku Band apfd Limits (Radio Regulations'98)	100
3.6	Ka Band apfd Limits (Radio Regulations'98)	101
3.7	Power Flux Density	104

3.8	Ku-Band NGSO FSS User Terminal Transmitter Antenna Radiation Patterns	125
3.9	Ku-Band NGSO FSS User Terminal Receiver Antenna Radiation Patterns	125
3.10	Ku-Band NGSO FSS Satellite Transmitter Antenna Radiation Patterns	126
3.11	Ku-Band NGSO FSS Satellite Receiver Antenna Radiation Patterns	126
3.12	Ka-Band NGSO FSS User Terminal Transmitter Antenna Radiation Patterns	127
3.13	Ka-Band NGSO FSS User Terminal Receiver Antenna Radiation Patterns	127
3.14	Ka-Band NGSO FSS Satellite Transmitter Antenna Radiation Patterns	128
3.15	Ka-Band NGSO FSS Satellite Receiver Antenna Radiation Patterns	128
4.1	Comparison of Uplink Interference Statistics	135
4.2	Uplink Single Entry Worst Case Interference Geometry	136
4.3	Comparison of Downlink Interference Statistics	140
4.4	Worst Case Single Entry Downlink Interference Without Mitigation	141
4.5	Assumed Worst Case Downlink Interference With GSO Arc Avoidance	142
4.6	Calculated Worst Case Downlink Interference With GSO Arc Avoidance	143
4.7	Comparison of Uplink Interference Statistics	150
4.8	Uplink Single Entry Worst Case Interference Geometry	151

4.9	Comparison of Downlink Interference Statistics	153
4.10	Downlink Single Entry Worst Case Interference Geometry	154
4.11	Satellite Transmitter Antenna Patterns	156
4.12	Comparison of Interference Statistics	158
4.13	$\text{epfd}_{\text{down}}$ at GSO Ku-1 Earth Station Receiver	162
4.14	Aggregation of Uplink Interference Statistics	164
4.15	Interference epfd_{up} Statistics	165
4.16	Aggregation of Downlink Interference Statistics	166
4.17	Interference $\text{epfd}_{\text{down}}$ Statistics	167
4.18	Conversion from Aggregate $\text{epfd}_{\text{down}}$ to Single Entry $\text{epfd}_{\text{down}}$	170
4.19	Comparison Against Linear Interpolated $\text{epfd}_{\text{down}}$ Limits	173
4.20	Comparison of $\text{epfd}_{\text{down}}$ Limits	174
4.21	Rain Degradation pdf	181
4.22	NGSO FSS Interference Degradation pdf	183
4.23	Overall Degradation pdf	183
4.24	Comparison of Calculated $\text{epfd}_{\text{down}}$ Values Against Article S.22 Limits	187
4.25	Comparison of Reference Patterns (Diameter = 0.6 metre, Frequency = 12 GHz, $D/\lambda = 24$)	194
4.26	Comparison of Reference Patterns (Diameter = 3 metre, Frequency = 12 GHz, $D/\lambda = 120$)	195
4.27	Simulation Algorithm	196
4.28	Random Off-axis Angle Assignment	197
4.29	NGSO Interference Path Random Pointing	199

4.30	Range Vector	199
4.31	Interference Path Off-axis Angle	200
4.32	Comparison of Relative Interference at 0.6m, 10° Elevated GSO FSS Receiver Antenna	201
4.33	Comparison of Relative Interference at 0.6m, 90° Elevated GSO FSS Receiver Antenna	202
4.34	Comparison of Relative Interference at 3m, 10° Elevated GSO FSS Receiver Antenna	202
5.1	Ku and Ka Band NGSO FSS Interference Paths into FS Links	213
5.2	Ku and Ka Band pfd Limits	215
5.3	Geographical Band Segmentation	235
5.4	Worst Case Interference Scenario	237
6.1	Downlink Interference Analysis Method	245
6.2	Potential Worst Case Single Entry Interference Alignments	253
6.3	Lowest Single Entry Interference Alignment	254
6.4	Aggregate Interference Statistics	257
6.5	-(N+I) Probability Density Function	258
6.6	FS Link Rain and Multipath Fading Statistics	259
6.7	FS Link Joint Fading Statistics	260
6.8	Extrapolated FS Link Joint Fading Statistics	261
6.9	FS Link Received Carrier Power Statistics	262
6.10	Convolved Probability Density Functions	263
6.11	Comparison of C/(N+I) Statistics Against FS Receiver Interference Criteria	264
6.12	Worst Case Interference Alignments	268

6.13	FS Receiver Antenna Patterns	271
6.14	Assumed Parameters for Diffraction Model	275
6.15	Maximum Line-of-sight Range	276
6.16	FS Exclusion Areas (from NGSO Ka-1 Earth Station Transmitter)	277
6.17	FS Exclusion Areas (from NGSO Ka-2 Earth Station Transmitter)	278
6.18	Interference Geometry	280
6.19	Base Station Receiver Elevation Antenna Pattern	282
6.20	Interference Statistics	287
6.21	Interference Statistics vs. NGSO FSS Earth Station Density	288
6.22	Interference Statistics vs. Interferer and Receiver Antenna Height	290

List of Tables

1.1	Comparison of FSS Orbits	16
2.1	Terrestrial Path Atmospheric Attenuation	56
2.2	Interference Path Assumptions	78
2.3	Overall Clear-air Path Loss Calculation	79
2.2	Interference Path Assumptions	80
3.1	Synchronisation Loss Criterion for Various Modulation and Coding Techniques	115
3.2	GSO FSS Ku Band System Parameters	117
3.3	GSO FSS Ka Band System Parameters	118
3.4	NGSO FSS Ku Band System Parameters	120
3.5	NGSO FSS Ka Band System Parameters	122
4.1	Implications of Uplink NGSO Ku-1 Aggregate Interference on End-to-end GSO Ku-1 Link Budget	138
4.2	Implications of Downlink NGSO Ku-1 Aggregate Interference on End-to-end GSO Ku-1 Link Budget	144
4.3	Single Entry Interference Benchmark Figures	154
4.4	Clear-sky $C/(N+I)_{TOTAL}$	177
4.5	Rain Attenuation	180
4.6	Calculated Parameters for NGSO FSS Degradation	184
4.7	Interpretation of Calculated Parameters for NGSO FSS Degradation	184
4.8	$epfd_{down}$ Values	187
4.9	Synchronisation Loss Analysis	206
4.10	Synchronisation Loss Criterion	207

5.1	Recommendations Defining Performance and Availability	
	Objectives of Digital and Analogue Fixed Service Links	218
5.2	Maximum Allowable Performance Degradations at 15 Mbps	223
5.3	Proposed Ku and Ka Band FS Interference Criteria for NGSO FSS Downlink Interference	229
6.1	Reference Link Parameters	246
6.2	Parameters for Rain and Multipath Fading Statistics	247
6.3	Representative FS Link Characteristics	248
6.4	Error Performance Objectives	250
6.5	Representative FS Link Performance Objectives	250
6.6	Allowable Degradations in Representative FS Link Performance Objectives	251
6.7	NGSO Ku-1 Downlink System Characteristics	252
6.8	Potential Worst Case Single Entry Interference Power Levels	253
6.9	Ka Band Receiver Characteristics	271
6.10	NGSO FSS Earth Station Transmitter Parameters	272
6.11	Exclusion Distances	276
6.12	Worst Case Interference Power	283
6-13	Radius of Simulation Area for Different Transmitter and Receiver Antenna Combinations	285

Declaration

This thesis is presented according to the regulations of the degree of Doctor of philosophy. The material contained in this thesis is the authors own work except where references are made. No part of it has been submitted for a degree at another university.

Acknowledgement

I am indebted to *Aegis Systems Limited* for allowing me to use the facilities available at the company. I would like to express my deep gratitude to *Paul Hansell*, *Iain Inglis* and *Richard Rudd* for sharing their wisdom. In particular, I am grateful to *Paul Hansell*, who took the time to review the chapters, for the guidance.

I extend my special thanks to *Professor David Hutchins* at University of Warwick for his helpful suggestions.

Thanks also to my mother-in-law, *Stavroula Konstantinou*, as this research would not have started without her encouragement and tremendous support.

I am especially grateful to my wife, *Chrysi Kirtay*, for her continuous support and indulgence in the completion of this research. My final thanks go to my father, *Sadettin Kirtay*, and my mother, *Cemile Kirtay*, both of whom worked very hard to bring me up.

List of Abbreviations

ACTS	Advanced Communication Technologies and Services
Apfd	Aggregate Power Flux Density
ASSET	Aegis Systems Spectrum Engineering Tool
ATPC	Automatic Transmitter Power Control
BBE	Background Block Error
BBER	Background Block Error Ratio
BER	Bit Error Rate
BFWA	Broadband Fixed Wireless Access
BS	Base Station
Cdf	Cumulative Distribution Function
CDMA	Code Division Multiple Access
CEPT	European Conference of Postal and Telecommunications Administrations
COST	Co-operation in the Field of Scientific and Technical Research
CRABS	Cellular Radio Access of Broadband Services
C/N	Carrier to Noise Ratio
C/(N+I)	Carrier to Noise Plus Interference Ratio
DCA	Dynamic Channel Assignment
D/ λ	Antenna Diameter/Wavelength Ratio
EB	Errored Block
EC	European Commission
EIRP	Effective Isotropic Radiated Power
Epfd	Equivalent Power Flux Density

$E_{\text{pfd}_{\text{down}}}$	Downlink Equivalent Power Flux Density
$E_{\text{pfd}_{\text{up}}}$	Uplink Equivalent Power Flux Density
ERC	European Radiocommunications Committee
ERO	European Radicommunications Office
ES	Errored Second
ESA	European Space Agency
ESR	Errored Second Ratio
ETSI	European Telecommunications Standards Institute
FCC	US Federal Communications Commission
FDMA	Frequency Division Multiple Access
FDP	Fractional Degradation in Performance
FM	Frequency Modulation
FS	Fixed Service
FSPL	Free Space Path Loss
FSS	Fixed Satellite Service
FWA	Fixed Wireless Access
GBS	Geographical Band Segmentation
GEO	Geostationary Earth Orbit
GSO	Geostationary
GSO FSS	Geostationary Fixed Satellite Service
G/T	Satellite Earth Station Figure of Merit
HPA	High Power Amplifier
HRC	Hypothetical Reference Circuits
HRDP	Hypothetical Reference Digital Path

I	Interference Power
IP	Internet Protocol
ISDN	Integrated Services Digital Network
ITU	International Telecommunications Union
ITU-D	International Telecommunications Union Development
ITU-R	International Telecommunications Union Radiocommunications
ITU-T	International Telecommunications Union Standardisation
JTG	Joint Task Group
LAN	Local Area Network
LEO	Low Earth Orbit
MEO	Medium Earth Orbit
MVDS	Multipoint Video Distribution Systems
N	Receiver Noise Power
$N_{\text{effective}}$	Effective Number of NGSO FSS Systems
N_{physical}	Actual Number of NGSO FSS Systems
NGSO	Nongeostationary
NGSO FSS	Nongeostationary Fixed Satellite Service
P_{fd}	Power Flux Density
PP	Point-to-point
PMP	Point-to-multipoint
PSK	Phase Shift Keying
QAM	Quadrature Amplitude Modulation
QPSK	Quadrature Phase Shift Keying
Rec.	Recommendation

Rx	Receiver
SCAT	Hydrometeor Scatter Prediction Model
SES	Severely Errored Seconds
SESR	Severely Errored Second Ratio
SSPA	Solid State Power Amplifiers
TDMA	Time Division Multiple Access
Tx	Transmitter
TWTA	Travelling Wave Tube Amplifiers
UN	United Nations
VSAT	Very Small Aperture Terminals
WP	Working Party
WRC	World Radio Conference

Abstract

This thesis presents research into the principles of spectrum sharing analysis methods developed for investigating implications of interference from Nongeostationary Fixed Satellite Service (NGSO FSS) systems into Geostationary Fixed Satellite Service (GSO FSS) systems and Fixed Service (FS) terrestrial radio systems operating or planned for operation in the 12 to 30 GHz frequency range.

Spectrum sharing is an effective way of allowing new services to operate without cancelling the existing allocations in the same part of the spectrum. The use of spectrum sharing results in re-use of the available spectrum among different services and, therefore, increases the efficient use of the radio frequencies. However, it is necessary to carry out extensive feasibility studies into technical or operational compatibility between the services involved. Often, sharing constraints are placed on systems, such as the power of emissions and the transmitter and receiver antenna pointings to reduce the interference into negligible levels.

Traditionally, radio spectrum allocated to GSO FSS has been shared with FS. In recent years, there has been a growing interest in the use of low Earth orbits and a number of NGSO FSS constellations has been designed to provide broadband data services. This has led to the allocation of certain bands used by the FS and GSO FSS systems to NGSO FSS.

In line with the new allocations, NGSO FSS, GSO FSS and FS systems are required to co-exist in parts of the 12 to 30 GHz frequency range. The primary objectives of this research were to identify principal factors affecting the feasibility of spectrum sharing and to develop spectrum sharing analysis methodologies to examine the implications of these factors with a view to identifying sharing constraints that would give rise to an acceptable sharing environment.

Publications

Use of Bessel Functions for the Representation of Earth Station Reference Antenna Patterns, Presented on Behalf of Eutelsat at 3rd ITU-R Joint Task Group 4-9-11 Meeting, California, January 1999.

Comments on the use of Methodology D in the Application of Recommendation ITU-R S.1323, Presented on Behalf of Eutelsat at 3rd ITU-R Joint Task Group 4-9-11 Meeting, California, January 1999.

On The Spectrum Efficiency of Distributed Architecture Radio Telephony Systems, Presented at 4th Communications Network Symposium, Manchester Metropolitan University, July 1997.

Preliminary Results of a Study of the Spectrum Efficiency of Randomly Distributed Circuit Switched Radio Networks, Presented at 3rd Communications Network Symposium, Manchester Metropolitan University, July 1996.

CHAPTER 1

INTRODUCTION

This chapter presents a review of fixed satellite and terrestrial service system characteristics concerning with frequency spectrum management. Initially, a brief introduction into the concept of spectrum management is provided together with a summary of international organisations responsible for the efficient use of the radio spectrum. This is followed by identification of key fixed satellite service system characteristics with regard to the use of the frequency spectrum. The basic parameter definitions related to satellite communications systems are also included in the review for the purposes of completeness. The characteristics of terrestrial fixed radio stations are then outlined. The final section explains the thesis structure.

1.1 Frequency Spectrum Management

Spectrum was originally introduced as an abstract mathematical idea by Jean Baptise Fourier in the early 19th century to bring solutions to differential equations. Peter Dirichlet and Georg Riemann had resolved initial doubts and since then the concept became a powerful tool used in applications including radiocommunications, signal processing and computing. Meanwhile, instruments were developed and the spectrum evolved into a measurable physical quantity. This was followed by the radio engineering and, today, the concept of radio spectrum is widely used [1].

The ability to carry energy and messages at a distance and at the speed of light make the spectrum of radiowaves a valuable natural resource with which another concept is associated namely satellite orbits. The radio spectrum and satellite orbits are common and limited resources. The concept of a free and unregulated access to limited resources brings about potential problems if the number of users starts to exceed certain limits. The regulation, coordination and management of the use of the spectrum and satellite orbits are, therefore, an unavoidable necessity [2,3].

As a consequence of an ever increasing demand, the issue of rational use, sharing and protection of the limited common resources is becoming a serious problem on the national and international scale. Therefore, radio spectrum management needs to embrace all activities related to regulations, planning, allocation, assignment, use and control of the radio spectrum and satellite orbits. There appears to be three main objectives: conveying policy goals, apportioning scarcity and avoiding conflicts [1].

The first international conference was held in Berlin in 1903 to regulate and manage the use of the radio spectrum by marine disaster relief applications. The primary aim of the conference was to prevent mutual interference and to allow for intercommunication. The first operational radiocommunications standard, stating that ships must be provided a communications service regardless of the system deployed, was agreed at the London conference in 1912.

For the provision of international regulations, the International Telecommunication Union (ITU) was set-up in 1932 which was then reorganised at the conference which took place at Atlantic City in 1947 and became a specialised agency of the United Nations (UN). The regulatory functions carried out by various ITU consultative committees were integrated and three sectors which are Radiocommunications (ITU-R), Telecommunication Standardisation (ITU-T) and Telecommunications Development (ITU-D) were created in 1992 [4].

The activities of the ITU falls into three main areas: radio spectrum management, consultation between telecommunications administrations and operators and technical assistance to developing countries. From the radio spectrum management point of view, among the major responsibilities of the ITU are to ensure that radio interference is avoided and that the spectrum and orbit resources are used efficiently. For these purposes, the Radio Regulations comprising articles, appendices, resolutions and recommendations are reviewed regularly at international World Radiocommunication Conferences (WRC). The Radio Regulations have the status of an international treaty and each government warrants that these regulations are respected by everybody under its jurisdiction [2].

The articles and appendices in the Radio Regulations include the agreements and procedures regulating the allocation of frequency bands to services and the technical measures to be taken to increase the efficiency of the use of the radio spectrum. The Radio Regulations resolutions and recommendations cover a wide range of subjects. In general, they are used for declaring the decisions and intentions agreed at WRC and for initiating studies in preparation for the future conferences.

In order to develop the Radio Regulations further, Study Groups (and their associated working groups, joint working parties and joint task groups) within the ITU-R undertake studies to investigate the use of the radio spectrum and satellite orbits in terrestrial and space radiocommunications. The results of these studies are presented in the form of draft ITU-R Recommendations which need to be approved by the member states to become ITU-R Recommendations. The implementation of the recommendations is not mandatory, however, as they are developed by the experts from national administrations, operators, industry and other organisations dealing with radiocommunications matters, their use is common worldwide. The ITU-R recommendations are divided into series according to the subjects they cover.

The scarcity of the radio spectrum causes conflicts between those who have access to it and those without it. In addition, conflicts also arise between proponents of competing uses of the spectrum as well as those who manage it and those who use it. The nature of these conflicts may be commercial, political, physical and interference. For those whose needs have already been satisfied, spectrum management should assure the continuation of the existing status. Therefore, any modification could result in a conflict. On the other hand, for the newcomers, the principal aim of spectrum management is to eliminate the obstacles that prevent them from entering the competition [1].

To solve spectrum scarcity and orbit congestion problems, numerous conferences and symposia are held every year by a number of international organisations. In addition to the ITU, in Europe, the European Commission (EC), the European Conference of Postal and Telecommunications Administrations (CEPT), the

European Radiocommunications Committee (ERC) and European Radiocommunications Office (ERO) are involved in radio frequency management activities.

Currently, the spectrum and orbit resources are treated as public in the international forum and no access fee mechanisms has been applied. The access to these resources are based on Table of Frequency Allocations of the Radio Regulations which is, as mentioned earlier, reviewed by all ITU member states at the regular conferences. However, on the national scene, the use of economic tools to overcome the spectrum congestion have been investigated. These include an analysis of the economic value of the spectrum, pricing the spectrum, allowing trading in spectrum and using competitions to grant spectrum [5].

In the US, Federal Communications Commission (FCC) deals with the national spectrum management issues [6]. Awarding licenses to the highest bidders was first implemented by the FCC in 1994 [7]. Currently, a number of methods are applied for granting licenses for the use of the radio spectrum including auctions and beauty contests (i.e. comparative evaluations). The economic implications of new licensing processes, in turn, makes the protection of a granted spectrum increasingly important. Spectrum monitoring and control equipment with an integrated spectrum management software are widely used in the field to measure channel occupancy and eliminate infringements due to interference [8].

In the Table of Frequency Allocations of the Radio Regulations, frequency bands in different parts of the spectrum (from 9 kHz to 275 GHz) are allocated for a number of radio services, giving the national administrations the opportunity to assign frequencies according to their individual needs. The formal definitions of “services” used in the Table of Frequency Allocations are given in the Radio Regulations Article 1 [9]. For the purposes of this research, the Fixed Satellite Service (FSS) and the Fixed Service (FS) are of particular interest. The Article 1 states that:

- *radiocommunication service* is a service involving the transmission, emission and/or reception of radiowaves for specific telecommunication purposes.
- *fixed service* is a radiocommunication service between specified fixed points.
- *fixed-satellite service* is a radiocommunication service between earth stations at given positions, when one or more satellites are used.

It is important to note that many frequency bands are allocated for more than one service, and are thus shared. As far as the protection from in-band interference is concerned, some services may not enjoy equal status in shared bands. The ITU recognises two categories of frequency allocation: primary and secondary. The Radio Regulations Article 5 states that the systems with secondary allocations should not cause interference to the systems with primary allocations and can not claim protection from interference from the systems with primary allocations. The systems within the same category, on the other hand, can claim interference protection from each other [10].

The use of sharing in the Allocation Table has grown greatly in recent years, in particular, since the introduction of satellite services. Currently, there are only few exclusive bands allocated to one service and some bands are shared by as many as six services.

Sharing allows major frequency allocations to be made to new services without cancelling the existing allocations in the same part of the spectrum. This, in turn, implies that the available spectrum is re-used among different services, increasing the efficient use of the radio frequencies. However, sharing requires extensive feasibility studies into technical or operational compatibility between the services involved. Often, limits are placed on parameters of systems, such as the power of emissions and the transmitter and receivers antenna pointings to reduce the interference into negligible levels. These limits are referred as sharing constraints.

Trends in the emerging technologies are towards the deployment of devices with an ability to co-exist without excessive mutual interference [11-13].

In addition to the sharing constraints, a formal frequency co-ordination procedure could be applied in order to facilitate the spectrum sharing. The frequency co-ordination is invoked before a new system is introduced. During the co-ordination process, negotiations are undertaken between interested parties with a view to making system adjustments or defining operational criteria that will ensure a mutually satisfactory frequency sharing environment. Examples of where co-ordination is likely to arise include between satellite networks, satellite Earth stations and terrestrial services in the territory of a different administration, satellite and terrestrial services and terrestrial services of neighbouring administrations.

It is also worth noting that, at an international level, it has sometimes been found convenient to allocate frequency bands to different services in different parts of the world although, in general, spectrum allocations are worldwide. For these purposes, the ITU divides the world into three regions. Each region is defined in the Radio Regulations Article 5 and illustrated in the following figure.

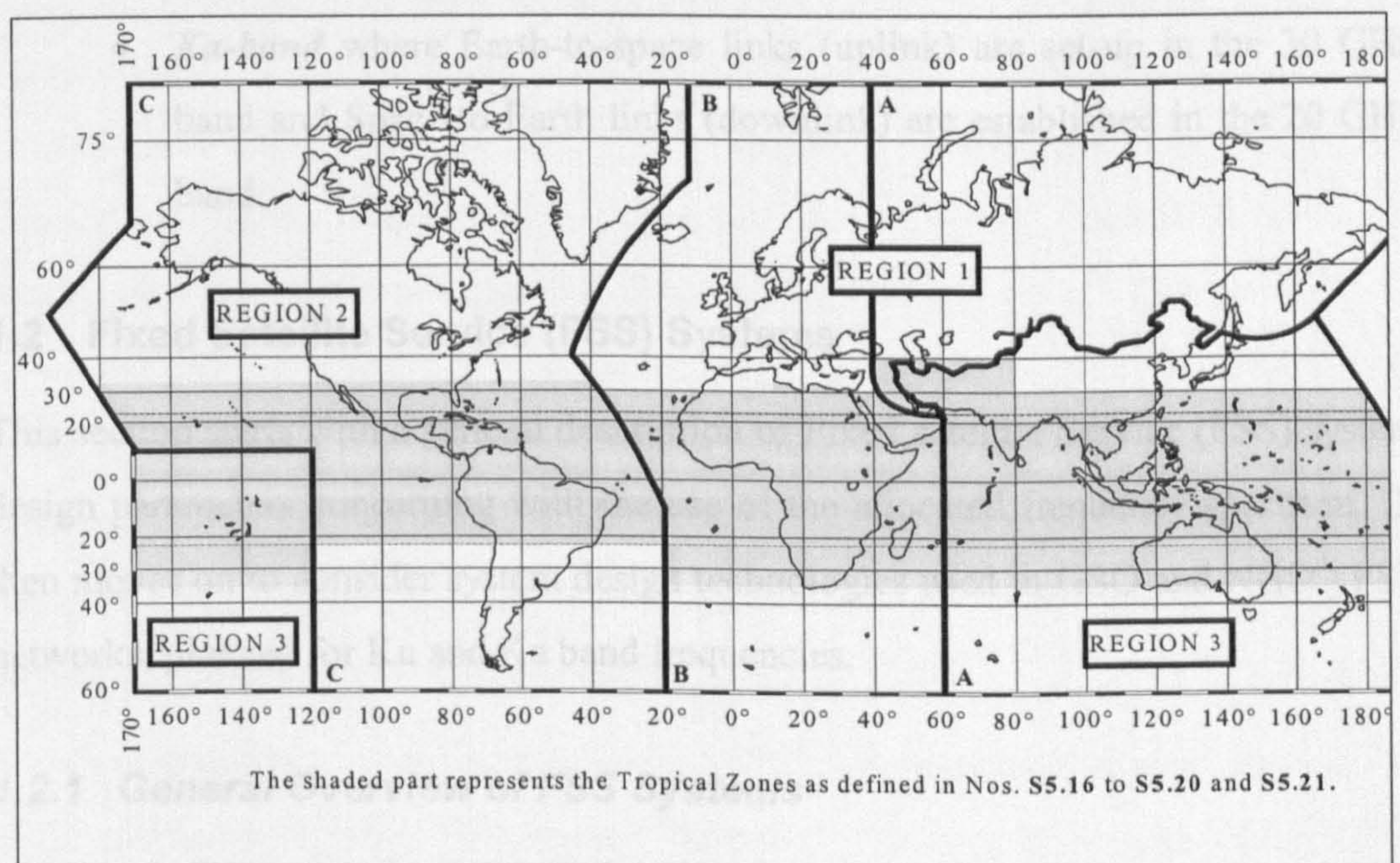


Figure 1.1: ITU Regions

Traditionally, radio spectrum allocated to terrestrial radio systems operating within the FS are shared with geostationary satellite systems of the fixed satellite service (GSO FSS). In recent years, there has been a growing interest in the use of low Earth orbits (i.e. nongeostationary orbits) and several constellation of satellite systems are proposed for the provision of broadband data services. In order to encourage the competition and to increase the efficient use of the spectrum, World Radio Conference'95 (WRC'95) revisited the radio regulations and decided to allocate certain bands used by the FS and the GSO FSS systems to nongeostationary fixed satellite service systems (NGSO FSS) on a primary basis.

It is the primary objective of this research to investigate the principles of the spectrum sharing analysis methods to be used for examining the implications of interference from the NGSO FSS systems into the GSO FSS systems and the FS systems operating/planned for operation in

- ***Ku-band*** where Earth-to-space links (uplink) are set-up in the 14 GHz band and Space-to-Earth links (downlink) are established in the 12 GHz band
- ***Ka-band*** where Earth-to-space links (uplink) are set-up in the 30 GHz band and Space-to-Earth links (downlink) are established in the 20 GHz band.

1.2 Fixed Satellite Service (FSS) Systems

This section starts with a general description of Fixed satellite Service (FSS) system design parameters concerning with the use of the allocated frequency spectrum. It then moves on to consider system design technologies used in GSO and NGSO FSS networks, planned for Ku and Ka band frequencies.

1.2.1 General Overview of FSS Systems

A fixed satellite communication system comprises a space and ground segment. Satellites and all terrestrial facilities for the control and monitoring of satellites

constitute an FSS system space segment. User terminals and gateways providing interconnections with other networks form an FSS system ground segment. The key space and ground segment elements are described in the following sections with a view to review issues related to the frequency spectrum.

1.2.1.1 Transponders

A satellite *transponder* is the subsystem which takes the received signal and converts it to a form suitable for retransmission. In most instances, a transponder refers to a chain of equipment on board the satellite which lies in a direct signal path between two ground terminals. In terms of transponder functionality, there are two types of satellites: *Transparent* and *Regenerative* [14].

In a typical transparent satellite application, a received carrier is passed through an RF front-end comprising a band pass filter (to reject spurious signals entering the transponder) and a low noise amplifier (to compensate for losses introduced on the uplink). The signal is then split into separate channels by a bank of band-pass filters. The frequency translation is then applied to each channel by feeding a microwave mixer with the output of the filter and an on-board generated continuous wave signal produced by a local oscillator unit. After the mixer, a new band-pass filter is introduced to each channel to reject the unwanted mixing products. The filter outputs are then amplified by high-power amplifiers (HPAs). Each HPA operates at maximum efficiency near saturation where the linearity is poor. This results in an intermodulation distortion. In order to minimise the impact of intermodulation products, HPAs do not operate near saturation (i.e. power back-off is introduced) and each channel is band-pass filtered after the non-linear high power amplification by another bank of filters. The filtered signals are then recombined and fed into a downlink transmitter antenna [14, 15].

It is worth noting that the amplification at a high frequency is more difficult to achieve than at a lower frequency. Therefore, the high power amplification is performed after the frequency translation where the resultant downlink signal frequency is lower than the received uplink signal frequency.

In some applications, transparent satellite design may employ different configurations where the positions of mixers, demultiplexer and amplifiers are interchanged [14, 15]. Some transparent transponders may also take a dual conversion approach where an incoming signal is translated into a lower intermediate frequency before demultiplexing, amplification and translation to the downlink transmitter frequency. This takes advantage of easy amplification and filtering at lower frequencies at the expense of an increased transponder hardware cost.

Regenerative satellites are employed to optimise the system capacity for applications where a flexible approach is required to meet the uplink and downlink traffic requirements. In a typical regenerative satellite application, an incoming signal is transmitted through an RF front-end and demultiplexed into a number of channels. At this stage, the downlink frequency translation process used in the transparent satellite design is replaced with downconversion to an intermediate frequency and demodulation to baseband on each channel. Processing is then performed on the baseband stream using baseband processors. The processing typically involves decoding, switching, routing, re-encoding and buffering. The processed data are then remodulated, upconverted to the transmit frequency and transmitted through a high power amplifier and a filter before recombined and fed to a downlink transmitter antenna [14-17].

The main advantage of employing regenerative satellite design is that an overall link degradation is not cumulative as it is in a transparent design since the uplink and downlink are considered independently. The major trade-off, on the other hand, is an increased satellite complexity due to the hardware and software requirements to implement on-board processing. Transparent and regenerative transponder configurations are illustrated in Figure 1.2.

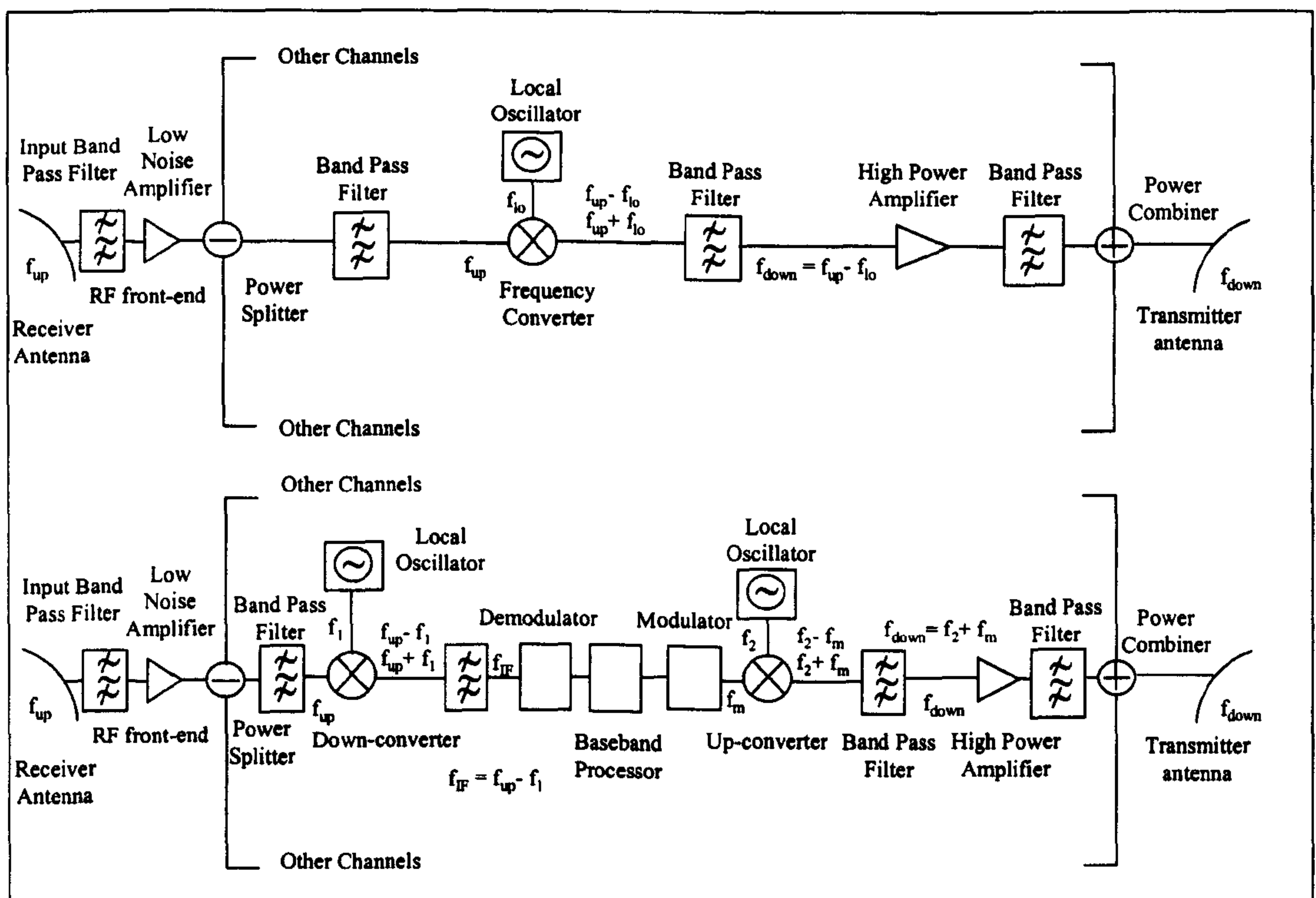


Figure 1.2: Transparent and Regenerative Configurations

1.2.1.2 High Power Amplifiers

Two types of power amplifier are used on satellites: Travelling Wave Tube Amplifiers (TWTAs) and Solid State Power Amplifiers (SSPAs). TWTAs operate by interaction between an electron beam and the radiowave. They satisfy the need for broadband capability, high output power and high efficiency (i.e. the ratio of radio frequency output power to electric power consumed). Therefore most satellite transponders today employ TWTAs as their main power amplifiers.

As power on-board the satellite is at a premium, it is desirable that TWTAs be operated as efficiently as possible, i.e. close or at saturation. However, this operation mode introduces non-linearity distortions due to non-linear relationship between output amplitude and phase and input amplitude. These include degradation of the bit-error-rate (BER) of the system (due to intersymbol interference) and spectral spreading of the transmitted signal which causes adjacent channel interference. In addition, when a number of carriers are at present at a given

transponder the output/input non-linearity causes intermodulation products. In these circumstances, input power to the amplifier is backed-off (i.e. input power is reduced relative to its value at saturation) resulting in reduced transmitter power which, in turn, represent a penalty, in particular, when transmitting to small Earth stations. Typically, TWTAs provide around 50 dB gain at saturation and their output powers are about 100 watt [17-21].

In general, SSPAs employ silicon bipolar transistor and GaAs MESFET. These amplifiers offer lower maximum output power and efficiency than TWTAs. However, they have the major advantages of greater linearity, higher reliability, lower mass and lower DC power supply requirements as compared to TWTAs. At Ku-band frequencies, recent improvements in SSPA technology has enabled power values around 30 watt to be achieved using GaAs MESFET components [22].

1.2.1.3 Earth Stations

Earth stations forming a ground segment of a typical FSS system comprise antenna, receiver and transmitter equipment [14, 15]. In Ku and Ka band applications, it is desirable that the Earth station receive antenna provides sufficient low noise gain and an efficient pointing capability. The receiver low noise front-end combined with the antenna amplifies the weak satellite signals to enable the following receiving stages (including demultiplexing, demodulation and baseband processing) to perform their functions with an adequate carrier-to-noise ratio. In the case of an Earth station transmitter, the multiplexed signals are modulated and upconverted to produce low-level output carriers in the appropriate uplink frequency band. The resultant upconverted signals are then amplified, filtered and combined to give a unified output to the transmit portion of the antenna feed. Depending on the terminal size, the power amplifiers range from SSPAs of a few watts output power to large TWTAs with output powers around hundreds of watts.

There are three key Earth station design parameters: antenna size, low noise amplifier noise temperature and high power amplifier output power. The ratio of the first two parameters is called “figure of merit” which is directly related to the

receiver Carrier-to-Noise ratio (C/N) and denoted by G/T . A three way balance needs to be struck between these parameters in that the antenna size and noise temperature should satisfy the Earth station receiver G/T requirement while antenna size should ensure that expensive high power amplifiers are not required to provide the required $EIRP$ when transmitting to the satellite [14, 15].

The *elevation angle* of an Earth station is the angle between the directions to the satellite and the horizon. When an elevation angle is too small, signals travel through much of the Earth's atmosphere and are degraded by high atmospheric attenuation and, in particular, high attenuation due to rainfall in Ku and Ka band [23].

Earth stations are distinguished by their size which varies according to the volume of traffic to be carried on the link [24]. The terms of *fixed* and *transportable* are also used to categorise FSS Earth stations. The definitions given in the Article 1 [9] state that the FSS provides radiocommunication service between Earth stations at given positions which may be specified fixed points or any fixed points within specified areas. Therefore, fixed and transportable Earth stations which are operated only when they are stationary within a specified area are included within the definition.

Small Earth stations providing a service directly to the user at a geographic location covered by a satellite beam are called very small aperture terminals (VSATs). VSATs do not require support from local terrestrial networks and can be powered from a portable supply and, therefore, could be transportable. The main advantages of VSAT networks include easy and rapid deployment, easily added or removed additional terminals and distance insensitive connection costs. Typically, a VSAT receiver comprises a parabolic antenna with a diameter less than $2m$, mostly $60cm$ to $90cm$, an outdoor unit including low-noise amplifier and downconverter and an indoor unit containing demodulator and decoder. In the transmitter case, an indoor unit includes encoder and modulator while an outdoor unit contains upconverter and solid state power amplifier with a saturated output about a few watts [14, 15, 25].

1.2.1.4 Satellite Orbits

The *orbit* is the trajectory followed by the satellite in equilibrium between two opposing forces which are the force of attraction due to Earth's gravitation and the centrifugal force associated with the curvature of the satellite's trajectory, as illustrated in Figure 1.3 [26].

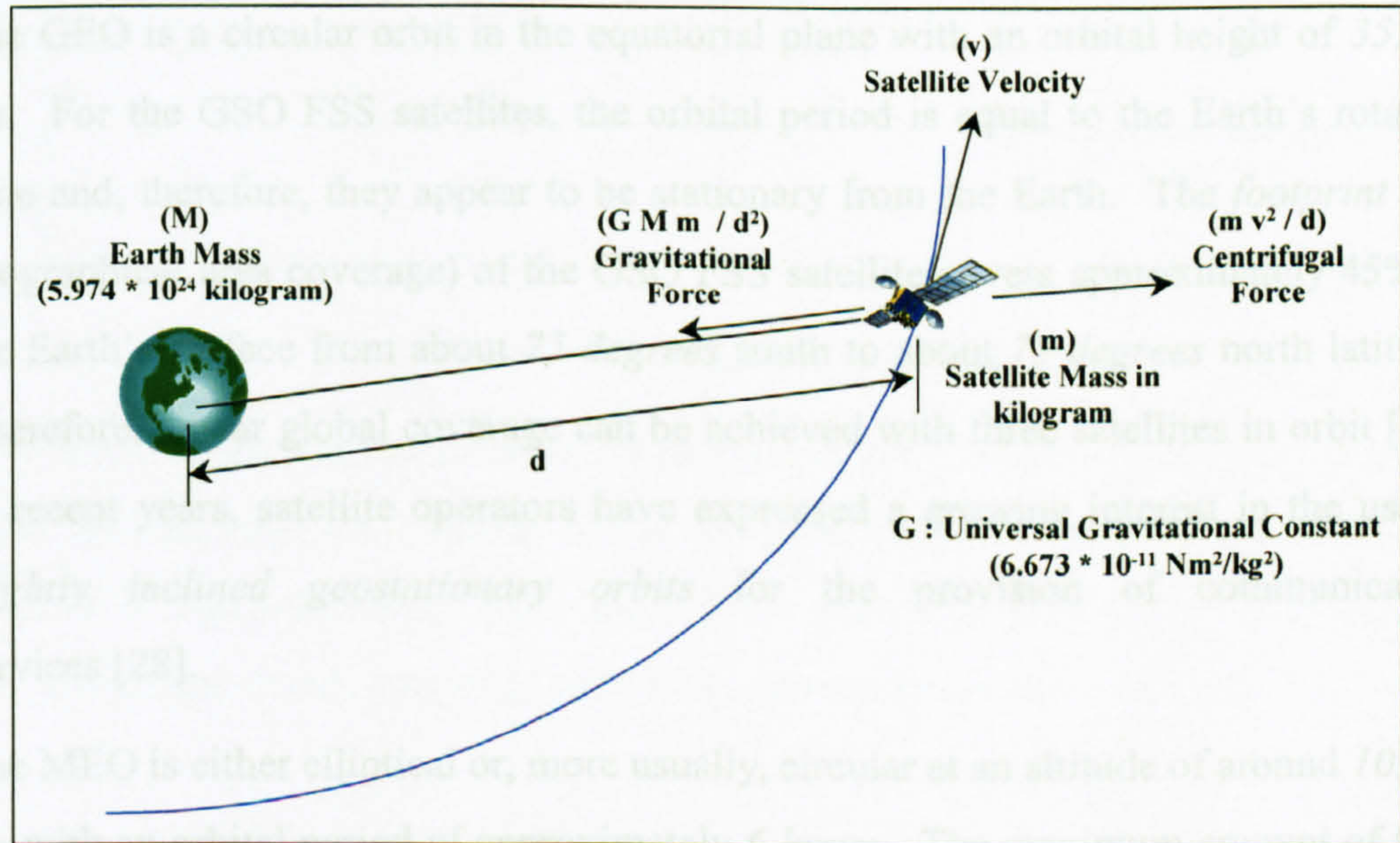


Figure 1.3: Forces Determining Satellite Trajectory

It is worth noting that the closer the satellite to the Earth, the stronger is the Earth's gravitational pull and the faster the satellite travels.

Amongst the factors that influence the FSS system orbit selection are the nature of services to be provided and their delay and data throughput requirements, the anticipated traffic levels and their geographical distributions, platform size and cost requirements and propagation factors. The orbits may be *circular* or *elliptical*. An elliptical orbit enables the satellites to spend a large fraction of orbital period over the regions located under the apogee. For a circular orbit, the altitude of the satellite is constant and equal portions of the orbital period is spent over the regions covered. The orbit may also have an *inclination* with respect to the equatorial plane to provide an optimum coverage for targeted regions of latitudes. In this context, the optimum refers to the probabilities associated with visibility of one, two or more satellites

with elevation angles greater than some specified operational minimum angle. Multiple inclined orbital planes generally provide a dense coverage over latitudes where highest traffic density is expected [23, 24, 26].

FSS systems may be deployed in three types of satellite orbits: Geostationary Earth Orbit (GEO), Medium Earth Orbit (MEO) and Low Earth Orbit (LEO).

The GEO is a circular orbit in the equatorial plane with an orbital height of 35,786 *km*. For the GSO FSS satellites, the orbital period is equal to the Earth's rotation time and, therefore, they appear to be stationary from the Earth. The *footprint* (i.e. geographical area coverage) of the GSO FSS satellite covers approximately 45% of the Earth's surface from about 75 *degrees* south to about 75 *degrees* north latitude. Therefore, a near global coverage can be achieved with three satellites in orbit [27]. In recent years, satellite operators have expressed a growing interest in the use of *slightly inclined geostationary orbits* for the provision of communication services [28].

The MEO is either elliptical or, more usually, circular at an altitude of around 10,000 *km* with an orbital period of approximately 6 *hours*. The maximum amount of time during which a satellite in a circular MEO is above the local horizon for an Earth station on the surface of the Earth is in the order of hours. Typically, an NGSO FSS system using MEO requires a modest number of satellites (≤ 20) operating in multiple inclined orbital planes (≤ 4) to provide global communications services.

Similarly, the LEO is either elliptical or, more commonly, circular at an altitude of less than 2000 *km* above the surface of the Earth. The orbit period at these altitudes is approximately less than 2 *hours*. For an Earth station operating within an NGSO FSS system deployed in a LEO, a given satellite is visible for less than 20 *minutes*. Therefore, when a satellite serving a user moves below the local horizon a handover to a succeeding satellite in the same or adjacent plane is required. A global NGSO FSS system deployed in LEO, typically, requires a large number of satellites (≤ 300) within a number of inclined orbits (≤ 20). Figure 1.4 shows illustrative GEO, MEO and LEO orbits.

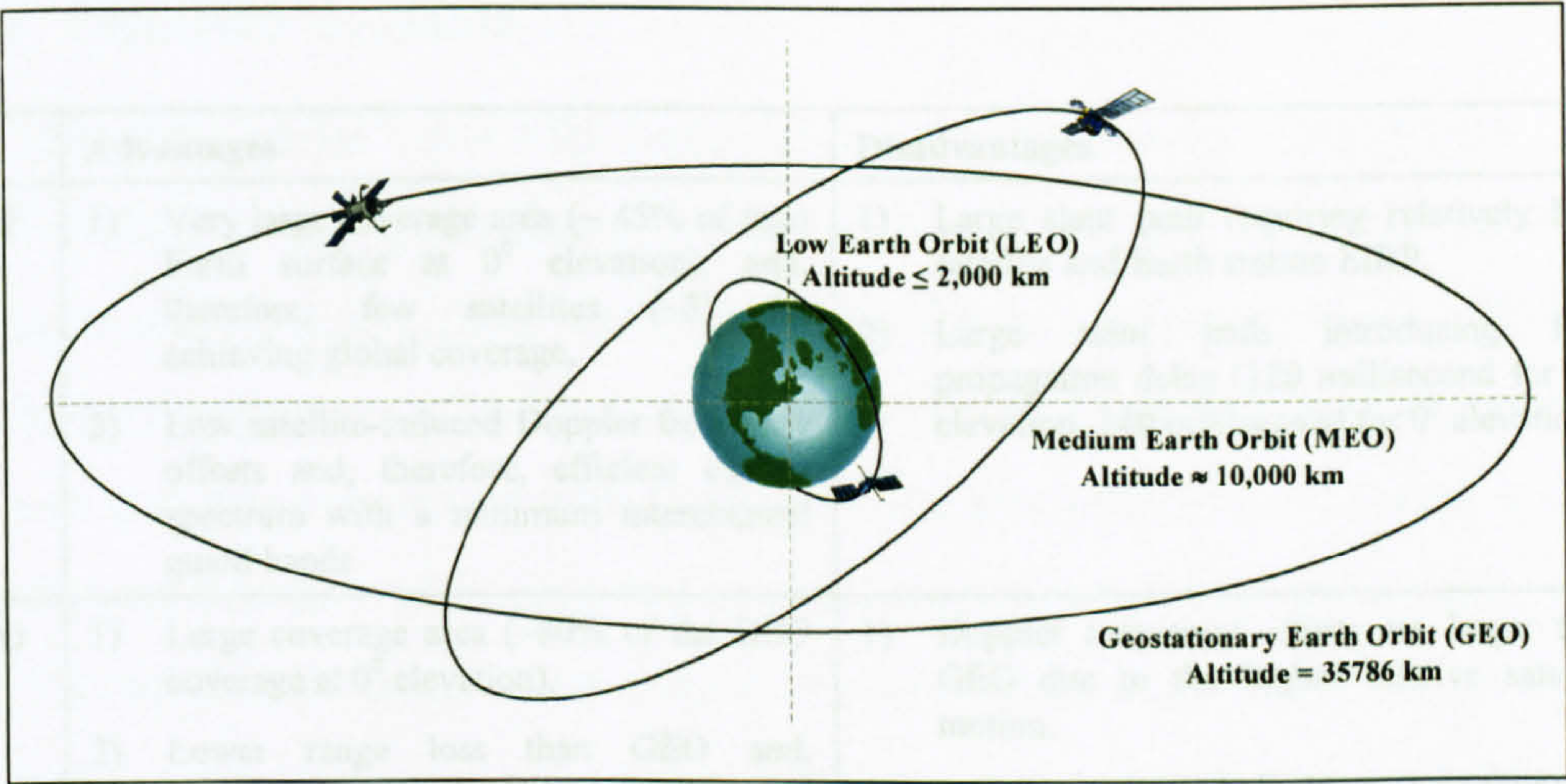


Figure 1.4: FSS System Orbits

It is worth noting that few satellite systems use circular orbits with altitudes between 2000 km and 9000 km . This is due to the harsh radiation environment associated with Van Allen radiation belts located at these altitudes [23]. The relative advantages and disadvantages of each FSS orbit are summarised in Table 1.1.

1) Lower propagation delay relative to both GEO and MEO, thereby comparable with long distance terrestrial links (e.g. a 700 km direct, 2.3 millisecond for 90 degrees, 10.3 millisecond for 9 degrees).	2) Low altitude resulting in small antenna diameter (1-50% of the GEO coverage is 9 degrees).
3) Large number of satellites than GEO and MEO for providing continuous global coverage.	4) Relatively higher probability of satellite failure as satellites remain visible for a few minutes.

Table 1.1: Comparison of FSS Orbits

Satellites in orbit may employ antennas forming a single beam covering a large geographical area or multiple spot beams each with smaller area coverage. Antenna beamwidth is usually used to refer to the angle between the directions in which the antenna gain falls to half its maximum value.

After this brief introduction, a summary of GSO FSS and NGSO FSS technologies employed in designing Ku and Ka band system constellations that are either in operation or being planned is provided together with the type of new services offered in the following sections.

	Advantages	Disadvantages
GEO	<div><div>1) Very large coverage area (~ 45% of total Earth surface at 0° elevation), and, therefore, few satellites (~3) for achieving global coverage,</div><div>2) Low satellite-induced Doppler frequency offsets and, therefore, efficient use of spectrum with a minimum interchannel guard bands.</div></div>	<div><div>1) Large slant path requiring relatively high satellite and Earth station EIRP,</div><div>2) Large slant path introducing long propagation delay (120 millisecond for 90° elevation, 140 millisecond for 0° elevation).</div></div>
MEO	<div><div>1) Large coverage area (~80% of the GEO coverage at 0° elevation),</div><div>2) Lower range loss than GEO and, therefore, relatively lower satellite and Earth station EIRP,</div><div>3) Lower propagation delay than GEO allowing system design for voice communications(at a 10,000 km altitude, 34 millisecond for 90° elevation, 51 millisecond for 0° elevation),</div><div>4) Less frequent intersatellite handover than required for LEO.</div></div>	<div><div>1) Doppler frequency offsets are larger than GEO due to the higher relative satellite motion,</div><div>2) Larger number of satellites than GEO for providing continuous global coverage</div></div>
LEO	<div><div>1) Lowest range allowing lowest satellite and Earth station EIRP requirement,</div><div>2) Lower propagation delay relative to both GEO and MEO, latency comparable with long distance terrestrial links (at a 700 km altitude, 2.3 millisecond for 90° elevation, 10.3 millisecond for 0° elevation).</div></div>	<div><div>1) Very high orbital velocity leading to large Doppler frequency offsets,</div><div>2) Low altitude resulting in small satellite coverage (~30% of the GEO coverage at 0° elevation),</div><div>3) Larger number of satellites than GEO and MEO for providing continuous global coverage,</div><div>4) Relatively higher probability of satellite handover as satellites remain visible for a few minutes.</div></div>

Table 1.1: Comparison of FSS Orbits

Satellites in orbit may employ antennas forming a single beam covering a large geographical area or multiple spot beams each with smaller area coverage. *Antenna beamwidth* is usually used to refer to the angle between the directions in which the antenna gain falls to half its maximum value.

After this brief introduction, a summary of GSO FSS and NGSO FSS technologies employed in designing Ku and Ka band system constellations that are either in operation or being planned is provided together with the type of new services offered in the following sections.

1.2.2 GSO FSS Systems

The first commercial GSO FSS satellites were employed in C-band (6/4 GHz), where 6 GHz is the approximate uplink frequency and 4 GHz is the downlink, because radio equipment was readily available for this frequency band. This was followed by migration to Ku-band in the 1980s due to the lack of existing spectrum at lower frequencies coupled with C-band orbital slot congestion. Today, the Ku-band frequencies are widely used and systems are planned for Ka-band deployment. Both Ku and Ka band system characteristics are reviewed in the following sections.

1.2.2.1 Ku-band System Characteristics

Currently, global satellite operators including Eutelsat, Astra, Panamsat and Intelsat as well as regional commercial satellite systems (for example, Italsat, Turksat, Chinasat, Brasilsat and Satmex) use Ku-band spectrum to provide fixed satellite services [29].

Ku-band GSO FSS satellites are equipped with multiple (typically, between 12 and 52) high power transponders each comprising transmitter and receiver equipment with typical bandwidths in the range 24 MHz to 72 MHz [17-20]. Most Ku-band transponders are transparent. The first commercial satellite, called *Hot Bird 4*, with an on-board processing unit operating in Ku-band was launched by Eutelsat in February 1998 [17, 30].

A transponder's available power and bandwidth are shared among a number of different carriers by employing conventional multiple access techniques, such as frequency division multiple access (FDMA), time division multiple access (TDMA) and code division multiple access (CDMA). These techniques may also be used in combination to provide efficient schemes for various traffic demands. In general, each carrier sharing the transponder may itself represent data from multiple users. Resources divided by frequency, time and codes may be assigned to the multiple sites permanently (fixed assignment) or dynamically based on the traffic (demand assignment). Fixed assignment is simple in implementation and leads to lower delay in connection set-up but does not achieve full bandwidth utilisation. Demand

assignment makes efficient use of the spectrum, however, it requires more complex network protocols and causes longer connection set-up delay with a non-zero blocking probability [25, 31, 32].

In a typical Ku band GSO FSS system, a satellite is located at a single orbital position on the geostationary arc to provide fixed multiple widebeam coverage over a very large geographical area. In addition to the multiple fixed widebeam transmit and receive coverage, steerable beam coverage may also be employed to establish a single satellite hop links between different geographical areas. The satellite payload equipment, therefore, includes fixed and steerable antennas with diameters, typically, within the range *1m* to *3m*. In order to maximise the system capacity, transponders support orthogonal polarised carriers [17-20].

In the following figure, the Eutelsat Atlantic Bird satellite (planned to be launched in 2001) multibeam downlink coverage map is illustrated [17].

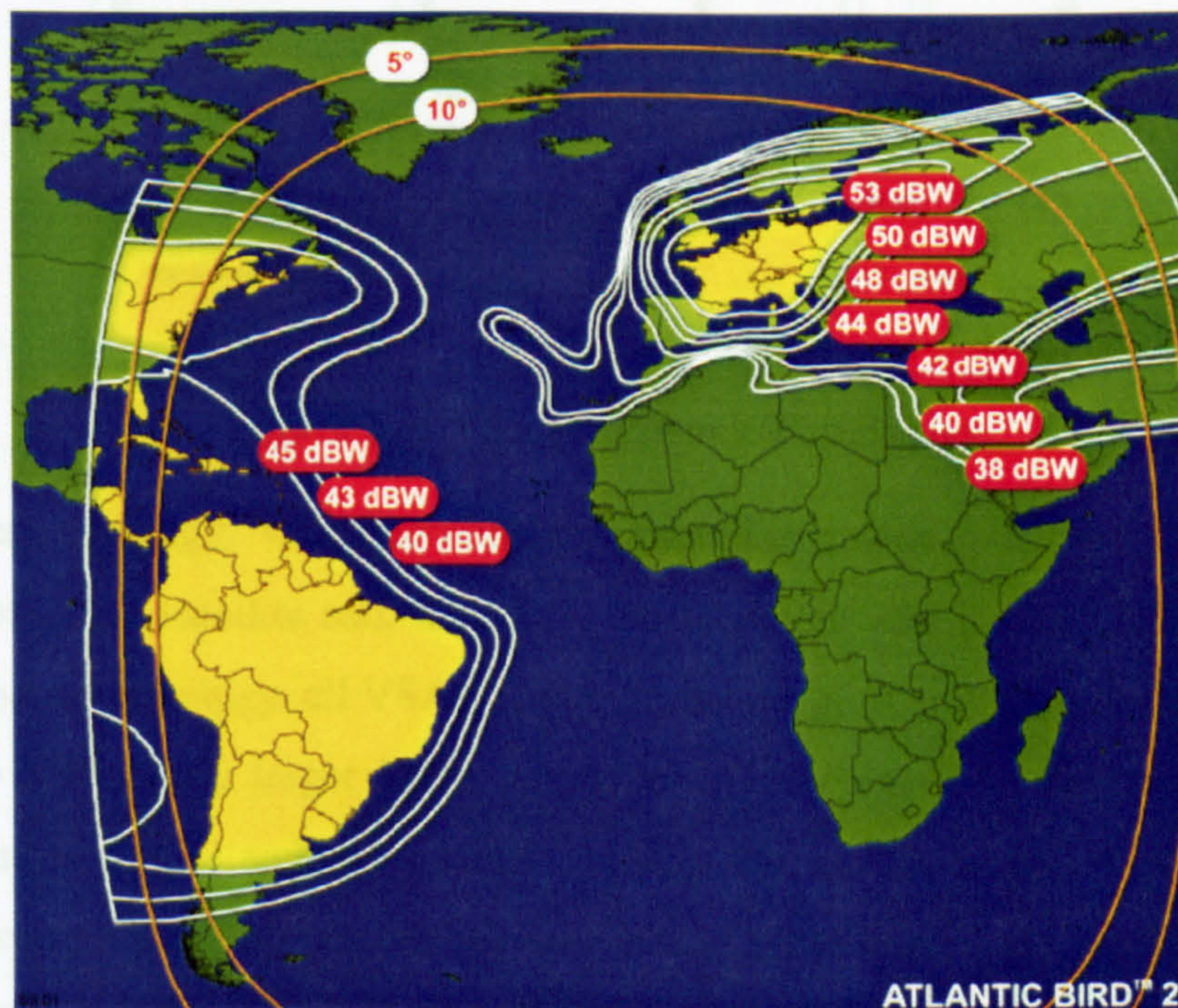


Figure 1.5: Example Multibeam Satellite Downlink Coverage

Ku band GSO FSS Earth stations may be connected to the end-user directly, for example VSATs, or via terrestrial networks. Depending on the type of applications

to be supported, Earth station antenna diameters satisfying G/T and $EIRP$ requirements may be as large as $10m$. Typical G/T values are 25 to 35 dB/K and typical $EIRP$ levels are 50 to 85 dBW per carrier [17-20].

In general, Ku-band VSAT terminals are used in networks of related users, for example, to establish private business networks to link offices of a global organisation distributed over a large geographical area. Corporations in banking, retail, transportation, financial services and energy industries employ VSAT networks for primarily data services which are less sensitive to transmission delay [25]. Two basic network topologies illustrated below are used by VSAT networks.

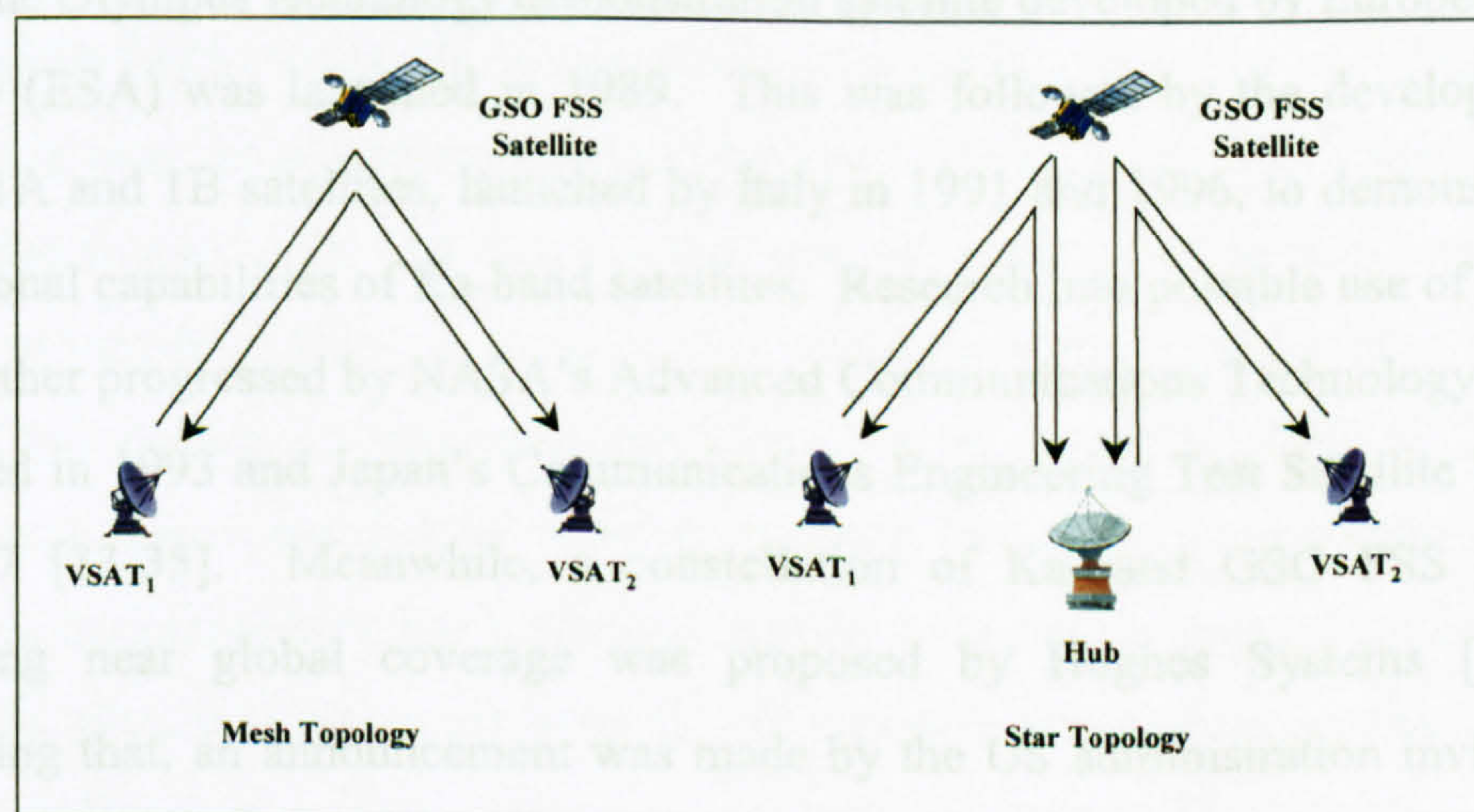


Figure 1.6: VSAT Network Topologies

In the mesh topology, VSAT terminals communicate with each other using direct paths through the satellite and, therefore, transmissions require only single satellite hop. In the star topology, all VSAT communications go through a hub station which is usually a relatively larger Earth station where, for example, data processing is carried out or central archive is stored. Using the star topology, VSAT-to-VSAT communications links are established with two satellite hops. It is worth noting that applications requiring little VSAT-to-VSAT communication, for example, if a hub station is located with a corporate headquarters and nearly all VSAT communications are to and from the headquarters, the use of star topology is an efficient solution. VSAT terminal transmit and receive data rates are limited by the

antenna size (typically less than $1m$) and the capability of the transmitter amplifier (typically, SSPA with an output power of few watts). Higher data rates are generally achieved using the star topology by employing large antennas and transmitter amplifiers at hub stations. In general, VSAT terminals transmit rates are 64 kbps to 512 kbps and the receive rates are between 64 kbps and 6 Mbps [25].

1.2.2.2 Ka-band System Characteristics

The first experimental Ka-band satellite (CS-2A) was launched by Japan in 1983 with a mission to quantify the potential rain attenuation at Ka-band frequencies. Later, the Olympus technology demonstration satellite developed by European Space Agency (ESA) was launched in 1989. This was followed by the development of Italsat 1A and 1B satellites, launched by Italy in 1991 and 1996, to demonstrate the operational capabilities of Ka-band satellites. Research into possible use of Ka-band was further progressed by NASA's Advanced Communications Technology Satellite launched in 1993 and Japan's Communications Engineering Test Satellite launched in 1997 [33-35]. Meanwhile, a constellation of Ka-band GSO FSS satellites providing near global coverage was proposed by Hughes Systems [36, 37]. Following that, an announcement was made by the US administration inviting Ka-band satellite applications with a filing deadline in November 1995. A total of twenty-three applications were made, some with global coverage, some limited to domestic US coverage, involving eighty-two geostationary satellites and over five hundred non-geostationary satellites. By 1998, fifty projects that required over three hundred geostationary orbit locations were filed with the ITU [29, 38, 39].

In line with these developments, existing global GSO FSS Ku-band operators made attempts to make use of the high capacity offered by the Ka-band to meet increasing bandwidth requirements resulting from demand for multimedia applications. For these purposes, new satellites designed to support both Ku and Ka band carriers have been ordered where the cross-connections between the Ku and Ka band coverage areas are established by coupling the corresponding carriers from both bands [17-19]. Astra-1H launched in June 1999 is the first commercial satellite employing

transparent Ka-band transponders to provide broadband interactive multimedia services [18, 40].

The primary concern in Ka-band satellite system design is that of overcoming rain fade. In general, proposed GSO FSS system designs seek to provide high link margins to overcome rain fading by employing high EIRP on board the satellite [38]. Therefore, many of Ka-band GSO FSS systems intend to employ regenerative satellites and the proposed constellation designs are based on the use of intersatellite links, digital beam forming networks producing multiple spot beams and digital processors for switching traffic among beams [21, 29, 33, 36, 40-44].

Intersatellite links are used to ensure global interconnectivity. The use of these links to provide long range communication between GSO FSS satellites reduces end-to-end transmission delay relative to the use of multi satellite hop connections involving terrestrial links. It is noted that establishing intersatellite links to nearby (within few degrees in longitude) satellites of other compatible GSO FSS satellite networks is also proposed in order to increase the global interconnectivity. In addition, dual-frequency Earth stations capable of communicating with compatible GSO FSS systems are planned to be able to access to the services provided by other systems [21].

The use of Ka-band frequencies for satellite applications imply relatively higher bandwidth carriers and require increased satellite EIRPs to compensate for increased fading. These features, in turn, have led to the possible requirement for a satellite antenna to radiate a large number of narrow spot beams where power and bandwidth resources are focused on the areas where they are needed [23]. In general, Ka-band GSO FSS system design proposals include multiple transmitter and receiver antennas ($\sim 1m$ in diameter) each with an offset reflector fed by an array of feed elements which are used to generate high power, shaped, multiple spot beams up to hundred per satellite. Alternative future antenna technology is the use of direct radiating phased array antennas where all the radiating elements contribute to each

of its spot beams [14]. These spot beams enable the systems to meet high data rate demand of densely populated areas [40].

It is worth noting that, in the presence of many beams, providing beam-to-beam connections is a complex procedure [38]. There are several methods proposed to achieve connectivity between different beams. The beam switching method is based on providing multiple switches on board the satellite to interconnect each spot beam to any other spot beam. This method becomes highly inefficient when there are more than a very few spot beams as the amount of hardware required increases significantly. An alternative method suggests that the address of the recipient could be included in the transmission as a header. The signal can then be demodulated to determine the destination. It is further suggested that the demodulation process could be implemented either on board the satellite or by relaying the signal to a gateway Earth station where signal is demodulated and the required information is transmitted back to the satellite. The first approach eliminates the need for the double hop at the expense of adding complexity on the satellite.

In general, the spot beams are positioned on a regular matrix and overlap at a crossover point close to their nominal half power beamwidth to afford contiguous coverage of the service area. The beamwidths are typically less than a degree and orthogonal polarisations are used to increase the system capacity [14, 15, 38]. It is worth noting that the use of dual polarisation may affect the unavailability of the links in comparison to single polarisation due to depolarisation induced interference resulting from adverse propagation characteristics [45, 46]. Figure 1.7 shows an illustrative geostationary satellite contiguous spot beam coverage.

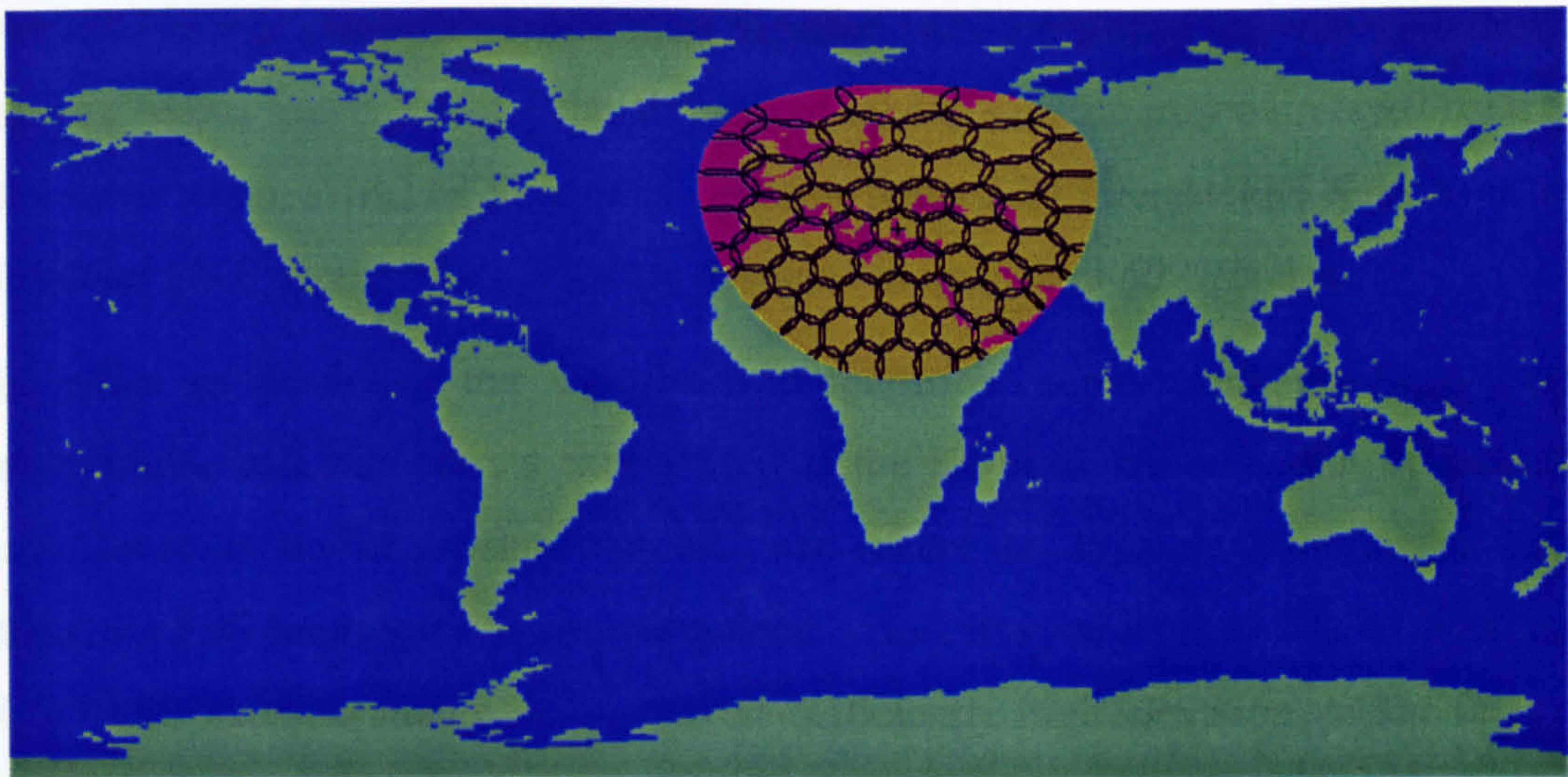


Figure 1.7: Illustrative Spot Beam Downlink Coverage

The use of very small spot beams also allows the high level of frequency re-use. For example, a proposed four-cell frequency re-use pattern ensures that no adjacent beams have the same frequencies allocated to them, and that every beam is isolated from a co-frequency beam by at least one beam spacing as illustrated in the following figure [21, 38].

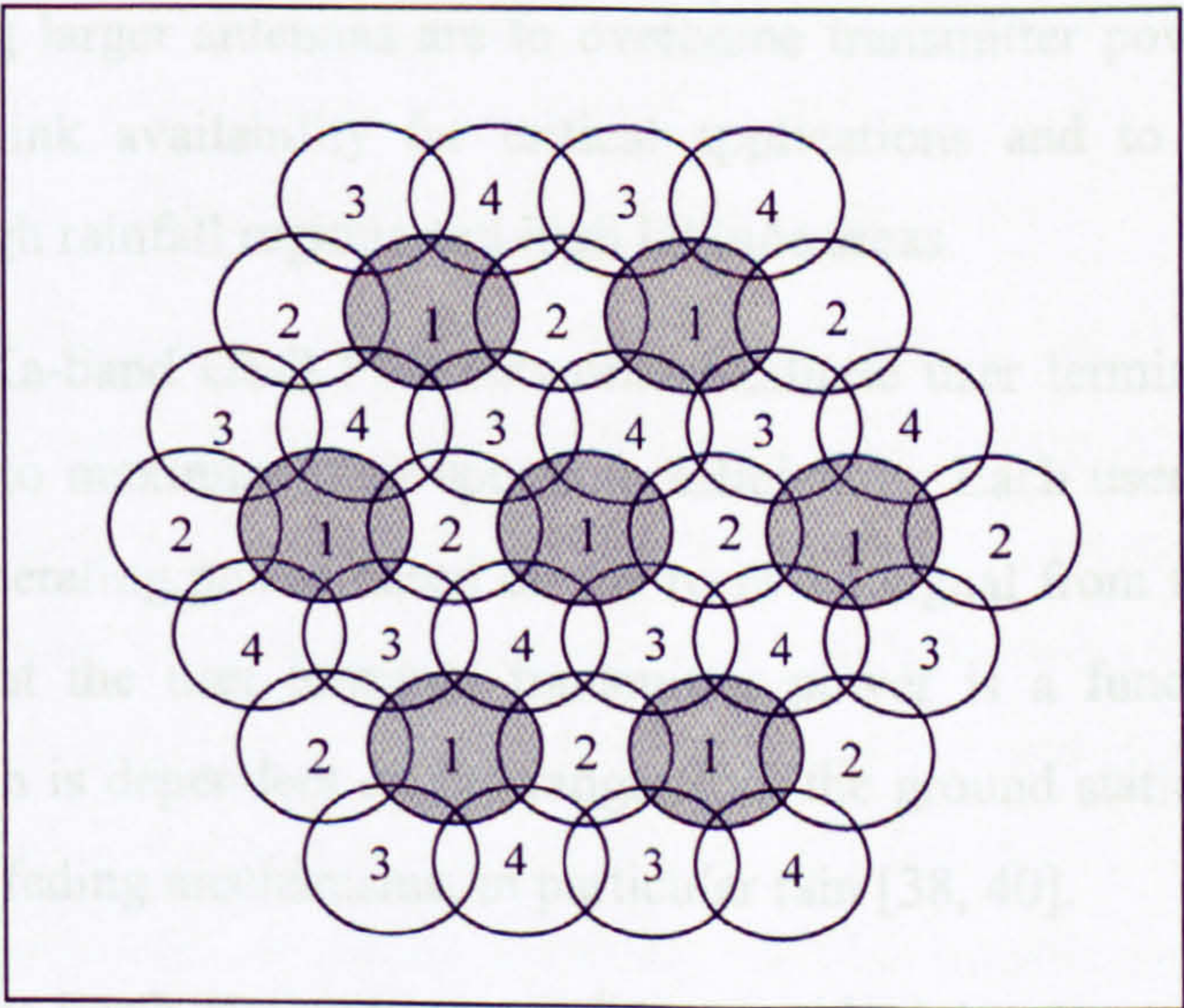


Figure 1.8: Four-cell Frequency Re-use Pattern

In general, beams are assigned a nominal wide bandwidth (for example, about 100MHz) to support multiple users operating within each service area. The use of

multiple beams and intersatellite links together with the ability to switch the traffic among beams suggests that a signal received by one satellite may be relayed back to the same beam, switched to another beam or relayed by intersatellite links to other satellites [43]. Intersatellite links are designed to operate in *60 GHz* band.

In order to minimise the significant propagation impairments resulting from atmospheric and rain effects experienced at the Ka-band, the selection of satellite orbit locations on the geostationary arc must ensure that high elevation angles from the GSO FSS Earth stations are maintained. This, in turn, implies that, at least one GSO FSS satellite should be viewed at sufficiently high elevation angles from a large proportion of the land areas of the Earth.

Ground segment of Ka-band GSO FSS networks comprises user terminals and gateway stations [21, 35, 41, 42, 44]. Different types of user terminals are used depending on the capacity requirement, location within the service area, elevation angle to the satellite and required service quality. It is noted that user terminals are planned for installation at customer premises for both residential and business applications. Typically, user antenna diameters range from *50 cm* to *2 m*. Primary reasons for using larger antennas are to overcome transmitter power limitation, to provide higher link availability for critical applications and to improve system availability in high rainfall regions and high latitude areas.

In most cases, Ka-band GSO FSS networks facilitate user terminal uplink power control in order to maximise their spectrum efficiency. Each user terminal adjusts its transmitter operating power based on the received signal from the satellite. It is worth noting that the user terminal transmitter power is a function of the path attenuation which is dependent on the range from the ground station to the satellite and propagation fading mechanisms, in particular rain [38, 40].

Ka-band gateway Earth stations are used to provide interconnection between the satellite network and terrestrial communication networks. Typically, each satellite coverage area includes at least one gateway with relatively larger antennas ($\sim 2.5\text{ m}$

to 5 m in diameter) using transmitter power level about tens of watts [21, 36, 41, 42, 44].

A number of Ka-band system configurations offering interactive communications are illustrated in the following figure.

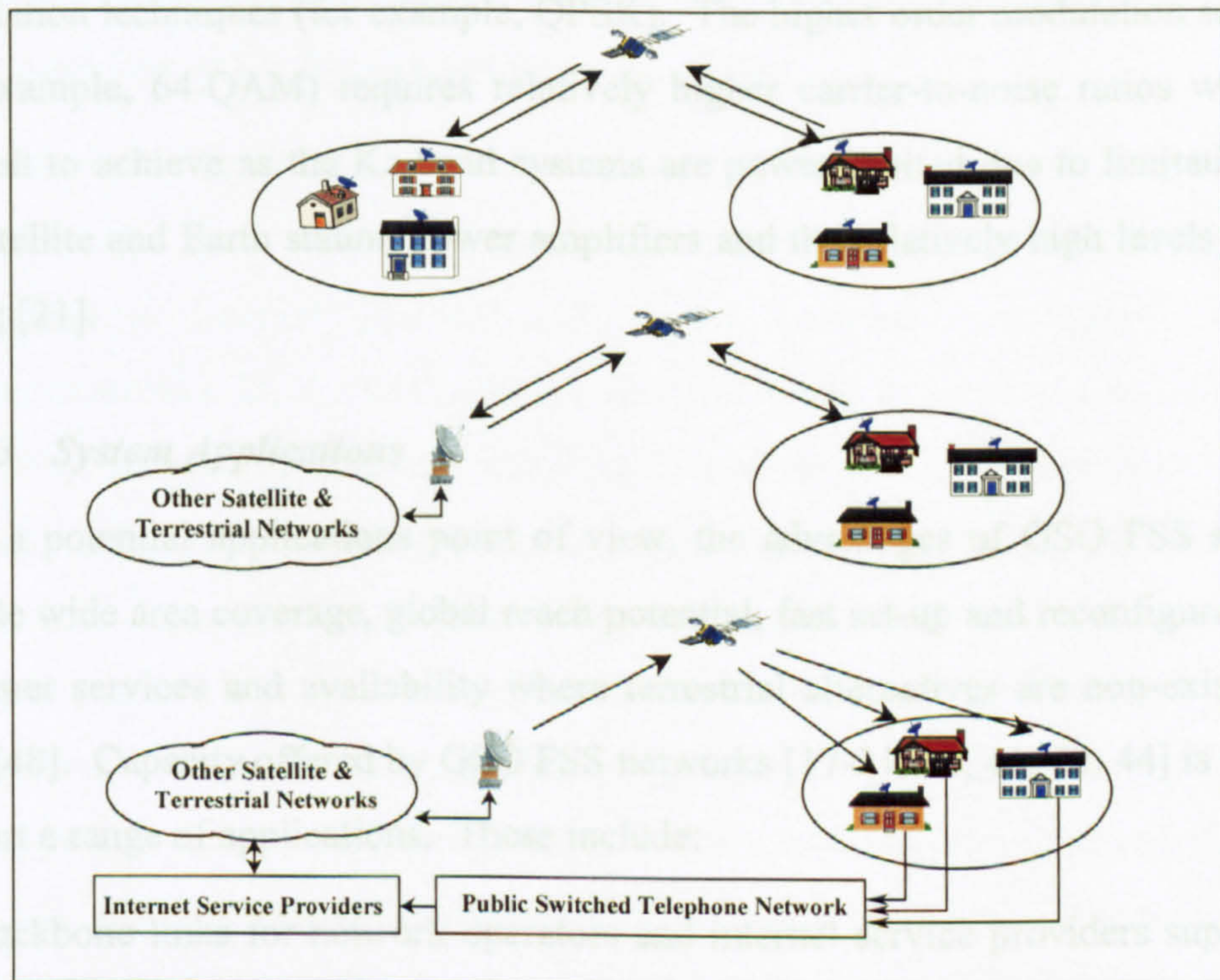


Figure 1.9: Ka-Band Configurations

Using the first configuration, it is possible to establish connection between any two or more terminals within the system. A typical application employing this approach may be provision of a private network for a global corporation. In the second configuration, connectivity between gateway and user terminals is provided through a satellite. This configuration may be used to support interactive data, video and audio applications. The third configuration where the return path is carried typically via the public switched telephone network may be suited for internet service providers to offer point-to-point and point-to-multipoint services as a typical internet link is asymmetric involving little amount of transmission in one direction and potentially large amounts of data in the opposite direction. It is worth noting that, in general, elements of the above configurations are combined to meet a given

requirement [47]. It should be noted that although it is possible to provide two-way communications using the first and second configurations with existing Ku-band VSAT technology, the Ka-band offers opportunity for high capacity.

Ka-band system proposals indicate that the networks will employ low order modulation techniques (for example, QPSK). The higher order modulation schemes (for example, 64-QAM) requires relatively higher carrier-to-noise ratios which is difficult to achieve as the Ka-band systems are power limited due to limitations on the satellite and Earth station power amplifiers and the relatively high levels of rain fading [21].

1.2.2.3 System Applications

From a potential applications point of view, the advantages of GSO FSS systems include wide area coverage, global reach potential, fast set-up and reconfiguration of customer services and availability where terrestrial alternatives are non-existent or poor [48]. Capacity offered by GSO FSS networks [17-21, 36, 41, 42, 44] is used to support a range of applications. These include:

- Backbone links for network operators and internet service providers supporting broadband services including internet access, videoconferencing, direct-to-home multimedia applications, telemedicine and distance learning.
- Capacity for private business network operators providing high speed networks for global organisations to support services including local area/wide area data network connections, corporate intranets and extranets, business videoconferencing between office locations, business data services (hotel, airline reservations, retail and banking), inventory tracking, inter-office file transfers and paging.
- Links for the extension of existing terrestrial networks to remote locations to provide basic telecommunications services.
- Capacity for Ku-band VSAT networks typically used to link together multiple store, factory and office locations of global organisations (for example,

manufacturers, corporations and supermarket chains) in private communications networks. Typical VSAT applications include credit authorisation, inventory control, fleet management, shipment tracking, electronic payment transactions, on-line trading, file/software updates, database access, pipeline monitoring, power line monitoring, internet access, corporate-mail, LAN internetworking, distance learning and brokerage services [25, 49].

- Provision of bandwidth-on-demand capability to provide interactive last-mile connections direct to customer premises. These connections are planned to be asymmetric Internet Protocol (IP) based Ka-band high speed two-way communication links where a star topology is formed between user terminals, the satellite and gateway stations providing connection to external networks. Global multimedia services offered include high speed direct internet access via satellite, interactive television [50], telebanking and investment services, multicasting where multimedia content (news, music, video, scientific data) is distributed dedicated user groups [51], interactive on-demand applications, monitoring remote data (environment, utility, security surveillance), database access (medical data, financial and business information), interactive tele-training.

1.2.3 NGSO FSS Systems

Deregulation of telecommunication services led to structural changes which created opportunities for the use of non-geostationary orbits to provide global satellite communication services. NGSO FSS constellations are a new type of system aiming to provide broadband satellite services to fixed or portable terminals [38, 40, 43, 52].

A number of NGSO FSS systems proposing to operate at Ku and Ka band frequencies have been filed with the ITU and FCC since early 1990s. These include *Skybridge*, Ku-band LEO constellation comprising 80 satellites; *Teledesic*, Ka-band constellation consisting of 288 LEO satellites; *@Contact*, Ka-band constellation consisting of 16 MEO satellites; *Spaceway-NGSO*, Ka-band MEO constellation comprising 20 satellites; *Rostelesat-N*, Ku-band LEO constellation of 91 satellites;

Rostelesat-V, Ka-band MEO constellation consisting of 24 satellites; *UsaKu-L1*, Ku-band LEO constellation of 80 satellites; *UsaKu-M1*, Ku-band MEO constellation comprising 20 satellites [53-58]. Many of these systems are still at the planning and fund raising stage. The best known NGSO FSS proposals under development with an increased likelihood of near future deployment are the Skybridge and Teledesic systems [38, 40, 43, 52, 59].

1.2.3.1 System Characteristics

Key NGSO FSS constellation design parameters include number of orbital planes, orbit altitude and inclination, number of satellites in each orbit, orbit spacing and relative phasing between satellites in adjacent orbital planes. These parameters together with operational system characteristics determine geographical area over which continuous system coverage is provided [52, 54-56, 60].

The primary objective of the system design is to provide sufficient coverage using the minimum number of satellites. For example, Skybridge, which is a constellation of 80 Ku-band LEO satellites in 20 circular planes each at 1469 km altitude and inclined at 53°, is designed to provide continuous coverage in the $\pm 68^\circ$ latitude band [53] while Teledesic, comprising 288 Ka-band LEO satellites in 12 slightly elliptical near polar orbital planes each at a nominal altitude of 1380 km and inclined at 84.7°, is planned for covering $\pm 72^\circ$ latitude band continuously [54]. Figure 1.10 illustrates both constellations.

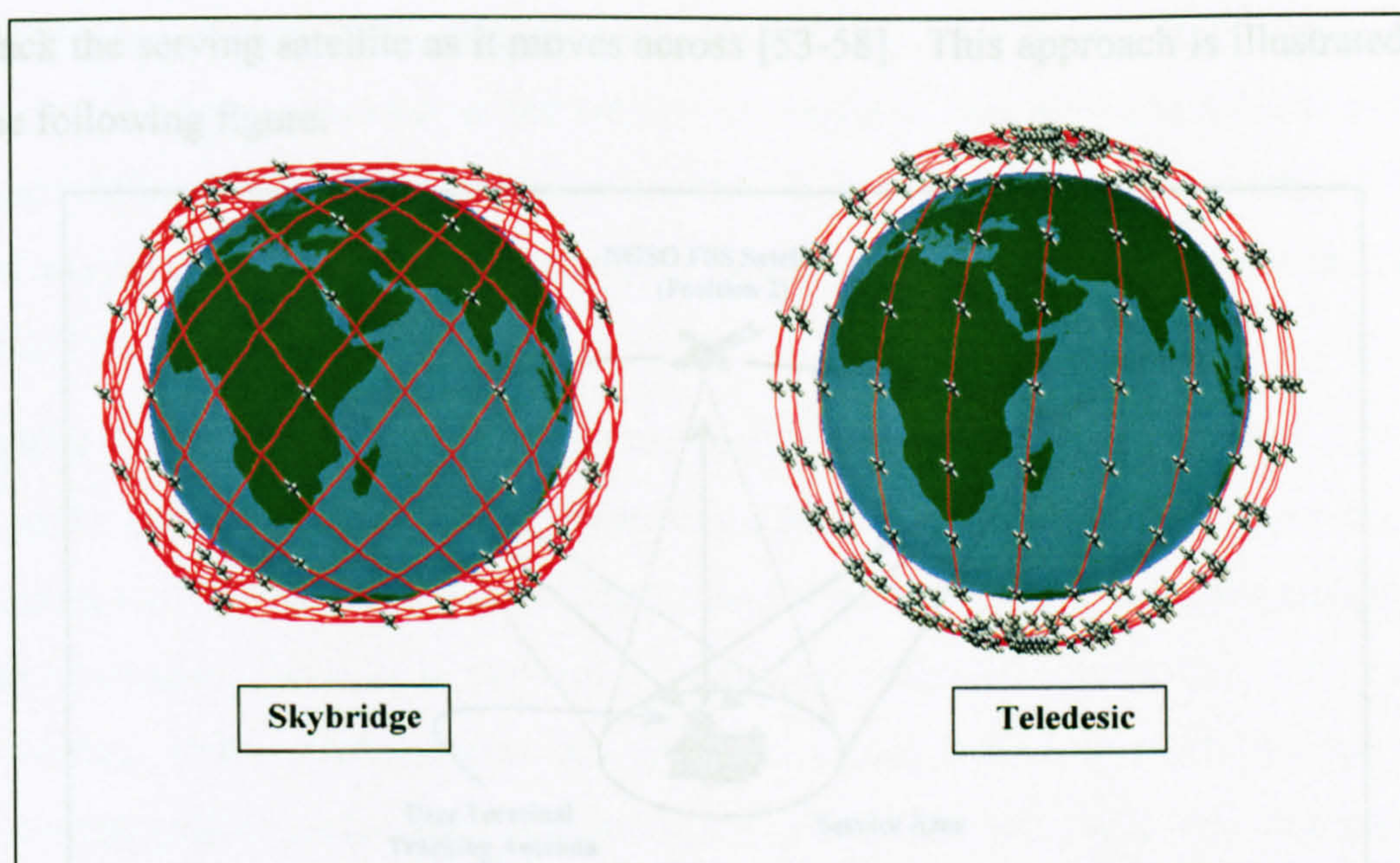


Figure 1.10: Skybridge and Teledesic Constellations

The use of multibeam satellites orbiting inclined multiple planes is a common approach taken by NGSO FSS system proposals [53-58]. Typically, the number of spot beams is in the order of tens per satellite in both uplink and downlink directions. Spot beams are, in general, produced by direct radiating arrays (i.e. phased arrays). These beams enable the system to use its limited power resources efficiently in providing sufficient degree of service quality. Each spot beam is dynamically assigned to illuminate a service area of typically a few hundred kilometre radius. This approach allows the system to re-use the allocated frequencies over sufficiently separated service areas.

It is worth noting that if small service areas were swept by LEO satellite nadir pointing fixed beams, the ground terminals would be served only a fraction of the satellite orbital period before traffic is handed over to other satellites. Frequent traffic handover limits the system capacity and implies increased processing costs. Therefore, NGSO FSS systems commonly employ an Earth-fixed service area design where spot beams are continuously steered over the service areas in order to remain fixed with respect to the ground. The ground terminals within each service area

track the serving satellite as it moves across [53-58]. This approach is illustrated in the following figure.

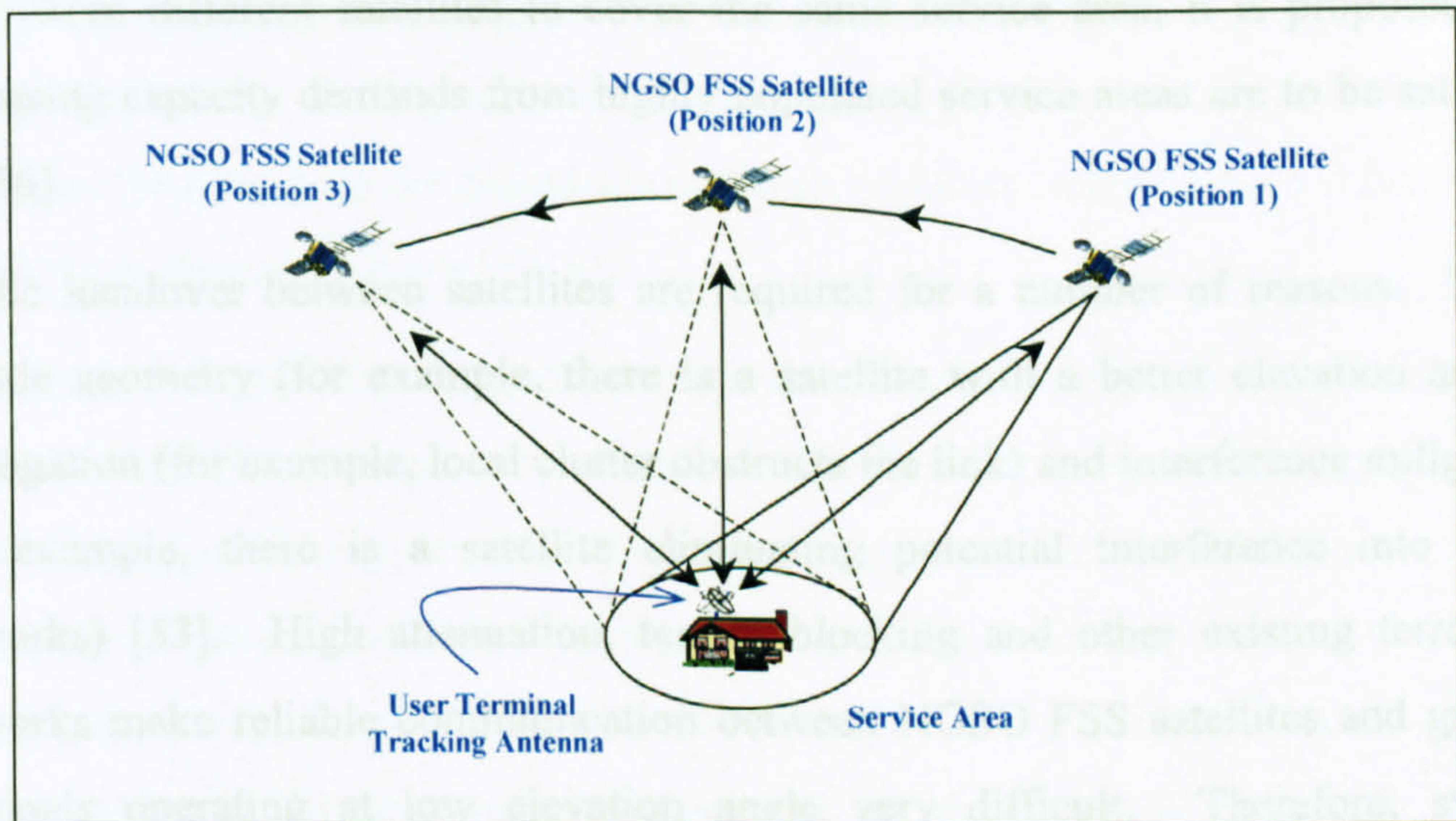


Figure 1.11: Spot Beam Steering

In a slightly different system design approach, satellites are designed to create a fixed contiguous beam pattern over the areas covered by their footprints [55, 58]. In these constellations, a fixed pattern is locked onto a service area and steered to remain fixed as satellite orbits in its orbital plane, as shown in Figure 1.12.

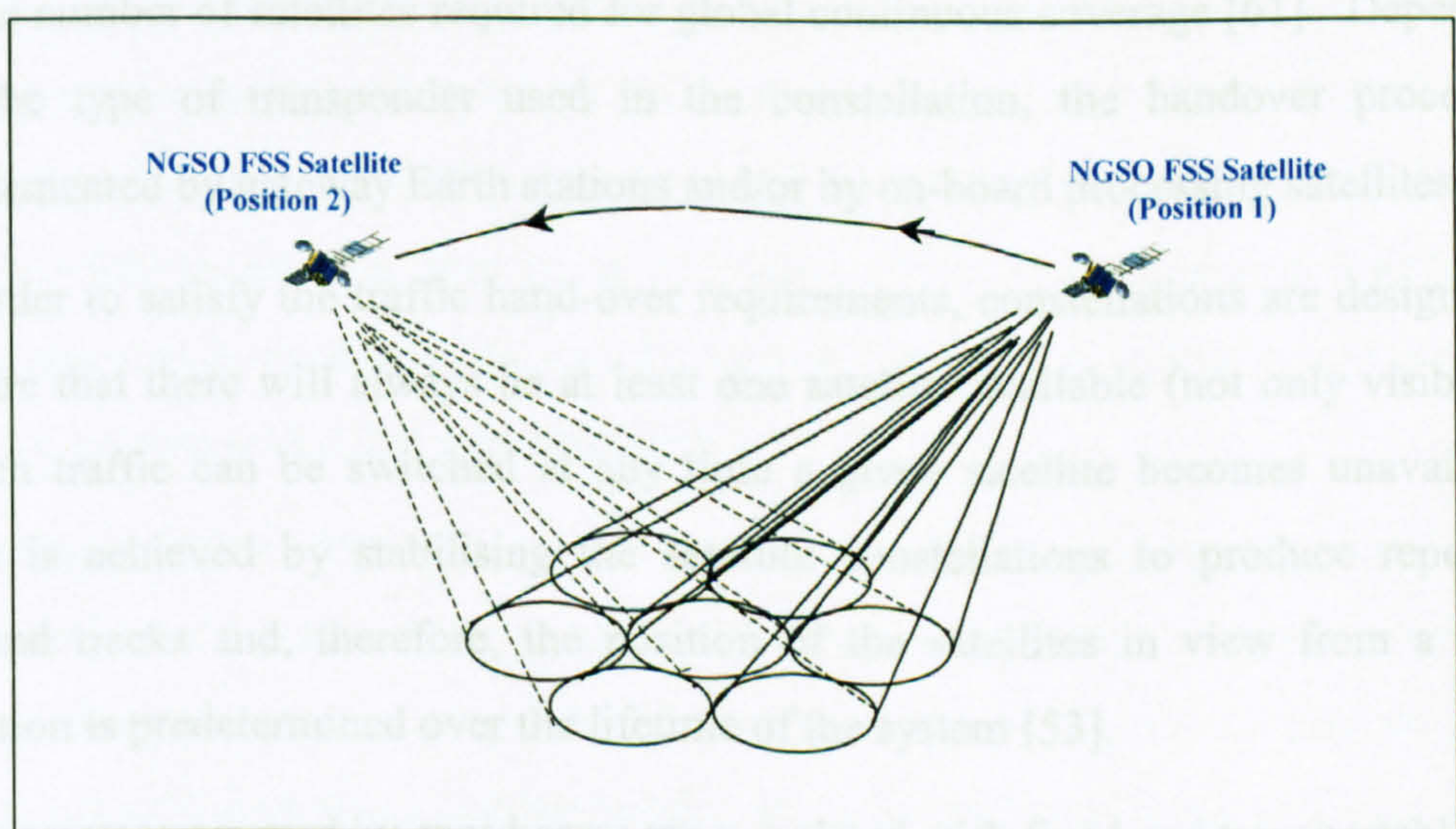


Figure 1.12: Fixed Beam Pattern

In most cases, NGSO FSS system design ensures that there is more than one satellite visible to a given location on the surface of the Earth. By allowing more than one beam from different satellites to cover the same service area, it is proposed that increasing capacity demands from highly populated service areas are to be satisfied [53-56].

Traffic handover between satellites are required for a number of reasons. These include geometry (for example, there is a satellite with a better elevation angle), propagation (for example, local clutter obstructs the link) and interference mitigation (for example, there is a satellite eliminating potential interference into other networks) [53]. High attenuation, terrain blocking and other existing terrestrial networks make reliable communication between NGSO FSS satellites and ground terminals operating at low elevation angle very difficult. Therefore, system proposals are incorporated with minimum operational ground terminal elevation angle requirements, typically between 10° and 40° [53-58].

A low Earth orbit altitude together with a high minimum elevation angle results in limited coverage areas which are being served by each satellite short periods of time. This implies an increased number of handovers which, in turn, suggests an increase in the number of satellites required for global continuous coverage [61]. Depending on the type of transponder used in the constellation, the handover process is implemented by gateway Earth stations and/or by on-board processing satellites.

In order to satisfy the traffic hand-over requirements, constellations are designed to ensure that there will always be at least one satellite available (not only visible) to which traffic can be switched at any time a given satellite becomes unavailable. This is achieved by stabilising the satellite constellations to produce repetitive ground tracks and, therefore, the position of the satellites in view from a given location is predetermined over the lifetime of the system [53].

Service areas covered by spot beams are populated with fixed and transportable user terminals of different sizes and gateway Earth stations. The gateway Earth station locations are selected to provide unobstructed view towards the satellites. They

provide connections to system control and monitoring centres and enable the NGSO FSS system to communicate with other networks. User terminals are primarily installed on rooftops to minimise the effects of obstacles limiting line-of-sight to satellite positions. Both gateways and user terminals employ directional antennas which, in turn, reduces the potential multipath problem caused by the reflection of signals from the local clutter [53-58].

In general, the use of mechanically steered multiple ground terminal antennas is proposed to enable the systems to implement satellite handover [53]. An alternative approach suggested is to employ active phased array ground terminal antennas with fast re-positioning or with dual beams [55, 56]. The downlink and uplink carriers are shared among the ground terminals according to the multiple access scheme combinations employed within the systems to make efficient use of limited bandwidth and power resources.

The required space and ground segment antenna sizes and transmitter power levels are determined by the operating frequency (i.e. Ku or Ka band), amount of traffic to be supported, terminal locations within the satellite footprint, availability requirements and type of orbit satellites operating (i.e. LEO or MEO). For example, the Spaceway system (Ka-band MEO) proposes to employ *32 cm* user antennas with *4 watt* solid state power amplifiers (SSPAs) to support data rates up to *2 Mbps*, *52 cm* antennas with *6 watt* SSPAs for data rates up to *10 Mbps* and *2 m* antennas with *25 watt* SSPAs for data rates up to *155 Mbps*. The system supports four phased array antennas at each satellite, two for transmit with *1.2 m* apertures and the other two for receive with *0.8 m* apertures [56].

In addition, NGSO FSS systems are generally designed with capability of varying satellite power levels and transmitter antenna gains to ensure a constant power flux density for each service area within a satellite footprint (i.e. to compensate for an increased path loss when serving service areas located near nadir and edge of the satellite footprint) [53-56]. For example, in the Skybridge (Ku-band LEO) constellation [53], the maximum satellite transmitter antenna gain for a service area

located at satellite nadir point is *15 dBi*. The gain is increased to *22.8 dBi* for the service area located at the edge of the satellite footprint. Similarly, the satellite transmitter power level is increased from *1.5* to *4.5 watt* for the 45 MHz carrier used in transmissions to the user terminals located in service areas around nadir point and edge of satellite footprint, respectively.

It is worth noting that Automatic Transmitter Power Control (ATPC) is commonly employed at NGSO FSS ground terminals, and at the satellites in some proposed systems [53, 55], so that the minimum amount of power is employed to carry out transmissions. When fading events occur (for example, under rain conditions) transmitter power is increased to compensate for the additional loss. The use of ATPC minimises power consumption under clear-sky conditions and, therefore, eases the spectrum sharing with other networks by reducing the potential interference [53-56].

Since NGSO FSS transmitters require EIRP levels less than those required by GSO FSS transmitters due to relatively short communication links, solid state power amplifier modules are proposed as high power amplifiers [53-56]. As mentioned previously, although these amplifiers produce less maximum output power in comparison to travelling wave tube amplifiers, they achieve greater linearity and higher reliability. In addition, solid state power amplifier technology enables small volume and mass amplifier components to be built which, in turn, reduces the satellite weight [14, 15, 22].

As far as typical amplifier output values are concerned, for example, Teledesic (Ka-band LEO constellation) user terminals (located at satellite nadir) with 35 dBi gain employ transmitter power of *0.8 watt* and *9.2 watt* under clear sky and rain conditions, respectively, for the transmission rate of *4.8 Mbps*. The gateway transmitters (located at satellite nadir) with *54 dBi* gain use *1.1 watt* and *12.1 watt* under clear sky and rain conditions, respectively, for the corresponding data transmission rate of *340 Mbps*. In addition, satellite carriers supporting 680 Mbps transmission rate to user terminals employ *45 watt* transmitter power and carriers

destined for gateway receivers with 340 Mbps transmission rate require 1.3 watt satellite transmitter power under both clear sky and rain conditions and for any terminal locations within the satellite footprint as ATPC is not employed in the downlink direction [54]. It is noted that @Contact (Ka-band MEO constellation) user terminals (located at satellite nadir point) with 41.9 dBi gain transmit 1 watt under clear sky and 21.87 watt for rain conditions to support transmission rate of 3.1 Mbps [55]. Comparison of Teledesic and @Contact user uplink power and antenna size values indicates the need for relatively larger user terminal EIRP requirement to support similar data transmission rates (using the same modulation technique, QPSK) when the constellation is designed for MEO.

1.2.3.2 Network Configurations

In NGSO FSS constellations employing transparent satellites [53, 57, 58], each uplink and downlink beam produced by, in general, phased array antennas are coupled via a transponder providing amplification, filtering and frequency conversion. All monitoring and control functions together with the allocation of satellite beams to different service areas are implemented on the ground using network operations control centre and gateway Earth stations. Transparent systems support direct links between user terminals and gateways (i.e. service links), and between gateways (infrastructure links), as shown in Figure 1.13.

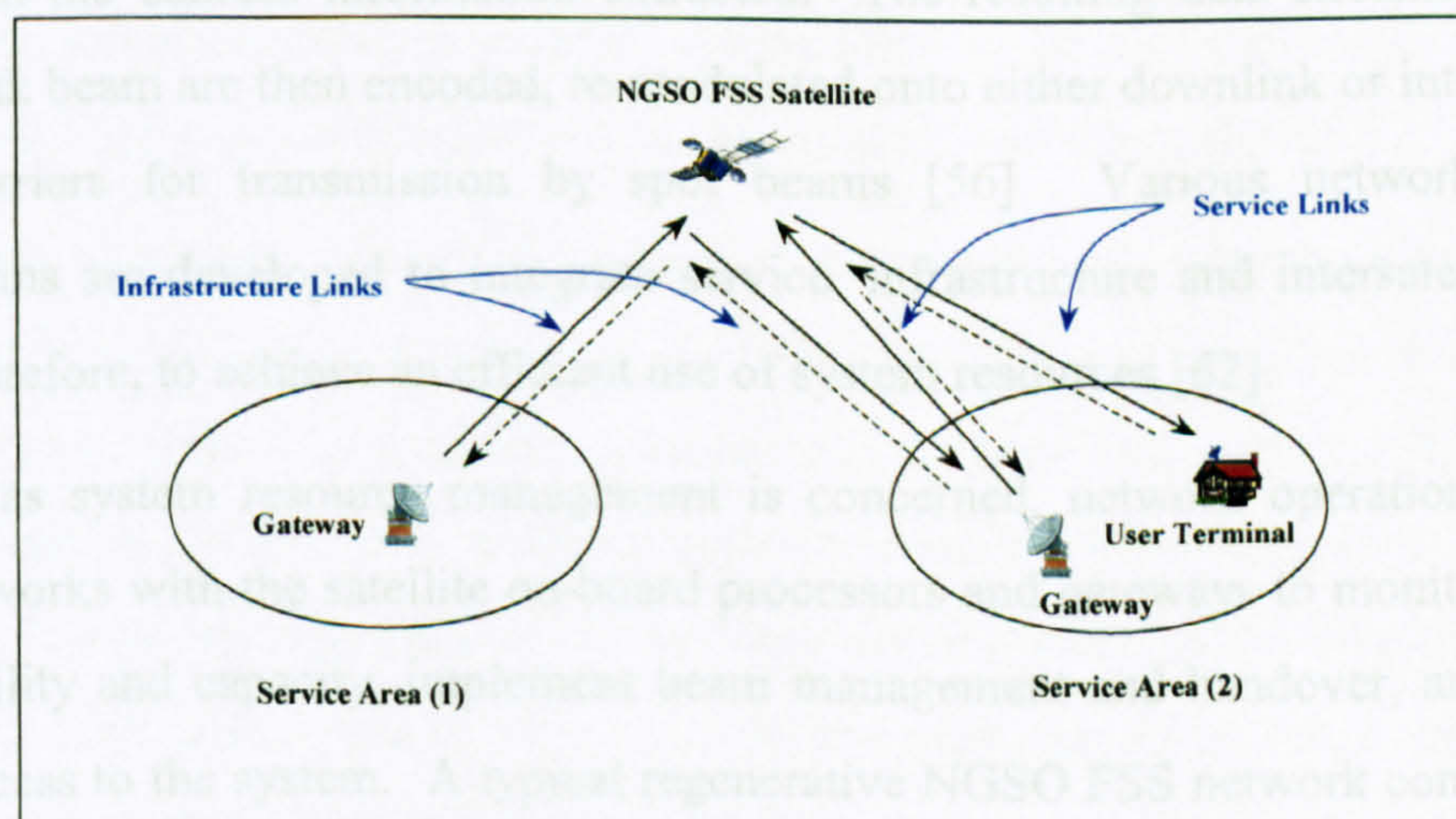


Figure 1.13: Links Supported by Typical Transparent NGSO FSS System

Service links interconnect a user terminal with an appropriate gateway providing the last mile connection between a user and other networks. Infrastructure links allow gateways placed at locations where there are not adequate terrestrial infrastructure to access terrestrial networks through another gateway. User terminal-to-user terminal interconnections within the same service area are established via a gateway using double hop to the satellite. In situations where both user terminals are not in the same service area, links are established through gateways and terrestrial networks. In general, systems are designed to handle unsymmetrical traffic patterns by assigning relatively large carriers to links originating from gateways as transmission rates from user terminals are expected to be significantly lower than those in the opposite direction.

Constellations employing regenerative satellites [54-58] allow service links between user terminals directly to be set-up in addition to the above mentioned connections supported by transparent constellations. Generally, regenerative constellations support multiple intersatellite links (typically, less 10 per satellite) planned for operation in 60 GHz band. The use of optical intersatellite links is also considered in some constellation designs [54, 56].

In a typical regenerative NGSO FSS satellite application, data packets recovered after demodulation and decoding are routed to the appropriate downlink data stream based on the address information extracted. The resulting data streams for each downlink beam are then encoded, re-modulated onto either downlink or intersatellite link carriers for transmission by spot beams [56]. Various network routing algorithms are developed to integrate service, infrastructure and intersatellite links and, therefore, to achieve an efficient use of system resources [62].

As far as system resource management is concerned, network operations control centre works with the satellite on-board processors and gateways to monitor service availability and capacity, implement beam management and handover, and control user access to the system. A typical regenerative NGSO FSS network configuration is illustrated in the following figure.

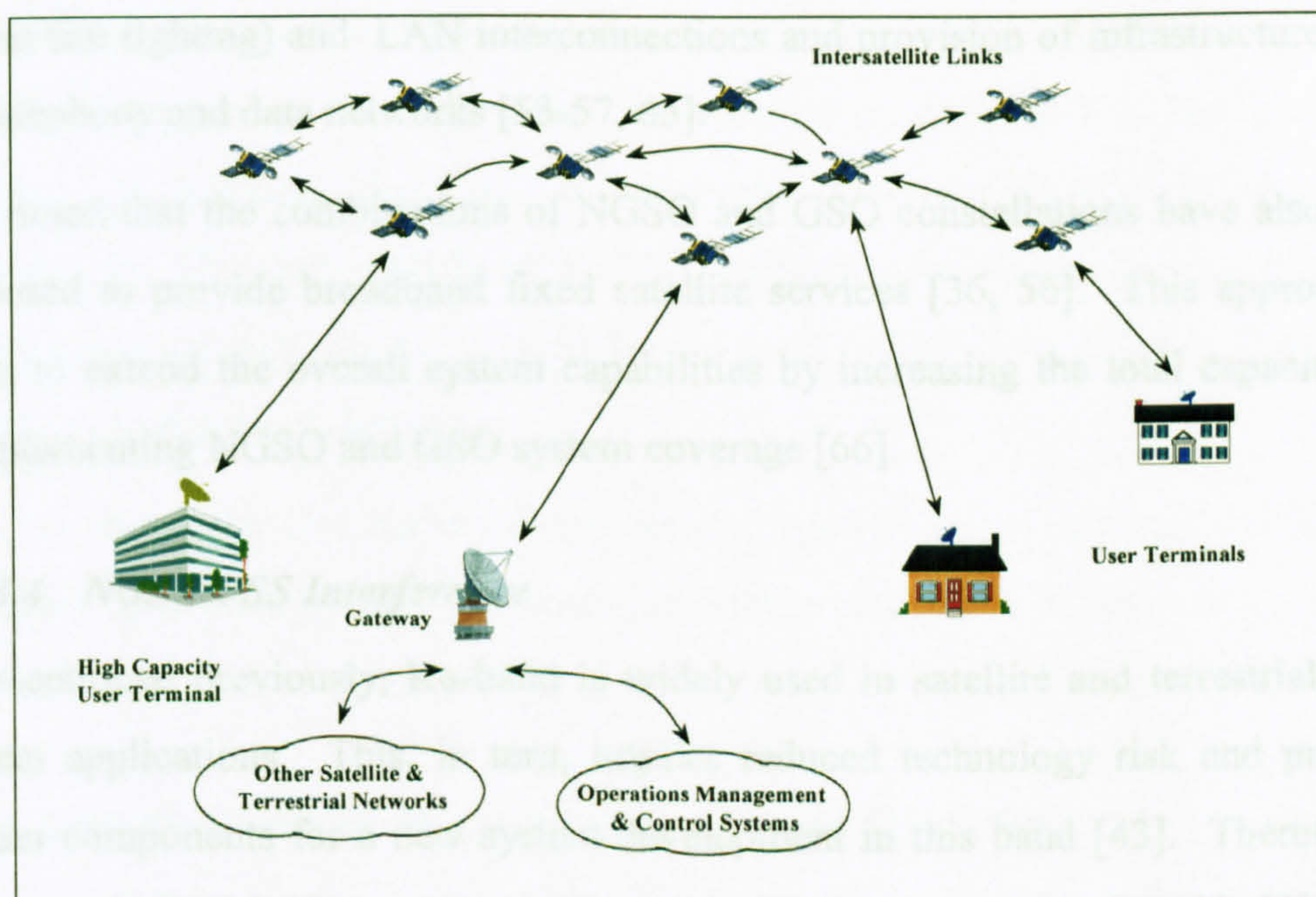


Figure 1.14: Regenerative NGSO FSS System Configuration

1.2.3.3 System Applications

NGSO FSS systems primarily aim to provide interactive real time multimedia applications direct to user premises by taking the advantage of relatively lower transmission delays than those associated with GSO FSS systems (uplink + downlink delay of *10 milliseconds* for an altitude of *1400 km* vs. *240 milliseconds* for an altitude of *35,786 km*). In addition, the hybrid use of NGSO FSS systems and terrestrial communications resources is considered to be an efficient and practical way of providing global wireless communication infrastructure [63-65].

The types of service offered by NGSO FSS networks are similar to those to be provided by GSO FSS systems. These include direct internet access, on line services (transactions, remote purchasing, telebanking, teletraining), videoconference and videotelephony, interactive entertainment services (video-on-demand, electronic games), telecommuting (access to business servers and LANs, file transfer, e-mailing), high speed access to large and complex databases (used in geology, engineering, meteorology and military applications), remote monitoring and control (electric utilities, nuclear power plants, oil and gas pipelines), disaster management

(forest fire fighting) and LAN interconnections and provision of infrastructure links for telephony and data networks [53-57, 65].

It is noted that the combinations of NGSO and GSO constellations have also been proposed to provide broadband fixed satellite services [36, 56]. This approach is taken to extend the overall system capabilities by increasing the total capacity and complementing NGSO and GSO system coverage [66].

1.2.3.4 NGSO FSS Interference

As mentioned previously, Ku-band is widely used in satellite and terrestrial radio system applications. This, in turn, implies reduced technology risk and price of system components for a new system development in this band [43]. Therefore, a number of NGSO FSS systems are planned for Ku-band operation [53, 57, 58].

One of the key issues related to Ku-band NGSO FSS system design is the requirement for spectrum sharing methods to solve potential interference problems with other systems currently in operation. For example, the ITU Radio Regulations state that “*non-geostationary satellite systems shall not cause unacceptable interference to geostationary satellite systems in the fixed satellite service....*” [67].

For these purposes, interference mitigation techniques are incorporated into NGSO FSS system design. In order to protect GSO FSS systems, NGSO FSS networks propose to cease transmissions in predetermined geographic zone (i.e. non-operating zone) within which transmissions to and from an NGSO FSS satellite may cause interference into GSO FSS systems. In such situations, all uplink and downlink transmissions are switched to other satellites in the constellation that are not in danger of causing interference. In addition, power limitations on satellite and ground terminal transmitters and requirement of ground terminal minimum operating elevation angle are imposed on NGSO FSS systems to eliminate potential interference into fixed radio stations of other networks operating on the surface of the Earth [68, 69].

In Ka-band, although there are very few currently operating GSO FSS links many systems are planned for near future deployment as explained in the preceding section. In addition, this band is commonly used for terrestrial fixed radio applications. Therefore, interference mitigation techniques similar to those proposed by Ku-band systems are to be used by Ka-band NGSO FSS systems [54-58] to facilitate the spectrum sharing.

It is worth noting that the development and application of analysis methods to evaluate the implications of proposed interference mitigation techniques are among the primary objectives this research.

1.3 Terrestrial Radio Systems Operating in Fixed Service

The first experimental point-to-point (PP) radio link was installed by Bell Laboratories between New York and Boston in 1947. This analogue point-to-point link utilised vacuum tubes for amplification and employed frequency modulation. The experimental system was further improved and, in 1950, the 4 GHz TD-2 system carrying the first commercial telephony service was developed. Through continuous improvements, this system expanded into a national long distance network of 6,500 km with 125 active repeaters connecting the East and West coasts of the USA in 1960 [70].

Point-to-point radio systems similar to the analogue TD-2 system were installed on major telephony backbone routes in Australia, Canada, France, Italy and Japan beginning in the early 1950s. The channel capacity of commercial systems reached 3,600 analogue voice circuits in Japan by 1979 and 6,000 in the USA by 1980.

The first digital point-to-point radio link was put into service in a short-haul network in Japan in 1968. This system operated at 2 GHz with a capacity of 240 circuits and employed 4-PSK (Phase Shift Keying) modulation. This development brought the issue of spectral efficiency to prominence as digital transmission required large amounts of spectrum for reliable and high quality communication of a large number of voice channels. Since the 1980s, high level modulation techniques leading to an

increased spectral efficiency (for example, 16-QAM (Quadrature Amplitude Modulation) and 64-QAM) have been implemented in digital fixed service links [70].

Among the major advantages of radio links are their ability for rapid installation, the possibility of easy expansion, the minimum maintenance requirement and the capability of re-using existing network structure. Today, fixed service radio links are, therefore, important parts of transmission media in all segments of national and international telecommunications networks. Typically, these links are deployed to form different portions of Integrated Services Digital Network (ISDN), to complement optical fibre and satellite networks, to establish infrastructure connections for mobile systems and to provide transportable systems for disaster recovery and relief operations.

Much standardisation work related to fixed service point-to-point radio links has been carried out within international organisations including ITU and ETSI. There exist a number of recommendations and standards on performance objectives, frequency channel arrangements, system architectures, equipment specifications and frequency sharing constraints.

Point-to-point radio links are employed in a wide range of frequency bands in each country. For example, in the UK, these links are employed in a number frequency bands in the range *1.3 GHz* to *60 GHz* [71]. Frequency channels are assigned on the basis of frequency assignment criteria defined for each frequency band. In the assignment process, the link details including site location, availability requirement, link length, type of service, bandwidth and equipment and antenna details are taken into account to calculate the required EIRP to achieve the link design objectives. Using the calculated value, it is then examined to see if the link under consideration could be accommodated without causing/receiving harmful interference to/from other links operating within the same band [72].

The choice of frequency band principally depends on link length and traffic capacity. Various frequency band assignment policies have been adopted by national

administrations. For example, in the UK, in order to conserve the spectrum in the lower frequency bands for the longer high capacity links the frequency channels are assigned in the highest frequency band compatible with meeting the radio planning requirements. Therefore, a minimum link length policy is adopted by the UK Radiocommunications Agency in selecting the appropriate frequency band for a given link. This policy is based on distances below which it would be reasonable to expect the next highest band available to be used [72].

Traditionally, the most difficult component of the telecommunications network to build and maintain cost effectively has proven to be the local access network. In recent years, a new approach, called Fixed Wireless Access (FWA), has been developed to provide wireless local access for potential residential and business customers. The primary objectives of FWA networks are to reduce the cost by eliminating the need of cables to the subscriber premises, to allow faster network deployment for providing high capacity services to new subscribers and to encourage competition by allowing new entrants to achieve fast coverage and roll-out [73].

The geography of the service area, user density, services offered and available technology are important parameters that enable operators to choose to deploy different technologies and network architectures to serve the potential users. Currently, Point-to-multipoint (PMP) and mesh type architectures are proposed for the FWA systems.

In general, point-to-multipoint networks are similar in design to cellular phone systems. The area to be served is split into a number of cells, with a base station located at the centre of each cell and its antenna typically mounted on a roof top or a pole to provide good line-of-sight to remote subscriber units situated at residential/commercial user premises. Cells are repeated in the form of a regular pattern to provide regional/national coverage.

A mesh architecture, on the other hand, distributes the base station functionality across the network and, therefore, removes the need for base station deployment. Mesh networks comprise an interconnected network of short point-to-point links and

each radio node can act as either a repeater station or a transmitter/receiver station. Basic network components of both architectures are illustrated in Figure 1.15.

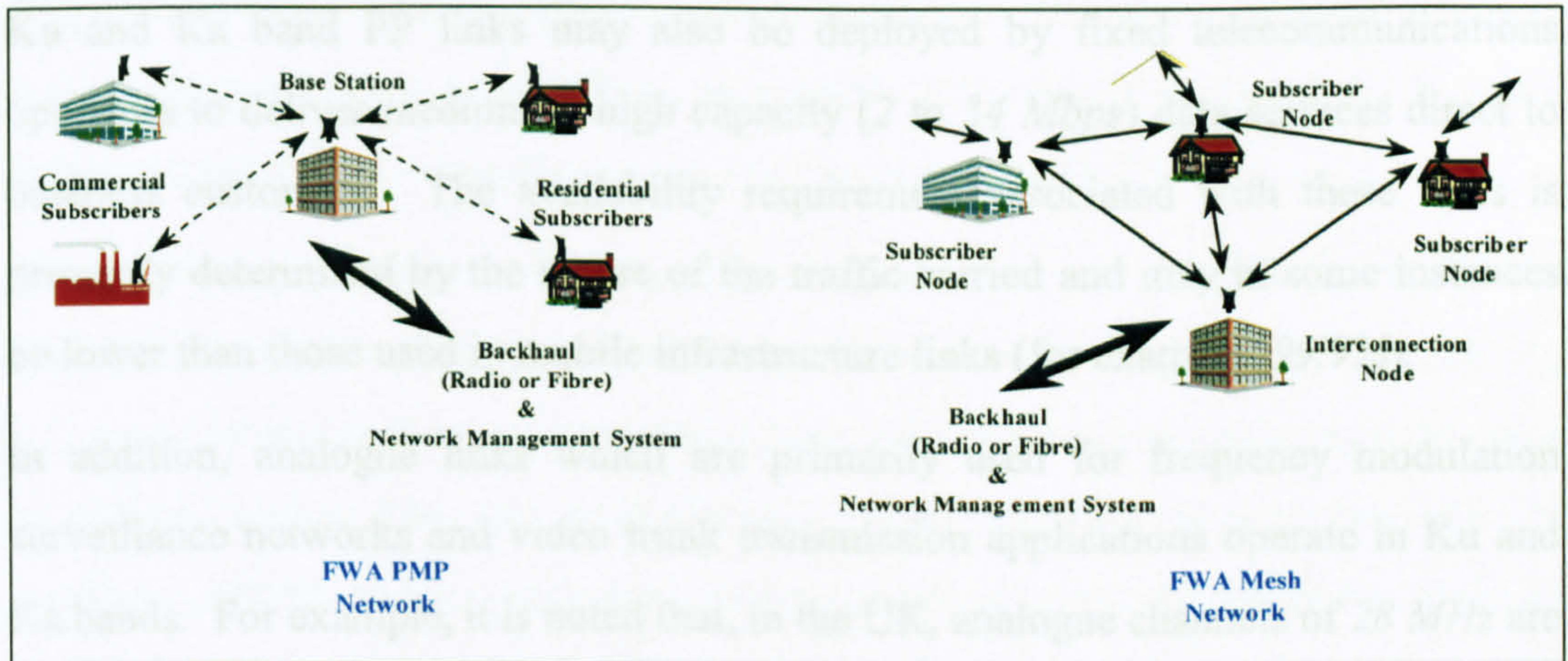


Figure 1.15: Point-to-Multipoint and Mesh System Configurations

Technical characteristics of fixed service links operating/planned for operation at Ku and Ka band frequencies are briefly discussed in the following sections.

1.3.1 Point-to-Point Radio Links

Ku and Ka band frequencies are extensively used for point-to-point radio links which are primarily deployed within the infrastructures of cellular networks to provide high capacity connections between, for example, base transceiver stations and base station controllers. In general, these links are designed to operate with a high availability (for example, 99.99% averaged throughout the year) as each link carries entire communication traffic from base transceiver stations. The transmitter power and antenna gain values are determined to overcome the effect of link fading events (for example, multipath and rain fading) and to achieve the required link availability objectives.

Within infrastructure links, typical data rates are in the range *2 Mbps* to *34 Mbps* and QPSK modulation is generally employed. Increasing numbers of micro and pico cells added to terrestrial mobile networks result in an increasing demand for higher capacity infrastructure links up to or beyond *155 Mbps*. These links are likely to use high level (for example *64-QAM*) modulation and may be required to have higher

availability criterion (for example, 99.999%) because of the greater proportion of network traffic being carried over each link.

Ku and Ka band PP links may also be deployed by fixed telecommunications operators to deliver medium to high capacity (2 to 34 *Mbps*) data services direct to business customers. The availability requirement associated with these links is primarily determined by the nature of the traffic carried and may in some instances be lower than those used in mobile infrastructure links (for example, 99.9%).

In addition, analogue links which are primarily used for frequency modulation surveillance networks and video trunk transmission applications operate in Ku and Ka bands. For example, it is noted that, in the UK, analogue channels of 28 *MHz* are employed to support these applications [71].

Typically, transmitter and receiver antennas are required to be highly directional, with tightly controlled side lobe emissions to maximise spatial re-use of frequencies. In Europe, ETSI standard *ETS 300 833* [74] has been developed to set minimum standards for antenna radiation patterns. This standard defines three classes of antenna, applicable to deployment environments where there is a low, high and very high probability of interference. In addition, generic antenna radiation patterns for high performance point-to-point links are defined within ITU recommendations [75, 76]. It is worth noting that the antenna elevation angles are typically close to zero although, in some instances, they may be few degrees.

As far as the typical link lengths and radio station equipment are concerned, the minimum link lengths in the UK vary from 2.5 *km* to 15 *km* at Ku and Ka band frequencies and the link equipment needs to comply with ETSI standards *EN 301 128*, *ETS 300 639* and *EN 300 431* [77-79].

1.3.2 Fixed Wireless Access Networks

At Ka band frequencies, fixed wireless access networks are being deployed in many countries. These networks are often referred as Broadband Fixed Wireless Access (BFWA) systems due to high bit rates supported through the network. The data

transmission rate is primarily determined by the type of service to be delivered to subscriber sites and the access technique employed within the network. Current BFWA networks aim to support maximum carrier transmission rates typically ranging from *14 Mbps* to *43 Mbps*. In general, this capacity is shared dynamically between a number of subscribers within the service area [80-83].

As mentioned previously, two types of architecture are proposed for BFWA deployments: *point-to-multipoint* and *mesh*. Due to the limited frequency spectrum, it is essential that both configurations use the available spectrum efficiently in order to achieve higher data rate transmissions. The frequency re-use plan, antenna radiation patterns, terrain conditions, power control schemes, multiplexing, multiple access and modulation techniques all play a significant role in determining the BFWA network spectral usage. Characteristics of both configurations are summarised in the following sections.

1.3.2.1 Point-to-multipoint Architecture

Most current networks use point-to-multipoint architecture. Ka band propagation requires that links are line-of-sight. Therefore, elevated base stations are employed to serve a number of subscribers in a given cell or sector. Local clutter (vegetation and buildings) and high capacity demand are two important factors limiting the cell size. Cell radius is typically in the range 2 to 5 *km* [80-82]. The need to ensure line of sight propagation within a cell area limits the single base station coverage. Therefore, the coverage is increased by allowing multiple base station coverage for service areas that cannot be served adequately by a single base station.

In the case of high local demand for service, i.e. urban deployment, each cell is split into sectors. In practice, 4 and 6 sector cells are most commonly deployed. In each sector, a specific set of radio frequencies together with wide antenna azimuth beamwidths are used. Base station azimuth beamwidths typically lie in the range 60° to 90° . Sectorisation reduces the likelihood of interference between cells because of the limited azimuth and narrow elevation beamwidth of the base station antenna. This, in turn, enables the network to re-use the available frequencies. The

correspondingly higher sectorized antenna gain (typically, between 16 to 22 dBi) also improves the link budget, enabling greater distances to be served. In rural applications, coverage and capacity objectives may be satisfied by unsectorized cells.

Base stations communicate with the cell's fixed subscriber units and the high capacity trunk network connecting the individual base stations to the centrally managed control centre. Although subscriber unit configurations may be somewhat different for various system designs, all configurations include outdoor mounted microwave equipment and digital equipment to support modulation, demodulation, control and interface functionality [80-82]. Narrow beam antennas (typically, 3 dB beamwidths of 2-4 degrees) directed towards the most appropriate cell sector are deployed at subscriber sites.

Each base station is connected to the control centre via high capacity backhaul links which could employ either wired or wireless technology. High capacity transmissions to/from other networks are provided through the control centre. Choice of backhaul links is an important economic factor in the broadband point-to-multipoint network design process and also has a bearing on overall spectrum efficiency. Point-to-multipoint network management facilitates the operations, administration, maintenance and provisioning of the network functions. Typically, a network manager workstation located at an appropriate point in the network enables operators to view and optimise the network performance [80-82].

1.3.2.2 Mesh Architecture

A different network topology known as mesh network is suggested for use in Ka band BFWA applications [83]. Unlike point-to-multipoint networks, mesh networks do not employ base stations. Instead, each subscriber station functions as a repeater station enabling traffic to be routed on an ad-hoc basis around an interconnected network of point-to-point links, or to be originated from or delivered to its subscribers. Transmissions are not broadcast to many subscriber stations over a wide area (as with point-to-multipoint base stations) but are conveyed between nodes.

In a typical mesh architecture, relatively short (≈ 1 km) inter-node connections are established using low power (1 to 5 milliwatts in a 1 MHz reference bandwidth), relatively narrow (3dB beamwidths of 9° to 12°) point-to-point radio beams [83]. Subscriber antennas are mounted at a roof-top to minimise the effect of local clutter and to ensure that there are line-of-sight paths in several directions for network interconnectivity. The direction of the links and the choice of frequencies for each link are determined by the traffic routing and channel assignment algorithms. Overall network performance can be significantly affected by the efficiency of these algorithms.

Mesh networks include specific system radio nodes in addition to subscriber radio nodes. The first set of specific nodes, often referred to as seed nodes, are used to provide initial inter-connectivity within a network when the number of subscribers is too low, for example at early stages of the network roll-out. The second set of specific nodes, referred as interconnection nodes, enable the network to connect to an infrastructure (trunk) network through which transmission to/from other networks is achieved. If the number of interconnection points is relatively small the bandwidth requirement could be large as the network traffic is concentrated at these nodes. The mesh network management system provides global network level control and monitors the performance of the mesh nodes [83].

1.3.2.3 Standardisation and Applications

In order to address issues related to BFWA system developments, technical activities are conducted within various study groups either at a national or international level. For example, ETSI has drafted two standards relating to BFWA networks, both based on point-to-multipoint technology: *EN 301 213* specifies system characteristics, *EN 301 215* defines antenna radiation patterns to be used in point-to-multipoint digital radio relay systems [84, 85].

It is worth noting that, due to cost implications, initial BFWA deployments are likely to target business customers by providing fast internet access, video conferencing and multimedia services. The residential market is likely to be addressed in the

longer term where additional services may include video-on-demand, interactive television and telephony services [80-83].

1.4 Thesis Structure

This research is concerned with spectrum sharing analysis methods to be used in examining the impact of interference from NGSO FSS systems into GSO FSS systems and FS terrestrial radio systems operating or planned for operation, at Ku and Ka band frequencies.

After this introduction chapter, the thesis is broken down into the following chapters:

- ***Chapter 2 [Propagation Characteristics]*** examines principal factors affecting propagation of radio signals in Ku and Ka band frequencies. This chapter also considers the implications of the use of propagation models defined in various ITU-R recommendations to investigate NGSO/GSO FSS and NGSO FSS / FS spectrum sharing issues.
- ***Chapter 3 [Review of Issues Related to Interference from Nongeostationary Fixed Satellite Service Systems Into Geostationary Fixed Satellite Service Systems]*** provides an overview of current regulations facilitating spectrum sharing between NGSO/GSO FSS systems. This chapter also includes a review of key mechanisms affecting the co-existence of these systems and summary of representative system characteristics to be used throughout this study.
- ***Chapter 4 [Sharing Analysis Between Geostationary and Nongeostationary Fixed Satellite Service Systems]*** presents the author's work into spectrum sharing methodologies used to examine the implications of interference from NGSO FSS systems into GSO FSS systems in the frequency range 12 to 30 GHz.
- ***Chapter 5 [Review of Issues Related to Interference from Nongeostationary Fixed Satellite Service Systems Into Fixed Service Systems]*** reviews current regulatory requirements and provides critical revision of methodologies employed in studies concerning NGSO FSS / FS spectrum sharing issues.

- ***Chapter 6 [Sharing Analysis Between Fixed Service and Nongeostationary Fixed Satellite Service Systems]*** presents the author's work concerning with development and application of analysis methodologies used to assess the feasibility of spectrum sharing between terrestrial radio systems operating in the fixed service and NGSO FSS systems in Ku and Ka band.
- ***Chapter 7 [Conclusions]*** identifies the key conclusions of this research.

CHAPTER 2

PROPAGATION CHARACTERISTICS

Radio frequency congestion has resulted in many frequency bands being shared by more than one radio service. In order to ensure satisfactory sharing conditions for terrestrial and space systems, it is necessary to be able to predict with reasonable accuracy the propagation behaviour at the frequencies of interest.

In this chapter, the principal factors affecting propagation of radio signals at the Ku and Ka band frequencies are examined. Within ITU-R, a number of recommendations has been developed to model terrestrial and space path propagation effects. These include [86-90]:

- **ITU-R Rec.676** (Attenuation by Atmospheric Gases) used for calculating terrestrial and slant path atmospheric attenuation,
- **ITU-R Rec.530** (Propagation Data and Prediction Methods Required for the Design of Terrestrial Line-of-Sight Systems) used for deriving terrestrial wanted path propagation statistics,
- **ITU-R Rec.452** (Prediction Procedure for the Evaluation of Microwave Interference Between Stations on the Surface of the Earth at Frequencies above about 0.7 GHz) used for deriving terrestrial interference path propagation statistics,
- **ITU-R Rec.618** (Propagation Data and Prediction Methods Required for the Design of Earth-Space Telecommunication Systems) used for deriving Earth-to-space and space-to-Earth wanted path propagation statistics,
- **ITU-R Rec.619** (Propagation Data Required for the Evaluation of Interference Between Stations in Space and Those on the Surface of the Earth) used for deriving Earth-to-space and space-to-Earth interference path propagation statistics,

The propagation statistics are calculated from empirical models based on long term measurements and are usually given in the form of cumulative distribution functions. Common problems in the use of prediction algorithms defined in the recommendations are their limited validity range in terms of frequency, path length and time percentages.

From the NGSO/GSO FSS and NGSO FSS / FS spectrum sharing point of view, the implications of the use of propagation models defined in each recommendation are reviewed in the following sections.

2.1 Atmospheric Gaseous Attenuation

Across the electromagnetic spectrum, absorption mechanisms by certain atmospheric gases take place due to molecular resonances. The absorption coefficient is dependent on the nature of the gas, its concentration, and its temperature [91]. Attenuation due to absorption mechanisms on terrestrial paths (between terrestrial stations) and slant paths (between space and terrestrial stations) can be calculated using estimation procedures defined in ITU-R Recommendation 676 (i.e. Rec.676).

The recommendation was recently modified and the new version (Rec.676-4) was released. From spectrum sharing point of view, the implications of the use of attenuation estimation procedures defined in previous and current versions are examined in this section.

In addition, a new ITU-R Recommendation (Rec.1395) has been developed within the ITU-R study group 4-9S. This recommendation describes a simplified approach for atmospheric attenuation calculations to be used in sharing studies concerning with slant paths (i.e. Space-to-Earth or Earth-to-space paths) [92]. In this section, the estimation methods defined in the new recommendation are also investigated.

2.1.1 ITU-R Rec.676

Two methods are described for the estimation of total terrestrial and slant path atmospheric attenuation. The first method is based on the calculation of specific

attenuation (dB/km) due to dry air and water vapour by applying line-by-line summation of the individual resonance lines mainly from oxygen and water vapour, at given values of pressure, temperature and humidity, up to 1000 GHz . The specific attenuation is then directly multiplied by the path length in order to obtain total attenuation on the terrestrial path. For the slant path, the specific attenuation is integrated through the layers of atmosphere at different pressures, temperatures and humidities.

The second method defines simplified algorithms to estimate terrestrial and slant path atmospheric attenuation up to 350 GHz . The specific attenuation calculation due to dry air and water vapour is formulated using a curve-fitting approach on the results of the line-by-line summation method. Figure 2.1 shows the specific attenuation at sea level for dry air and water vapour [86].

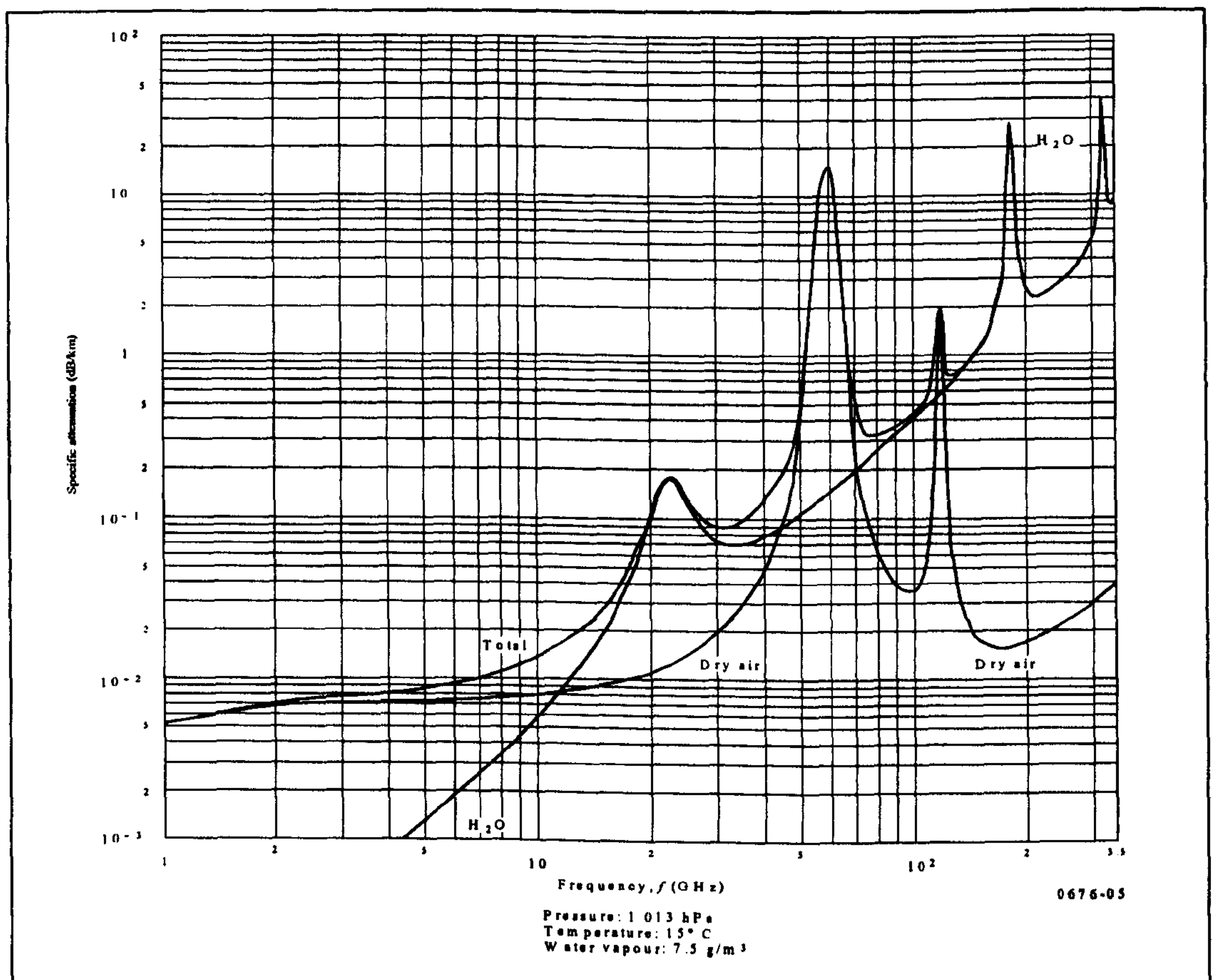


Figure 2.1: Specific Attenuation

The curves illustrate that specific attenuation has strong peaks at around 20, 60, 120, 180 and 320 GHz. These frequencies include oxygen and water vapour molecular rotational resonance lines at which the attenuation increases sharply.

In the application of the simplified method, the attenuation on a terrestrial path is calculated by multiplying the specific attenuation with a path length. For the slant path attenuation, a concept of “equivalent height” is introduced for dry air and water vapour. The specific attenuation is multiplied by the equivalent height to derive zenith path attenuation. Slant path attenuation at elevation angles other than zenith is then determined using set of formulae given in the recommendation.

Comparison of Rec.676-3 (previous version) and Rec.676-4 (current version) suggests that the simplified estimation methods are modified while the line summation method remains unchanged. Algorithms defined in both versions indicate that attenuation varies with operating frequency, path elevation angle, antenna altitude, humidity, pressure and temperature. In the absence of local meteorological parameters (humidity, pressure and temperature), it is recommended that values given in Rec.835 [93] should be used.

2.1.1.1 *Slant Path Attenuation*

A simulation model employing the line summation method is developed for slant path attenuation modelling. The simulation modelling is carried out using Aegis Systems Spectrum Engineering Tool (ASSET) software.

ASSET is developed at Aegis Systems Limited and capable of modelling a range of sharing scenarios involving both space and terrestrial systems. The software is well known internationally and has been used as a key element in spectrum sharing studies for many years. The line summation method is built into the software to evaluate the implications of atmospheric attenuation in examining sharing scenarios.

Assuming that a ground terminal receiver is located at a sea level, atmospheric attenuation values are obtained at every 5 degrees elevation in the frequency bands 14/12 GHz (Ku-band) and 30/20 GHz (Ka-band).

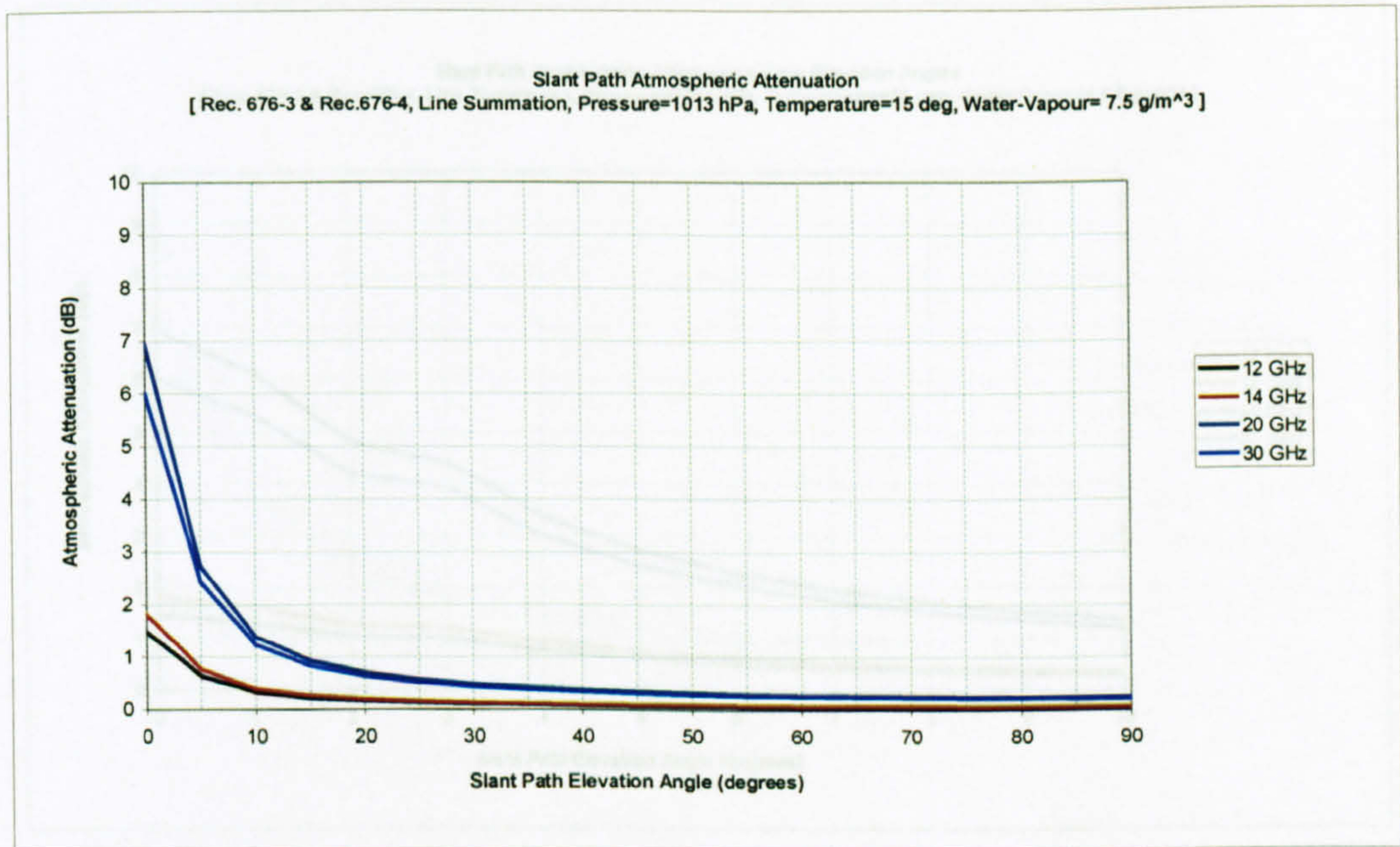


Figure 2.2: Total Slant Path Atmospheric Attenuation (Line Summation)

As expected, the slant path attenuation is higher at low elevation angles as the length of the path travelling through the atmosphere is much longer. In particular, the horizon paths are faded by some 7 dB in the Ka band. On the other hand, the results suggest that the atmospheric attenuation is insignificant ($\leq 2\text{ dB}$) for elevation angles greater than 10 degrees .

The same simulation scenario is repeated using an elevation interval of 1 degree to illustrate the atmospheric attenuation for elevation angles less than 10 degrees . The results are shown in Figure 2.3.

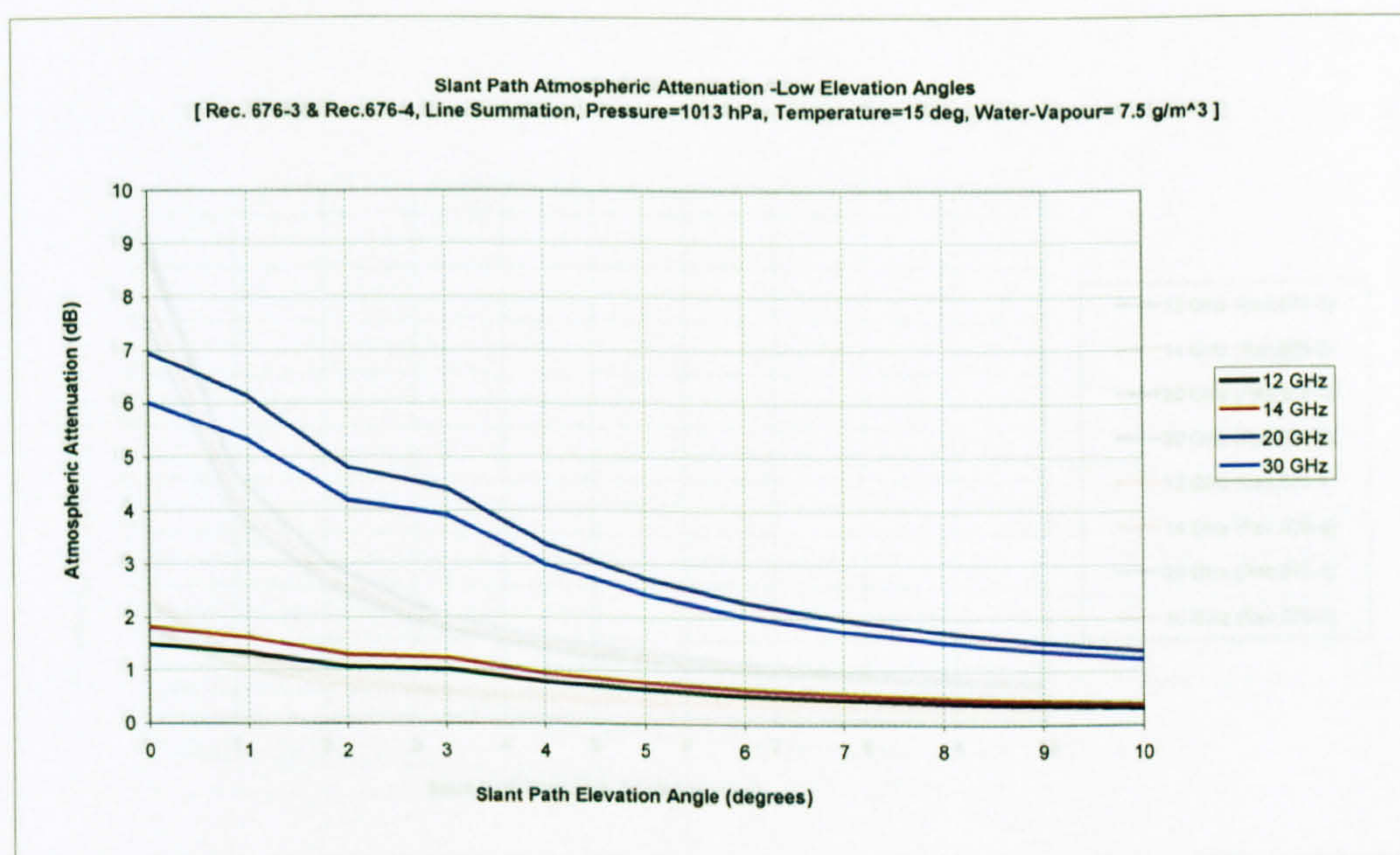


Figure 2.3: Total Slant Path Atmospheric Attenuation (Line Summation, Low Elevation Angles)

It is interesting to note that the total attenuation at *20 GHz* is slightly higher than that of at *30 GHz*. This is the result of the peak due to water vapour resonance lines located at *22.235 GHz* (see Figure 2.1).

For the purposes of comparison, the simplified prediction algorithms defined in both versions of Rec.676 are implemented using Mathcad software package. The following figure illustrates corresponding attenuation curves for elevation angles less than *10 degrees*.

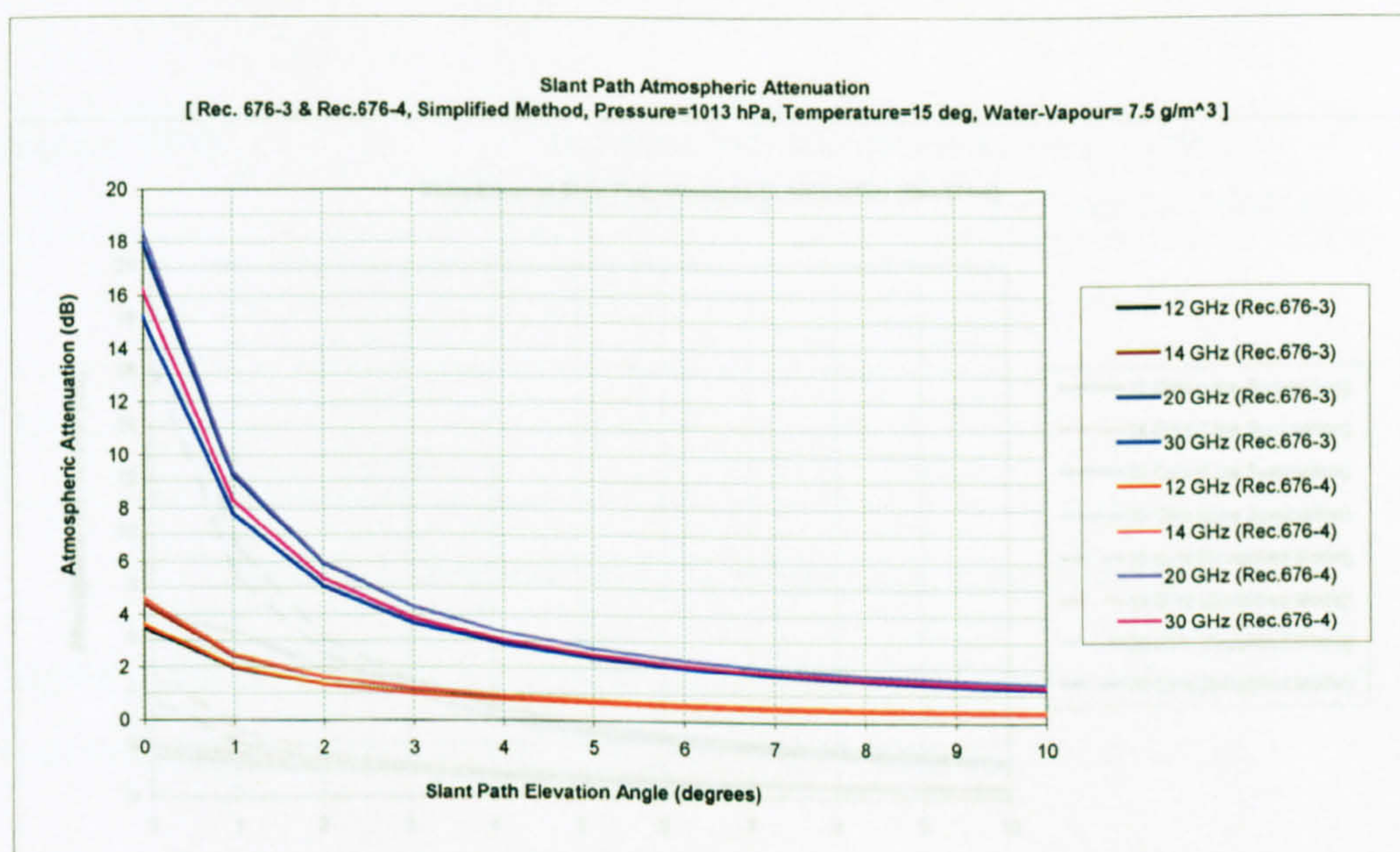


Figure 2.4: Total Slant Path Atmospheric Attenuation (Simplified Model, Low Elevation Angles)

The plots indicate that, as far as Ku and Ka band sharing analysis is concerned, the use of both models would not make a significant difference as the attenuation values are very close to each other for the same frequency. Figure 2.5 compares the line summation and simplified methods defined in Rec.676-4 for low elevation angles.

2.1.1.2 Terrestrial Path Attenuation

Atmospheric attenuation on terrestrial radio paths could be significant under certain atmospheric conditions. Table 2.1 presents terrestrial path attenuation values obtained from the line summation and simplified methods defined in Rec.676-4. The meteorological parameters are assumed to be Pressure=1013 hPa, Temperature=15 °C, Water Vapour=7.5 g/m³.

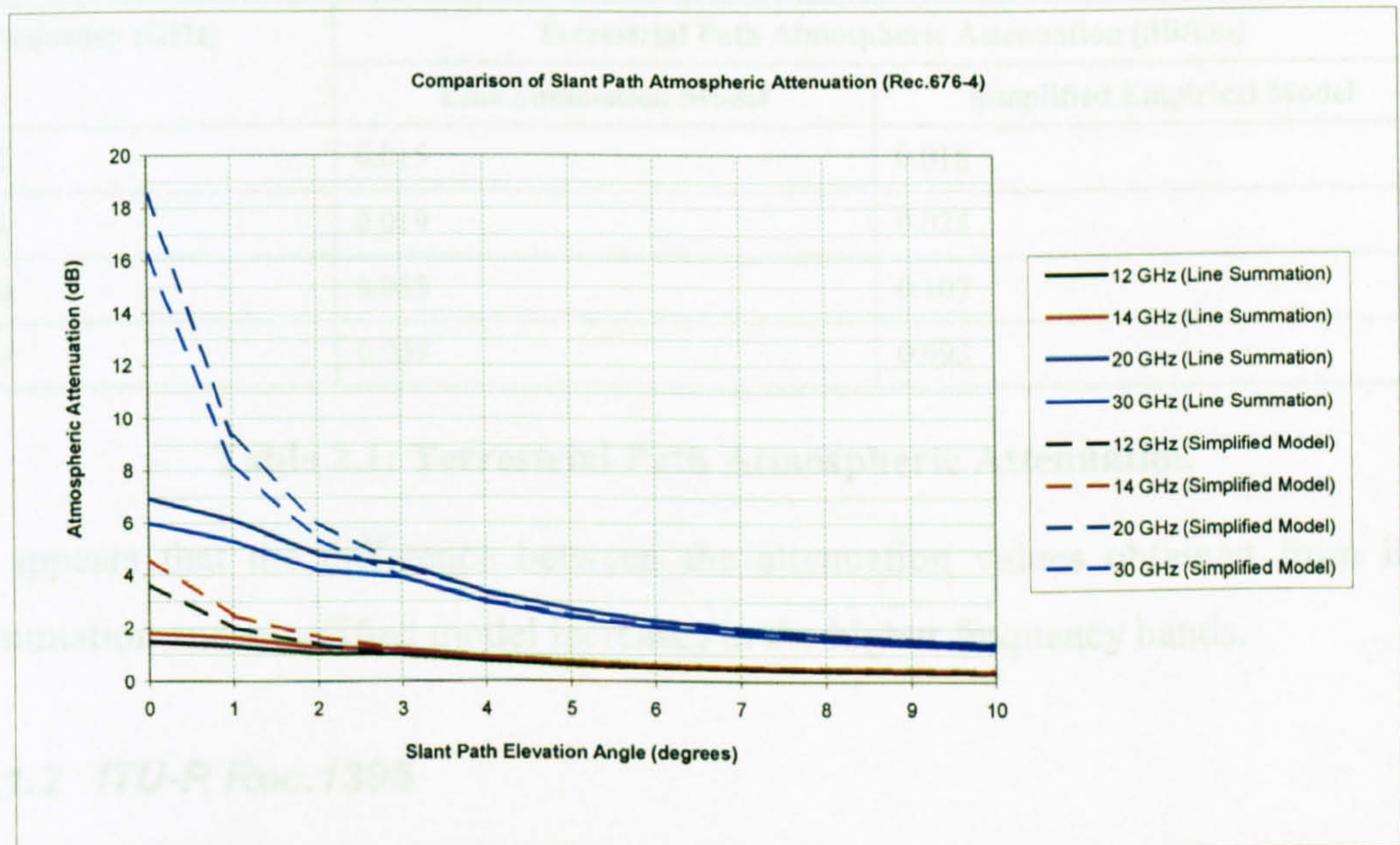


Figure 2.5: Comparison of Total Slant Path Atmospheric Attenuation (Line Summation and Simplified Model, Low Elevation Angles)

The line summation and simplified model results are in close agreement for elevation angles greater than 3 *degrees*. The simplified model results in greater attenuation than the line summation method for very low elevations. As can be seen, the difference is significant at Ka band.

2.1.1.2 Terrestrial Path Attenuation

Atmospheric attenuation on terrestrial radio paths could be significant under certain atmospheric conditions. Table 2.1 presents terrestrial path attenuation values obtained from the line summation and simplified models defined in Rec.676-4. The meteorological parameters are assumed to be: *Pressure*=1013 hPa, *Temperature*=15 C°, *Water Vapour*=7.5 g/m³.

Frequency (GHz)	Terrestrial Path Atmospheric Attenuation (dB/km)	
	Line Summation Model	Simplified Empirical Model
12	0.015	0.018
14	0.019	0.024
20	0.083	0.107
30	0.069	0.093

Table 2.1: Terrestrial Path Atmospheric Attenuation

It appears that the difference between the attenuation values obtained from line summation and simplified model increases in the higher frequency bands.

2.1.2 ITU-R Rec.1395

Rec. 1395 provides a set of formulae for the estimation of slant path atmospheric attenuation [92]. Three regions are defined as a function of latitude for each frequency band.

- low latitudes within 22.5° of the Equator,
- mid-latitudes greater than 22.5° and less than 45° from the Equator
- high-latitudes greater than 45° from the Equator

For a given frequency band, each region is associated with a formula that is based on the line summation method described in Rec.676 together with the driest month meteorological parameters specified in Rec.835. The calculation method requires an antenna altitude and a path elevation angle as input parameters.

Figure 2.6 compares the slant path attenuation calculated from Rec.1395, implemented in Mathcad, against those derived from the line summation method. It is assumed that the ground terminal is located at a sea level in the high latitude region.

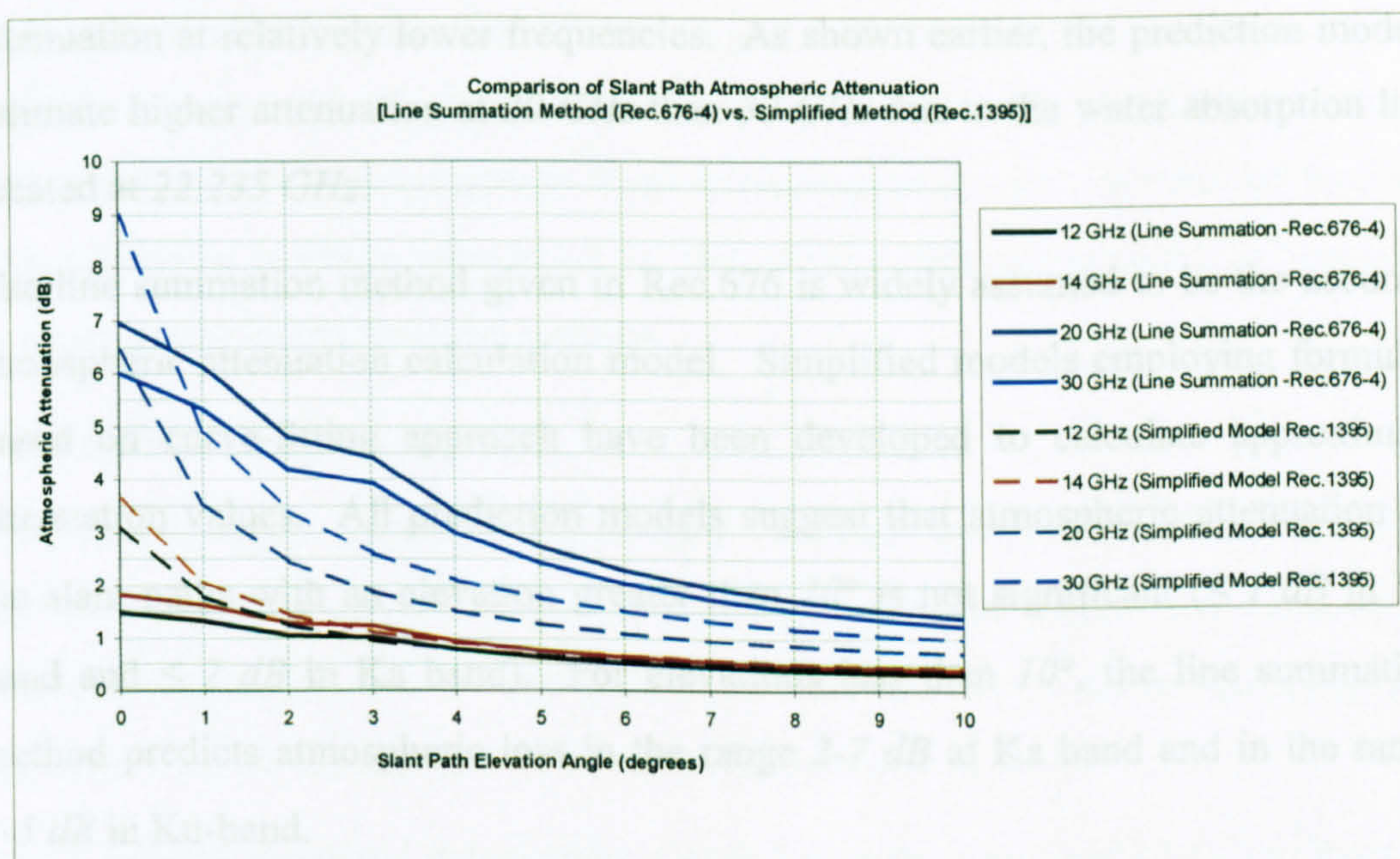


Figure 2.6: Comparison of Total Slant Path Atmospheric Attenuation (Line Summation (Rec.676-4) and Simplified Model (Rec.1395), Low Elevation Angles)

The plots indicate that the simplified model does not consider the impact of water absorption peak at 22.235 GHz as the attenuation levels at 30 GHz are greater than those calculated for 20 GHz . Therefore, the differences are in order of few dBs in the Ka band results. The Ku-band attenuation values are in good agreement for the slant paths elevated at greater than 2 degrees .

2.1.3 Discussion

The attenuation due to atmospheric gas is primarily determined by meteorological parameters (pressure, temperature and humidity), operating frequency and path length. For slant path attenuation, the path elevation angle determines the length of the path travelling through the atmosphere. A small path elevation angle implies that the propagation path traverses a longer cross-section of the atmosphere, hence the attenuation due to atmospheric gases is higher. In general, an increasing frequency gives rise to a larger attenuation. However, the oxygen and water absorption lines cause attenuation peaks, which, in turn, results in relatively higher

attenuation at relatively lower frequencies. As shown earlier, the prediction models estimate higher attenuation at 20 GHz than 30 GHz due to the water absorption line located at 22.235 GHz.

The line summation method given in Rec.676 is widely assumed to be the accurate atmospheric attenuation calculation model. Simplified models employing formulae based on curve-fitting approach have been developed to calculate approximate attenuation values. All prediction models suggest that atmospheric attenuation on the slant paths with an elevation greater than 10° is not significant (≤ 1 dB in Ku band and ≤ 2 dB in Ka band). For elevations less than 10° , the line summation method predicts atmospheric loss in the range 2-7 dB at Ka band and in the range 1-5 dB in Ku-band.

The analysis suggests that the attenuation values obtained from empirical models defined in Rec.676-3 and Rec.676-4 are very close to each other in the frequency bands of interest. The comparison of the line summation and the simplified model defined in the Rec.676-4 shows that the latter predicts higher attenuation for elevation angles less than 3° . In addition, Rec.1395 defines a simplified approach for determining the slant path attenuation. Comparison of Rec.1395 results against the attenuation values obtained from Rec.676-4 line summation model indicates that the difference is a few dBs, at Ka band.

In the context of NGSO/GSO FSS and NGSO FSS / FS spectrum sharing, implications of atmospheric attenuation can be summarised by taking wanted (i.e. planned) and interfering paths into consideration as following:

NGSO/GSO FSS Sharing:

From the wanted path perspective, the minimum operating elevation angles for NGSO FSS systems are typically $\geq 10^\circ$ while the Radio Regulations implies that the minimum elevation angle for GSO FSS links should be $\geq 3^\circ$ [94]. The line summation and simplified prediction models of Rec.676-4 suggest that GSO and NGSO FSS wanted paths will be faded at most by some 4 dB in Ka-band and 1 dB in Ku-band.

From the interfering path point of view, paths exist down to the horizon for which considerable atmospheric attenuation may apply. For example, the Ka band horizon path attenuation is approximately 7 dB according to the line summation method. This additional isolation introduced by atmospheric attenuation could be beneficial in terms of protection from interference.

NGSO FSS / FS Sharing:

Atmospheric loss is not significant on the FS wanted paths as Ku and Ka band links are relatively short (5 to 15 km). According to the line summation method, for example, attenuation due to atmospheric gas remains below 1 dB in both frequency bands for a 10 km FS link (see Table 2-1).

In the case of terrestrial interference paths, the attenuation could be considerable. For example, 100 km interfering path will be faded by some 8 dB at 20 GHz on the basis of the line summation method. Attenuation due to atmospheric gas might prove useful in that the NGSO FSS / FS spectrum utilisation might be enhanced.

2.2 Terrestrial Path Propagation

In terrestrial path propagation analysis, influences of atmosphere and terrain need to be taken into account. The degree to which these influences affect propagation depends primarily on the operating frequency. At the frequencies of interest, the atmospheric events occurring in the troposphere, which is the lowest region of the atmosphere, play a significant role [87, 88, 91].

The radio refractive index of the troposphere varies with height due to changes of temperature, pressure and humidity. The way these variations take place influences radiowave propagation. The refractive index generally decreases with height. This gives rise to a slight downward *refraction* of radiowaves which, in turn, allows propagation to distances slightly beyond the optical horizon. When the variation of refractive index is sufficiently large and extends over a sufficient height interval and horizontal extent, the atmospheric *ducts*, in which radiowaves are transmitted far beyond the normal horizon, may occur. In addition, partial *reflection* of radiowaves

may occur when there is an abrupt change in the refractive index over a large horizontal area. Both ducting and reflection mechanisms may lead to multipath events on line-of-sight terrestrial paths and interference events on beyond horizon paths [87, 88, 91, 95].

Randomly distributed small scale spatial fluctuations of refractive index about local mean value result in weak signal levels being present at large distances beyond the horizon. This phenomenon is referred to as *tropospheric scattering*. These small refractive index irregularities may also cause rapid fading or *scintillation* on line-of-sight paths [87, 88, 91, 95].

The implications of terrain structure and clutter (i.e. hills, buildings, vegetation etc.) are frequency dependent and include *reflection*, *scatter*, *diffraction* and *absorption* of transmitted radiowaves. It is also important to note that *absorption* and *scatter* due to hydrometeors occurring in the troposphere also have significant effects on the terrestrial radiowave propagation in Ku and Ka bands [87, 88, 95, 96].

In line with the above discussions, implications of wanted and interference path propagation mechanisms are investigated in the following sections. The terrestrial wanted path mechanisms are considered in the context of fixed service link planning while the interference path propagation effects are examined from an NGSO FSS / FS spectrum sharing point of view.

2.2.1 Wanted Path Propagation Effects

Fading due to multipath and rain mechanisms need to be considered in Ku and Ka band fixed service link planning. For a terrestrial line-of-sight link, there may often be a ground reflected radiowave in addition to the direct ray. There may also be reflected radiowaves due to abrupt change of tropospheric refractive index with height. Multipath fading is the result of the direct radiowaves combined with reflected radiowaves [87].

Water is present in the atmosphere in a variety of phases: as gas, liquid droplets and solid particles. These phases include particles of rain, snow, ice crystals, hail, fog

and clouds. Precipitation is generally recognised as rain, snow and hail. Precipitation molecules interact with radiowaves in different ways depending on the phase. These interactions cause radiowaves to be absorbed and scattered. As far as the fixed service wanted path is concerned, absorption due to rain is the most significant precipitation effect which needs to be taken into account at the frequencies of interest [87, 91, 95, 96].

The prediction models for multipath and rain effects are defined in Rec.530 (currently at version 8) [87].

2.2.1.1 *Multipath Fading*

The multipath fading prediction algorithm described in the recommendation is not path profile dependent and is widely used for terrestrial link design purposes. The prediction algorithm, initially, produces fading distribution for large fade depths in the average worst month in any part of the world. An interpolation procedure is then defined for small fade depths. In addition, a conversion method from average worst month to average annual statistics is also described.

The multipath fading algorithm requires an estimate of “geoclimatic factor (K)” for the average worst month from the measurements for the path location in question. If measured data is not available, empirical expressions are defined for K for inland links and coastal links over/near large and medium sized bodies of water.

Having determined the geoclimatic factor K , large fade depths (for example >25 dB) for the average worst month are calculated from the following expression:

$$p_w = K d^{3.6} f^{0.89} (1 + |\epsilon_p|)^{-1.4} 10^{-A/10} \quad (2-1)$$

where

d is the path length, km

f is the frequency, GHz

ϵ_p is the path inclination, mrad, calculated from

$$|\epsilon_p| = |h_r - h_e| / d$$

where

h_r is the receiver antenna height above sea level, m

h_e is the transmitter antenna height above sea level, m

A is the fade depth (dB) exceeded for the percentage time p_w in the average worst month.

On the basis of Equation 2-1, an interpolation method is defined for deriving a percentage of time for which any fade depth is exceeded. It is noted that the interpolation method has been modified in the latest version of the recommendation (Rec.530-8). Both previous and current methods are summarised below.

Previous Interpolation Method (Rec.530-7):

- Using Equation 2-1, calculate p_w for a fade depth of $A=35$ dB,
- Calculate q'_a for $A=35$ dB and the corresponding p_w from

$$q'_a = -20 \log \left[-\ln \left(\frac{100 - p_w}{100} \right) \right] / A \quad (2-2)$$

- Calculate q_t from

$$q_t = (q'_a - 2) / \left[\left(1 + 0.3 \cdot 10^{-A/20} \right) 10^{-0.016A} \right] - 4.3 \left(10^{-A/20} + A/800 \right) \quad (2-3)$$

- If $q_t > 0$, repeat preceding steps for $A=25$ to obtain the definitive value of q_t
- If the definitive value of q_t is obtained from $A=35$, calculate p_w for $A>35$ using Equation 2-1. For $A<35$, calculate p_w from

$$p_w = 100 \left[1 - \exp \left(-10^{-q_a A / 20} \right) \right] \quad (2-4)$$

where

$$q_a = 2 + \left(1 + 0.3 \cdot 10^{-A/20} \right) \left(10^{-0.016A} \right) \left(q_t + 4.3 \left(10^{-A/20} + A/800 \right) \right) \quad (2-5)$$

- If the definitive value of q_t is obtained from $A=25$, calculate p_w for $A>25$ using Equation 2-1. For $A<25$, calculate p_w from Equations 2-4 & 2-5.
- Apply the following procedure for to convert the average worst month exceedence percentage (p_w) into the average year exceedence percentage (p):
- Calculate the logarithmic geoclimatic conversion factor from

$$\Delta G = 10.5 - 5.6 \log \left(1.1 \pm |\cos(2\xi)|^{0.7} \right) - 2.7 \log d + 1.7 \log(1 + |\varepsilon_p|) \quad (2-6)$$

where

$\Delta G \leq 10.8$ dB and positive sign in the equation is used for $\xi \leq 45^\circ$,
 ξ is the latitude,
 d is the path length,
 ε_p is the path inclination

- Calculate the average year exceedence percentage (p) from

$$p = 10^{-\Delta G/10} p_w \quad (2-7)$$

Current Interpolation Method (Rec.530-8):

- Using Equation 2-1, calculate the multipath occurrence factor (p_o) from

$$p_o = K d^{3.6} f^{0.89} (1 + |\varepsilon_p|)^{-1.4} \quad (2-8)$$

- Calculate the value of fade depth, A_t , at which the transition between the deep fading distribution and the shallow fading distribution occurs from

$$A_t = 25 + 1.2 \log(p_o) \text{ dB} \quad (2-9)$$

- If the required fade depth $A \geq A_t$, calculate the percentage of time for which A is exceeded in the average worst month from

$$p_w = p_o * 10^{-A/10} \quad (2-10)$$

- If the required fade depth $A < A_t$ apply the following algorithm:
 - Calculate the percentage of time, p_t , that A_t is exceeded in the average worst month from

$$p_t = p_o * 10^{-A_t/10} \quad (2-11)$$

- Calculate q'_a from

$$q'_a = -20 \log \left[-\ln \left(\frac{100 - p_t}{100} \right) \right] / A_t \quad (2-12)$$

- Calculate q_t from

$$q_t = (q'_a - 2) / \left[\left(1 + 0.3 * 10^{-A_t/20} \right) 10^{-0.016 A_t} \right] - 4.3 \left(10^{-A_t/20} + A_t / 800 \right) \quad (2-13)$$

- Calculate q_a from

$$q_a = 2 + \left(1 + 0.3 * 10^{-A/20} \right) \left(10^{-0.016 A} \right) \left(q_t + 4.3 \left(10^{-A/20} + A / 800 \right) \right) \quad (2-14)$$

- Calculate the percentage of time for which A is exceeded in the average worst month from

$$p_w = 100 \left[1 - \exp \left(-10^{-q_a A / 20} \right) \right] \quad (2-15)$$

- Apply the same conversion procedure as described in Rec.530-7 for the conversion of the average worst month exceedence percentage (p_w) into the average year exceedence percentage (p).

Comparison:

Ku and Ka band multipath fading statistics obtained from both methods are compared in Figure 2.8. Modelling is based on the following assumptions:

$d := 5$	path length, km
$C_0 := 1.7$	constant, assume lower antenna altitude in 0-400 metre above mean sea level
$C_{lat} := 0$	constant, assume latitude is ≤ 53 degrees
$C_{lon} := 3$	constant, assume longitude is in Europe
$p_L := 5$	from Rec.453-6
$h_r := 10$	antenna height above sea level, m
$h_e := 10$	antenna height above sea level, m
$\xi := 52$	link latitude, degrees

Figure 2.7: Assumptions For Multipath Fading Modelling

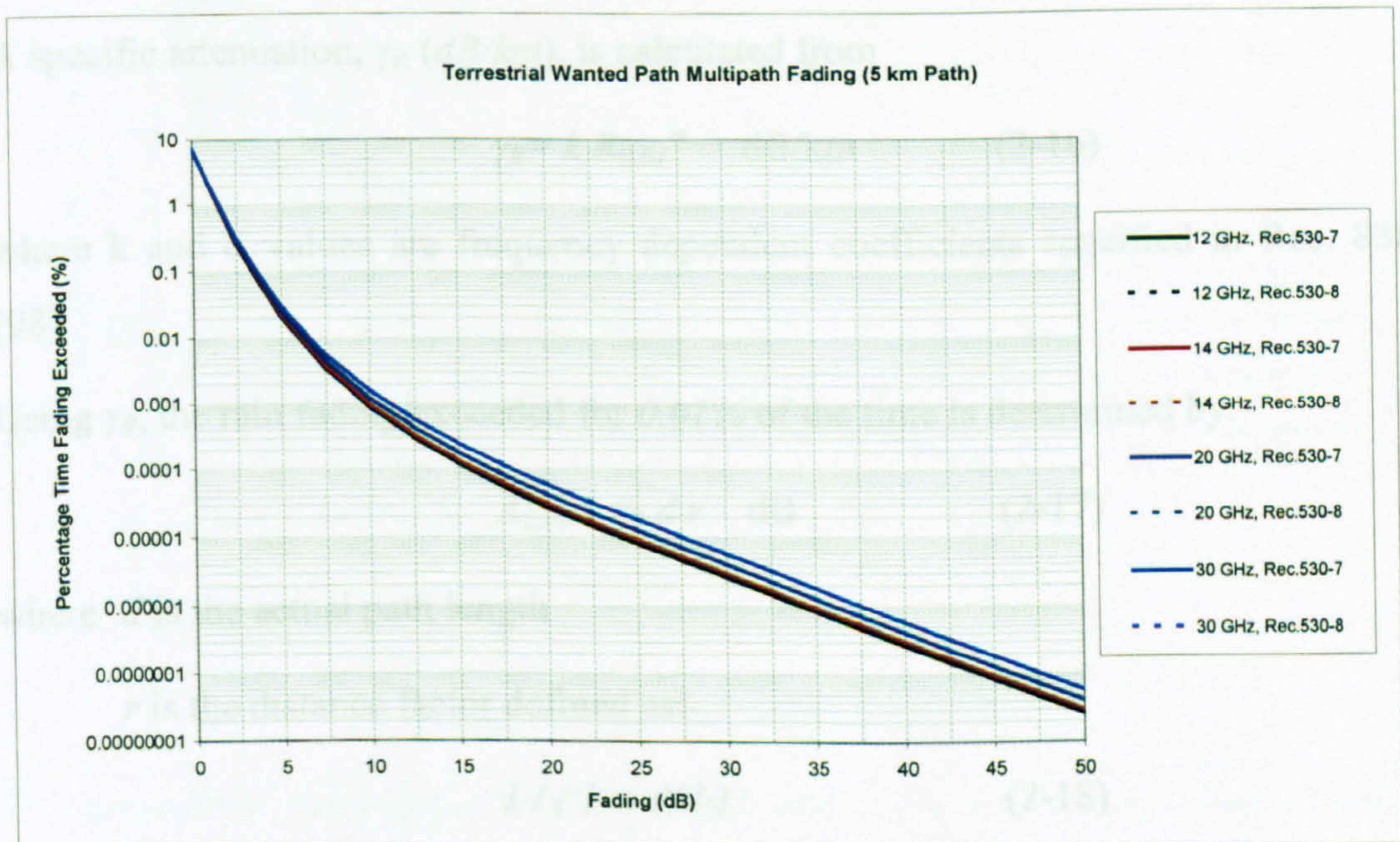


Figure 2.8: Multipath Fading Statistics

Fading distributions obtained from both models are the same at a given frequency and, therefore, both models could be used in multipath fading prediction in Ku and Ka bands.

The plots indicate that fading due to multipath effects does not vary significantly with frequency for the assumed parameter values. For example, when the operating

frequency increases from 12 GHz to 30 GHz , the fading increase remains below 2 dB at an exceedence percentage of 0.01% .

2.2.1.2 Rain Fading

The rain fading procedure is valid for frequencies up to 40 GHz and path lengths up to 60 km . In addition, fading statistics are defined for percentage times in the range 0.001% to 1% . The long term terrestrial path rain fading statistics are dependent on rainfall rate, $R\text{ (mm/h)}$. Rainfall rate exceeded for 0.01% ($R_{0.01}\text{ (mm/h)}$), is used in the prediction algorithms. An estimate of $R_{0.01}$ is obtained from Rec.837 [97] in which rainfall rate distributions are specified in terms of longitude and latitude of the terrestrial link, if the local rainfall rate is not available.

A specific attenuation, $\gamma_R\text{ (dB/km)}$, is calculated from

$$\gamma_R = k R_{0.01}^\alpha \quad \text{dB/km} \quad (2-16)$$

where k and α values are frequency dependent coefficients specified in Rec. 838 [98].

Using γ_R , the rain fading exceeded for 0.01% of the time is determined by:

$$A_{0.01} = \gamma_R d r \quad \text{dB} \quad (2-17)$$

where d is the actual path length

r is the distance factor defined as:

$$1 / (1 + d/d_0) \quad (2-18)$$

where d_0 is given by

$$35 \exp(-0.015 R_{0.01}) \quad (2-19)$$

In Rec.530-7, the expression for rain fading exceeded for other annual percentages of time (p) in the range $0.001\% - 1\%$ is given as:

$$\frac{A_p}{A_{0.01}} = 0.12 p^{-(0.546 + 0.043 \log p)} \quad (2-20)$$

It is noted that the new version (Rec.530-8) includes an additional expression to be used for latitudes less than 30° :

$$\frac{A_p}{A_{0.01}} = 0.12 p^{-(0.546 + 0.043 \log p)} \quad \text{if radio links located in latitudes } \geq 30^\circ \text{ (North or South)} \quad (2-21)$$

$$\frac{A_p}{A_{0.01}} = 0.07 p^{-(0.855 + 0.139 \log p)} \quad \text{if radio links located in latitudes } < 30^\circ \text{ (North or South)}$$

The rain fading statistics derived from both versions are compared in Figure 2.9 for a 5 km FS link located at *Latitude* = 20° and *Longitude* = 80° .

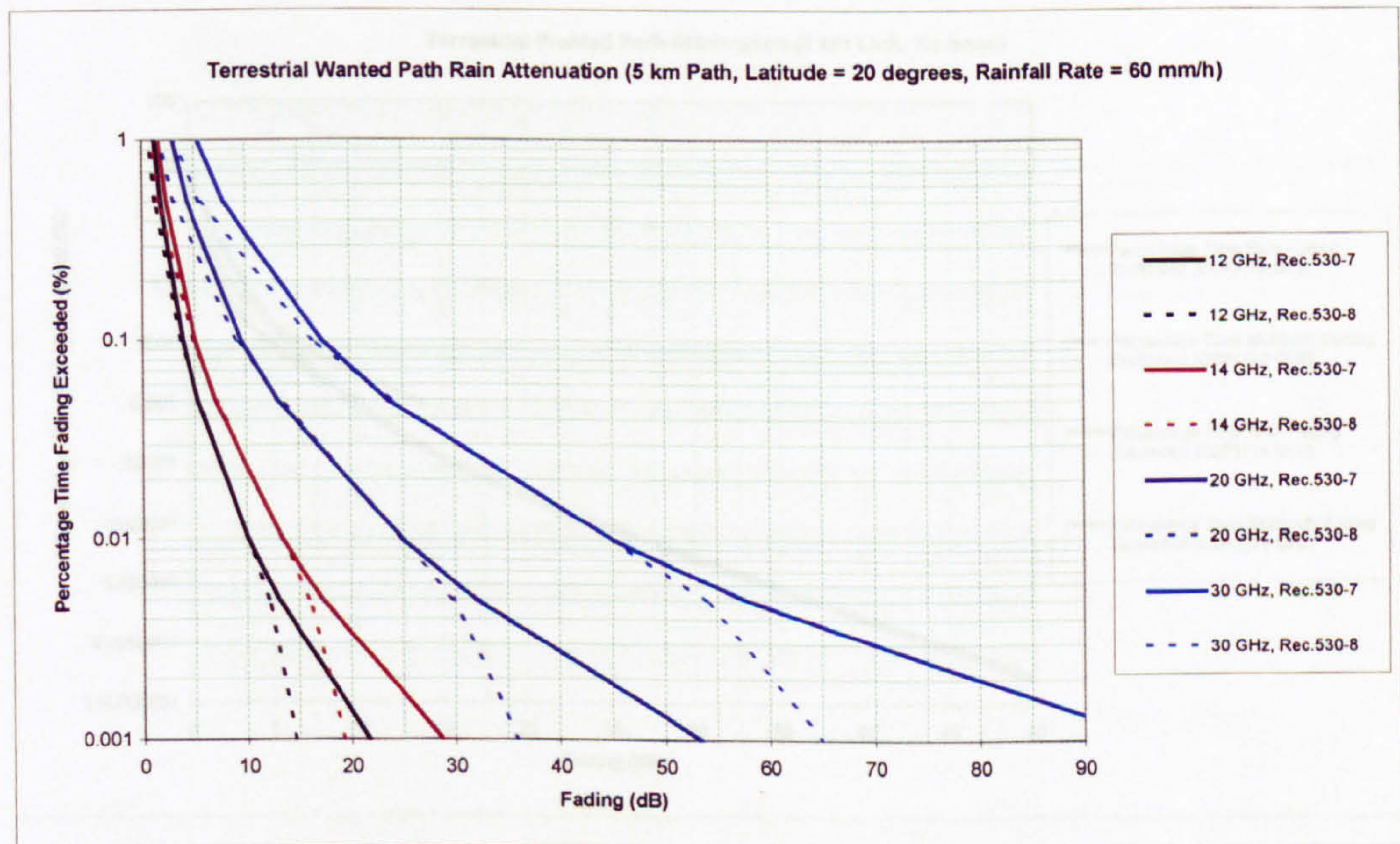


Figure 2.9: Rain Fading Statistics

For exceedence percentages between 0.01% and 0.1% , the fading values obtained from both models are very close to each other. Outside this range, Rec.530-8 predicts lower rain fading for a given percentage time. Typically, FS links are required to operate reliably for 99.99% of the time averaged over a year. The results illustrate that the level of rain attenuation which is likely to be exceeded for 0.01% of the time varies in the range $10\text{-}45\text{ dB}$ depending on the operating frequency band.

Depending on rain cell size, relatively longer links may be severely restricted by the rain attenuation and, therefore, radio relay systems comprising multiple short hop links need to be deployed for establishing long distance links.

2.2.1.3 Combined Effects of Multipath and Rain Fading

Rec.530 notes that the exceedence percentages for a given fading value corresponding to rain and multipath fading can be added to derive combined fading statistics.

On the basis of the assumptions shown in Figure 2.7, the following rain and multipath fading distributions are produced from Rec.530-8 for a 5 km FS link located at 52 degrees latitude.

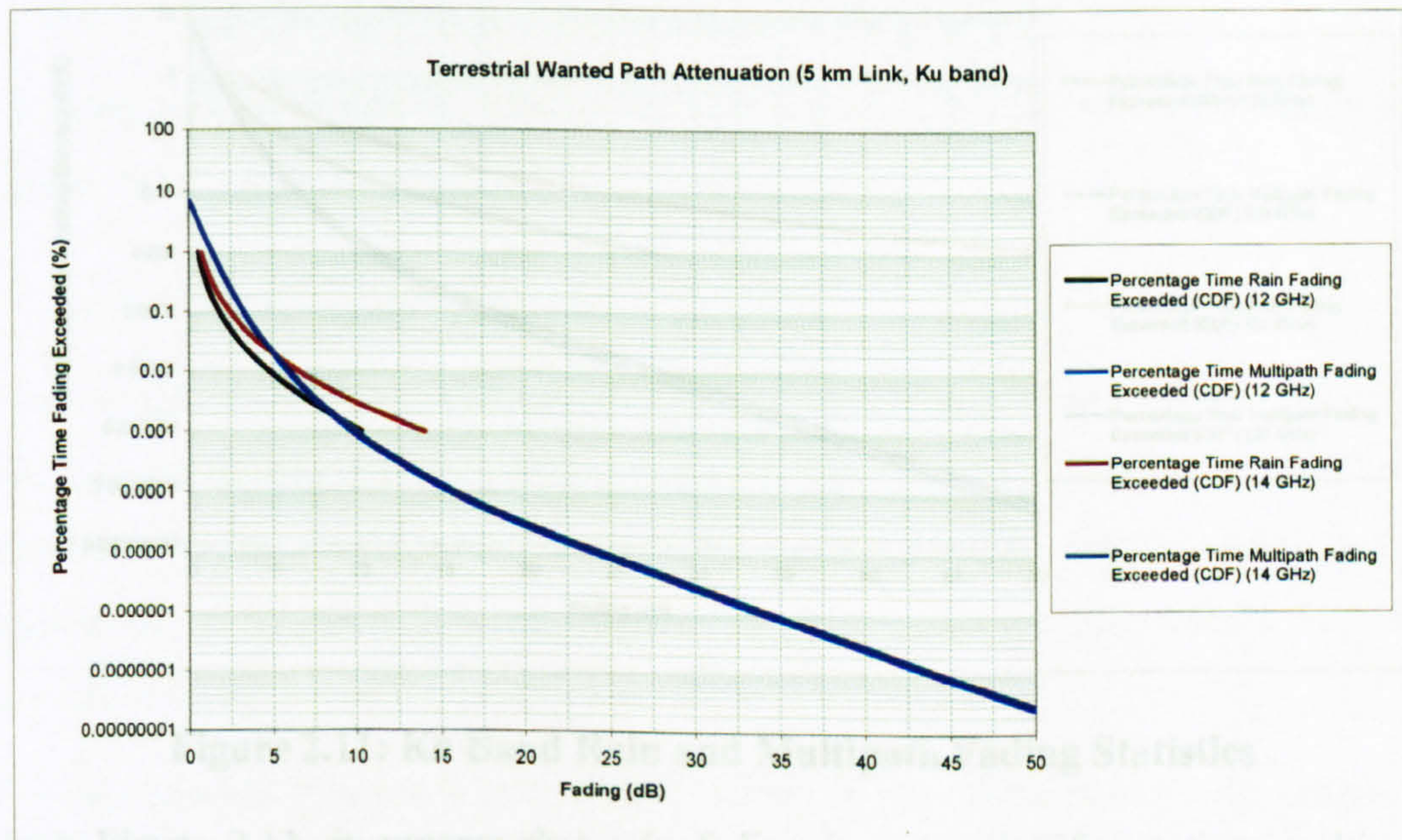


Figure 2.10: Ku Band Rain and Multipath Fading Statistics

The plots suggest that both rain and multipath fading need to be considered in Ku band FS link design as the fading statistics are close to each other. For example, at 12 GHz, the rain fading value of 5 dB is exceeded for 0.01% of the time while the same amount of fading caused by multipath effects is exceeded for 0.02% of the time. Therefore, the link should have a fading margin of 5 dB to be used for 0.03% of the time to accommodate rain and multipath fading.

It is important to note that if the FS link requires higher availability (i.e. unavailability < 0.03%) then the margin needs to be increased (for example, 10 dB margin ensures 0.002% unavailability at 12 GHz) providing that an adequate

transmitter power is available. If there is a restriction on the available power then the bit rate can be decreased so that the required power is lowered and the link margin is increased.

Figure 2.11 illustrates Ka band fading statistics derived by using the same path parameter values.

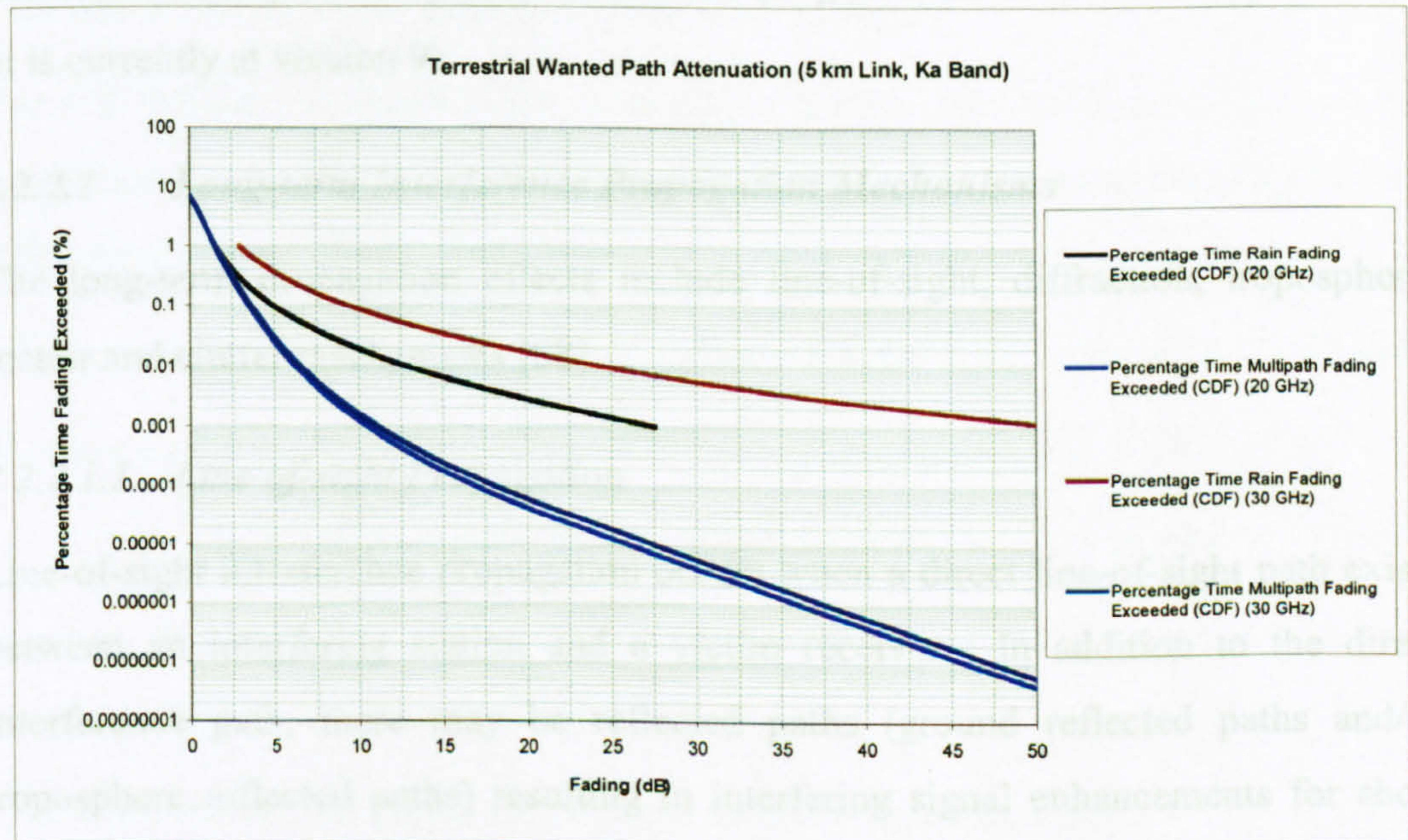


Figure 2.11: Ka Band Rain and Multipath Fading Statistics

From Figure 2.11, it appears that rain fading is more significant than multipath fading at Ka band frequencies. For example, at 30 GHz, rain fading is 25 dB exceeded for 0.01% of time. For the same fading value, multipath effects cause an unavailability of 0.00001%. It is, therefore, clear that the significant portion of the total unavailability of 0.01001% is the result of fading due to rain.

2.2.2 Interference Path Propagation Effects

Propagation mechanisms may cause interference for short or long periods of time depending on frequency and path characteristics. Therefore, both long-term and short-term terrestrial path propagation mechanisms affecting NGSO FSS / FS spectrum sharing are detailed in this section.

The implications of each propagation mechanism are summarised together with prediction methods defined in Rec.452 [88], which is used for examining the interference paths between radio stations located on the surface of the Earth operating at frequencies between 0.7 GHz and 30 GHz . This recommendation was developed during the European Co-operation in the Field of Scientific and Technical Research (COST) 210 project of 1984-1991 [99], and has been constantly reviewed (it is currently at version 9).

2.2.2.1 *Long-term Interference Propagation Mechanisms*

The long-term propagation effects include line-of-sight, diffraction, tropospheric scatter and clutter mechanisms [88].

2.2.2.1.1 *Line-of-sight Propagation*

Line-of-sight interference propagation occurs when a direct line-of-sight path exists between an interfering station and a victim receiver. In addition to the direct interference path, there may be reflected paths (ground reflected paths and/or troposphere reflected paths) resulting in interfering signal enhancements for short periods of time.

The line-of-sight loss prediction model defined in Rec.452 combines the effects of direct and reflected interference paths. The basic transmission loss ($L_{b0}(p)$) not exceeded for the average annual percentage time $p\%$ due to line-of-sight propagation is given by:

$$L_{b0}(p) = 92.5 + 20 \log(f) + 20 \log(d) + A_g + E_s(p) \quad (\text{dB}) \quad (2-22)$$

where f is the operating frequency in GHz , d is the line-of-sight interference path length in km and A_g is the atmospheric loss in dB .

$E_s(p)$ accounts for the multipath correction and is defined as a function of the interference path length and percentage time:

$$E_s(p) = 2.6(1 - e^{-d/10}) \log(p/50) \quad (\text{dB}) \quad (2-23)$$

2.2.2.1.2 Diffraction

Where a line-of-sight interference path does not exist, diffraction over terrain or obstacles will limit the path loss. Therefore, under normal atmospheric conditions, diffraction mechanisms dominate the long-term interference beyond the line-of-sight. The diffraction loss is at a minimum for a single knife edge obstruction and at a maximum for a smooth spherical Earth [88, 91, 95].

Rec.452 defines a diffraction loss calculation method applicable to average annual percentage times up to 50%. The basic transmission loss not exceeded for $p\%$ for a diffraction path is calculated from:

$$L_{bd}(p) = 92.5 + 20 \log(f) + 20 \log(d) + E_{sd}(p) + L_d(p) + A_g \quad (\text{dB}) \quad (2-24)$$

In above equation, $E_{sd}(p)$ represents the multipath correction and is defined by:

$$E_{sd}(p) = 2.6(1 - e^{-(d_{lt} + d_{lr})/10}) \log(p/50) \quad (\text{dB}) \quad (2-25)$$

where d_{lt} & d_{lr} are the distance in km from the interfering transmitter and the victim receiver antennas to their respective horizons.

$L_d(p)$ accounts for the excess diffraction loss and is calculated from:

$$L_d(p) = L_d(50\%) - F_i(p) [L_d(50\%) - L_d(\beta_0\%)] \quad (\text{dB}) \quad (2-26)$$

where

$L_d(50\%)$ and $L_d(\beta_0\%)$ are the excess diffraction loss values calculated from algorithms defined in Rec.526 [100] for $p=50\%$ and $p \leq \beta_0\%$.

β_0 is a radio meteorological parameter representing the time percentage for which radio refractivity index lapse rates exceeding 100 N-units/km can be expected in the first 100 metres of the atmosphere. The recommendation includes a set of empirical expressions to calculate the appropriate β_0 value for a given interference path.

$F_i(p)$ is the interpolation factor based on a log-normal distribution of diffraction loss over the range $\beta_0\% < p < 50\%$. The recommendation includes an annex for the expressions to be used for calculating $F_i(p)$ values.

2.2.2.1.3 Tropospheric Scatter

Small scale tropospheric refractive index irregularities cause tropospheric scattering which, in turn, result in a relatively low level of interference at a victim receiver for path lengths greater than *100 km* where interference due to diffraction becomes very weak [88]. Rec.452 employs a generalised empirical approach to predict basic transmission loss due to troposcatter over the range of average annual time percentages *p* from *0.001%* to *50%*. The loss expression is given by:

$$L_{bs}(p) = 190 + L_f + 20 \log(d) + 0.573\theta - 0.15N_o + L_c + A_g - 10.1[-\log(p/50)]^{0.7} \quad (\text{dB}) \quad (2-27)$$

where θ is the interference path angular distance in miliradian and N_o is the interference path centre sea level surface refractivity.

L_f represents frequency dependent loss and is defined as:

$$L_f = 25 \log(f) - 2.5 [\log(f/2)]^2 \quad (\text{dB}) \quad (2-28)$$

The procedure applies the following expression for aperture to medium coupling loss:

$$L_c = 0.051 e^{0.055(G_t + G_r)} \quad (\text{dB}) \quad (2-29)$$

where G_t and G_r are the interfering transmitter and the victim receiver antenna gains in the direction of the interfering path (*dB*i).

2.2.2.1.4 Additional Clutter Loss

Local clutter including buildings and vegetation can provide additional diffraction losses [88, 91, 95]. The calculation methods are defined for both ends of the interference path where the local clutter scenario is known. Rec.452 notes that if the clutter environment is not known the additional clutter loss should not be included into the calculations. In this research, generic NGSO FSS / FS spectrum sharing scenarios are considered and, therefore, the implications of local clutter effects are not taken into account.

2.2.2.2 *Short-term (Anomalous) Interference Propagation Mechanisms*

The significant anomalous propagation effects include ducting and layer reflection and hydrometeor scatter [88].

2.2.2.2.1 *Ducting and Layer Reflection*

The tropospheric refractivity N varies with height and has a median lapse rate of approximately 40. As explained earlier, this leads to the curvature of radio waves towards the Earth, allowing propagation to distances beyond the optical horizon. For values of lapse rate greater than 157 N/km , radio waves will be curved towards the Earth's surface to the extent that extremely long-range propagation is possible due to ducting effect. This mechanism occurs in well mixed atmospheres only for a small percentage time. The meteorological conditions giving rise to these phenomena are most often encountered over bodies of water or in flat, coastal, areas [88, 91, 95].

The layer reflection occurs when a radiowave is incident on a boundary between media with different electrical properties. The reflected energy is dependent on Fresnel coefficients relating to the media, the frequency and the geometry of the situation [91].

In Rec.452, the following function is defined to predict the basic transmission loss occurring during short periods of time due to ducting and layer reflection:

$$L_{ba}(p) = A_f + A_d(p) + A_g \quad (\text{dB}) \quad (2-30)$$

A_f represents fixed coupling losses between antennas and the anomalous tropospheric propagation structure while $A_d(p)$ is time and angular-distance dependant losses within the anomalous tropospheric propagation structure. A_g is the atmospheric attenuation.

A_f is calculated from:

$$A_f = 102.45 + 20 \log f + 20 \log (d_{lt} - d_{lr}) + A_{st} + A_{sr} + A_{ct} + A_{cr} \quad (\text{dB}) \quad (2-31)$$

where

d_{lt} & d_{lr} are the distance in km from the interfering transmitter and the victim receiver antennas to their respective horizons,

A_{st} & A_{sr} are site shielding diffraction losses in dB for the interfering transmitter and the victim receiver.

A_{ct} & A_{cr} are over-sea surface duct coupling corrections in dB for the interfering transmitter and the victim receiver.

The recommendation includes empirical expressions for calculating A_{st} , A_{sr} and A_{ct} , A_{cr} . It is noted that for radio stations with a horizon below the local horizontal, site shielding diffraction losses are equal to zero. Similarly, if the stations are located more than 5 km from the coast the over-sea surface duct coupling corrections will not apply.

The time and angular-distance dependant losses are given by:

$$A_d(p) = \gamma_d \theta' + A(p) \quad (\text{dB}) \quad (2-32)$$

where γ_d is the specific attenuation defined by $(5 \times 10^{-5} \times \text{effective Earth radius} \times f^{1/3})$, θ' is the angular distance and $A(p)$ is the cumulative distribution function accounting for the time variability.

$A(p)$ is defined in relation to β_0 which is the radio meteorological parameter representing the time percentage for which the radio refractivity index lapse rate can be expected to exceed 100 N-units/km. β_0 is defined as a simple function of latitude and is corrected using empirical expressions for terrain roughness and path geometry to give β . The time variability is calculated from the following expression:

$$A(p) = -12 + (1.2 + 3.7 \cdot 10^{-3} d) \log(p/\beta) + 12 (p/\beta)^\Gamma (\text{dB}) \quad (2-33)$$

Γ is a function of β and the interference path length d . It is noted that the expression used for Γ is modified within the new version of Rec.452 (version 9).

The expression

$$\Gamma = \left[\frac{-1.079 + \log(142 - (1.2 + 3.7 \times 10^{-3} \times d) \times (2 - \log(\beta)))}{2 - \log(\beta)} \right] \quad (2-34)$$

used in Rec.452-8 replaced with the expression

$$\Gamma = \left[\frac{1.076}{(2.0058 - \log(\beta))^{1.012}} \right] \times e^{-\left(9.51 - 4.8 \log(\beta) + 0.198 (\log(\beta))^2\right) \times 10^{-6} \times d^{1.13}} \quad (2-35)$$

in Rec.452-9.

In order to examine the implications of this modification with respect to Ku and Ka band propagation modelling, interference path loss statistics due to ducting and layer reflection are derived for 100 km interference path. Figure 2.12 shows the assumed parameter values.

$f_1 := 14$	$f_2 := 30$	Frequency GHz
$v := 3 \cdot 10^8$		Light velocity, m/sec
DistanceBetweenTxAndRx := 100		kilometre
$\phi_t := 50.000$		Latitude of transmitter antenna, degrees.
$\phi_r := 50.000$		Latitude of receiver antenna, degrees.
$\psi_t := 0.000$		Longitude of transmitter antenna, degrees.
$\psi_r := 0.000$		Longitude of receiver antenna, degrees.
$h_{tg} := 10$		Transmitter antenna centre height above ground level, m
$h_{rg} := 10$		Receiver antenna centre height above ground level, m
$h_{ts} := 10$		Transmitter antenna centre height above mean sea level, m
$h_{rs} := 10$		Receiver antenna centre height above mean sea level, m
$\Delta N := 45$		Average radio-refractive index lapse rate through the lowest 1 km of the atmosphere, N-units/km. Taken from a world map given in Rec.452 for 50 degrees latitude
$N_o := 325$		Sea level surface refractivity. Taken from a world map given in Rec.452 for 50 degrees latitude
$d_b := 0$		Aggregate length of the separation path sections over water (km).
$\varepsilon := 3.5$		Coefficient
$h_m := 0$		terrain roughness, m
$p_{676} := 1013$		pressure, hPa
$t_{676} := 15$		temperature, C
$R_e := 6378.145$		Earth Radius, kilometre
$h_{te} := 10$		Effective transmitter antenna height above terrain, m
$h_{re} := 10$		Effective receiver antenna height above terrain, m

Figure 2.12: Assumptions For Ducting and Layer Reflection Modelling

The results are compared in Figure 2.13.

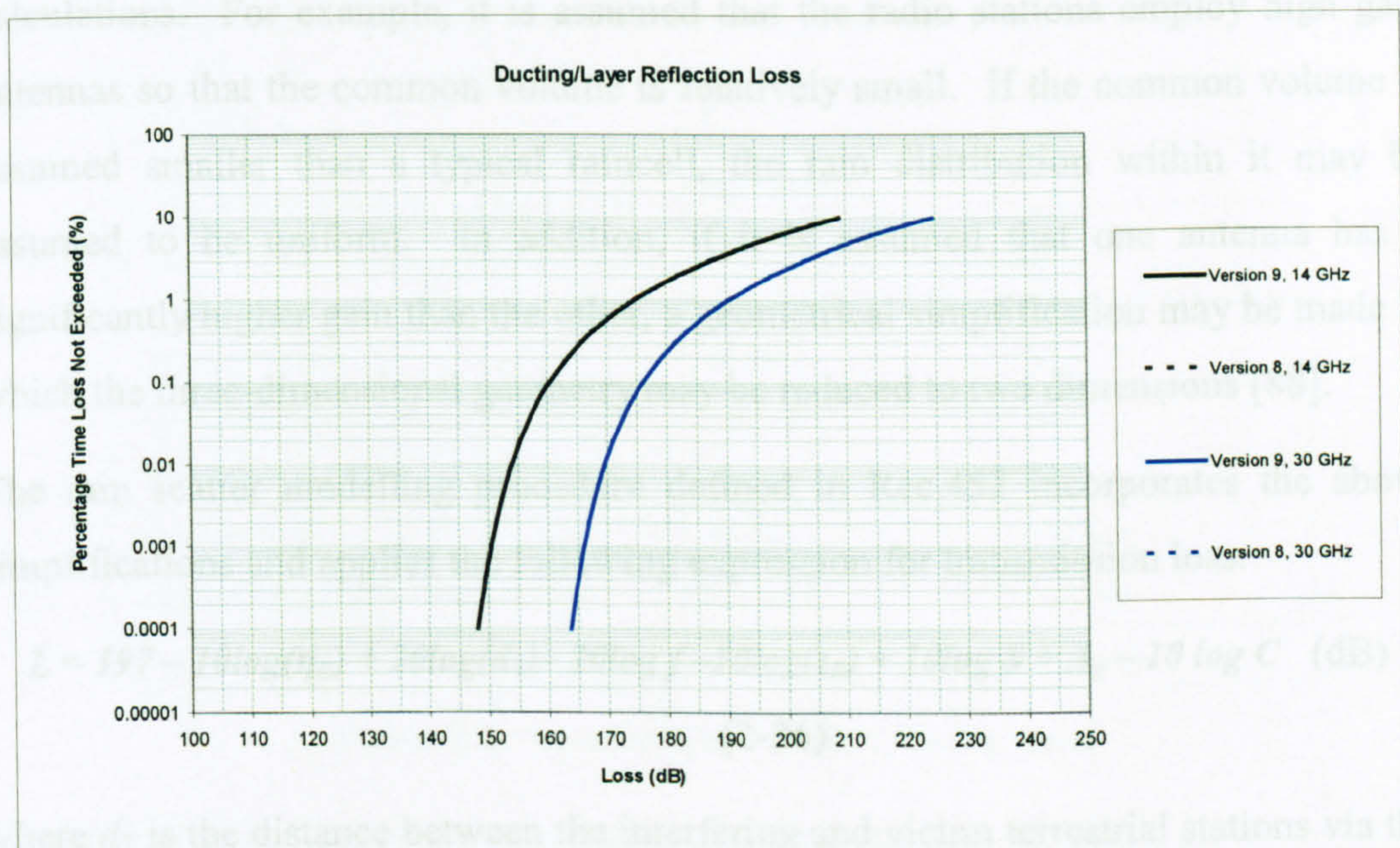


Figure 2.13: Comparison of Ducting and Layer Reflection Interference Path Loss Statistics

The plots indicate that the resultant loss statistics are the same and, therefore, both versions could be used in Ku and Ka band terrestrial path interference analysis without affecting sharing analysis conclusions.

2.2.2.2.2 Hydrometeor Scatter

At Ku and Ka band frequencies, hydrometeor scatter is dominated by rain scatter which is the result of interactions between rain molecules and radiowaves. The modelling of rain scatter requires evaluation of the reflectivity of an assumed form of rainfall distributions within the common volume defined by the intersection of interfering and victim terminal antenna beams [88, 91, 96].

It is important to note that the calculation procedure would be extremely complex if a generalised model, where antennas may have any gain, and be related arbitrarily with respect to each other, and rain may be distributed over any volume, were to be used [88].

In Rec.452 certain simplifying assumptions are made for the purposes of interference calculations. For example, it is assumed that the radio stations employ high gain antennas so that the common volume is relatively small. If the common volume is assumed smaller than a typical raincell, the rain distribution within it may be assumed to be uniform. In addition, if it is assumed that one antenna has a significantly higher gain than the other, a geometrical simplification may be made in which the three-dimensional geometry may be reduced to two dimensions [88].

The rain scatter modelling procedure defined in Rec.452 incorporates the above simplifications and applies the following expression for transmission loss:

$$L = 197 - 10\log(\eta_E) + 20\log(d_T) - 20\log f - 10\log(z_R) + 10\log S + A_g - 10\log C \quad (\text{dB})$$

(2-36)

where d_T is the distance between the interfering and victim terrestrial stations via the scattering volume, η_E represents the antenna efficiency, S models the difference between Rayleigh and Mie scattering (negligible at frequencies less than 10 GHz), z_R is the reflectivity for a given rainfall rate (calculated for the %-time of interest). A_g attenuation due to gasses and C is the ‘scatter transfer function’, which captures the geometry of the situation, the antenna directivity and rain attenuation. The calculation of C involves integration over the heights of interest.

Because of the modelling complexity, the rain scatter model is provided by the ITU-R in the form of a computer programme: Hydrometeor Scatter Prediction Model (SCAT) [101]. The software is able to model scattering effects for both short and long interference paths. The model output is the cumulative distribution function of transmission loss calculated by summing the individual probabilities of all rainfall rate/rain height combinations leading to the same transmission loss which gives the overall probability for that loss.

Using the assumptions given in Table 2.2, rain scattering transmission loss statistics are obtained from SCAT simulations. It is important to note that the assumed transmitter characteristics are based on the NGSO FSS user terminal parameters

given in Ku and Ka band system filings while the assumed receiver characteristics are taken from Rec.758 [102] where FS system parameters are defined.

Rain Zone	E	
Latitude	50 degrees	
Path Length	100 km	
	Ku Band (14 GHz)	Ka Band (30 GHz)
Transmitter Gain	37 dBi	37.3 dBi
Transmitter Antenna Radiation Pattern	App. 29	Rec.465
Transmitter Elevation	10 degrees	40 degrees
Receiver Gain	49 dBi	47.7 dBi
Receiver Antenna Radiation Pattern	Rec.699	Rec.699
Receiver Elevation	0 degrees	0 degrees

Table 2.2: Interference Path Assumptions

Figure 2.14 illustrates the resultant distributions in Ku and Ka bands for the assumed interference path parameter values.

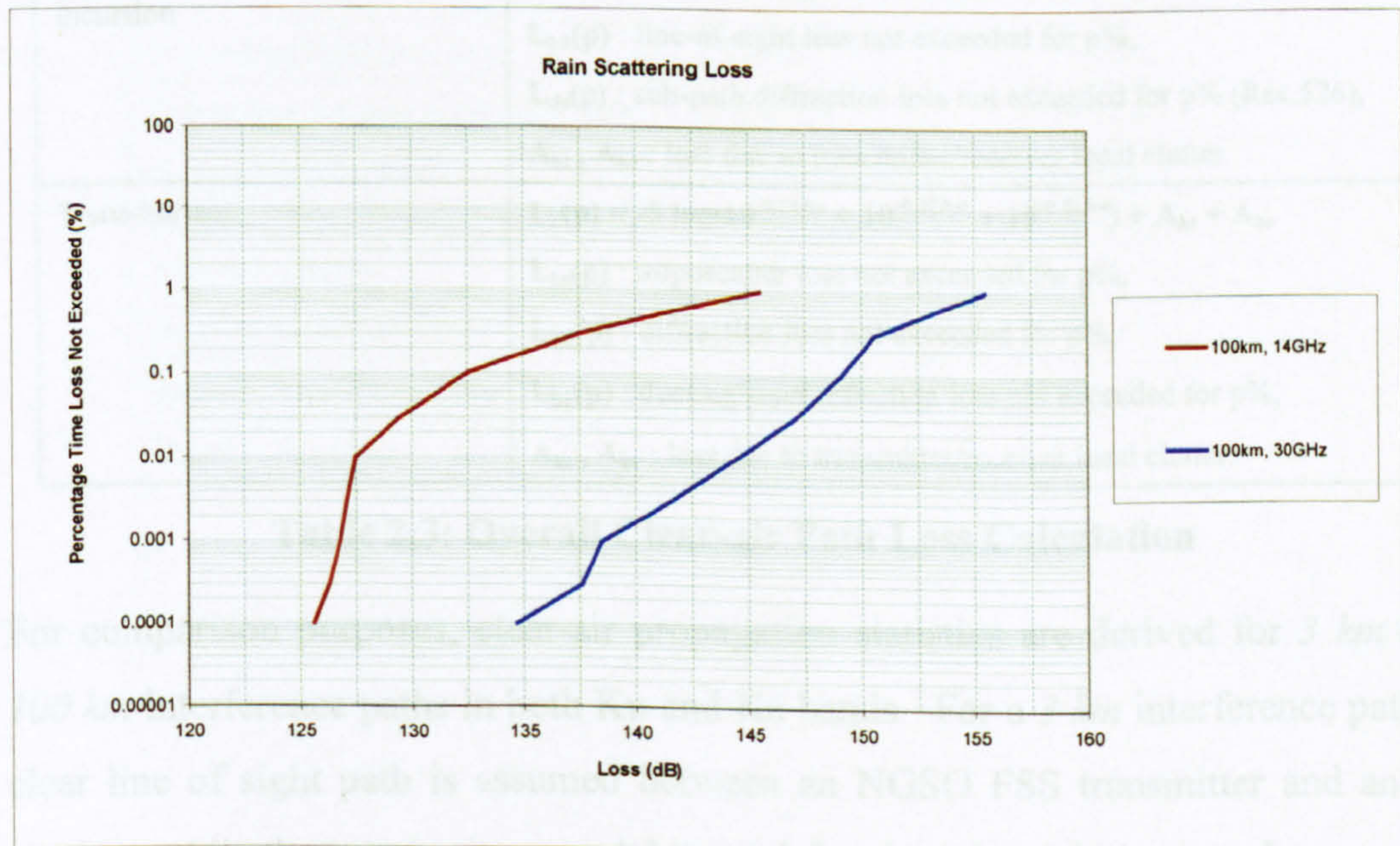


Figure 2.14: Rain Scattering Path Loss Statistics

The plots suggest that an increasing frequency results in an increased loss for a given percentage time. For example, at Ka band, a loss value of 145 dB will not be exceeded for 0.01% of the annual time (i.e. path loss will exceed 145 dB for 99.99%

of the time) for the assumed parameters due to scattering effects. At Ku band, the statistics indicate that the assumed interference path will be subject to 127.5 dB loss not exceeded for the same percentage.

2.2.2.3 Combined Effects of Individual Interference Propagation Mechanisms

Rec. 452 defines a method for combining individual clear-air propagation mechanisms in order to derive an overall interference path loss statistics. This method is based on identifying the interference path type and associating appropriate propagation mechanisms with the path. Table 2-3 summarises the combination procedure [88].

Path Type	Predicted Overall Loss Not Exceeded for p%, $L_b(p)$
Clear line-of-sight	$L_b(p) = L_{bo}(p) + A_{ht} + A_{hr}$ $L_{bo}(p)$: line-of-sight loss not exceeded for p%, A_{ht}, A_{hr} : loss due to transmitter/receiver local clutter.
Line-of-sight with terrain incursion	$L_b(p) = L_{bo}(p) + L_{ds}(p) + A_{ht} + A_{hr}$ $L_{bo}(p)$: line-of-sight loss not exceeded for p%, $L_{ds}(p)$: sub-path diffraction loss not exceeded for p% (Rec.526), A_{ht}, A_{hr} : loss due to transmitter/receiver local clutter.
Trans-horizon	$L_b(p) = -5 \log(10^{-0.2L_{bs}} + 10^{-0.2L_{bd}} + 10^{-0.2L_{ba}}) + A_{ht} + A_{hr}$ $L_{bs}(p)$: troposcatter loss not exceeded for p%, $L_{bd}(p)$: diffraction loss not exceeded for p%, $L_{ba}(p)$: ducting/layer reflection loss not exceeded for p%, A_{ht}, A_{hr} : loss due to transmitter/receiver local clutter.

Table 2.3: Overall Clear-air Path Loss Calculation

For comparison purposes, clear-air propagation statistics are derived for 3 km and 100 km interference paths in both Ku and Ka bands. For a 3 km interference path, a clear line of sight path is assumed between an NGSO FSS transmitter and an FS receiver while the transhorizon model is used for obtaining 100 km interference path loss statistics. For both cases, terrain effects are not considered by assuming smooth Earth between the transmitter and receiver. Table 2.4 summarises assumed parameter values.

Transmitter/Receiver Antenna Latitude	50 degrees	
Transmitter/Receiver Antenna Longitude	0 degrees	
Transmitter/Receiver Antenna Centre Height Above Ground Level	10 m	
Transmitter/Receiver Antenna Centre Height Above Mean Sea Level	10 m	
Transmitter/Receiver Antenna Effective Height Above Terrain	10 m	
Average radio-refractive index lapse rate through the lowest 1 km of the atmosphere (Taken from a world map given in Rec.452)	45 N-units/km	
Sea level surface refractivity (Taken from a world map given in Rec.452)	325	
Aggregate length of the separation path sections over water	0 km	
Coefficient, ϵ	3.5	
Terrain Roughness	0 m	
Pressure	1013 hPa	
Temperature	15 C	
	Ku Band (14 GHz)	Ka Band (30 GHz)
Transmitter Maximum Gain	37 dBi	37.3 dBi
Transmitter Antenna Radiation Pattern	App. 29	Rec.465
Transmitter Elevation	10 degrees	40 degrees
Transmitter Antenna Gain Towards Receiver Antenna	12.53 dBi	-8.05 dBi
Receiver Maximum Gain	49 dBi	47.7 dBi
Receiver Antenna Radiation Pattern	Rec.699	Rec.699
Receiver Elevation	0 degrees	0 degrees

Table 2.4: Interference Path Assumptions

Figure 2.15 shows the line-of-sight statistics for an assumed 3 km interference path.

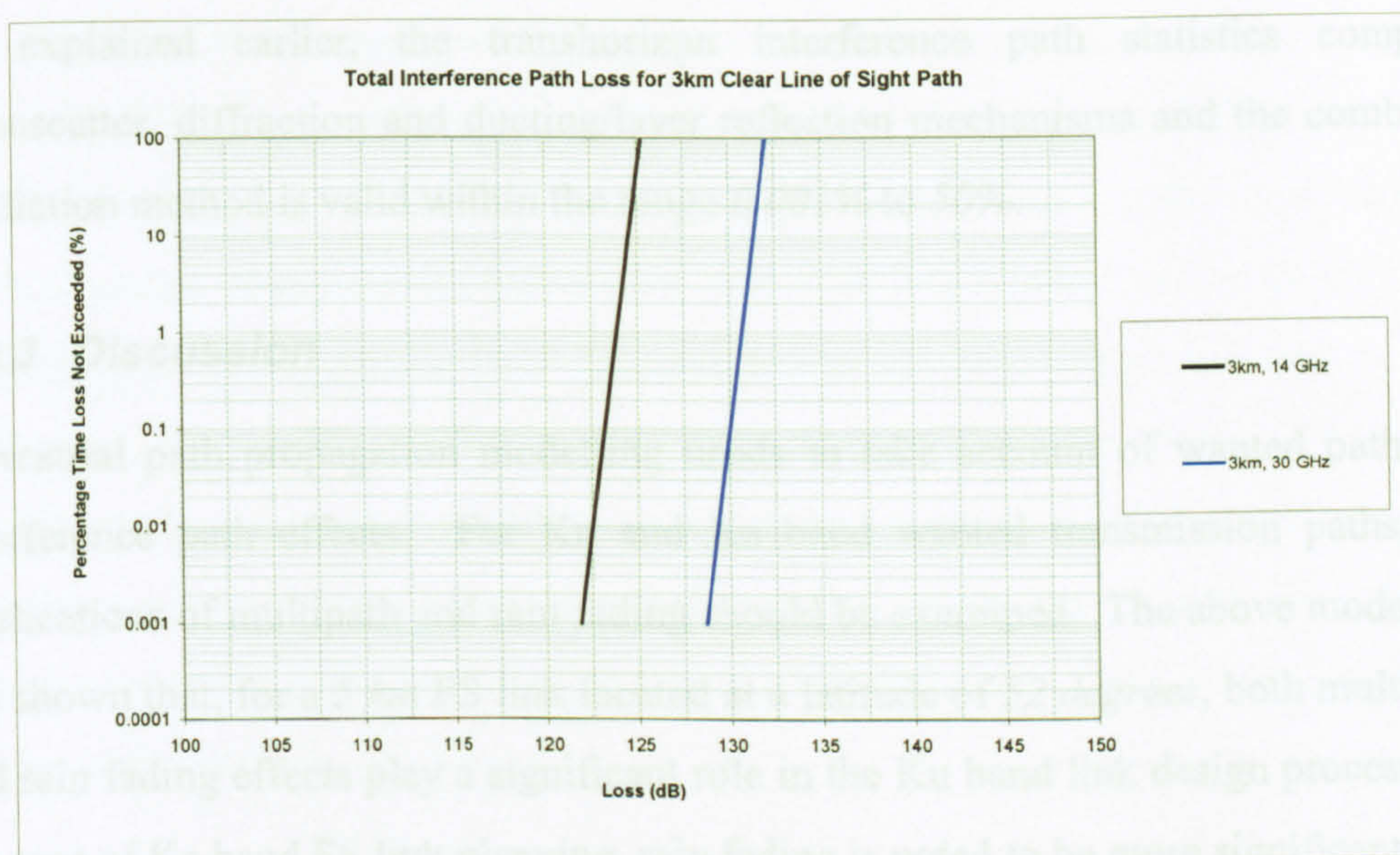


Figure 2.15: Line-of-sight Path Loss Statistics

The plots indicate that, for the assumed parameter values, the line-of-sight prediction model (including short-term enhancements due to multipath effects) results in path loss variations less than 5 dB over percentages from 0.001% to 100%. The statistical behaviour of the total loss for an assumed 100 km transhorizon interference path is illustrated in Figure 2.16.



Figure 2.16: Trans-Horizon Path Loss Statistics

As explained earlier, the transhorizon interference path statistics comprise troposcatter, diffraction and ducting/layer reflection mechanisms and the combined prediction method is valid within the range 0.001% to 50% .

2.2.3 Discussion

Terrestrial path propagation modelling needs to take account of wanted path and interference path effects. For Ku and Ka band wanted transmission paths, the implications of multipath and rain fading should be examined. The above modelling has shown that, for a 5 km FS link located at a latitude of 52 degrees , both multipath and rain fading effects play a significant role in the Ku band link design process. In the case of Ka band FS link planning, rain fading is noted to be more significant than multipath fading.

In order to compensate for propagation fading, a fixed margin is included in link budget calculations when a link employs a fixed transmit power. This means that most of the time a transmitter power will be much higher than needed as the link will be attenuated by rain for only fraction of a time (i.e. the rain margin is not needed for clear sky conditions). From the spectrum sharing point of view, transmitting an unnecessarily higher power for most of the time, in turn, increases interference into other systems operating in the same band. In order to reduce the impact of interference, transmitters employ Automatic Transmitter Power Control (ATPC) where the nominal power of the transmitted signal is reduced when there is no rain and increased to overcome attenuation events i.e. when there is rain. This reduces the potential interference generated by the transmitter.

The rain fading statistics of wanted paths derived from previous (Rec.530-7) and revised prediction models (Rec.530-8) indicate that, for links located below 30° latitude, predicted fading values are different within the range 0.001% to 0.01% and 0.1% to 1% in that the revised model gives lower fading estimates. Both models use the same empirical expressions for links located at latitudes greater than 30 degrees .

For terrestrial interference paths, propagation mechanisms causing short and long term interference are reviewed taking path loss prediction models defined in ITU-R Rec.452 into account. It is noted that the free space path loss together with loss due to local clutter is applied for calculating total path loss when interference paths are line-of-sight. For transhorizon interference paths, the effects of troposcatter, diffraction, ducting/layer reflection and local clutter effects are combined to derive overall interference path loss statistics. It is further noted that interference caused by scattering which occurs when transmitter and receiver beams form a common volume within the part of atmosphere where a rain cell exists could be significant for short periods of time.

2.3 Space Path Propagation

Space path propagation involves Earth-to-space and space-to-Earth wanted and interference paths, for example, transmissions between satellites in geostationary and nongeostationary orbits and radio stations operating on the Earth surface. In space path propagation analysis, the implications of rain fading, atmospheric absorption and tropospheric effects need to be considered depending on the operating frequency, geographic location (i.e. longitude and latitude) and path elevation angle [89, 90, 103-105].

Space path fading introduced by atmospheric gases is the result of absorption and mainly depends of frequency, elevation angle, altitude above sea level and humidity. Its impact increases at low elevation angles as the path length travelling through the atmosphere increases [86, 103-105]. The detailed examination of atmospheric attenuation on the space path is presented previously in § 2.1.

The variations in tropospheric refractive index give rise to a number of propagation effects. The regular decrease of refractive index with height causes space paths to bend towards the Earth's surface which, in turn, results in a defocusing of an antenna beam. For low elevation space paths (for example, less than 5°), the small scale variations in refractive index lead to scintillation effects. Irregularities in the refractive index structure also give rise to a decrease in effective antenna gain due to

phase decorrelation across the antenna aperture. In specific cases where the space path is over water or in coastal areas and the path elevation angle is very small (i.e. less than 3°), multipath effects may also be significant for very short periods of time [89].

In line with the above discussions, the implications of space path propagation mechanisms are examined in the following sections.

2.3.1 Wanted Path Propagation Effects

Wanted space paths are designed to be line-of-sight and, therefore, clear-air propagation is modelled by free space path loss and gas attenuation. The most important space path propagation mechanism is rain fading, particularly at Ka band [96, 106-108]. In general, both GSO FSS and NGSO FSS systems operate at elevation angles greater than 10° to overcome the adverse rain effects. Therefore, in comparison to rain fading, atmospheric absorption and tropospheric effects are unlikely to introduce serious loss into space-to-Earth and Earth-to-space GSO FSS and NGSO FSS links operating in Ku and Ka band.

The rain fading calculation methods are defined in Rec.618 [89]. These methods are empirical and based on long term rain fading measurements stored in ITU-R data bank.

2.3.1.1 Rain Fading

The latest version of Rec.618 (version 6) includes modified rain attenuation prediction methods. In the previous version, the rain model was valid for frequencies up to 30 GHz and statistical distributions were generated for percentage times ranging from 0.001% to 1% . Propagation studies carried out in ITU-R Study Group 3 for the purposes of revising Rec.618 are incorporated into the new version which defines an empirical calculation method valid up to 55 GHz for percentage times in the range of 0.001% to 5% . The revised recommendation proposes a new statistical model fit to the data in the ITU-R data bank. It is stated that the new

model performs particularly well when used with rain contour maps included in the revised Rec.837 (version 2) [97].

Many steps used for the evaluation of rain effects on slant paths are similar to those used for terrestrial paths. The most significant difference is that the propagation paths are no longer horizontal. This requires calculation of “rain height”, at which the phase of water changes from liquid to solid [89]. Figure 2.17 illustrates the parameters used for the slant path rain attenuation prediction model.

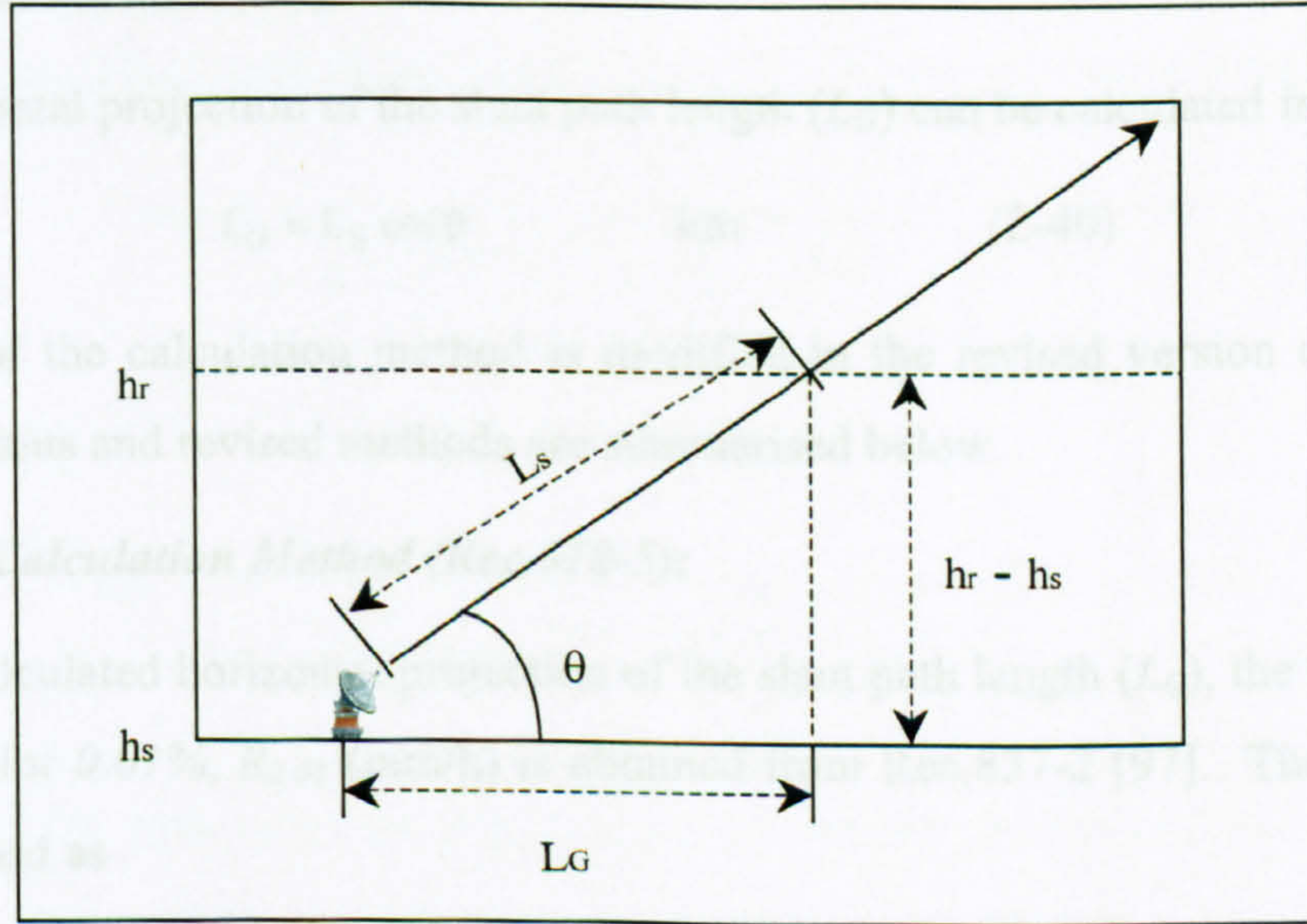


Figure 2.17: Slant Path Geometry

The rain height (h_R) is dependent on the latitude (φ) of a ground terminal and is expressed as following:

$$h_R = \left\{ \begin{array}{ll} 5 - 0.075(\varphi - 23) & \text{for } \varphi > 23^\circ \\ 5 & \text{for } 0^\circ \leq \varphi \leq 23^\circ \\ 5 & \text{for } 0^\circ \geq \varphi \geq -21^\circ \\ 5 + 0.1(\varphi + 21) & \text{for } -71^\circ \leq \varphi < -21^\circ \\ 0 & \text{for } \varphi < -71^\circ \end{array} \right\} \quad \text{km} \quad (2-37)$$

h_R is then used in calculating the slant path length (L_s). For greater elevation angles, $\theta \geq 5^\circ$:

$$L_S = \frac{(h_R - h_S)}{\sin \theta} \quad \text{km} \quad (2-38)$$

For small elevation angles, $\theta < 5^\circ$:

$$L_S = \frac{2(h_R - h_S)}{\left(\sin^2 \theta + \frac{2(h_R - h_S)}{Re} \right)^{1/2} + \sin \theta} \quad \text{km} \quad (2-39)$$

where Re is the effective Earth radius (8500 km) and h_S is the ground terminal height above mean sea level (km).

The horizontal projection of the slant path length (L_G) can be calculated from

$$L_G = L_S \cos \theta \quad \text{km} \quad (2-40)$$

The rest of the calculation method is modified in the revised version of Rec.618. Both previous and revised methods are summarised below.

Previous Calculation Method (Rec.618-5):

Having calculated horizontal projection of the slant path length (L_G), the rainfall rate exceeded for 0.01% , $R_{0.01}$ (mm/h) is obtained from Rec.837-2 [97]. The parameter L_o is defined as

$$L_o = 35 \exp(-0.015 R_{0.01}) \quad (2-41)$$

Taking the parameters L_G and L_o into account, the reduction factor is determined from

$$r_{0.01} = \frac{1}{1 + \left(\frac{L_G}{L_o} \right)} \quad (2-42)$$

A specific attenuation, γ_R (dB/km), is then calculated from

$$\gamma_R = k R_{0.01}^\alpha \quad \text{dB/km} \quad (2-43)$$

where k and α values are frequency dependent coefficients defined in Rec.838 [98].

The rain fading exceeded for 0.01% of an average year is obtained from:

$$A_{0.01} = \gamma_R L_S r_{0.01} \quad \text{dB} \quad (2-44)$$

An expression for rain fading exceeded for other annual percentages of time (p) in the range 0.001% to 1% is defined as:

$$\frac{A_p}{A_{0.01}} = 0.12 p^{-(0.546 + 0.043 \log p)} \quad (2-45)$$

Revised Calculation Method (Rec.618-6):

Having calculated horizontal projection of the slant path length (L_G), a specific attenuation, γ_R (dB/km), is obtained from the equation (2-43). The horizontal reduction ($r_{0.01}$) and vertical adjustment ($v_{0.01}$) factors are then calculated as:

$$r_{0.01} = \frac{1}{1 + 0.78 \sqrt{\frac{L_G \gamma_R}{f} - 0.38(1 - e^{-2L_G})}} \quad (2-46)$$

and

$$v_{0.01} = \frac{1}{1 + \sqrt{\sin(\theta)} \left(31(1 - e^{-(\theta(1+\chi))}) \sqrt{\frac{L_R \gamma_R}{f^2}} - 0.45 \right)} \quad (2-47)$$

where θ is the path elevation angle as seen from the ground terminal and χ is a function of the latitude (φ) of the ground terminal and defined as

$$\begin{aligned} \chi &= 36 - |\varphi| & \text{if } |\varphi| < 36^\circ \\ \chi &= 0 & \text{else} \end{aligned} \quad (2-48)$$

L_R (km) is calculated from:

$$\begin{aligned} L_R &= \frac{L_G r_{0.01}}{\cos \theta} & \text{if } \zeta > \theta \\ L_R &= \frac{h_R - h_S}{\sin \theta} & \text{else} \end{aligned} \quad (2-49)$$

where $r_{0.01}$ is the horizontal reduction factor, h_R is calculated from the equation.2-37, h_S is the ground terminal height above mean sea level in km and ζ (degrees) is calculated from:

$$\zeta = \tan^{-1} \left(\frac{h_r - h_s}{L_G r_{0.01}} \right) \quad (2-50)$$

The slant path attenuation exceeded for 0.01% of the time is obtained from:

$$A_{0.01} = \gamma_R L_R \nu_{0.01} \quad dB \quad (2-51)$$

The estimated long term statistics of the slant path attenuation to be exceeded for other percentages (p) of an average year in the range 0.001% to 5% is derived from the following formula:

$$A_p = A_{0.01} \left(\frac{p}{0.01} \right)^{-(0.655+0.033\ln(p)-0.045\ln(A_{0.01})-\beta(1-p)\sin(\theta))} \quad dB \quad (2-52)$$

where β is determined from:

$$\begin{aligned} \beta &= 0 & \text{if } p \geq 1\% \text{ or } |\phi| \geq 36^\circ \\ \beta &= -0.005(|\phi| - 36) & \text{if } p < 1\% \text{ and } |\phi| < 36^\circ \text{ and } \theta \geq 25^\circ \\ \beta &= -0.005(|\phi| - 36) + 1.8 - 4.25\sin(\theta) & \text{otherwise} \end{aligned}$$

Comparison:

Rain fading statistics obtained from both versions are compared in Figure 2.18 for an Earth station located at a sea level and a latitude of 50° (Rainfall rate = 25 mm/h). It is assumed that the station operates with an elevation of 10° .

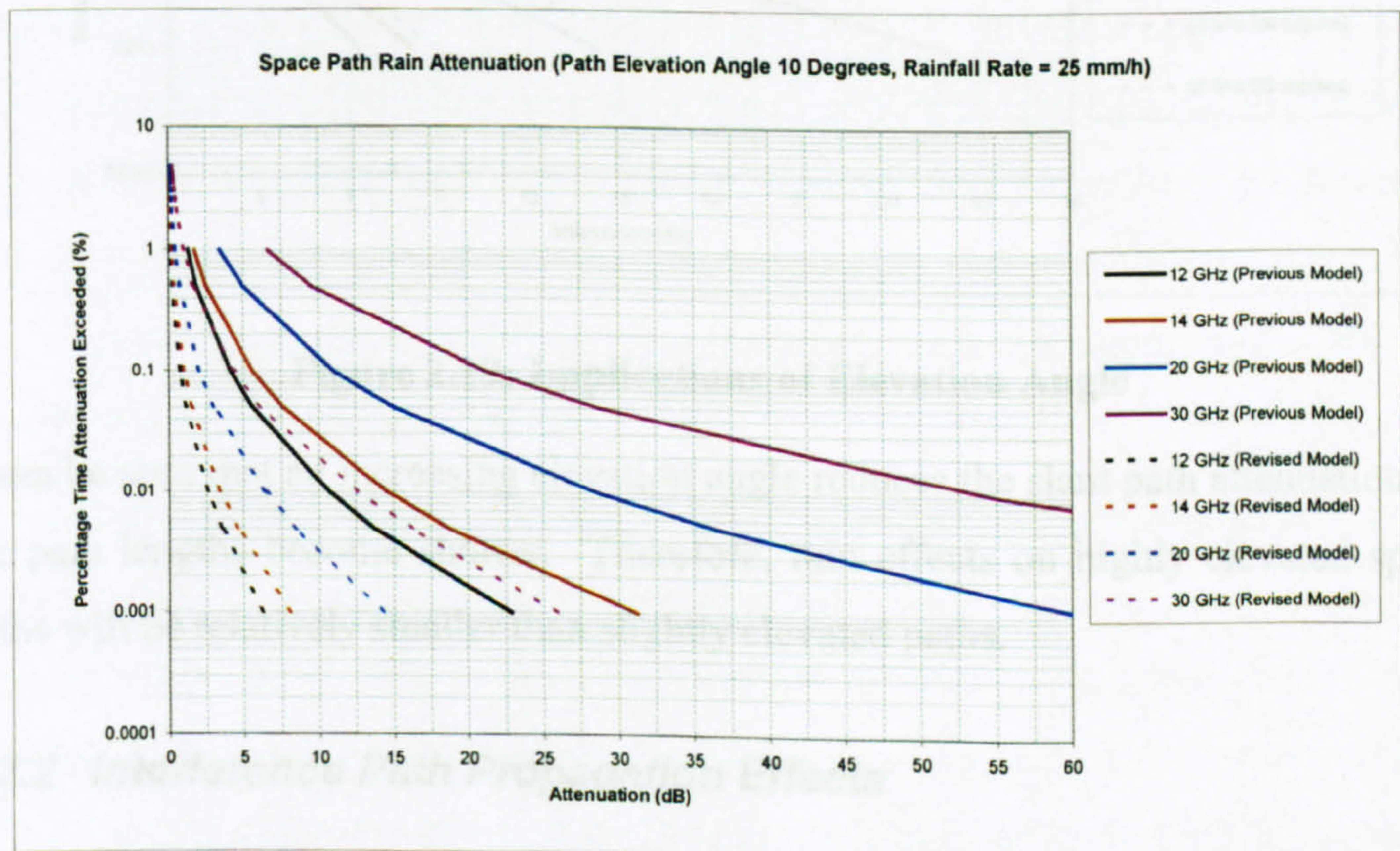


Figure 2.18: Comparison of 10° Elevation Space Path Rain Attenuation

The results indicate that estimated attenuation values obtained from the revised model are significantly lower than those derived from the previous model. At an exceedence percentage of 0.01% , the revised model predicts attenuation values in the range 2.5 to 12.5 dB for frequencies between 12 GHz and 30 GHz. For the same percentage and frequency range, the previous model estimates are in the range 10.5 to 55 dB range. It should be borne in mind that the revised model is valid up to 5% while the previous model is used for estimating attenuations up to 1% .

Using the revised rain prediction model, the impact of increasing elevation angle is examined by comparing the results obtained for 10° elevation against those obtained for 20° elevation.

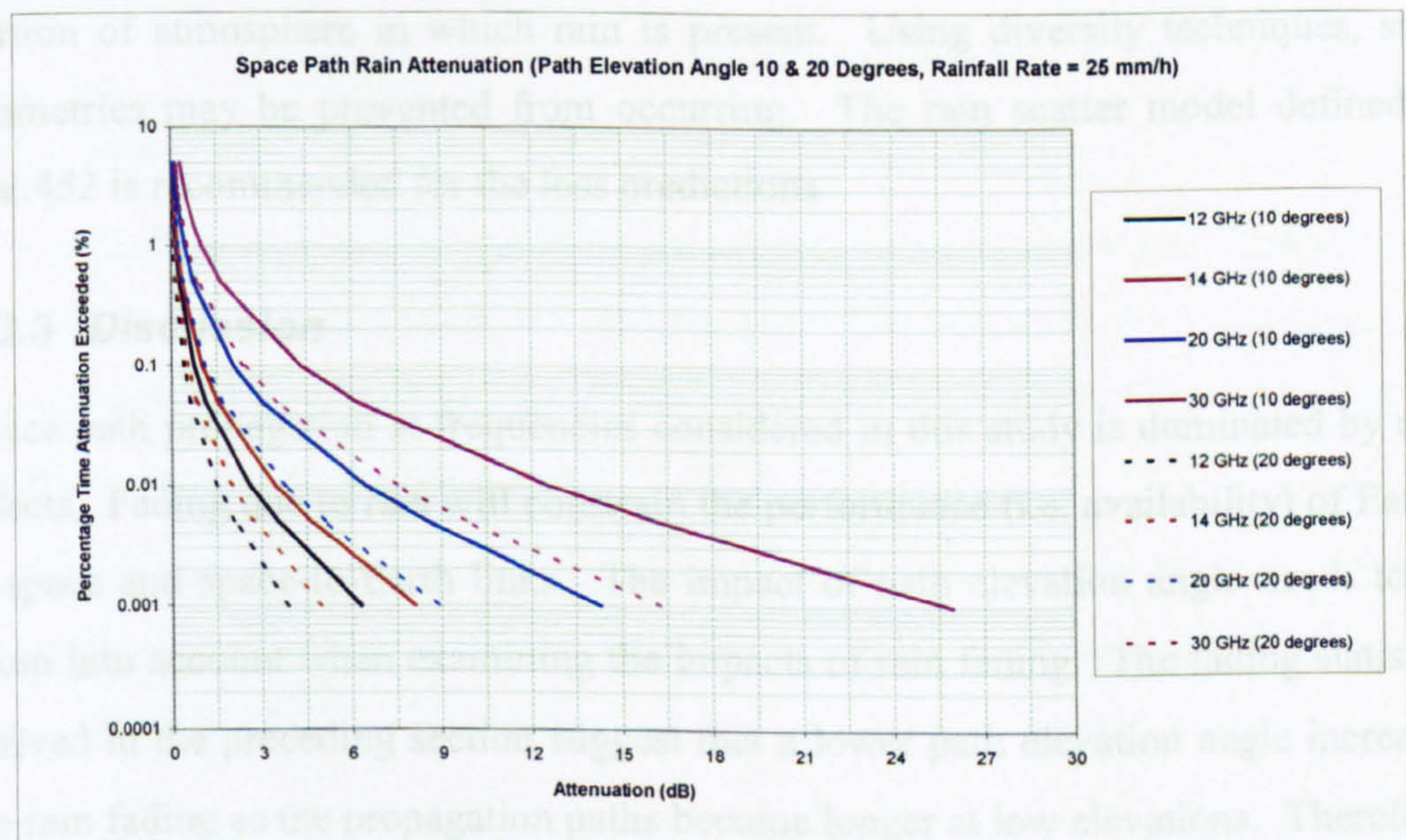


Figure 2.19: Implications of Elevation Angle

It can be seen that an increasing elevation angle reduces the slant path attenuation, as the path lengths become shorter. Therefore, rain effects on highly elevated space paths will be relatively smaller than slightly elevated paths.

2.3.2 Interference Path Propagation Effects

Clear-air propagation and rain scatter are two principal impairment mechanisms giving rise to space path interference. Rec.619 (currently at version 1) summarises

important propagation effects applicable to interference paths between ground terminals and space stations [90].

Rec.619 defines a basic transmission loss formula including free space path loss and atmospheric absorption. It notes that variations in the tropospheric refractivity index causes scintillation and diffraction effects (including ray bending, beam spreading and low angle fading) which may be significant at very low elevation angles (typically less than 4°). It refers to the loss prediction methods defined in Rec.452 [88] for modelling these effects.

The recommendation further notes that enhanced levels of unwanted signals may result when the main beams of interfering and victim systems intersect within the portion of atmosphere in which rain is present. Using diversity techniques, such geometries may be prevented from occurring. The rain scatter model defined in Rec.452 is recommended for the loss predictions.

2.3.3 Discussion

Space path propagation at frequencies considered in this study is dominated by rain effects. Fading due to rain will constrain the performance (i.e. availability) of Earth-to-space and space-to-Earth links. The impact of path elevation angle needs to be taken into account when examining the impacts of rain fading. The fading statistics derived in the preceding section suggest that a lower path elevation angle increases the rain fading as the propagation paths become longer at low elevations. Therefore, for a given required availability, the minimum path elevation angle will be constrained by the rain attenuation.

In the space path propagation analysis, empirical prediction methods defined in the previous (version 5) and revised (version 6) Rec.618 are compared. Both models are generic and based on long term rain attenuation measurements stored in the ITU-R data bank. It is noted that the revised model is valid up to 55 GHz for percentages 0.001% to 5% while the previous method is applicable up to 30 GHz in the range 0.001% to 1% . The comparison of rain statistics derived from both models indicates

that, for the assumed parameter values, the revised method predicts lower attenuation for a given exceedence percentage. This, in turn, implies that when the revised method is employed in the link design process a link would require a relatively lower EIRP, as the rain margin is smaller, to achieve its performance objectives (i.e. availability targets).

As far as interference paths are concerned, in a typical GSO/NGSO FSS sharing scenario, aggregate interference will be determined by line-of-sight paths. Therefore, free space propagation is applied to model fading on a given interfering path. It is also worth noting that additional loss may result from the atmospheric absorption when a path elevation angle is very small, as shown previously in Figure 2.3.

2.4 Conclusions

One of the key aspects that has to be considered in the examination of interference between systems operating at Ku and Ka band frequencies is that of propagation impairments. It is, therefore, important to establish the impact of these propagation mechanisms on the spectrum sharing.

In this chapter, propagation mechanisms affecting GSO/NGSO FSS and NGSO FSS/FS spectrum sharing are reviewed primarily taking prediction models defined in ITU-R recommendations into account.

In line with the overall structure, the key conclusions that can be drawn from the modelling carried out in this chapter are summarised below.

- Atmospheric absorption is dependent on frequency, path length and location. Atmospheric loss generally increases with increasing frequency and path length. At Ku band, space path loss is less than 2 dB for all elevation angles while a 10 km terrestrial link is faded by some 1 dB . At Ka band, space path loss remains below 7 dB and a 10 km terrestrial path fading is approximately 1 dB . In comparison to other fading mechanisms, the atmospheric absorption is not a

dominant factor but does have a limited impact at the frequencies considered in this study.

- Terrestrial path propagation is affected by tropospheric and terrain effects. Both give rise to refraction, reflection and scattering of radiowaves. In addition, absorption and scatter effects caused by rain play a significant role in terrestrial path propagation. At the frequencies of interest, it is noted that multipath and rain fading mechanisms need to be considered in the design of terrestrial links. At Ku band, a 5 km link located at 52 degrees latitude is faded by some 5 dB for 0.01% of an average year due to rain and 0.02% of an average year due to multipath effects, leading to total percentage time of 0.03% for which 5 dB fading is exceeded. At Ka band, the same link is subject to 25 dB rain fading for 0.01% and multipath fading for 0.0001% of time indicating that a significant portion of total unavailability time is attributed to the rain fading. From an interference path point of view, the combined effects of individual propagation mechanisms need to be considered depending on the type of interference path. An overall loss for a clear line-of-sight path is determined by free space propagation, atmospheric loss and fading due to local clutter. An obstructed line-of-sight path will be subject to additional sub-path diffraction loss. The impacts of interference paths beyond the horizon are modelled by combining troposcatter, diffraction, ducting/layer reflection and local clutter effects. In addition, interference paths resulting from rain scatter may also be significant in some situations.
- In designing Earth-to-space and space-to-Earth links, rain fading is the most significant effect to consider in Ku and Ka band. Rain fading determines the minimum path elevation angle below which links could not sustained due to excessive loss. During investigations carried out in this chapter, the implications of the use of previous and revised rain attenuation prediction methods defined in Rec.618 are examined. It is noted that, for a given percentage time, the predictions from the revised method are lower than those obtained from the previous method. Furthermore, in the revised method, the maximum frequency

for which the prediction model is valid is noted to be improved from *30 GHz* to *55 GHz* and the maximum percentage time from *1%* to *5%*. From an interference paths perspective, interfering space paths will be line-of-sight. Therefore, the analysis should take account of free space path loss, atmospheric absorption and, in some cases, clutter loss.

CHAPTER 3

REVIEW OF ISSUES RELATED TO INTERFERENCE FROM NONGEOSTATIONARY FIXED SATELLITE SERVICE SYSTEMS INTO GEOSTATIONARY FIXED SATELLITE SERVICE SYSTEMS

In this chapter, the key aspects of the Ku and Ka band interference paths from NGSO FSS systems into GSO FSS systems are reviewed. These interference paths are illustrated in Figure 3.1.

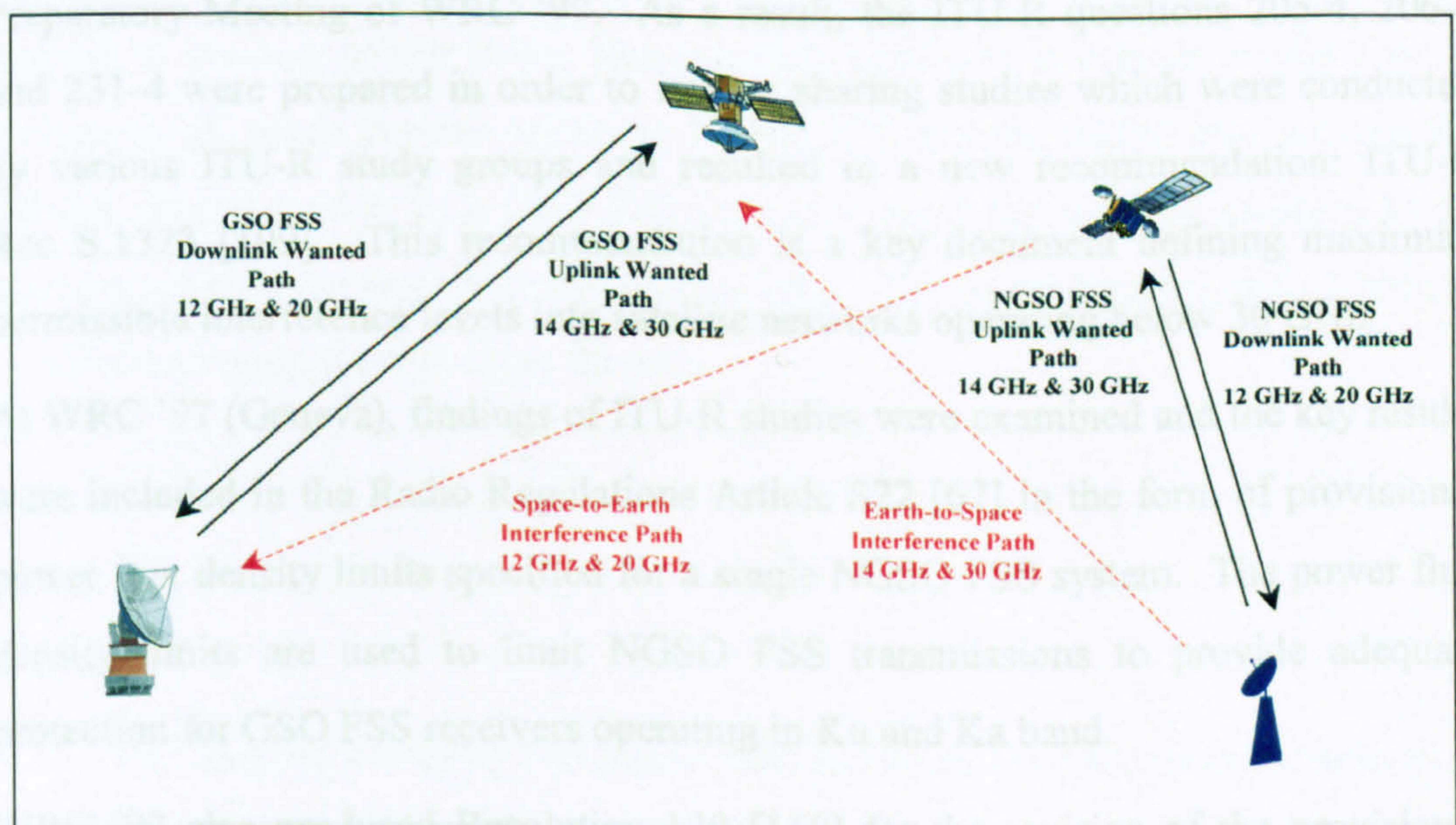


Figure 3.1: NGSO FSS Interference Paths into GSO FSS links in Ku and Ka Band

Firstly, an overview of current regulatory requirements facilitating Ku and Ka band NGSO/GSO FSS frequency sharing is given. Then, on the basis of literature research carried out, the key sharing topics are identified together with critical revision of sharing methodologies applied. This is followed by the presentation of

representative system characteristics used during the course of this research. The final section outlines conclusions of the review.

3.1 Current Regulations

This section summarises historic development of GSO/NGSO FSS spectrum sharing regulations and examines the key documents defining the current sharing requirements.

3.1.1 Brief History

The World Radio Conference '95 (WRC '95) produced resolutions in order to address outstanding issues related to feasibility of spectrum sharing between GSO FSS and NGSO FSS systems. These resolutions were considered in the Conference Preparatory Meeting of WRC '97. As a result, the ITU-R questions 205-4, 206-4 and 231-4 were prepared in order to initiate sharing studies which were conducted by various ITU-R study groups and resulted in a new recommendation: ITU-R Rec. S.1323 [109]. This recommendation is a key document defining maximum permissible interference levels into satellite networks operating below 30 GHz.

At WRC '97 (Geneva), findings of ITU-R studies were examined and the key results were included in the Radio Regulations Article S22 [67] in the form of provisional power flux density limits specified for a single NGSO FSS system. The power flux density limits are used to limit NGSO FSS transmissions to provide adequate protection for GSO FSS receivers operating in Ku and Ka band.

WRC '97 also produced Resolution 130 [110] for the revision of the provisional limits. In response, within the ITU-R, Joint Task Group 4-9-11 (JTG 4-9-11) was set-up to study the implications of NGSO FSS interference into GSO FSS links together with the other working group ITU-R Working Party 4A (WP-4A).

3.1.2 ITU-R Radio Regulations Article S.22 (Based on Regulations Published in Geneva '98)

Article S.22 is concerned with the efficient use of the frequency spectrum allocated to space services. In order to control the interference to GSO satellite systems, it is stated that NGSO satellite systems shall not cause unacceptable interference to GSO satellite systems in the fixed satellite service operating in accordance with the Radio Regulations.

In line with the above requirement, Article S.22 [67] includes definitions of equivalent power flux density (epfd) to protect GSO FSS Earth stations and aggregate power flux density (apfd) to protect GSO FSS satellites from NGSO FSS interference.

Equivalent Power Flux Density (epfd): The equivalent power flux-density is defined as the sum of the power flux-densities produced at a point on the Earth's surface by all space stations within an NGSO FSS system, taking into account the off-axis discrimination of a GSO FSS reference receiving antenna assumed to be pointing towards the geostationary-satellite orbit. The equivalent power flux density is calculated using the following formula:

$$\boxed{epfd = 10 \log \left[\sum_{i=1}^{N_s} 10^{pfd_i / 10} \frac{G_r(\theta_i)}{G_{\max}} \right]} \quad (3-1)$$

where:

N_s : number of NGSO FSS space stations visible from the point considered at the Earth's surface, within an elevation angle greater than or equal to 0° ;

i : index of the NGSO FSS space station considered;

pfd_i : power flux density produced at the point considered on the Earth's surface in $\text{dB(W/m}^2\text{)}$ in the reference bandwidth;

θ_i : off-axis angle between the direction considered towards the geostationary satellite orbit and the direction of the interfering space station in the NGSO FSS satellite system;

$G_r(\theta_i)$: off-axis gain of the GSO FSS ground terminal receiver reference antenna

G_{max} : maximum gain of the GSO FSS ground terminal receiver reference antenna;

epfd: computed equivalent power flux-density in dB(W/m²) in the reference bandwidth.

Aggregate power flux density (apfd): The aggregate power flux-density is defined as the sum of the power flux densities produced at a point in the geostationary-satellite orbit by all the earth stations of an NGSO FSS satellite system. The aggregate power flux density is computed by means of the following formula:

$$\boxed{apfd = 10 \log \left[\sum_{i=1}^{N_e} 10^{P_i/10} \frac{G_i(\theta_i)}{4 \pi d_i^2} \right]} \quad (3-2)$$

where:

N_e : number of earth stations in the NGSO FSS satellite system with an elevation angle greater than or equal to 0°, from which the point considered in the geostationary satellite orbit is visible;

i : index of the earth station considered in the NGSO FSS satellite system;

P_i : RF power at the input of the transmitting antenna of the earth station considered in the NGSO FSS satellite system in dBW in the reference bandwidth;

θ_i : off-axis angle between the boresight of the earth station considered in the NGSO FSS satellite system and the direction of the point considered in the geostationary satellite orbit;

$G_r(\theta_i)$: transmit antenna gain of the earth station considered in the NGSO FSS satellite system in the direction of the point considered in the geostationary satellite orbit;

d_i : distance in metres between the earth station considered in the NGSO FSS satellite system and the point considered in the geostationary satellite orbit;

$apfd$: aggregate power flux-density in dB(W/m²) in the reference bandwidth.

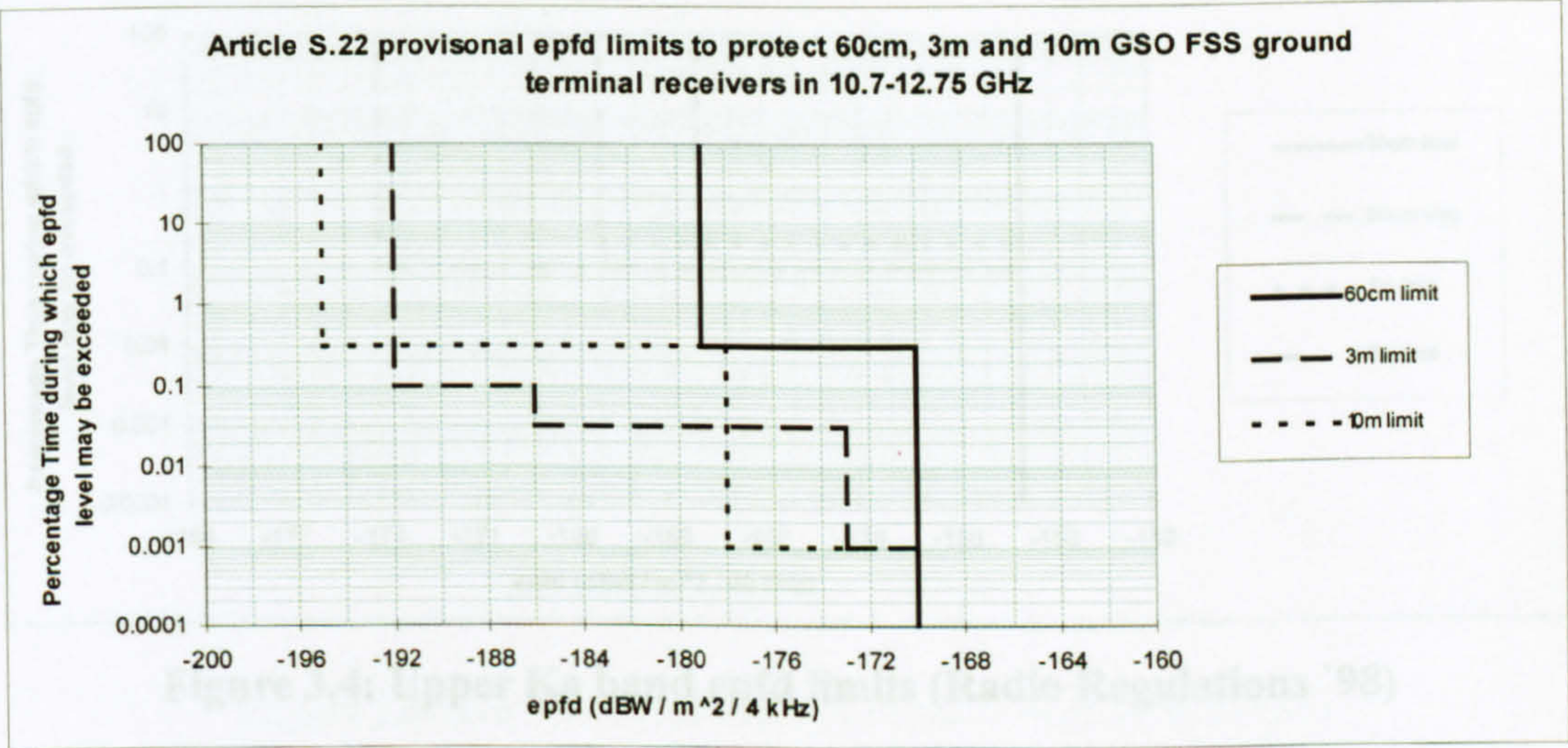
The above definitions can be summarised as follows:

- $epfd$ is a constraint on the NGSO FSS downlink (i.e. at the GSO FSS Earth station) and takes account of the interference generated by all NGSO FSS satellites in a given system and also the antenna discrimination of the GSO FSS Earth station with respect to each of the interference entries from the satellites of the given NGSO FSS system.
- $apfd$ is a constraint on the NGSO FSS uplink (i.e. at the GSO FSS satellite) and takes account of the interference generated by all the Earth stations in a given NGSO FSS system. It is assessed at a point on the geostationary orbit and therefore no account is taken of any satellite receive antenna discrimination with respect to each of the interference entries from the Earth stations of the given NGSO FSS system

On the basis of above definitions, provisional $epfd$ and $apfd$ limits have been incorporated into the Article S.22. It is important to note that these limits are specified for interference from a single NGSO FSS system, i.e. single entry $epfd/apfd$ limits.

The Ku band $epfd$ limits are defined for 60cm, 3m and 10m GSO FSS Earth station receivers. Two sets of $epfd$ limits are defined for Ka band. The first set intends to provide protection for 30cm, 70cm, 90cm, 1.5m, 5m, 7.5m and 12m GSO FSS Earth stations operating in lower Ka band (17.8-18.6 GHz) while the second set is specified for 30cm, 90cm, 2m and 5m receivers operating in upper Ka band (19.7-20.2 GHz).

The following plots illustrate these limits in terms of “a percentage time for which a given interference $epfd$ level may be exceeded”.



3.2: Ku band epfd limits (Radio Regulations '98)

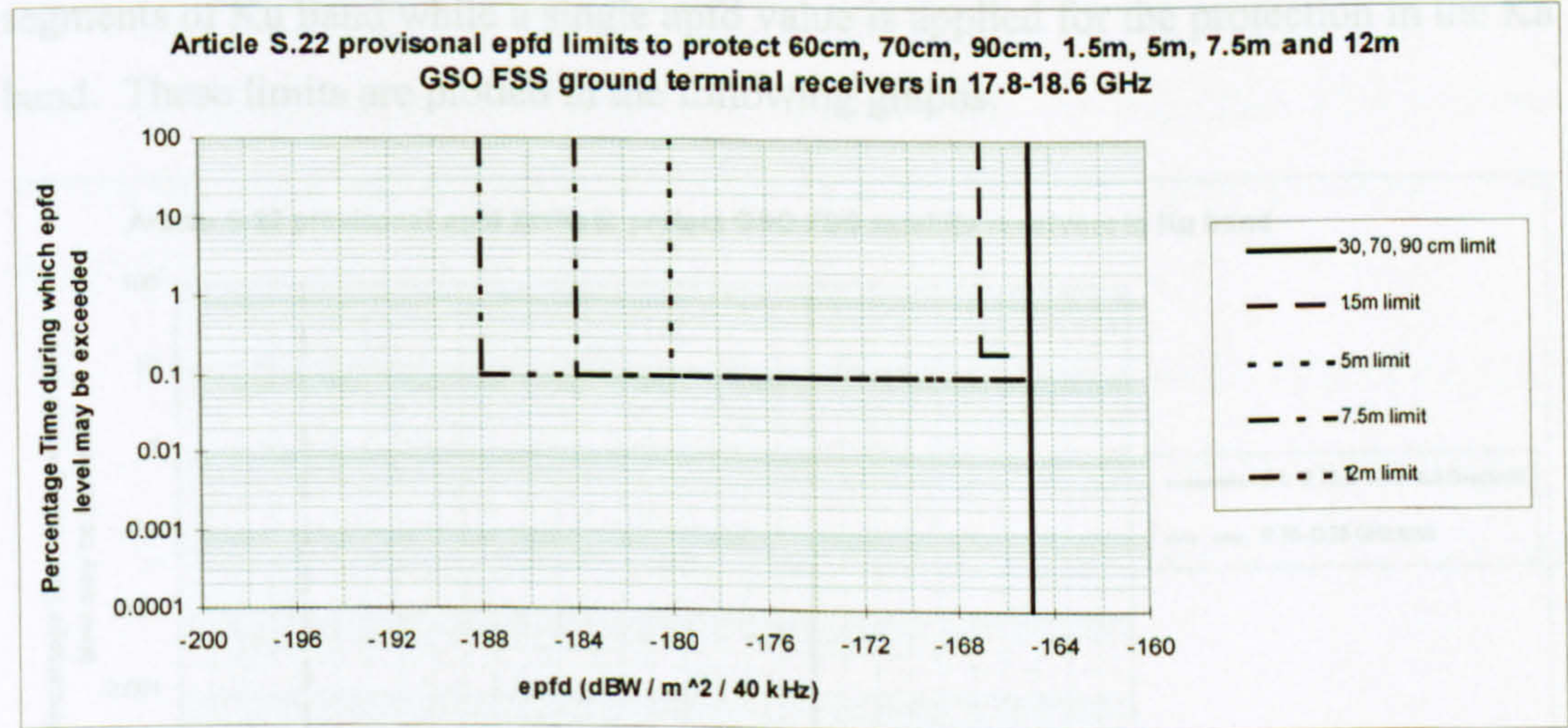


Figure 3.3: Lower Ka band epfd limits (Radio Regulations '98)

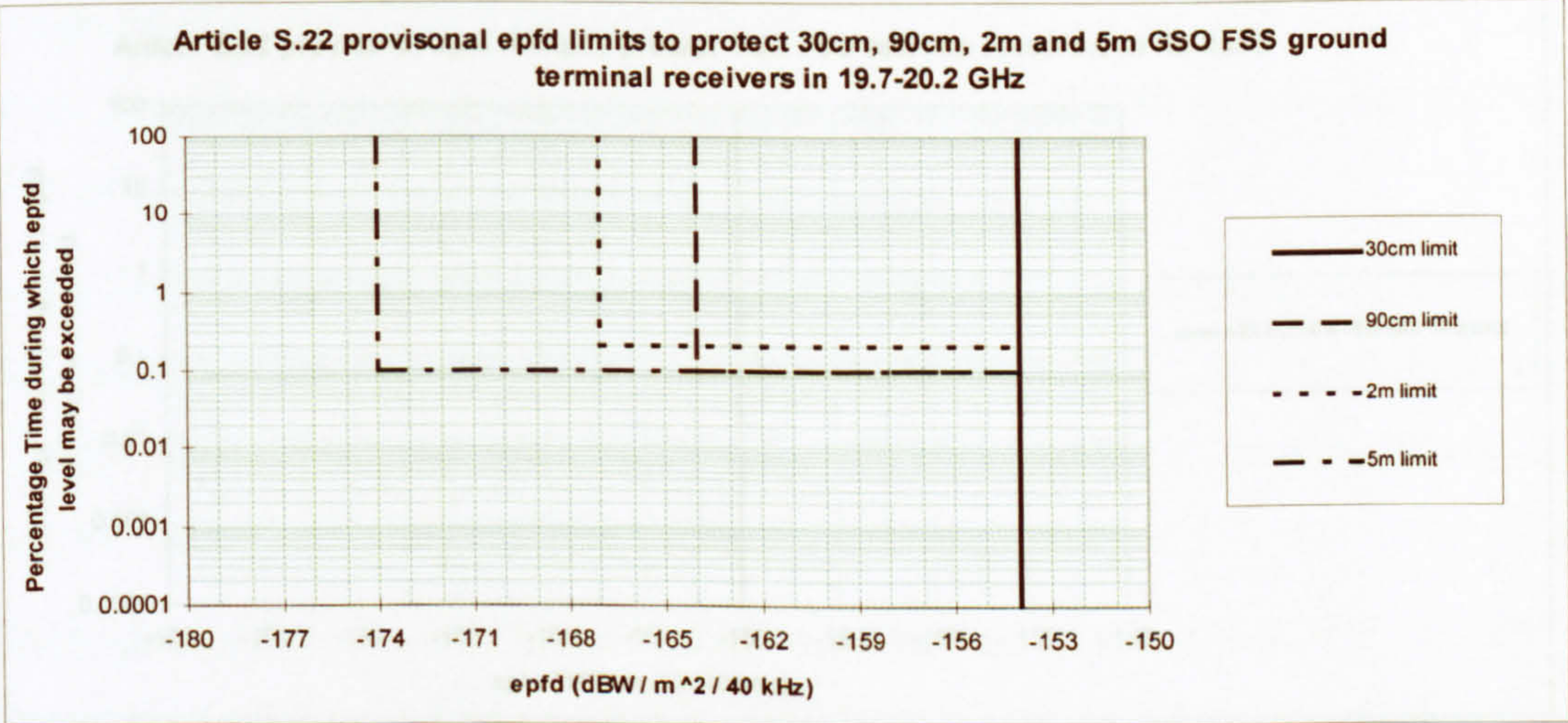


Figure 3.4: Upper Ka band epfd limits (Radio Regulations '98)

As can be seen, the provisional epfd limits are specified in “staircase” form. In examining the impact of NGSO FSS interference on a given GSO FSS link, any calculated epfd value on the left side of the epfd limits indicates that the provisional limits would not provide adequate protection for the examined GSO FSS link.

As far as apfd limits are concerned, two values are specified provisionally for three segments of Ku band while a single apfd value is applied for the protection in the Ka band. These limits are plotted in the following graphs.

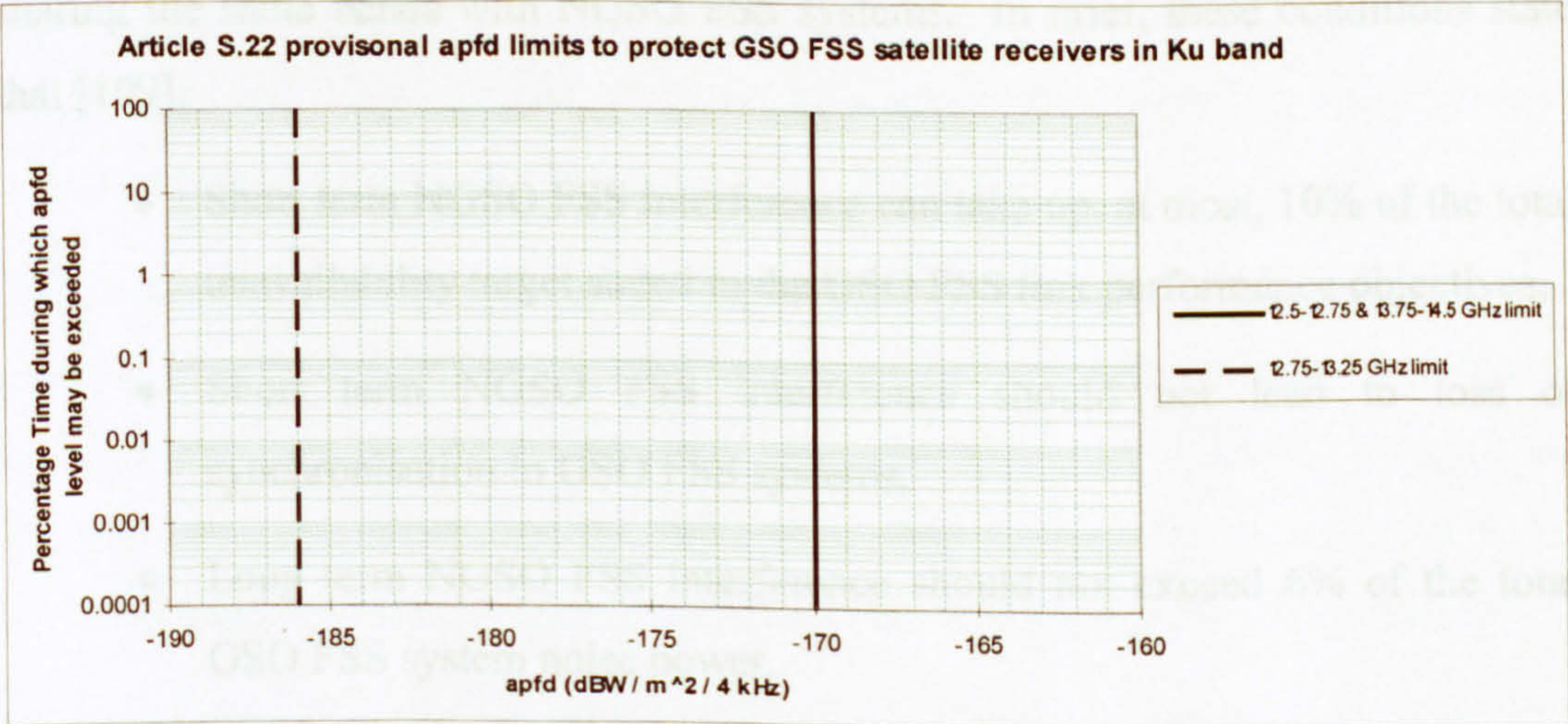


Figure 3.5: Ku band apfd limits (Radio Regulations '98)

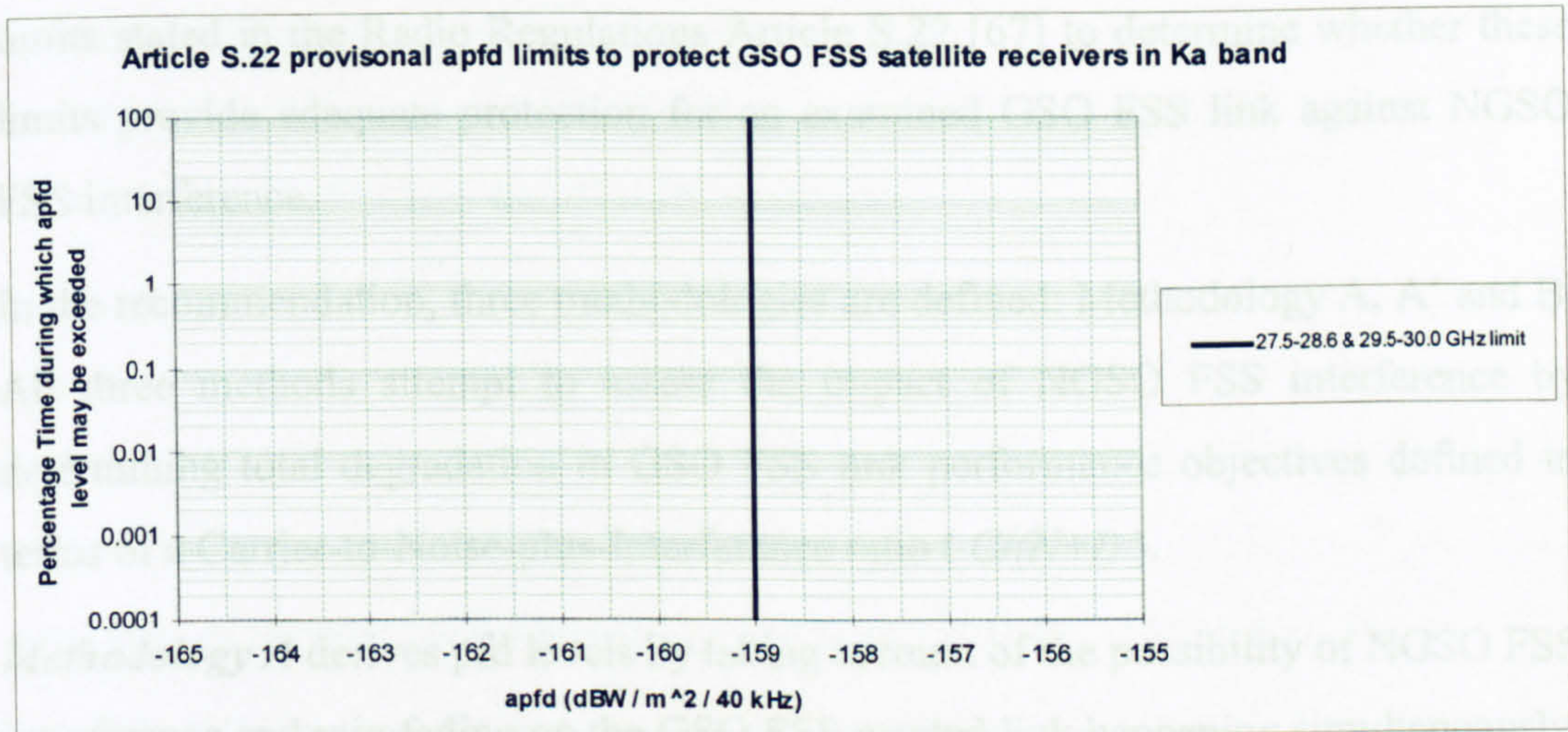


Figure 3.6: Ka band apfd limits (Radio Regulations '98)

The apfd plots show that the Article S.22 limits are specified for 100% of a time. Once more, any calculated apfd value on the left side of these limits indicates that the provisional apfd limits would not protect the GSO FSS satellite receivers adequately from the NGSO FSS ground terminal interference.

3.1.3 ITU-R Recommendation 1323

Rec.1323 defines minimum protection requirements for the GSO FSS systems sharing the same bands with NGSO FSS systems. In brief, these conditions state that [109]:

- Short term NGSO FSS interference can take up, at most, 10% of the total unavailability target stated in the GSO FSS link performance objectives,
- Short term NGSO FSS interference should not lead to loss of synchronisation in GSO FSS systems,
- Long term NGSO FSS interference should not exceed 6% of the total GSO FSS system noise power.

The recommendation includes a number of methods to determine maximum tolerable power flux density (pfd) levels for a given GSO FSS link characteristics and performance objectives. Calculated pfd levels are then compared against pfd

limits stated in the Radio Regulations Article S.22 [67] to determine whether these limits provide adequate protection for an examined GSO FSS link against NGSO FSS interference.

In the recommendation, three methodologies are defined: Methodology A, A' and B. All three methods attempt to assess the impact of NGSO FSS interference by determining total degradation in GSO FSS link performance objectives defined in terms of a Carrier-to-Noise-plus-Interference ratio ($C/(N+I)$).

Methodology A derives pfd levels by taking account of the possibility of NGSO FSS interference and rain fading on the GSO FSS wanted link happening simultaneously. The method is based on the assumption of statistically independent GSO FSS link fading and NGSO FSS interference probability density functions. These functions are convolved in order to determine the maximum allowed aggregate interference pfd levels.

Methodology A' is an attempt to simplify the Methodology A. In this method, the probability distribution functions are simplified and parameterised in order to implement an analytical convolution which gives rise to two equations with two unknowns.

Methodology B assumes that degradations in the GSO FSS link performance due to interference and fading do not occur simultaneously and, therefore, the impact of interference and fading should be considered separately.

The method derives a link margin by subtracting the GSO FSS link $C/(N+I)$, required to provide a threshold Bit Error Rate (BER) (which can only be exceeded for a particular percentage time, p), from the clear sky $C/(N+I)$. Aggregate interference power flux density values are then derived by assuming that the available margin is used by aggregate NGSO FSS interference for 10% of time p .

In sharing scenarios where multiple NGSO FSS systems occupy the same band with the victim GSO FSS link, this methodology suggests that maximum tolerable pfd level attributed to a single NGSO FSS system can be calculated by simply dividing the "10% of p " figure by the number of interfering NGSO FSS systems. This

simplified assumption implies that there will be no simultaneous NGSO FSS interference entry peaks from the different interfering systems and that their interference contributions are all at the same level.

In addition to the above mentioned methodologies, Rec.1323 includes a procedure (*Procedure D*) implementing verification of compliance with the minimum GSO FSS link protection requirements and refinement of pfd limits developed using any of three methodologies. This procedure aims to determine a suitable set of pfd limits from a set of proposed pfd statistics by applying a trial and error approach.

Procedure D implementation involves convolution of the uplink and downlink rain fading statistics with the proposed pfd statistics, representing aggregate interference originating from NGSO FSS systems, and the comparison of the resultant $C/(N+I)$ ratios with the performance objectives of the examined GSO FSS link. Using this procedure, a value of 'relative availability reduction' due to NGSO FSS interference is calculated. In situations where the relative availability reduction is greater than the 10% criterion, the pfd limits are considered to provide insufficient protection, and are modified until the relative availability reduction is less than 10%.

3.2 Previous Work

This section briefly looks at studies concerning with Ku and Ka band NGSO/GSO FSS spectrum sharing with a view to identify key issues and to examine sharing analysis techniques employed. It is noted that investigations carried out within ITU-R Working Party 4A (WP-4A) and Joint Task Group 4-9-11 (JTG 4-9-11) are of particular interest.

Literature review has indicated that there are a number of topics which may affect the feasibility of frequency sharing. These may be categorised into the following:

- Possible modification to the Article S.22 epfd and apfd definitions,
- Implications of NGSO FSS interference mitigation techniques,
- Revision of the Article S.22 provisional epfd/apfd limits,

- Refinement of GSO FSS reference antenna radiation patterns to be used in sharing analysis,
- Examination of aggregate interference statistics from multiple NGSO FSS systems and identification of algorithms for converting aggregate epfd/apfd limits (originating from multiple NGSO FSS systems) into single entry limits (originating from a single NGSO FSS system),
- Provision of protection for GSO FSS links designed with very large ground terminal receiver antennas,
- Investigation of short term NGSO FSS interference peaks.

Brief discussions on each of the above topics together with analysis methodologies applied in earlier studies are provided in the following sections.

3.2.1 Epfd and Apfd Definitions

Prior to explaining the need for the use of epfd and apfd concepts, it is necessary to define power flux density (pfd). It can be shown that [15] a surface of effective area A situated at a distance R from the transmitting subtends to a solid angle A/R^2 at the transmitting antenna, as illustrated below.

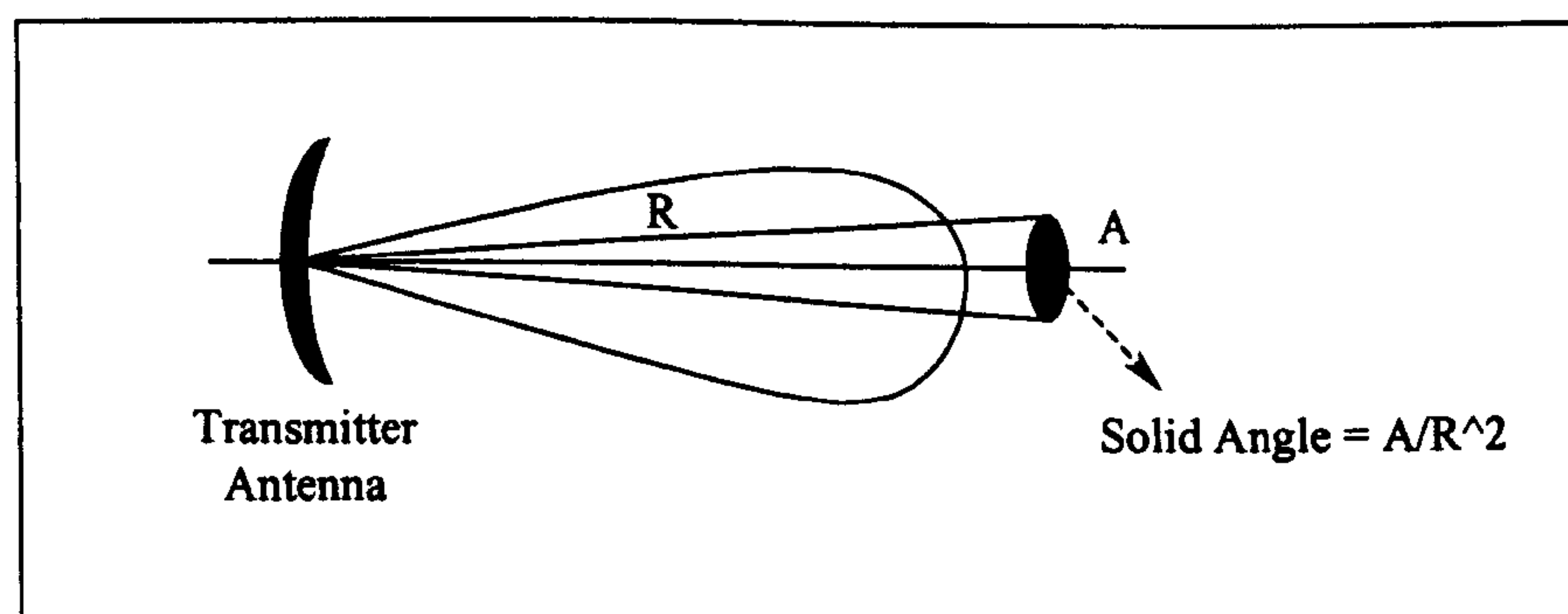


Figure 3.7: Power Flux Density

Assuming transmitter antenna radiates power of P_T (watts) in a direction where the value of antenna gain is G_T , it can be shown that the total power spread over A is equal to

$$P_R = \frac{P_T G_T}{4\pi R^2} A \quad \text{Watts} \quad (3-3)$$

The magnitude of $\frac{P_T G_T}{4\pi R^2}$ is called “power flux density” and expressed in watts/m² (or in logarithmic terms $pdf \text{ (dBW/m}^2\text{)} = 10\log(P_T) + 10\log(G_T) - 10\log(4\pi R^2)$) [15].

Traditionally, pdf limits are used to restrict GSO FSS satellite downlink transmissions in order to protect radio stations operating over the Earth’s surface. These limits relate to the power flux density which would be obtained under assumed free space propagation conditions. They are specified as a function of downlink path elevation angle as seen from a point on the Earth’s surface [94]. Typically, sharing methodologies applied for assessing implications of pdf limits are based on calculating interference at a given terrestrial radio station or satellite Earth station receiver location by employing analytic approach or static simulation analysis where GSO FSS satellite transmissions are represented by pdf masks.

However, interference scenarios involving NGSO FSS and GSO FSS systems require a different approach because the sharing environment is no longer static. Therefore, the concept of epfd is introduced to reflect the dynamic nature of the sharing environment by taking account of both transmitter and receiver antenna pointings that are time varying parameters.

As stated in § 3.1.3, WRC ’97 apfd limits, set for the protection of GSO FSS satellite receivers, are in the form of single power limits to be met for 100% of the time and do not take account of a satellite receiver antenna discrimination. Interference studies, based on simulation analysis, have indicated that this approach results in relatively higher interference statistics [111-114]. Therefore, it is suggested that the apfd definition should include a GSO FSS satellite receiver antenna discrimination to obtain more realistic interference statistics. This modification, in turn, leads to a single equivalent power flux density “epfd” definition [115, 116]:

Equivalent Power Flux Density (epfd): The equivalent power flux-density is defined as the sum of the power flux-densities produced at a GSO receive station on the Earth surface or in the geostationary orbit, as appropriate, by all the transmit stations within a NGSO satellite system, taking into account the off-axis discrimination of a reference receiving antenna assumed to be pointing in its nominal direction. The equivalent power flux density is calculated using the following formula:

$$epfd = 10 * \log \left[\sum_{i=1}^{N_a} 10^{\frac{P_i}{10}} * \frac{G_t(\theta_i)}{4 * \pi * d_i^2} * \frac{G_r(\phi_i)}{G_{r,max}} \right] \quad (3-4)$$

where:

N_a : the number of NGSO FSS transmitter stations that are visible from the GSO receiver station on the Earth's surface or in the geostationary orbit, as appropriate;

i : the index of the NGSO FSS transmitter station;

P_i : the RF power at the antenna input of the NGSO FSS transmitter station, dBW in the reference bandwidth;

θ_i : the off-axis angle between the boresight of the NGSO FSS transmitter station and the direction of the GSO FSS receiver station;

$G_t(\theta_i)$: the transmitter antenna gain (as a ratio) of the NGSO FSS station in the direction of the GSO FSS receiver station;

ϕ_i : the off-axis angle between the boresight of the GSO FSS receiver station and the direction of the i^{th} transmitter station considered in the NGSO FSS system;

$G_r(\phi_i)$: the receiver antenna gain (as a ratio) of the GSO FSS receiver station in the direction of the i^{th} transmit station considered in the NGSO FSS system;

d_i : the distance between the NGSO FSS transmitter and the GSO FSS receiver stations, in metres;

$G_{r,max}$: the maximum gain (as a ratio) of the GSO FSS station receiver antenna;

$epfd$: the computed equivalent power flux-density in dB(W/m²) in the reference bandwidth.

The terms $epfd_{up}$ and $epfd_{down}$ are adopted to distinguish between the uplink and downlink $epfd$, respectively [115, 116]. In line with these modifications, the new terminology is used in this research when referring to uplink and downlink power flux densities in assessing implications of NGSO FSS interference on GSO FSS links.

3.2.2 NGSO/GSO Interference Mitigation Techniques

The NGSO FSS system descriptions suggest that there are several mitigation techniques proposed for reducing potential interference into GSO FSS links [53-58]. It is worth noting that the choice of mitigation technique has a significant impact on the NGSO FSS system design complexity, cost and capacity. These factors will eventually determine the viability of incorporating proposed mitigation techniques into NGSO FSS system designs [117].

The use of satellite diversity is suggested as a possible mitigation technique to avoid main-beam-to-main beam interference coupling mechanism [118]. These situations are avoided by an NGSO FSS system either selecting another visible satellite in view or simply switching off transmission whenever such in-line coupling instances occur. In the former case, it is necessary that an NGSO FSS system is designed to provide a multiple satellite coverage when serving a given ground terminal location on the surface of the Earth. In the latter case, an NGSO FSS system design should be capable of accepting the loss of coverage and the interruption of links whenever in-line event occurs.

It is noted that NGSO FSS systems plan to implement satellite diversity by introducing geostationary arc avoidance angles. Both ground and satellite based avoidance angle, for which switching to another satellite or total cessation of transmission occurs, are proposed for use in mitigating NGSO FSS interference [119, 120]. In addition, satellite selection procedures are described for implementing satellite diversity mitigation technique with satellite switching. For example, a new satellite to which traffic is switched may be selected either randomly or by applying a selection criterion, for example, highest elevation angle or largest separation angle away from GSO arc [117].

The use of high performance NGSO FSS satellite antennas is suggested to be an efficient mitigation technique to reduce the impact of downlink interference into GSO FSS Earth stations. Antennas with low side-lobe radiation pattern reduce the impact of long term interference on GSO FSS links. This, in turn, decreases the required avoidance angle and increases the NGSO FSS system capacity at the expense of increased antenna design cost [118].

It is worth noting that the development and application of sharing methodologies to examine the implications of the above mentioned mitigation techniques in improving Ku and Ka band NGSO/GSO FSS sharing environment are among the primary objectives of this research.

3.2.3 Article S.22 Limits

As stated previously, epfd limits are defined in staircase (discontinuous) form which does not entirely represent actual statistical behaviour of the NGSO FSS interference as, in practice, interference statistics would be in the form of continuous curves. Therefore, it is suggested that the use of staircase limits in assessing the impact of NGSO FSS interference on GSO FSS links may not be appropriate and this, in turn, may affect NGSO FSS system operational characteristics, design and implementation cost.

In addition, Article S.22 $\text{epfd}_{\text{down}}$ limits are defined for certain GSO FSS Earth station antenna diameters. It is pointed out that there is a need for operators to be able to check the degree of protection afforded by the limits for Earth station antennas with diameters other than those included in the current regulations.

To address these issues, the development of continuous curves of equivalent power flux densities versus antenna diameter of the GSO FSS Earth station to be protected is considered [121, 122]. Possible solutions suggested include:

- the development of continuous curves of equivalent power flux densities through application of curve-fitting techniques to the provisional limits in Article S.22 of the Radio Regulations.
- setting of a constant value for the ratio of interference power spectral density to noise power spectral density as a long term interference criteria (assuming sidelobe gains of GSO FSS Earth station antennas are constant regardless of antenna size) and calculation of long term epfd limits as a function of antenna size based on maintaining this constant value.

In addition, linear interpolation between points defined in epfd limits is suggested to obtain continuous curves for antenna diameters included in the Article S.22 [123].

As far as the revision of Article S.22 epfd values are concerned, as many sharing scenarios comprising wide range of system characteristics as possible need to be examined to provide satisfactory sharing conditions for both NGSO FSS and GSO FSS systems. This primarily suggests an investigation of all possible interference alignments together with propagation mechanisms affecting wanted and interference paths.

For the purposes of revising Article S.22 epfd values, the GSO FSS community was requested to provide link budgets to be used in sharing studies (Circular Letter CR-92). Responses were incorporated into an ITU-R GSO FSS link database that is now commonly used in sharing investigations. This database was extended by responses to a second circular letter (Circular Letter CR-116) requesting additional link budgets. GSO FSS links stored in the ITU-R database are called “CR-116 links”.

Representative GSO FSS links characteristics used in this research are based on CR-116 links.

It is noted that a number of information documents [124-132] has been produced by both NGSO FSS and GSO FSS system proponents proposing modifications to Article S.22 epfd values to protect largely their commercial interests. In general, simulation analysis and analytical approach are employed for deriving epfd limits. In simulation analysis, epfd levels are obtained from interference statistics produced by simulation modelling. A common approach taken in implementing analytical method is the application of *Methodology A'* and *Procedure D* defined in Rec.1323 [109].

3.2.4 GSO FSS Antenna Reference Radiation Patterns

The GSO FSS Earth station reference antenna pattern defined in ITU-R Rec.1323 is based on Rec.580 [133] and Rec.465 [134]. These patterns represent an envelope of 90% of the side lobe peaks and are developed to model worst case geometrical configurations used in determining peak interference levels between GSO FSS and terrestrial systems operating in the fixed service.

It is argued that the interference events no longer correspond to static geometry in the case of NGSO/GSO FSS interference analysis and the use of peak envelope antenna reference pattern in modelling interference from dynamic multiple interference sources may result in pessimistic interference levels at GSO FSS Earth stations. Therefore, it is suggested that there is a need to characterise more accurately the Earth station antenna patterns to be used in frequency sharing studies for GSO FSS and NGSO FSS systems [135].

The issue of developing an appropriate reference antenna pattern is addressed by a number of ITU-R studies [136-139]. It is suggested that NGSO FSS interfering satellites move in and out of the peaks and troughs of the actual GSO FSS Earth station antenna radiation pattern. Therefore, measurements are carried out to derive a reference pattern describing an average gain envelope taking both peaks and

troughs into account. The use of theoretical Bessel function-based antenna radiation patterns is also considered and comparisons with measured data are performed to validate the theoretical models.

The results of these studies are incorporated into a new recommendation (Rec.1428) proposing a new Earth station reference antenna envelope to be used in interference assessment involving NGSO FSS systems operating in the 10.7-30 GHz band [140].

3.2.5 Co-existence of Multiple NGSO FSS Systems

As well as avoiding interference into GSO FSS systems, NGSO FSS systems need to achieve a satisfactory sharing environment among themselves. Several techniques are studied for co-existence of multiple NGSO FSS systems in the same frequency band [141-147].

One of the proposed mitigation techniques is to employ NGSO FSS systems in homogenous orbits. Investigations suggest that the number of NGSO FSS systems sharing a given frequency band may be increased by using nearly identical orbital parameters including height and inclination (i.e. by employing plane or satellite interleaving). It is argued that plane or satellite interleaving using the same altitude and inclination remove the possibility of an in-line event where one NGSO satellite is directly between an Earth station and another NGSO satellite. It is, however, worth mentioning that this degree of similarity between different NGSO FSS operators would highly unlikely to occur.

An avoidance of in-line events plays a significant role in facilitating sharing among inhomogeneous constellations. It is suggested that mainbeam-to-mainbeam events can be avoided by either switching to another satellite whenever a satellite becomes closer to an in-line event with a satellite operating in another NGSO FSS system or simply ceasing transmission and accepting the outage.

The complexity of satellite avoidance increases if the number of NGSO FSS systems becomes larger. It is also argued that systems operating with satellite diversity require more satellites than those filed with the ITU-R (or operational) earlier as the

NGSO FSS co-ordination procedure defined in ITU radio regulations [148] places the obligation for implementing mitigation techniques on the systems filed later. The relatively larger constellation requirement, in turn, brings the economic viability into question.

The use of various satellite selection strategies, satellite and ground terminal antenna sidelobe modifications, frequency channelisation and alternate polarisation are suggested as alternative mitigation techniques.

It is noted that a new recommendation (Rec.1431) is produced comprising key conclusions of the studies concerning with interference among NGSO FSS systems [149].

3.2.6 Cumulative Effect of Multiple NGSO FSS Systems

Rec.1323 states that “*aggregate interference from all NGSO FSS systems should not account for more than 10% of the short term time allowance stated in the GSO FSS link performance requirements*” [109]. The use of the 10% criterion, therefore, results in aggregate epfd levels accounting for cumulative interference from all in-band NGSO FSS systems. On the other hand, the approach used in Article S.22 [67] is to specify single entry interference limits (i.e. epfd attributed to a single NGSO FSS system) as defining an aggregate limit in the Radio Regulations could lead to a situation where the first comer taking all of the acceptable allowance for itself would prevent other systems to access the frequency band [150]. Therefore, it is agreed that a method is needed to derive single entry epfd statistics from aggregate epfd statistics [110].

Studies suggest that, in order to convert aggregate epfd statistics into single entry epfd statistics, boundaries where:

- interference from multiple NGSO FSS systems aggregates on a power basis,
- interference from multiple NGSO FSS systems aggregates on a time basis,

- interference from multiple NGSO FSS systems approaches the interference from a single NGSO FSS system causing the worst case single entry

have to be identified [151-153].

It is also suggested that the most important issue to be considered when relating single entry epfd to aggregate epfd is the number of NGSO FSS systems each causing similar single entry epfd levels into GSO FSS systems [154]. It is generally agreed that the aggregate interference from N actual NGSO FSS systems ($N_{physical}$) will likely be different from the interference caused by one system multiplied by a factor of N since the impact of each NGSO FSS system will not be identical. Therefore, a concept of “equivalent NGSO FSS systems ($N_{effective}$)” is introduced [115].

On the basis of sharing studies concerning with interference between NGSO FSS and GSO FSS systems as well as among NGSO FSS systems, it is recommended that a value of $N_{effective}$ should be assumed to be 3.5 in order to convert epfd statistics from aggregate to single entry or from single entry to aggregate [155]. Based on the use of number of equivalent NGSO FSS systems and the identification of power and time aggregation boundaries, a conversion method [156] is proposed to determine the final values of single entry epfd from an aggregate epfd.

3.2.7 Interference into Large GSO FSS Earth Stations

It is recognised that GSO FSS links with Earth stations using very large ground terminal antennas are more sensitive to NGSO FSS downlink interference (due to relatively higher antenna gain) and the $epfd_{down}$ limits may not provide adequate protection in such situations [157]. Simulation analysis studies [158-161] conclude that coordination procedures may need to be developed to ensure satisfactory interference protection. In line with the findings of these studies, a threshold size of a diameter of 18 metre [162] is agreed to be a value at which the coordination procedure [163] is triggered.

On the basis of the link characteristics stored within the ITU-R GSO FSS database, it is argued that there will be few cases requiring coordination as the number of GSO FSS links having Earth station antennas greater than *18 metre* is limited [162].

In addition to the antenna diameter, it is decided to include the condition of the $epfd_{down}$ radiated by the NGSO FSS satellites to trigger coordination for the protection of GSO FSS links using very large antennas [164, 165]. Development of $epfd_{down}$ coordination trigger is based on limiting interference peaks from NGSO FSS satellites which are dependent on the NGSO FSS system orbital characteristics. It is argued that these events are likely to occur over a small proportion of the Earth's surface. However, if multiple NGSO FSS systems having different orbital parameters share the same band, the locations of interference peaks from each system are likely to be different. Therefore, the proportion of the Earth surface subject to NGSO FSS interference peaks increases which, in turn, may lead to an increasing number of cases requiring coordination.

3.2.8 Synchronisation Loss

It is argued that very short term NGSO FSS downlink interference peaks may cause loss of GSO FSS Earth station modem synchronisation. It is further argued that while the duration of interference events might be very small, the loss of synchronisation and consequently time taken to resynchronise effectively magnifies (in time) the interference event which, in turn, increases the link unavailability [166].

Most of the recent work [167-171] on this issue investigated the level of interference that would cause loss of synchronisation, amount of time required to resynchronise and frequency of synchronisation loss events. These studies report on measurements of actual modems operating in the presence of simulated interference peaks. The results show that the point at which GSO FSS ground terminal receiver synchronisation is lost largely depends on the type of modulation and coding used on the GSO FSS link examined.

On the basis of material presented to the ITU-R, it is argued that the NGSO FSS interference peaks result in two distinct modes of GSO FSS receiver modem behaviour. Less severe interference events cause loss of synchronisation. In such cases, the recovery time is of order of a few seconds. For more severe interference events, carrier is lost and is recovered by a search mechanism. In these instances, there appears to be a significant difference in reacquisition time.

The following table illustrates the results obtained for various types of modulation and coding techniques and for links with data rates less than 34 Mbps to determine a generally valid level of GSO FSS link $C/(N+I)$ below which synchronisation loss might be expected to occur.

Modulation and Coding	$C/(N+I)$ (dB)
QPSK rate 7/8	6.0
QPSK rate 3/4	5.3
QPSK rate 1/2	3.5
8-PSK	8.1
16-QAM	11.0

Table 3.1: Synchronisation Loss Criterion for Various Modulation and Coding Techniques

It is important to note that when $C/(N+I)$ performance objective of a GSO FSS link is specified with values lower than those given above, the ITU-R agreed to assume that the synchronisation loss level is 1 dB less than the lowest GSO FSS link performance objective [172].

3.3 Representative GSO/NGSO FSS System Characteristics

This section presents representative system parameters used in applying NGSO/GSO FSS sharing analysis methods developed during the course of this research. These parameters are based on information gathering on the technical and service characteristics of both GSO FSS and NGSO FSS systems. Mainly, information is collected from public domain sources, including standards bodies such as the ITU-R and the US Federal Communications Commission (FCC). For NGSO FSS system

characteristics, the original NGSO FSS system filings together with amendments to the filings are obtained [53-58]. Specific technical and service information are then extracted from the filings. A number of relevant latest published technical documents are also used to obtain detailed and up to date information on technical and regulatory developments. For the GSO FSS system characteristics, the ITU-R GSO FSS link database is used as a primary information resource. Additionally, GSO FSS system operators web sites together with system filings are also considered to derive relevant modelling parameters [17-21, 36, 41, 42, 44].

3.3.1 GSO FSS System Characteristics

The following tables illustrate Ku & Ka band GSO FSS link parameters. As mentioned earlier, the parameter values are derived from ITU-R CR-116 GSO FSS links database. It has been assumed that Earth station antenna radiation patterns follow ITU-R Rec. IS.847 [173] while space station antenna radiation patterns follow ITU-R Rec. S.672 [174] with -20 dB sidelobe envelope.

It is worth noting that, from an interference point of view, GSO FSS systems are designed for provide compatibility with 2° orbit spacing from co-frequency and co-coverage adjacent GSO FSS satellites. This is achieved using high performance satellite and Earth station antennas and employing power control schemes to limit the effective isotropic radiated power (EIRP) levels.

	GSO Ku-1	GSO Ku-2
UPLINK		
Operating Frequency (GHz)	14	14
Carrier Bandwidth (MHz)	32.93	0.77
Earth Station Transmitter Antenna Maximum Gain (dBi)	37.02 (0.6m, 65%)	51 (3m, 65%)
Earth Station Transmitter Maximum Power (dBW / Carrier)	36.58	11.03
Earth Station Transmitter Antenna Radiation Pattern	Rec. IS 847	Rec. IS 847
Space Station Receiver Antenna Maximum Gain (dBi)	32.33 (0.35m, 65%)	23.73 (0.13, 65%)
Space Station Receiver Noise Temperature (K)	500	470
Space Station Receiver Antenna Radiation Pattern	Rec.672 (Ls = -20 dB)	Rec.672 (Ls = -20 dB)
Earth Station Transmitter Antenna Pointing Loss (dB)	0.5	0.5
Earth Station Transmitter Latitude (degrees)	51.5 (Rain Zone E)	51.5 (Rain Zone E)
Earth Station Transmitter Elevation Angle (degrees)	29.8	10.14
Earth Station Transmitter Intermodulation C / I (dB)	100	100
Earth Station Transmitter Polarisation Isolation C / I (dB)	100	35
Space Station Receiver Cross Polarisation Isolation C / I (dB)	26.72	30
Space Station Receiver Frequency Re-use Isolation C / I (dB)	24.5	100
Uplink Clear-sky C / I due to Other GSO FSS Networks (dB)	29.28	23.95
Uplink Clear-sky C / I due to FS Networks (dB)	100	100
DOWNLINK		
Transponder Type	Transparent	Transparent
Operating Frequency (GHz)	12	12
Carrier Bandwidth (MHz)	32.93	0.77
Space Station Transmitter Antenna Maximum Gain (dBi)	31 (0.35m, 65%)	22.39 (0.13, 65%)
Space Station Transmitter Maximum Power (dBW / Carrier)	17.69	4.46
Space Station Transmitter Antenna Radiation Pattern	Rec.672 (Ls = -20 dB)	Rec.672 (Ls = -20 dB)
Earth Station Receiver Antenna Maximum Gain (dBi)	35.68 (0.6m, 65%)	49.66 (3m, 65%)
Earth Station Receiver Noise Temperature (K)	153	150
Earth Station Receiver Antenna Radiation Pattern	Rec. IS 847	Rec. IS 847
Earth Station Receiver Antenna Pointing Loss (dB)	0.5	0.5
Earth Station Receiver Latitude (degrees)	38.72 (Rain Zone K)	43 (Rain Zone A)
Earth Station Receiver Elevation Angle (degrees)	39.60	36.94
Space Station Transmitter Cross Polarisation Isolation C / I (dB)	21.5	30
Space Station Transmitter Frequency Re-use Isolation C / I (dB)	100	100
Space Station Adjacent Transponder Isolation C / I (dB)	100	100
Space Station Transmitter Intermodulation C / I (dB)	100	24.1
Earth Station Receiver Polarisation Isolation C / I (dB)	100	35
Downlink Clear-sky C / I due to Other GSO FSS Networks (dB)	14.72	23.95
Downlink Clear-sky C / I due to FS Networks (dB)	100	100

Table 3.2 GSO FSS Ku Band System Parameters

	GSO Ka-1	GSO Ka-2
UPLINK		
Operating Frequency (GHz)	30	30
Carrier Bandwidth (MHz)	0.375	1.69
Earth Station Transmitter Antenna Maximum Gain (dBi)	47.16 (0.9m, 65%)	53.18 (1.8m, 65%)
Earth Station Transmitter Maximum Power (dBW / Carrier)	-6.39	-13.73
Earth Station Transmitter Antenna Radiation Pattern	Rec. IS 847	Rec. IS 847
Space Station Receiver Antenna Maximum Gain (dBi)	48.07 (1.0m, 65%)	47.16 (0.9m, 65%)
Space Station Receiver Noise Temperature (K)	1100	700
Space Station Receiver Antenna Radiation Pattern	Rec.672 (Ls = -20 dB)	Rec.672 (Ls = -20 dB)
Earth Station Transmitter Antenna Pointing Loss (dB)	1.125	0
Earth Station Transmitter Latitude (degrees)	50.73 (Rain Zone E)	28 (Rain Zone A)
Earth Station Transmitter Elevation Angle (degrees)	31.63	55
Earth Station Transmitter Intermodulation C / I (dB)	100	100
Earth Station Transmitter Polarisation Isolation C / I (dB)	100	20
Space Station Receiver Cross Polarisation Isolation C / I (dB)	20.43	27
Space Station Receiver Frequency Re-use Isolation C / I (dB)	22.17	17.2
Uplink Clear-sky C / I due to Other GSO FSS Networks (dB)	24.52	15
Uplink Clear-sky C / I due to FS Networks (dB)	100	18
DOWNLINK		
Transponder Type	Transparent	Regenerative
Operating Frequency (GHz)	20	20
Carrier Bandwidth (MHz)	0.375	81.03
Space Station Transmitter Antenna Maximum Gain (dBi)	44.55 (1.0m, 65%)	43.64 (0.9m, 65%)
Space Station Transmitter Maximum Power (dBW / Carrier)	-9.23	1.51
Space Station Transmitter Antenna Radiation Pattern	Rec.672 (Ls = -20 dB)	Rec.672 (Ls = -20 dB)
Earth Station Receiver Antenna Maximum Gain (dBi)	43.64 (0.9m, 65%)	49.66 (1.8m, 65%)
Earth Station Receiver Noise Temperature (K)	205	250
Earth Station Receiver Antenna Radiation Pattern	Rec. IS 847	Rec. IS 847
Earth Station Receiver Antenna Pointing Loss (dB)	1.125	0
Earth Station Receiver Latitude (degrees)	50.9 (Rain Zone E)	28 (Rain Zone A)
Earth Station Receiver Elevation Angle (degrees)	31.43	57.31
Space Station Transmitter Cross Polarisation Isolation C / I (dB)	23.64	27
Space Station Transmitter Frequency Re-use Isolation C / I (dB)	30	23.5
Space Station Adjacent Transponder Isolation C / I (dB)	100	100
Space Station Transmitter Intermodulation C / I (dB)	17.96	100
Earth Station Receiver Polarisation Isolation C / I (dB)	100	20
Downlink Clear-sky C / I due to Other GSO FSS Networks (dB)	29.21	13.84
Downlink Clear-sky C / I due to FS Networks (dB)	100	16.84

Table 3.3 GSO FSS Ka Band System Parameters

3.3.2 NGSO FSS System Characteristics

As mentioned earlier, a significant number of NGSO satellite system applications have been filed to the regulatory bodies (ITU-R and FCC) for the provision broadband services using Ku & Ka band frequencies. Taking account of system filings and published studies, the following tables are generated to summarise the representative NGSO FSS system characteristics.

	NGSO Ku-1	NGSO Ku-2
CONSTELLATION		
<i>Number of Planes</i>	20 (Circular)	7 (Circular)
<i>Number of Satellites per Plane</i>	4	13
<i>Plane Inclination (degrees)</i>	53	82
<i>Orbit Height (kilometre)</i>	1469	700
<i>Satellite Phasing Between First Satellites of Adjacent Planes (degrees)</i>	67.5	13.85
<i>Maximum Number of Possible Beams per Satellite</i>	24	37
<i>Maximum Number of Co-frequency Co-polar Beams per Satellite</i>	6	13
LINK CONFIGURATION STRATEGIES		
	<div>1) User terminals track satellites, 2) Satellite receive/transmit beams are steerable, 3) Satellite transmit power and antenna gain varies with elevation to provide constant pfd on the surface of the Earth, 4) User terminals transmit/receive when there is an available satellite at an elevation >10 degrees (i.e. minimum operating elevation angle is 10 degrees), 5) User terminals transmit/receive when there is an available satellite not within ±10 degrees of GSO arc (i.e. GSO arc avoidance is 10 degrees).</div>	<div>1) User terminals track satellites, 2) Downlink beams employ transmitter power control, 3) User terminals transmit/receive when there is an available satellite at an elevation >10 degrees (i.e. minimum operating elevation angle is 10 degrees), 4) Satellite receive/transmit beams follow a fixed pattern where a 37-beam fixed pattern locks on to service area when minimum elevation requirement is satisfied, 5) User terminals transmit/receive when there is an available satellite not within ±10 degrees of GSO arc (i.e. GSO arc avoidance is 10 degrees).</div>

Table 3.4 (1) NGSO FSS Ku Band System Parameters

	NGSO Ku-1	NGSO Ku-2
UPLINK		
Operating Frequency (GHz)	14	14
Carrier Bandwidth (MHz)	2.93	4.16
User Terminal Transmitter Antenna Maximum Gain (dBi)	37 (0.6m, 65%) (professional user Tx)	32 (0.34m, 65%)
User Terminal Transmitter Maximum Power (dBW / Carrier)	1.12	8.7
User Terminal Transmitter Antenna Radiation Pattern	See Figure 3.8 (RR Appendix 29)	See Figure 3.8 (Rec. S.465)
User Terminal Transmitter Minimum Elevation Angle (degrees)	10	10
Space Station Receiver Antenna Maximum Gain (dBi)	13.2	16.4
Space Station Receiver Noise Temperature (K)	455	400
Space Station Receiver Antenna Radiation Pattern	See Figure 3.11	See Figure 3.11
DOWNLINK		
Transponder Type	Transparent	Regenerative
Operating Frequency (GHz)	12	12
Carrier Bandwidth (MHz)	22.6	4.92
Space Station Transmitter Antenna Maximum Gain (dBi)	15	16.4
Space Station Transmitter Maximum Power (dBW / Carrier)	1.4	-4.5 (90°), -2.7 (65°), 1.2 (45°), 5 (20°)
Space Station Transmitter Antenna Radiation Pattern	See Figure 3.10	See Figure 3.10
User Terminal Receiver Antenna Maximum Gain (dBi)	30.8 (0.34m, 65%) (residential user Rx)	30.8 (0.34m, 65%)
User Terminal Receiver Noise Temperature (K)	182	200
User Terminal Receiver Antenna Radiation Pattern	See Figure 3.9 (RR Appendix 29)	See Figure 3.9 (Rec. S.465)
User Terminal Receiver Minimum Elevation Angle (degrees)	10	10

Table 3.4 (2) NGSO FSS Ku Band System Parameters

	NGSO Ka-1		NGSO Ka-2	
CONSTELLATION				
Number of Planes	12 (Elliptical)		4 (Circular)	
Number of Satellites per Plane	24		4	
Plane Inclination (degrees)	Plane No	Inclination (degrees)	45	
	1	84.724		
	2	84.719		
	3	84.714		
	4	84.709		
	5	84.705		
	6	84.700		
	7	84.695		
	8	84.690		
	9	84.686		
	10	84.681		
	11	84.676		
	12	84.671		
Orbit Height (km)	Plane No	Apogee (km)	Perigee (km)	10400
	1	1372.5	1357.5	
	2	1374.5	1359.5	
	3	1376.5	1361.5	
	4	1378.5	1363.5	
	5	1380.5	1365.5	
	6	1382.5	1367.5	
	7	1384.5	1369.5	
	8	1386.5	1371.5	
	9	1388.5	1373.5	
	10	1390.5	1375.5	
	11	1392.5	1377.5	
	12	1394.5	1379.5	

Table 3.5 (1) NGSO FSS Ka Band System Parameters

		NGSO Ka-1		NGSO Ka-2
Satellite Phasing Between First Satellites of Adjacent Planes (degrees)	Plane No	Argument of Perigee (degrees)	Right Ascension of Ascending Node (degrees)	22.5
	1	90	0.00	
	2	90	15.36	
	3	90	30.72	
	4	90	46.08	
	5	90	61.44	
	6	90	76.80	
	7	90	92.16	
	8	90	107.52	
	9	90	122.88	
	10	90	138.24	
	11	90	153.60	
	12	90	168.96	
Maximum Number of Possible Beams per Satellite	364 (Uplink) 16 (Downlink)		61	
Maximum Number of Co-frequency Co-polar Beams per Satellite	52 (Uplink) 16 (Downlink)		10	
LINK CONFIGURATION STRATEGIES				
	1) User terminals track satellites, 2) Uplink receive beams follow a fixed pattern, 3) Each beam covers an area of 160*160 km ² comprising 7 cells, 4) User terminals transmit/receive when there is an available satellite at an elevation >40 degrees (i.e. minimum operating elevation angle is 40 degrees), 5) Satellite transmit power and antenna gain varies with elevation to provide constant pfd on the surface of the Earth.		1) User terminals track satellites, 2) User terminals transmit/receive when there is an available satellite at an elevation >20 degrees (i.e. minimum operating elevation angle is 20 degrees), 3) Satellite receive/transmit beams follow a fixed pattern where a 61-beam fixed pattern locks on to service area when minimum elevation requirement is satisfied, 4) When satellites are within ±15 degrees latitude of the equator neither satellites nor associated user terminals transmits (i.e. Latitude avoidance is 15 degrees).	

Table 3.5 (2) NGSO FSS Ka Band System Parameters

	NGSO Ka-1	NGSO Ka-2
UPLINK		
Operating Frequency (GHz)	30	30
Carrier Bandwidth (MHz)	3.1	1.43
User Terminal Transmitter Antenna Maximum Gain (dBi)	35.2 (0.23m, 65%)	41.9 (0.49m, 65%)
User Terminal Transmitter Maximum Power (dBW / Carrier)	-0.6	-3.94
User Terminal Transmitter Antenna Radiation Pattern	See Figure 3.12 (Rec. S.465)	See Figure 3.12
User Terminal Transmitter Minimum Elevation Angle (degrees)	40	20
Space Station Receiver Antenna Maximum Gain (dBi)	36.1	37.1
Space Station Receiver Noise Temperature (K)	546	724
Space Station Receiver Antenna Radiation Pattern	See Figure 3.15	See Figure 3.15
DOWNLINK		
Transponder Type	Transparent	Transparent
Operating Frequency (GHz)	20	20
Carrier Bandwidth (MHz)	270	63.6
Space Station Transmitter Antenna Maximum Gain (dBi)	35.7	37.1
Space Station Transmitter Maximum Power (dBW / Carrier)	16.5	6.3
Space Station Transmitter Antenna Radiation Pattern	See Figure 3.14	See Figure 3.14
User Terminal Receiver Antenna Maximum Gain (dBi)	31.8 (0.23m, 65%)	38.3 (0.49m, 65%)
User Terminal Receiver Noise Temperature (K)	250	172
User Terminal Receiver Antenna Radiation Pattern	See Figure 3.13 (Rec. S.465)	See Figure 3.13
User Terminal Receiver Minimum Elevation Angle (degrees)	40	20

Table 3.5 (3) NGSO FSS Ka Band System Parameters

Both Ku and Ka band NGSO FSS system user terminal and satellite antenna radiation patterns are illustrated in the following figures.

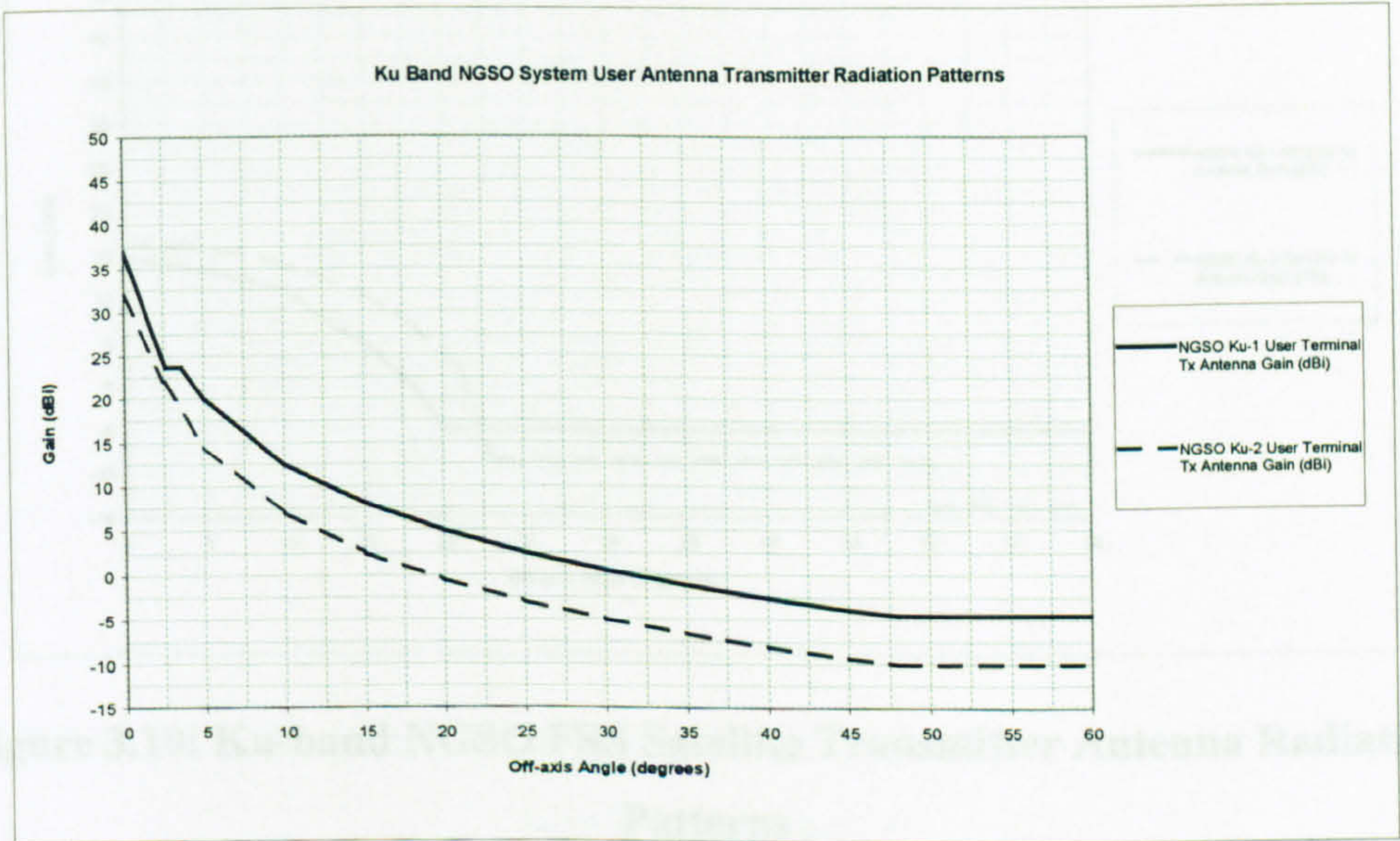


Figure 3.8: Ku-band NGSO FSS User Terminal Transmitter Antenna Radiation Patterns

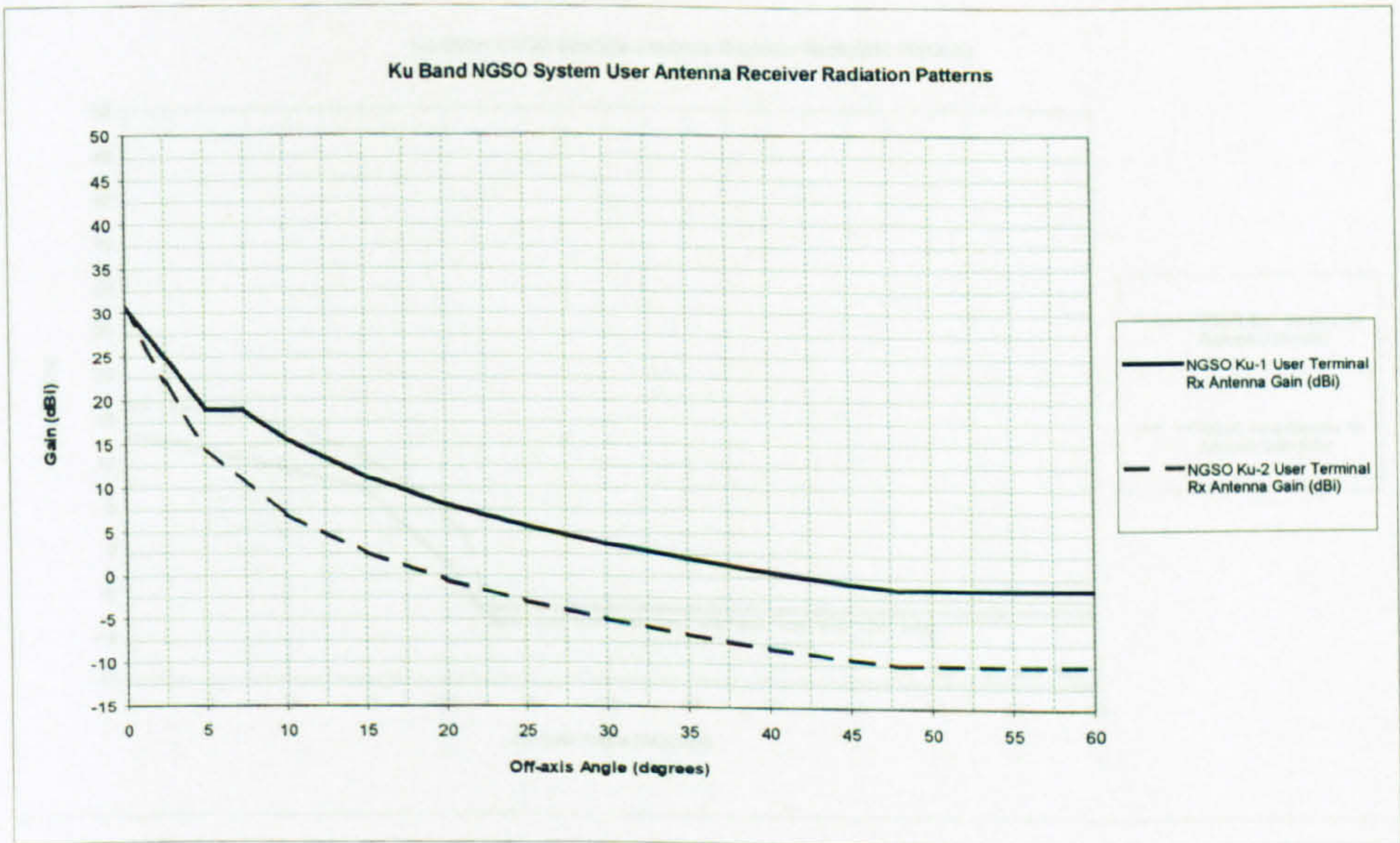


Figure 3.9: Ku-band NGSO FSS User Terminal Receiver Antenna Radiation Patterns

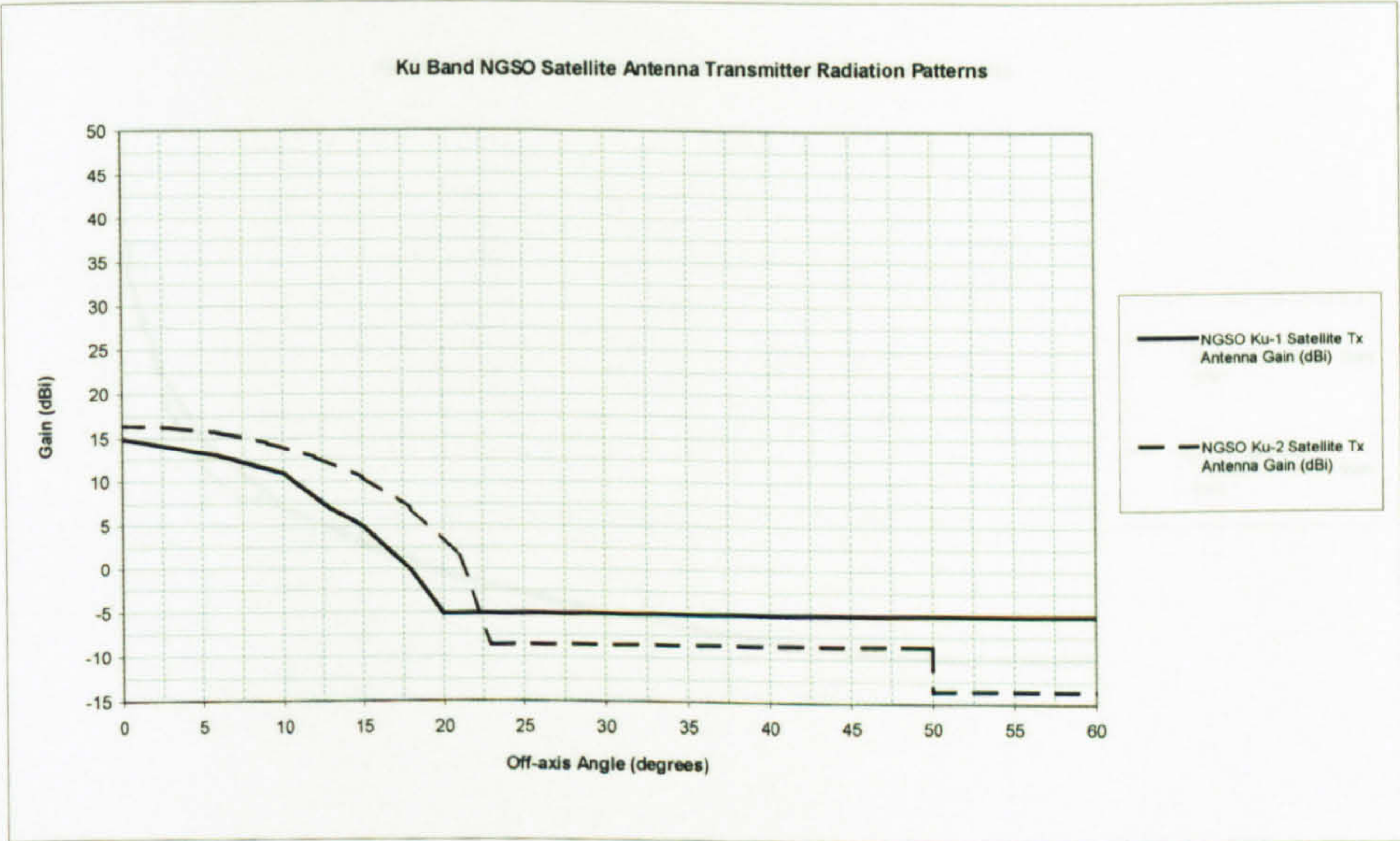


Figure 3.10: Ku-band NGSO FSS Satellite Transmitter Antenna Radiation Patterns

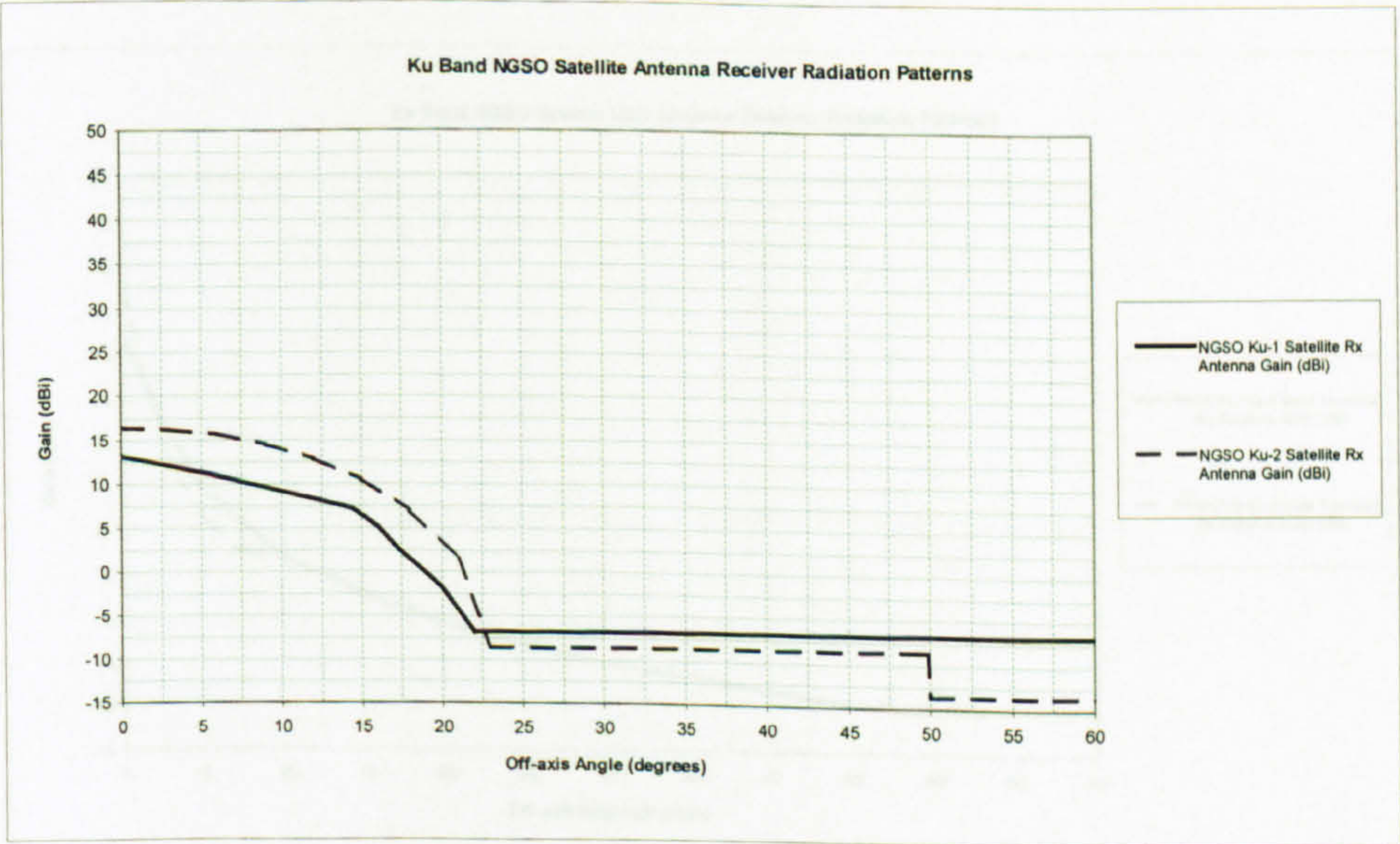


Figure 3.11: Ku-band NGSO FSS Satellite Receiver Antenna Radiation Patterns

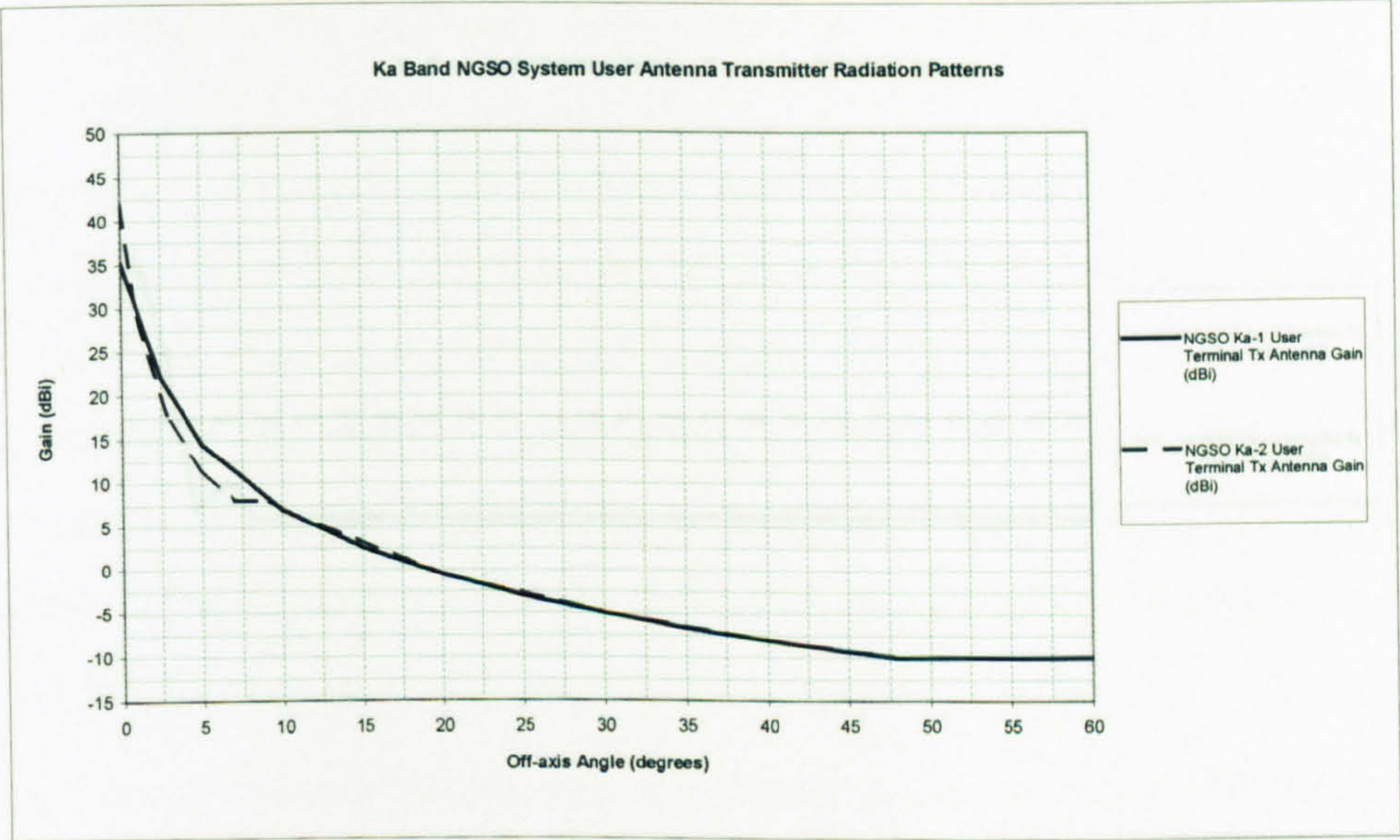


Figure 3.12: Ka-band NGSO FSS User Terminal Transmitter Antenna Radiation Patterns

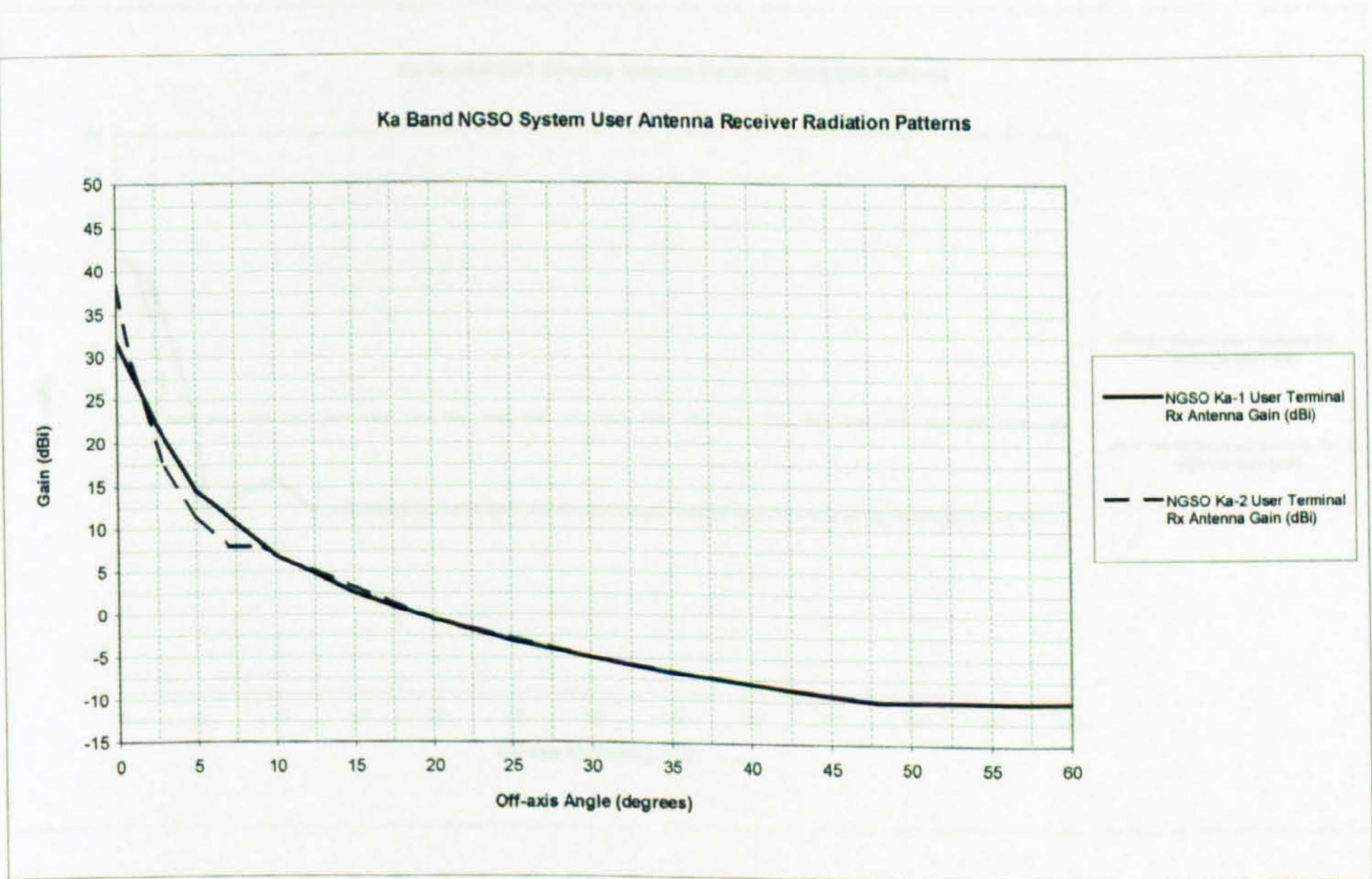


Figure 3.13: Ka-band NGSO FSS User Terminal Receiver Antenna Radiation Patterns

3.4 Conclusions

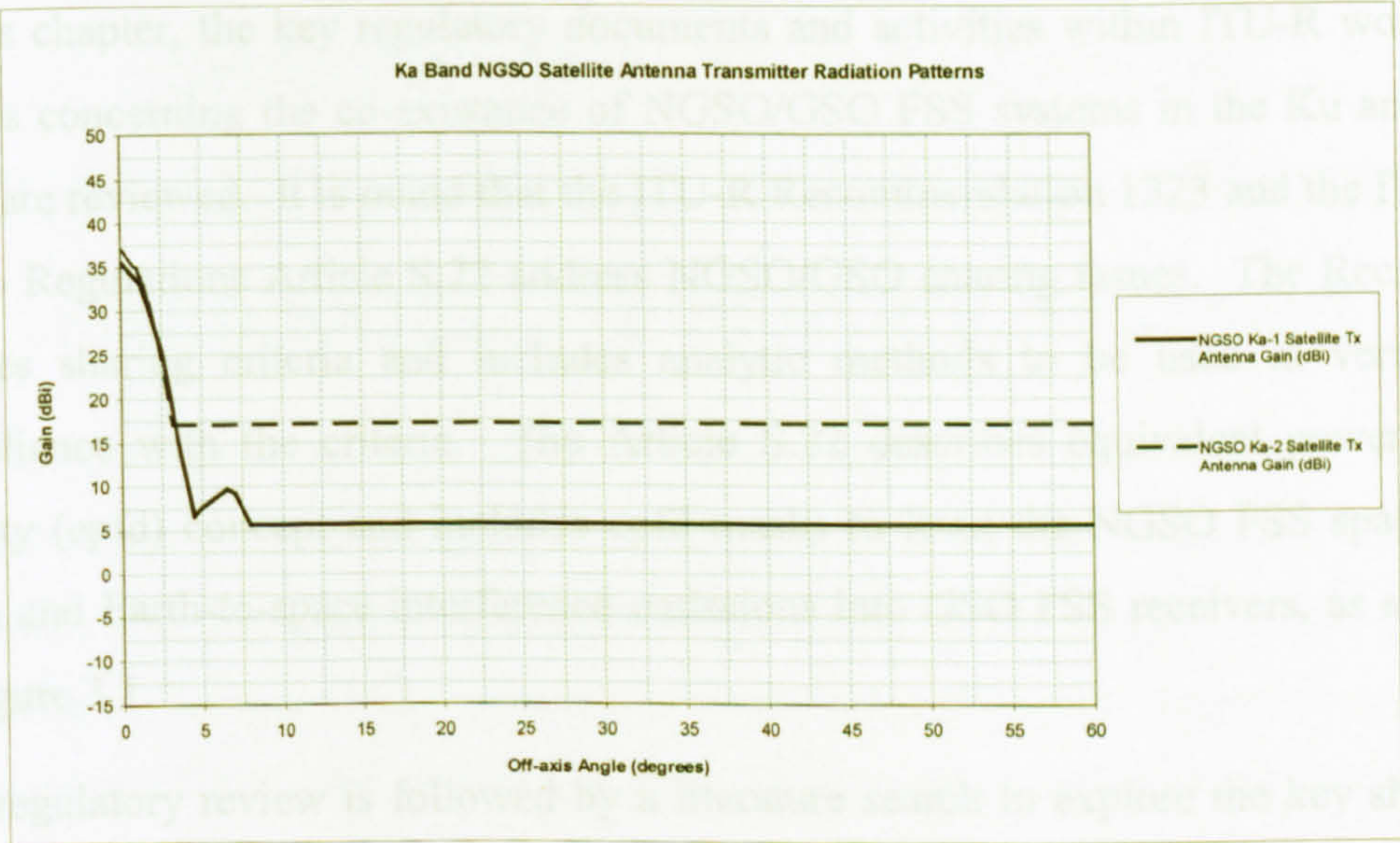


Figure 3.14: Ka-band NGSO FSS Satellite Transmitter Antenna Radiation Patterns

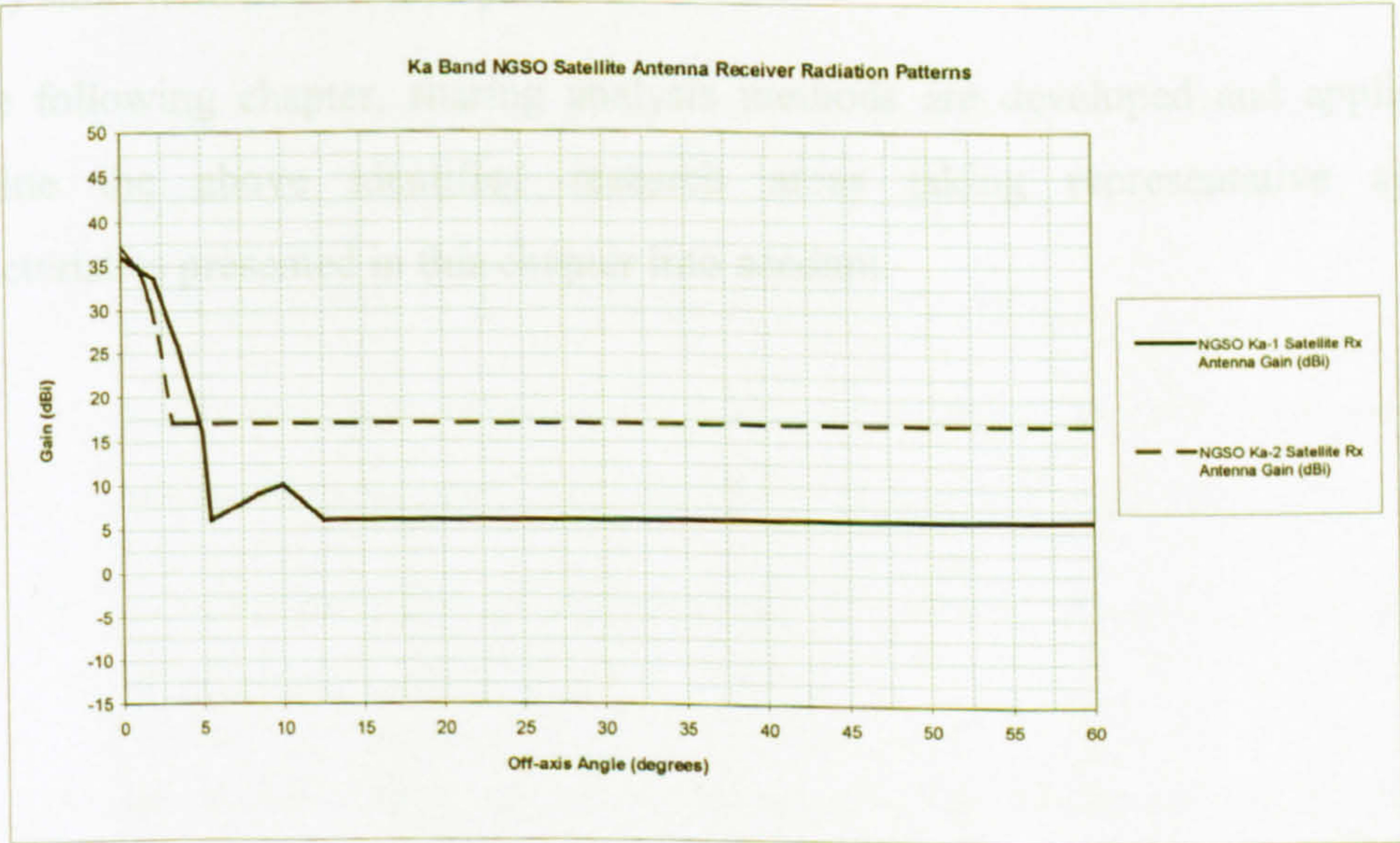


Figure 3.15: Ka-band NGSO FSS Satellite Receiver Antenna Radiation Patterns

3.4 Conclusions

In this chapter, the key regulatory documents and activities within ITU-R working groups concerning the co-existence of NGSO/GSO FSS systems in the Ku and Ka band are reviewed. It is noted that the ITU-R Recommendation 1323 and the ITU-R Radio Regulations Article S.22 address NGSO/GSO sharing issues. The Rec.1323 defines sharing criteria and includes analytic methods to be used in verifying compliance with the criteria. The Article S.22 describes equivalent power flux density (epfd) concept and includes epfd masks to limit the NGSO FSS space-to-Earth and Earth-to-space interference emissions into GSO FSS receivers, as shown in Figure 3.1.

The regulatory review is followed by a literature search to explore the key sharing issues. The contributions to the ITU-R study groups Joint Task Group 4-9-11 & Working Party 4A proved to be valuable information sources. It is recognised that a number of issues need to be investigated include implications of the use of epfd limits, examination of interference mitigation techniques, impact of cumulative NGSO FSS interference, refinement of antenna reference patterns and implications of very short term interference peaks.

In the following chapter, sharing analysis methods are developed and applied to examine the above identified research areas taking representative system characteristics presented in this chapter into account.

CHAPTER 4

SHARING ANALYSIS BETWEEN GEOSTATIONARY AND NONGEOSTATIONARY FIXED SATELLITE SERVICE SYSTEMS

This chapter presents the author's work concerning with spectrum sharing methodologies used to examine the feasibility of GSO and NGSO FSS system co-existence at Ku and Ka band frequencies. Sharing methods are developed and applied to the representative systems (described in the preceding chapter) to evaluate the impact of both the downlink (from NGSO FSS satellite transmitters into GSO FSS Earth stations) and the uplink (from NGSO FSS Earth Station transmitters into GSO FSS satellites) interference paths.

Initially, the implications of NGSO FSS mitigation techniques are examined by employing analytic and simulation analysis methods. Further modelling work related to the revision of Article S.22 *epfd* limits [67] is then carried out. The work involves:

- an application of an analytic conversion algorithm defined for deriving aggregate $epfd_{down} / epfd_{up}$ statistics from aggregate interference statistics,
- an examination of the use of continuous *epfd* limits,
- an investigation of the validity of the conversion algorithm proposed for converting aggregate *epfd* statistics to single entry *epfd* statistics,
- an implementation of Methodology A' [109] for assessing the aggregate NGSO FSS interference,
- an identification of shortcomings of the Methodology A' and an investigation of possible modifications to overcome implementation difficulties.

Next, investigations are directed towards examining the implications of the revised GSO FSS Earth station reference antenna pattern [140]. For these purposes, a simulator employing a probabilistic interference analysis approach is developed. This is followed by a description of an analytical method applied for examining the impact of NGSO FSS interference peaks. The method is based on determining whether any proposed $epfd_{down}$ limit could degrade a GSO FSS link $C/(N+I)$ ratio to a point where a receiver synchronisation loss is likely to occur. In the final section, conclusions are presented with a view to evaluate if an acceptable sharing environment can be achieved among NGSO FSS and GSO FSS systems at Ku and Ka band frequencies.

It is worth noting that, in order to apply interference analysis methods to NGSO/GSO FSS sharing scenarios, a number of analysis tools have been developed during the course of this research. These include mathematical models for an examination of the interference mitigation techniques, calculation of the worst case interference levels, implementation of the $epfd$ methodologies, evaluation of the conversion algorithms, investigation of the power flux density interpolation algorithms for different antenna diameters and examination of the interference peaks.

In addition, interference scenarios requiring detailed deterministic (i.e. time-based) simulations are primarily carried out by employing the Aegis Systems Spectrum Engineering Toolkit (ASSET). As mentioned previously, ASSET is capable of simulating a wide range of interference scenarios involving both space and terrestrial systems. It includes satellite diversity and satellite selection strategy features and allows antenna pattern modifications. Furthermore, a Monte Carlo approach is taken in order to implement probabilistic simulations where a random selection of system input parameter values from presumed statistical distributions are employed.

4.1 Implications of NGSO FSS Mitigation Techniques

In order to facilitate spectrum sharing with other services, NGSO FSS systems propose to employ a number of interference mitigation techniques. The implications

of these techniques are examined by sharing analysis methods developed during the course of this research.

It is important to note that in the sharing scenarios where simulation analysis approach is employed, the resultant interference statistics are in the form of cumulative distribution functions illustrating percentage times for which given interference levels are exceeded. The following points should be considered when interpreting the results:

- For a distribution corresponding to a very simple scenario where there is a single interference entry, one end of the distribution will represent a high level of interference occurring for a short period of time (caused by some form of main beam-to-main beam alignment) while the other end will show a continuous (long term) level of interference.
- For a distribution corresponding to a complex scenario where there are multiple interference entries, the long term interference level will increase because of power aggregation from multiple interfering paths (represented by a horizontal movement in the resultant distribution) whereas the short term interference level will remain the same because simultaneous power aggregation through a boresight alignment is unlikely to happen. However, the short term interference is likely to happen more often as there are more interference entries. This will result in aggregation in time (represented by a vertical movement in the resultant distribution).
- When there are a large number of interference entries at a particular level (for example through a sidelobe plateau in an antenna pattern) a near vertical jump will occur in the resultant statistics.
- In some instances, an expected highest interference level may not be achieved during a simulation run. This is due to limited simulated time period which is often the result of an increasing computation time required to simulate complex sharing scenarios.

- In general, the distribution functions presented in this study use 1 dB wide bins centred on 0.5 dB values. Therefore, the highest interference level, for example -100.5 dBW , actually represents anything between -101 and -100 dBW .

4.1.1 GSO Arc Avoidance

The GSO Arc avoidance is a mitigation technique involving a non-operating exclusion zone which is defined to be α° on either side of the GSO arc as seen by a GSO FSS Earth station [53, 57, 58]. The deterministic simulation analysis is employed to examine the implications of the use of this technique. This method is based on determining the position of each satellite in a given NGSO FSS constellation at regular time intervals (typically one second) over a simulation period (typically long enough to cover the large portion of the NGSO FSS constellation orbit shell). From this data, interference calculations are implemented and the results are then analysed statistically to be presented in the form of cumulative distribution functions.

The interference scenarios considered in this section comprise the NGSO Ku-1 and GSO Ku-1 systems whose characteristics are presented in Chapter 3. The primary objective of the interference analysis is to derive the uplink and downlink interference statistics by modelling the NGSO Ku-1 constellation with and without the GSO arc avoidance technique.

4.1.1.1 Simulation Model Description

In this section, the key system parameters are outlined and the interference scenario modelling approach developed to examine the uplink and downlink sharing scenarios is explained.

The NGSO Ku-1 constellation (see Table 3.4 in Chapter 3) consists of 80 LEO satellites orbiting at 1469 km in 8 circular planes inclined at 53° . The constellation is divided into two identical parts. The sub-constellations have offset of -18° in right ascension and 22.5° in mean anomaly. Each satellite employs steerable spot beams

and antenna gain varies with elevation to compensate for the increased path loss and to provide constant EIRP on the surface of the Earth. The number of co-frequency beams per satellite is 6.

The NGSO Ku-1 system applies 10° GSO arc avoidance to mitigate interference into GSO FSS systems. When the path to an NGSO Ku-1 satellite from a user terminal lies within 10° of the GSO Arc, no circuit is established with the satellite and the traffic is being transferred to another satellite further from the GSO Ku-1 link.

The NGSO Ku-1 system also employs a minimum operating elevation angle of 10° for all Earth stations. In the interference analysis scenarios, each NGSO Ku-1 Earth station seeks to establish a link with a satellite chosen randomly from those satisfying the elevation and arc avoidance constraints. Having allocated links to as many Earth station as the constellation supports, the simulation model sustains these links until they become untenable due to low elevation angles ($<10^\circ$) or due to angular proximity to the GSO FSS link ($<10^\circ$).

It is important to note that the simulation models include fully loaded NGSO Ku-1 co-frequency beams operating simultaneously and the simulation runs are reasonably long to explore as many geometric alignments as possible. These aim to ensure that the resultant interference statistics contain likely worst case interference levels which might be significant in determining whether interference exceeds victim receiver antenna interference criteria.

In line with above discussions, the number of NGSO Ku-1 Earth station receivers representing a fully loaded network is calculated to be approximately 500 using the total number of satellites (80) and the number of co-frequency beams (6) in modelling uplink interference into the GSO Ku-1 satellite receiver. The Earth station receivers are assumed to follow random uniform worldwide distribution.

In downlink interference modelling, a cluster of service areas surrounding the victim GSO Ku-1 Earth station receiver antenna is modelled. It is noted that the NGSO Ku-1 constellation ensures that there are maximum 4 satellites visible from a point on the surface of the Earth at any time. As the maximum number of co-frequency

terminal are modelled to load all visible beams pointing towards these service areas. Each service area is calculated to be an area of radius 350 km taking account of the NGSO Ku-1 satellite 3 dB beamwidth and altitude. The victim receiver is assumed to be co-located with an NGSO Ku-1 Earth station receiver at the centre of the cluster of service areas at latitude of 50 degrees .

4.1.1.2 Uplink Simulation Analysis

The above explained uplink sharing scenario has been simulated using deterministic simulation analysis method. Interference power statistics corresponding to scenarios with and without GSO arc avoidance mitigation are illustrated in Figure 4.1. The results are based on a simulated time period of $100,000$ seconds (approx. 28 hours) using 1 second time steps. For comparison, the figure also includes the receiver noise floor which is calculated as follows:

Satellite Receiver Noise Floor = Boltzmann Constant + Receiver Noise Temperature + Receiver Bandwidth

Satellite Receiver Noise Floor = $(10 * \log(1.38 * 10^{-23})) + (10 * \log(500)) + (10 * \log(32.93 * 10^6))$

Satellite Receiver Noise Floor = $-126.4\text{ dBW}/32.93\text{ MHz}$

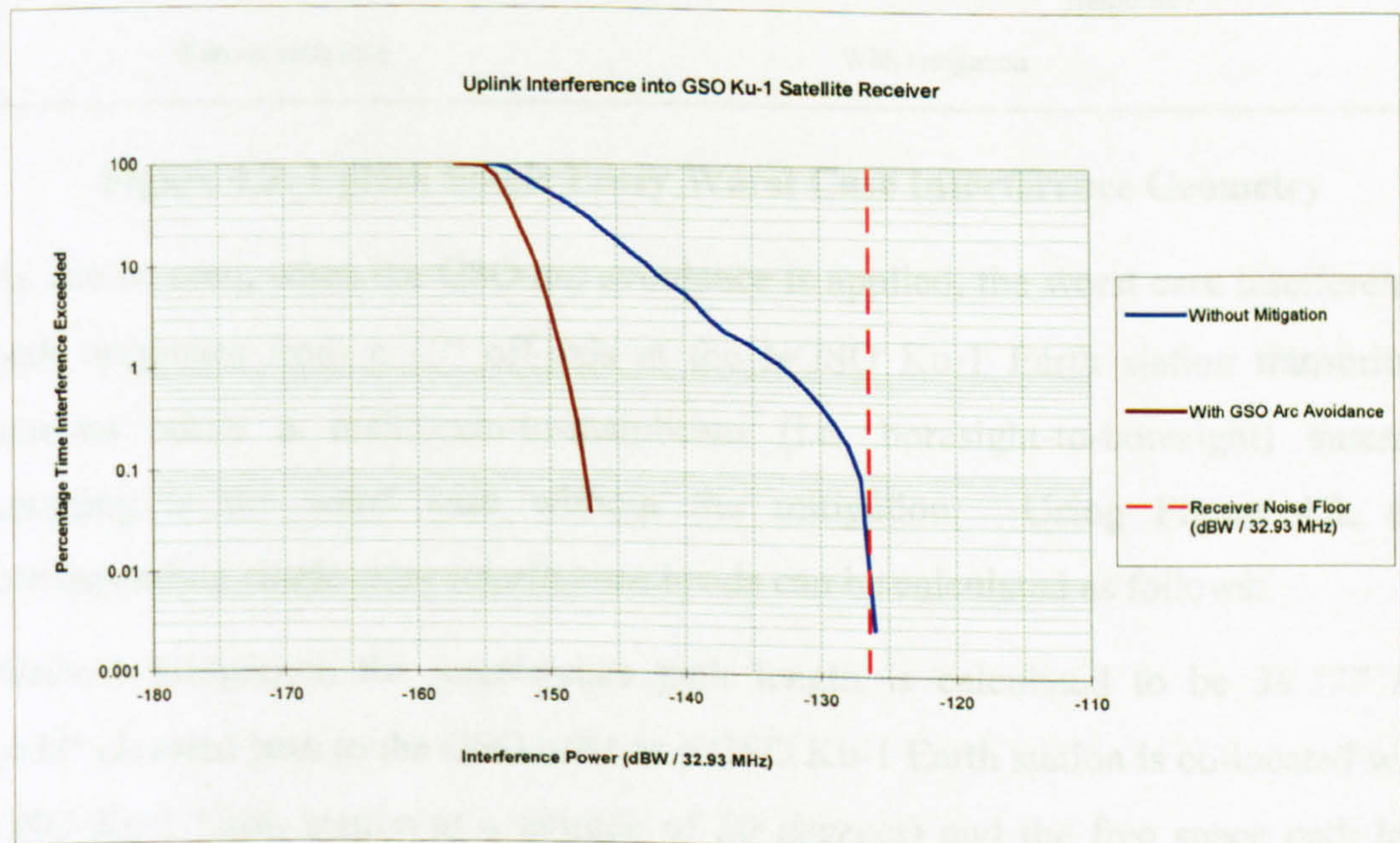


Figure 4.1: Comparison of Uplink Interference Statistics

The plots suggest that the use of the GSO arc avoidance technique for the NGSO FSS uplink paths reduces the level of interference into GSO FSS satellite receivers. This is examined in detail by employing analytical methods in the remaining of this section.

The following figure illustrates the geometry of the worst case single interference entry with and without GSO arc avoidance.

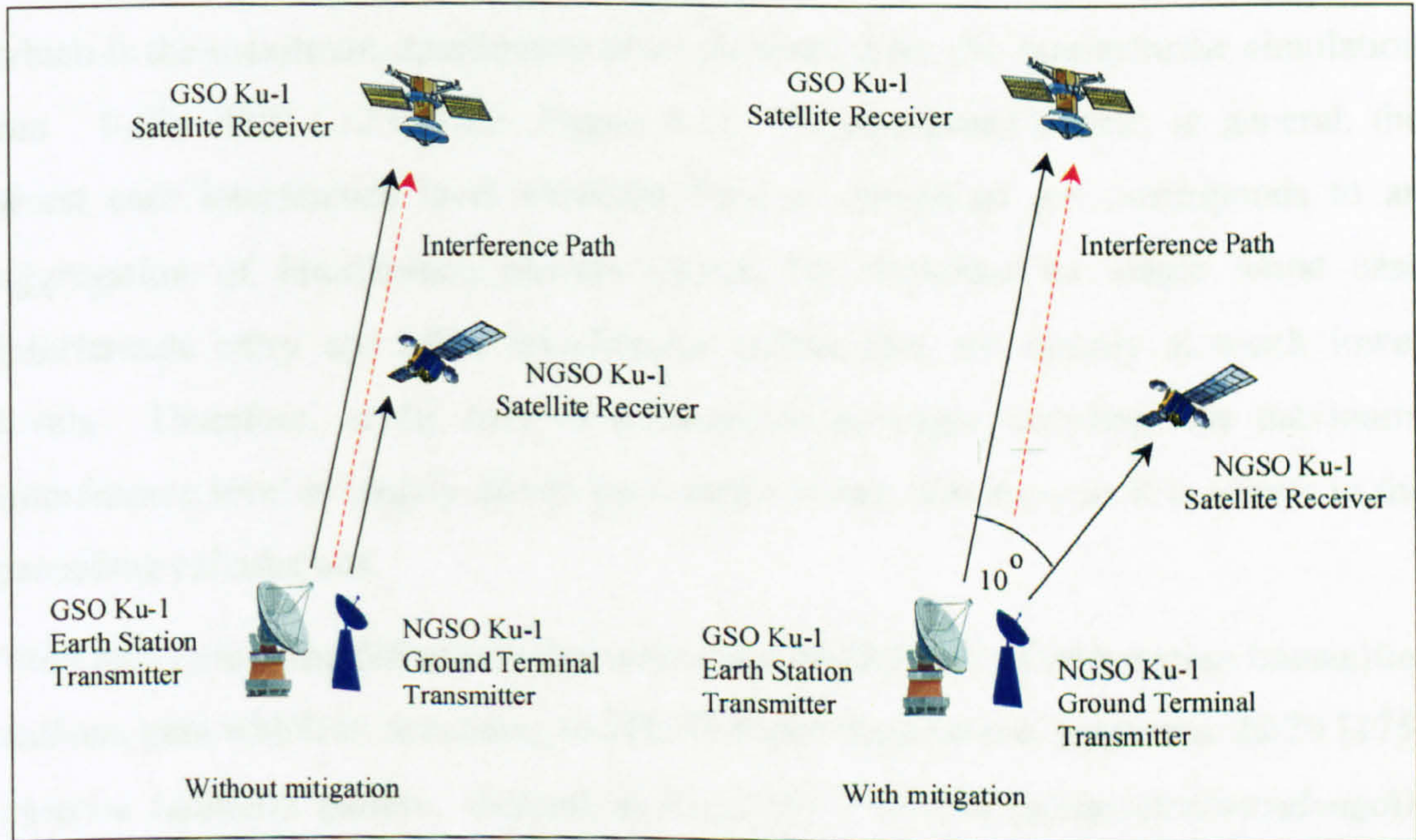


Figure 4.2: Uplink Single Entry Worst Case Interference Geometry

As can be seen, when the GSO arc avoidance is applied, the worst case interference path originates from a 10° off-axis at the NGSO Ku-1 Earth station transmitter antenna while a mainbeam-to-mainbeam (i.e. boresight-to-boresight) antenna coupling is the worst case without the mitigation. Using Figure 4.2, the corresponding single entry interference levels can be calculated as follows:

Without mitigation, the interference path length is calculated to be $38,377 \text{ km}$ ($\approx 33^\circ$ elevated path to the GSO orbit as NGSO Ku-1 Earth station is co-located with GSO Ku-1 Earth station at a latitude of 50 degrees) and the free space path loss (FSPL) is 207.1 dB . The slant path atmospheric loss at 14 GHz is approximately 0.13 dB for the 33° elevated Earth-to-space path. The GSO Ku-1 space station

receiver boresight gain is $G_{RX}(0^\circ) = 32.33 \text{ dBi}$. The NGSO Ku-1 Earth station transmitter antenna boresight gain is $G_{TX}(0^\circ) = 37 \text{ dBi}$. The resulting worst case interference can then be calculated as:

$$I_{\text{worst}} = P_{\text{TX}} + G_{\text{TX}}(0^\circ) - \text{Path Loss} + G_{\text{RX}}(0^\circ) - \text{Atm Loss}$$

$$I_{\text{worst}} = 11.63 \text{ dBW} / 32.93\text{MHz} + 37 \text{ dBi} - 207.1 \text{ dB} + 32.33 \text{ dBi} - 0.13 \text{ dB}$$

$$I_{\text{worst}} = -126.3 \text{ dBW} / 32.93 \text{ MHz}$$

which is the maximum interference level obtained from the deterministic simulation run $(-126 \text{ dBW} / 32.93\text{MHz})$, Figure 4.1). As mentioned earlier, in general, the worst case interference level obtained from a simulation run corresponds to an aggregation of interference powers caused by simultaneous single worst case interference entry and other interference entries that are usually at much lower levels. Therefore, in the case of boresight-to-boresight coupling, the maximum interference level is largely driven by a single worst case entry as it is shown in the preceding calculations.

With mitigation, the difference lies within the NGSO Ku-1 Earth station transmitter antenna gain which is, according to ITU-R Radio Regulations Appendix 28/29 [175] antenna radiation pattern, defined as $G_{TX}(10^\circ) = 52 - 10\log(\text{diameter}/\text{wavelength}) - 25\log(10^\circ) = 12.44 \text{ dBi}$ and the worst case interference is then calculated to be:

$$I_{\text{worst}} = P_{\text{TX}} + G_{\text{TX}}(10^\circ) - \text{Path Loss} + G_{\text{RX}}(0^\circ) - \text{Atm Loss}$$

$$I_{\text{worst}} = 11.63 \text{ dBW} / 32.93\text{MHz} + 12.44 \text{ dBi} - 207.1 \text{ dB} + 32.33 \text{ dBi} - 0.13 \text{ dB}$$

$$I_{\text{worst}} = -150.8 \text{ dBW} / 32.93 \text{ MHz}$$

which is approximately 3 dB lower than the value obtained from the simulation run $(-147 \text{ dBW}/32.93\text{MHz})$. This suggest that the worst case simulation result shown in Figure 4.1 corresponds to an aggregation of multiple simultaneous interference entries two of which may be at the calculated single entry worst case interference level.

A further analysis is applied to examine the implications of the use of GSO arc avoidance mitigation technique. The method is based on the determination of the

overall performance degradation within GSO Ku-1 clear-sky link budget due to NGSO Ku-1 uplink interference with and without GSO arc avoidance. Table 4.1 illustrates the application of the method step by step.

UPLINK			
GSO Ku-1 Earth Station EIRP (dBW/32.93MHz)		73.6	
Antenna Pointing Loss (dB)		0.5	
Free Space Path Loss Between GSO Ku-1 Earth Station Transmitter and GSO Ku-1 Satellite Receiver (dB)		207.1 (38,377 km at 14 GHz)	
Atmospheric Attenuation (dB) (Rec.676, Simplified Model)		0.2 (Path Elevation ≈ 33 degrees)	
GSO Ku-1 Satellite Receiver Antenna Gain (dBi)		32.33	
Received Carrier Power (dBW/32.93MHz)		(C _{up}) = 73.6 – 0.5 – 207.1 – 0.2 + 32.33 = -101.9	
GSO Ku-1 Satellite Receiver Noise Level (dBW/32.93 MHz)		(N _{up})= k T _{sat} B = -126.4	
(C/N) _{up} (dB)		-101.9 – (-126.4) = 24.5	
GSO Ku-1 Earth Station Transmitter Intermodulation (C/I) ₁ (dB)		100	
GSO Ku-1 Earth Station Transmitter Polarisation Isolation (C/I) ₂ (dB)		100	
GSO Ku-1 Satellite Receiver Cross Polarisation Isolation (C/I) ₃ (dB)		26.72	
GSO Ku-1 Satellite Receiver Frequency Re-use Isolation (C/I) ₄ (dB)		24.5	
GSO Ku-1 Uplink Clear-sky C/I due to Other GSO FSS Networks (C/I) ₅ (dB)		29.28	
GSO Ku-1 Uplink Clear-sky C/I due to FS Networks (C/I) ₆ (dB)		100	
		(without mitigation)	(with mitigation)
NGSO Ku-1 Interference Exceeded for 0.3% (dBW/32.93 MHz) (Assuming GSO Ku-1 Performance Requirement is given for 99.7%) (Simulation Results in Figure 4.1)		-129	-148
C/I due to NGSO Ku-1 Interference (dB) (C _{up} /I _{NGSO})		-101.9 – (-129) = 27.1	-101.9 – (-148) = 46.1
Calculation of (C/(N+I))UPLINK TOTAL:			

Table 4.1 (a) Implications of Uplink NGSO Ku-1 Aggregate Interference on End-to-end GSO Ku-1 Link Budget

DOWNLINK			
GSO Ku-1 Satellite EIRP (dBW/32.93MHz)		48.69	
GSO Ku-1 Earth Station Receiver Antenna Pointing Loss (dB)		0.5	
Free Space Path Loss Between GSO Ku-1 Satellite Transmitter and GSO Ku-1 Earth Station Receiver (dB)		205.7 (38,377 km at 12 GHz)	
Atmospheric Attenuation (dB) (Rec.676, Simplified Model)		0.1 (Path Elevation ≈ 33 degrees)	
GSO Ku-1 Earth Station Receiver Antenna Gain (dBi)		35.68	
Received Carrier Power (dBW/32.93MHz)		$(C_{down}) = 48.69 - 0.5 - 205.7 - 0.1 + 35.68 = -121.93$	
GSO Ku-1 Earth Station Receiver Noise Level (dBW/32.93 MHz)		$(N_{down})= k T_{ES}B = -131.6$	
$(C/N)_{down}$ (dB)		$-121.93 - (-131.6) = 9.65$	
GSO Ku-1 Space Station Transmitter Cross Polarisation Isolation $(C/I)_1$ (dB)		21.5	
GSO Ku-1 Space Station Transmitter Frequency Re-use Isolation $(C/I)_2$ (dB)		100	
GSO Ku-1 Space Station Adjacent Transponder Isolation $(C/I)_3$ (dB)		100	
GSO Ku-1 Space Station Transmitter Intermodulation $(C/I)_4$ (dB)		100	
GSO Ku-1 Earth Station Receiver Polarisation Isolation $(C/I)_5$ (dB)		100	
GSO Ku-1 Downlink Clear-sky C / I due to Other GSO FSS Networks $(C/I)_6$ (dB)		14.72	
GSO Ku-1 Downlink Clear-sky C / I due to FS Networks $(C/I)_7$ (dB)		100	
Calculation of (C/(N+I))DOWNLINK TOTAL:			
Degradation	dB	numeric	1 / (numeric degradation)
$(C/N)_{down}$	9.65	9.2257	0.1084
$(C/I)_1$	21.5	141.2538	0.0071
$(C/I)_2$	100	10^{10}	10^{-10}
$(C/I)_3$	100	10^{10}	10^{-10}
$(C/I)_4$	100	10^{10}	10^{-10}
$(C/I)_5$	100	10^{10}	10^{-10}
$(C/I)_6$	14.72	29.6483	0.0337
$(C/I)_7$	100	10^{10}	10^{-10}
$(1 / (C / (N+I)))$ DOWNLINK TOTAL (numeric)			0.1492
$(C / (N+I))$ DOWNLINK TOTAL (numeric)			6.7
$(C / (N+I))$ DOWNLINK TOTAL (dB)			8.26
Calculation of END-TO-END LINK (C / (N+I))			
$(1 / (C / (N+I)))$ TOTAL (numeric) = $(1 / (C / (N+I)))$ UPLINK TOTAL (numeric) + $(1 / (C / (N+I)))$ DOWNLINK TOTAL (numeric)			
	(without mitigation)		(with mitigation)
$(1 / (C / (N+I)))$ TOTAL (numeric)	0.0123 + 0.1492 = 0.1615		0.0104 + 0.1492 = 0.1596
$(C / (N+I))$ TOTAL (numeric)	6.19		6.26
$(C / (N+I))$ TOTAL (dB)	7.92		7.97

Table 4.1 (b) Implications of Uplink NGSO Ku-1 Aggregate Interference on End-to-end GSO Ku-1 Link Budget

The use of the GSO arc avoidance mitigation technique reduces the impact of NGSO Ku-1 uplink interference by increasing the GSO Ku-1 uplink $C/N+I$ from 19.1 dB to 19.8 dB . The calculations show that the downlink $C/N+I$ is 8.26 dB which, in turn, indicates that the overall link performance is largely determined by the downlink as the $C/(N+I)$ ratio of 8.26 dB is much lower than 19.1 dB (or 19.8 dB). Therefore, the improvement in the end-to-end GSO Ku-1 $C/(N+I)$ due to mitigation is an increase of 0.05 dB (from 7.92 dB to 7.97 dB).

4.1.1.3 Downlink Simulation Analysis

Similar to the uplink analysis, the downlink sharing scenario outlined in § 4.1.1.1 has been simulated using deterministic simulation analysis method. Interference statistics corresponding to models with and without GSO arc avoidance mitigation are illustrated in Figure 4.3. The simulation runs are based on a simulated time period of $700,000$ seconds (approx. 8 days) with 0.5 second step size. As before, the results are also compared against the receiver noise floor which is calculated as follows:

Ground Terminal Noise Floor = Boltzmann Constant + Receiver Noise Temperature + Receiver Bandwidth

Ground Terminal Noise Floor = $(10 \cdot \log(1.38 \cdot 10^{-23})) + (10 \cdot \log(153)) + (10 \cdot \log(32.93 \cdot 10^6))$

Ground Terminal Noise Floor = $-131.6 \text{ dBW}/32.93 \text{ MHz}$

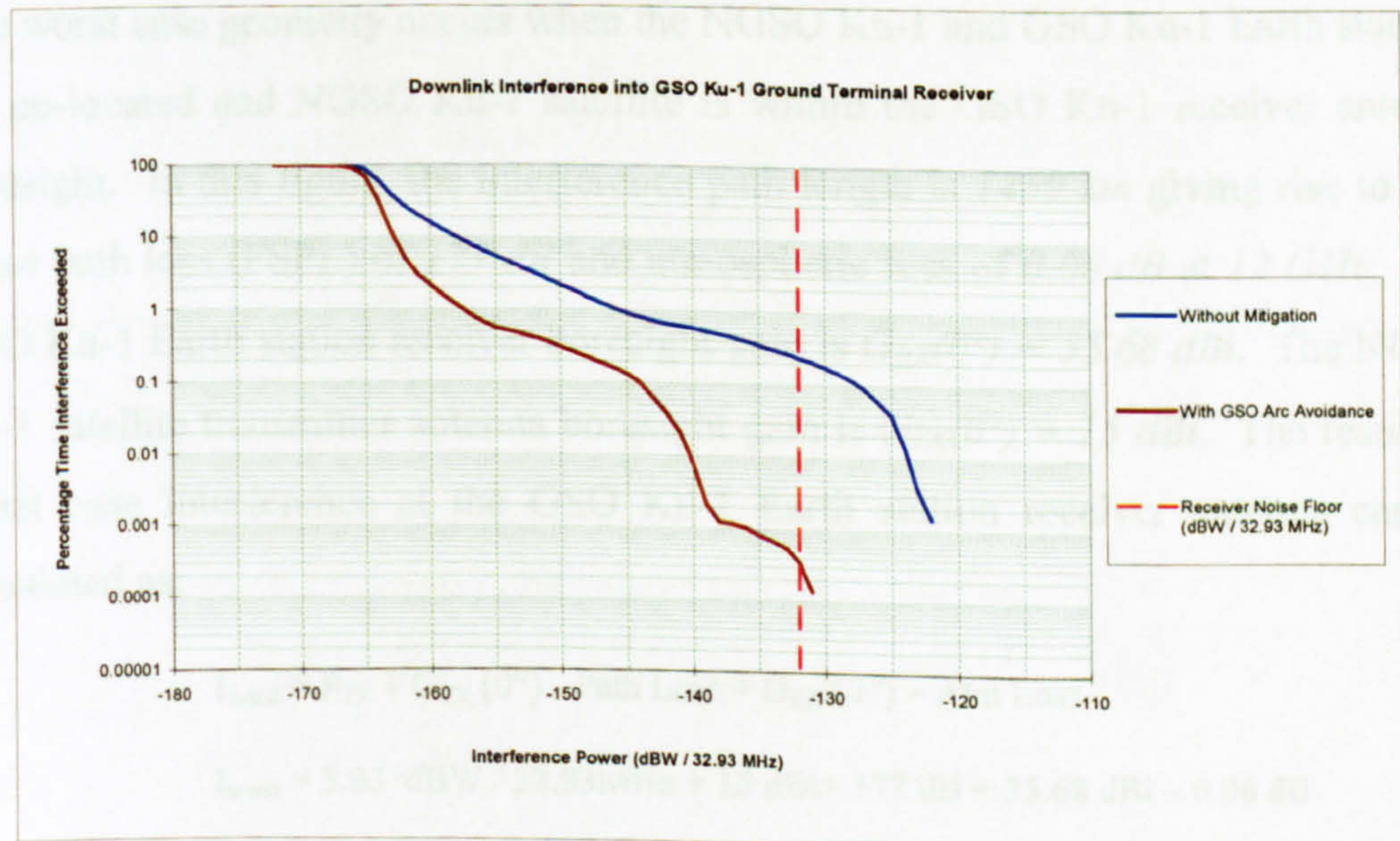


Figure 4.3: Comparison of Downlink Interference Statistics

The results indicate that the short term interference is reduced by some 10 dB by the use of GSO arc avoidance though the receiver noise level is still exceeded for both cases. Figure 4.4 illustrates the worst case single interference entry geometry without the use of mitigation.

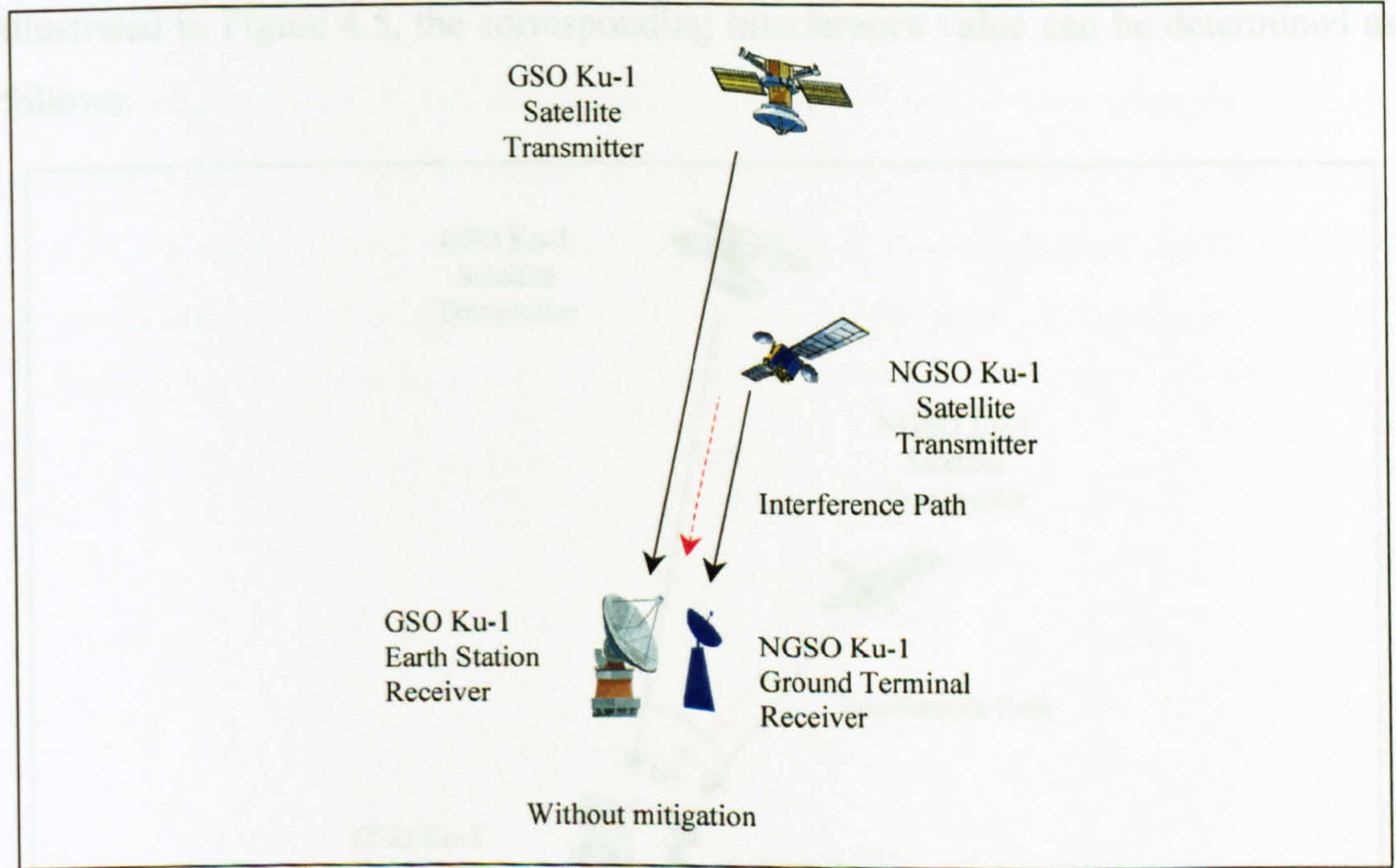


Figure 4.4: Worst Case Single Entry Downlink Interference Without Mitigation

The worst case geometry occurs when the NGSO Ku-1 and GSO Ku-1 Earth stations are co-located and NGSO Ku-1 satellite is within the GSO Ku-1 receiver antenna boresight. In this figure, the interference path length is 1469 km giving rise to free space path loss (FSPL) of 177 dB and atmospheric loss of 0.06 dB at 12 GHz . The GSO Ku-1 Earth station receiver boresight gain is $G_{RX}(0^\circ) = 35.68\text{ dBi}$. The NGSO Ku-1 satellite transmitter antenna boresight gain is $G_{TX}(0^\circ) = 15\text{ dBi}$. The resulting worst case interference at the GSO Ku-1 Earth station receiver antenna can be calculated as:

$$I_{\text{worst}} = P_{\text{TX}} + G_{\text{TX}}(0^\circ) - \text{Path Loss} + G_{\text{RX}}(0^\circ) - \text{Atm Loss}$$

$$I_{\text{worst}} = 3.03\text{ dBW} / 32.93\text{ MHz} + 15\text{ dBi} - 177\text{ dB} + 35.68\text{ dBi} - 0.06\text{ dB}$$

$$I_{\text{worst}} = -123.3\text{ dBW} / 32.93\text{ MHz}$$

which is in agreement with the maximum interference value obtained from the simulation run, shown in Figure 4.3.

When the GSO arc avoidance is applied, if the worst case single entry geometry is assumed to be the case where GSO and NGSO FSS Earth stations are co-located as illustrated in Figure 4.5, the corresponding interference value can be determined as follows:

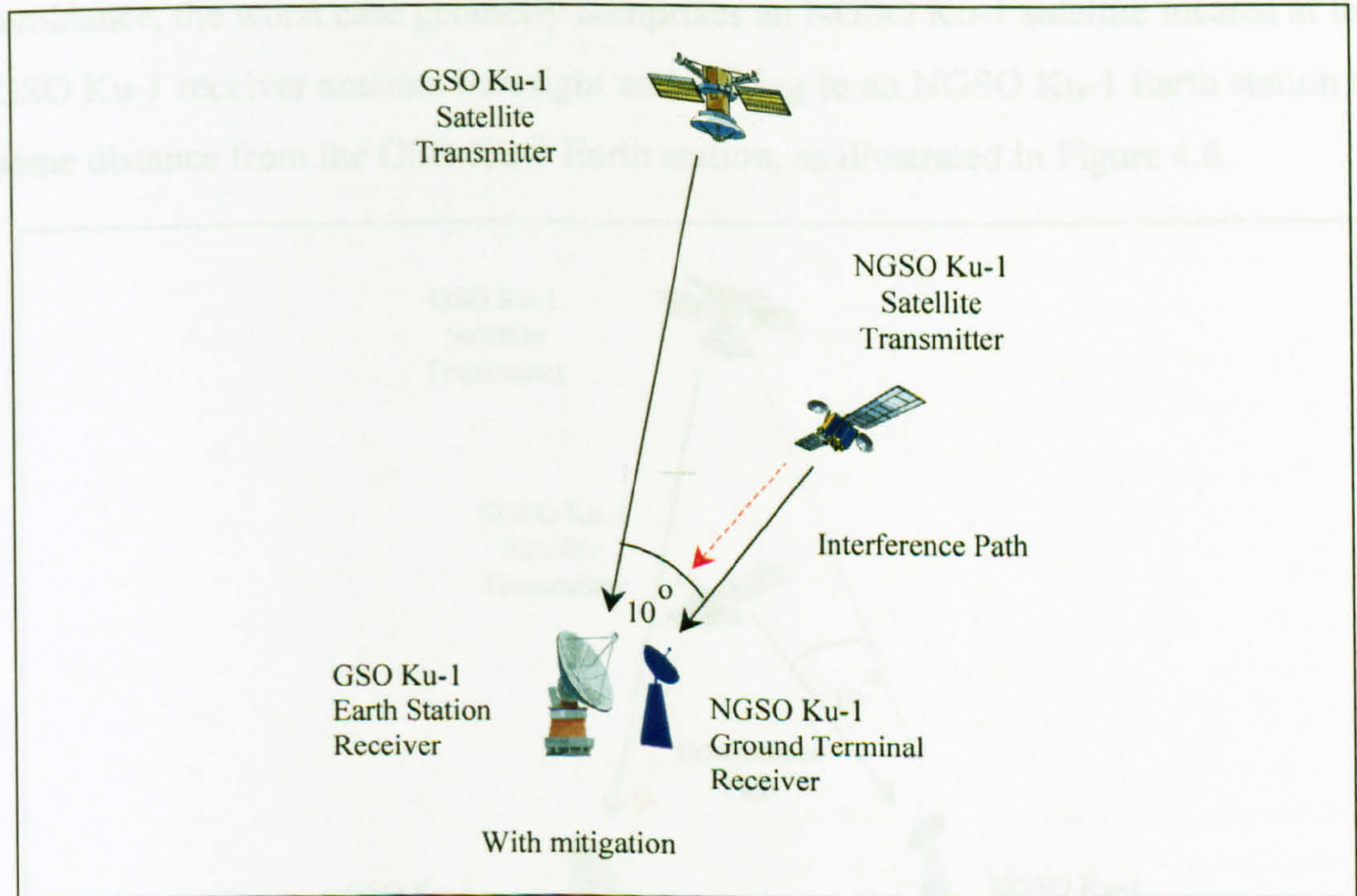


Figure 4.5: Assumed Worst Case Downlink Interference With GSO Arc Avoidance

In this case, the interference path is 1492 km ($FSPL = 177.5 \text{ dB}$ at 12 GHz) and the GSO Ku-1 Earth station receiver off-beam gain is $G_{RX}(10^\circ) = 4 \text{ dBi}$. Using these figures, the interference level is calculated to be

$$I = P_{TX} + G_{TX}(0^\circ) - \text{Path Loss} + G_{RX}(10^\circ) - \text{Atm Loss}$$

$$I = 3.03 \text{ dBW} / 32.93 \text{ MHz} + 15 \text{ dBi} - 177.5 \text{ dB} + 4 \text{ dBi} - 0.06$$

$$I = -155.5 \text{ dBW} / 32.93 \text{ MHz}$$

The worst case interference with GSO arc avoidance obtained from the simulation modelling (shown in Figure 4.3) is approximately $-131 \text{ dBW}/32.93 \text{ MHz}$ (by some 25 dB higher than the calculated worst case level of $-155.5 \text{ dBW}/32.93 \text{ MHz}$) suggesting that the GSO arc avoidance does not reduce the short term interference to the expected level.

The detailed analysis of the simulation results has revealed that, with the GSO arc avoidance, the worst case geometry comprises an NGSO Ku-1 satellite located at the GSO Ku-1 receiver antenna boresight and linking to an NGSO Ku-1 Earth station at some distance from the GSO Ku-1 Earth station, as illustrated in Figure 4.6.

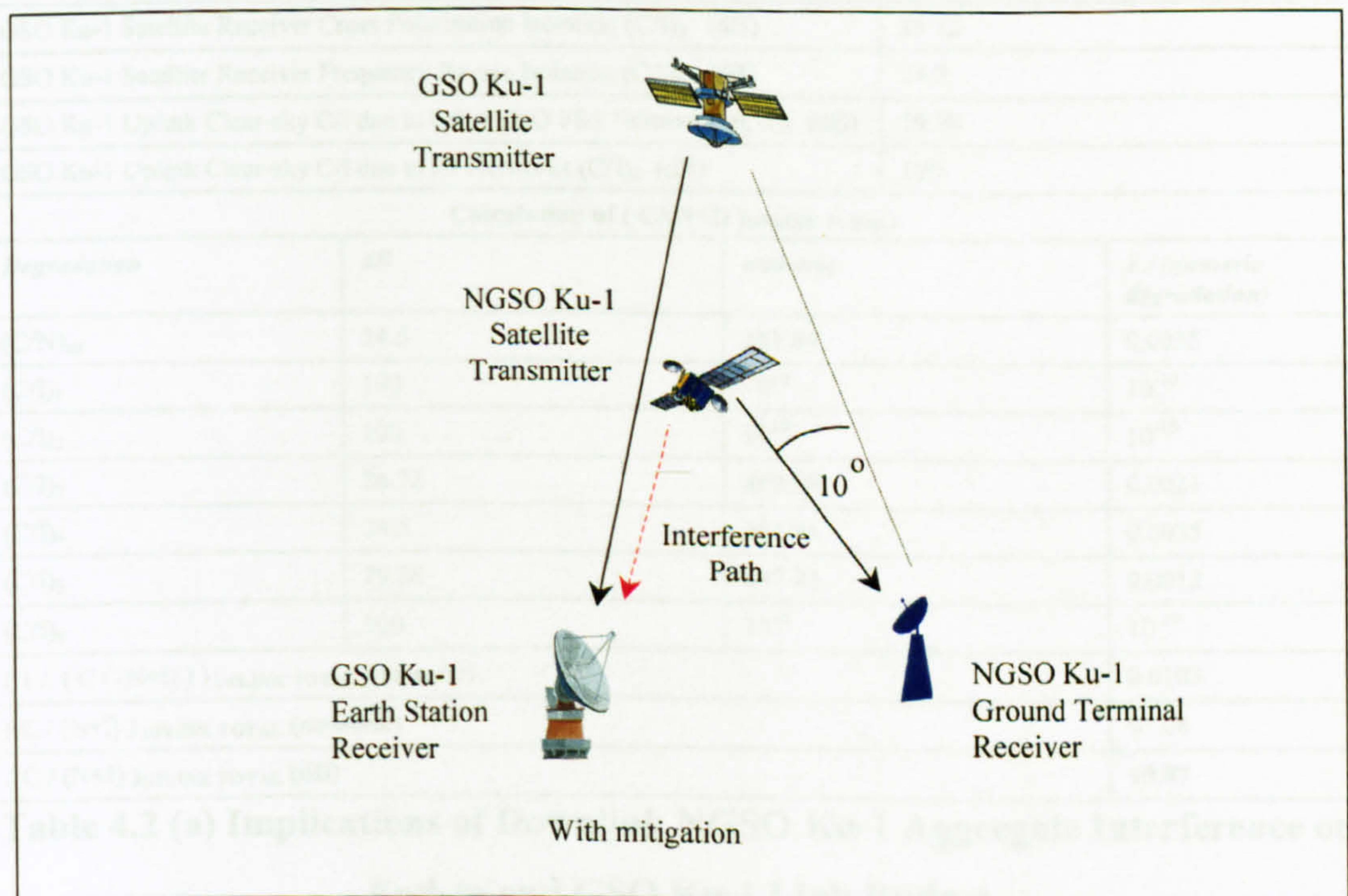


Figure 4.6: Calculated Worst Case Downlink Interference With GSO Arc Avoidance

The GSO Ku-1 end-to-end link performance degradation due to NGSO Ku-1 downlink interference can be calculated with and without mitigation. Table 4.2 shows the calculations.

UPLINK			
GSO Ku-1 Earth Station EIRP (dBW/32.93MHz)		73.6	
Antenna Pointing Loss (dB)		0.5	
Free Space Path Loss Between GSO Ku-1 Earth Station Transmitter and GSO Ku-1 Satellite Receiver (dB)		207.1 (38,377 km at 14 GHz)	
Atmospheric Attenuation (dB) (Rec.676, Simplified Model)		0.2 (Path Elevation ≈ 33 degrees)	
GSO Ku-1 Satellite Receiver Antenna Gain (dBi)		32.33	
Received Carrier Power (dBW/32.93MHz)		$(C_{up}) = 73.6 - 0.5 - 207.1 - 0.2 + 32.33 = -101.9$	
GSO Ku-1 Satellite Receiver Noise Level (dBW/32.93 MHz)		$(N_{up})= k T_{SAT}B = -126.4$	
$(C/N)_{up}$ (dB)		$-101.9 - (-126.4) = 24.5$	
GSO Ku-1 Earth Station Transmitter Intermodulation $(C/I)_1$ (dB)		100	
GSO Ku-1 Earth Station Transmitter Polarisation Isolation $(C/I)_2$ (dB)		100	
GSO Ku-1 Satellite Receiver Cross Polarisation Isolation $(C/I)_3$ (dB)		26.72	
GSO Ku-1 Satellite Receiver Frequency Re-use Isolation $(C/I)_4$ (dB)		24.5	
GSO Ku-1 Uplink Clear-sky C/I due to Other GSO FSS Networks $(C/I)_5$ (dB)		29.28	
GSO Ku-1 Uplink Clear-sky C/I due to FS Networks $(C/I)_6$ (dB)		100	
Calculation of $(C/(N+I))_{UPLINK TOTAL}$:			
Degradation	dB	numeric	$1 / (numeric degradation)$
$(C/N)_{up}$	24.5	281.84	0.0035
$(C/I)_1$	100	10^{10}	10^{-10}
$(C/I)_2$	100	10^{10}	10^{-10}
$(C/I)_3$	26.72	469.89	0.0021
$(C/I)_4$	24.5	281.84	0.0035
$(C/I)_5$	29.28	847.22	0.0012
$(C/I)_6$	100	10^{10}	10^{-10}
$(1 / (C / (N+I)))_{UPLINK TOTAL}$ (numeric)			0.0103
$(C / (N+I))_{UPLINK TOTAL}$ (numeric)			97.08
$(C / (N+I))_{UPLINK TOTAL}$ (dB)			19.87

Table 4.2 (a) Implications of Downlink NGSO Ku-1 Aggregate Interference on End-to-end GSO Ku-1 Link Budget

DOWNLINK		
GSO Ku-1 Satellite EIRP (dBW/32.93MHz)	48.69	
GSO Ku-1 Earth Station Receiver Antenna Pointing Loss (dB)	0.5	
Free Space Path Loss Between GSO Ku-1 Satellite Transmitter and GSO Ku-1 Earth Station Receiver (dB)	205.7 (38,377 km at 12 GHz)	
Atmospheric Attenuation (dB) (Rec.676, Simplified Model)	0.1 (Path Elevation ≈ 33 degrees)	
GSO Ku-1 Earth Station Receiver Antenna Gain (dBi)	35.68	
Received Carrier Power (dBW/32.93MHz)	$(C_{down}) = 48.69 - 0.5 - 205.7 - 0.1 + 35.68 = -121.93$	
GSO Ku-1 Earth Station Receiver Noise Level (dBW/32.93 MHz)	$(N_{down}) = k T_{ES} B = -131.6$	
$(C/N)_{down}$ (dB)	$-121.93 - (-131.6) = 9.65$	
GSO Ku-1 Space Station Transmitter Cross Polarisation Isolation $(C/I)_1$ (dB)	21.5	
GSO Ku-1 Space Station Transmitter Frequency Re-use Isolation $(C/I)_2$ (dB)	100	
GSO Ku-1 Space Station Adjacent Transponder Isolation $(C/I)_3$ (dB)	100	
GSO Ku-1 Space Station Transmitter Intermodulation $(C/I)_4$ (dB)	100	
GSO Ku-1 Earth Station Receiver Polarisation Isolation $(C/I)_5$ (dB)	100	
GSO Ku-1 Downlink Clear-sky C / I due to Other GSO FSS Networks $(C/I)_6$ (dB)	14.72	
GSO Ku-1 Downlink Clear-sky C / I due to FS Networks $(C/I)_7$ (dB)	100	
	(without mitigation)	(with mitigation)
NGSO Ku-1 Interference Exceeded for 0.3% (dBW/32.93 MHz) (Assuming GSO Ku-1 Performance Requirement is given for 99.7%) (Simulation Results in Figure 4.3)	-134	-150
C/I due to NGSO Ku-1 Interference (dB) (C_{down}/I_{NGSO})	$-121.93 - (-134) = 12.1$	$-121.93 - (-150) = 28.1$

Table 4.2 (b) Implications of Downlink NGSO Ku-1 Aggregate Interference on End-to-end GSO Ku-1 Link Budget

Calculation of (C/(N+I))DOWNLINK TOTAL:							
(without mitigation)				(with mitigation)			
Degradation	dB	numeric	1 / (numeric degradation)	Degradation	dB	numeric	1 / (numeric degradation)
(C/N) _{down}	9.65	9.2257	0.1084	(C/N) _{down}	9.65	9.2257	0.1084
(C/I) ₁	21.5	141.2538	0.0071	(C/I) ₁	21.5	141.2538	0.0071
(C/I) ₂	100	10 ¹⁰	10 ⁻¹⁰	(C/I) ₂	100	10 ¹⁰	10 ⁻¹⁰
(C/I) ₃	100	10 ¹⁰	10 ⁻¹⁰	(C/I) ₃	100	10 ¹⁰	10 ⁻¹⁰
(C/I) ₄	100	10 ¹⁰	10 ⁻¹⁰	(C/I) ₄	100	10 ¹⁰	10 ⁻¹⁰
(C/I) ₅	100	10 ¹⁰	10 ⁻¹⁰	(C/I) ₅	100	10 ¹⁰	10 ⁻¹⁰
(C/I) ₆	14.72	29.6483	0.0337	(C/I) ₆	14.72	29.6483	0.0337
(C/I) ₇	100	10 ¹⁰	10 ⁻¹⁰	(C/I) ₇	100	10 ¹⁰	10 ⁻¹⁰
(C _{down} /I _{NGSO})	12.1	16.2181	0.0617	(C _{down} /I _{NGSO})	28.1	645.6542	0.0015
(1 / (C / (N+I))) DOWNLINK TOTAL (numeric)			0.2109	(1 / (C / (N+I))) DOWNLINK TOTAL (numeric)			0.1507
(C / (N+I)) DOWNLINK TOTAL (numeric)			4.74	(C / (N+I)) DOWNLINK TOTAL (numeric)			6.64
(C / (N+I)) DOWNLINK TOTAL (dB)			6.76	(C / (N+I)) DOWNLINK TOTAL (dB)			8.22
Calculation of END-TO-END LINK (C / (N+I))							
(1 / (C / (N+I))) TOTAL (numeric) = (1 / (C / (N+I))) UPLINK TOTAL (numeric) + (1 / (C / (N+I))) DOWNLINK TOTAL (numeric)							
			(without mitigation)	(with mitigation)			
(1 / (C / (N+I))) TOTAL (numeric)			0.0103 + 0.2109= 0.2212		0.0103 + 0.1507= 0.1610		
(C / (N+I)) TOTAL (numeric)			4.52		6.21		
(C / (N+I)) TOTAL (dB)			6.55		7.93		

Table 4.2 (c) Implications of Downlink NGSO Ku-1 Aggregate Interference on End-to-end GSO Ku-1 Link Budget

As can be seen, with the use of the GSO arc avoidance mitigation technique, the C_{down}/I_{NGSO} is improved by $28.1-12.1=16\text{ dB}$ which is approximately 3 dB less than that of obtained in the uplink case (C_{up}/I_{NGSO} is calculated to be 27.1 dB without mitigation and 46.1 dB with mitigation as shown in Table 4.1). This suggests that, for the assumed parameters, the use of the GSO arc avoidance technique improves the carrier-to-interference ratio for both the uplink and downlink directions.

The calculated degradation figures also suggest that the end-to-end link performance improvement is $7.93 - 6.55 = 1.38\text{ dB}$ which is higher than that of obtained from the uplink case (0.05 dB). As explained earlier, this is due to the dominance of the $C/(N+I)_{DOWNLINK}$ in the $C/(N+I)_{TOTAL}$ calculations.

4.1.1.4 Discussion

The key system parameters need to be taken into account when designing simulation scenarios for the deterministic simulation analysis include constellation parameters (number of satellites, altitude, inclination and satellite phasing), beam frequency reuse pattern, operational characteristics (mitigation techniques, power control and minimum elevation angle), transmitter and receiver power and antenna characteristics and beam coverage area size.

To examine the implications of the GSO arc avoidance, the deterministic simulation method has been applied to the uplink and downlink sharing scenarios where, in each direction, the NGSO FSS constellation is modelled with and without the mitigation. The simulation results have been benchmarked against the worst case interference levels which are derived analytically. Further analysis method has been developed and applied to assess the impact of the use of the GSO arc avoidance. It is based on the calculation and comparison of the GSO FSS link overall performance degradation using the interference statistics derived from the simulation analysis with and without the GSO arc avoidance.

The analysis carried out using representative system characteristics has shown that the use of GSO arc avoidance does not prevent near on-beam hits into the GSO FSS Earth station receiver antennas. It allows interference alignments where the NGSO FSS satellite is in the GSO FSS receive Earth station boresight and transmitting towards an NGSO FSS user terminal, satisfying the geostationary arc avoidance requirement, placed at some distance from the GSO FSS Earth station receiver. It is noted that this conclusion is in line with the results of studies carried out within ITU-R [176-178].

For the assumed availability target (99.7%), the GSO FSS link performance degradation analysis (based on the simulation results) has suggested that the GSO arc avoidance improves C/I_{NGSO} ratio for both the uplink and downlink sharing scenarios.

4.1.2 Latitude Avoidance

Latitude avoidance requires that neither the NGSO FSS satellites nor the associated NGSO FSS Earth stations transmit when the NGSO FSS satellites are within the volume defined by $\pm\theta^\circ$ in latitude [55, 58]. The implications of this technique have been investigated using both the deterministic simulation modelling and analytic approach. These methods have been implemented to examine the interference paths from the NGSO Ka-2 system into the GSO Ka-2 system.

4.1.2.1 Simulation Model Description

The NGSO Ka-2 system (see Table 3.5 in Chapter 3) consists of 16 satellites orbiting at 10,400 km in 4 circular planes inclined at 45°. The system employs fixed beam pattern comprising 61 beams to provide service to user terminals. Each satellite is capable of operating with 10 co-frequency beams within its fixed beam pattern.

The system serves users having minimum elevation angles of 20°. When a service area satisfies the minimum elevation angle requirement the 61-beam pattern locks on to that area and the beams are steered as the satellite passes over. When the minimum elevation angle requirement is not satisfied the beam pattern is switched to cover another service area and the existing links are handed over to the next available satellite.

The interference mitigation technique requires that when a satellite passes through the volume defined by $\pm 15^\circ$ in latitude, all transmissions should be turned off. In such circumstances, the service area is served by a satellite satisfying the latitude avoidance requirement.

For the uplink interference scenario, taking account of the orbital height and the beamwidth figures, an area covered by 61 beams is calculated to be approximately 12 million km² (corresponding to an area of radius of 2000 km). As any satellite within the constellation supports 10 co-frequency beams, it is assumed that the user density should be based on 10 users over an area of 2000 km radius. This gives rise

to total number of 93 user terminals uniformly randomly distributed worldwide to represent fully loaded NGSO Ka-2 network. The GSO Ka-2 Earth station transmitter is assumed to be co-located with an NGSO Ka-2 transmitter at *50 degrees* latitude.

In the downlink simulation model, the number of user terminals is assumed to be 10 since there are 10 co-frequency beams operating within the fixed *61-beam* pattern. Each user terminal is modelled to have tracking antennas in order to represent the beam steering over the service area. These terminals are placed at pre-determined locations so that the beam pattern could be simulated. The victim GSO Ka-2 Earth station is assumed to be co-located with an NGSO Ka-2 Earth station receiver at the centre of the beam pattern at *40 degrees* latitude.

It is worth noting that in order to assess the implications of the GSO FSS Earth station location on the resultant interference statistics, the GSO Ka-2 Earth station is assumed to be co-located with an NGSO Ka-2 Earth station at 50° and 40° latitudes in the uplink and downlink scenarios, respectively.

4.1.2.2 Uplink Simulation Analysis

On the basis of the above explained scenario, the uplink simulation analysis has been implemented. The statistics plotted in Figure 4.7 are based on a simulated time of *1,000,000 seconds* (approx. *12 days*) using *1 second* simulation time steps.

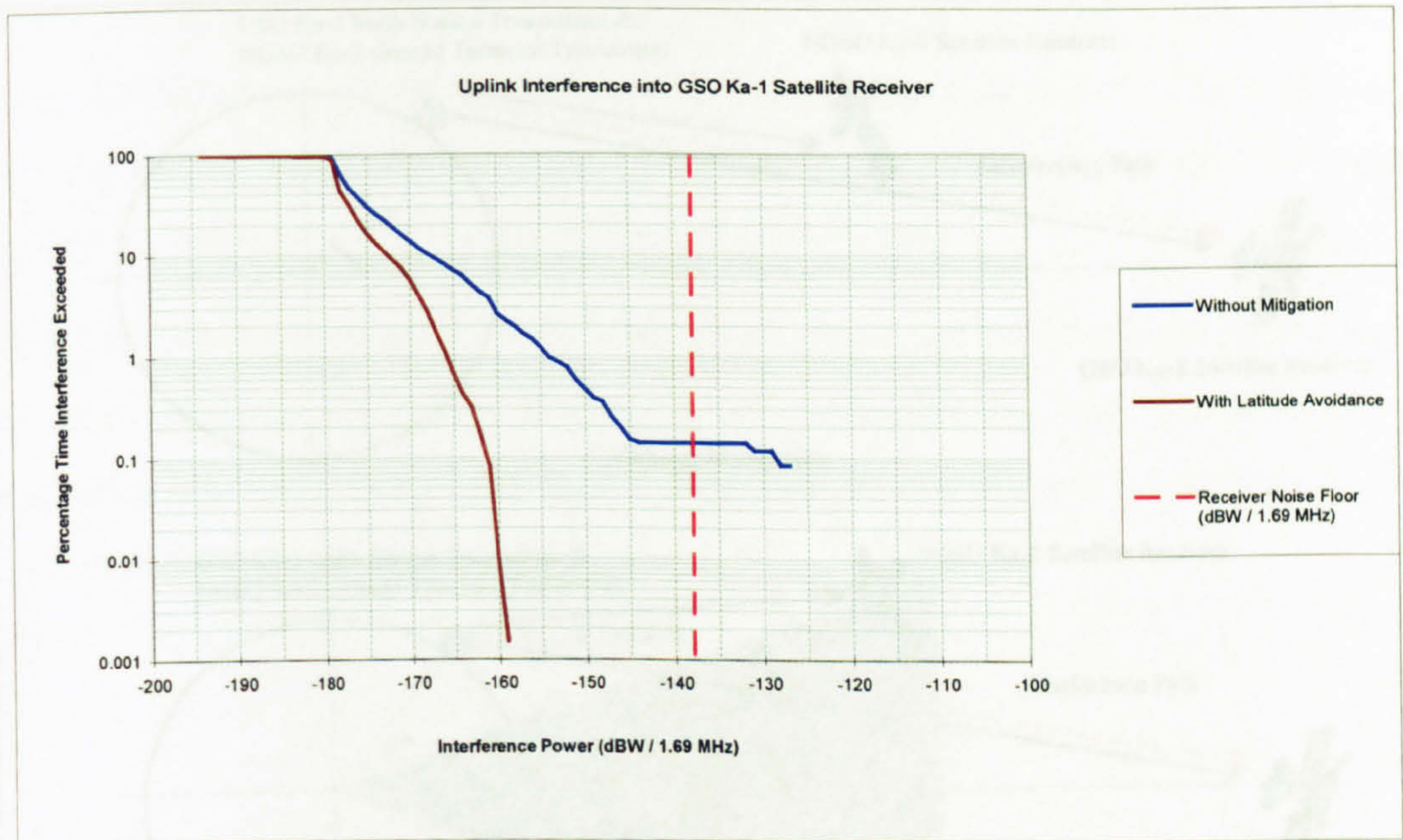


Figure 4.7: Comparison of Uplink Interference Statistics

As can be seen, the use of the latitude avoidance mitigation technique significantly reduces the aggregate uplink interference into the GSO FSS satellites. In order to validate the simulation results, the following analysis has been implemented.

Figure 4.8 compares the worst case single entry interference geometry with and without the mitigation.

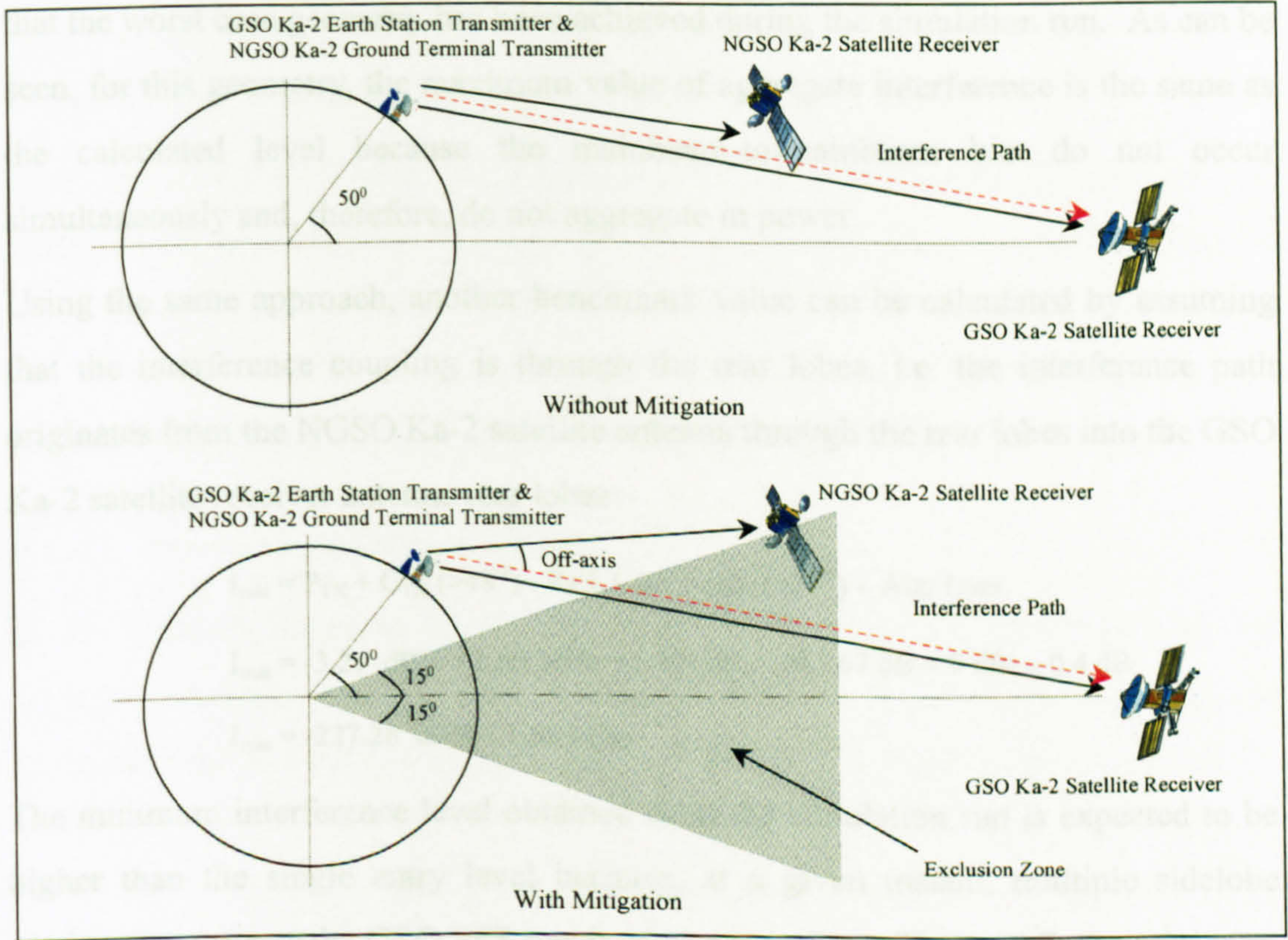


Figure 4.8: Uplink Single Entry Worst Case Interference Geometry

Without mitigation, the worst case geometry comprises mainbeam-to-mainbeam coupling between the co-located NGSO Ka-2 and GSO Ka-2 Earth station transmitters and the satellite receivers. It can be shown that the interference path length is $38,377 \text{ km}$ resulting in 213.67 dB path loss and 0.4 dB atmospheric gaseous attenuation at 30 GHz . The system characteristics (given in Tables 3.3 and 3.5 in Chapter 3) indicate that the NGSO Ka-2 Earth station maximum antenna gain is 41.9 dBi while the GSO Ka-2 satellite receiver antenna gain is 47.16 dBi . Using these figures, the worst case single entry interference level can be calculated as:

$$I_{\text{worst}} = P_{\text{TX}} + G_{\text{TX}} (0^\circ) - \text{Path Loss} + G_{\text{RX}} (0^\circ) - \text{Atm Loss}$$

$$I_{\text{worst}} = -3.21 \text{ dBW} / 1.69 \text{ MHz} + 41.9 \text{ dBi} - 213.67 \text{ dB} + 47.16 \text{ dBi} - 0.4 \text{ dB}$$

$$I_{\text{worst}} = -128.22 \text{ dBW} / 1.69 \text{ MHz}$$

The comparison of this benchmark figure against the maximum aggregate interference level obtained from the simulation run ($-128 \text{ dBW}/1.69 \text{ MHz}$) suggest

that the worst case geometry has been achieved during the simulation run. As can be seen, for this geometry, the maximum value of aggregate interference is the same as the calculated level because the mainbeam-to-mainbeam hits do not occur simultaneously and, therefore, do not aggregate in power.

Using the same approach, another benchmark value can be calculated by assuming that the interference coupling is through the rear lobes, i.e. the interference path originates from the NGSO Ka-2 satellite antenna through the rear lobes into the GSO Ka-2 satellite receiver antenna rear lobes:

$$I_{\min} = P_{\text{TX}} + G_{\text{TX}}(>48^\circ) - \text{Path Loss} + G_{\text{RX}}(>77^\circ) - \text{Atm Loss}$$

$$I_{\min} = -3.21 \text{ dBW} / 1.69 \text{ MHz} + (-10) \text{ dBi} - 213.67 \text{ dB} + 0 \text{ dBi} - 0.4 \text{ dB}$$

$$I_{\min} = -227.28 \text{ dBW} / 1.69 \text{ MHz}$$

The minimum interference level obtained from the simulation run is expected to be higher than the single entry level because, at a given instant, multiple sidelobe entries aggregate at the GSO FSS receiver antenna. From Figure 4.7, the minimum interference level obtained from the simulation run is approximately $-191 \text{ dBW}/1.69 \text{ MHz}$ which is by some 36 dB higher than the calculated single rear lobe-to-rear lobe interference entry.

With mitigation, the worst case geometry occurs when Earth stations and satellites are at the same longitude, and the NGSO FSS satellite is at the edge of the 15° latitude exclusion zone, as shown in Figure 4.8. For the assumed GSO Ka-2 Earth station latitude of 50° , the off-axis angle at the NGSO FSS Earth station transmitter antenna can be calculated to be 4.7° which gives rise to transmitter antenna gain of $G_{\text{TX}}(4.7^\circ) = 12.19 \text{ dBi}$. Using this figure, the expected worst case single entry interference level can be calculated as:

$$I_{\text{worst}} = P_{\text{TX}} + G_{\text{TX}}(5.2^\circ) - \text{Path Loss} + G_{\text{RX}}(0^\circ) - \text{Atm Loss}$$

$$I_{\text{worst}} = -3.21 \text{ dBW} / 1.69 \text{ MHz} + 12.19 \text{ dBi} - 213.67 \text{ dB} + 47.16 \text{ dBi} - 0.4 \text{ dB}$$

$$I_{\text{worst}} = -157.93 \text{ dBW} / 1.69 \text{ MHz}$$

which is the same as the maximum interference value of $-158 \text{ dBW}/1.69\text{MHz}$ obtained from the deterministic simulation model (Figure 4.7).

From the GSO Ka-2 link performance point of view, assuming that the link performance objective is defined for 99.7% of the time, the comparison of interference levels exceeded for 0.3% with ($\approx -163 \text{ dBW}/1.69\text{MHz}$) and without ($\approx -147 \text{ dBW}/1.69\text{MHz}$) mitigation suggests that the use of latitude avoidance would improve the uplink C/I_{NGSO} degradation by some 16 dB.

4.1.2.3 Downlink Simulation Analysis

In the downlink direction, interference statistics shown in Figure 4.9 are obtained from the simulation scenario described in § 4.1.2.1. As in the uplink scenarios, the simulated time is 1,000,000 seconds (approx. 12 days) with step size of 1 second.

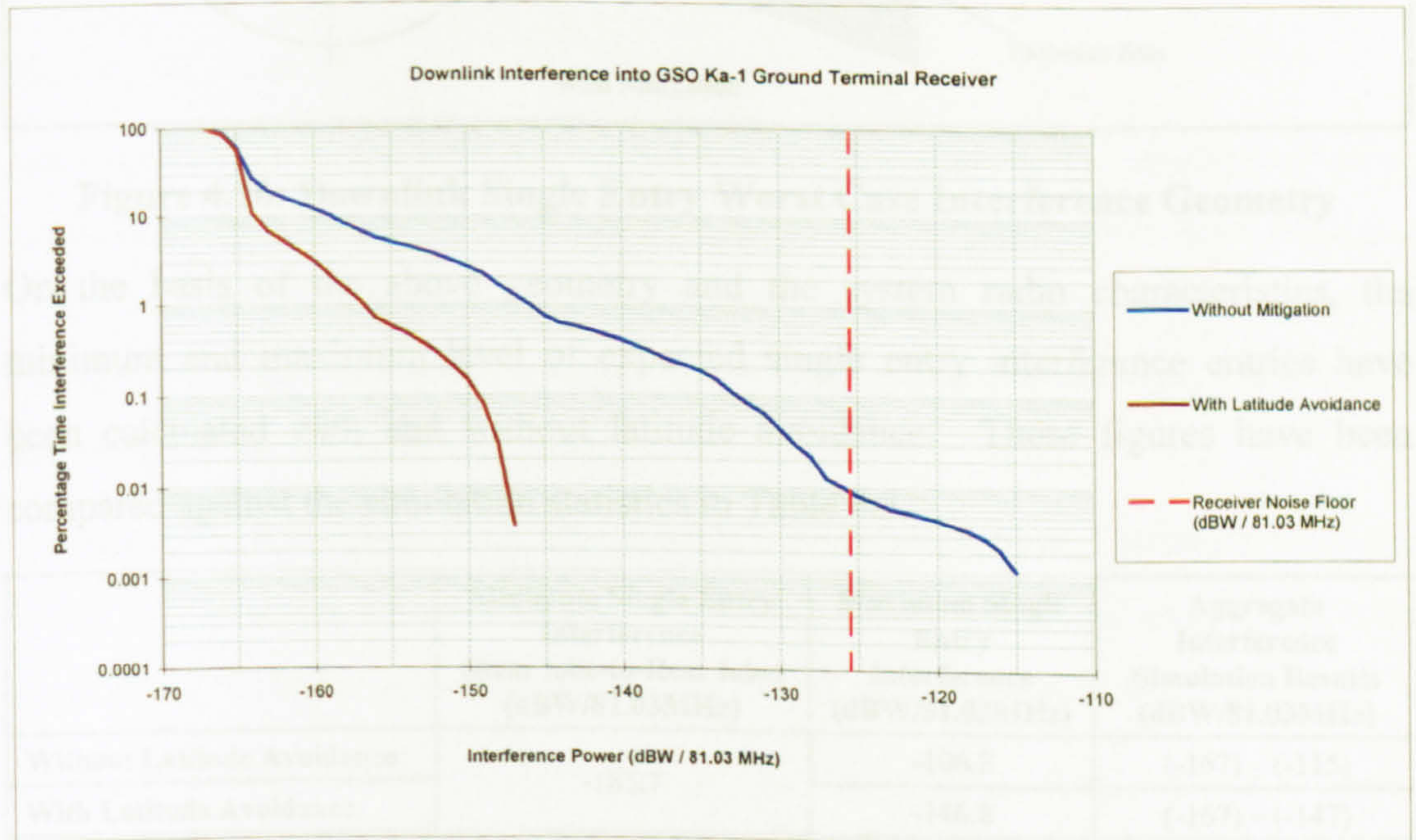


Figure 4.9: Comparison of Downlink Interference Statistics

The plots suggest that the latitude avoidance technique results in 10-30 dB reduction in the short term aggregate interference level at the GSO Ka-2 Earth station receiver antenna for percentage times less than 1%. In order to verify the results, the worst case alignments shown in Figure 4.10 are considered.

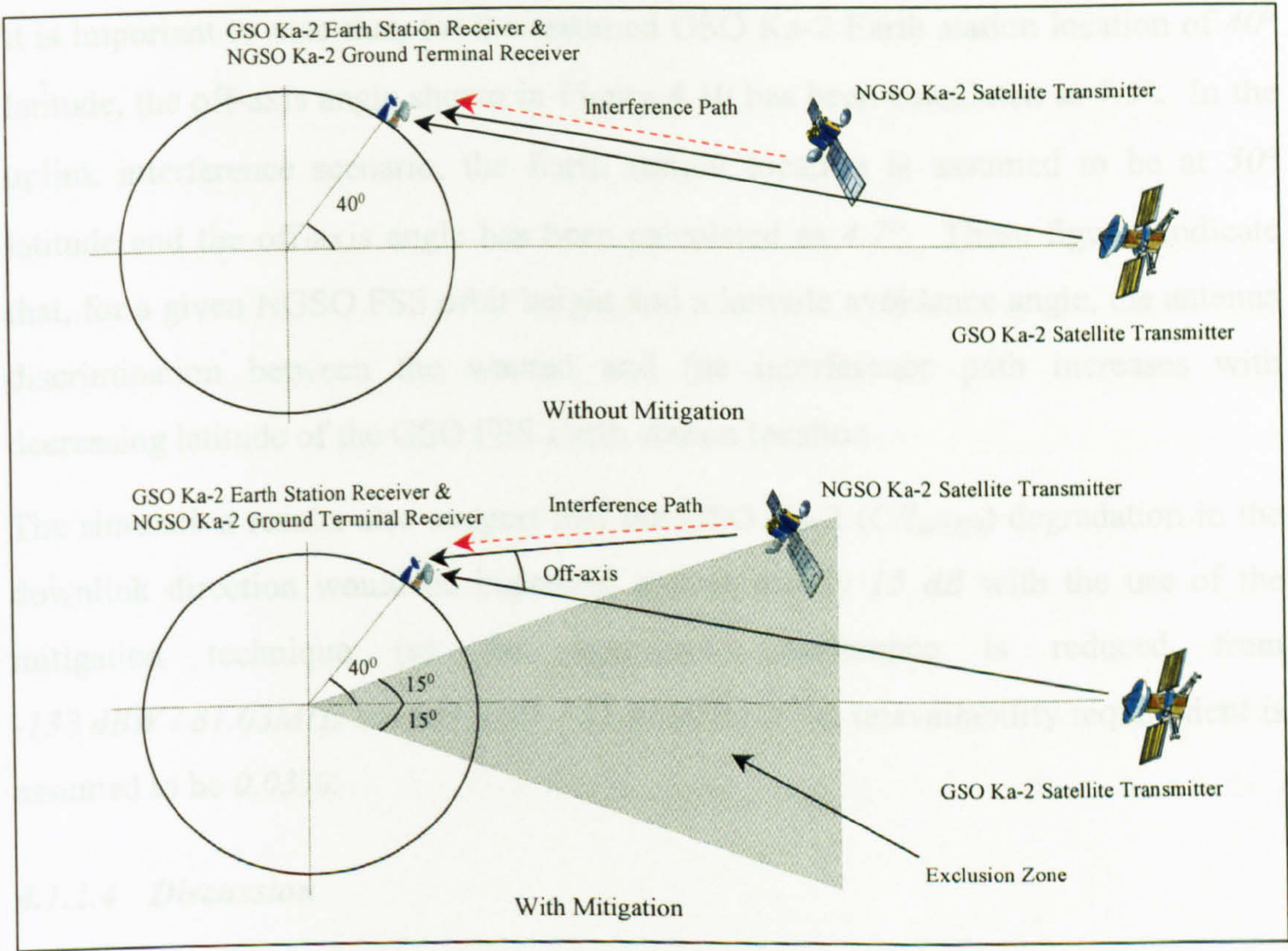


Figure 4.10: Downlink Single Entry Worst Case Interference Geometry

On the basis of the above geometry and the system radio characteristics, the minimum and maximum level of expected single entry interference entries have been calculated with and without latitude avoidance. These figures have been compared against the simulation statistics in Table 4.3.

	Minimum Single Entry Interference (Rear lobe-to-Rear lobe) (dBW/81.03MHz)	Maximum Single Entry Interference (dBW/81.03MHz)	Aggregate Interference Simulation Results (dBW/81.03MHz)
Without Latitude Avoidance	-185.7	-106.2	(-167) – (-115)
With Latitude Avoidance		-146.8	(-167) – (-147)

Table 4.3 Single Entry Interference Benchmark Figures

As can be seen, the simulation results fall within the calculated range. As expected, the sidelobe entries aggregate in power whereas the aggregate worst case interference is close to the calculated single entry level.

It is important to note that, for the assumed GSO Ka-2 Earth station location of 40° latitude, the off-axis angle shown in Figure 4.10 has been calculated as 7.5° . In the uplink interference scenario, the Earth station location is assumed to be at 50° latitude and the off-axis angle has been calculated as 4.7° . These figures indicate that, for a given NGSO FSS orbit height and a latitude avoidance angle, the antenna discrimination between the wanted and the interference path increases with decreasing latitude of the GSO FSS Earth station location.

The simulation results also suggest that the GSO Ka-2 (C/I_{NGSO}) degradation in the downlink direction would be improved approximately 15 dB with the use of the mitigation technique (as the aggregate interference is reduced from $-138\text{ dBW} / 81.03\text{MHz}$ to $-153\text{ dBW} / 81.03\text{MHz}$) if the unavailability requirement is assumed to be 0.03% .

4.1.2.4 Discussion

The implications of the latitude avoidance technique have been investigated using the deterministic simulation method. The simulation scenarios have been designed on the basis of the representative system characteristics given in Chapter 3 and the results have been validated taking the mainbeam-to-mainbeam and rearlobe-to-rearlobe interference alignments into account.

The results have indicated that the latitude avoidance technique prevents both the uplink and downlink mainbeam-to-mainbeam coupling. This conclusion agrees with the findings of the studies conducted by the ITU-R study groups [179, 180].

It has been noted that the off-axis angle at the GSO FSS receiver antenna between the wanted and the interfering path is dependent on the NGSO FSS system orbit height, the latitude of the co-located Earth stations and the value of the latitude avoidance angle. A larger off-axis gives rise to an improved antenna discrimination and, therefore, an increased reduction in the aggregate interference level.

4.1.3 High Performance NGSO FSS Satellite Antennas

In order to reduce the impact of the downlink interference into the GSO FSS Earth station receivers, NGSO FSS satellite antenna radiation patterns may be improved. In this section, the implications of this technique have been analysed by comparing the aggregate interference statistics obtained for each radiation pattern considered. For these purposes, the downlink interference from the NGSO Ku-2 constellation into the GSO Ku-2 receiver has been simulated for three different space station radiation patterns.

The first pattern considered here [181] is proposed in the ITU-R Study Group 4A while the second pattern is defined in ITU-R Rec.672 [174] for space stations operating in Fixed Satellite Service. The final pattern corresponds to that given in the NGSO Ku-2 system description document [57]. Figure 4.11 illustrates all three radiation patterns.

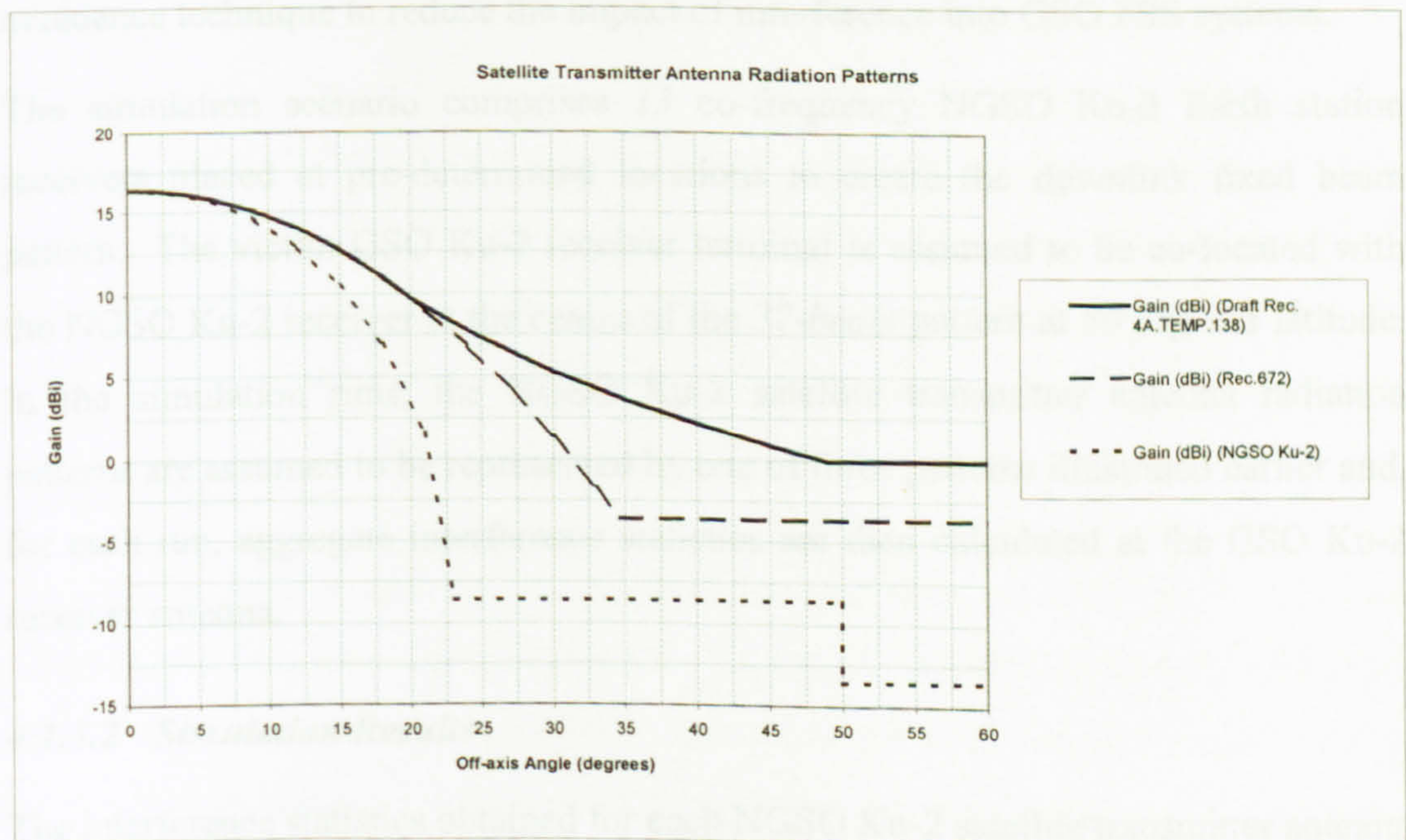


Figure 4.11: Satellite Transmitter Antenna Patterns

4.1.3.1 Simulation Model Description

The NGSO Ku-2 network orbital constellation includes 91 satellites in circular orbits of 700 km in altitude and 82° in inclination. The satellites are placed into 7 orbital planes of 13 satellites each. The radio traffic is established through a steerable 37-beam antenna which provides the tracking of geographically fixed cells at the Earth surface. Each satellite is capable of using 13 co-frequency beams within its fixed beam pattern.

A minimum operating elevation angle for a service zone is defined as 10 degrees. When a service area satisfies the minimum elevation angle requirement the fixed beam pattern locks on to that area and the beams are steered as the satellite passes over. When the minimum elevation angle requirement is not satisfied the beam pattern is switched to cover another service area and the existing links are handed over to the next available satellite. The system also employs a 10° GSO arc avoidance technique to reduce the impact of interference into GSO FSS systems.

The simulation scenario comprises 13 co-frequency NGSO Ku-2 Earth station receivers placed at pre-determined locations to create the downlink fixed beam pattern. The victim GSO Ku-2 receiver terminal is assumed to be co-located with the NGSO Ku-2 receiver at the centre of the 37-beam pattern at 50 degrees latitude. In the simulation runs, the NGSO Ku-2 satellite transmitter antenna radiation patterns are assumed to be represented by one of three patterns illustrated earlier and, for each run, aggregate interference statistics are then calculated at the GSO Ku-2 receiver antenna.

4.1.3.2 Simulation Results

The interference statistics obtained for each NGSO Ku-2 satellite transmitter antenna radiation pattern are compared in Figure 4.12. Each scenario is simulated for 1,000,000 seconds (approx. 12 days) with 1 second time step.

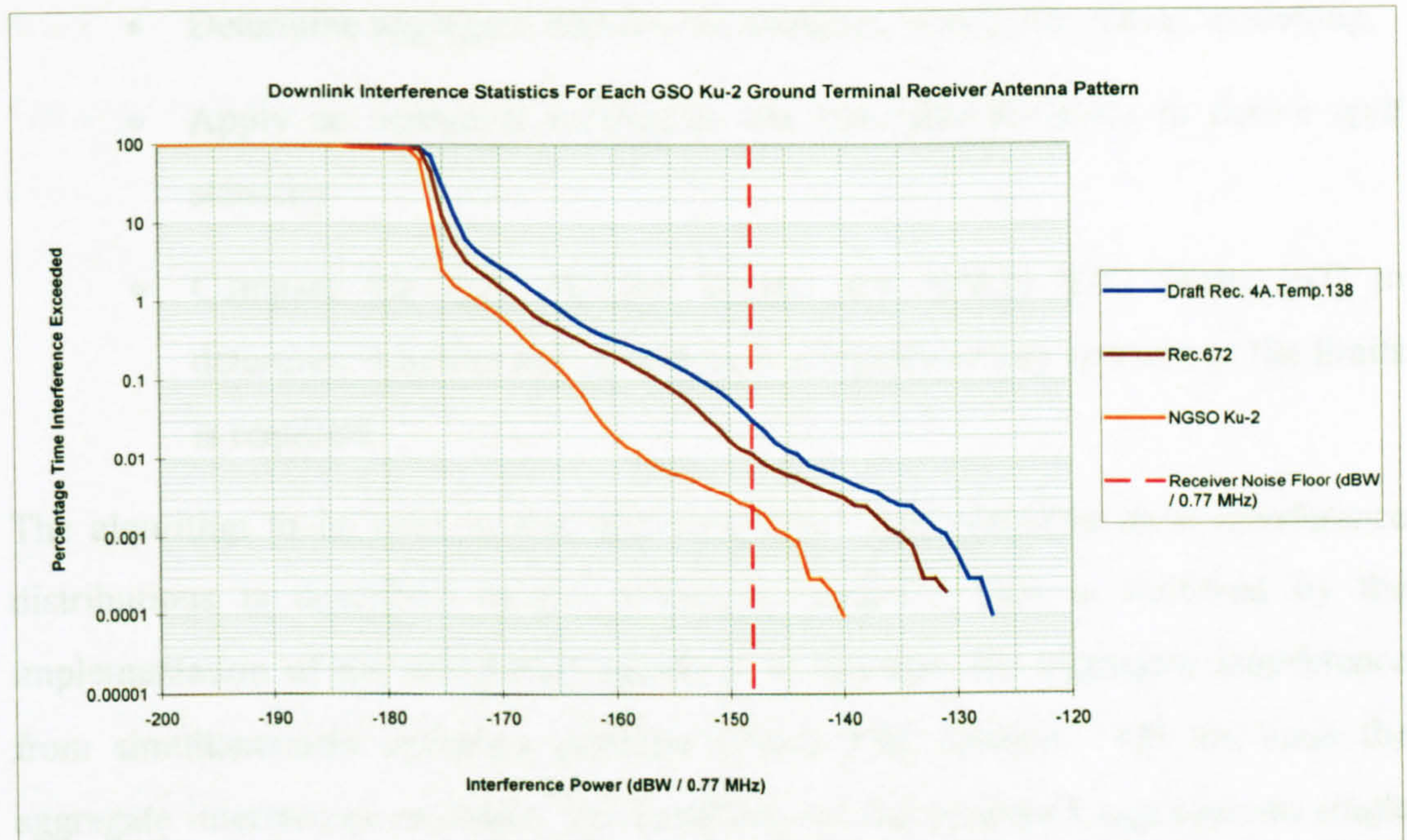


Figure 4.12: Comparison of Interference Statistics

Although, for all patterns, the aggregate interference exceeds the receiver noise floor, the third pattern gives rise to the lowest interference. This is the result of this pattern's improved/suppressed near sidelobe and rearlobe envelopes for off-axis angles $> 5^\circ$. For the Rec.672 pattern, the reduced sidelobes (for off-axis angles $> 20^\circ$) compared against the first radiation pattern also gives rise to improvement of in order of 4 dB in the resultant interference statistics.

4.1.3.3 Discussion

The results suggest that the NGSO FSS space station antennas with improved sidelobe performance reduce the amount of aggregate interference into the GSO FSS Earth station receivers and, therefore, increase the efficient use of the spectrum. It is, however, important to note that, in general, this achievement is at the expense of an increased antenna design cost.

4.2 Revision of epfd Limits

In this research, the implications of two methods have been examined. The first method is a simulation approach and requires the following steps to be implemented:

- Determine aggregate interference statistics from a simulation modelling,
- Apply an analytical method to the interference values to derive *epfd* statistics
- Compare the *epfd* statistics against the Article S.22 limits [67] to determine whether the protection is adequate or any revision to the limits is required.

The algorithm to be used in deriving continuous *epfd* statistics from interference distributions is described in the following section. This is followed by the implementation of the simulation approach to examine the aggregate interference from simultaneously operating multiple NGSO FSS systems. On the basis the aggregate interference statistics, the feasibility of the proposed aggregate-to-single entry *epfd* conversion algorithm [156] has been examined. Then, the *epfd* statistics have been used to assess the implications of comparing the continuous *epfd* curves against the discontinuous (staircase) *epfd* limits. Finally, the implications of the interpolation/extrapolation algorithm proposed for deriving *epfd* limits corresponding to antenna diameters not included in the current Article S.22 *epfd* limits have been investigated.

The second method is an analytical approach. It is based on the implementation of the Methodology A', which is defined in ITU-R Rec.1323 [109], to verify compliance with the protection requirement stating that the interference from all NGSO FSS systems should not exceed 10% of total GSO FSS link unavailability target. As mentioned previously in §3.1.3, the methodology considers the probability of simultaneous rain fades and interference events. The implementation involves a convolution of simplified interference and fading probability density functions to derive the *epfd* levels which are then compared against the Article S.22 limits.

4.2.1 Conversion from interference to *epfd*

The *epfd* is defined as the sum of the power flux densities produced at a GSO FSS receiver station by all NGSO FSS transmitters taking account of receiver antenna off-axis discrimination and formulated as [67]:

$$epfd = 10 * \log \left[\sum_{i=1}^{N_a} 10^{\frac{P_i}{10}} * \frac{G_t(\theta_i)}{4 * \pi * d_i^2} * \frac{G_r(\phi_i)}{G_{r,max}} * \frac{RefBandwidth}{TxBandwidth} \right] \quad (4-1)$$

where:

N_a : the number of NGSO FSS transmitter stations that are visible from the GSO FSS receiver station on the Earth's surface or in the geostationary orbit, as appropriate;

i : the index of the NGSO FSS transmitter station;

P_i : the RF power at the antenna input of the NGSO FSS transmitter station, *dBW* in the transmitter bandwidth (*TxBandwidth*);

θ_i : the off-axis angle between the boresight of the NGSO FSS transmitter station and the direction of the GSO FSS receiver station;

$G_t(\theta_i)$: the transmitter antenna gain (as a ratio) of the NGSO FSS station in the direction of the GSO FSS receiver station;

ϕ_i : the off-axis angle between the boresight of the GSO FSS receiver station and the direction of the i^{th} transmitter station considered in the NGSO FSS system;

$G_r(\phi_i)$: the receiver antenna gain (as a ratio) of the GSO FSS receiver station in the direction of the i^{th} transmit station considered in the NGSO FSS system;

d_i : the distance between the NGSO FSS transmitter and the GSO FSS receiver stations, in metres;

$G_{r,max}$: the maximum gain (as a ratio) of the GSO FSS station receiver antenna;

epfd: the equivalent power flux-density in *dBW/m²* in the reference bandwidth (*RefBandwidth*).

Similarly, the aggregate interference produced at a GSO FSS receiver station by all NGSO FSS transmitters can be expressed as:

$$I = 10 * \log \left[\sum_{i=1}^{N_a} 10^{\frac{P_i}{10}} * \frac{G_t(\theta_i) * G_r(\phi_i)}{\left(\frac{4 * \pi * d_i}{\lambda} \right)^2} * \frac{RxBandwidth}{TxBandwidth} \right] \quad (4-2)$$

where I is the aggregate interference at the GSO FSS receiver, dBW in the receiver bandwidth ($RxBandwidth$). The *epfd* can be defined in terms of the aggregate I taking the above two equations into account as following:

$$epfd = I + 10 \log \frac{4\pi}{\lambda^2} - 10 \log G_{r,max} + 10 \log \left(\frac{RefBandwidth}{RxBandwidth} \right) \quad (4-3)$$

The formula 4-3 is used to translate the aggregate interference statistics obtained from the simulation analysis into the *epfd* statistics defined in dBW in the reference bandwidth. Using this formula, *epfd_{down}* statistics at the GSO Ku-1 Earth station receiver have been derived from the aggregate interference statistics illustrated in Figure 4.3 in § 4.1.1. Figure 4.13 shows the *epfd_{down}* statistics and compares them against the Article S.22 single entry *epfd* limits to verify the compliance with the regulations.

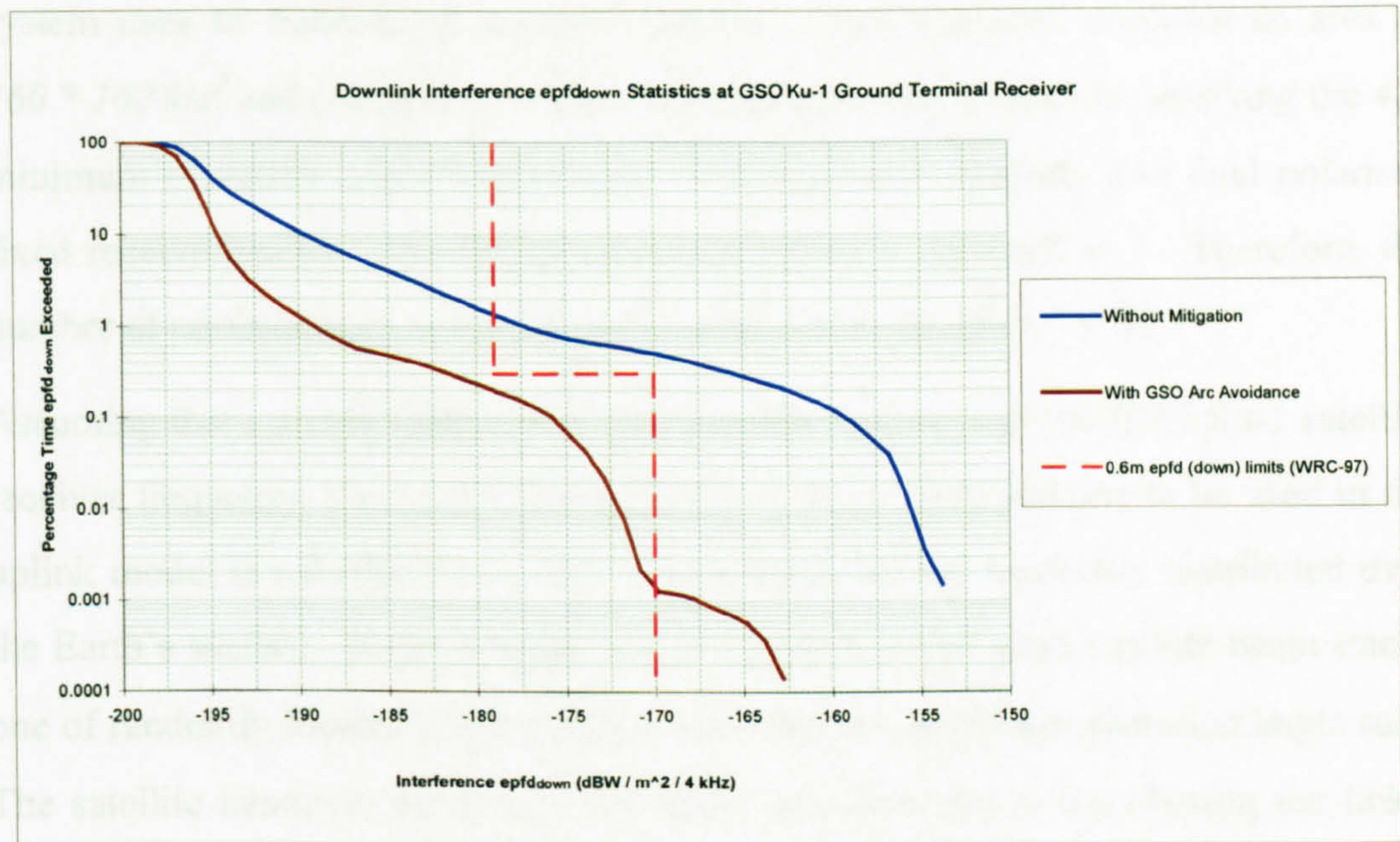


Figure 4.13: $epfd_{down}$ at GSO Ku-1 Earth station Receiver

For this example, the comparison indicates that the current limits do not provide adequate protection for the GSO Ku-1 Earth station receiver from the NGSO Ku-1 downlink interference. Without mitigation, the $epfd_{down}$ statistics exceed the limits at the 1% level while the use of arc avoidance reduces the percentage time at which the limits are exceeded to 0.001%.

4.2.2 Multiple NGSO FSS System Interference

This section outlines the investigations carried out in this study concerning with the mechanisms by which interference from multiple NGSO FSS systems aggregate. For these purposes, both the uplink and downlink interference paths are examined.

4.2.2.1 Uplink $epfd$

For the uplink $epfd$ analysis, interference statistics from the NGSO Ka-1 and NGSO Ka-2 Earth station transmitters into the GSO Ka-1 satellite receivers have been derived.

The NGSO Ka-1 constellation has the largest number of satellites (288) operating in elliptical orbits at approximately 1,400km altitude (see Table 3.5 in Chapter 3). The

system uses an Earth-fixed supercell pattern. Each supercell occupies an area of $160 * 160 \text{ km}^2$ and comprises 7 cells. A cell is served by a satellite satisfying the 40° minimum elevation angle requirement. Each satellite supports 364 dual polarised fixed receive beams. The frequency re-use within a supercell is 7. Therefore, the number of co-frequency uplink beams is modelled to be $364 / 7 = 52$.

Assuming that a single Earth station per supercell operates at the GSO Ka-1 satellite receiver frequency, the total number of NGSO Ka-1 Earth stations to be used in the uplink model is calculated as 6293. These terminals are randomly distributed over the Earth's surface. In the simulations, it is assumed that each satellite beam tracks one of randomly located Earth stations using the 40° minimum elevation angle rule. The satellite handover process is simplified and involves in transferring the links, becoming unavailable due to low elevation angles, to a satellite meeting the minimum elevation criteria. In addition, the satellite spot beam antenna gain is modelled as varying with path elevation angle.

The NGSO Ka-2 simulation model is identical to that used in the latitude avoidance mitigation analysis (see § 4.1.2). The constellation comprises 16 satellites each supporting 10 co-frequency beams at an altitude of 10,400 km.

In order to reduce the computational complexity due to the large number of Earth stations involved, the scenarios have been simulated for 20,400 seconds (approx. 6 hours) which translates as a requirement of an approximately 10 days real simulation time on a 500 MHz PC. Figure 4.14 illustrates the interference statistics. For the comparison purposes, interference statistics from each constellation also have been obtained and shown in the same figure.

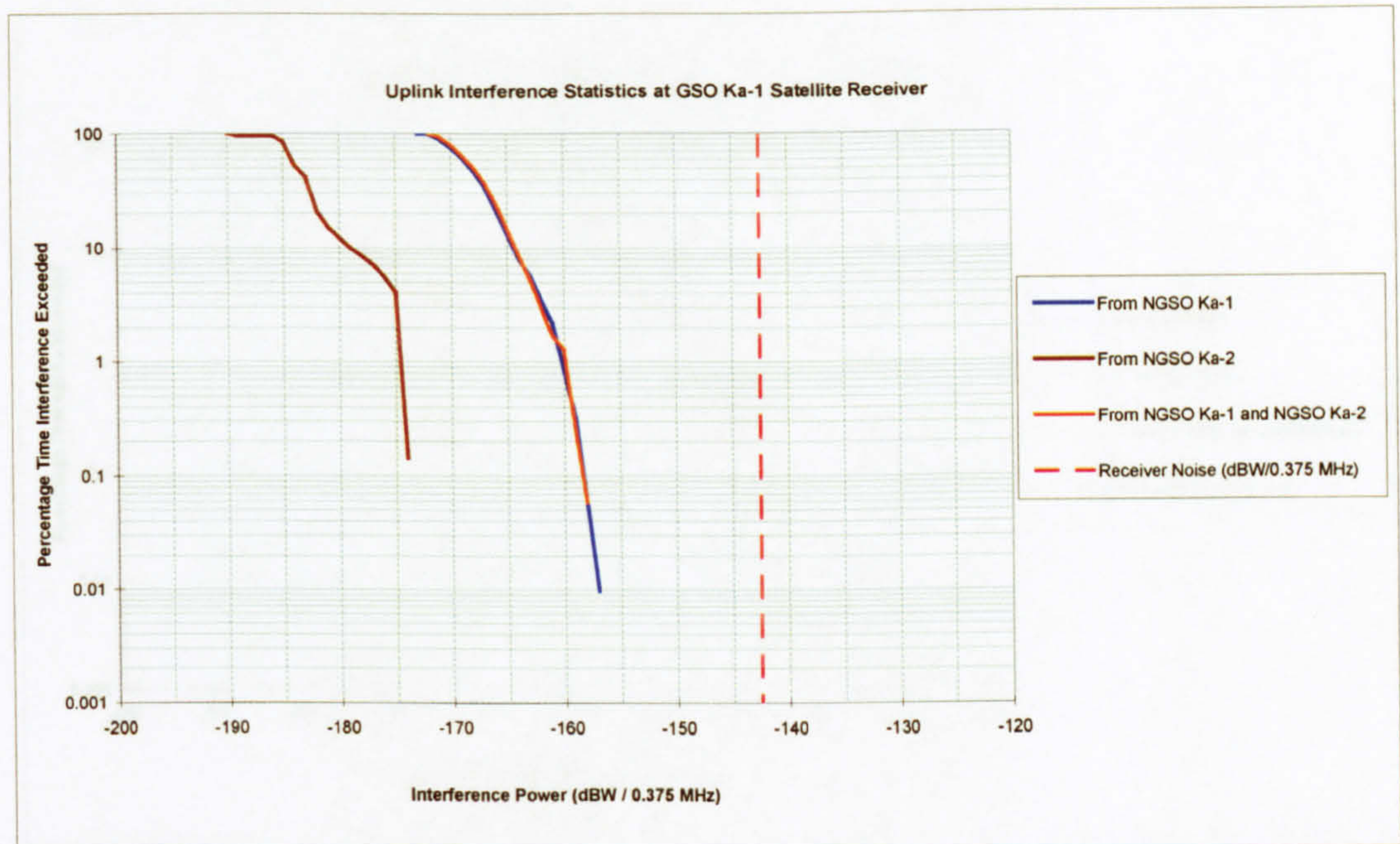


Figure 4.14: Aggregation of Uplink Interference Statistics

Comparison of the NGSO Ka-1 and NGSO Ka-2 system parameters indicate that these systems are inhomogeneous as both constellations are significantly different (see Table 3.5 in Chapter 3). Therefore, the aggregate interference statistics from NGSO Ka-1 and NGSO Ka-2 systems are entirely dominated by the NGSO Ka-1 which is the larger constellation.

Using the conversion method defined in the preceding section, the aggregate interference statistics have been translated to $epfd_{up}$ statistics and compared against the Article S.22 limits specified for GSO FSS space stations operating in the upper Ka-band (19.7-20.2 GHz) in Figure 4.15.

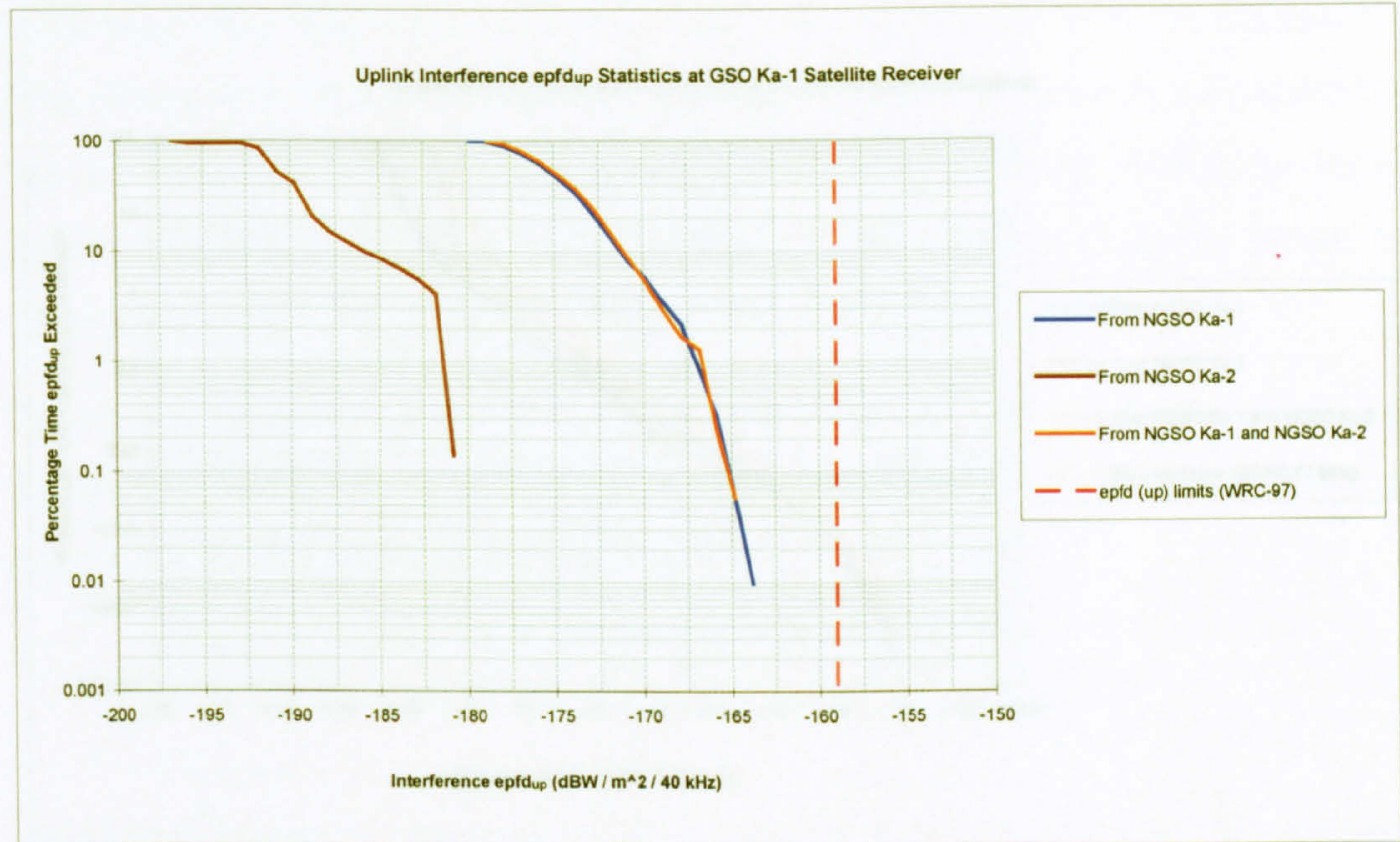


Figure 4.15: Interference $epfd_{up}$ Statistics

For the simulated time period, the $epfd_{up}$ statistics are dominated by the interference originating from the NGSO Ka-1 interference paths and remain below the $epfd_{up}$ limit.

4.2.2.2 Downlink $epfd$

For the downlink $epfd$ analysis, multiple NGSO FSS aggregate interference has been investigated using NGSO Ku-1 and NGSO Ku-2 constellations. Simulation descriptions are the same as those used in the NGSO FSS mitigation technique analysis detailed in § 4.1. The interference statistics at the GSO Ku-2 Earth station receiver, obtained from the simulation runs of 2,000,000 seconds (approx. 23 days), are shown in figure 4.16. As before, for the comparison purposes, interference statistics from each constellation also are included in the figure.

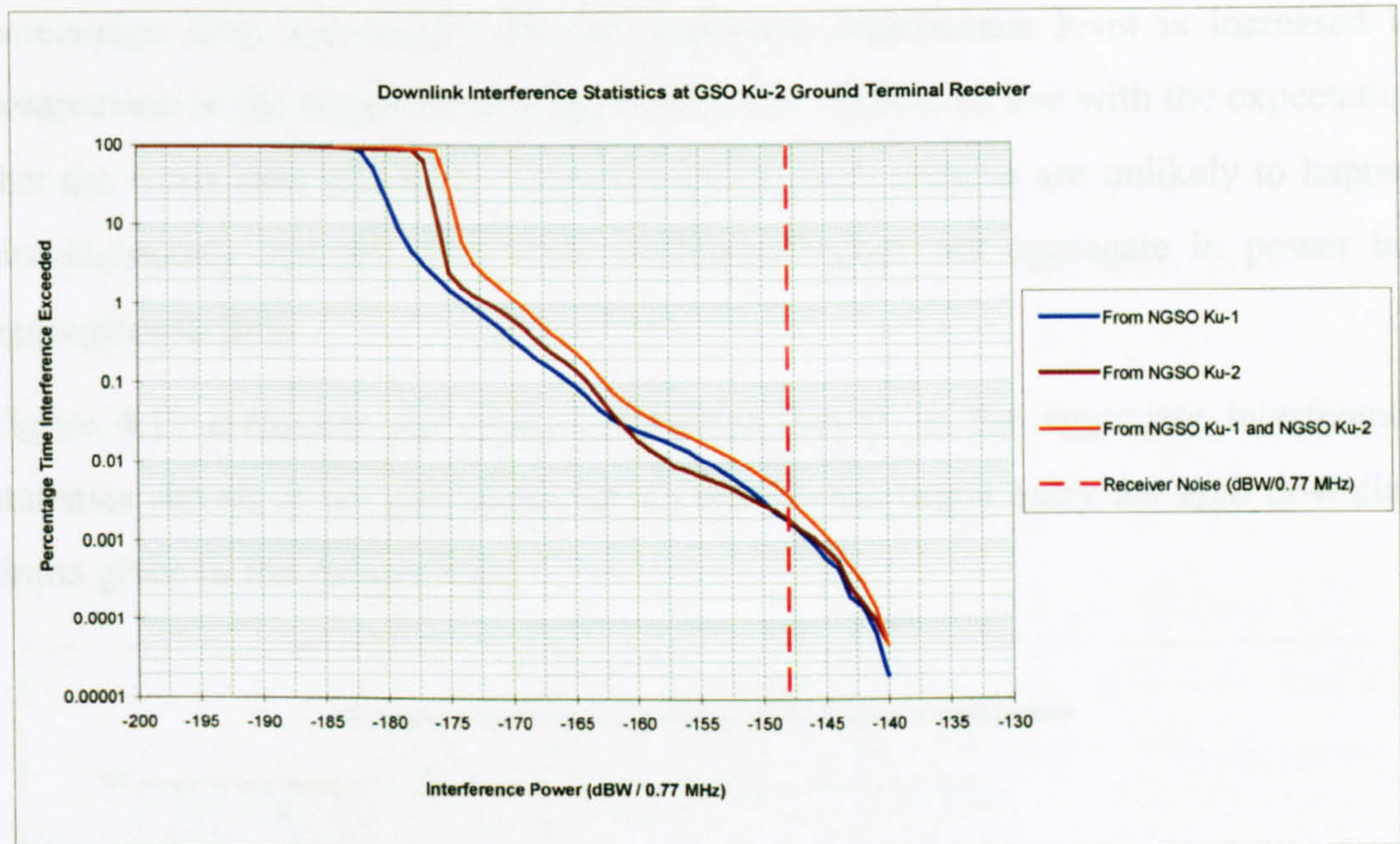


Figure 4.16: Aggregation of Downlink Interference Statistics

Comparison of the NGSO Ku-1 and NGSO Ku-2 parameters suggests that the system characteristics do not differ significantly (see Table 3.4 in Chapter 3). Constellations comprise approximately 80 satellites and both systems employ *10 degrees* minimum elevation angle together with the GSO arc avoidance mitigation technique.

Figure 4.16 indicates that the long term interference (left end of the curves) is increased in the scenario modelling interference from the NGSO Ku-1 and NGSO Ku-2 systems as the number of interference entries through the sidelobes of the GSO Ku-2 receiver antenna are higher than those obtained from the scenarios where interference from a single constellation is considered. This suggests that the long term interference aggregates in power when several homogeneous NGSO FSS interferes with a GSO FSS Earth station receiver.

As far as the short term interference (right end of the curves) is concerned, the aggregate power level obtained from the NGSO Ku-1 and NGSO Ku-2 interference scenario is the same as those obtained from the single constellation scenarios. On the other hand, in the NGSO Ku-1 and NGSO Ku-2 interference scenario, the

percentage time associated with the maximum interference level is increased in comparison to the single constellation scenarios. This is in line with the expectation that the worst case interference alignments for both systems are unlikely to happen simultaneously and the short term interference does not aggregate in power but aggregates in time.

Figure 4.17 compares the $epfd_{down}$ statistics, based on the aggregate interference statistics shown in the preceding figure, against the single entry $3m$ $epfd$ downlink limits given in the Article S.22.

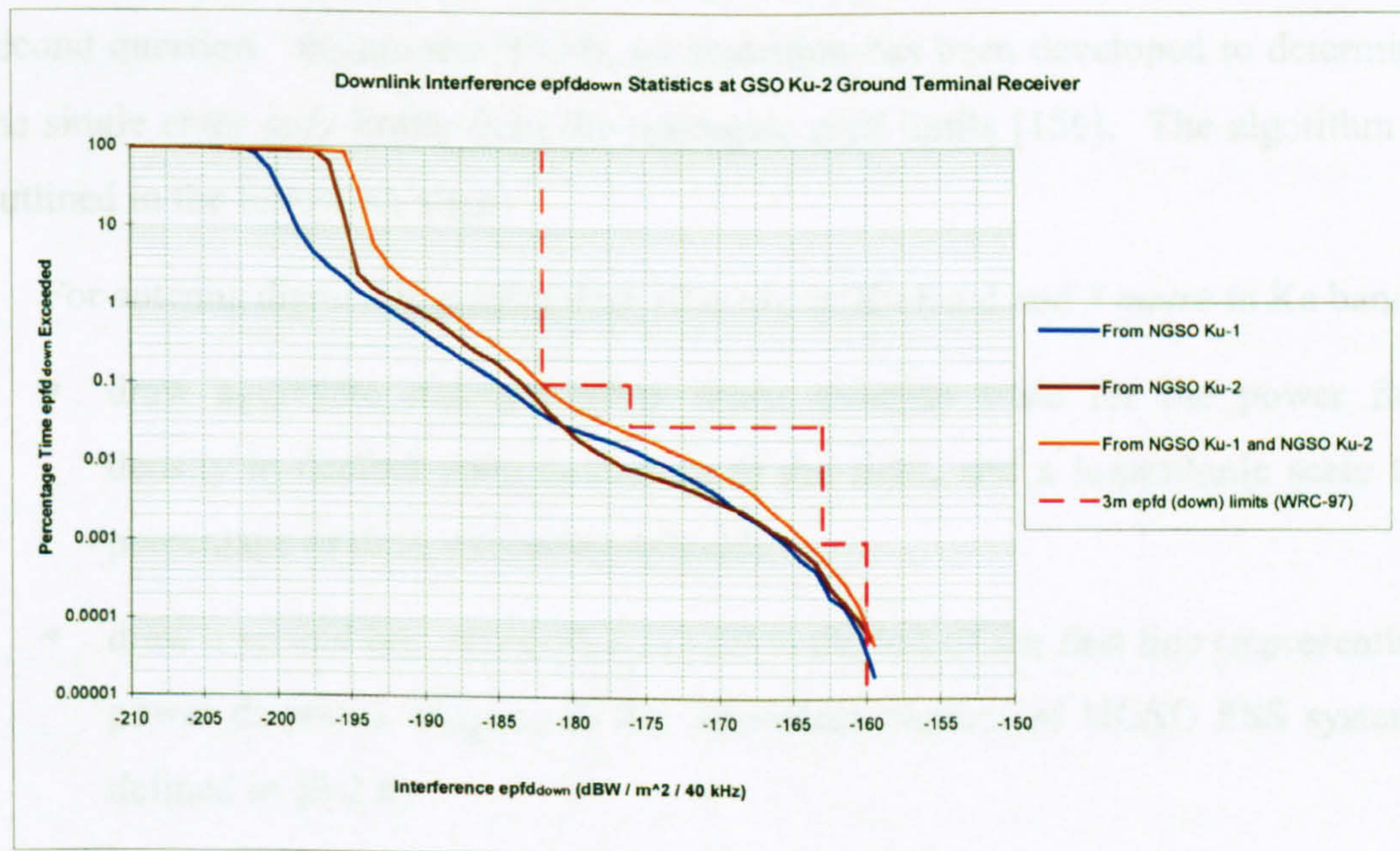


Figure 4.17: Interference $epfd_{down}$ Statistics

As can be seen, for the simulated time period and assumed system parameters, the $3m$ $epfd$ downlink limits are satisfied for the most but very short period of time ($<0.0001\%$).

4.2.3 Conversion from Aggregate-to-Single Entry $epfd$

As shown in the preceding section, the compliance with the $epfd$ limits is checked by comparing the continuous aggregate $epfd$ statistics derived from interference scenarios where a single NGSO FSS system or multiple NGSO FSS systems

interfere with a GSO FSS Earth station receiver against the single entry discontinuous *epfd* limits stated in Article S.22. This raises two questions:

- Is it possible to convert the *epfd* statistics based on several NGSO FSS systems to the single entry *epfd* statistics based on a single NGSO FSS system so that the comparison against the Article S.22 single entry limits is meaningful?
- What are the implications of comparing the single entry continuous *epfd* statistics against the discontinuous Article S.22 single entry limits?

This section deals with the first question while the next section is concerned with the second question. Within the ITU-R, an algorithm has been developed to determine the single entry *epfd* limits from the aggregate *epfd* limits [156]. The algorithm is outlined in the following steps:

- For antenna diameters greater than *10 metre* in Ku band and *5 metre* in Ka band:
 - draw aggregate statistics using linear abscissa scale for the power flux density in decibel units increasing to the right, and a logarithmic scale for percentage of time increasing upwards,
 - draw a second line $10\log(N_{\text{effective}})$ dB to the left of the first line (representing power division), ($N_{\text{effective}}$ is the equivalent number of NGSO FSS systems defined in §3.2.6)
 - draw a third line by dividing the first line by a factor of $N_{\text{effective}}$ (representing time division),
 - draw the single entry statistics by
 - taking the second line from 100% of time to the point where it crosses the third line,
 - taking the third line from that point and the point where the third line reaches 0.01% of time,
 - taking the first line for percentages of time below 0.001%,

- drawing a straight line between the 0.01% of time and the 0.001% of time,
- For smaller antenna diameters:
 - apply the same procedure but take the third line for all percentages of time less than the point where it crosses the second line.

In the cases where the second (power shifted) and the third (time shifted) curves do not intersect, the following procedure is recommended:

- select a point (P) that is greater than or equal to the 1% of time on the aggregate curve,
- connect the corresponding point (P) on the power shifted and the corresponding point (P) time shifted curves,
- form the single entry statistics by using the power shifted portion for percentage times between 100% and $P\%$, the segment created in the previous step for percentage times between $P\%$ and $(P/N_{effective})\%$ and the time shifted segment for times less than $(P/N_{effective})\%$.

Based on the results presented in the preceding section, the implementation of the above algorithm and the comparison with the resultant single entry statistics with those obtained from the single constellation simulation runs are shown in Figures 4.18 (a), (b), (c) and (d). In the analysis, two values are assumed for the $N_{effective}$: 3.5 (representing the agreed value in ITU-R) and 2 (representing the actual number of simultaneously operating NGSO FSS systems considered in this study).

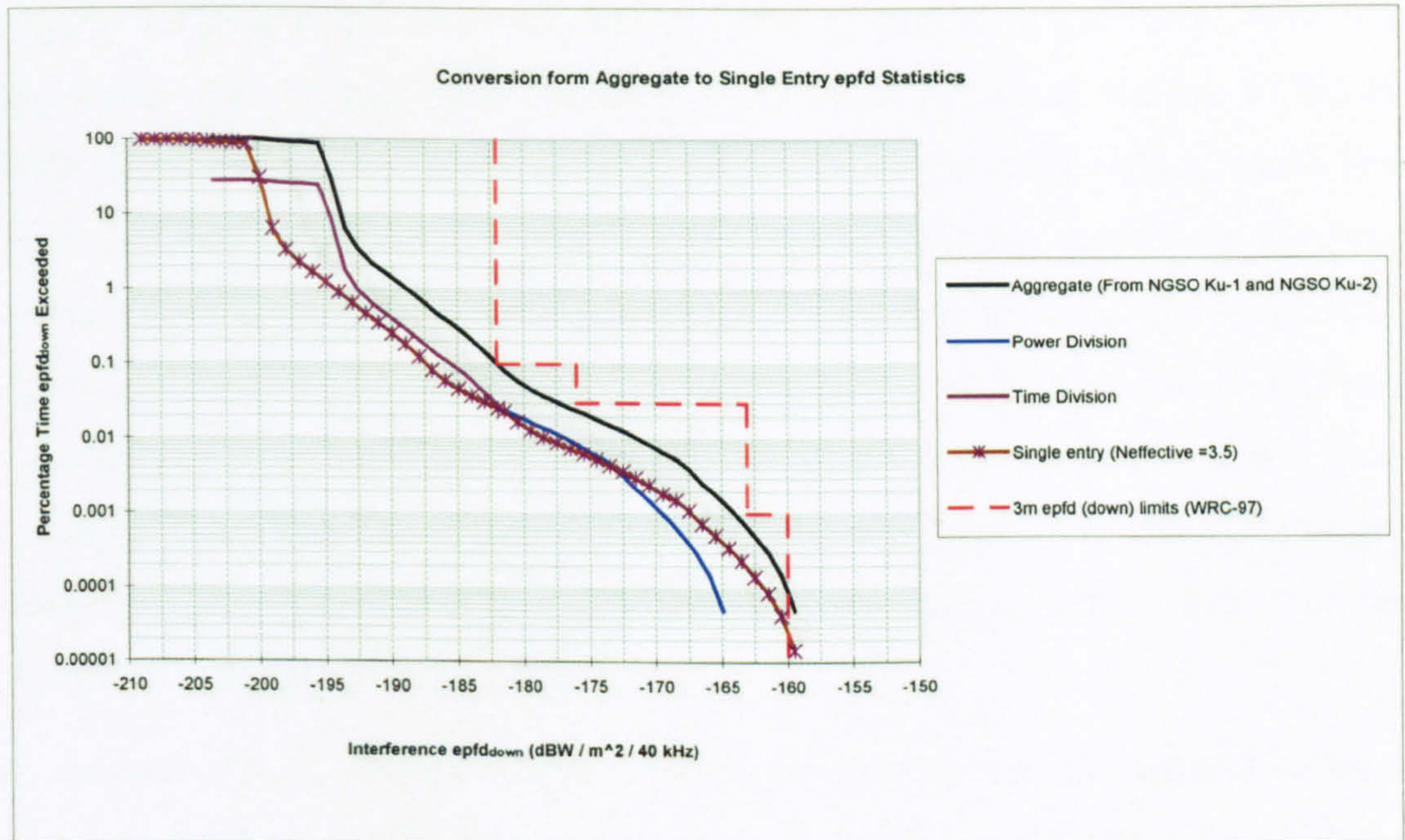


Figure 4.18 (a) : Conversion from Aggregate $epfd_{down}$ to Single Entry $epfd_{down}$
($N_{effective}=3.5$)

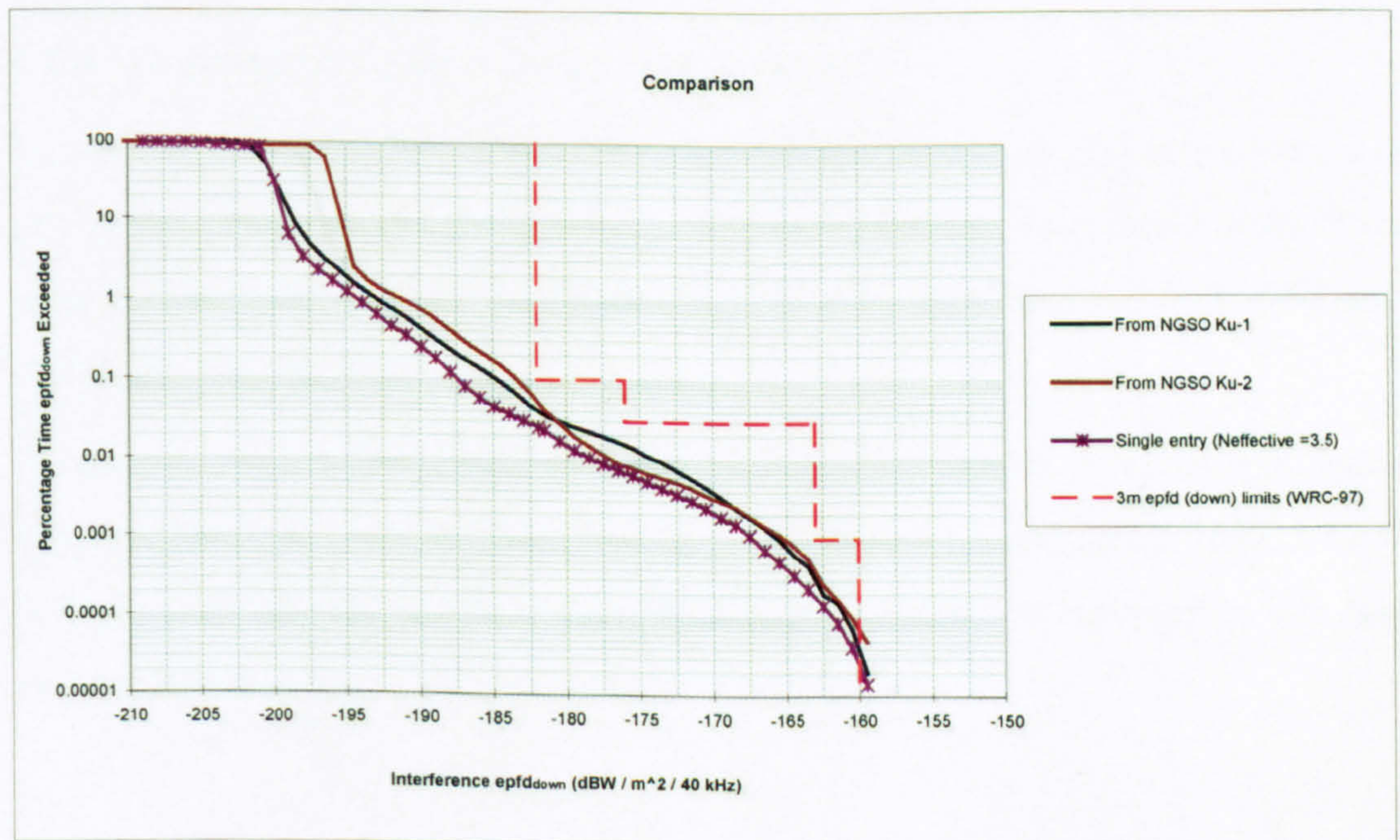


Figure 4.18 (b) : Comparison of Single Entry $epfd_{down}$ Against Simulation
Results ($N_{effective}=3.5$)

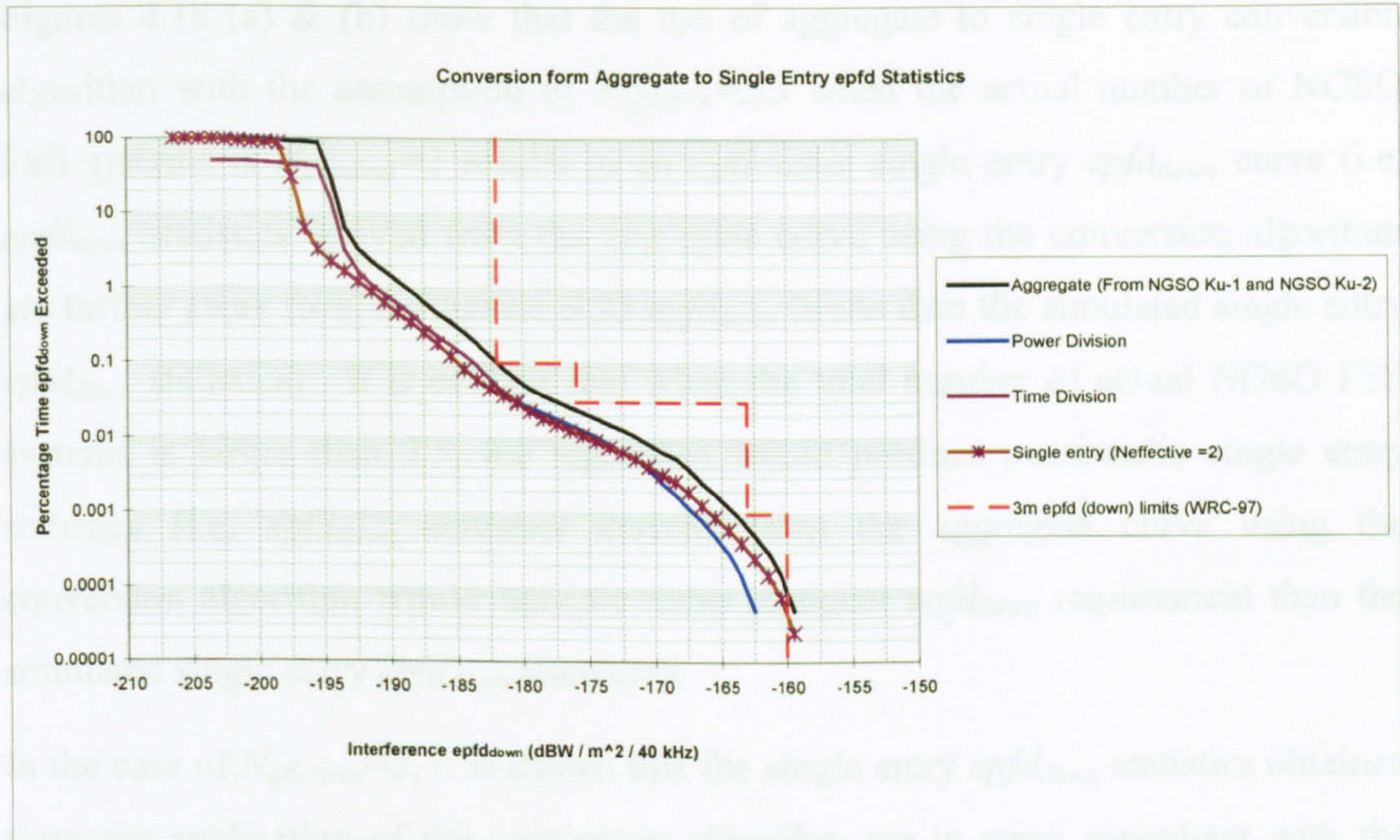


Figure 4.18 (c) : Conversion from Aggregate $epfd_{down}$ to Single Entry $epfd_{down}$ ($N_{effective}=2$)

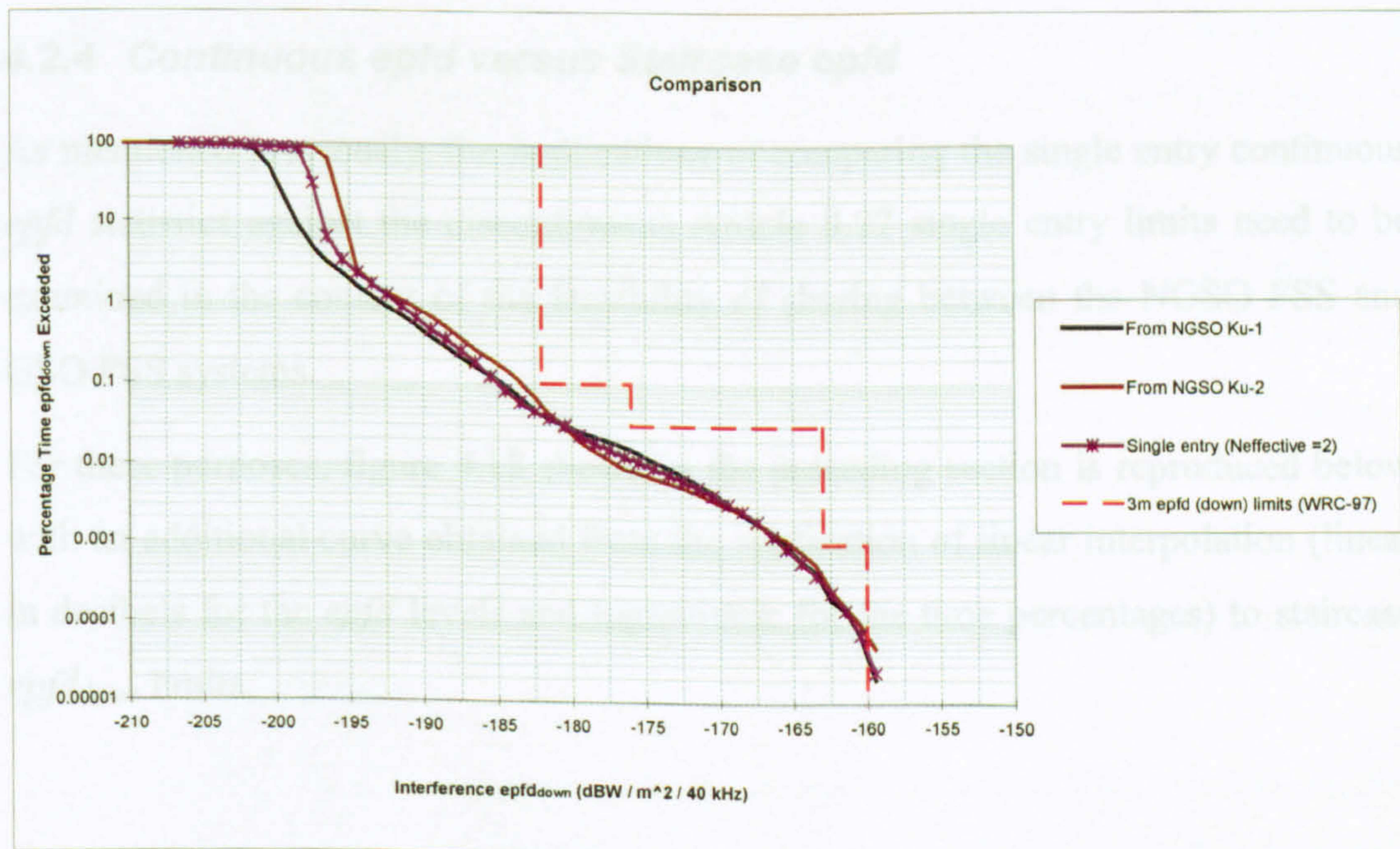


Figure 4.18 (d) : Comparison of Single Entry $epfd_{down}$ Against Simulation Results ($N_{effective}=2$)

Figures 4.18 (a) & (b) show that the use of aggregate to single entry conversion algorithm with the assumption of $N_{effective}=3.5$ when the actual number of NGSO FSS systems is $N_{physical}=2$ results in an optimistic single entry $epfd_{down}$ curve (i.e. $epfd_{down}$ statistics derived from the aggregate curve using the conversion algorithm are further away from the Article S.22 $epfd_{down}$ limits than the simulated single entry $epfd_{down}$ statistics). It is evident that when the total number of actual NGSO FSS systems is larger than 3.5, the algorithm would produce pessimistic single entry statistics (i.e. $epfd_{down}$ statistics derived from the aggregate curve using the conversion algorithm would indicate more stringent $epfd_{down}$ requirement than the simulated single entry $epfd_{down}$ statistics).

In the case of $N_{effective}=2$, it is shown that the single entry $epfd_{down}$ statistics obtained from the application of the conversion algorithm are in good agreement with the $epfd_{down}$ statistics obtained from single entry simulation runs as the difference remains below 2 dB for the most percentages.

4.2.4 Continuous $epfd$ versus Staircase $epfd$

As mentioned previously, the implications of comparing the single entry continuous $epfd$ statistics against the discontinuous Article S.22 single entry limits need to be examined in the context of the feasibility of sharing between the NGSO FSS and GSO FSS systems.

For these purposes, figure 4.18 shown in the preceding section is reproduced below with an additional curve obtained from the application of linear interpolation (linear in decibels for the $epfd$ levels and logarithmic for the time percentages) to staircase $epfd_{down}$ limits.

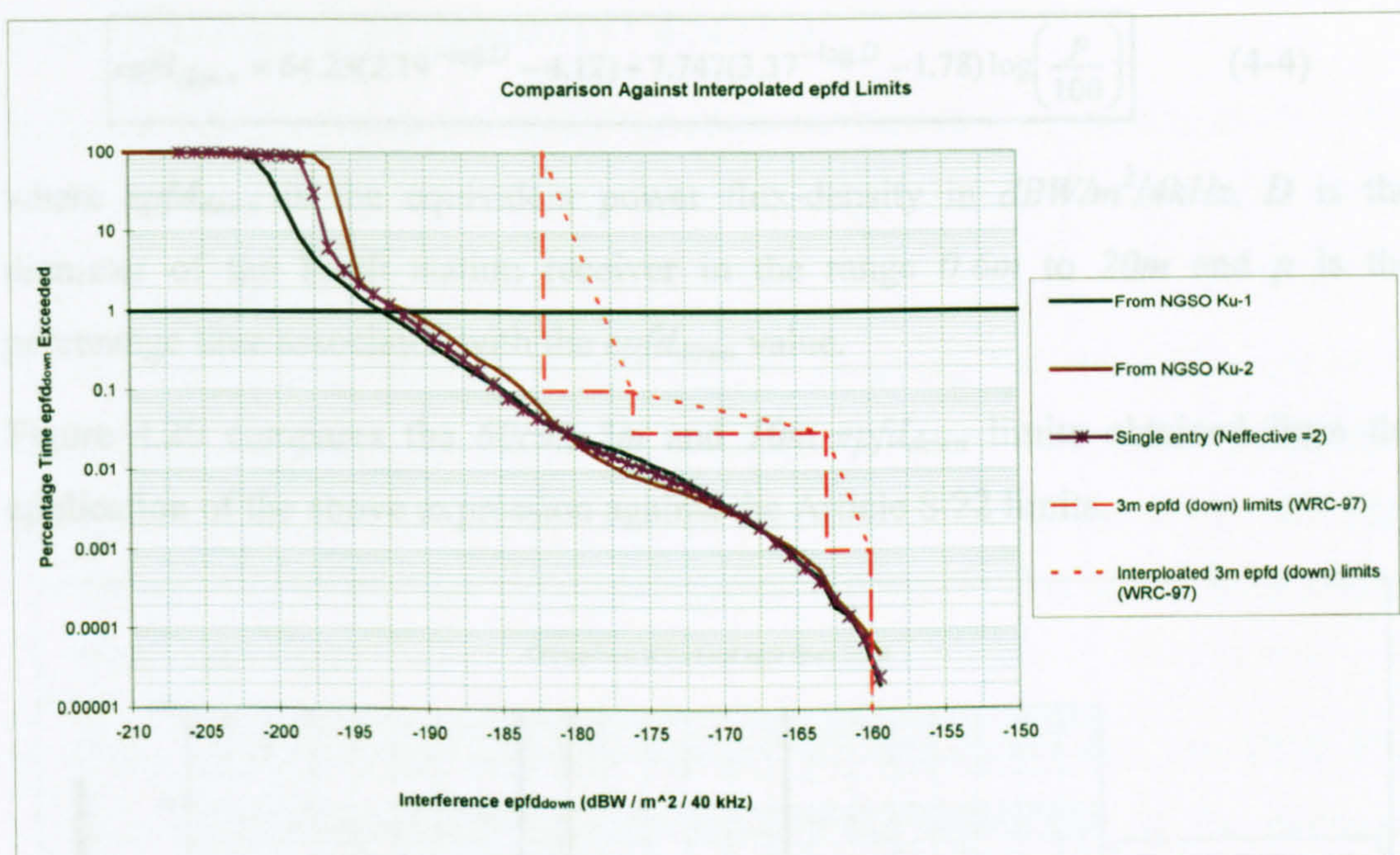


Figure 4.19: Comparison Against Linear Interpolated $epfd_{down}$ Limits

The plots in Figure 4.19 illustrate that, for example, there is a margin of by some 10 dB between the $epfd_{down}$ statistics and the staircase $epfd_{down}$ limits for an exceedance percentage of 1% . It is further illustrated that the margin would be 15 dB if the continuous $epfd$ curves were employed in the analysis.

It is, therefore, evident that the use of discontinuous $epfd$ masks to check the NGSO FSS interference compliance is a pessimistic approach. Additionally, the actual interference $epfd$ statistics are in continuous form and comparison against continuous $epfd$ masks is more realistic.

4.2.5 Derivation of Limits for Antenna Diameters not Included in Radio Regulations

As shown in §3.1.2, the $epfd_{down}$ limits are defined for certain Earth station receiver antenna diameters. For diameters other than those specified, the ITU-R adopted the following empirical expression to be used in estimating short-term $epfd$ limits (0.001% to 1%) for downlinks operating in the Ku band [115, 117].

$$epfd_{down} = 64.23(2.19^{-\log D} - 4.12) + 7.747(3.37^{-\log D} - 1.78) \log\left(\frac{p}{100}\right) \quad (4-4)$$

where $epfd_{down}$ is the equivalent power flux-density in $dBW/m^2/4kHz$, D is the diameter of the Earth station receiver in the range $0.6m$ to $20m$ and p is the percentage time associated with the $epfd_{down}$ value.

Figure 4.20 compares the $60cm$, $3m$ and $10m$ $epfd_{down}$ limits obtained from the application of the above expression against the Article S.22 limits.

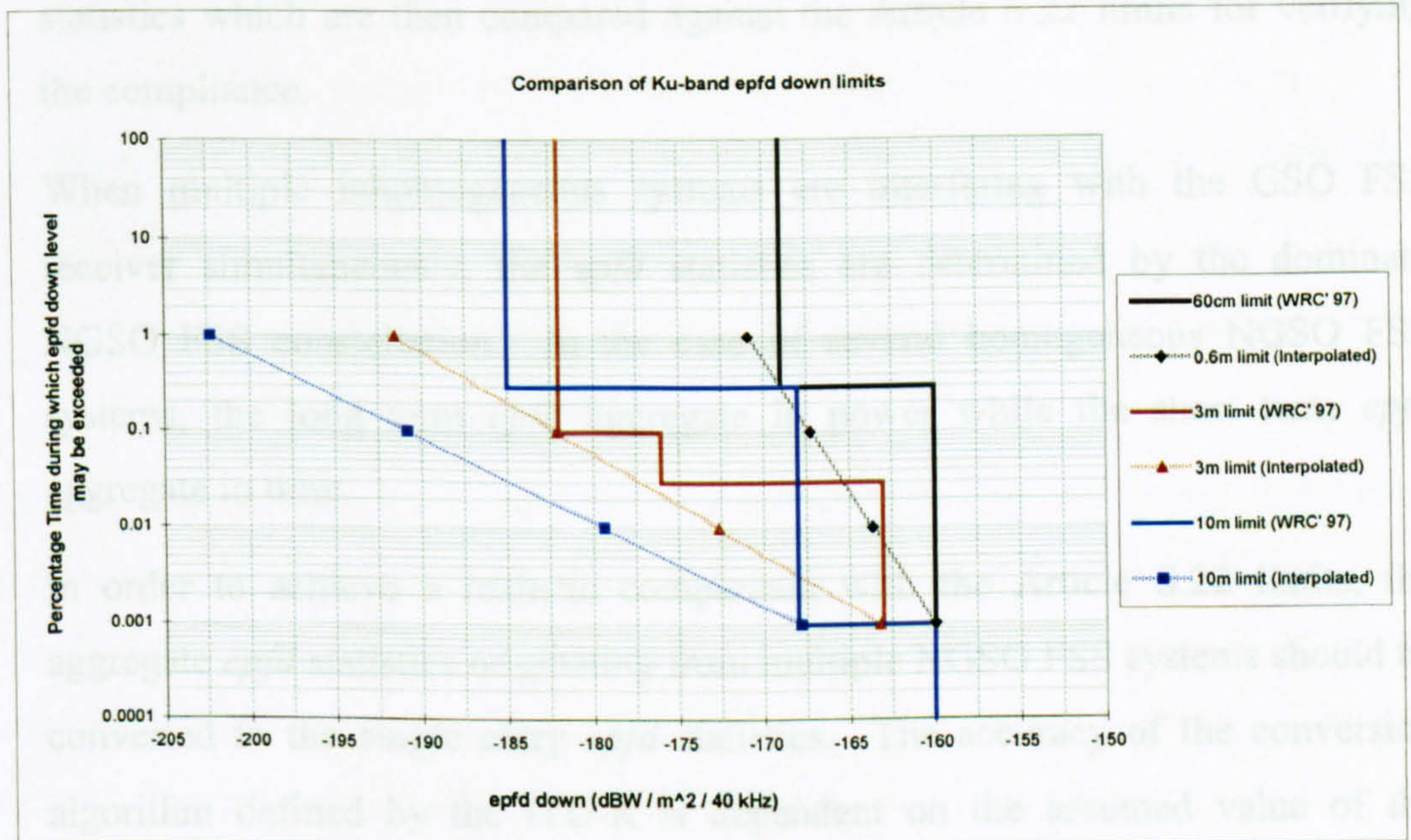


Figure 4.20: Comparison of $epfd_{down}$ limits

From the NGSO/GSO FSS spectrum sharing point of view, the $epfd_{down}$ limits derived from the empirical formula are not less stringent than those specified in the Article S.22. This indicates that the use of the above expression to derive $epfd_{down}$ limits for different antenna diameters does not result in $epfd_{down}$ limits that will make the Ku-band GSO FSS links more vulnerable against the NGSO FSS interference.

4.2.6 Discussion on Simulation Analysis

In the preceding sections, the use of the simulation analysis approach to examine the issues related to the revision of the Article S.22 *epfd* limits has been investigated. From the analysis presented, it is shown that:

- The GSO FSS parameters comprising the operating frequency, the maximum receiver antenna gain and the bandwidth are used to translate the aggregate interference statistics obtained from the simulation analysis into the *epfd* statistics which are then compared against the Article S.22 limits for verifying the compliance.
- When multiple inhomogeneous systems are interfering with the GSO FSS receiver simultaneously, the *epfd* statistics are determined by the dominant NGSO FSS constellation. In the case of several homogeneous NGSO FSS systems, the long term *epfd* aggregate in power while the short term *epfd* aggregate in time.
- In order to achieve a realistic comparison with the Article S.22 limits, the aggregate *epfd* statistics originating from multiple NGSO FSS systems should be converted to the single entry *epfd* statistics. The accuracy of the conversion algorithm defined by the ITU-R is dependent on the assumed value of the effective number of NGSO FSS systems. For example, when the actual number of NGSO FSS systems is less than the assumed value, the resultant single entry statistics are further away from the *epfd* limits than the actual single entry statistics.
- The use of the discontinuous *epfd* limits to check the compliance with the Article S.22 limits results in pessimistic conclusions as far as the NGSO FSS systems are concerned. The comparison against the continuous *epfd* limits based on the linear interpolation between the breakpoints is more realistic as, in practice, the NGSO FSS interference statistics are in the continuous form.

- The application of the empirical formula developed by the ITU-R to derive $epfd_{down}$ limits for the GSO FSS receiver antenna diameters not included in the Article S.22 has indicated that the resultant $epfd_{down}$ limits do not make the Ku-band GSO FSS links more vulnerable against the NGSO FSS interference than those specified in the Article S.22.

4.2.7 Implementation of Methodology A'

In this section, the primary objectives are:

- To present the use of an analytical approach to examine the feasibility of NGSO/GSO FSS spectrum sharing by implementing Methodology A', defined in Rec.1323 [109],
- To investigate the implications of the modifications to the rain fading prediction model, described in Rec.618 [89].

For the analysis purposes, two versions of Methodology A' model have been implemented and applied to the GSO Ku-2 link (parameters given in Table 3.2 in Chapter 3) to calculate the $epfd_{down}$ values at the Earth station receiver. The first version is based on the previous Rec.618 rain model while the second version employs the revised model. It should be noted that both prediction models are detailed in Chapter 2.

In order to apply Methodology A', it is necessary in the first instance to calculate the overall clear-sky GSO FSS link performance ($C/(N+I)_{TOTAL}$) and compare that figure against the short term link performance objectives to determine the available link margins. The calculated margins are then attributed to degradations due to propagation and aggregate NGSO FSS interference.

The GSO Ku-2 end-to-end link short term performance objectives are assumed to be: *13.5 dB to be exceeded for 98%* and *13.0 dB to be exceeded for 99%*. Table 4.4 illustrates the calculation procedure for the GSO Ku-2 clear-sky $C/(N+I)_{TOTAL}$.

UPLINK			
GSO Ku-2 Earth Station EIRP (dBW/0.77 MHz)	62.03		
Antenna Pointing Loss (dB)	0.5		
Free Space Path Loss Between GSO Ku-2 Earth Station Transmitter and GSO Ku-2 Satellite Receiver (dB)	207.1 (38,518 km at 14 GHz, Lat=51.5°)		
Atmospheric Attenuation (dB) (Rec.676, Simplified Model)	0.12 (Path Elevation ≈ 31 degrees)		
GSO Ku-2 Satellite Receiver Antenna Gain (dBi)	23.73		
Received Carrier Power (dBW/0.77 MHz)	$(C_{up}) = 62.03 - 0.5 - 207.1 - 0.12 + 23.73 = -121.96$		
GSO Ku-2 Satellite Receiver Noise Level (dBW/0.77 MHz)	$(N_{up})= k T_{SAT}B = -143.01$		
$(C/N)_{up}$ (dB)	$-121.96 - (-143.01) = 21.05$		
GSO Ku-2 Earth Station Transmitter Intermodulation $(C/I)_1$ (dB)	100		
GSO Ku-2 Earth Station Transmitter Polarisation Isolation $(C/I)_2$ (dB)	35		
GSO Ku-2 Satellite Receiver Cross Polarisation Isolation $(C/I)_3$ (dB)	30		
GSO Ku-2 Satellite Receiver Frequency Re-use Isolation $(C/I)_4$ (dB)	100		
GSO Ku-2 Uplink Clear-sky C/I due to Other GSO FSS Networks $(C/I)_5$ (dB)	23.95		
GSO Ku-2 Uplink Clear-sky C/I due to FS Networks $(C/I)_6$ (dB)	100		
Calculation of $(C/(N+I))_{UPLINK TOTAL}$:			
Degradation	dB	numeric	$1 / (numeric degradation)$
$(C/N)_{up}$	21.05	127.35	0.0079
$(C/I)_1$	100	10^{10}	10^{-10}
$(C/I)_2$	35	3162.28	0.0003
$(C/I)_3$	30	1000	0.0010
$(C/I)_4$	100	10^{10}	10^{-10}
$(C/I)_5$	23.95	248.31	0.0040
$(C/I)_6$	100	10^{10}	10^{-10}
$(1 / (C / (N+I)))_{UPLINK TOTAL}$ (numeric)			0.0132
$(C / (N+I))_{UPLINK TOTAL}$ (numeric)			75.78
$(C / (N+I))_{UPLINK TOTAL}$ (dB)			18.79

Table 4.4 (a): Clear-sky $C/(N+I)_{TOTAL}$

DOWNLINK			
GSO Ku-2 Satellite EIRP (dBW/0.77 MHz)		26.85	
GSO Ku-2 Earth Station Receiver Antenna Pointing Loss (dB)		0.5	
Free Space Path Loss Between GSO Ku-2 Satellite Transmitter and GSO Ku-2 Earth Station Receiver (dB)		205.6 (37,751 km at 12 GHz , Lat=43°)	
Atmospheric Attenuation (dB) (Rec.676, Simplified Model)		0.1 (Path Elevation ≈ 40.4 degrees)	
GSO Ku-2 Earth Station Receiver Antenna Gain (dBi)		49.66	
Received Carrier Power (dBW/0.77 MHz)		(C _{down}) = 26.85 – 0.5 – 205.6 – 0.1 + 49.66 = -129.69	
GSO Ku-2 Earth Station Receiver Noise Level (dBW/0.77 MHz)		(N _{down})= k T _{ES} B = -147.97	
(C/N) _{down} (dB)		-129.69 – (-147.97) = 18.28	
GSO Ku-2 Space Station Transmitter Cross Polarisation Isolation (C/I) ₁ (dB)		30	
GSO Ku-2 Space Station Transmitter Frequency Re-use Isolation (C/I) ₂ (dB)		100	
GSO Ku-2 Space Station Adjacent Transponder Isolation (C/I) ₃ (dB)		100	
GSO Ku-2 Space Station Transmitter Intermodulation (C/I) ₄ (dB)		24.1	
GSO Ku-2 Earth Station Receiver Polarisation Isolation (C/I) ₅ (dB)		3511.5	
GSO Ku-2 Downlink Clear-sky C / I due to Other GSO FSS Networks (C/I) ₆ (dB)		23.95	
GSO Ku-2 Downlink Clear-sky C / I due to FS Networks (C/I) ₇ (dB)		100	
Calculation of (C/(N+I))DOWNLINK TOTAL:			
Degradation	dB	numeric	1 / (numeric degradation)
(C/N) _{down}	18.28	67.30	0.0149
(C/I) ₁	30	1000	0.0010
(C/I) ₂	100	10 ¹⁰	10 ⁻¹⁰
(C/I) ₃	100	10 ¹⁰	10 ⁻¹⁰
(C/I) ₄	24.1	257.04	0.0039
(C/I) ₅	35	3162.28	0.0003
(C/I) ₆	23.95	248.31	0.0040
(C/I) ₇	100	10 ¹⁰	10 ⁻¹⁰
(1 / (C / (N+I))) DOWNLINK TOTAL (numeric)			0.0241
(C / (N+I)) DOWNLINK TOTAL (numeric)			41.51
(C / (N+I)) DOWNLINK TOTAL (dB)			16.18
Calculation of END-TO-END LINK (C / (N+I))			
(1 / (C / (N+I))) TOTAL (numeric) = (1 / (C / (N+I))) UPLINK TOTAL (numeric) + (1 / (C / (N+I))) DOWNLINK TOTAL (numeric)			
(1 / (C / (N+I))) TOTAL (numeric)		0.0132+0.0241 = 0.0373	
(C / (N+I)) TOTAL (numeric)		26.82	
(C / (N+I)) TOTAL (dB)		14.28	

Table 4.4 (b): Clear-sky $C/(N+I)_{\text{TOTAL}}$

As the end-to-end link short term performance requirements suggest that the $C/(N+I)_{TOTAL}$ should remain above 13.5 dB for 98% of the time and 13.0 dB for 99% of the time, the available margins are calculated to be :

- $14.28\text{ dB} - 13.5\text{ dB} \approx 0.78\text{ dB}$ not to be used by propagation and NGSO FSS interference for more than $100\% - 98\% = 2\%$ of the time,
- $14.28\text{ dB} - 13.0\text{ dB} \approx 1.28\text{ dB}$ not to be used by propagation and NGSO FSS interference for more than $100\% - 99\% = 1\%$ of the time.

The rain fading is the most significant space-to-Earth propagation mechanism at the Ku band frequencies. The Methodology A' requires the percentage time for which the available margin associated with the second short term GSO FSS link performance requirement (13.0 dB for 99% of the time) is exceeded due to rain fading.

As detailed in Chapter 2, the revised Rec.618 rain attenuation prediction model is valid in the range 0.001% to 5% (1% in the previous version). The rain degradations experienced on the uplink and the downlink should be convolved (assuming that the uplink and the downlink rain statistics are uncorrelated) if the end-to-end rain degradation statistics are required. The convolution process requires two complete rain fading statistics (i.e. probability density functions defined over all time percentages). Since the rain models are only valid over a very small range of time percentages, the rain degradation values corresponding to time percentages outside this range would have to be assumed if the convolution were applied.

In this research, it is assumed that the rain fading occurs on the uplink only or on the downlink only but not simultaneously. This approach removes the necessity of the convolution process and the ambiguity that would be introduced to the results because of the assumptions that would have to be made in deriving complete uplink and downlink rain fading statistics in the absence of rain models valid for all time percentages.

Table 4.5 illustrates parameter values calculated from the application of the previous and revised Rec.618 rain models.

Parameter	Previous Rec.618		Revised Rec.618	
	Uplink	Downlink	Uplink	Downlink
Rain Zone	E	A	E	A
$R_{0.01}$ (mm/h)	22	8	22	8
h_R (km)	2.8625	3.5	2.8625	3.5
L_S (km)	16.28	5.82	16.28	5.82
L_G (km)	16.02	4.65	16.02	4.65
L_O	25.16	31.04	-	-
$r_{0.01}$	0.61	0.87	0.697	0.172
L_R	-	-	11.36	5.82
$\eta_{0.01}$	-	-	0.26	0.34
k	0.027	0.018	0.027	0.018
α	1.15	1.21	1.15	1.21
γ_R (dB/km)	0.95	0.23	0.95	0.23
A_S (dB)	-	-	0.0457	0.0044
A_I (dB)	1.1336	0.1399	0.1693	0.0188
$A_{0.1}$ (dB)	3.6096	0.4456	0.8192	0.1096
$A_{0.01}$ (dB)	9.4466	1.1663	2.7938	0.4515
$A_{0.001}$ (dB)	20.2049	2.4945	6.7144	1.3106
Percentage time "p" for which $A_p = 1.28$ dB is exceeded	0.7920%	0.0076%	0.0463%	0.0011%

Table 4.5: Rain Attenuation

In addition to the rain fading, the overall link thermal noise temperature and the effective overall link noise temperature figures can be calculated on the basis of the information provided in the link budget:

- the transmission gain from the satellite receiver to the Earth station receiver is calculated from $C_{down} - C_{up} = (-129.69) - (-121.96) = -7.73$ dB, which is 0.169 numerically,
- the overall link thermal noise temperature is then calculated from *(Satellite Receiver Noise Temperature * Transmission Gain) + Earth Station Receiver Noise Temperature* = $(470 * 0.169) + 150 = 230$ K.
- the effective noise power in the receiver bandwidth is calculated from $C_{down} - (C/(N+I))_{TOTAL\ clear-sky} = (-129.69) - 14.28 = -143.97$ dBW/0.77MHz,
- the effective overall link noise temperature is then calculated from *Effective Noise Power (dBW/0.77MHz) – Boltzmann's Constant(dBW/KHz) –*

$10 \cdot \log(\text{Receiver Bandwidth (Hz)}) = -143.97 - (-228.6) - (10 \cdot \log(0.77 \cdot 10^6)) = 25.77 \text{ dBK}$ which is 378 K numerically.

It is important to note that the effective overall link noise temperature takes account of all degradations used in $C/(N+I)_{\text{TOTAL}}$ calculation and, therefore, should be used as a system noise temperature when translating maximum tolerable degradations (due to NGSO FSS interference) to equivalent power flux densities.

As mentioned previously, the Methodology A' uses simplified probability distribution functions (pdfs) to represent degradations due to the propagation effects and the NGSO FSS interference.

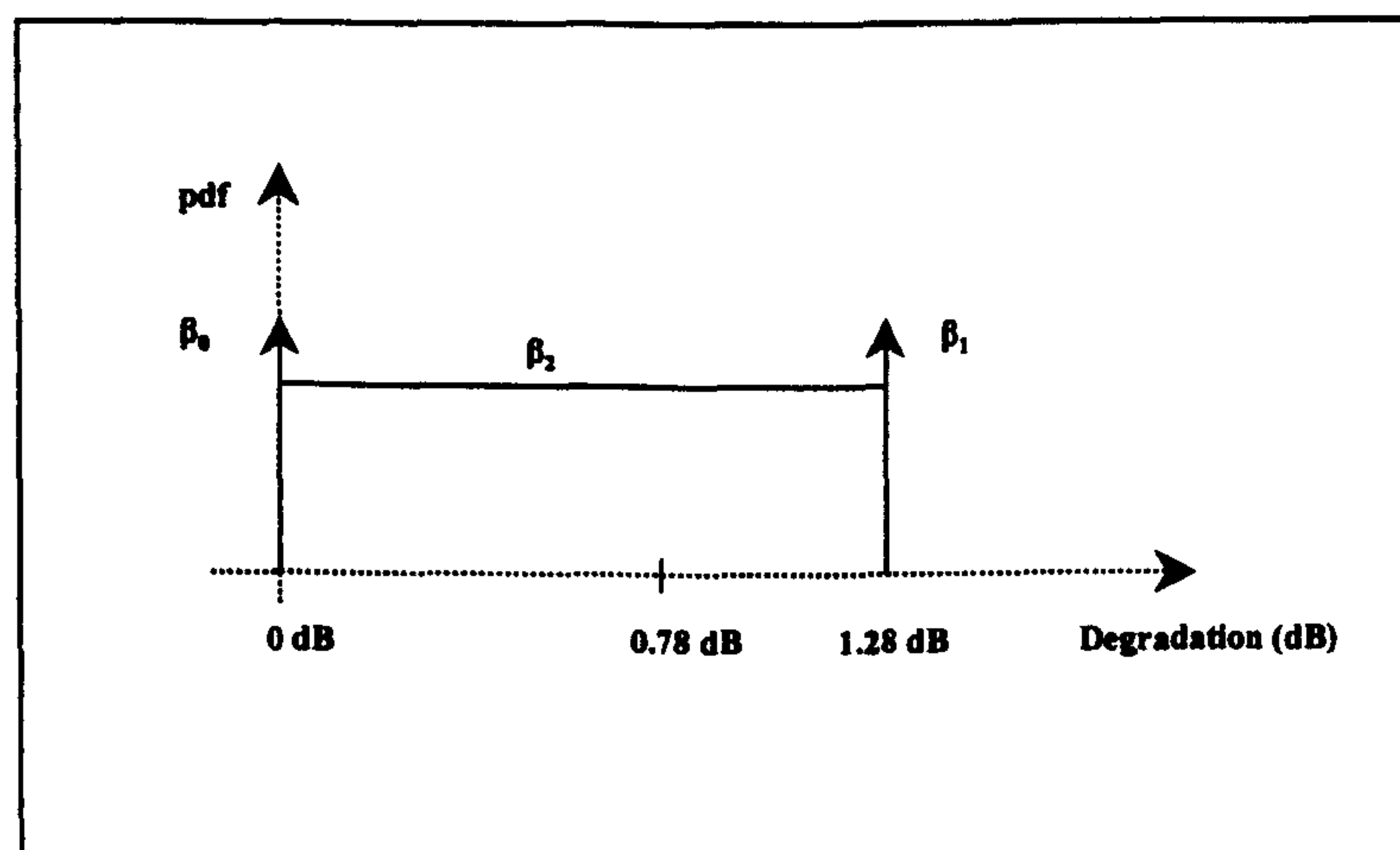


Figure 4.21: Rain Degradation pdf

The rain degradation pdf is represented by two arrows and a rectangle. It is important to note that:

- the distribution has to be defined across the range 0 to 1.28 dB as the largest margin available is 1.28 dB.
- the right hand side arrow represents the sum of any fades greater than 1.28 dB. According to rain fading calculations presented in Table 4.5, the previous Rec.618 rain model indicates that fades greater than 1.28 dB occur for 0.792% (i.e. $\beta_1 = 0.00792$) on the uplink or 0.0076% (i.e. $\beta_1 = 0.000076$) on the downlink. For the revised Rec.618 rain model, the associated percentages are calculated to

be 0.0463% (i.e. $\beta_1 = 0.000463$) on the uplink or 0.0011% (i.e. $\beta_1 = 0.000011$) on the downlink.

- the left hand side arrow represents the amount of time that there is no rain attenuation. It is important to note that the assumption for the value of percentage time for which no rain fading occurs (β_0) should be based on two criteria:
 - $\beta_0 \leq 100$ - unavailability percentage time (1%) associated with the second criterion (13 dB for 99% of the time)
 - and
 - $\beta_0 \geq 99\%$ in the previous Rec.618 model and $\beta_0 \geq 95\%$ in the revised Rec.618 model
- the probabilities between two arrows are represented by a rectangle where β_2 represents the average time percentage for the range of attenuation values 0 dB to 1.28 dB. The integral of the probability density function must equal unity, therefore, β_2 can be calculated from:

$$\beta_2 = ((1 - \beta_0) - \beta_1) / 1.28 \quad (4-5)$$

- Using the above equation, it can be shown that:

$$\beta_2 = ((1 - 0.99) - 0.00792) / 1.28 = 0.001625 \text{ (previous Rec.618, rain on the uplink)}$$

$$\beta_2 = ((1 - 0.99) - 0.000076) / 1.28 = 0.007753 \text{ (previous Rec.618, rain on the downlink)}$$

$$\beta_2 = ((1 - 0.98) - 0.000463) / 1.28 = 0.015214 \text{ (revised Rec.618, rain on the uplink)}$$

$$\beta_2 = ((1 - 0.98) - 0.000011) / 1.28 = 0.015566 \text{ (revised Rec.618, rain on the downlink)}$$

Using the similar approach, degradations in the GSO Ku-2 link performance due to the aggregate NGSO FSS interference are calculated.

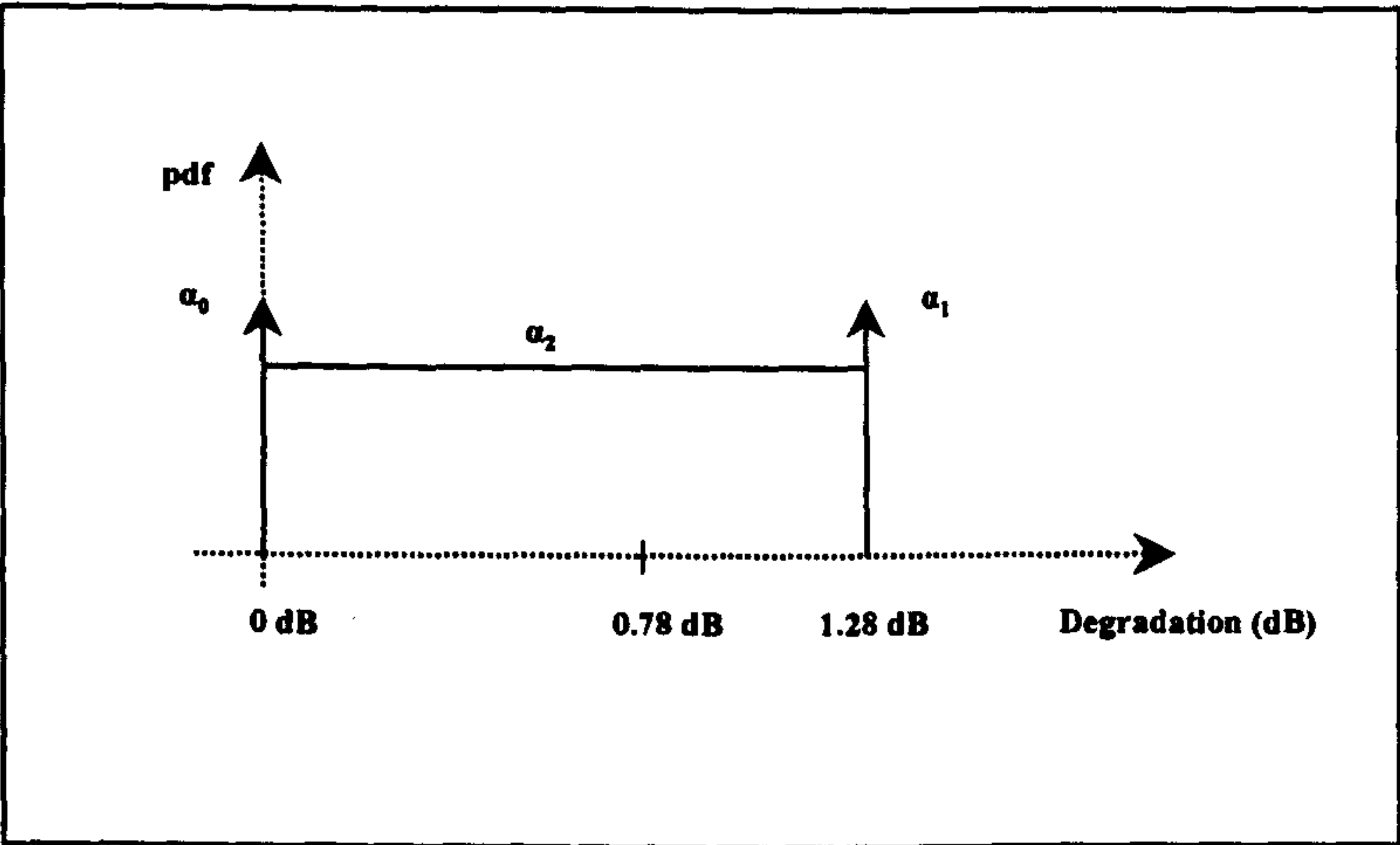


Figure 4.22: NGSO FSS Interference Degradation pdf

As before, the arrow on the right hand side indicates that interference degradation values greater than 1.28 dB occur for $100\alpha_1\%$ of the time. The left arrow represents the amount of time ($100\alpha_0\%$) that there is no degradation due to short term interference. The value α_2 represents the average percentage for degradation values in the range of 0 dB to 1.28 dB and can be calculated from:

$$\alpha_0 = 1 - \alpha_1 - 1.28\alpha_2 \tag{4-6}$$

In order to assess the joint effects of the rain and the NGSO FSS interference, two pdfs need to be convolved. The resultant overall degradation pdf is illustrated below.

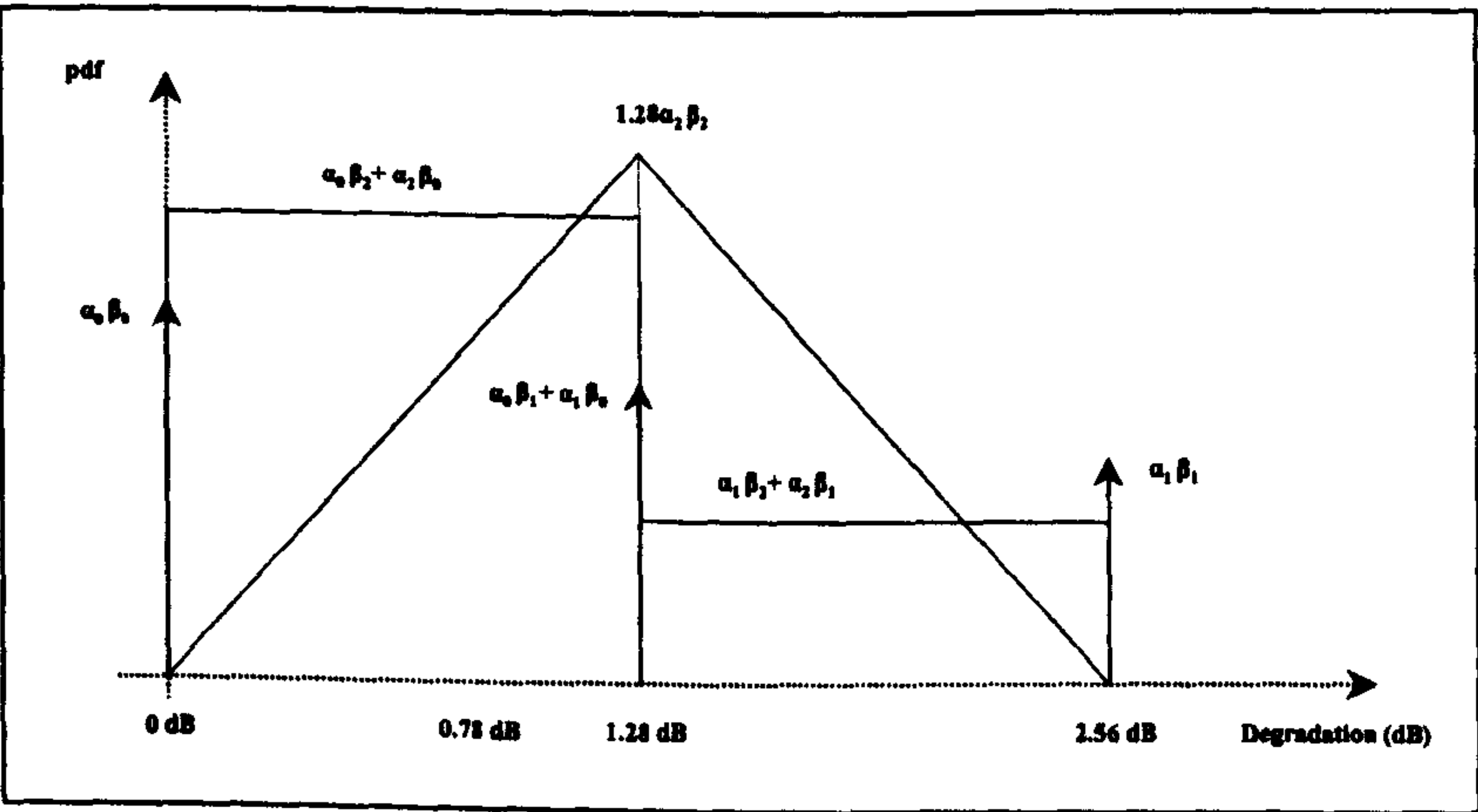


Figure 4.23: Overall Degradation pdf

On the basis of the second short term GSO Ku-2 performance criterion (*13.0 dB* for 99%), the integration of the overall degradation pdf from *1.28 dB* upwards must be equal to or less than $100\% - 99\% = 1\%$ (i.e. *0.01*) if the total degradation is to remain below *1.28 dB* for 99% of the time. This can be represented by the following expression:

$1.28 \alpha_2 \beta_2 (2.56-1.28)/2 + \alpha_0 \beta_1 + \alpha_1 \beta_0 + (\alpha_1 \beta_2 + \alpha_2 \beta_1) (2.56-1.28) + \alpha_1 \beta_1 = 0.01 \quad (4-7)$

Similarly, on the basis of the first short term link performance criterion (*13.5 dB* for 98%), the integration of the convolution pdf between *0.78 dB* and *1.28 dB* must be equal to or less than $0.02-0.01$ if total degradation is to remain below *0.78 dB* for 98% of the time. This can be represented by the following expression:

$1.28 \alpha_2 \beta_2 (1.28-0)/2 - 0.78 \alpha_2 \beta_2 (0.78-0)/2 + (1.28-0.78) (\alpha_0 \beta_2 + \alpha_2 \beta_0) = 0.02-0.01 \quad (4-8)$

Substituting α_0 with $(1 - \alpha_1 - 1.28 \alpha_2)$ and using appropriate values for β_0 , β_1 and β_2 it is possible to solve the equations for α_1 and α_2 . Table 4.6 illustrates α_0 , α_1 and α_2 values calculated for the previous and revised Rec.618 rain models:

	α_0	α_1	α_2
Previous Rec.618, Uplink Rain	0.974072	0.002071	0.018577
Previous Rec.618, Downlink Rain	0.974106	0.009845	0.012498
Revised Rec.618, Uplink Rain	0.984035	0.009478	0.005051
Revised Rec.618, Downlink Rain	0.984034	0.009929	0.004701

Table 4.6: Calculated Parameters for NGSO FSS Degradation

Taking these values into account, Table 4.7 can be constructed:

	Maximum percentage time for which NGSO FSS short term interference can cause a degradation > 1.28 dB ($100\alpha_1\%$)	Maximum percentage time for which NGSO FSS short term interference can cause a degradation > 0.78 dB ($100\{\alpha_1+[1.28-0.78] \alpha_2 \}$)	Percentage time for which there should be no degradation due to NGSO FSS short term interference ($100\alpha_0$)
Previous Rec.618, Uplink Rain	0.21%	1.14%	97.41%
Previous Rec.618, Downlink Rain	0.98%	1.61%	97.41%
Revised Rec.618, Uplink Rain	0.95%	1.20%	98.40%
Revised Rec.618, Downlink Rain	0.99%	1.23%	98.40%

Table 4.7: Interpretation of Calculated Parameters for NGSO FSS Degradation

As can be seen, the percentage times are associated with the degradations due to the NGSO FSS interference. Therefore, a conversion algorithm needs to be defined for obtaining $epfd_{down}$ values from the GSO FSS link degradations. The algorithm used in this study, initially, relates the interference degradations to the GSO FSS link I/N ratio and, then, defines the $epfd$ as a function of I/N . The following steps summarise the algorithm:

- Assume that the degradation in GSO FSS link's C/N due to NGSO FSS interference (I) is X dB,
- This can be expressed as:

$$10 \log \left(\frac{C}{N} \right) - 10 \log \left(\frac{C}{N+I} \right) = X \text{ dB} \quad (4-9)$$

- It is then possible to determine I/N (dB) ratio in terms of X (dB) as following:

$$\begin{aligned} 10 \log \left(\frac{C}{N} \right) - 10 \log \left(\frac{C}{N+I} \right) &= X \text{ dB} \\ 10 \log \left(\frac{\frac{C}{N}}{\frac{C}{N+I}} \right) &= X \text{ dB} \\ 10 \log \left(1 + \frac{I}{N} \right) &= X \text{ dB} \\ \frac{I}{N} &= 10^{\left(\frac{X(\text{dB})}{10} \right)} - 1 \\ \frac{I}{N} (\text{dB}) &= 10 \log \left(10^{\left(\frac{X(\text{dB})}{10} \right)} - 1 \right) \end{aligned} \quad (4-10)$$

- In § 4.2.1, it is shown that

$$epfd = I + 10 \log \frac{4\pi}{\lambda^2} - 10 \log G_{r,\max} + 10 \log \left(\frac{\text{RefBandwidth}}{\text{RxBandwidth}} \right) \quad (4-11)$$

where $epfd$ is the equivalent power flux-density in (dBW/m^2 in the reference bandwidth (RefBandwidth)), I is the aggregate interference at the GSO FSS receiver (in dBW in the receiver bandwidth (RxBandwidth)), $G_{r,\max}$ is the

maximum gain (as a ratio) of the GSO FSS station receiver antenna and λ is the wavelength (in metres).

- The above equation can be re-written as:

$$I = epfd - 10 \log \frac{4\pi}{\lambda^2} + 10 \log G_{r,\max} - 10 \log \left(\frac{\text{RefBandwidth}}{\text{RxBandwidth}} \right) \quad (4-12)$$

- The $epfd$ can be expressed as a function of I/N ratio as following:

$$\begin{aligned} \left(\frac{I}{N} \right) + N &= epfd - 10 \log \frac{4\pi}{\lambda^2} + 10 \log G_{r,\max} - 10 \log \left(\frac{\text{RefBandwidth}}{\text{RxBandwidth}} \right) \\ \left(\frac{I}{N} \right) + 10 \log(kTB) &= epfd - 10 \log \frac{4\pi}{\lambda^2} + 10 \log G_{r,\max} - 10 \log \left(\frac{\text{RefBandwidth}}{\text{RxBandwidth}} \right) \end{aligned} \quad (4-13)$$

- Hence,

$$epfd = \left(\frac{I}{N} \right) + 10 \log(kTB) + 10 \log \frac{4\pi}{\lambda^2} - 10 \log G_{r,\max} + 10 \log \left(\frac{\text{RefBandwidth}}{\text{RxBandwidth}} \right) \quad (4-14)$$

where $epfd$ is the equivalent power flux-density (dBW/m² in the reference bandwidth), I is the aggregate interference at the GSO FSS receiver (dBW in the receiver bandwidth), N is the noise power at the GSO FSS receiver (dBW in the receiver bandwidth), k is the Boltzmann constant ($1.379 * 10^{-23}$ W/KHz), T is the effective overall link noise temperature (in Kelvin), B is the receiver bandwidth (Hz), $G_{r,\max}$ is the maximum gain (as a ratio) of the GSO FSS station receiver antenna, λ is the wavelength (in metres).

Taking the results given in Table 4.7 and the above described conversion algorithm into account, the $epfd_{down}$ values at the GSO Ku-2 Earth station receiver are calculated and illustrated in Table 4.8.

Degradation (dB)	I/N (dB)	$epfd_{down}$ (dBW m ² / 4 kHz)	% time for which $epfd_{down}$ may be exceeded			
			Previous Rec.618, Uplink Rain	Previous Rec.618, Downlink Rain	Revised Rec.618, Uplink Rain	Revised Rec.618, Downlink Rain
1.28	-4.63	-178.04	0.21	0.98	0.95	0.99
0.78	-7.04	-180.44	1.14	1.61	1.20	1.23

Table 4.8: $epfd_{down}$ Values

As the GSO Ku-2 Earth station antenna size is 3 metre, the calculated $epfd_{down}$ values can directly be compared against the Ku-band limits defined for 3 m antennas in the Article S.22 [67].

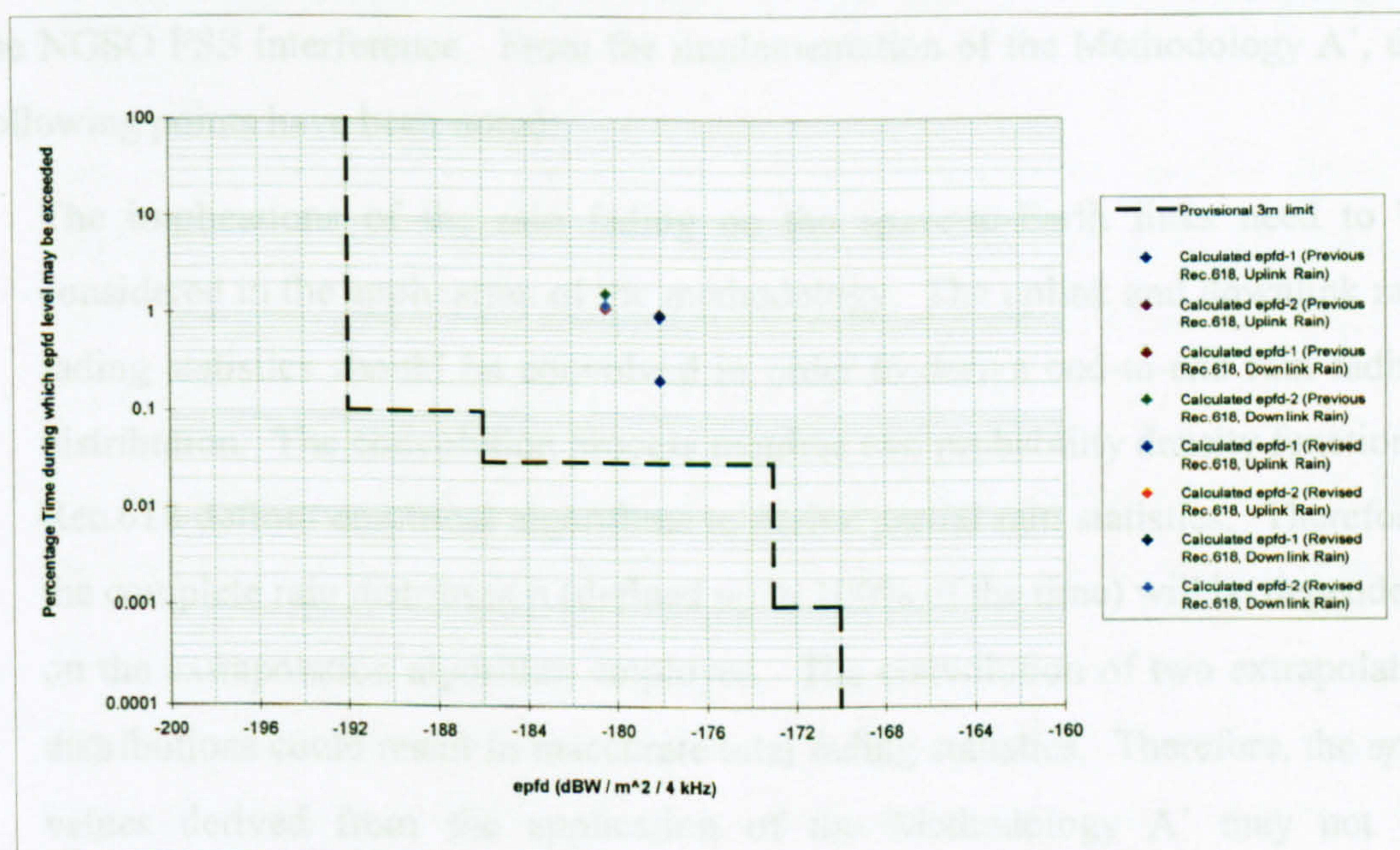


Figure 4.24: Comparison of Calculated $epfd_{down}$ Values Against Article S.22 Limits

The figure includes eight $epfd_{down}$ results corresponding to different combinations of the assumptions related to the rain fading model and whether the fading occurs on the downlink or the uplink only. It is important to note that the points representing $epfd_{down}$ values correspond to the level of maximum interference acceptable to the GSO Ku-2 link. Therefore, any calculated $epfd_{down}$ level on the right-hand side of the limits indicates that the link will be protected sufficiently. The results suggest

that, for the GSO Ku-2 link, the $epfd_{down}$ limits given in the Article S.22 provide adequate protection from the aggregate NGSO FSS interference.

4.2.8 Discussion on Analytic Approach

In the preceding section, the use of the analytical approach to investigate the Article S.22 $epfd$ limits has been presented by implementing the Methodology A'. It has been shown that the methodology is based on the calculation of the maximum tolerable interference $epfd$ levels on the basis of the GSO FSS link performance requirements. The calculated values are compared against the regulatory limits to determine whether the GSO FSS link examined will be sufficiently protected from the NGSO FSS interference. From the implementation of the Methodology A', the following points have been noted:

- The implications of the rain fading on the space-to-Earth links need to be considered in the application of the methodology. The uplink and downlink rain fading statistics should be convolved in order to derive end-to-end rain fading distribution. The convolution process requires two probability density functions. Rec.618 defines empirical algorithms to derive partial rain statistics. Therefore, the complete rain distribution (defined up to 100% of the time) will be dependent on the extrapolation algorithm employed. The convolution of two extrapolated distributions could result in inaccurate total fading statistics. Therefore, the $epfd$ values derived from the application of the Methodology A' may not be representative. One way of getting around this problem is the assumption of the rain fading occurring on the uplink and downlink separately, but not simultaneously. This assumption eliminates the ambiguity that would be introduced when deriving complete rain fading statistics.
- The rain fading prediction model defined in the revised Rec.618 employs the following formulae to calculate the rain fading for a given percentage time:

$$\beta(p) := \begin{cases} (-0.005(|\phi| - 36)) & \text{if } (p < 1) \cdot (|\phi| < 36) \cdot (\theta \geq 25) \\ 0 & \text{if } (p \geq 1) + (|\phi| \geq 36) \\ ((-0.005(|\phi| - 36)) + 1.8 - (4.25 \sin(\theta_{\text{rad}}))) & \text{otherwise} \end{cases}$$

$$A(p) := A_{0.01} \left(\frac{p}{0.01} \right)^{-\left[0.655 + (0.033 \cdot \ln(p)) - (0.045 \cdot \ln(A_{0.01})) - (\beta(p) \cdot (1 - p) \cdot \sin(\theta_{\text{rad}}))\right]}$$

(4-15)

where ϕ is the latitude of GSO FSS Earth station (in degrees), θ is the GSO FSS Earth station elevation angle (in degrees), p is the percentage time for which rain fading exceeds the value of $A(p)$, $A_{0.01}$ is the fading exceeded for 0.01%.

- The revised model does not specify any algorithm to be used to derive a percentage time for which a given rain fading value is exceeded. Therefore, a bisection method, in which an exceedence percentage is obtained iteratively by bisecting the rain fading function, has been implemented.
- In the analysis, in order to ensure protection against the worst case NGSO FSS interference levels, it is assumed that rain fading occurs on the wanted path but not on the interfering paths.
- Rec.1323 allows, at most, an unavailability due to NGSO FSS interference to be 10% of the total stated GSO FSS link unavailability objectives. Therefore, for example, the GSO Ku-2 link would tolerate 1.28 dB degradation due to the NGSO FSS interference at most 0.1% of the time as the total stated unavailability time associated with the link performance criterion is 1%. However, the analysis has shown that the rain fades occur very short periods of time (e.g. 0.0011% for the revised Rec.618 downlink rain (see Table 4.5)) and the total stated unavailability time attributed to the rain fading (e.g. 0.9%) is not entirely taken up by rain. Therefore, unavailability due to the NGSO FSS interference takes up the greatest share of the total stated unavailability (e.g. 0.99% for the revised Rec.618 downlink rain case (see Table 4.7)). In order to

comply with the 10% criterion, the total unavailability target should be equal to the sum of the “*total achieved unavailability*” (derived from the Rec.618 rain models) and 10% of the “*total stated unavailability*”.

- In some cases, the GSO FSS link margin may be greater than the maximum rain fading obtained for 0.001%. In those circumstances, it is reasonable to assume that the rain fading function is uniform for exceedence percentages less than 0.001%.
- The methodology does not include any statement with regard to the value of percentage time for which no rain fading occurs (β_o). Two criteria should be taking into account for the assumption of β_o value:
 - 1) $\beta_o \leq 100$ - unavailability percentage time associated with the second short term performance criteria,
 - 2) $\beta_o \geq 99\%$ in the previous Rec.618 model and $\beta_o \geq 95\%$ in the revised Rec.618 model.
- The translation from the GSO FSS link degradation to the *epfd* should take account of all degradations in the GSO FSS link budget. Therefore, the effective overall link noise temperature should be used as the system noise temperature.
- The Article S.22 limits are defined for limiting interference from a single NGSO FSS system while Methodology A' considers the implications of aggregate NGSO FSS interference.

4.3 Impact of GSO FSS Earth Station Reference Antenna Patterns

The GSO FSS Earth station reference radiation pattern defined in Rec.1323 [109] represents an envelope of the side-lobe peaks. Peak envelope reference patterns are required for interference analysis involving a single fixed transmitter and receiver to ensure that the worst case interference scenario is covered. With the introduction of the NGSO FSS systems, it is argued that sharing studies should be based on reference patterns taking account of troughs and peaks in the gain pattern as the level

of interference will vary substantially with the time due to dynamic nature of the sharing environment.

In line with this requirement, Rec.1428 [140] defining a new Earth station reference antenna pattern based on the average gain envelope has been developed for use in the interference analysis involving NGSO FSS systems operating in the 10.7-30 GHz band.

In this research, a Monte Carlo simulator has been designed to simulate the interference models aiming to examine the implications of the use of both patterns in a typical NGSO/GSO FSS sharing scenario.

4.3.1 Reference Radiation Patterns

The GSO FSS Earth station reference antenna pattern defined in Rec.1323 is formulated as following:

$\text{Rec1323ReferencePattern}(\phi) :=$	$ \begin{aligned} & G_{\max} - \left[2.5 \cdot 10^{-3} \cdot \left(\frac{D}{\lambda} \cdot \phi \right)^2 \right] \quad \text{if } 0 \leq \phi < \phi_m \\ & G_1 \quad \text{if } \phi_m \leq \phi < \phi_r \\ & 29 - (25 \cdot \log(\phi)) \quad \text{if } \phi_r \leq \phi < 36.3 \\ & -10 \quad \text{if } 36.3 \leq \phi \leq 180 \end{aligned} $
---	---

(4-16)

where

D antenna diameter λ wavelength $G_1 := (-1) + \left(15 \cdot \log \left(\frac{D}{\lambda} \right) \right)$ $\phi_m := \left(20 \cdot \frac{\lambda}{D} \right) \cdot \sqrt{G_{\max} - G_1}$ $\phi_r := 15.85 \left(\frac{D}{\lambda} \right)^{-0.6}$

(4-17)

It is noted that the Rec.1323 reference pattern, as it stands, does not “work” for the situations where $D/\lambda < 100$ because the angle breakpoints become discontinuous.

The Rec.1323 reference pattern originates from the APS8 Annex III pattern and it is obtained by suppressing sidelobe envelopes, defined for $D/\lambda \geq 100$, by 3 dB. In order to have a complete antenna pattern, i.e. to include the cases where $D/\lambda < 100$, the APS8 Annex III pattern (defined for $D/\lambda < 100$) is modified by applying the same 3 dB reduction approach. The formulae representing the complete Rec.1323 antenna pattern are shown below.

$\text{Rec1323CompleteReferencePattern}(\phi) :=$	$\begin{aligned} &\text{if } \frac{D}{\lambda} < 100 \\ &\quad \left \begin{aligned} &G_{\max} - \left[2.5 \cdot 10^{-3} \cdot \left(\frac{D}{\lambda} \cdot \phi \right)^2 \right] \quad \text{if } 0 \leq \phi < \phi_m \\ &G_l \quad \text{if } \phi_m \leq \phi < 100 \cdot \frac{\lambda}{D} \\ &49 - \left(10 \cdot \log \left(\frac{D}{\lambda} \right) \right) - (25 \cdot \log(\phi)) \quad \text{if } 100 \cdot \frac{\lambda}{D} \leq \phi < 36.3 \\ &10 - \left(10 \cdot \log \left(\frac{D}{\lambda} \right) \right) \quad \text{if } 36.3 \leq \phi \leq 180 \end{aligned} \right. \\ &\text{if } \frac{D}{\lambda} \geq 100 \\ &\quad \left \begin{aligned} &G_{\max} - \left[2.5 \cdot 10^{-3} \cdot \left(\frac{D}{\lambda} \cdot \phi \right)^2 \right] \quad \text{if } 0 \leq \phi < \phi_m \\ &G_l \quad \text{if } \phi_m \leq \phi < \phi_r \\ &29 - (25 \cdot \log(\phi)) \quad \text{if } \phi_r \leq \phi < 36.3 \\ &-10 \quad \text{if } 36.3 \leq \phi \leq 180 \end{aligned} \right. \end{aligned}$
---	--

(4-18)

The Rec.1428 pattern is described as following:

Proposed_Pattern (ϕ , D) :=	<div data-bbox="948 435 1147 517">if $20 \leq \frac{D}{\lambda} \leq 25$</div> <div data-bbox="1002 538 1831 1040"> $\left \begin{array}{l} G_{\max_F}(D) - \left[2.5 \cdot 10^{-3} \cdot \left(\frac{D}{\lambda} \cdot \phi \right)^2 \right] \text{ if } 0 \leq \phi < \phi_{m_F}(D) \\ G_{l_F}(D) \text{ if } \phi_{m_F}(D) \leq \phi < 95 \cdot \frac{\lambda}{D} \\ 29 - 25 \cdot \log(\phi) \text{ if } 95 \cdot \frac{\lambda}{D} \leq \phi < 33.1 \\ (-9) \text{ if } 33.1 \leq \phi < 80 \\ (-5) \text{ if } 80 \leq \phi \leq 180 \end{array} \right$ </div> <div data-bbox="948 1061 1168 1143">if $25 < \frac{D}{\lambda} \leq 100$</div> <div data-bbox="1002 1164 1831 1735"> $\left \begin{array}{l} G_{\max_F}(D) - \left[2.5 \cdot 10^{-3} \cdot \left(\frac{D}{\lambda} \cdot \phi \right)^2 \right] \text{ if } 0 \leq \phi < \phi_{m_F}(D) \\ G_{l_F}(D) \text{ if } \phi_{m_F}(D) \leq \phi < 95 \cdot \frac{\lambda}{D} \\ 29 - 25 \cdot \log(\phi) \text{ if } 95 \cdot \frac{\lambda}{D} \leq \phi < 33.1 \\ (-9) \text{ if } 33.1 \leq \phi < 80 \\ (-4) \text{ if } 80 \leq \phi < 120 \\ (-9) \text{ if } 120 \leq \phi \leq 180 \end{array} \right$ </div> <div data-bbox="948 1756 1106 1838">if $\frac{D}{\lambda} > 100$</div> <div data-bbox="1002 1859 1831 2398"> $\left \begin{array}{l} G_{\max_S}(D) - \left[2.5 \cdot 10^{-3} \cdot \left(\frac{D}{\lambda} \cdot \phi \right)^2 \right] \text{ if } 0 \leq \phi < \phi_{m_S}(D) \\ G_{l_S}(D) \text{ if } \phi_{m_S}(D) \leq \phi < \phi_{r_S}(D) \\ 29 - 25 \cdot \log(\phi) \text{ if } \phi_{r_S}(D) \leq \phi < 10 \\ 34 - 30 \cdot \log(\phi) \text{ if } 10 \leq \phi < 34.1 \\ (-12) \text{ if } 34.1 \leq \phi < 80 \\ (-7) \text{ if } 80 \leq \phi < 120 \\ (-12) \text{ if } 120 \leq \phi \leq 180 \end{array} \right$ </div>
-----------------------------------	---

(4-19)

where

$$\begin{aligned}
 G1_F &:= 29 - 25 \cdot \log \left(95 \cdot \frac{\lambda}{D} \right) \\
 Gmax_F &:= \left(20 \cdot \log \left(\frac{D}{\lambda} \right) \right) + 7.7 \\
 \phi m_F &:= \left(20 \cdot \frac{\lambda}{D} \right) \cdot \sqrt{Gmax_F - G1_F} \\
 G1_S &:= -1 + 15 \cdot \log \left(\frac{D}{\lambda} \right) \\
 Gmax_S &:= \left(20 \cdot \log \left(\frac{D}{\lambda} \right) \right) + 8.4 \\
 \phi m_S &:= \left(20 \cdot \frac{\lambda}{D} \right) \cdot \sqrt{Gmax_S - G1_S} \\
 \phi r_S &:= 15.85 \cdot \left(\frac{D}{\lambda} \right)^{-0.6}
 \end{aligned}
 \tag{4-20}$$

Figures 4.25 and 4.26 illustrate both patterns for the small and large antennas where $D/\lambda < 100$ and $D/\lambda \geq 100$.

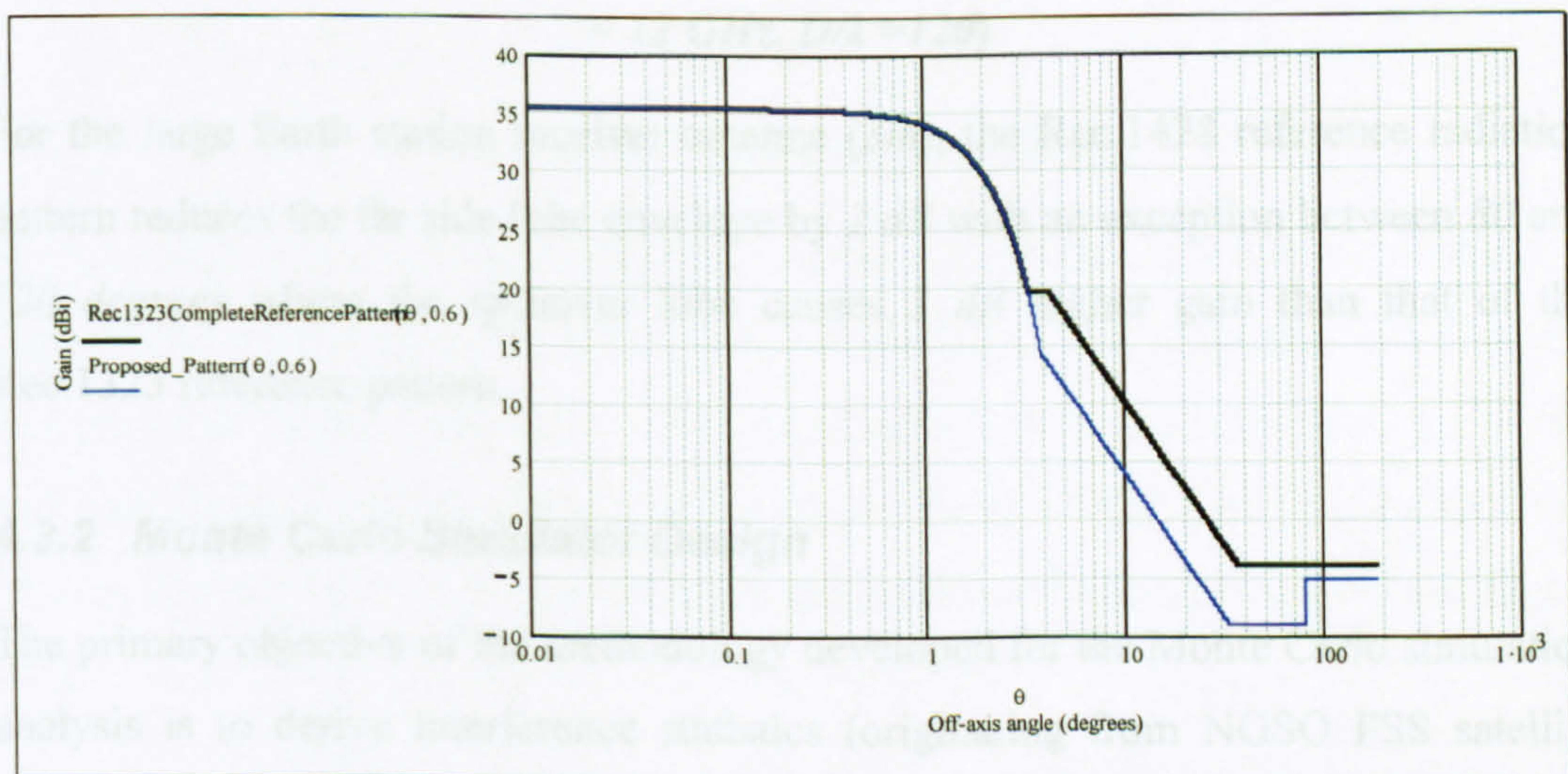


Figure 4.25: Comparison of Reference Patterns (*Diameter* = 0.6 metre, *Frequency* = 12 GHz, $D/\lambda = 24$)

For the small Earth station receiver antenna ($0.6m$), the comparison of two patterns indicates that the Rec.1428 reference pattern sidelobes are reduced by some 5 dB. The far side lobe envelope has a peak between 80 - 180 degrees off-axis angles, which is attributed to the “spillover effect”. This effect decreases the amount of far side lobe suppression to 1 dB.

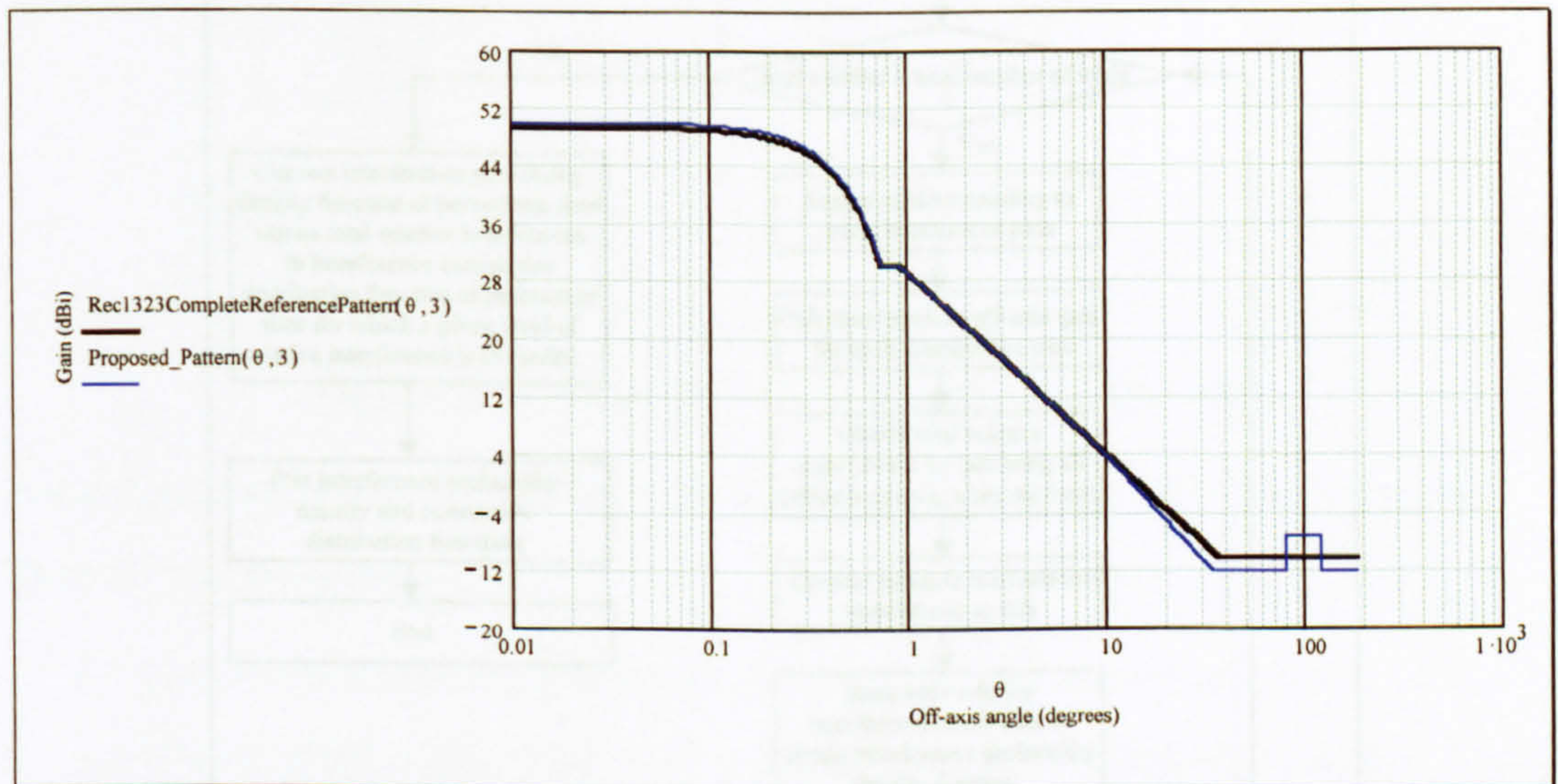


Figure 4.26: Comparison of Reference Patterns (*Diameter* = 3 metre, *Frequency* = 12 GHz, $D/\lambda = 120$)

For the large Earth station receiver antenna ($3m$), the Rec.1428 reference radiation pattern reduces the far side lobe envelope by 2 dB with an exception between 80 and 120 degrees where the spillover lobe causes 3 dB higher gain than that of the Rec.1323 reference pattern.

4.3.2 Monte Carlo Simulator Design

The primary objective of the methodology developed for the Monte Carlo simulation analysis is to derive interference statistics (originating from NGSO FSS satellite transmitters) at Earth station receivers operating with GSO FSS satellites. The analysis algorithm requires input parameters including an NGSO FSS system orbit height, a GSO FSS Earth station receiver elevation angle and a number of NGSO FSS interference paths to be considered in each simulation trial. The procedure

illustrated in Figure 4.27 is then applied to produce both interference probability density and cumulative distribution functions.

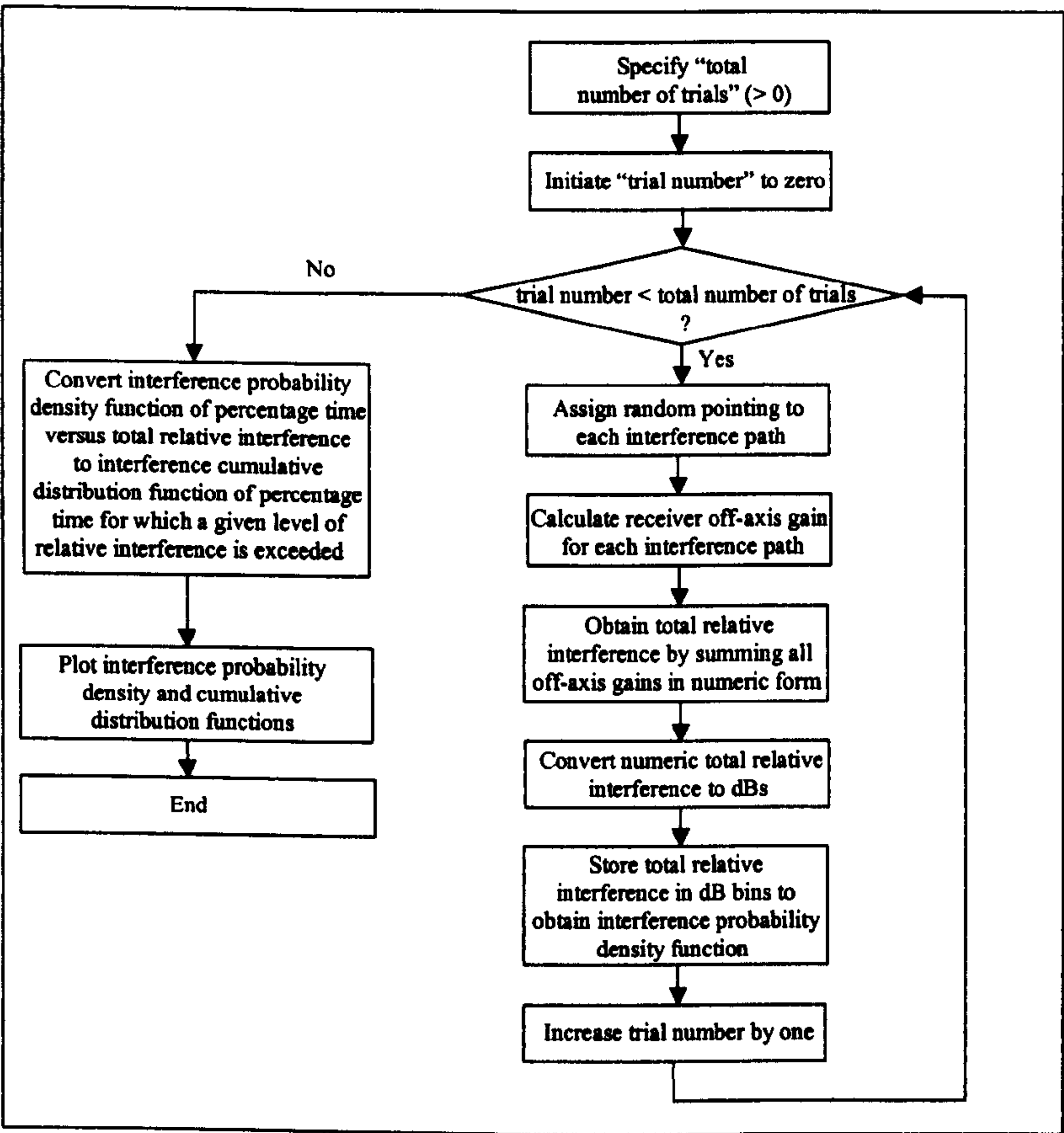


Figure 4.27: Simulation Algorithm

The key step in the simulation algorithm is the assignment of a random pointing to each NGSO FSS interference path in simulation trials. This algorithm needs to take account of the higher probability of an interference entry originating from an NGSO FSS satellite at a lower elevation angle as seen from a GSO Earth station receiver. The principles of the algorithm can be explained using the geometry shown in Figure 4-28..

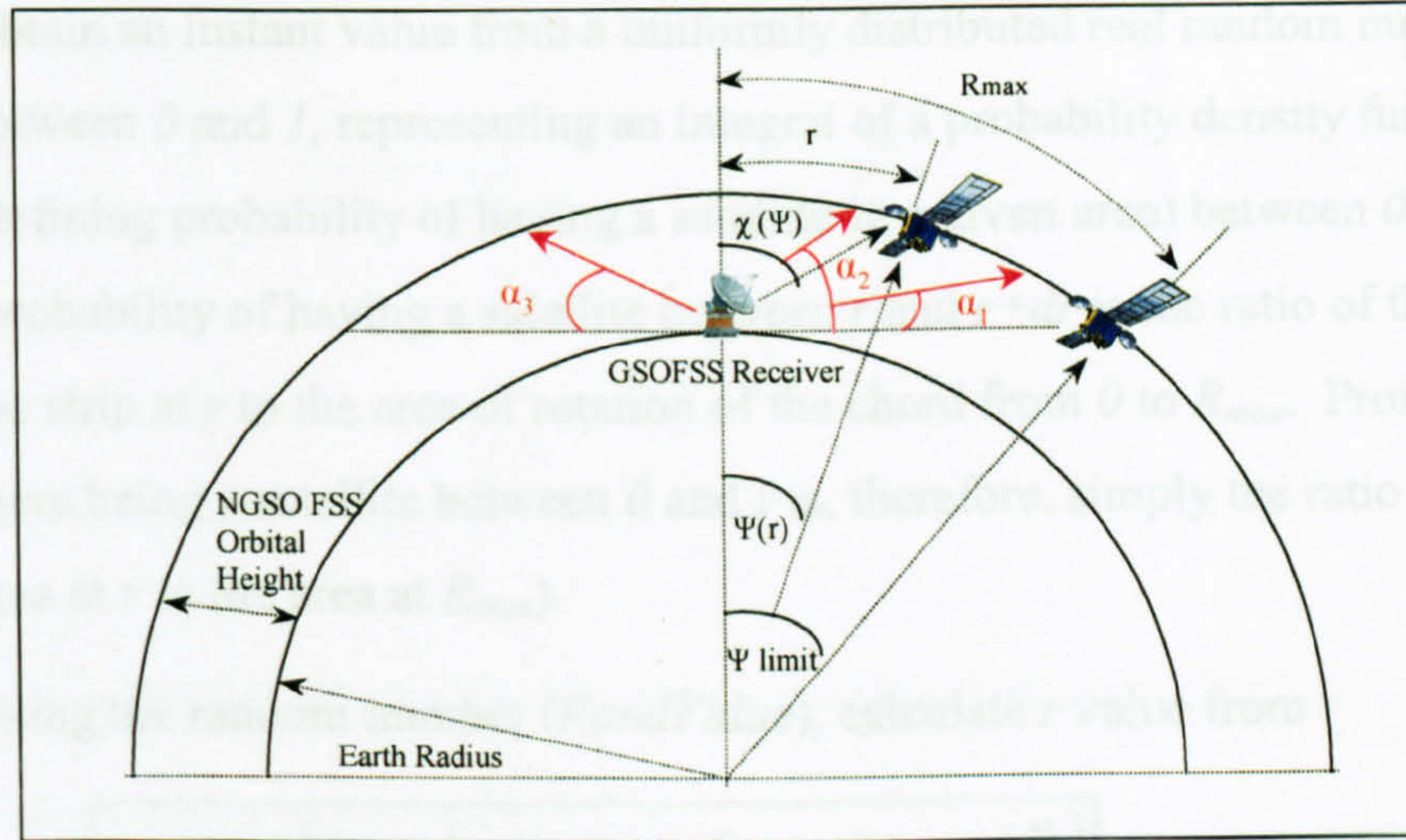


Figure 4.28: Random Off-axis Angle Assignment

Assuming that the NGSO satellite is in the same plane as the GSO Earth station receiver and positioned at ' \mathbf{r} ':

- Interference path off-axis angle at the GSO Earth station receiver is $(90 - \alpha_1 - \chi(\psi))$, if the GSO Earth station receiver elevation angle is α_1 .
- Interference path off-axis angle at the GSO Earth station receiver is $(\alpha_2 - 90 + \chi(\psi))$, if the GSO Earth station receiver elevation angle is α_2 .
- Interference path off-axis angle at the GSO Earth station receiver is $(\chi(\psi) + 90 - \alpha_3)$, if the GSO Earth station receiver elevation angle is α_3 .

In order to accommodate all three cases, the random off-axis assignment algorithm uses the NGSO FSS satellite and the GSO FSS Earth station position vectors. The algorithm is based on the vector analysis and explained below:

- Using the NGSO FSS satellite altitude, calculate ψ_{limit} corresponding to the maximum angle, as seen from the Earth centre, between the GSO Earth station receiver location and a point on the orbit shell for which the Earth station elevation angle is 0 degrees.
- From ψ_{limit} , calculate R_{max} corresponding to the radius of an area over the surface of the part of the orbit shell visible from the GSO Earth station.

- Obtain an instant value from a uniformly distributed real random number between 0 and 1, representing an integral of a probability density function (defining probability of having a satellite in a given area) between 0 and r (probability of having a satellite between r and $r+dr$ is the ratio of the area of the strip at r to the area of rotation of the chord from 0 to R_{max} . Probability of there being a satellite between 0 and r is, therefore, simply the ratio of the area at r to the area at R_{max}).
- Using the random number (*RandValue*), calculate r value from

$$r = (R_e + h) \left[\cos^{-1} \left\{ 1 - \text{RandValue} \left[1 - \cos \left(\frac{R_{max}}{R_e + h} \right) \right] \right\} \right] \quad (4-21)$$

where R_e is the Earth radius and h is the orbital height.

- From r , calculate $\psi(r)$ corresponding to the angle, as seen from the Earth centre, between the GSO Earth station receiver location and a point on the orbit shell where an NGSO satellite is randomly located.
- Introduce a uniform random variable (*Long*) varying between 0 and 2π to represent the longitude of the NGSO satellite.
- Calculate the satellite position vector \vec{S} from

$$\begin{aligned} S_x &= (R_e + h) \cos(\text{Lat}) \cos(\text{Long}) \\ S_y &= (R_e + h) \cos(\text{Lat}) \sin(\text{Long}) \\ S_z &= (R_e + h) \sin(\text{Lat}) \\ \text{where Lat} &= 90 - \psi(r) \end{aligned} \quad (4-22)$$

on the basis of Figure 4-29 shown below.

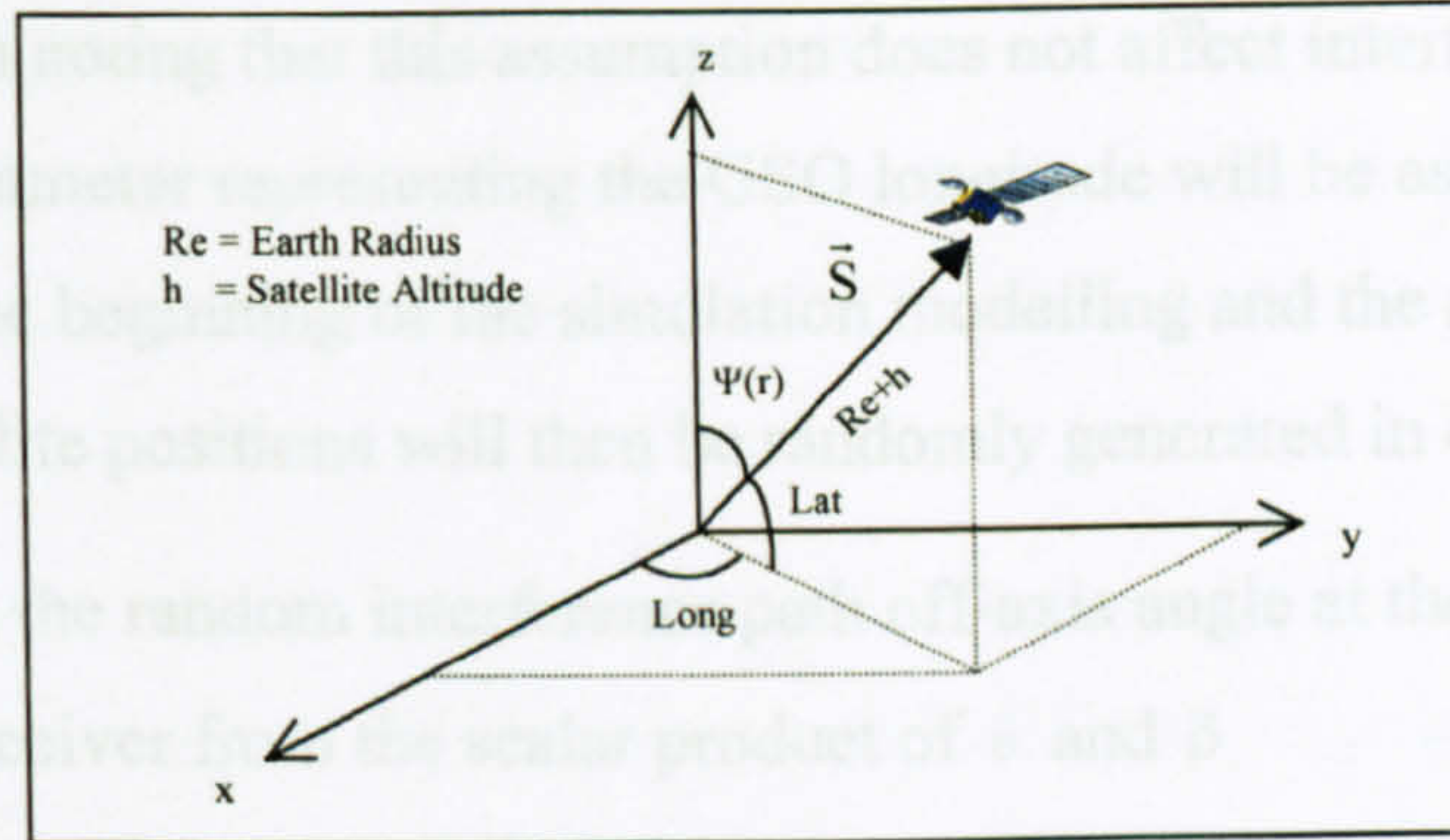


Figure 4-29: NGSO Interference Path Random Pointing

- Calculate the range vector $\vec{\rho}$ from

$$E_x = 0, E_y = 0, E_z = Re$$

$$\vec{\rho} = \vec{S} - \vec{E}$$

Therefore :

$$\rho_x = (Re + h) \cos(Lat) \cos(Long)$$

$$\rho_y = (Re + h) \cos(Lat) \sin(Long)$$

$$\rho_z = (Re + h) \sin(Lat) - Re$$

(4-23)

on the basis of Figure 4-30.

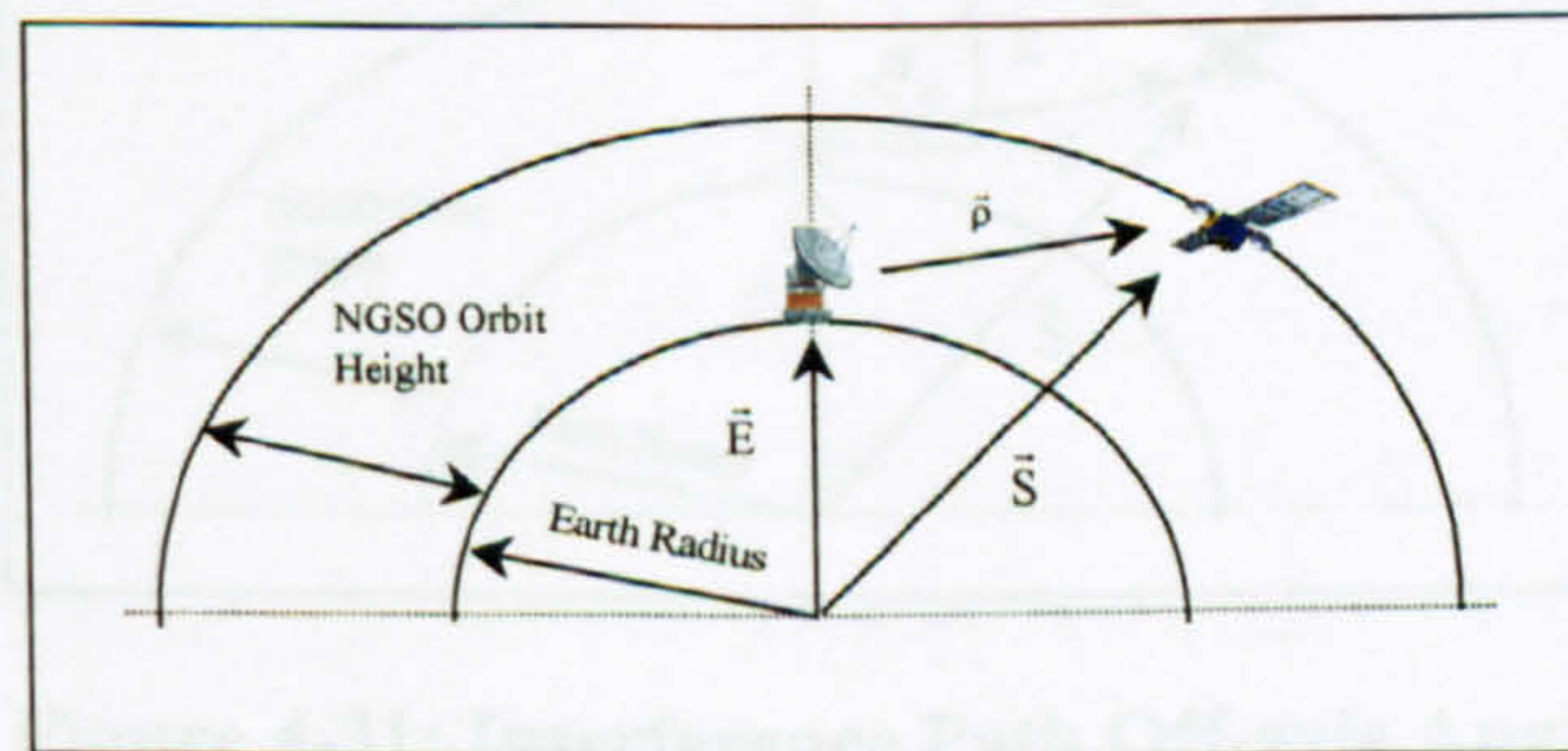


Figure 4-30: Range Vector

- Assuming the Earth station receiver is in the YZ plane (i.e. the longitude is 90 degrees), calculate the elevation vector \vec{e} from

$$e_x = 0$$

$$e_y = \cos(\beta)$$

$$e_z = \sin(\beta)$$

where β is the GSO Earth station receiver antenna elevation angle

(4-24)

It is worth noting that this assumption does not affect interference statistics as the parameter representing the GSO longitude will be assigned a value at once in the beginning of the simulation modelling and the relative NGSO FSS satellite positions will then be randomly generated in each trial.

- Calculate the random interference path off-axis angle at the GSO Earth station receiver from the scalar product of \vec{e} and $\vec{\rho}$

$$\vec{\rho} \cdot \vec{e} = |\rho| |\vec{e}| \cos(\chi)$$

where χ is interference path off axis angle at the GSO receiver antenna

$$\chi = \cos^{-1} \left(\frac{\vec{\rho} \cdot \vec{e}}{|\rho| |\vec{e}|} \right)$$

$$\text{as } \vec{\rho} \cdot \vec{e} = \rho_x e_x + \rho_y e_y + \rho_z e_z$$

$$|\vec{e}| = 1 \text{ then}$$

$$\chi = \cos^{-1} \left(\frac{\rho_x e_x + \rho_y e_y + \rho_z e_z}{|\rho|} \right)$$

(4-25)

as illustrated below

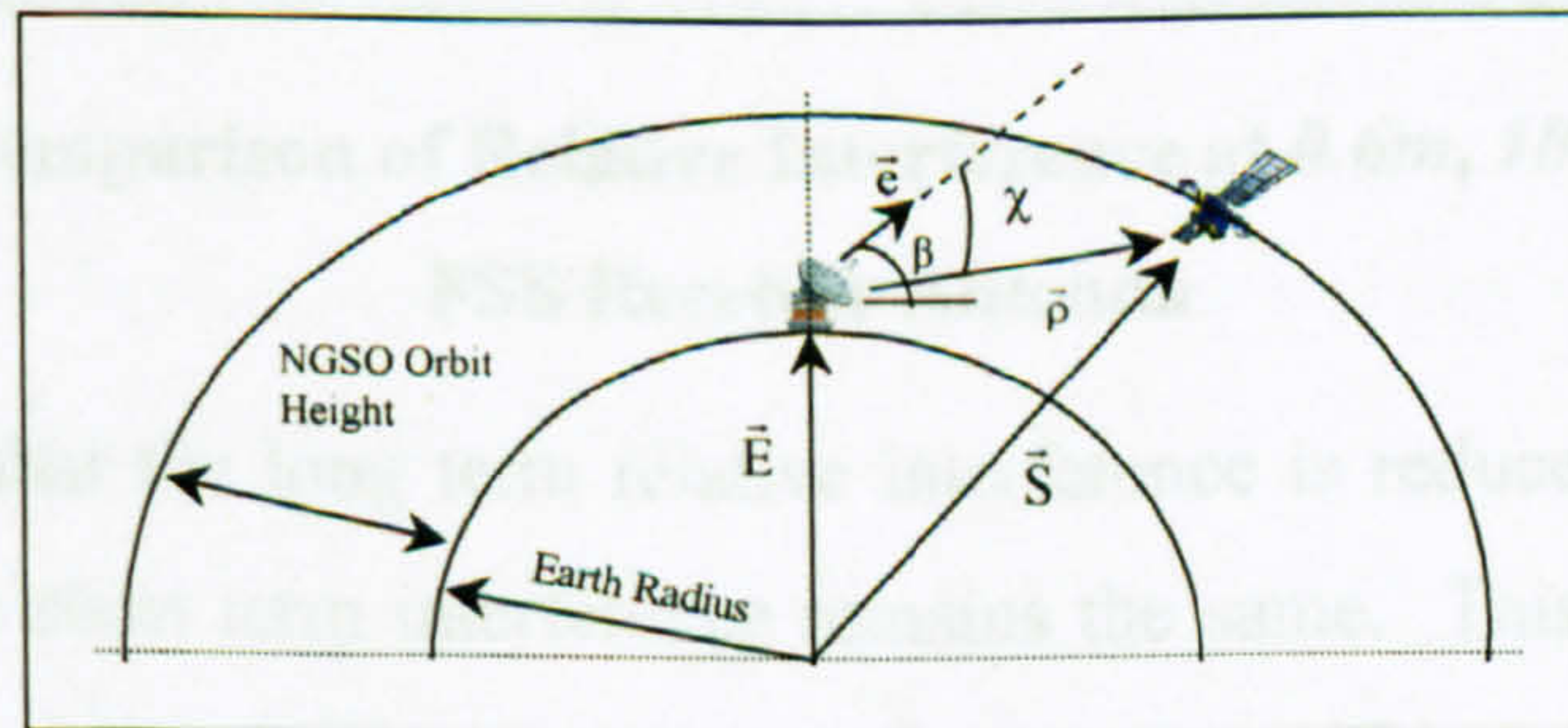


Figure 4-31: Interference Path Off-axis Angle

4.3.3 Monte Carlo Simulation Analysis

The above described Monte Carlo simulator has been configured to demonstrate the differences in the interference statistics obtained at the reference radiation patterns for the $0.6m$ and $3m$ antenna diameters.

The parameters of the NGSO FSS system is taken from the NGSO FSS Ku-2 characteristics given in Chapter 3. It is assumed that satellites are at an altitude of $700 km$ and there are 13 co-frequency NGSO FSS interference entries at the GSO

FSS receiver antenna input. All simulation runs are based on 3,000,000 Monte Carlo trials. It is worth noting that the derivation of the interference distribution functions has involved the replacement of “0”s with “minimum y axis value” in order to avoid “ $\log 0$ ”.

Figure 4.32 compares the cumulative distribution function of the relative interference at the 10 degrees elevated, 0.6m GSO FSS receiver antenna.

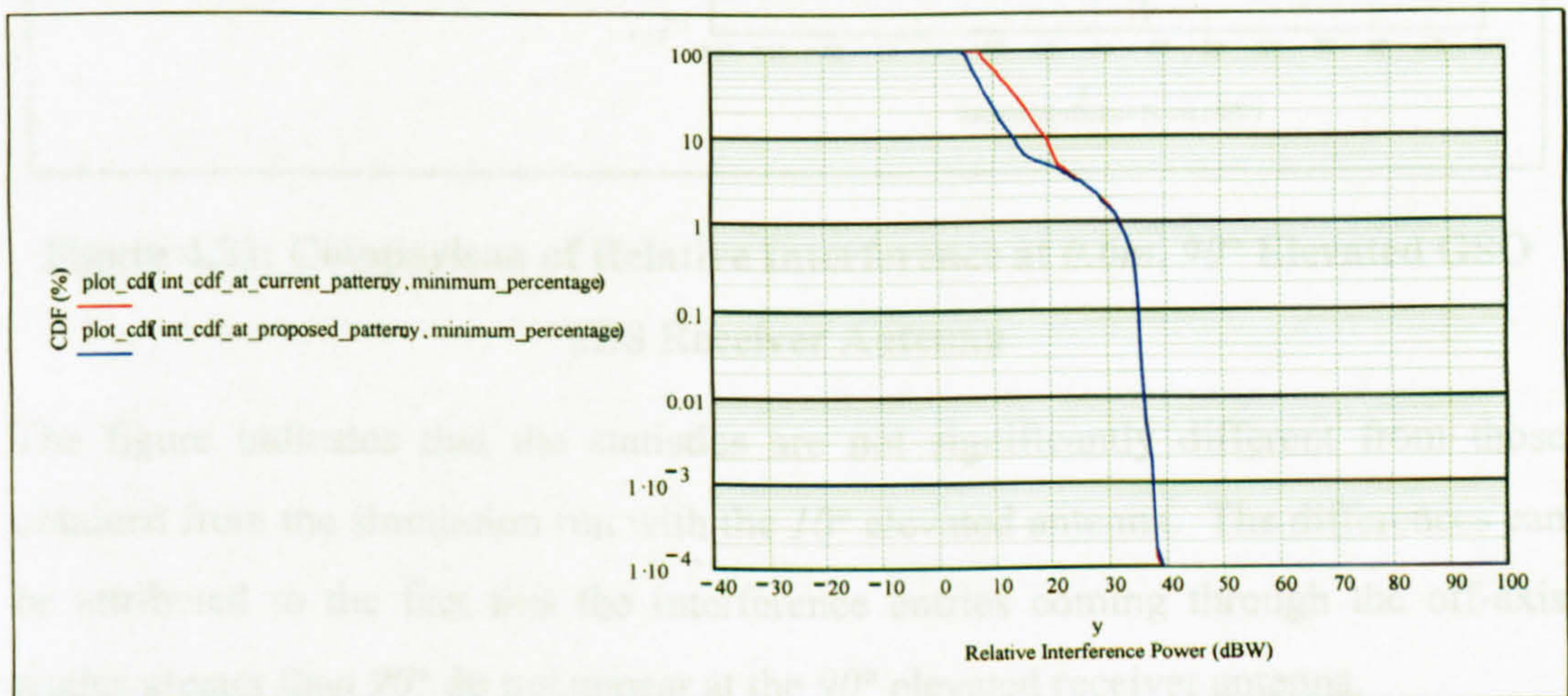


Figure 4.32: Comparison of Relative Interference at 0.6m, 10° Elevated GSO FSS Receiver Antenna

The plots show that the long term relative interference is reduced at the Rec.1428 pattern while the short term interference remains the same. This behaviour can be explained by considering the antenna radiation patterns illustrated in Figure 4.25. The long term interference is reduced due to decreased sidelobe and far lobe envelopes of the Rec.1428 pattern. The short term interference remains unchanged as both patterns have the same main lobe radiation pattern.

For the same scenario, a second simulation run is carried out assuming the receiver is elevated at 90° in order to examine the variations in interference statistics with the receiver elevation angle. The results are illustrated in Figure 4.33.

Figure 4.34: Comparison of Relative Interference at 3m, 10° Elevated GSO FSS Receiver Antenna

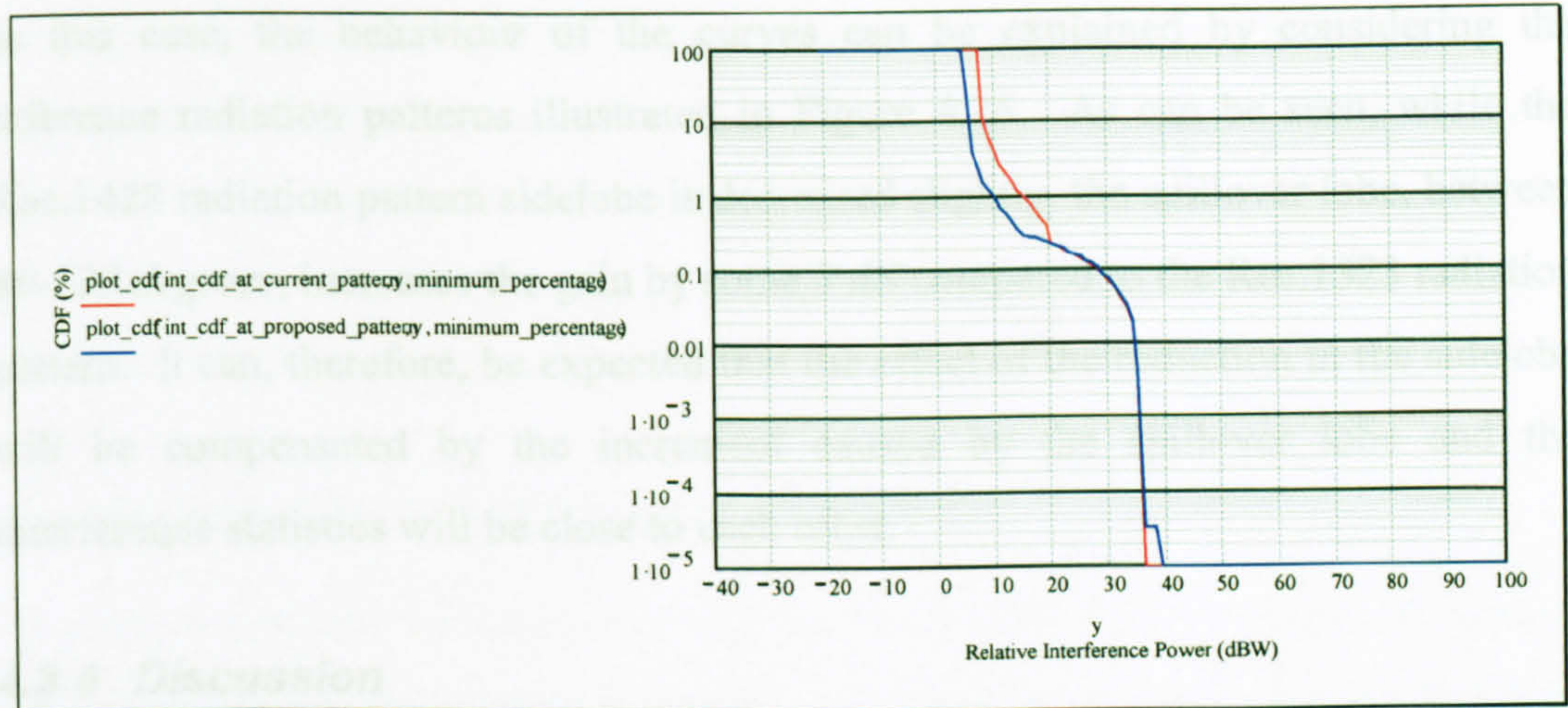


Figure 4.33: Comparison of Relative Interference at 0.6m, 90° Elevated GSO FSS Receiver Antenna

The figure indicates that the statistics are not significantly different from those obtained from the simulation run with the 10° elevated antenna. The differences can be attributed to the fact that the interference entries coming through the off-axis angles greater than 90° do not appear at the 90° elevated receiver antenna.

Using similar approach, the interference statistics at the 3m receiver antenna are examined. The following figure illustrates the interference statistics at the receiver antenna with an elevation angle of 10°.

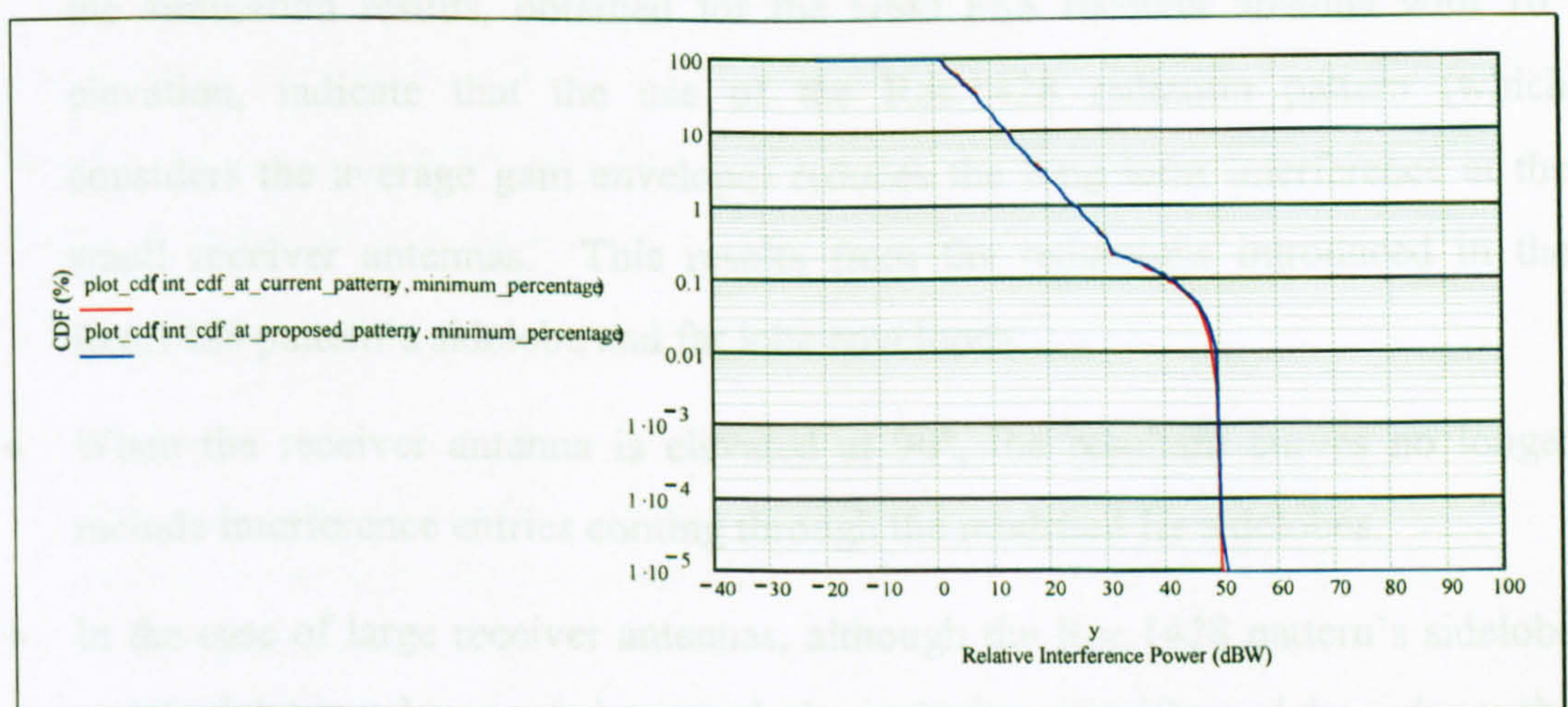


Figure 4.34: Comparison of Relative Interference at 3m, 10° Elevated GSO FSS Receiver Antenna

In this case, the behaviour of the curves can be explained by considering the reference radiation patterns illustrated in Figure 4.26. As can be seen, while the Rec.1428 radiation pattern sidelobe is decreased slightly, the spillover lobe, between *80-120 degrees*, increases the gain by some *3 dB* compared to the Rec.1323 radiation pattern. It can, therefore, be expected that the effect of the reduction in the sidelobe will be compensated by the increment caused by the spillover lobe and the interference statistics will be close to each other.

4.3.4 Discussion

In the preceding sections, the Monte Carlo simulator has been defined and applied for the examination of the interference at the GSO FSS Earth station receiver antennas. The use of the probabilistic approach in the preliminary analysis of the modifications to the GSO FSS receiver reference antenna radiation patterns reduces the computational complexity encountered in the deterministic modelling of large constellations.

From the application of the probabilistic simulation analysis, it has been noted that:

- Bearing in mind the assumptions made for the Rec.1323 reference antenna in order to have a complete antenna pattern in particular with regard to $D/\lambda < 100$, the simulation results, obtained for the GSO FSS receiver antenna with 10° elevation, indicate that the use of the Rec.1428 radiation pattern (which considers the average gain envelope) reduces the long term interference at the small receiver antennas. This results from the reductions introduced in the Rec.1428 pattern's sidelobe and far lobe envelopes.
- When the receiver antenna is elevated at 90° , the resultant curves no longer include interference entries coming through the modified far sidelobes.
- In the case of large receiver antennas, although the Rec.1428 pattern's sidelobe and far lobe envelopes are decreased, the inclusion of spillover lobe reduces the impact of this modification on the mid-term and long term interference. Therefore, very similar interference statistics are obtained at both antennas.

- From the NGSO/GSO FSS sharing point of view, it can be concluded that the impact of the replacement of the Rec.1323 GSO FSS reference receiver antenna pattern with the Rec.1428 radiation pattern is not significant with regard to the calculation of $epfd_{down}$ limits as the short term interference statistics obtained from the Monte Carlo analysis for both patterns are very close to each other.

4.4 Impact of NGSO FSS Interference Peaks

In order to evaluate the sensitivity of a particular GSO FSS Earth station receiver modem to NGSO FSS interference peaks, it is necessary to carry out measurements. As mentioned previously in § 3.2.8, the results of measurements on a variety of modems with different coding and modulation types have been presented to the ITU-R study groups and the typical $C/(N+I)$ threshold values at which the synchronisation loss is expected to occur have been produced.

In this research, an analytic method relating the synchronisation loss to the $epfd_{down}$ limits has been presented. This method is then applied to examine the impact of NGSO FSS interference peaks on the representative GSO Ka-2 system whose characteristics are given in Chapter 3.

4.4.1 Calculation Method

The method is based on determining the $C/(N+I)$ ratio of the GSO FSS link taking account of the maximum tolerable interference level derived from the $epfd_{down}$ limits. The following steps summarise the calculation procedure:

- Calculate the carrier level (C) at the GSO FSS Earth station from:

$$C \text{ (dBW / Receiver bandwidth)} = \text{Satellite EIRP (dBW / Transmitter bandwidth)} - \text{Free Space Path Loss (dB)} - \text{Atmospheric Attenuation (dB)} - \text{Receiver Antenna Pointing Loss (dB)} - \text{Receiver Feeder Loss (dB)} + \text{Receiver Antenna Gain (dBi)} + 10\log(\text{Receiver Bandwidth (Hz)} / \text{Transmitter Bandwidth (Hz)})$$

- Calculate the maximum tolerable NGSO FSS interference (I) in terms of the $epfd_{down}$ as following

$$I \text{ (dBW / Reference bandwidth)} = epfd_{down} \text{ (dBW / Reference Bandwidth)} - 10\log(4\pi/\lambda^2) + \text{Maximum Receiver Antenna Gain (dBi)}$$

where λ is the wavelength

- Calculate the carrier-to-maximum tolerable NGSO FSS interference ratio (C/I) from:

$$C/I \text{ (dB)} = C \text{ (dBW / Reference bandwidth)} / I \text{ (dBW / Reference bandwidth)}$$

- Determine the GSO FSS link $C/(N+I)$ taking account of all degradations (thermal noise, intermodulation, interference from other networks, cross polarisation etc.) but the NGSO FSS interference,
- Combine $C/(N+I)$ and C/I to derive the GSO FSS link $C/(N+I)$ in the presence of the maximum allowed NGSO FSS interference (obtained from $epfd_{down}$),
- Compare the calculated $C/(N+I)$ against the $C/(N+I)$ threshold at which the GSO FSS link synchronisation is lost.

4.4.2 Implementation of the Calculation Method

Article S.22 $epfd_{down}$ limits applicable to upper Ka-band (19.7-20.2 GHz) indicate that the maximum allowed $epfd_{down}$ is $-154 \text{ dBW/m}^2/40\text{kHz}$ (see Figure 3.4 in Chapter 3). Taking the GSO Ka-2 link characteristics (given in Table 3.3 in Chapter 3) into account, the implications of the NGSO FSS interference peaks corresponding to the $epfd$ level of $-154 \text{ dBW/m}^2/40\text{kHz}$ are examined here. It should be noted that the GSO Ka-2 link employs a regenerative transponder. Table 4.9 illustrates the calculation procedure.

DOWNLINK			
GSO Ka-2 Satellite EIRP (dBW/81.03 MHz)	45.15		
GSO Ka-2 Earth Station Receiver Antenna Pointing Loss (dB)	0		
Free Space Path Loss Between GSO Ka-2 Satellite Transmitter and GSO Ka-2 Earth Station Receiver (dB)	209.75 (36,655 km at 20 GHz , Lat=28°)		
Atmospheric Attenuation (dB) (Rec.676, Simplified Model)	0.3 (Path Elevation ≈ 57.31 degrees)		
Feeder Loss Between GSO Ka-2 Earth Station Receiver Antenna and Front-end Amplifier (dB)	0.5		
GSO Ka-2 Earth Station Receiver Antenna Gain (dBi)	49.66 (1.8m)		
Received Carrier Power (dBW/81.03 MHz)	(C) = 45.15 – 0 – 209.75 – 0.3 – 0.5 + 49.66 = -115.74		
GSO Ka-2 Earth Station Receiver Noise Level (dBW/81.03 MHz)	(N)= k T _{ES} B = -125.53		
(C/N) (dB)	-115.74 – (-125.53) = 9.79		
GSO Ka-2 Space Station Transmitter Cross Polarisation Isolation (C/I) ₁ (dB)	27		
GSO Ka-2 Space Station Transmitter Frequency Re-use Isolation (C/I) ₂ (dB)	23.5		
GSO Ka-2 Space Station Adjacent Transponder Isolation (C/I) ₃ (dB)	100		
GSO Ka-2 Space Station Transmitter Intermodulation (C/I) ₄ (dB)	100		
GSO Ka-2 Earth Station Receiver Polarisation Isolation (C/I) ₅ (dB)	20		
GSO Ka-2 Downlink Clear-sky C / I due to Other GSO FSS Networks (C/I) ₆ (dB)	13.84		
GSO Ka-2 Downlink Clear-sky C / I due to FS Networks (C/I) ₇ (dB)	16.84		
Calculation of (C/(N+I)) without NGSO FSS Interference:			
Degradation	dB	numeric	1 / (numeric degradation)
(C/N)	9.79	9.528	0.1050
(C/I) ₁	27	501.187	0.0020
(C/I) ₂	23.5	223.872	0.0045
(C/I) ₃	100	10 ¹⁰	10 ⁻¹⁰
(C/I) ₄	100	10 ¹⁰	10 ⁻¹⁰
(C/I) ₅	20	100	0.01
(C/I) ₆	13.84	24.21	0.0413
(C/I) ₇	16.84	48.306	0.0207
1 / (C / (N+I)) (numeric)			0.1835
C / (N+I) (numeric)			5.45
C / (N+I) (dB)			7.36

Table 4.9 (a): Synchronisation Loss Analysis

Calculation of Degradation due to NGSO FSS Interference			
epfd _{down} (dBW/ m ² / 40 kHz)	-154		
λ (metre)	0.015		
10log(4π/λ ²)	47.47		
GSO Ka-2 Earth Station Receiver Antenna Gain (dBi)	49.66 (1.8m)		
I (dBW / Reference bandwidth) = epfd _{down} (dBW / Reference Bandwidth) – 10log(4π/λ ²) + Maximum Receiver Antenna Gain (dBi)			
I (dBW/ 40 kHz)	-151.81		
C(dBW/ 81.03 MHz)	-115.74		
C(dBW/ 40 kHz)	-148.81		
C/I (dB)	3		
Calculation of C/(N+I) in the Presence of Maximum Allowed NGSO FSS Interference			
	<i>dB</i>	<i>numeric</i>	<i>1 / (numeric degradation)</i>
C / (N+I) (dB) (without NGSO FSS Interference)	7.36	5.445	0.1835
C/I (dB)	3	1.995	0.5012
1 / (C / (N+I)) (numeric)			0.6847
C / (N+I) (numeric)			1.4605
C / (N+I) (dB)			1.65

Table 4.9 (b): Synchronisation Loss Analysis

The results suggests that the NGSO FSS interference peaks reduces the $C/(N+I)$ from 7.36 dB to 1.65 dB. The $C/(N+I)$ threshold values agreed by the ITU-R for different modulation and coding schemes are re-produced in the following table for the purposes of comparison.

Modulation and Coding	C/(N+I) (dB)
QPSK rate 7/8	6.0
QPSK rate 3/4	5.3
QPSK rate ½	3.5
8-PSK	8.1
16-QAM	11.0

Table 4.10: Synchronisation Loss Criterion

It is clear that the GSO Ka-2 link would suffer from the synchronisation loss due to NGSO FSS interference peaks for the modulation and coding techniques included in Table 4.10.

4.4.3 Discussion

For the purposes of this research, an analytical method has been implemented to relate the $epfd_{down}$ limits to the $C/(N+I)$ ratio (at the GSO FSS Earth station receiver) for which the NGSO FSS interference peaks resulting from the alignments where interference entries come through the receiver antenna near boresight cause the synchronisation loss.

The application of the method to the representative GSO Ka-2 system has shown that the NGSO FSS interference peaks can reduce the GSO FSS link $C/(N+I)$ significantly. This is in line with the findings of various ITU-R studies [167-171]. Depending on the type of modulation and coding, the reduction could be so severe that the Earth station modem might lose synchronisation. It is possible to prevent these events by tightening the $epfd_{down}$ limits.

In the case of large GSO FSS receiver antennas, the situation may get worse and a significant reduction in the level of $epfd_{down}$ limits may be needed to prevent the synchronisation loss events. This, in turn, could put excessive burden on the NGSO FSS systems. In such cases, the NGSO FSS operators may choose to apply the co-ordination procedure [163].

4.5 Conclusions

In this chapter, the implications of interference from the NGSO FSS systems into the GSO FSS links operating or planned for operation at Ku and Ka band frequencies have been examined. For these purposes, deterministic and probabilistic simulation analysis and analytical methodologies have been developed. The methods have been applied for the investigation of a number of topics affecting the feasibility of the NGSO/GSO FSS system co-existence. The analysis has been based on the representative system characteristics given in Chapter 3. The work provided in this chapter together with the key conclusions can be summarised as following:

- **Implications of NGSO FSS mitigation techniques:** To examine the implications of the mitigation techniques, deterministic simulation analysis models have been

implemented. This has been supported by the analytical models developed for the verification of the simulation results. These have included the analysis of the worst case interference levels and the calculation and comparison of the GSO FSS link overall performance degradation due to the interference derived from the simulation analysis. It has been shown that the GSO arc avoidance mitigation technique does not prevent near on-beam interference couplings which increases the short term interference level significantly at the GSO FSS Earth station receivers. The latitude avoidance mitigation technique, on the other hand, prevents the main beam-to-main beam interference alignment which, in turn, improves the $C/(N+I)$ ratio of the GSO FSS link. It has also been shown that the use of the NGSO FSS transmitter antennas with improved sidelobes reduces the impact of long term interference. However, the trade-off between the improved radiation pattern and the antenna design cost needs to be considered carefully.

- **Revision of *epfd* limits:** Two methods have been considered. The simulation method has been based on determining the aggregate interference statistics from a simulation modelling and applying the analytical method to the interference statistics to derive the *epfd* statistics which are then compared against the Article S.22 limits to determine whether the protection is adequate or any revision to the limits is necessary. This approach has been employed to examine the implications of the aggregate interference from simultaneously operating multiple NGSO FSS systems, the feasibility of the proposed aggregate-to-single entry *epfd* conversion algorithm, the implications of comparing the continuous *epfd* curves against the discontinuous (staircase) *epfd* limits and the interpolation/extrapolation algorithm proposed for deriving *epfd* limits corresponding to antenna diameters not included in the current Article S.22 *epfd* limits. The revision of the *epfd* limits using analytical approach has been based on the implementation of the Methodology A'. It has been shown that the methodology is based on the calculation of the maximum tolerable interference *epfd* levels on the basis of the GSO FSS link performance requirements. The

calculated values are compared against the Article S.22 limits to determine the adequacy of these limits. In the application of the methodology, issues related to the convolution of the uplink and downlink rain fading statistics, the modifications to the rain fading prediction model, the relation between the GSO FSS link “achieved” and “stated” unavailability targets, the percentage time limitations of the rain fading model, the use of percentage representing no rain fading, the effective overall link noise temperature and the single and aggregate interference limits have been addressed.

- ***Impact of GSO FSS Earth station reference antenna patterns:*** A Monte Carlo simulation technique has been developed for the examination of the interference at the GSO FSS Earth station receiver antennas. It has been shown that the application of the probabilistic simulation approach to evaluate the modifications to the GSO FSS receiver reference antenna radiation patterns is feasible and involves less computation than that required by the deterministic simulation modelling. The probabilistic analysis has suggested that the use of the reference radiation envelopes based on the antenna sidelobe peaks and the average of the sidelobe troughs and peaks would not have a significant impact on the calculation of the $epfd_{down}$ limits as the resultant short term interference statistics would be very close to each other. The analysis has also suggested that the differences at the aggregate interference statistics are dependent on the antenna diameter and the elevation angle of the GSO FSS receiver.
- ***Impact of NGSO FSS interference peaks:*** An analytical approach with the objectives of determining the reduction in the GSO FSS link $C/(N+I)$ due to the NGSO FSS interference peaks and relating this to the $epfd_{down}$ limits has been implemented. In the application of the method, the GSO FSS $C/(N+I)$ is calculated when the NGSO FSS interference corresponds to the maximum allowed $epfd$. The results are compared against the synchronisation loss criterion defined for the modulation and coding used in the GSO FSS link. It has been shown that the near on-beam entries at the receiver antennas may reduce the $C/(N+I)$ to a level where the modem may lose synchronisation. The degree of

severity is largely determined by the type of modulation and coding employed in the GSO FSS link. It is worth noting that the protection of the large GSO FSS receiver antennas with the use of *epfd* limits may not be feasible without imposing excessive restrictions on the NGSO FSS systems. Therefore, the coordination procedure may be required to ensure adequate protection from the interference peaks in these situations.

CHAPTER 5

REVIEW OF ISSUES RELATED TO INTERFERENCE FROM NONGEOSTATIONARY FIXED SATELLITE SERVICE SYSTEMS INTO FIXED SERVICE SYSTEMS

This section provides a review of key issues concerned with the spectrum sharing between nongeostationary fixed satellite service (NGSO FSS) systems and terrestrial radio stations operating in the fixed service (FS) within the 12-30 GHz band (i.e. Ku and Ka band). The technical characteristics of the systems operating in both services are outlined in Chapter 1.

In the sharing scenarios where NGSO FSS transmitter stations operate, FS systems are potentially exposed to high levels of time varying aggregate interference which could affect their performance and availability. For the space path interference analysis, where interference from NGSO FSS satellites into FS receivers is investigated, the spectrum sharing is primarily facilitated by limiting an NGSO FSS satellite transmitter power. For the terrestrial path interference analysis, where interference from NGSO FSS Earth stations into FS receivers is examined, possible means for reducing interference to permissible levels are an introduction of a minimum separation distance between an NGSO FSS transmitter and an FS receiver and a limitation of an NGSO FSS Earth station maximum power radiated at low angles of elevation.

Figure 5.1 illustrates NGSO FSS interference paths into FS links operating at Ku and Ka band frequencies. It is important to note that, for the purposes of this study, sharing situations involving both point-to-point (PP) and point-to-multipoint (PMP) FS systems have been investigated.

After this brief introduction, the current regulatory requirements together with the relevant ITU-R recommendations are summarised in the following section. This is

followed by a brief outline on the findings of a literature review carried out to examine the studies concerning with the NGSO FSS / FS spectrum sharing issues. A critical revision of the methodologies employed in these studies is presented in the discussion section. Finally, the key conclusions are provided in the last section.

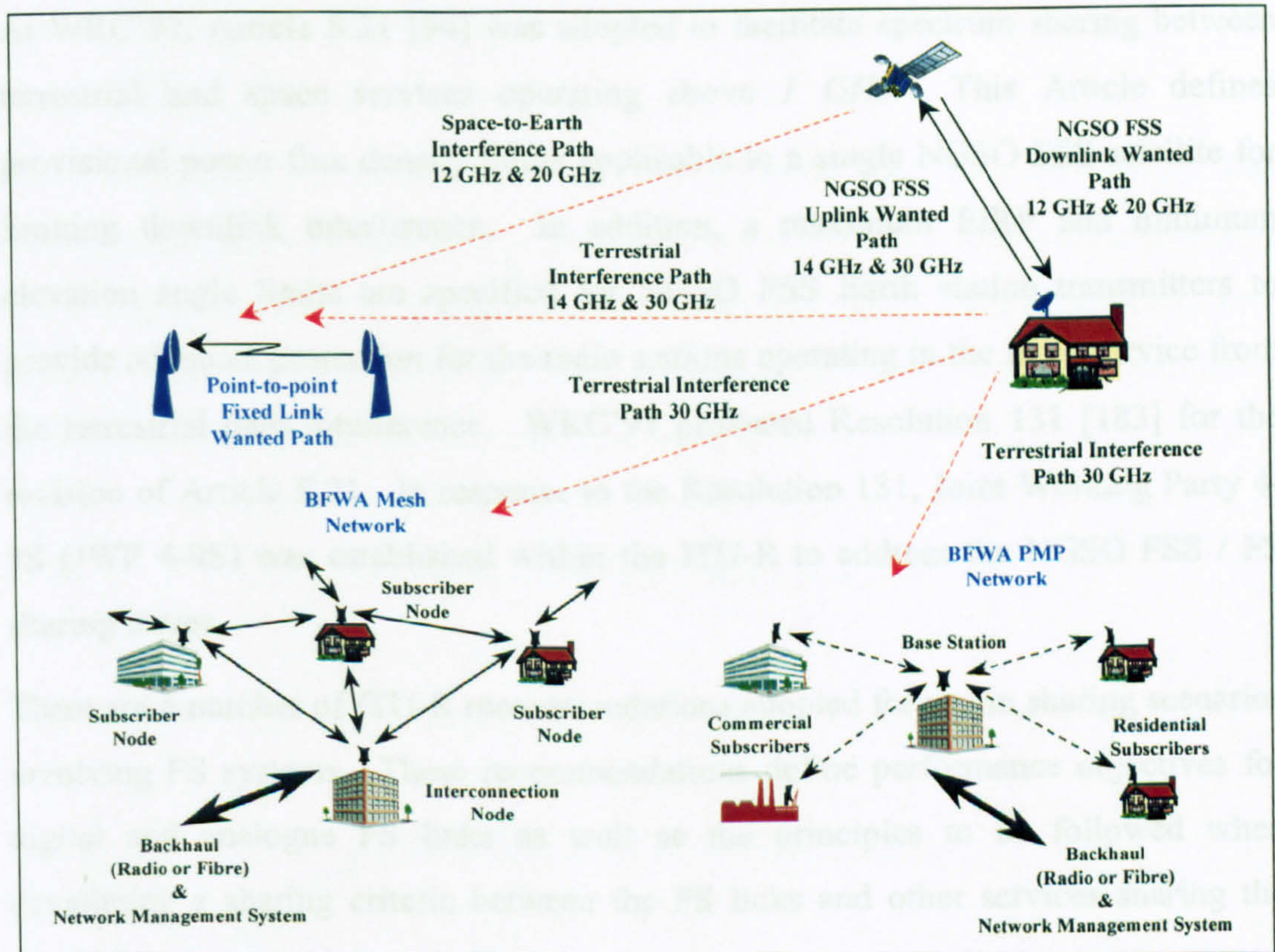


Figure 5.1: Ku and Ka Band NGSO FSS Interference Paths into FS links

5.1 Current Regulations

This section summarises the current regulations facilitating the spectrum sharing between NGSO FSS and FS systems.

5.1.1 Brief History

Traditionally, frequency bands allocated to FS systems are shared with GSO FSS systems. Therefore, most of the existing regulations and recommendations are derived from the studies involving GSO FSS and FS systems. In order to open a way for an NGSO FSS system development, World Radio Conference'95 (WRC'95)

revisited the Radio Regulations and decided to allocate on a primary basis certain FS bands to FSS systems operating with NGSO satellites. The Resolution 118 [182] produced by the conference was considered in Conference Preparatory Meeting of WRC'97 and the ITU-R studies were initiated.

At WRC'97, Article S.21 [94] was adopted to facilitate spectrum sharing between terrestrial and space services operating above 1 GHz . This Article defines provisional power flux density limits applicable to a single NGSO FSS satellite for limiting downlink interference. In addition, a maximum EIRP and minimum elevation angle limits are specified for NGSO FSS Earth station transmitters to provide adequate protection for the radio stations operating in the fixed service from the terrestrial path interference. WRC'97 produced Resolution 131 [183] for the revision of Article S.21. In response to the Resolution 131, Joint Working Party 4-9S (JWP 4-9S) was established within the ITU-R to address the NGSO FSS / FS sharing issues.

There are a number of ITU-R recommendations adopted for use in sharing scenarios involving FS systems. These recommendations define performance objectives for digital and analogue FS links as well as the principles to be followed when developing a sharing criteria between the FS links and other services sharing the same band.

The following sections summarise the regulations and recommendations concerned with the NGSO FSS / FS spectrum sharing issues.

5.1.2 ITU-R Radio Regulations Article S.21 (Based on Regulations Published in Geneva '98)

Article S.21 [94] defines regulatory requirements for terrestrial and space services sharing frequency bands above 1 GHz . It includes the maximum EIRP and minimum elevation angle limits applicable to the FSS Earth station transmitters in order to protect FS links from the terrestrial interference paths. In the frequency bands of interest, the maximum values of the EIRP transmitted in any direction

towards the horizon by an FSS Earth station transmitter are given as: 64 dBW/1MHz for an elevation angle (θ) less than 0° and $64+3\theta \text{ dBW/1MHz}$ for θ values up to 5° . No limit is defined for the elevation angles greater than 5° . For the minimum elevation angle, it is stated that the Earth station antenna should not be employed for a transmission at elevation angles of less than 3° measured from the horizontal plane to the direction of maximum radiation.

From the space-to-Earth transmissions point of view, the provisional power flux density (pfd) limits are specified to limit the interference. The pfd limits are defined for a single satellite as a function of an interference path elevation angle as seen from a point on the surface of the Earth. Figure 5.2 illustrates the pfd limits corresponding to the Ku and Ka band frequencies.

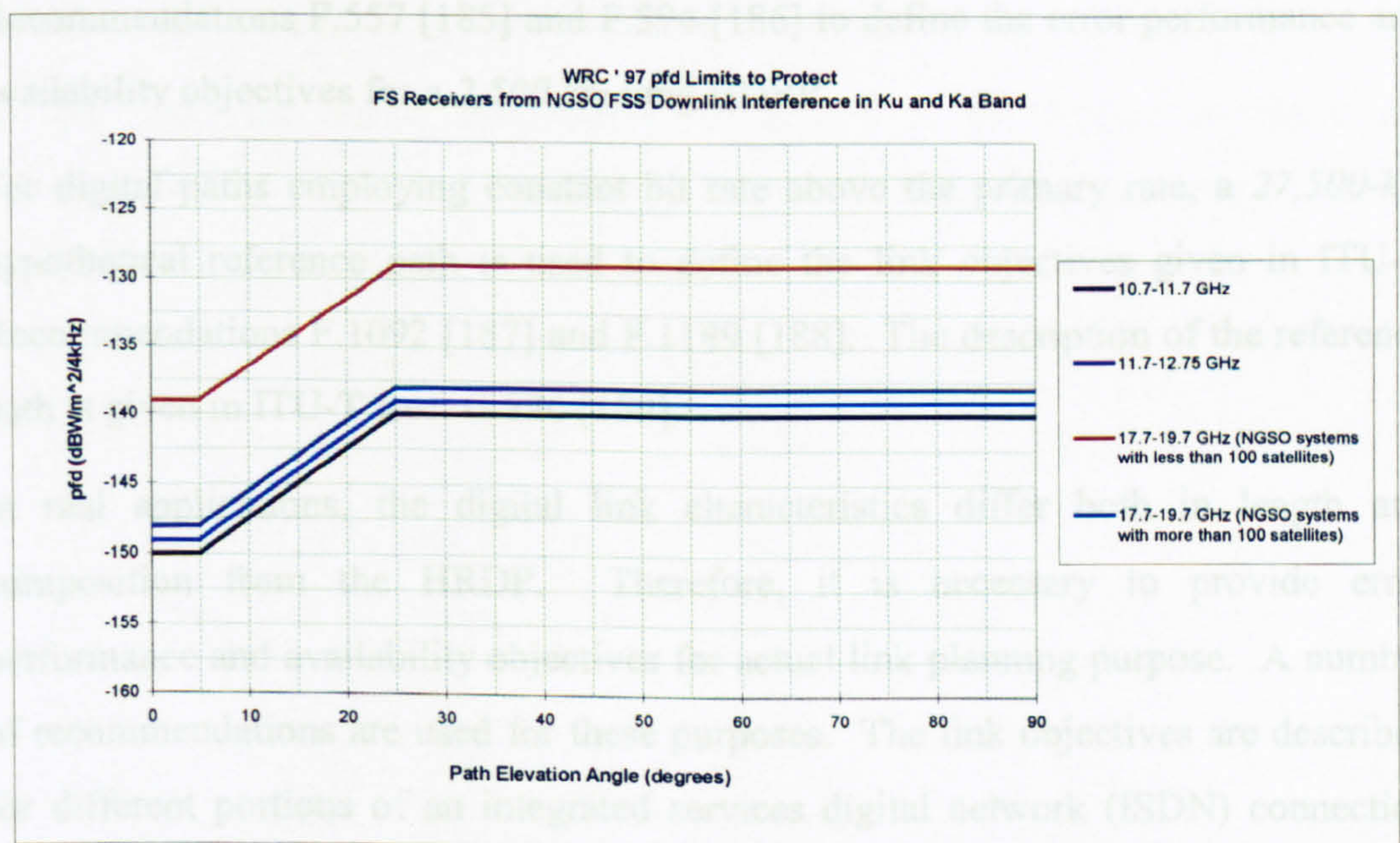


Figure 5.2: Ku and Ka band pfd limits

It is interesting to note that two sets of provisional limits are defined for Ka band depending on the number of satellites forming the NGSO FSS constellations.

5.1.3 ITU-R Recommendations for Analogue/Digital FS System Performance and Availability Objectives

The maximum level of tolerable interference is primarily determined by the permissible degradations in the FS link performance and availability objectives.

For digital systems, link objectives are defined for hypothetical reference digital paths (HRDPs) and real links. A hypothetical reference digital path at a bit rate below the primary rate has been described in ITU-T Rec. G.821 [184]. The primary rate is the European *E1* rate of 2.048 Mbps or the American *T1* rate of 1.544 Mbps (i.e. the lowest bit rate of a hierarchical system). The reference path is sub-divided into portions of different circuit quality, termed “high grade”, “medium grade” and “local grade”. It is noted that the high grade portion is used in ITU-R Recommendations F.557 [185] and F.594 [186] to define the error performance and availability objectives for a 2,500 km long HDRP.

For digital paths employing constant bit rate above the primary rate, a 27,500-km hypothetical reference path is used to define the link objectives given in ITU-R Recommendations F.1092 [187] and F.1189 [188]. The description of the reference path is given in ITU-T Rec. G.826 [189].

In real applications, the digital link characteristics differ both in length and composition from the HRDP. Therefore, it is necessary to provide error performance and availability objectives for actual link planning purpose. A number of recommendations are used for these purposes. The link objectives are described for different portions of an integrated services digital network (ISDN) connection employing bit rates below the primary rate.

For analogue FS links, the link objectives are noise and availability. It is argued that the total noise power in the analogue links is dependent on both equipment design and path propagation characteristics which, in turn, are determined by the atmospheric conditions and terrain irregularities. As for the digital links, the analogue link objectives are defined for hypothetical reference circuits (HRCs) and

real links. The definitions of HRCs for telephony, television and trans-horizon radio relay systems are provided in the following recommendations:

- ITU-T Rec. G.212 [190] General definition
- ITU-R Rec. F.391, 392 [191, 192] Telephony
- ITU-R Rec. S.352 [193] Television
- ITU-R Rec. F.396 [194] Trans-horizon telephony.

It is noted that the hypothetical reference circuits are *2,500 km* long and built from homogeneous sections of equal length each comprising interconnected channels, groups, supergroups and mastergroups. As in the case of digital links, the analogue link noise and availability requirements are also defined in a number of recommendations by taking account of real link compositions and lengths.

In line with the above discussions, Table 5.1 is constructed to show the recommendations to be used in defining the performance and availability objectives of digital and analogue fixed service links.

PERFORMANCE AND AVAILABILITY OBJECTIVES OF DIGITAL LINKS						
Objective	Integrated Services Digital Network (ISDN) Connection Below Primary Rate				Digital Path Above Primary Rate	
	Hypothetical Reference Digital Path (HRDP) (Defined in ITU-R Rec. F.556 and ITU-T Rec. G.821) (High Grade, 2,500 km)	Real Links			Hypothetical Reference Digital Path (HRDP) (Defined in ITU-T Rec. G.826) (27,500km)	
		High Grade	Medium Grade	Local Grade	International	National
Error Performance	Rec. F.594	Rec. F.634	Rec. F.696	Rec. F.697	Rec. F.1092	Rec. F.1189
Availability	Rec. F.557	Rec. F.695	Rec. F.696	Rec. F.697	Rec. G.826	Rec. G.826
PERFORMANCE AND AVAILABILITY OBJECTIVES OF ANALOGUE LINKS						
Objective		Telephony	Television		Trans-Horizon	
Noise	Hypothetical Reference Circuit (HRC)	Rec. F.393	Rec. F.555		Rec. F.397	
	Real Links	Rec. F.395	-		Rec. F.593	
Availability		Rec. F.557	-		-	

Table 5.1: Recommendations Defining Performance and Availability Objectives of Digital and Analogue Fixed Service Links

A review of the above recommendations suggests that:

- For the digital links, error performance is assessed in terms of the events errored seconds (ES) and severely errored seconds (SES) and the parameters errored second ratio (ESR) and severely errored second ratio (SESR). ES is defined as 1-second period in which one or more bits are in error while SES is described as 1-second period which has a bit error rate greater than 1×10^{-3} . ESR and SESR are then defined as ratio of ES and SES to total seconds in the measurement interval (ITU-T Rec. G.821 [184]). In line with the above descriptions, ITU-R Rec. F.697 [195], for example, states that the ESR should not exceed 0.012 and SESR should remain below 0.00015 in any month for local grade portion of a real ISDN connection at bit rate below the primary rate.

- For the analogue links, allowable noise power is defined in terms of psophometrically weighted mean power not to be exceeded for a given percentage in any month. For example, ITU-R Rec.593 [196] states that psophometric mean noise power at a point of zero relative level in real circuits of multi-channel trans-horizon FM systems of less than 2,500 km should remain $10 \times \text{path length (picowatts)}$ for 80% of the time.
- For both digital and analogue links, availability is primarily dependent on the equipment reliability and the propagation conditions. The concept of unavailability for a hypothetical reference digital path is defined as “the period of time beginning at the onset of ten consecutive SES events in at least one direction of transmission”. For the analogue links, it is stated that the link is unavailable “if the level of the baseband frequencies falls by 10 dB or more from reference level for at least 10 consecutive seconds and/or if any telephone channel the unweighted noise power with an integrating time of 5 ms is greater than 10^6 pW0 within at least 10 consecutive seconds”. Taking the above definitions into account, Rec. F.557 [185], for example, recommends that the availability objective for 2,500 km HRDP and HRC should be 99.7% of the time. The recommendation notes that the objective is provisional and, depending on applications, the availability may be within the range 99.5%-99.9%.

It is important to note that the total allowable degradation of any system must be shared among the thermal noise, interference within the system and interference from other systems sharing the same frequency band. The above recommendations provide performance, noise and availability requirements to overcome combined effects of all causes. It is, therefore, necessary that the allowable degradations in the performance and availability of an FS system due to interference from NGSO FSS systems are expressed in terms of a permissible fraction of the total allowable degradation in performance and availability. This is examined in the following section.

5.1.4 ITU-R Recommendations for Fixed Service System Protection

This section summarises reference ITU-R recommendations concerning with the protection of FS systems from NGSO FSS interference.

5.1.4.1 ITU-R Rec. F.758

Rec. F.758 [102] provides basic sharing criteria between the fixed service and other services sharing the same bands. It includes a set of representative FS system parameters to be employed in sharing studies. System characteristics have been under constant review to include new FS systems and to amend the existing ones. The last draft revision document (Doc. 9/1022 dated 3.Feb.2000) provides new information on representative point-to-multipoint FS links and also includes amendments to the existing systems in the *10-30 GHz* range.

FS link characteristics comprise basic transmitter and receiver parameters. Carrier frequency, EIRP, bandwidth, modulation, capacity, antenna radiation patterns, noise figure and nominal receiver input level values corresponding to a range of links in different bands are specified. It is important to note that, for the point-to-point links, indicated EIRP values are at maximum. These values are not associated with any path length, which given that they are maximum values might be expected to be large. For shorter links requiring a smaller fade margin, it is reasonable to assume that relatively lower gain antennas and lower levels of EIRP are used. The use of generic antenna radiation pattern defined in Rec. F.699 [75] is recommended in cases where the measured patterns are not available.

The recommendation notes that the spectrum sharing principle should be based on determining the maximum allowable values of performance and availability degradations of the FS links due to interference from other services sharing the same band. It is further noted that the time varying nature of the interference makes it necessary to define a long term and short term interference criteria. The short-term interference is due to the existence of anomalous propagation conditions, and typically consists of very large levels of interference which occur rarely, and exist for short periods of time. The long-term interference arises from sources within

line-of-sight of the victim receiver, and is typically low in level and constant in value.

As guidance for sharing studies, a long-term interference criterion is defined for 20% of a time while a short-term criterion is specified for $< 1\%$. The derivation of a maximum level of tolerable interference associated with a long term time percentage is simplified by considering the degradation in the FS link fade margin due to interference. Two degradation values are specified for the FS links included in the recommendation: 0.5 dB and 1 dB . Taking these figures into account, a maximum allowed interference is defined relative to the receiver noise level. A 0.5 dB degradation corresponds to an interference-to-receiver noise ratio of -10 dB ($I/N = -10\text{ dB}$) while a 1 dB degradation leads to an I/N of -6 dB .

It is important to note that, for the detailed sharing analysis, the use of performance objectives of an FS link under consideration is recommended for deriving a long term interference criterion. It is also recognised that the derivation of the maximum allowed short term interference level and the exact time percentage associated with it requires the FS link performance objectives.

5.1.4.2 ITU-R Recs. SF.357 & SF.615

Rec. SF.357 and 615 [197, 198] define the maximum permissible values of interference from systems operating in the FSS into $2,500\text{ km}$ long analogue and digital HRC / HRDP, respectively.

Rec. SF.357 notes that the interference noise power at a point of zero relative level caused by the aggregate emissions from Earth stations and satellites of the FSS systems should not exceed $1,000\text{ pW0p}$ psophometrically-weighted 1 minute mean power for more than 20% of any month and $50,000\text{ pW0p}$ psophometrically-weighted 1 minute mean power for 0.01% of any month.

Rec. SF.615 states that the allowable degradation in performance and availability of $2,500\text{-km}$ HRDP resulting from the aggregate interference from the FSS systems should comply with the following limits:

- The period of time in any month during which the *BER* exceeds 10^{-3} not to be increased by more than 0.0054%,
- The period of unavailability not to be increased by more than 0.03% of any year,
- The number of *ES* measured at 64 kbps interface not to be increased by more than 0.032% in any month.

5.1.4.3 ITU-R Recs. F.1241 & F.1398

Rec. F.1241 and 1398 [199, 200] define maximum allowed performance degradations due to interference in the digital FS systems forming part of the international and national portion of the 27,500 km hypothetical reference path, respectively, with a constant bit rate at or above the primary rate.

Rec. SF.1241 argues that the maximum allowable performance degradation represents more stringent requirement than the allowable degradation in availability. It states that the performance degradation in the international portion of a reference path due to interference from other services should be expressed as a permissible fraction of the error performance objectives given in Rec. F.1092 [187]. The objectives for the degradation of performance due to interference are then defined in terms of the *ESR* and *SESR* for various constant bit rates.

For example, the recommendation suggests that, for an FS link of L km in the international portion of a path with a constant bit rate up to 5 Mbps, the *ESR* and *SESR* due to interference should not exceed the following limits:

$$\bullet \quad ESR < 0.004 * (F_L + B_L), \quad (5-1)$$

$$\bullet \quad SESR < 0.0002 * (F_L + B_L) \quad (5-2)$$

where F_L and B_L are distance and block allowance factors varying with path length L .

Similarly, Rec. SF 1398 states that the performance degradation in the national portion of a reference path due to interference from other services should be expressed as a permissible fraction of the error performance objectives given in Rec.

F.1189 [188]. The objectives for the degradation of performance are then defined for the long-haul, short haul and access network sections of the national portion of the reference path operating at or above the primary rate.

For example, it is recommended that, the performance degradation in a digital path of L km with a 15 Mbps constant rate should not exceed the limits shown in Table 5.2.

	Long-haul	Short-haul	Access
ESR	$0.005 * A$	$0.005 * B$	$0.005 * C$
SESR	$0.0002 * A$	$0.0002 * B$	$0.0002 * C$
Notes	<p>A is block allowance for long haul section and formulated as:</p> $(A_1 + 0.01 * L_r / 500)$ <p>where $0.01 < A_1 < 0.02$ & L_r is the actual path length rounded up to the next multiple of 500 km.</p>	<p>B is block allowance for short haul section and $0.075 < B < 0.085$.</p>	<p>C is block allowance for access section and $0.075 < B < 0.085$.</p>

Table 5.2: Maximum Allowable Performance Degradations at 15 Mbps

5.1.4.4 ITU-R Recs. IS.847, IS.849 & P.620

These recommendations are relevant to the analysis of terrestrial interference paths between NGSO FSS Earth stations and FS links. Rec. IS.847 [173] is used for determining the co-ordination area of a GSO FSS Earth station and defines a methodology together with simplified propagation models for the co-ordination distance calculations. The method assumes a constant Earth station antenna gain in the direction of horizon. In the case of Earth stations operating with NGSO space stations, the gain of their antenna towards the horizon varies with time in a manner determined by the orbital parameters of the operational space station and the geographic location of the Earth station antenna. These issues are addressed in Rec. IS.849 [201] which describes methods for calculating co-ordination distances for NGSO FSS Earth stations. Rec. P.620 [202] provides propagation data required for the evaluation of co-ordination distances.

Rec. IS 849 points out that the frequencies shared by NGSO FSS and FS services need to be co-ordinated in order to avoid interference. The co-ordination takes place within an area surrounding the NGSO FSS Earth station and extending to distances beyond which the possibility of interference is assumed to be negligible. The co-ordination area calculations are based on the evaluation, for each azimuth from the Earth station, of the distance that would be required to afford adequate protection to a receiving FS site. The calculated distances are joined to form the required co-ordination contour [201].

The co-ordination area calculations consider the transmitter power, antenna gain, receiver interference threshold, path propagation mechanisms, distance and terrain profile. From the propagation modelling point of view, clear-air and hydrometeor scatter mechanisms need to be taken into account. The key recommendation defining both mechanisms is Rec. P.452 [88] which is detailed in Chapter 2. It is, however, important to note that the method defined in Rec. P.452 is intended for use in detailed (e.g. bi-literal) interference calculations, where site and path specific details are available. Therefore, Rec. P.452 is not directly suitable for the calculation of co-ordination contour where site, terminal and path specific data is, by definition, not known.

Rec. IS.849 notes that the propagation elements required for co-ordination are embodied in Rec. IS.847 which includes simple, largely empirical, models for both clear-sky and hydrometeor scatter modes of propagation. The co-ordination distance calculation requires a value of transmission loss to be exceeded for all but $p\%$ of the time which is given as:

$$L_b(p) = P_t + G_t + G_r - P_r(p) \quad (5-3)$$

where P_t is the transmitter power level, G_t and G_r are the transmitter and receiver antenna gains respectively and $P_r(p)$ is the interference threshold power level not to be exceeded for more than $p\%$ of the time [173].

For the clear-air and hydrometeor scatter mechanisms, the co-ordination distances which will result in a value of transmission loss equal to $L_b(p)$ are calculated. In the

case of clear-air propagation, the terrain is categorised as coastal land/inland, warm sea/cold sea and simplified propagation model is applied iteratively for calculating the distance at which $L_b(p)$ is achieved. The model is valid within the range 0.001% to 10% of the time. For the hydrometeor scatter case, Rec. IS.847 includes empirical transmission loss formulae defined for determining, iteratively, the distance between the region of scattering and the location of an FS station on the co-ordination contour.

It is noted that ITU-R Rec. P.620 (currently at version 4) also provides propagation methods for the evaluation of co-ordination distance and is constantly updated by ITU-R Study Group 3. The revised propagation models defined in Rec. P.452 and P.620 are intended for use in detailed interference and the co-ordination area calculations, respectively.

The current version of Rec. P.620 includes clear-air propagation loss prediction model for three ranges of frequency. For the purposes of this research, the range 850 MHz to 60 GHz is of interest and the model is valid for 0.001% to 50% . As for Rec. P.452 (see Chapter 2), a radio meteorological parameter, β , is used to reflect the relative incidence of anomalous propagation and is derived in a similar way, as a simple function of latitude. As Rec. P.620 is not a path specific method, the terrain details are captured by a simple categorisation as coastal land/inland/ warm sea/cold sea. In addition, factors for site shielding and coupling to over-sea ducts are modelled as in Rec. P.452, but in a simplified manner. The calculation for the time and distance dependent losses uses the same model as that in Rec. P.452 in which a cumulative distribution function relating *transmission loss* and *%-time* is translated to reflect path and radiometeorological parameters [202].

For the hydrometeor scatter mode, in the method of Rec. P.620, a coordination contour is determined by the iterative application of an expression for basic path loss, L :

$$L = 168 - 20 \log(d) - 20 \log(f) - G_t - 13.2 \cdot R + S + A_g - C + \Gamma \quad (5-4)$$

where d is the distance from the terrestrial station to the scattering volume, A_g attenuation due to gasses, G_t represents the FS station antenna gain, R is the rainfall rate, S models the difference between Rayleigh and Mie scattering ($0 \text{ at } \leq 10 \text{ GHz}$) in a simpler expression than that in Rec. P.452. The scatter transfer function, C , is a simplified version of that in Rec. P.452, in which an Earth station elevation of 20° is assumed. C and Γ allow for rain attenuation inside and outside the rain cell, respectively. It is important to note that the basic path loss expression is similar to that of Rec. P.452.

Rec. IS.849 provides three methods for deriving a co-ordination contour around the co-ordinating NGSO FSS Earth station. It is stated that the co-ordination distances obtained for hydrometeor scatter are found to be smaller than the clear-air distances and, therefore, these methods take account of the clear-air propagation mechanisms. The recommendation also refers to Rec. IS.847 for the reference characteristics to be used in representing the (by definition) unknown receiving FS. The summary of all three methods [201] is given below:

Composite Method:

The method is based on deriving the joint statistics of path loss and Earth station horizon antenna gain for each azimuth around the NGSO FSS Earth station. These statistics are determined by performing a convolution of the gain statistics with the fading characteristics predicted for a specific path length. The path length is iteratively increased, and the convolution repeated, until the joint statistics offer sufficient overall loss for a sufficient percentage time to meet the limit. It is important to note that although the method is conceptually simple it is the most complex in implementation owing to the need for convolution of two probability density functions.

“3%” Method:

This method also makes use of antenna horizon gain statistics for the NGSO Earth station. Rather than developing joint statistics, however, the value of horizon gain

exceeded for 3% of the time is determined (for each azimuth) and this figure is then used in the iteration procedure determining the co-ordination distance.

Time Invariant Gain Method:

In this option, the difference between the maximum and minimum gains of the NGSO FSS Earth station antenna towards the horizon (on each azimuth) is determined. For a difference of 20 dB or less, the maximum horizon gain is assumed, between 20 dB and 30 dB difference the minimum value plus 20 dB is assumed, and for 30 dB or greater difference, the maximum value minus 10 dB is used. As for the 3% method, these values are then applied in the iteration procedure.

5.1.4.5 ITU-R Recs. F.1494 and F.1495

These recommendations have been recently produced by the Joint Working Party 4-9S (JWP 4-9S) for the development of interference criteria to protect FS links from NGSO FSS satellites operating at Ku and Ka band [203, 204].

Rec.1494 defines a method for deriving protection criteria at 11/12 GHz band (i.e. Ku band). It is proposed that the short term interference criterion of “*I/N=20 dB to be exceeded for not more than 0.001% of the time*” provides an adequate protection for the majority of the FS links operating in Ku band from the NGSO FSS space-to-Earth interference paths.

In order to check the validity of this assumption the probabilities of the simultaneous effect of short term interference and propagation fading (assumed to be dominated by multipath fading) are calculated for a number of FS links assuming both are not correlated. These probabilities are then compared against the allowable degradations in the performance of FS links due to interference. The allowable degradation is defined as “*10% of the total Error Performance Objectives (ES & SES) stated in the ITU-R Recommendations F.1241 and F.1398*”. FS links, for which degradation probabilities are calculated to be less than the allowable degradations, are assumed to be adequately protected from the NGSO FSS interference.

For long term interference, it is recommended that *Fractional Degradation in Performance (FDP)* should be used. The FDP is defined in ITU-R Rec. F.1108 [205] as following:

$$FDP = \sum_i \left(\frac{I_i * f_i}{N_T} \right) \quad (5-5)$$

where I_i is the interference power at i^{th} event,

f_i is the fraction of time that the interference had a power I_i ,

N_T is the receiver noise power

It is stated that the FDP due to long term interference from NGSO FSS satellites should remain below 10% in order to protect FS links operating in the Ku band [203].

Rec.1495 derives protection criteria for FS links operating at 17.7-19.3 GHz band (i.e. Ka band). It is assumed that the FS link fading due to propagation effects (dominated by rain fading) and NGSO FSS downlink interference do not occur simultaneously. Therefore, an outage of the FS link is assumed to occur when the interference level is greater than the link fade margin (defined in dBs for a given bit-error-rate (BER)).

In line with the above assumptions, the interference criteria are calculated by apportioning the effect of interference on the total allowable FS link degradations, defined as 10% of the total Error Performance Objectives. For these purposes, it is assumed that 20% of the link degradation is attributed to the long term interference while the remaining 80% are allocated to the short term interference.

The short-term interference criteria are then derived by linking the FS link fade margin to performance degradations (i.e. *ES* and *SES*). In this process, it is assumed that fade margins for *ES* and *SES* are respectively 5 dB and 1 dB lower than the FS link fade margin referenced to the *BER* at 10^{-3} level.

In the recommendation, it is argued that a 19 dB fade margin (defined for BER of 10^{-3}) can be taken as a representative value since more than 80% of FS links

operating in Ka band in the UK and France are with fade margins greater than 19 dB [204]. It is further argued that a short haul inter-exchange network section composed of 5 hops of 8 kilometres with data rates from 15 to 55 Mbps is assumed to be a representative link associated with the above fade margin. The allowable *ES* and *SES* degradations due to short term NGSO FSS interference are then calculated to be:

ES allowable to short term interference $9.6 * 10^{-3} \%$

SES allowable to short term interference $2.6 * 10^{-4} \%$

Two short term criteria are defined by associating the *ES* and *SES* and the corresponding fade margins:

Criterion 1: *I/N*=14 dB not to be exceeded for 0.0096%

Criterion 2: *I/N*=18 dB not to be exceeded for 0.00026%

For the long term interference, it is recommended that the criterion based on 0.5 dB degradation of the fade margin (defined in Rec.758 [102]) should be used.

Table 5.3 summarises the proposed Ku and Ka band interference criteria for the assumptions made in the new recommendations [203, 204].

	Short term	Long term
Ku Band	<i>I/N</i> should not exceed 20 dB for more than 0.001%	Fractional Degradation Performance (FDP) should be less than 10%
Ka Band	<i>I/N</i> should not exceed 14 dB for more than 0.01% of the time, <i>I/N</i> should not exceed 18dB for more than 0.0003% of the time	<i>I/N</i> should not exceed -10 dB for more than 20% of the time

Table 5.3: Proposed Ku and Ka Band FS Interference Criteria for NGSO FSS
Downlink Interference

5.2 Previous Work

This section briefly looks at the studies concerning with the NGSO FSS / FS sharing in the 12-30 GHz band. It has been noted that the investigations carried out within the ITU-R Working Party 4-9S are of particular interest.

5.2.1 Space-to-Earth Interference Paths

A review of documents examining the NGSO FSS Earth-to-space interference paths has shown that most studies employ simulation analysis approach. The following is a summary of these studies [206-214].

- The primary objective of the simulation analysis approach is to address the suitability of the Article S.21 limits or other power flux density (pfd) masks proposed for the protection of the FS links. Interference scenarios are based on the assumption that the NGSO FSS satellites transmit continuously 100% of the simulated time and each satellite transmission is represented by a pfd mask. Interference at an FS receiver from a single satellite is then calculated from:

$$I = PFD + 10 \log (\lambda^2/4\pi) + Rx \text{ Antenna Gain} - \text{Atmospheric Loss} - Rx \text{ Feeder Loss} \quad (5-6)$$

- At a given instant, the aggregate interference power is determined by adding interference entries (defined in the equation 5-6) from all satellites visible to an FS receiver. Interference statistics are presented in the form of cumulative distribution of received interference power level with time.
- Interference statistics are dependent on the radio characteristics of both the transmitter and receiver as well as the latitude, longitude and a pointing direction of the FS receiver. In particular, the pointing azimuth of an FS receiver antenna plays a significant role in deriving a maximum likely interference level. The FS pointing azimuth value resulting in the highest interference statistics (i.e. the worst case interference) is determined by the NGSO FSS system orbital parameters and the FS receiver latitude and the pointing elevation.
- An analytical method has been developed to estimate the worst case azimuths for a given NGSO FSS constellation and FS receiver characteristics. The methodology is incorporated into Rec. S.1257 [215]. It is noted that the method is based on calculating the probability (i.e. percentage of time) of finding a satellite of a constellation in an area in an orbit shell. In the NGSO FSS/FS

spectrum sharing context, this area may be thought of as part of the NGSO FSS orbit shell illuminated by the FS receiver antenna beam. Having determined the area on the orbit shell for a given antenna beam, the probability of a satellite being in this area is calculated taking the orbital characteristics into account. This probability is expressed as:

$$P = \frac{A}{2\pi^2} \frac{1}{\sin \alpha} \frac{1}{\cos L} \quad (5-7)$$

where A is the area on the NGSO FSS orbit shell (*steradian*), α is the angle between ground track and latitude line (*radian*) and L is the latitude of a centre of the area on the orbit shell projected to the Earth surface (*radian*). At a given FS receiver elevation, the worst case azimuths are those corresponding to the highest probability and defined as following:

$$\begin{aligned} \theta_\varepsilon &= \text{ArcCos} \left(\cos(\text{elev}_{FS}) \frac{R}{R+h} \right) - \text{elev}_{FS} \\ \Delta_1 &= \text{ArcCos} \left(\frac{\sin i - \cos \theta_\varepsilon \sin L_o}{\sin \theta_\varepsilon \cos L_o} \right) \\ \Delta_2 &= 2\pi - \Delta_1 \\ \Delta_3 &= \text{ArcCos} \left(\frac{-\sin i - \cos \theta_\varepsilon \sin L_o}{\sin \theta_\varepsilon \cos L_o} \right) \\ \Delta_4 &= 2\pi - \Delta_3 \end{aligned} \quad (5-8)$$

where elev_{FS} is the pointing elevation of the FS antenna (*radian*), R is the Earth radius (*km*), h is the NGSO FSS constellation altitude (*km*), i is the NGSO FSS orbit inclination (*radians*) and L_o is the latitude of the FS station (*radian*). Δ_1 , Δ_2 and Δ_3 , Δ_4 are symmetrical with respect to the North ($\Delta=0^\circ$) and the South ($\Delta=180^\circ$). The worst case azimuths exist if $\text{ArcCos}(x)$ function exists which requires that $|x| \leq 1$. If this condition is not met then corresponding equations do not apply and give no worst case azimuth.

- The studies employ FS link parameters based on either representative values specified in Rec.758 [102] or real system values provided by the FS link

operators. Generic FS receiver antenna radiation patterns defined in Rec. F.699 [75] and Rec. F.1245 [76] are used in the most of the reviewed documents.

- It is generally assumed that a long term interference (corresponding to 20% of the time) should not degrade an FS link C/N ratio more than 0.5 dB at Ku band and 1 dB at Ka band. This is based on information given in Rec. F.758. In order to establish a short term interference criteria, a number of recommendations are taken as references. These include recommendations F.758 [102], F.1190 [216] and IS.847 [173]. The most commonly assumed short-term criteria is $I/N=20$ dB to be exceeded for no more than 0.001% time. FS links are assumed to be adequately protected if both short term and long term criteria are met. The implications of NGSO FSS interference on digital FS receivers have also been considered by calculating the Fractional Degradation in Performance (FDP). On the basis of Rec. F.1108 [205], it is generally accepted that the digital FS receivers are adequately protected if the FDP produced by a NGSO FSS constellation is less than 10%.

5.2.2 Terrestrial Interference Paths

The following key points are derived from the review of documents describing studies concerning with the Ku and Ka band terrestrial interference paths from the NGSO FSS Earth stations into the terrestrial radio stations operating in the fixed service [217-222].

- Separation distances are required to avoid harmful interference between NGSO FSS transmitters and FS receivers. Using the transmitter and receiver characteristics, minimum required distance calculations are carried out assuming clear line-of-sight propagation conditions. This represents the worst-case as far as interference paths are concerned, as the propagation effects that would be introduced by man-made and natural terrain are not taken into account. By repeating the separation distance calculations for the FS receiver azimuth angles from 0° to 360°, a two dimensional “exclusion zone” is calculated. An exclusion zone represents a region around an FS receiver where an operation of NGSO

FSS Earth station is not possible without risk of causing unacceptable interference.

- A number of potential interference mitigation techniques is suggested to ease the NGSO FSS/ FS sharing situation as far as terrestrial path interference is concerned:
 - *Use of higher performance antennas* to improve the antenna sidelobe performance and, hence, to reduce the off-axis transmitted or received interference power,
 - *Operation with increased antenna gain* to reduce the power into the antenna required to achieve the same performance and consequently reducing off-axis interference power from the antenna,
 - *Use of Automatic Transmit Power Control (ATPC)* to reduce the nominal power of a transmitted signal and only transmit an increased power level to overcome fading events when they occur,
 - *Careful siting of terminals* to take advantage of the high levels of additional isolation that can be achieved by siting terminals such that natural and/or man-made obstacles are located on the interfering path,
 - *Operation with minimum elevation angle* to prevent the higher levels of off-axis EIRP from the near sidelobes being transmitted along the interfering terrestrial path,
 - *Use of dynamic channel assignment (DCA)* to avoid unacceptable interference by detecting its presence and moving to another available frequency,
 - *Operation with increased interference margin* to increase the transmitted power on a link in order to provide a higher tolerable degradation.
- Studies have been conducted to examine the technical feasibility and to quantify the costs and benefits offered by possible mitigation techniques. For example, it is argued that while a reasonable advantage can be obtained by introducing

relatively higher minimum operational elevation angles the amount of visible orbit shell from NGSO FSS Earth station will be decreased. This implies that the number of satellites in the NGSO FSS constellation needs to be increased. Similar arguments also apply for the use of high performance antennas, ATPC and DCA, all of which have technical and economical implications.

As mentioned previously, in the 30 GHz band where NGSO FSS Earth station transmitters are planned for operation, FS systems are proposed for the broadband fixed wireless access (BFWA) applications for the provision of multimedia type of services, requiring large bandwidths. This brings about potential sharing situations where a large number of FS radio stations operate in the same band and geographical area as the NGSO FSS Earth stations. It has been noted that a number of studies have been carried out concerning with the implications of terrestrial path interference between the BFWA systems and the NGSO FSS Earth stations [223-226].

It is observed from the reviewed studies that investigations are mainly concerned with interference paths into point-to-multipoint (PMP) FS base station and subscriber receivers. Propagation characteristics associated with this band enable both PMP FS and NGSO FSS systems to employ smaller antennas which, in turn, increases the possibility of widespread system deployment. From the spectrum sharing point of view, the large terminal numbers imply that the dominant interfering paths will generally be line-of-sight. It is, therefore, noted that the propagation effects are modelled taking account of free-space path loss, atmospheric loss and, in some cases, clutter loss.

The PMP system parameters and long term interference criteria ($I/N = -10$ dB for 20%) defined in Rec. F.758 are widely used in the sharing studies. It is generally agreed that both the base stations and user terminals are likely to experience significant long-term interference from the NGSO FSS Earth stations, in particular, in urban deployment scenarios. The degree of interference is a function of the

terminal separation, antenna discrimination, NGSO FSS Earth station output power and interference allowance associated with the base station or user terminal receiver.

It is argued that the protection of PMP FS systems from NGSO FSS terrestrial interference will not be possible if both systems operate in the same geographical area [225]. On this basis, it is suggested that the band segmentation may be a suitable solution to facilitate effective use of the spectrum. In order to improve the sharing conditions and avoid a strict segmentation of the 30 GHz band, the use of Geographical Band Segmentation (GBS) has been proposed.

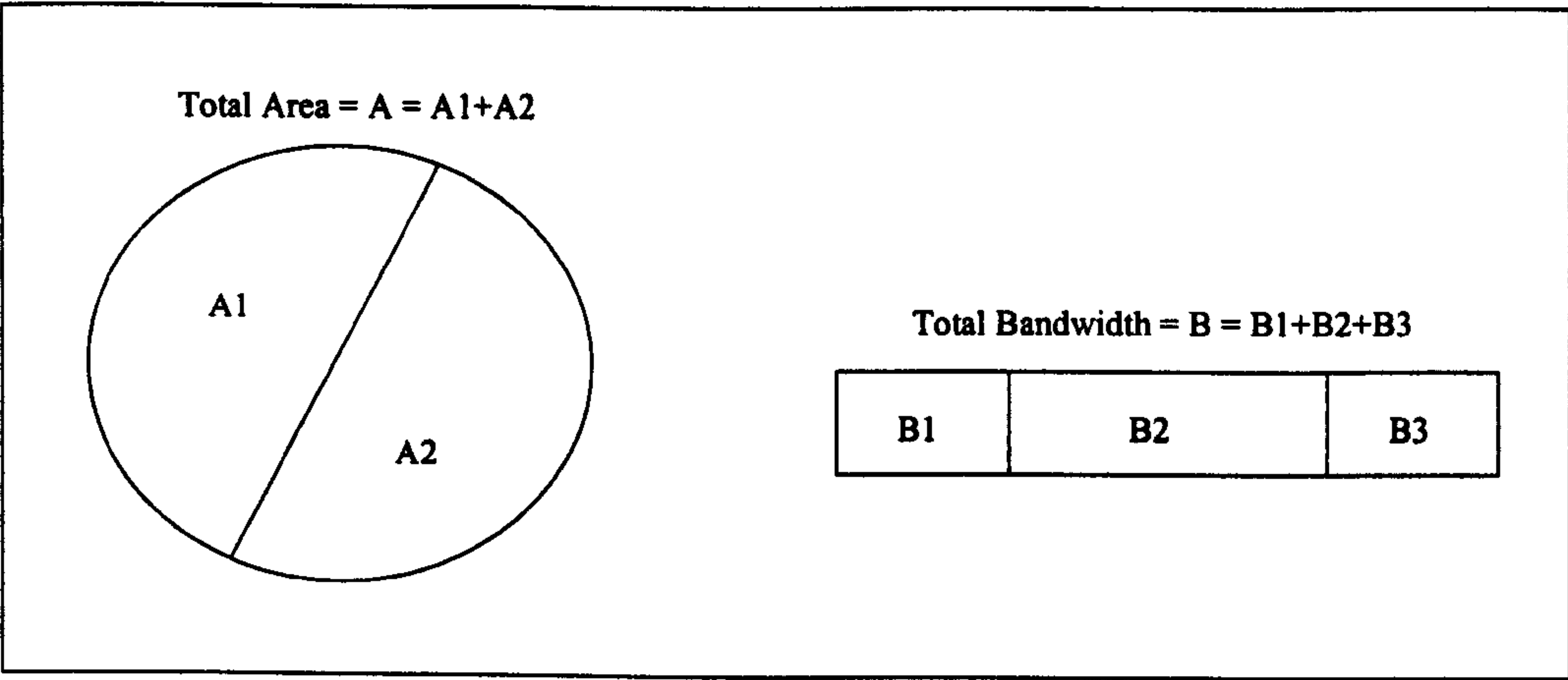


Figure 5.3: Geographical Band Segmentation

In Figure 5.3, the total bandwidth of B is apportioned over an area A using the GBS which results in:

- NGSO FSS system being exclusive in band $B1$ in area $A1+A2$,
- BFWA system being exclusive in band $B3$ in area $A1+A2$,
- NGSO FSS system being able to use band $B2$ in area $A1$,
- BFWA system being able to use band $B2$ in area $A2$.

In the above scenario, $B1$ and $B3$ are respectively NGSO FSS and FS exclusive bands and $B2$ is the conditional band. In the band $B2$, the exclusion of NGSO FSS transmitters from the area $A2$ decreases the aggregate interference into BFWA base stations and user terminals, ideally, to an acceptable level.

In addition to the GBS, it is also argued that the use of ATPC, improved antenna radiation patterns, high minimum operational elevation angle and careful positioning of the NGSO FSS Earth stations should be considered as further mitigation techniques to improve the sharing environment in the conditional bands [226].

5.3 Discussion

This section provides a brief discussion on the downlink and terrestrial path spectrum sharing analysis methods applied in the above discussed studies.

5.3.1 Space-to-Earth Interference Paths

As far as space-to-Earth interference paths are concerned, Article S.21 limits relate to the power flux density which would be obtained under assumed clear-sky free space propagation conditions. By applying these limits to known NGSO FSS systems it is possible to assess the worst case interference into FS receivers if each satellite were to meet the limits. Therefore, the use of pfd masks to calculate aggregate interference is a conservative approach as all visible satellites are assumed to be transmitting at the maximum pfd limit towards the same point where an FS receiver is assumed to be located.

In order to derive likely actual levels of downlink interference, it is necessary to model NGSO FSS constellations fully, accounting for individual beam patterns and EIRP. In this case, the worst case interference level will be determined by an interference entry either originating from an NGSO FSS satellite antenna sidelobe located very close to an FS receiver antenna boresight or originating from an NGSO FSS satellite antenna boresight located very close to an FS receiver antenna rearlobe, as shown in Figure 5.4.

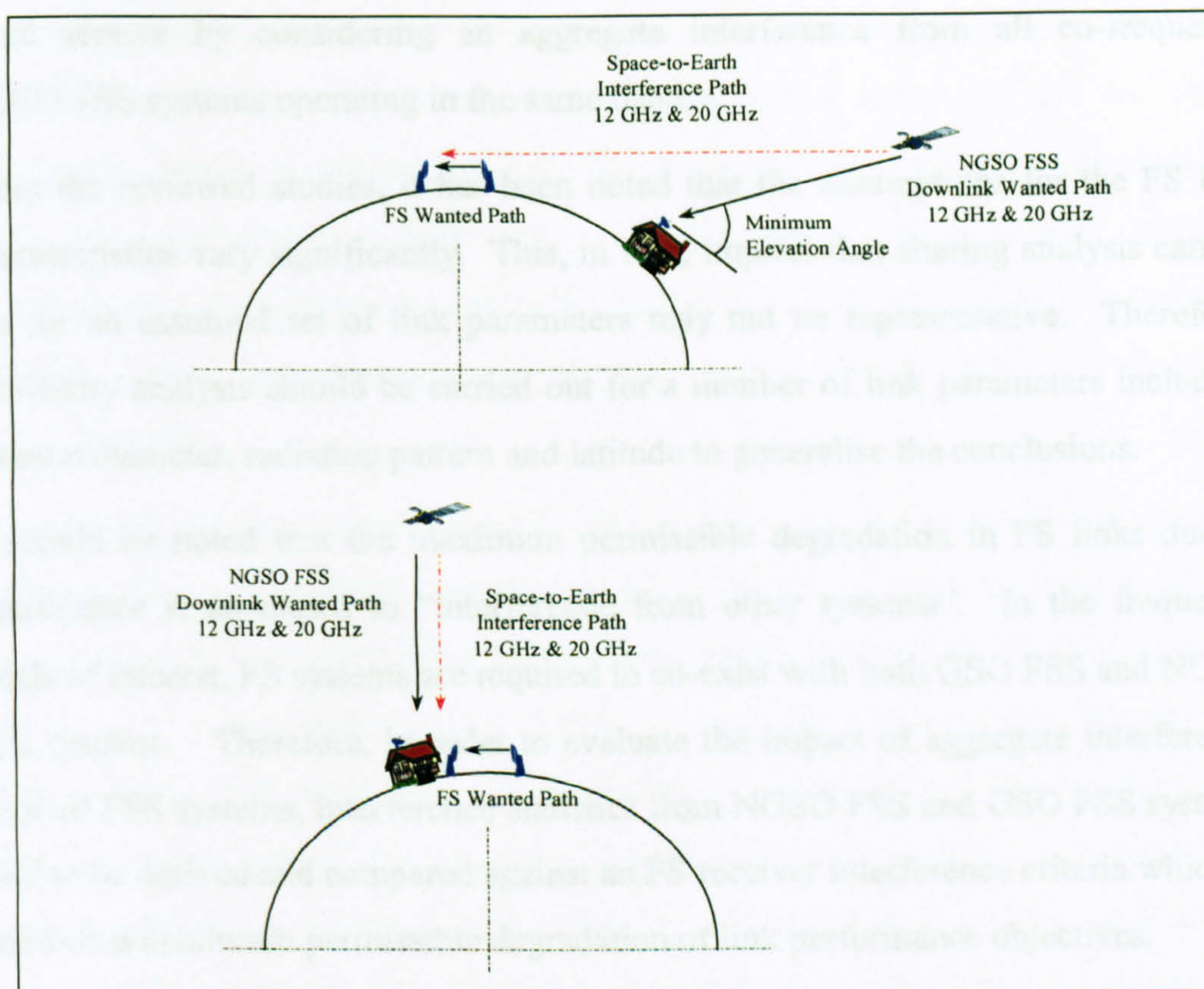


Figure 5.4: Worst Case Interference Scenarios

Although the use of worst case azimuth approach aims to provide a maximum protection for the FS receivers operating in the same band as the NGSO FSS satellite transmitters, it is important to note that the worst case azimuth for the FS receivers will be different for each of the NGSO FSS constellations as the projected development of NGSO FSS usage at Ku and Ka bands indicates that systems will not be homogenous, i.e. the constellation and radio characteristics will not be similar. Therefore, the simulation approach used in the pfd analysis needs to consider the worst case azimuth corresponding to each given constellation.

Recently approved radio regulations suggest that, for the sharing studies involving NGSO FSS systems, the number of non-homogenous systems operating within the same frequency band should be assumed to be in the range 3 to 5 which is the result of the restrictions that the self-interference would impose on the NGSO FSS systems. Therefore, the pfd limits defined on a per satellite basis should be able to provide an adequate protection for the terrestrial radio stations operating within the

fixed service by considering an aggregate interference from all co-frequency NGSO FSS systems operating in the same band.

From the reviewed studies, it has been noted that the assumptions for the FS link characteristics vary significantly. This, in turn, implies that sharing analysis carried out for an assumed set of link parameters may not be representative. Therefore, sensitivity analysis should be carried out for a number of link parameters including antenna diameter, radiation pattern and latitude to generalise the conclusions.

It should be noted that the maximum permissible degradation in FS links due to interference is attributed to “interference from other systems”. In the frequency bands of interest, FS systems are required to co-exist with both GSO FSS and NGSO FSS systems. Therefore, in order to evaluate the impact of aggregate interference from all FSS systems, interference statistics from NGSO FSS and GSO FSS systems need to be derived and compared against an FS receiver interference criteria which is based on a maximum permissible degradation of link performance objectives.

5.3.2 Terrestrial Interference Paths

From terrestrial interference paths point of view, compatibility studies suggest that the risk of interference between terrestrial radio stations of the fixed service and NGSO FSS Earth stations may not be significant in low populated areas. However, the risk increases in densely populated areas and, therefore, the sharing may be difficult in some hot spot areas where both systems are densely deployed. Under such circumstances, either one or both services may be excessively constrained or prevented from offering a viable service. Various mitigation techniques are proposed to improve the sharing situation by reducing the potential of interference. The implications of proposed mitigation techniques need to be examined in realistic deployment scenarios. The feasibility of potential mitigation techniques and their relative effectiveness are related to technical, economic and regulatory trade-offs.

It is noted that the calculation methods defined in Rec. IS.849 [201] are used to determine co-ordination areas around transmitting NGSO Earth stations for an

unknown receiving FS station. The co-ordination area calculations are based on conservative assumptions and the primary objective is to determine an area beyond which interference is negligible. Any FS station operating within a co-ordination area may experience interference. Under such circumstances, detailed (e.g. bi-literal) interference calculations need to be carried out taking site and path specific details into account and employing propagation models defined in Rec. P.452 [88].

It is noted from the reviewed studies that the terrestrial path interference analysis involving NGSO FSS Earth stations and FS terminals is based on determining an “exclusion area” around an FS receiver where the operation of an NGSO FSS Earth station may cause interference. These studies assume clear-sky line-of-sight propagation in each direction. It is, however, important to note that the exclusion area calculations should take account of transhorizon path propagation mechanisms if initial calculations results in beyond line-of-sight exclusion distances. In addition, if surrounding clutter and shielding information is available it should be incorporated into an analysis and the Rec. P.452 propagation loss prediction models should be used to obtain required separation distances.

In addition to the exclusion area analysis, implications of interference aggregating from simultaneously operating multiple NGSO FSS Earth stations need to be considered. For these purposes, a statistical analysis approach where input parameters are defined by various probability distribution functions could be employed.

5.4 Conclusions

Interference from the NGSO FSS transmitters will degrade the FS link performance objectives. Therefore, the maximum level of tolerable interference is primarily determined by the permissible degradation levels associated with the FS link performance objectives, which are defined in a number of ITU-R recommendations. Allowable degradations attributable to the NGSO FSS interference are expressed as a permissible fraction of the total allowable degradation which is attributed to the

thermal noise, intra-system interference and interference from other systems sharing the same frequency band.

The ITU-R recommendations addressing issues related to the protection of FS links from the NGSO FSS interference describe methodologies for deriving maximum permissible interference levels which are defined for both hypothetical paths and real links. In addition, the co-ordination area calculation methods based on simplified propagation models are described to determine the areas surrounding FS receivers where the operation of an NGSO FSS Earth station transmitter may cause interference. These methods take account of implications of the transmitter power, variation in NGSO FSS Earth station antenna gain towards the horizon, terrain profile, receiver interference threshold and path propagation mechanisms. In the interference situations where the FS receivers operate within a co-ordination area, detailed interference calculations need to be carried out using the site and path specific details.

It is noted that the impact of the space-to-Earth NGSO FSS interference is limited by the pfd masks imposed on the satellite transmitters. Sharing studies are mainly concerned with deriving pfd masks that would provide adequate protection for the majority of operational FS links while not imposing excessive burden on planned NGSO FSS systems. For the terrestrial path interference, it is suggested that the NGSO FSS Earth station transmissions should be restricted by setting up minimum separation distances towards the FS receivers for each azimuth considered, which, in turn, implies establishing NGSO FSS Earth station maximum EIRP limits in the direction of the FS receivers. Furthermore, a number of interference mitigation techniques are identified to reduce the impact of terrestrial path interference. These include the use of higher performance antennas, automatic transmit power control and dynamic channel assignment techniques, careful siting of terminals and operation with higher minimum elevation angle.

In the 30 GHz band, planned FS systems include PMP and Mesh type broadband fixed wireless access networks which are primarily designed for providing

broadband multimedia type services to the commercial and residential end users. The findings of the sharing studies indicate that the co-existence of NGSO FSS Earth stations and PMP access systems may not be feasible in the same geographical area due to potential for the high density deployment. Therefore, it is stated that the band segmentation may be a suitable solution to facilitate efficient use of the available spectrum.

In line with the information gathered from the critical examination of the available literature, the author's work into the examination of NGSO FSS / FS spectrum sharing issues is presented in the following chapter.

CHAPTER 6

SHARING ANALYSIS BETWEEN FIXED SERVICE AND NONGEOSTATIONARY FIXED SATELLITE SERVICE SYSTEMS

This chapter presents the author's work concerned with spectrum sharing methodologies used to assess the feasibility of Fixed Service (FS) and Nongeostationary Fixed Satellite Service (NGSO FSS) system co-existence in the frequency range *12 to 30 GHz*. During the course of this research, sharing methods have been developed and applied to the representative systems to examine the implications of both the downlink (from NGSO FSS satellite transmitters into terrestrial radio systems operating within FS) and uplink (from NGSO FSS Earth Station transmitters into terrestrial radio systems operating within FS) interference paths.

In the following section, a downlink interference analysis method is described to derive an FS link Carrier-to-Noise Ratio ($C/(N+I)$) statistics which are then compared against a link performance objectives to determine if a performance degradation due to interference is within acceptable limits. The method considers the joint effects of aggregate NGSO FSS interference power and FS link fading statistics by applying a convolution procedure. The implications of the use of the method have been investigated by carrying out a sharing analysis using the representative system characteristics assumed to be operating in the Ku band. The downlink sharing analysis is followed by a discussion outlining issues related to the application of the analysis method.

In the next section, single entry and aggregate interference analysis methods, developed for investigating the impact of NGSO FSS Earth station terrestrial interference paths into FS receivers, are presented. The single entry interference analysis method is based on integrating free space and diffraction propagation

effects. This is used to derive exclusion areas, where the co-existence of both an NGSO FSS Earth station transmitter and an FS receiver is not possible without causing a risk of unacceptable interference. The aggregate interference analysis method is a statistical approach, where a Monte Carlo simulation analysis technique is combined with a generic building blockage prediction method to calculate an aggregate interference statistics from a randomly positioned interferer population. Both analysis methods have been applied to examine the problem of NGSO FSS terrestrial path interference, using the representative systems assumed to be operating in the Ka band. As in the case of downlink analysis, a discussion section is presented to summarise the implications of the use of the analysis methods.

Finally, the key conclusions at the end of the chapter bring out an overview of the sharing methodologies described in this phase of the research.

6.1 Interference from NGSO FSS Satellites into Terrestrial Radio Systems Operating within FS

As stated in Chapter 5, ITU-R studies examining the NGSO FSS / FS downlink interference analysis are based on deriving aggregate interference statistics at a given FS receiver, when a receiver antenna is pointing at its worst-case azimuth. These studies assume that NGSO FSS satellites transmit at either pfd limits or power levels stated in the system filings. For both assumptions, the resultant interference statistics are compared against an FS interference criterion, which is a maximum allowable interference power level defined relative to a receiver noise power, to check if the adequate protection is achieved. In addition, interference statistics are compared against each other to address the implications of the use of the pfd approach as opposed to the full system characteristics approach [207-214].

It is important to note that when FS links are deployed, the transmitter power, at each end, is adjusted at an initial link set-up according to distance. In general, the carrier level at the receiving end is not constant, with the observed variations being determined by propagation mechanisms causing a transmitted/wanted signal fading.

Therefore, methods employed for the NGSO FSS / FS downlink sharing analysis should take account of fading statistics affecting an FS wanted path.

6.1.1 Interference Analysis Approach

The analysis method developed in this study for assessing the impact of NGSO FSS downlink interference into an FS link is based on calculating joint effects of aggregate NGSO FSS interference and FS link received power statistics. Aggregate interference statistics are derived from a deterministic simulation analysis, where an NGSO FSS constellation is modelled fully by taking individual beam patterns and transmission characteristics into account.

In order to derive worst-case aggregate interference statistics, an FS receiver is assumed to be pointing at its worst-case azimuth, and interfering paths are assumed to be line-of-sight. Therefore, interference path propagation is modelled by assuming that free-space and atmospheric loss mechanisms are present.

At an FS receiver, wanted power statistics are determined by link fading mechanisms. At the Ku and Ka band frequencies, fading due to multipath and rain mechanisms need to be considered. Prediction models for the multipath and rain effects are defined in Recommendation P.530 [87]. Note that the derivation of multipath and rain fading statistics was detailed earlier in Chapter 2.

The interference analysis method is completed by convolving the aggregate NGSO FSS downlink interference probability density function (pdf) and the FS link joint rain and multipath fading pdf, as illustrated in Figure 6.1.

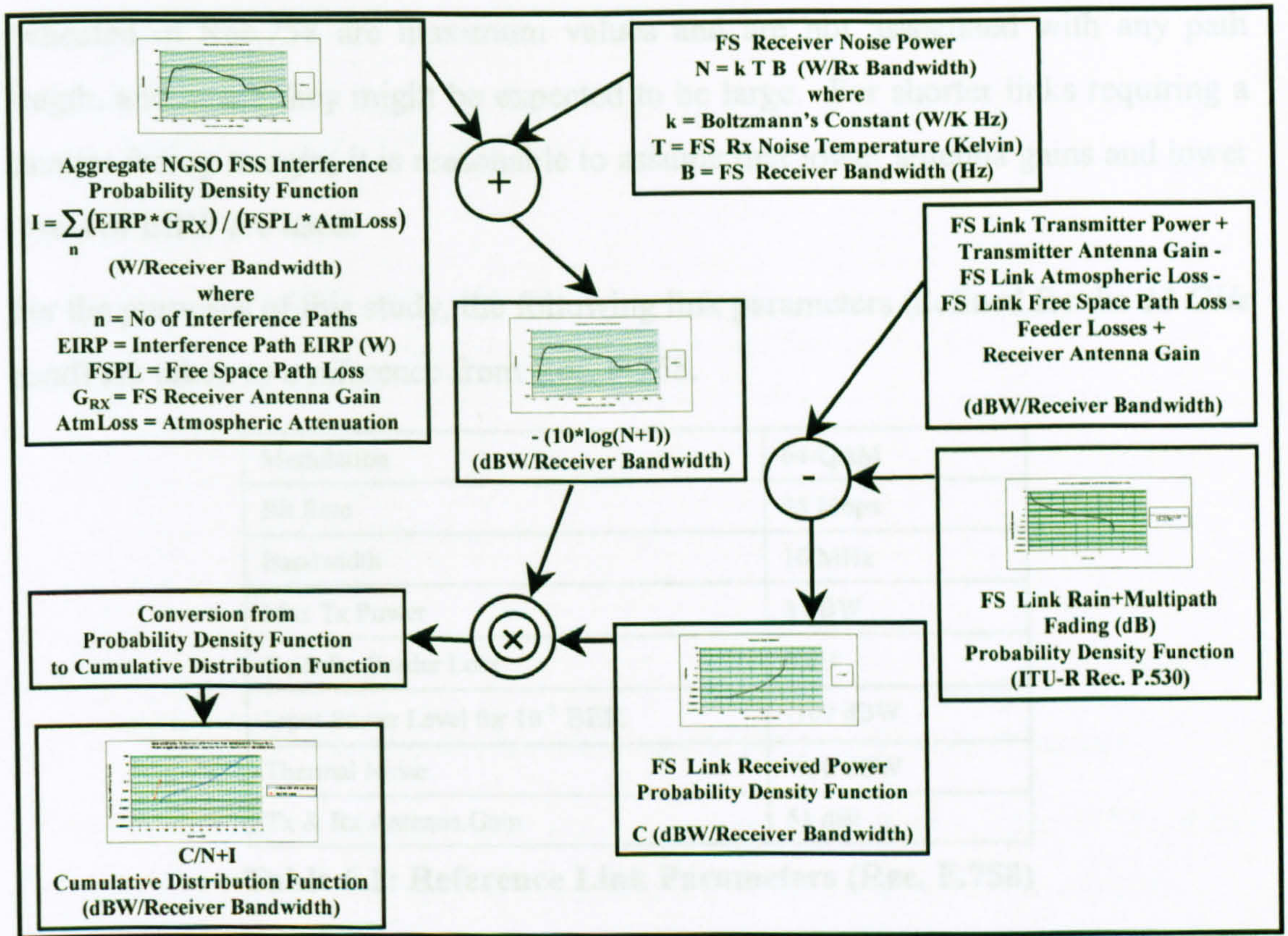


Figure 6.1: Downlink Interference Analysis Method

6.1.2 Interference Analysis

In this section, a link design process has been applied for deriving representative FS link parameters. For the representative link, the author describes an interference criteria derivation method using the new definitions for FS link performance objectives defined by ITU-T. The NGSO FSS space-to-Earth transmission parameters given in Chapter 3 are also summarised for completeness. The interference analysis method, shown in Figure 6.1, has been applied to investigate the impact of downlink interference by taking representative system characteristics into account.

6.1.2.1 Representative FS Link

The FS link characteristics defined in Rec. F.758 [102] are commonly used in sharing studies involving FS systems. It is important to note that EIRP values

indicated in Rec.758 are maximum values and are not associated with any path length, and hence they might be expected to be large. For shorter links requiring a smaller fading margin, it is reasonable to assume that lower antenna gains and lower levels of EIRP are used.

For the purposes of this study, the following link parameters (defined for the *12 GHz* band) are taken as a reference from Rec. F.758.

Modulation	64-QAM
Bit Rate	45 Mbps
Bandwidth	10 MHz
Max Tx Power	3 dBW
Tx & Rx Feeder Loss	0 dB
Input Power Level for 10^{-3} BER	-109 dBW
Thermal Noise	-130 dBW
Tx & Rx Antenna Gain	51 dBi

Table 6.1: Reference Link Parameters (Rec. F.758)

On the basis of the above parameter values, the following steps are implemented to derive appropriate link parameter values for an assumed link length of 10km.

- It is assumed that :
 - The link is operating at *12 GHz*,
 - The required link availability is *99.99%*,
 - Tx & Rx Antenna Gains are *40 dBi* corresponding to *1m* dish at each end,
 - Tx & Rx feeder loss is *1 dB*,
 - The minimum C/N required for 10^{-3} BER is *23 dB* (64-QAM) [227].
- Additional parameters required for the derivation of rain and multipath fading statistics are shown in Table 6.2 below:

Rainfall rate	25 mm/h
Path elevation angle	0 degrees
Polarisation tilt angle relative to horizontal	0 degrees
Latitude	50 degrees
Longitude	0 degrees
Lower antenna altitude above mean sea level	0 metre
Percentage time that the refractivity gradient in the lowest 100 m of the atmosphere is more negative than -100 N units/km	5 %
Path type	Inland
Receiver antenna height above mean sea level	10 metre
Transmitter antenna height above mean sea level	10 metre
Atmospheric pressure	1013 hPa
Temperature	15 C
Water vapour density	10 g/m ³

Table 6.2: Parameters for Rain and Multipath Fading Statistics

- Using rain and multipath fading estimation methods defined in Rec. P.530, it can be shown that for a *10 km* link operating at *12 GHz* with *99.99%* availability:
 - Multipath Fading = *10.11 dB* exceeded for *0.00696%* of time
 - Rain Fading = *10.11 dB* exceeded for *0.00306%* of time

Therefore, the link fade margin is assumed to be *~11dB*.

- Assuming rain and multipath fading do not occur simultaneously, the unavailability caused by propagation fading is *0.00696% + 0.00306% ≈ 0.01%*, which suggests that the multipath fading contributes more than the rain fading to the total unavailability for the link considered here. In practice, some links may operate with more margin to make allowance for other fading mechanisms.
- *Atmospheric Loss* is calculated to be *0.2 dB* from the simplified atmospheric attenuation estimation model described in Rec. P.676-4 [86].
- *Free Space Path Loss* is given by

$$10 \log(4 \pi \text{ Path Length} / \lambda)^2 \quad (6-1)$$

where λ is the wavelength.

- Using the above formula, for a *10 km* link operating at *12 GHz*, *Free Space Path Loss* is calculated to be *134 dB*.
- The objective is to determine a required *EIRP* corresponding to parameter values given in Table 6.1 and 6.2. The following equation forms the basis for the calculations (all expressed in dBs):

$$TxPower = C/N \text{ Required for } 10^{-3} \text{ BER} + Rx \text{ Noise Power} + Tx \text{ Feeder Loss} + \text{Free Space Path Loss} + \text{Atmospheric Loss} + \text{Fade Margin} + Rx \text{ Feeder Loss} - Tx \text{ Gain} - Rx \text{ Gain}$$

(6-2)

- Taking the calculated parameter values into account, it can be shown that required transmitter power (*Tx Power*) is $\approx -40 \text{ dBW/10MHz}$ and, therefore, required *EIRP* is *0 dBW/10MHz*.

In line with the above calculations, parameter values shown in Table 6.3 are assumed to be the representative FS transmitter characteristics:

Link Length (km)	10 km
Tx and Rx Antenna Gain (dBi)	40
Tx and Rx Antenna Radiation Pattern (on the basis of Rec.758)	Rec.699
Tx and Rx Feeder Loss (dB)	1
Carrier Bandwidth (MHz)	10
Transmitter Power (dBW/10MHz)	-40
Maximum EIRP (dBW/10MHz)	0
Thermal Noise (dBW/10MHz)	-130
Tx and Rx Mean Antenna Height (a.g.l.) (m)	10

Table 6.3: Representative FS Link Characteristics

6.1.2.2 FS Link Interference Criteria

As stated previously, point-to-point links operating within the fixed service are deployed in infrastructure of cellular networks, for example to link base station transceivers to base station controllers, in the *12 GHz* band. Furthermore, the ITU-R Radio Relay Systems Handbook [70] states that the short haul inter-exchange section of national digital path includes connections used in cellular infrastructure networks.

Therefore, for the purposes of the present analysis, an FS link interference criteria is derived assuming that the representative link considered here is a real link, and forms a short haul section of national portion constant bit rate digital path, operating above the primary rate. Note that the representative FS link bit rate is *45 Mbps* which is above the primary rate of *2.048 Mbps*.

It is noted that the performance objectives for short haul links operating above the primary rate are defined in the recent ITU-R Recommendation F.1491 [228]. These performance objectives are derived from the new recommendation ITU-T G.826 [189]. A major change in the new recommendation is the subdivision of seconds into blocks, to allow straightforward in-service testing of links. A block is defined as “a set of consecutive bits associated with the transmission path” and each second of the transmission is subdivided into *N* blocks. In line with the block definition, the new recommendation replaces the previous ES and SES definitions (see Chapter 5) with the following:

- *Errored Block (EB)* : a block with one or more bits in error,
- *Errored Second (ES)* : a one second period with one or more errored blocks,
- *Severely Errored Seconds (SES)* : a one second period with more than 30% errored blocks,
- *Background Block Error (BBE)* : an errored block not within a SES. This parameter provides a limit for long-term interference effects.

The corresponding error ratios are specified as *ESR*, *SESR* and *BBER*. It might seem that the *ES* criterion remains unchanged, as a single bit-error is sufficient to cause an errored block. However, the block concept makes the distribution of errors critical. A cluster of errors may have no more impact than a single error, if they fall in the same block, but a few errors falling in different blocks may lead to an unacceptable *ES* rate. In the case of the *SES* definition, the criterion is quite different in that the 30% limit aims to capture random errors. It is important to note that the *BBER* corresponds to the old *RBER* defined in ITU-R Rec. F.634 [229] as the *BER* in the

absence of short-term fading on a radio link. The *BBER*, however, no longer excludes events associated with short-term propagation [189].

On the basis of Rec. F.1491, the error performance objectives for the real FS links which form the short haul network section of the national portion of the digital path operating at or above the primary rate are shown in Table 6.4:

Bit Rate (Mbps)	1.5 to 5	>5 to 15	>15 to 55	>55 to 160	>160 to 3,500
ESR	0.04 B	0.05 B	0.075 B	0.16 B	For further study
SESR	0.002 B	0.002 B	0.002 B	0.002 B	0.002 B
BBER	$2 * B * 10^{-4}$	$2 * B * 10^{-4}$	$2 * B * 10^{-4}$	$2 * B * 10^{-4}$	$1 * B * 10^{-4}$

Table 6.4: Error Performance Objectives (from Rec. F.1491)

The value of B is agreed to be in the range of 0.075 and 0.085. For the assumed single hop representative FS link, the bit rate is given as 45 Mbps and, therefore, the parameters given for 15-55 Mbps need to be used. Assuming B is 0.08, the link performance objectives can be calculated as:

ESR	0.006
SESR	0.00016
BBER	0.000016

Table 6.5: Representative FS Link Performance Objectives

The above objectives are defined to include the effects of interference and all other sources of performance degradations. The allowable degradation in the performance of FS systems due to interference from other services sharing the same frequency bands on a primary basis are expressed as a permissible fraction of the total error performance objectives.

ITU-R Rec. SF.615 [198] states that the allowable degradation due to interference should be 10% of the total error performance objectives. Furthermore, the ITU-R Radio Relay Systems Handbook [70] notes that in the frequency bands shared by services other than FS and FSS on a primary basis, the value of 10% should be further subdivided into these services. For the analysis purposes, it is assumed that the frequency band under consideration is shared among FS and FSS systems. The

allowable degradations in the representative FS link’s performance objectives due to aggregate interference from FSS systems are then calculated to be the 10% of the values shown in Table 6.5 and illustrated in Table 6.6.

ESR	0.0006
SESR	0.000016
BBER	0.0000016

Table 6.6: Allowable Degradations in Representative FS Link Performance Objectives

Using the new definitions of error performance objectives, it has been shown that the new SES corresponds to seconds where the *BER* is $>1.7*10^{-5}$. It is further shown that both the new ES and BBER requirements can be met if the *BER* is $<10^{-12}$ [230].

In this study, these *BER* figures have been used to derive the FS link short-term and long-term interference criteria. As the representative link employs 64-QAM modulation technique, it can be shown from the corresponding modulation/demodulation performance curves derived in the presence of *Additive White Gaussian Noise* [227] that the *BER* of $1.7*10^{-5}$ requires the $(C/N+I)_1$ ratio of 28 dB while the *BER* of 10^{-12} requires the minimum $(C/N+I)_2$ ratio of 30 dB.

Taking the $(C/N+I)_1$ value and the maximum allowed *SESR* degradation figure shown in Table 6.6 into account, the short term interference criterion for the representative FS link is calculated as :

$$C/N+I= 28\text{ dB (not to be exceeded for 0.0016\% of the time)}$$

As stated earlier, the $(C/N+I)_2$ value can be associated with the long-term interference effects. The conventional criterion for the long term interference percentage time is defined as 20% in ITU-R Rec.758 [102]. Using the calculated $(C/N+I)_2$ and the percentage time of 20%, the long term interference criterion for the representative FS link is calculated as:

$$C/N+I= 30\text{ dB (not to be exceeded for 20\% of the time)}$$

6.1.2.3 NGSO FSS System Parameters

Interference scenarios considered here employ individual beam patterns and transmitter powers to derive likely downlink interference levels. The system characteristics representing the NGSO Ku-1 system (given in Chapter 3) have been used as the representative system. For completeness, the downlink parameters are reproduced in Table 6.7.

No of Planes	20
No of Satellites per Plane	4
Maximum Number of Co-frequency Co-polar Beams per Satellite	6
Orbit Height	1469 km
Inclination	53 degrees
Frequency	12 GHz
Carrier Bandwidth	22.6 MHz
Maximum Satellite Transmitter Antenna Gain	15 dBi
Maximum Satellite Transmitter Power	1.4 dBW
Satellite Transmit Antenna Pattern	Based on contours given in the system filing (see Figure 3.10 in Chapter 3)

Table 6.7: NGSO Ku-1 Downlink System Characteristics

Using the representative FS and NGSO FSS system characteristics together with the FS interference criteria, single entry interference levels have been calculated to gain an initial insight of the sharing environment. Interference modelling has been carried out by employing a deterministic simulation approach. The FS link fading distributions have been derived using the prediction models defined in Rec. P.530 [87]. Simulation results and FS link fading statistics have been then used to apply the method described in Figure 6.1 for obtaining the representative link C/N+I statistics. These statistics have been compared against the interference criteria to assess the impact of interference.

6.1.2.4 Single Entry Interference Levels

This section is concerned with the calculation of maximum and minimum expected single entry interference levels from the NGSO Ku-1 satellite transmitter. For the

potential worst-case single interference entry, alignments shown in Figure 6.2 have been considered.

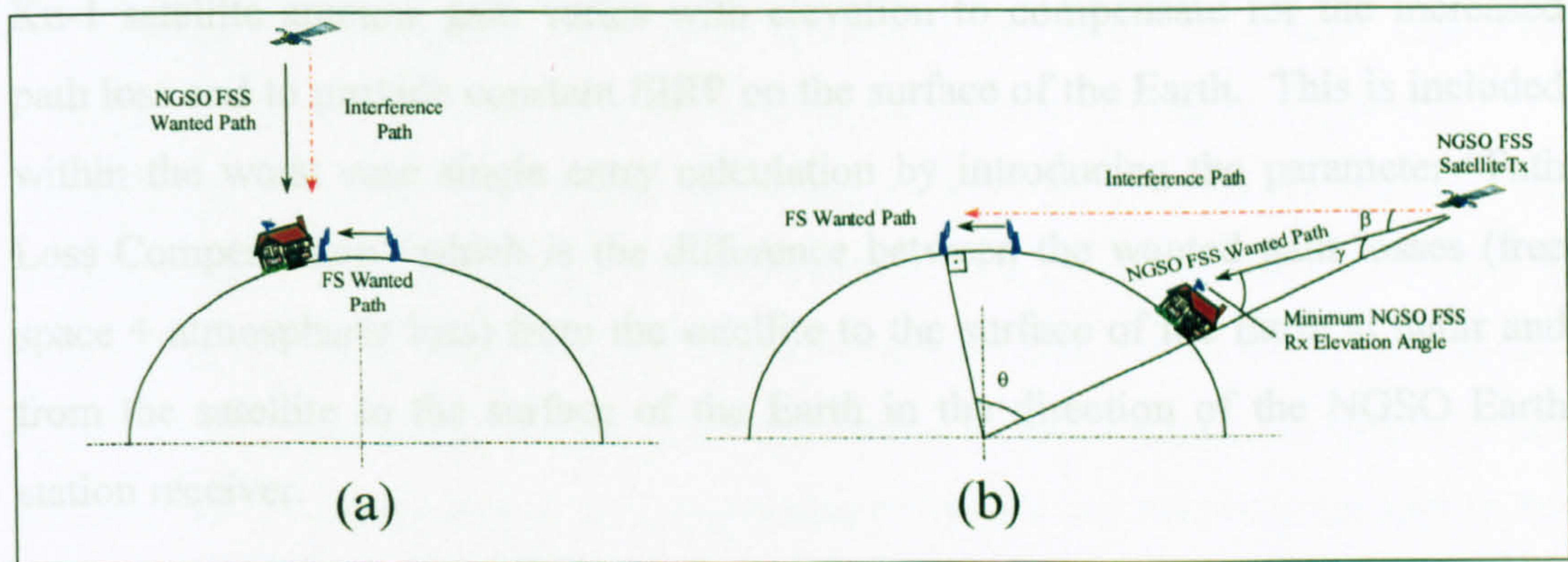


Figure 6.2 (a) (b): Potential Worst-case Single Entry Interference Alignments

Parameters shown in Table 6.8 have been calculated from the above interference alignments.

(a)	(b)
NGSO Earth station receiver elevation angle = 90 degrees	Minimum NGSO Earth station receiver elevation angle = 10 degrees
Off-axis angle from NGSO satellite transmitter to fixed terrestrial link receiver = 0 degrees	Off-axis angle from NGSO satellite transmitter to fixed terrestrial link receiver, $\beta = 1.2$ degrees
Off-axis gain at NGSO satellite transmitter = 15 dBi	Off-axis gain at NGSO satellite transmitter = 14.7 dBi
Interference path length = 1469 km	Interference path length = 4570 km
Interference path free space propagation loss = 177.3 dB	Interference path free space propagation loss = 187.2 dB
Wanted path length = 1469 km	Wanted path length = 3596 km
Wanted path free space propagation loss = 177.3 dB	Wanted path free space propagation loss = 185.2 dB
Atmospheric loss = 0.05 dB	Wanted path atmospheric loss = 0.4 dB
Fixed terrestrial link receiver antenna gain (rearlobe) = -5.96 dBi	Path loss compensation = $(185.2 - 177.3) + (0.4 - 0.05) = 8.3$ dB
Single Entry Interference Power = -170.4 dBW/10 MHz	Interference path atmospheric loss = 1.4 dB
	Fixed terrestrial link receiver antenna gain (boresight) = 40 dBi
	Single Entry Interference Power = -127.7 dBW/10 MHz

Table 6.8: Potential Worst Case Single Entry Interference Power Levels

It seems that the worst case single entry interference is the result of an alignment where the satellite transmitter is within the FS receiver antenna boresight and the

Earth station, located at some distance from the FS receiver, is receiving at its minimum allowed elevation, 10° degrees. It is important to note that the NGSO FSS Ku-1 satellite antenna gain varies with elevation to compensate for the increased path loss and to provide constant EIRP on the surface of the Earth. This is included within the worst case single entry calculation by introducing the parameter “Path Loss Compensation” which is the difference between the wanted path losses (free space + atmospheric loss) from the satellite to the surface of the Earth at nadir and from the satellite to the surface of the Earth in the direction of the NGSO Earth station receiver.

For the minimum single interference entry at the FS receiver, the interference alignment shown in Figure 6.3 has been considered.

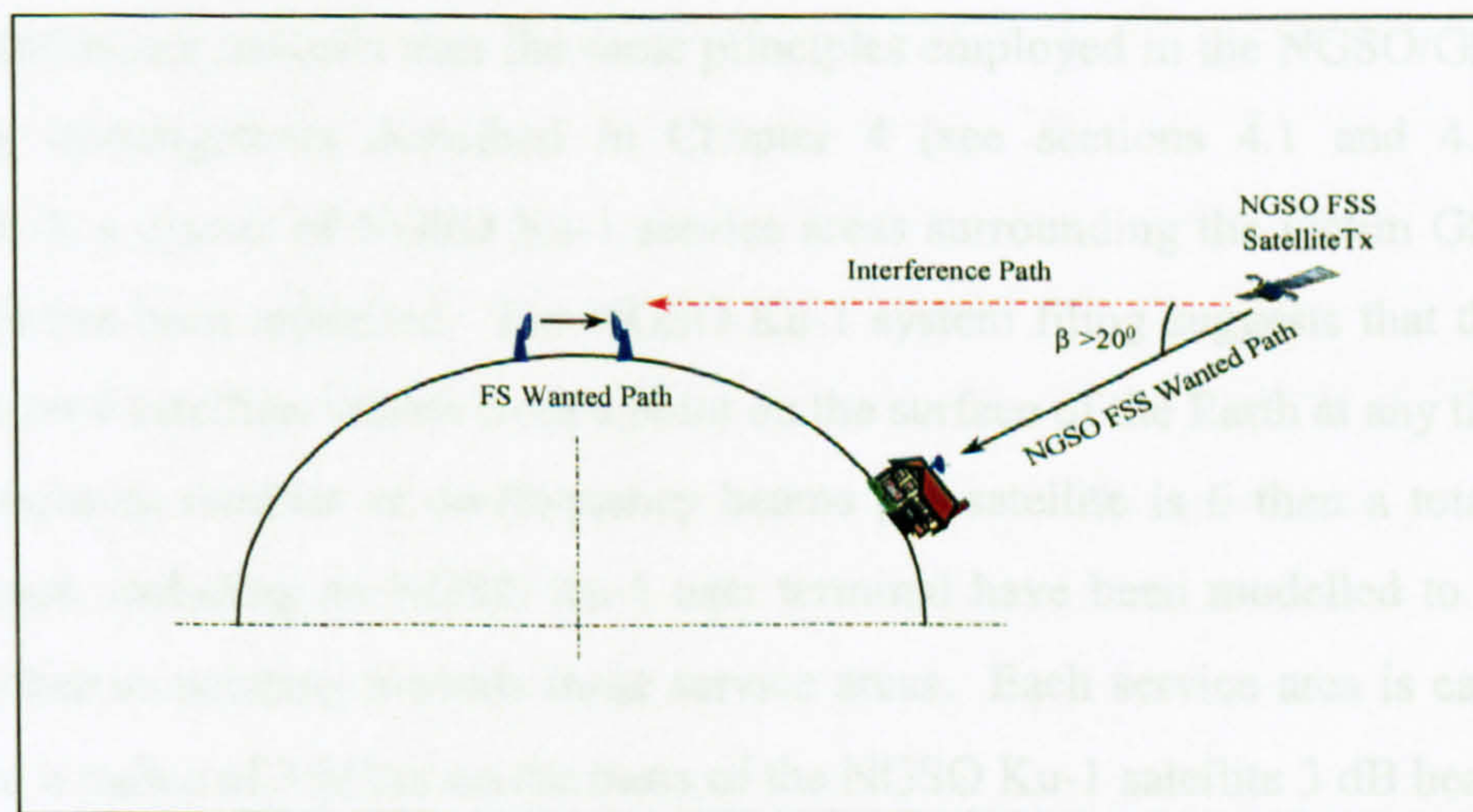


Figure 6.3: Lowest Single Entry Interference Alignment

Satellite transmitter antenna radiation patterns (given in Figure 3.10 in Chapter 3) indicate that when interference path from the NGSO Ku-1 satellite is at an off-axis angle of $>20^\circ$ the antenna gain is at its lowest level, -5 dBi . In addition, the FS receiver antenna pattern is represented by an envelope defined in Rec. F.699 [75] which suggests that the rearlobe antenna gain is -5.96 dBi . Taking these figures into account, it can be shown that the minimum single interference entry level is -201.7 dBW/10MHz .

6.1.2.5 *Interference Scenario*

An interference scenario comprising the NGSO Ku-1 constellation and the representative FS receiver has been simulated in order to obtain aggregate interference statistics to be used in the analysis method shown in Figure 6.1. As stated earlier, the sharing scenarios involving NGSO FSS systems are dynamic. In the simulation run, the position of each satellite in a given NGSO FSS system is determined at regular time intervals over an extended time period and from this data a series of “interference events” are calculated. Time intervals are typically one second. The events are then analysed statistically and the results presented in the form of graphs showing interference level against the percentage of time over the simulated period for which that level was exceeded.

The interference analysis uses the same principles employed in the NGSO/GSO FSS sharing investigations described in Chapter 4 (see sections 4.1 and 4.2). In Chapter 4, a cluster of NGSO Ku-1 service areas surrounding the victim GSO FSS receiver has been modelled. The NGSO Ku-1 system filing suggests that there are maximum 4 satellites visible from a point on the surface of the Earth at any time. As the maximum number of co-frequency beams per satellite is 6 then a total of 24 areas each including an NGSO Ku-1 user terminal have been modelled to load all visible beams pointing towards these service areas. Each service area is calculated to be of a radius of 350 km on the basis of the NGSO Ku-1 satellite 3 dB beamwidth and the orbit height. The victim GSO FSS receiver has been assumed to be co-located with an NGSO Ku-1 ground terminal receiver at the centre of the cluster of service areas at latitude of 50 degrees.

It is, however, important to note that, in the NGSO/GSO FSS sharing scenario, the victim receiver points towards the geostationary orbit (i.e. the wanted link has been modelled as an elevated path). Therefore, NGSO FSS Earth stations distributed within a total area of $24 * \pi * 350^2$ (corresponding to a radius of approximately 1700km) are sufficient to explore the worst-case interference alignments. Here, the victim FS receiver is at 0° elevation. This, in turn, implies that the number of

NGSO FSS Earth stations and the area over which they are distributed need to be increased to explore all likely interference alignments. It is noted that in order to increase the likelihood of achieving the worst case interference alignment shown in Figure 6.2 (b), the distance between the FS receiver and the NGSO Ku-1 Earth station operating at the minimum elevation needs to be approximately *4000 km*. Therefore, in the simulation scenario, the number of NGSO Ku-1 Earth stations has been increased by approximately 4 times by increasing the area of radius to *4000 km*.

As in the NGSO/GSO FSS sharing scenarios, the victim FS receiver is assumed to be co-located with the NGSO Ku-1 Earth station receiver at the centre of the cluster of service areas at latitude of *50 degrees*. It is worth noting that each NGSO FSS constellation will produce higher levels of cumulative interference over time at some azimuths than at others, for a given latitude and elevation. This is essentially due to the visibility statistics of the satellites, which in turn depend on the orbital characteristics. Therefore, interference statistics arising from multiple satellite interferers are dependent on the azimuth pointing angle of the FS receiver antenna and the worst case azimuth must be determined for the sharing scenario examined.

An analytic method for the derivation of the worst case azimuth as seen from an FS receiver is presented previously in Chapter 5. By applying this method to the NGSO Ku-1 constellation, the worst case azimuths with respect to the North are calculated to be 62° and 298° assuming that the FS receiver is located at 50° latitude and elevated at 0° .

6.1.2.6 Simulation Results

Using the above defined simulation model, a run of *700,000* steps of *1* second each, corresponding to time required for travelling NGSO Ku-1 orbit *100* times, has been implemented. The resultant aggregate interference statistics are illustrated in Figure 6.4.

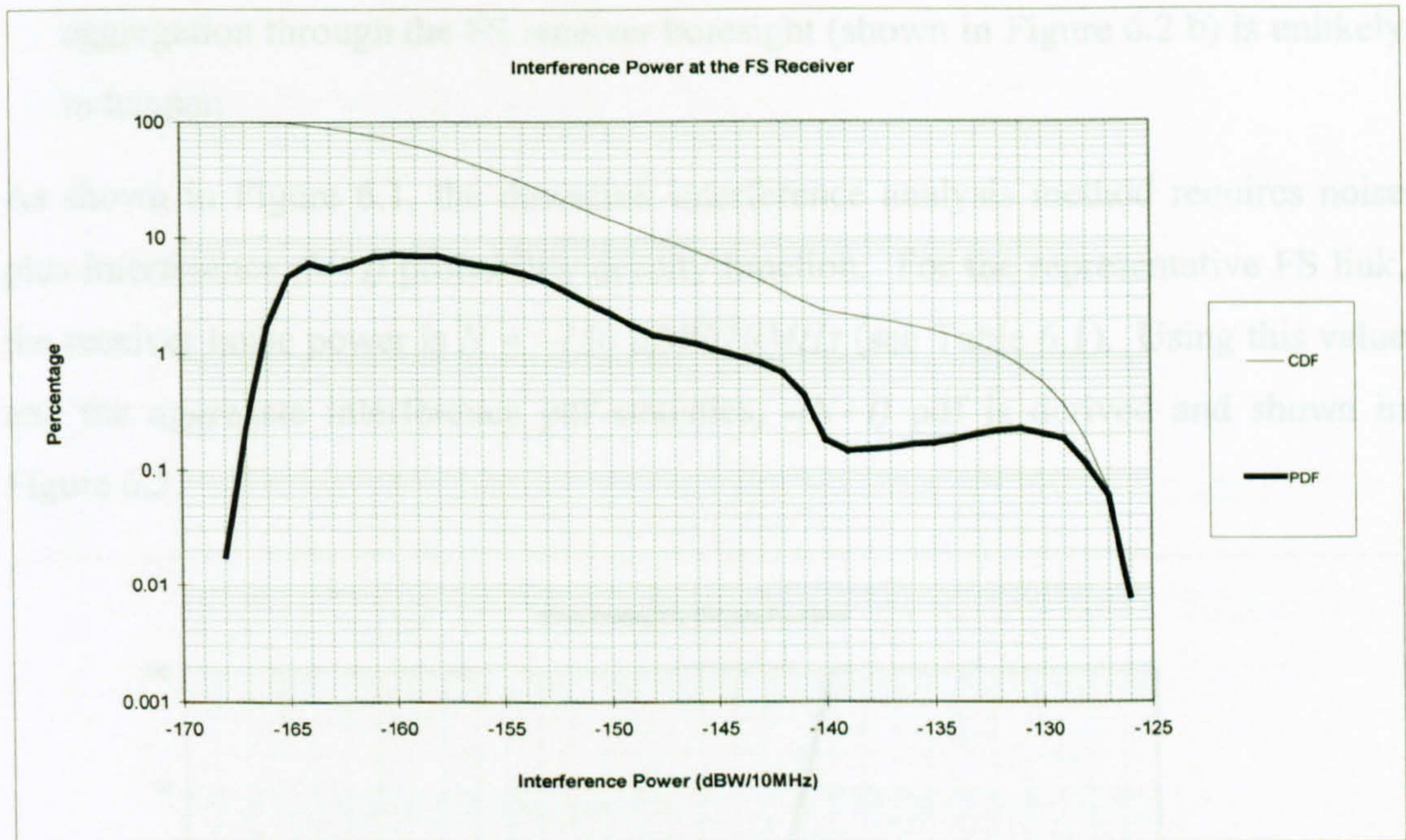


Figure 6.4: Aggregate Interference Statistics

The interference statistics are plotted in the form of cumulative distribution function (cdf) and probability density function (pdf). The cdf indicates that, for example, interference power exceeds -127 dBW/10MHz for 0.07% of the simulated time. The pdf plot suggests that, for example, the probability of interference power being between -127.5 dBW/10MHz and -126.5 dBW/10MHz is 0.06% as the statistics are based on interference values stored in 1dB wide bins.

The simulation results show that the aggregate interference power received at the receiver varies between -168 dBW/10MHz and -126 dBW/10MHz . Comparison of these figures against the corresponding single entry interference values which are calculated previously to be -201.7 dBW/10MHz and -127.7 dBW/10MHz , indicates that when multiple interference entries are considered:

- the long term interference level (left end of the aggregate interference cdf shown in Figure 6.4) increases because of power aggregation from multiple interfering paths
- the short term interference (right end of the aggregate interference cdf shown in Figure 6.4) remains at a similar level the same because simultaneous power

aggregation through the FS receiver boresight (shown in Figure 6.2 b) is unlikely to happen

As shown in Figure 6.1, the downlink interference analysis method requires noise plus interference $(N+I)$ probability density function. For the representative FS link, the receiver noise power is $N = -130 \text{ dBW}/10\text{MHz}$ (see Table 6.1). Using this value and the aggregate interference pdf statistics, $-(N+I)$ pdf is derived and shown in Figure 6.5.

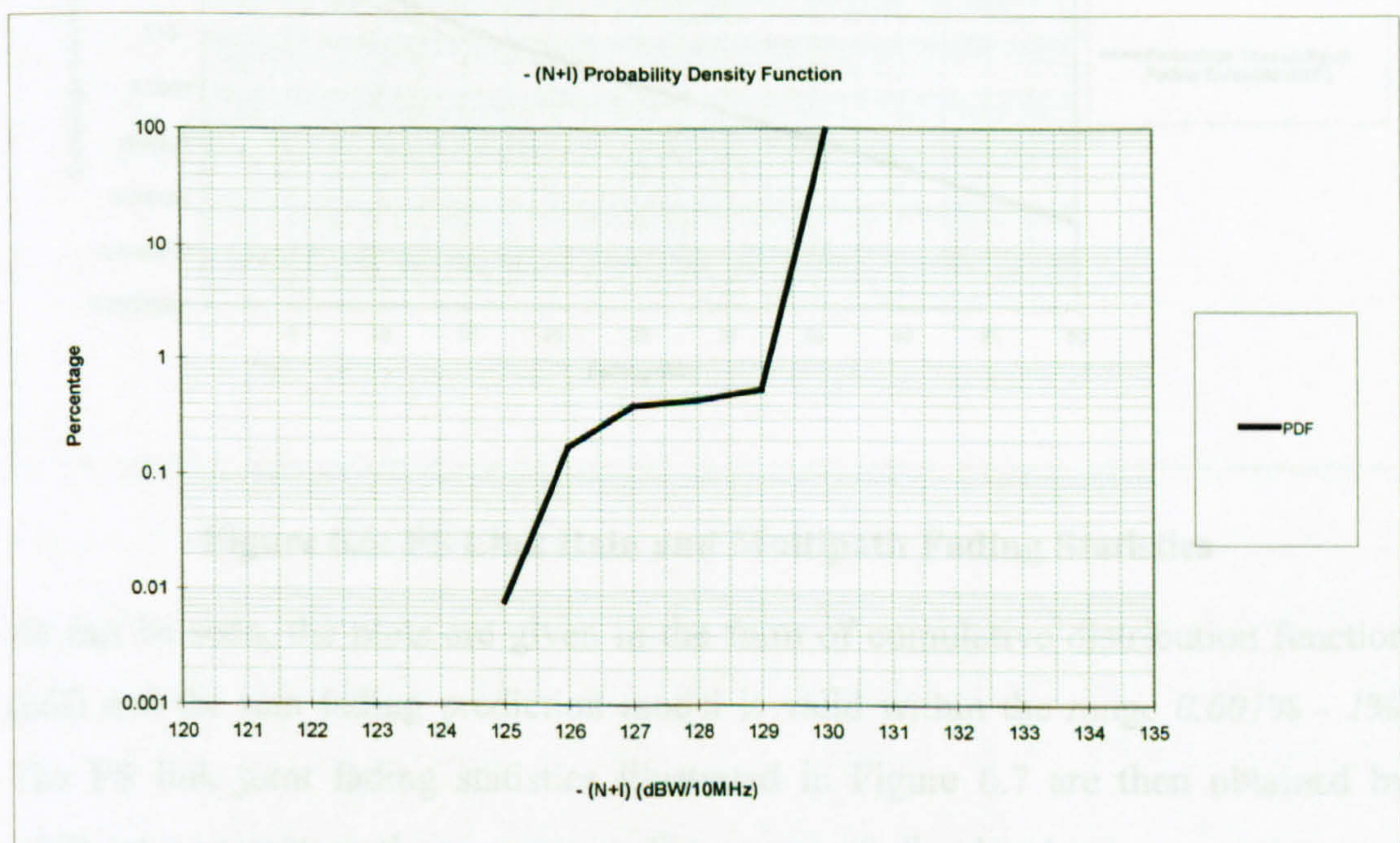


Figure 6.5: $-(N+I)$ Probability Density Function

In deriving $-(N+I)$ pdf, the aggregate interference and noise levels are converted into numeric terms and added before converting back to logarithmic terms. It can be noted that the resultant curve is largely dominated by the receiver noise power and varies within $125 \text{ dBW}/10\text{MHz}$ and $130 \text{ dBW}/10\text{MHz}$.

6.1.2.7 FS Fading Statistics

Next step involves derivation of the FS link fading statistics. For these purposes, the rain and multipath fading prediction models of Rec. P.530 [87] have been used. These prediction models are detailed in Chapter 2. Figure 6.6 illustrates the fading

statistics obtained for the *10km* representative link considered here. Assumed FS link parameter values are the same as those given in Table 6.2.

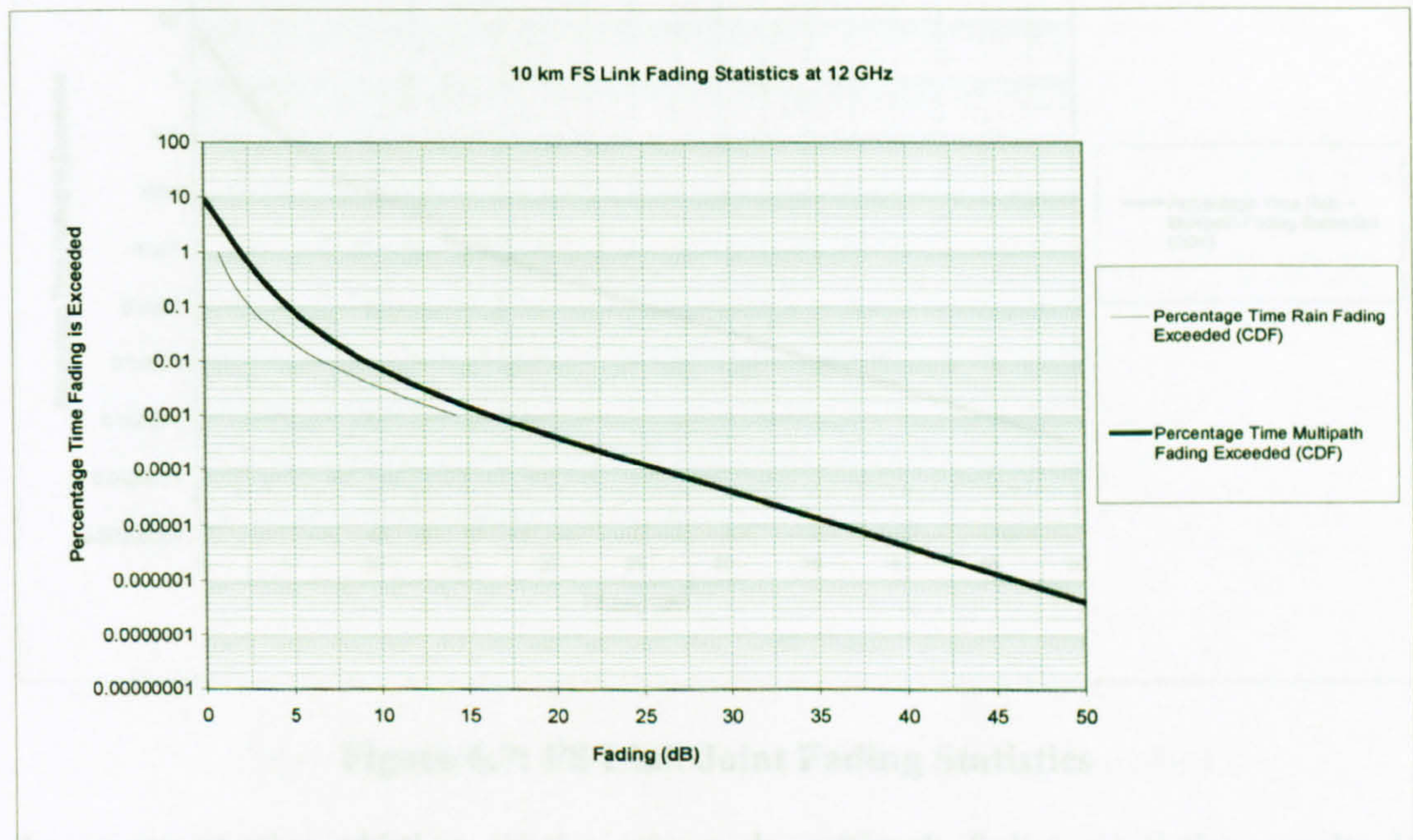


Figure 6.6: FS Link Rain and Multipath Fading Statistics

As can be seen, the plots are given in the form of cumulative distribution function (cdf) and the rain fading prediction model is valid within the range *0.001%* - *1%*. The FS link joint fading statistics illustrated in Figure 6.7 are then obtained by adding the percentage times corresponding to same fading level.

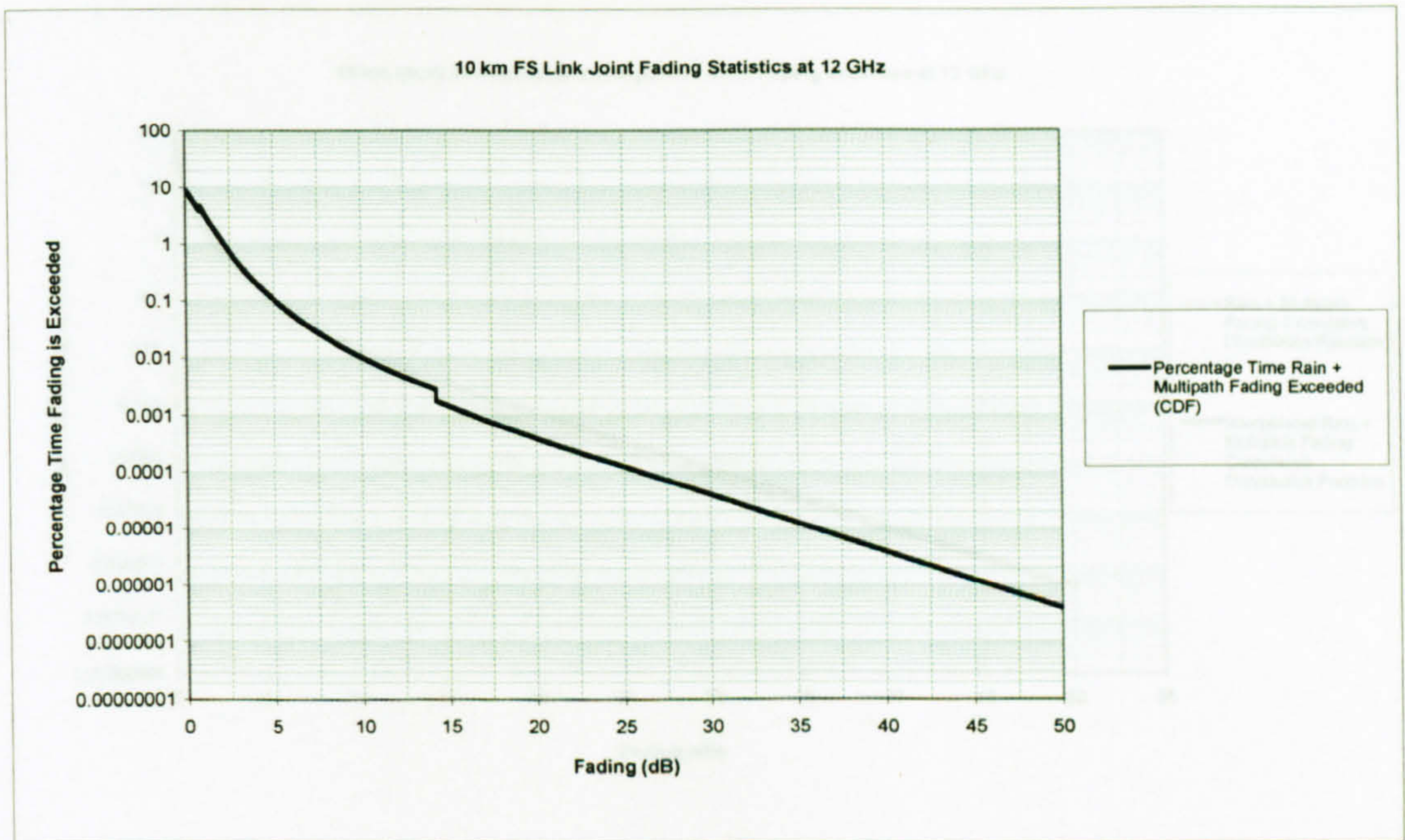


Figure 6.7: FS Link Joint Fading Statistics

As expected, the addition of the rain and multipath fading statistics results in discontinuity at percentage times beyond which rain fading model is not valid. In addition, the analysis method requires that the joint fading statistics be convolved with the interference plus noise power ($N+I$) statistics shown in Figure 6.5. The convolution process requires complete (i.e. defined up to 100%) distribution functions. Therefore, linear interpolation is applied to the FS link joint statistics to remove the discontinuity and to obtain a complete cumulative distribution function. The interpolated statistics are illustrated in Figure 6.8 below.

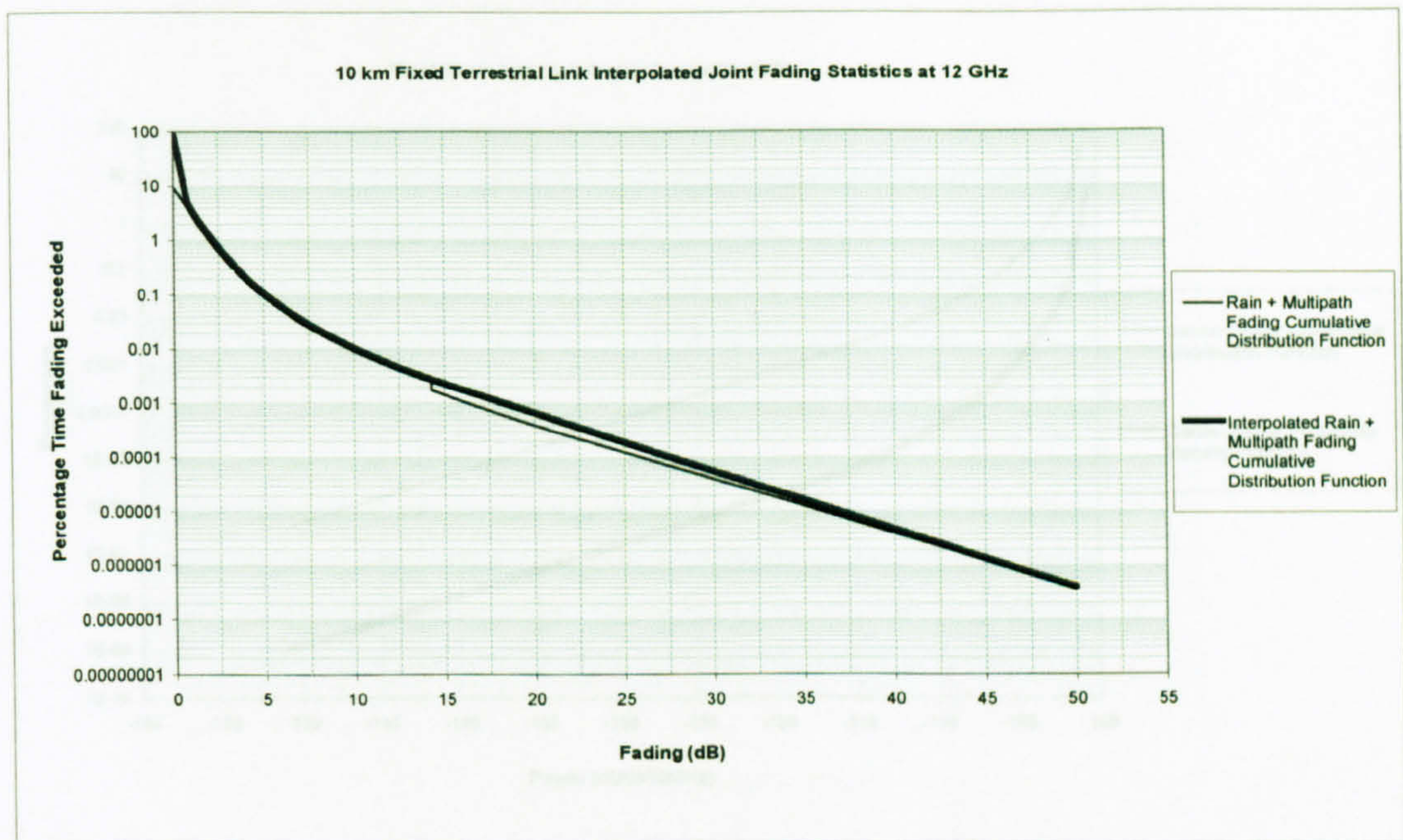


Figure 6.8: Interpolated FS Link Joint Fading Statistics

In line with the interference analysis method, shown in Figure 6.1, the interpolated joint fading statistics are further processed to obtain the carrier power statistics by using:

- interpolated link fading statistics (illustrated in Figure 6.8),
- FS link transmitter power of $-40 \text{ dBW}/10\text{MHz}$ (given in Table 6.1),
- Transmitter and receiver antenna gain of 40 dBi (given in Table 6.1),
- Transmitter and receiver feeder loss of 1 dB (given in Table 6.1),
- Free space path loss of 134 dB (10km link operating at 12GHz),
- Atmospheric loss of 0.2 dB (10km link operating at 12GHz).

in the following expression:

$$\begin{aligned} \text{Received carrier power} = & \text{Transmitter power} + \text{Transmitter antenna gain} - \text{Joint rain and} \\ & \text{multipath fading} - \text{Free space loss} - \text{Atmospheric loss} + \text{Receiver antenna gain} - \\ & \text{Transmitter feeder loss} - \text{Receiver feeder loss} \end{aligned}$$

Figure 6.9 illustrates the carrier power statistics at the terrestrial link receiver.

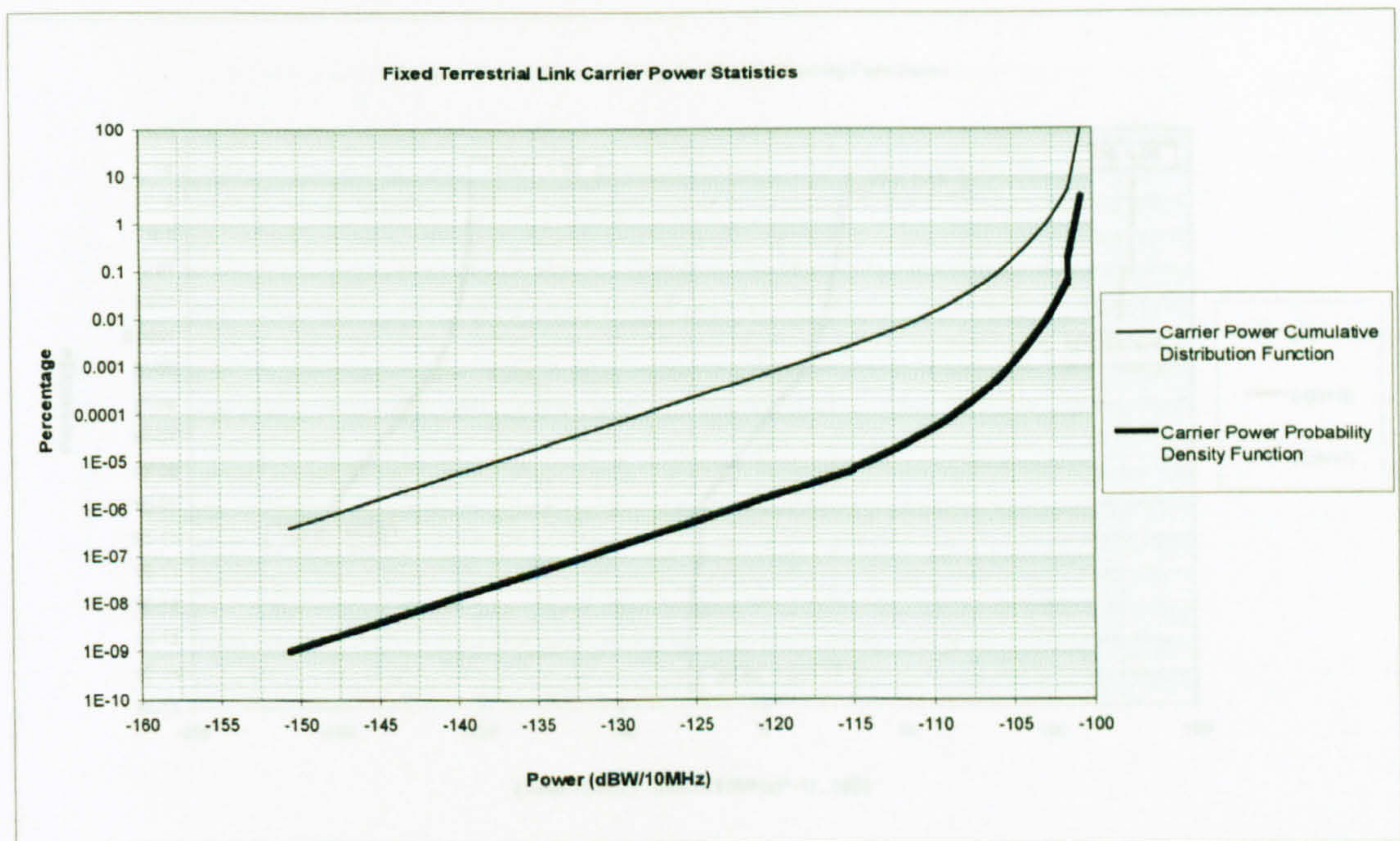


Figure 6.9: FS Link Received Carrier Power Statistics

6.1.2.8 Convolution Results

The next step in the interference analysis method is the convolution of the carrier power (C) pdf, illustrated in Figure 6.9, and the noise+interference ($-(N+I)$) pdf, shown in Figure 6.5. It is worth noting that the numeric convolution procedure requires both the carrier power and the noise+interference pdfs have the same bin/step size. The carrier power statistics are based on the fading distributions derived from the Rec.530 using a bin/step size of 0.01 dB to obtain an accurate representation of the path fading. The noise+interference statistics are based on the interference distribution obtained from the simulation modelling where interference values are stored in 1 dB wide bins. Therefore, before the convolution, the noise+interference pdf is interpolated linearly to obtain a bin/step size of 0.01 dB. Both pdfs and the resultant carrier-to-noise+interference ratio ($C/N+I$) pdf are illustrated in Figure 6.10.

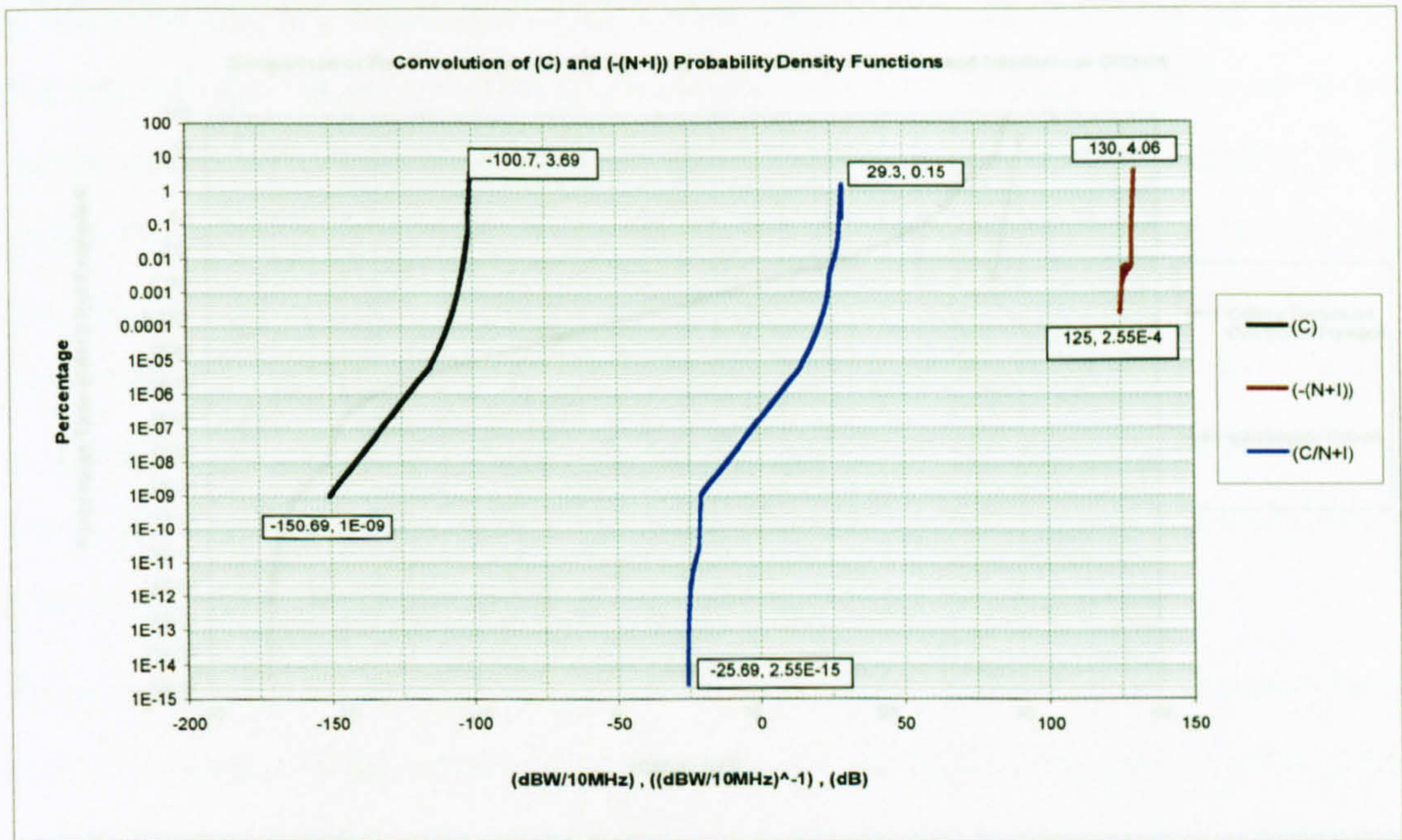


Figure 6.10: Convolved Probability Density Functions

The minimum and maximum values in each pdf are provided for validation purposes. The convolution procedure requires that the minimum level and corresponding percentage in the resultant $C/N+I$ pdf be calculated by adding the minimum levels from the C and $-(N+I)$ pdfs (which are in dBs) and by multiplying and normalising (i.e. by dividing 100) the corresponding percentages. The same approach is applicable for calculating the maximum level and its percentage in the $C/N+I$ pdf.

As a final step, the $C/N+I$ cdf is calculated from the $C/N+I$ pdf and compared against the fixed terrestrial link interference criteria derived in § 6.1.2.2. This is illustrated in Figure 6.11.

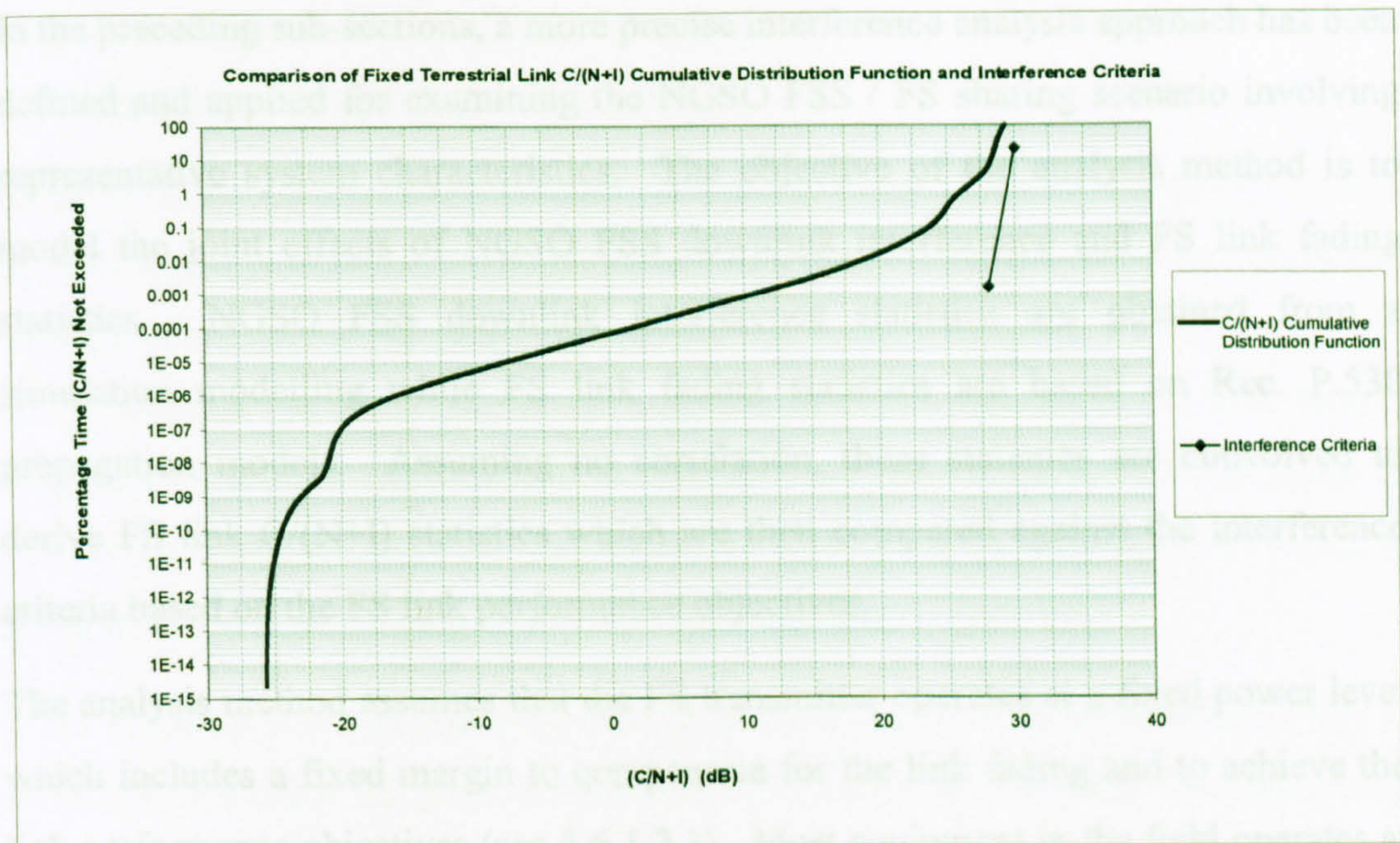


Figure 6.11: Comparison of $C/(N+I)$ Statistics Against FS Receiver Interference Criteria

For the short term interference, the $C/(N+I)$ is greater than 12.5 dB for $(100-0.0016)\%=99.9984\%$ of time whereas the minimum $C/(N+I)$ requirement for the same percentage is 28 dB which is 15.5 dB higher than what is achieved. In the case of long term interference, the $C/(N+I)$ cdf curve does not exceed 28.5 dB for 20% of the time, however, the minimum required $C/(N+I)$ not to be exceeded for the same percentage is 30 dB . Therefore, it is reasonable to conclude that the performance degradation in the representative terrestrial link due to aggregate NGSO interference is not within the acceptable limits.

6.1.3 Discussion

The review of the literature has indicated that the analysis of interference originating from NGSO FSS satellites into terrestrial radio systems operating in the fixed service has involved calculating and comparing aggregate interference statistics against an FS link short-term and long-term interference criteria which are defined relative to an FS receiver noise power. This approach provides an initial insight into the NGSO FSS / FS downlink sharing environment.

In the preceding sub-sections, a more precise interference analysis approach has been defined and applied for examining the NGSO FSS / FS sharing scenario involving representative system characteristics. The objective of the analysis method is to model the joint effects of NGSO FSS downlink interference and FS link fading statistics. NGSO FSS downlink interference statistics are obtained from a simulation modelling while FS link fading statistics are based on Rec. P.530 propagation models. Assuming no correlation, these statistics are convolved to derive FS link $C/(N+I)$ statistics which are then compared against the interference criteria based on the FS link performance objectives.

The analysis method assumes that the FS transmitter operates at a fixed power level which includes a fixed margin to compensate for the link fading and to achieve the link performance objectives (see § 6.1.2.1). Most equipment in the field operates at a fixed power level [208]. It is noted that recent studies examine the implications of introducing Automatic Transmitter Power Control (ATPC) into new FS links. When a link employs ATPC, the transmitter power is set at a level less than that used by the same link with a fixed margin. In the case of fading, the transmitter power is increased to achieve a minimum FS link received carrier power objective. In theory, under such situations, it is reasonable to assume that an FS link received carrier power is at a constant level. This, in turn, simplifies the analysis method in that the convolution is replaced by summation as the fixed carrier power, C (in dBW), and $-(N+I)$ (in dBW) statistics can be added together to arrive at overall FS link $C/N+I$ statistics. In practice, however, the ATPC range is limited (to the order of 15 to 20 dB) and, therefore, an FS link still requires a fixed margin to compensate for deep fades.

It is worth noting that there are significant implications when introducing new FS links using ATPC into an environment already populated by FS links operating with a fixed margin. In particular, potential interference from an FS transmitter employing a fixed margin (and therefore transmitting at a relatively high level) into an FS receiver associated with a link employing ATPC is likely to cause intra-system interference problems.

6.2 Interference from NGSO FSS Earth Stations Into Terrestrial Radio Systems Operating within FS

Traditional use of the fixed satellite service has been based on a relatively small number of Earth stations. Frequency sharing between these terminals and terrestrial stations operating in the fixed service has not been difficult due to the relatively small numbers involved. As stated in early chapters, a number of Ka-band NGSO FSS satellite systems are proposed to provide cost effective data communications to individuals and businesses on a significantly large scale. This is likely to result in the high density deployment of NGSO FSS Earth station terminals.

From the fixed service system deployment point of view, in addition to the point-to-point (PP) FS links, the point-to-multipoint (PMP) broadband fixed wireless access (BFWA) systems are planned for the Ka band operation. This also implies that the number of base stations and subscribers are likely to be significant. In these circumstances, the NGSO FSS / FS spectrum sharing issues become more complex than those involving small number of terminals.

Sharing analysis methodologies described in this section are concerned with examining the implications of single entry and aggregate interference from NGSO FSS Earth station transmitters into FS receivers operating in the Ka band. For the single entry interference analysis, an exclusion area derivation approach has been employed while a statistical method has been used for examining the impact of interference aggregating from multiple NGSO FSS Earth station transmitters.

6.2.1 Analysis Approach

In this section, both single entry and aggregate interference analysis methods are described in detail.

6.2.1.1 Single Entry Interference Analysis Method

The common approach in the assessment of single entry interference from NGSO FSS Earth stations into both PP and PMP FS receivers is to derive exclusion areas in

which the NGSO FSS transmitters could not operate without risk of causing interference [217-226].

For the purposes this research, initial investigations have been directed towards determining exclusion distances for the worst case interference scenarios, i.e. where an NGSO FSS Earth station is transmitting at a minimum elevation in the same azimuth plane as an FS station is operating. For these scenarios, the worst case single interference entry corresponds to an alignment where the transmitter is within the receiver antenna mainlobe.

Determination of an exclusion distance between an FS receiver and an NGSO FSS Earth station transmitter requires a comparison of a required transmission loss with a loss contributed by the propagation medium. This is an iterative process and the exclusion distance is the distance at which these two loss values become equal. Using the calculated exclusion distances, the exclusion areas around the representative FS receivers have been determined by summing the area of sector wedges each *5-degree* wide with a radius equal to the exclusion distance at each *5-degree* azimuth.

As already mentioned, the NGSO FSS Earth station terminals are expected to be deployed in high densities. The starting assumption for the interference analysis is therefore that the interfering paths will generally be line-of-sight. Because of this, it is largely only necessary to consider long-term interference and propagation effects. The interference analysis in the remainder of this chapter takes account of free-space path loss, atmospheric loss and, in some cases, diffraction loss. The FS receiver interference criterion is based on long term considerations (i.e. $\geq 20\%$ of time).

It will be seen that some of the exclusion distances calculated on the basis of the line-of-sight assumption outlined earlier are in fact beyond the horizon. These situations are related to an NGSO FSS Earth station transmitter being located on or very near to an FS receiver main lobe. In these instances, the exclusion area calculations should take account of transhorizon propagation mechanisms (see Chapter 2). It can, however, be argued that if sharing considerations are having to

consider separation distances beyond the horizon the prospects for large numbers of FS and NGSO FSS terminals coexisting are not good.

In general, PMP FS system base station antennas are mounted on a top of a high building roof or a pole to provide good line-of-sight paths for the subscriber stations. In some cases, this may lead to interference situations where a base station receiver is located on a highly elevated location (*50-100 metres*) very close to an NGSO FSS Earth station transmitter whose height is constrained by the rooftop height of the subscriber's premises which may be as little as *5 metres*. For such alignments, there is an increased likelihood of an NGSO FSS boresight interference entry into a base station receiver. Therefore, the implications of the relative height difference between the transmitter and receiver making such alignments possible have been also briefly investigated within the single entry interference analysis.

Figure 6.12 illustrates the worst case interference alignments considered in the single entry interference analysis.

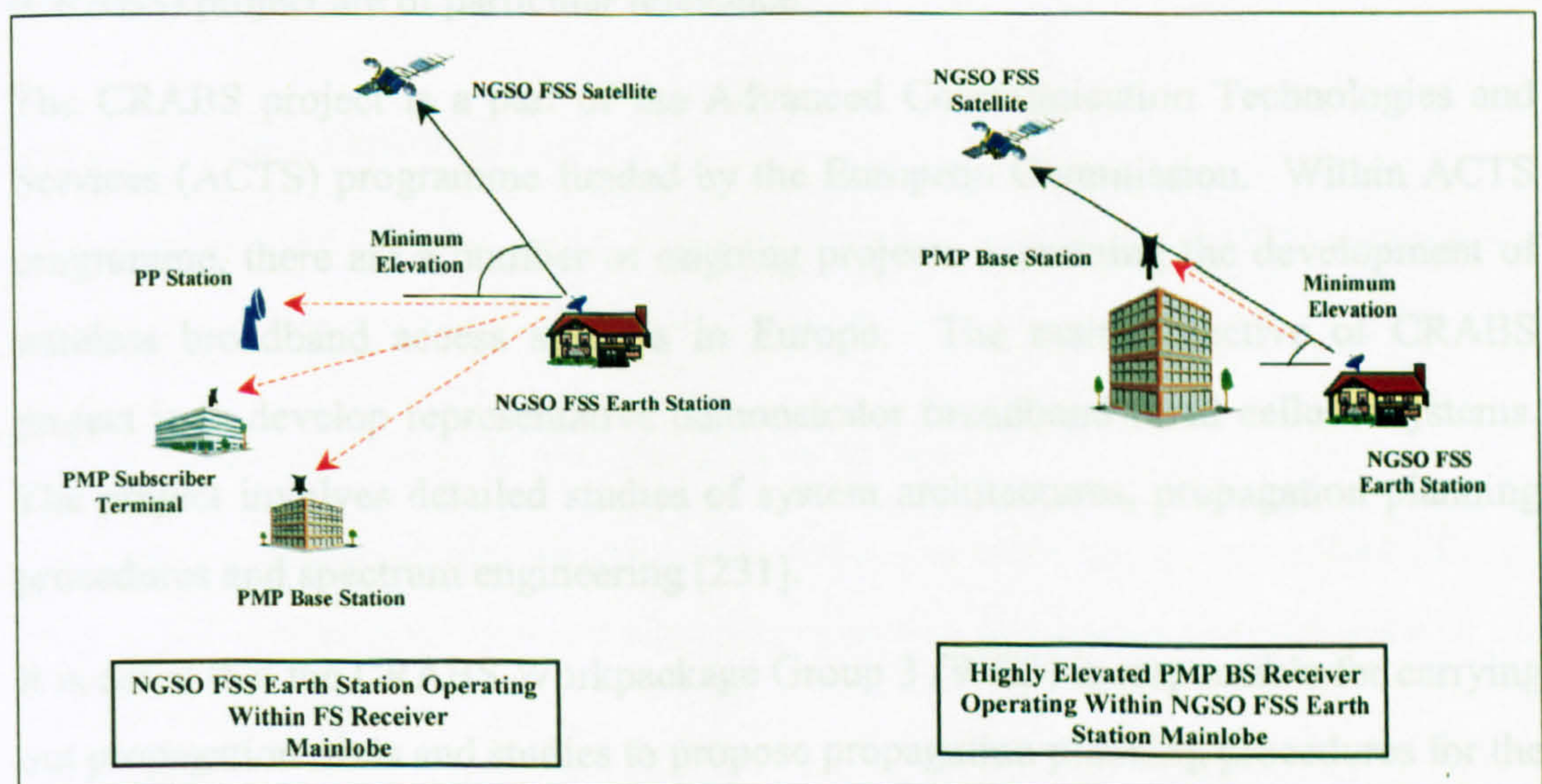


Figure 6.12 : Worst Case Interference Alignments

6.2.1.2 Aggregate Interference Analysis Method

A Monte Carlo simulation approach used to assess the impact of multiple interfering sources has been applied for examining the implications of aggregate interference.

In the interference scenario simulations, for each of a large number of trials, a population of potentially interfering NGSO FSS Earth station transmitters are randomly located, at a specified geographic density, within an area of a specified radius. A single FS receiver is positioned at the centre of the simulation area. Interference from the randomly pointing transmitter population is then aggregated at the victim receiver taking account of propagation effects. The output of the simulation model is in the form of a cumulative distribution function (cdf), indicating the proportion of FS receiver locations that are likely to suffer a particular level of interference from multiple NGSO FSS Earth station in-band transmissions.

As the sharing environment is expected to be dominated by line-of-sight interfering paths, the question of “how many of the NGSO FSS Earth stations within an area simulated are likely to have line-of-sight propagation path to the FS receiver ?” needs to be investigated. The review of relevant documents revealed that the results of the trials carried out in the Cellular Radio Access of Broadband Services (CRABS) project are of particular relevance.

The CRABS project is a part of the Advanced Communication Technologies and Services (ACTS) programme funded by the European Commission. Within ACTS programme, there are a number of ongoing projects examining the development of wireless broadband access systems in Europe. The main objective of CRABS project is to develop representative demonstrator broadband fixed cellular systems. The project involves detailed studies of system architectures, propagation planning procedures and spectrum engineering [231].

It is noted that the CRABS Workpackage Group 3 (WG3) is responsible for carrying out propagation trials and studies to propose propagation planning procedures for the design of broadband wireless access systems. The findings of this group has led to a new ITU-R Recommendation P.1410 [232]. In particular, the recommendation includes a statistical model for calculating building blockage probability based on very simple characterisation of buildings. The model is provided for use in planning purposes when building and terrain databases are not available.

The building blockage statistical model is based on calculating the probability that a line-of-sight path exists for given transmitter and receiver positions. The model takes account of the ratio of land covered by buildings to total land, the density of buildings (*buildings/km²*) and the distribution of building height. Using these parameters, the line-of-sight probability is calculated by combining the probabilities that each building lying in the propagation path is below the height of the propagation path joining the transmitter and receiver. The building height distribution is assumed to be Rayleigh and the terrain is assumed to be flat over the area of interest.

The Monte Carlo simulator used in the analysis presented this research includes the above described model in order to take account of the line-of-sight path probability between an NGSO FSS Earth station transmitter and an FS receiver. By applying the free space propagation model to each line-of-sight interfering path, an aggregate interference level is determined at each Monte Carlo trial for the interference scenario simulated.

6.2.2 System Characteristics

Representative FS receiver and NGSO FSS transmitter parameter values required for the sharing analysis are presented in this section.

6.2.2.1 Representative FS Receiver Characteristics

The receiver characteristics shown in the following table are based on real PP and PMP fixed service links that are currently operating or planned for operation in the 30 GHz band [80].

	PP Link Receiver Station (Taken from 4-9S/UK 2-E)	PMP Base Station Receiver (Based on Hughes AIReach BFWA System)	PMP Subscriber Receiver (Based on Hughes AIReach BFWA System)
Carrier Bandwidth (MHz)	21	12.5	12.5
Maximum Antenna Gain (dBi)	45	16 (90° sector antenna)	35
Receiver Noise Figure (dB)	11	7	7
Antenna pattern	Rec. 699	EN 301 215	EN 301 215

Table 6.9: Ka-band Receiver Characteristics

As can be seen, a relatively low gain base station sector antenna has been taken into account as this will have the widest beamwidth and hence will have the greatest probability of receiving on beam interference. The associated antenna pattern for each representative receiver is illustrated in Figure 6.13.

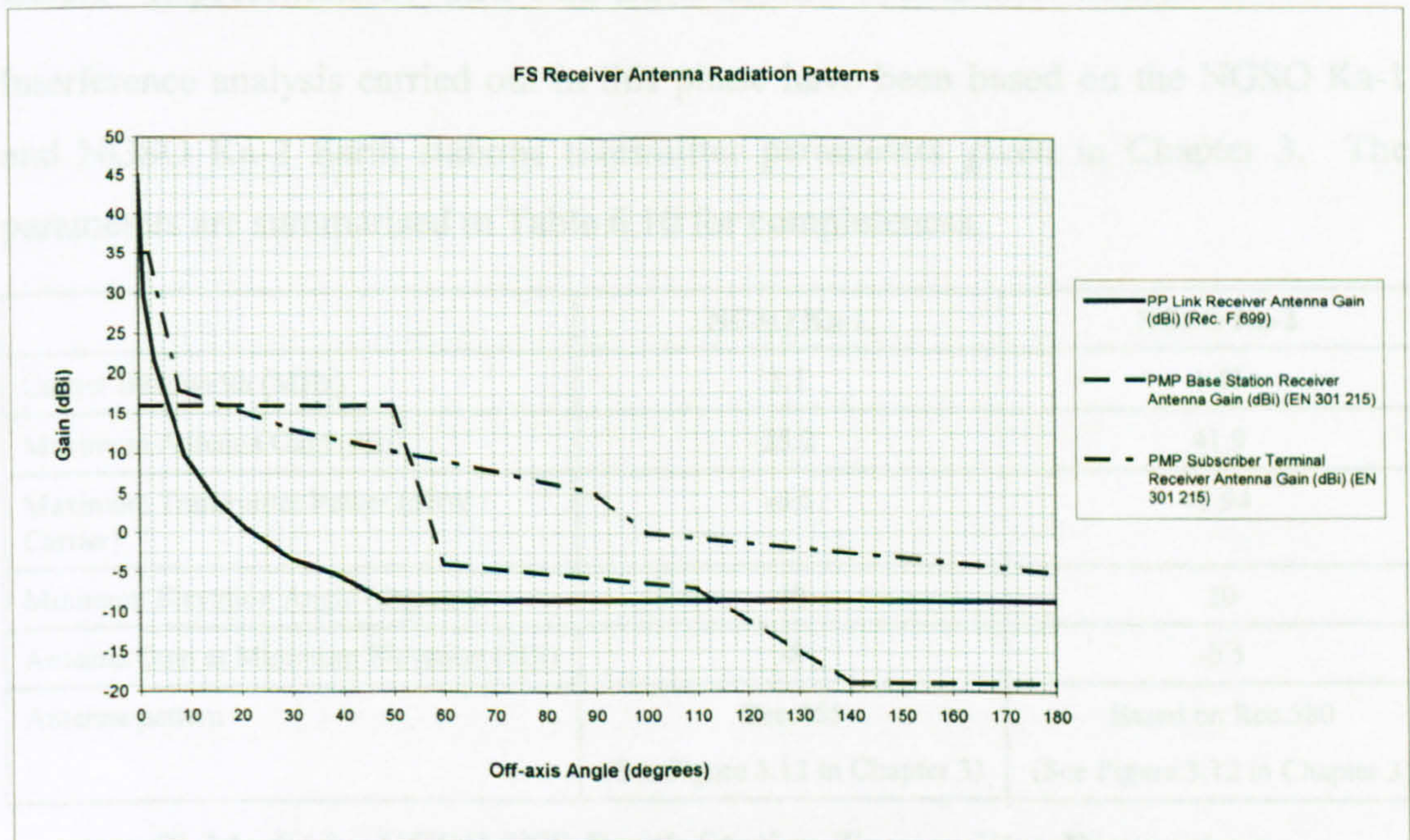


Figure 6.13 : FS Receiver Antenna Patterns

It is worth noting that EN 301 215 is a draft ETSI standard defining transmitter and receiver antenna characteristics for use in PMP digital radio relay systems operating in the 24 GHz to 30 GHz frequency band [85]. The document notes that the

subscriber antenna pattern is the same for both azimuth and elevation planes whereas the sectored base station antenna pattern is described for the azimuth plane. The standard does not define an elevation pattern for the base station receiver antenna. The elevation pattern is, therefore, assumed to confirm the UK Radicommunications Agency standard MPT 1560 [233] which is detailed in the single entry interference analysis in the following section. The PP FS link receiver antenna pattern is represented by Rec.699 [75] which defines a circular radiation envelope.

As explained in the preceding section, interference into the above FS receivers will be dominated by line-of-sight entries and, therefore, the long term interference criterion needs to be taken into account. In line with Rec.758 [102], it has been assumed that maximum allowed interference should be 10% of the receiver noise level to be exceeded for not more than 20% of time.

6.2.2.2 Representative NGSO FSS Earth Station Transmitter Characteristics

Interference analysis carried out in this phase have been based on the NGSO Ka-1 and NGSO Ka-2 Earth stations transmitter parameters given in Chapter 3. The parameters are summarised in Table 6.10 for completeness.

	NGSO Ka-1	NGSO Ka-2
Carrier Bandwidth (MHz)	3.1	1.43
Maximum Antenna Gain (dBi)	35.2	41.9
Maximum Transmitter Power (dBW / Carrier)	-0.6	-3.94
Minimum Elevation Angle (degrees)	40	20
Antenna Gain at Minimum Elevation (dBi)	-8	-0.5
Antenna pattern	Rec.465 (See Figure 3.12 in Chapter 3)	Based on Rec.580 (See Figure 3.12 in Chapter 3)

Table 6.10 : NGSO FSS Earth Station Transmitter Parameters

6.2.3 Single Entry Interference Analysis

Initially, the implications of an interference entry from the NGSO FSS Earth station operating within the same azimuth plane as the FS receiver have been examined by

calculating an exclusion area around the FS receiver. This has been followed by a worst case interference analysis corresponding to situations where the PMP FS system base station (BS) receiver positioned at a highly elevation location is within the NGSO FSS transmitter antenna boresight.

6.2.3.1 NGSO FSS Earth Station Operating Within FS Receiver Azimuth Plane

The exclusion distance calculations are based on the following assumptions:

- The NGSO FSS Earth station is at a minimum elevation and transmitting a maximum power,
- Propagation medium is clear-sky,
- The FS receiver is operating at 0° elevation and the NGSO FSS Earth station is transmitting towards the azimuth of the FS receiver antenna,
- The maximum allowed interference is 10% of the FS receiver noise power level.

Using the above assumptions, the following interference scenarios have been considered for the analysis:

1. NGSO Ka-1 Earth station at 40° elevation into PP FS link receiver
2. NGSO Ka-1 Earth station at 40° elevation into PMP BS receiver
3. NGSO Ka-1 Earth station at 40° elevation into PMP subscriber receiver
4. NGSO Ka-2 Earth station at 20° elevation into PP FS link receiver
5. NGSO Ka-1 Earth station at 20° elevation into PMP BS receiver
6. NGSO Ka-1 Earth station at 20° elevation into PMP subscriber receiver

For each scenario, the exclusion distance from the FS receiver has been calculated iteratively assuming a starting distance of *250 metre* and a distance increment size of *250 metre*. At each distance, the required loss has been compared against the loss contributed by the propagation medium. The distance calculations are based on smooth Earth assumption; i.e. no terrain irregularities have been taken into account.

For the calculated distances, where there is a line-of-sight between the transmitter and receiver, the propagation loss has been modelled by the free space path loss, beyond this an additional spherical Earth diffraction loss has been taken into account. The required loss has been calculated using the following equation (where all parameters are numeric) by assuming the maximum allowed interference power is 10% of the receiver noise power:

$$\text{RequiredLoss} := 10 \cdot \log \left[\frac{10^{\frac{\text{NGSOFSSSTxPower}}{10}} \cdot 10^{\frac{\text{FSRxGaindB}(\text{OffAxis})}{10}} \cdot 10^{\frac{\text{NGSOFSSSTxGaindB}}{10}} \cdot (\text{NumericBandwidthCorrection})}{10^{\frac{\text{MaximumAllowedInterference}}{10}}} \right]$$

(6-3)

The iteration process has been carried out until the propagation loss is equal to or greater than the required loss. The exclusion distances have been calculated at each 5-degrees azimuth. The total area has been then determined by summing the area of sector wedges.

Although high density deployment implies an increased likelihood of free space propagation for the interfering paths, the impact of transhorizon propagation has been incorporated into the exclusion distance calculation model by taking diffraction over spherical Earth into account, for which empirical prediction methods are defined in the ITU-R Rec. P.526-6 [100]. The Rec.526 loss prediction methods have been used to calculate an additional path loss attributable to the diffraction over spherical Earth. This approach results in more realistic exclusion distances between the FS receiver and the NGSO FSS transmitter than those would be obtained by applying only the free space propagation loss model to the distances beyond the line-of-sight.

It should be noted that, in practice, both the NGSO FSS and FS systems will mainly be deployed in urban areas where the clutter loss due to man-made and natural obstacles is significant. In sharing situations where deployment area details are available, the loss mechanisms that are dependent on a specific path profile should be considered. Under these circumstances, the exclusion distances will potentially

be less than those calculated using the diffraction model. Therefore, the use of Rec.526 is still conservative but resultant distances are more generic than those representing particular cases.

The parameter values listed in Figure 6.14 have been assumed for the diffraction model.

$a_{e_526} := 8500$	Effective Earth radius, km
$\epsilon_{526} := 15$	Effective relative permittivity
$\sigma_{526} := 10^{-3}$	Effective conductivity, (S/m)
$h1_{526} := 10$	FS receiver antenna height, metre
$h2_{526} := 10$	NGSO FSS transmitter antenna height, metre
$d_{min_526} := 0.25$	Assumed minimum separation, km
$d_{max_526} := 1000$	Assumed maximum separation, km
$d_h := 0.5$	Horizon distance as viewed from FS transmitter antenna, km (if no information $d_h=0.5$ km)
$\theta_h := 0$	Horizon angle, as viewed from FS transmitter antenna, between the horizontal plane and a ray that grazes the physical horizon in the direction concerned, degrees

Figure 6.14 : Assumed Parameters for Diffraction Model

For the assumed *10 metre* antenna heights, the maximum line-of-sight range is approximately *22 km* on the basis of smooth Earth assumption, as shown in Figure 6.15. As stated earlier, in situations where the required exclusion distance is beyond *22 km*, the additional spherical Earth diffraction loss has been included into the calculations.

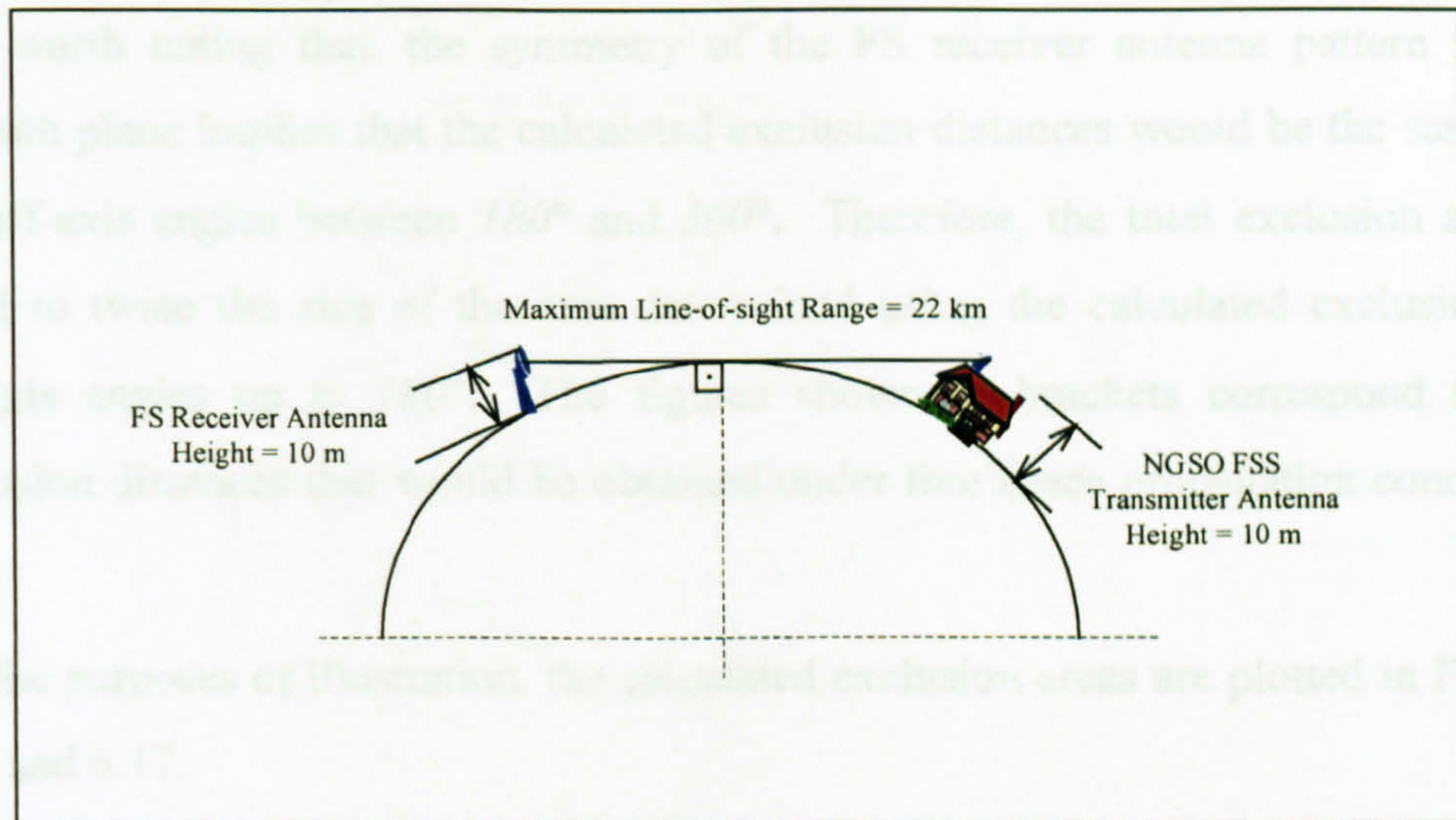


Figure 6.15 : Maximum Line-of-sight Range

Table 6.11 illustrates the exclusion distances and total exclusion areas calculated for each scenario.

Off-axis at FS Receiver in Azimuth Plane	Exclusion Distance (km)					
	Scenario 1	Scenario 2	Scenario 3	Scenario 4	Scenario 5	Scenario 6
0°	27 (168)	13.25	25.75 (117)	28.25 (272)	21.5	27.25 (189)
5°	6	13.25	23 (44)	9.75	21.5	24.5 (71)
10°	2.5	13.25	15.75	4.25	21.5	22.25 (25)
20°	1.25	13.25	12.25	1.75	21.5	19.75
30°	0.75	13.25	9.5	1.25	21.5	15.25
40°	0.5	13.25	8	0.75	21.5	13
50°	0.5	13.25	7	0.75	21.5	11.25
60°	0.5	1.5	6	0.75	2.25	9.5
70°	0.5	1.25	5.25	0.75	2	8.25
80°	0.5	1.25	4.5	0.75	2	7
100°	0.5	1	2.25	0.75	1.75	3.5
120°	0.5	0.75	2	0.75	1	3
140°	0.5	0.25	1.75	0.75	0.5	2.75
160°	0.5	0.25	1.5	0.75	0.5	2.25
180°	0.5	0.25	1.25	0.75	0.5	2
Total Exclusion Area (km ²)	68.46	171.79	219.01	82.17	451.90	399.02

Table 6.11: Exclusion Distances

It is worth noting that, the symmetry of the FS receiver antenna pattern in the azimuth plane implies that the calculated exclusion distances would be the same for the off-axis angles between 180° and 360° . Therefore, the total exclusion area is equal to twice the size of the area determined using the calculated exclusion for off-axis angles up to 180° . The figures shown in brackets correspond to the exclusion distances that would be obtained under free space propagation conditions only.

For the purposes of illustration, the calculated exclusion areas are plotted in Figures 6.16 and 6.17.

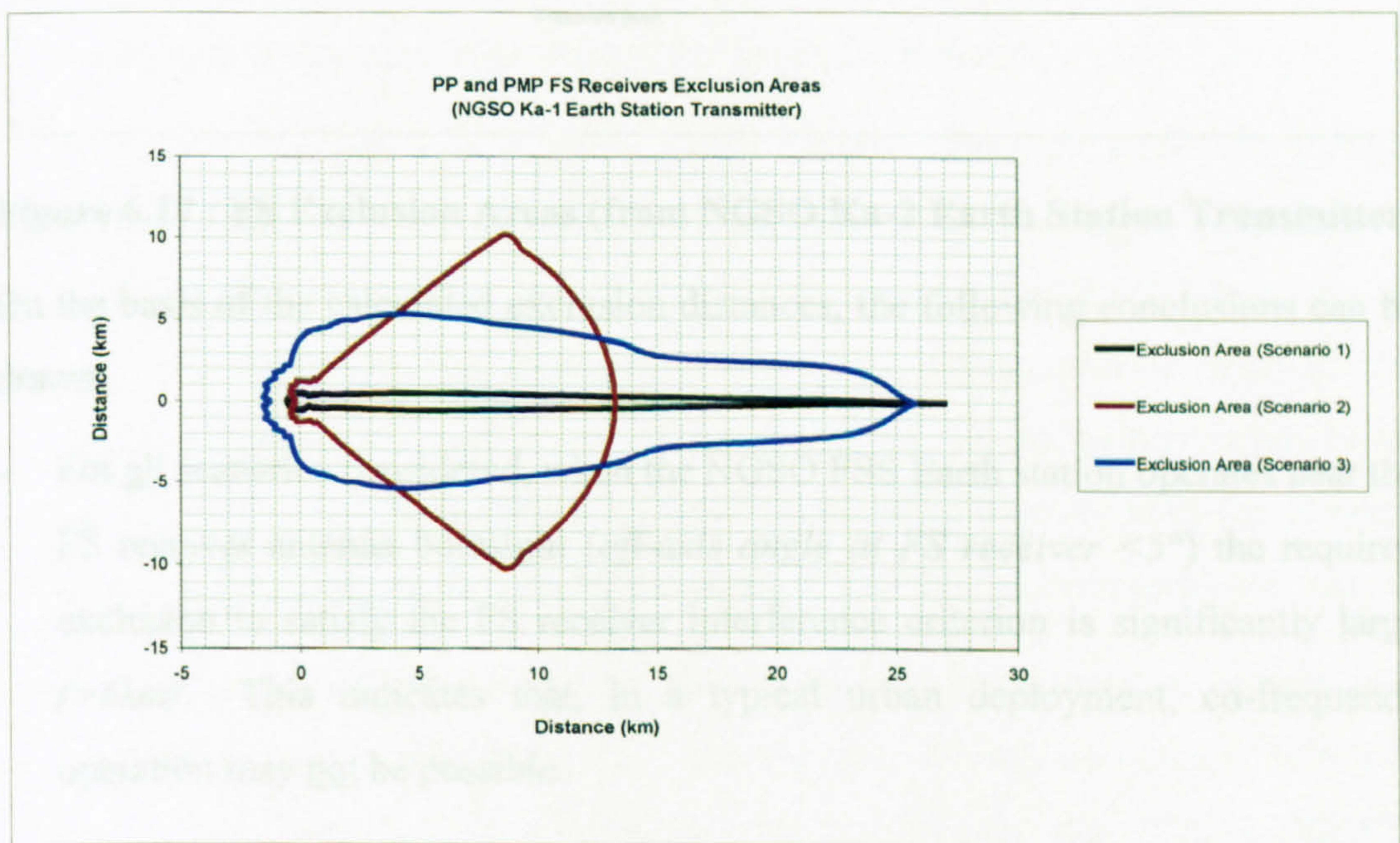


Figure 6.16 : FS Exclusion Areas (from NGSO Ka-1 Earth Station Transmitter)

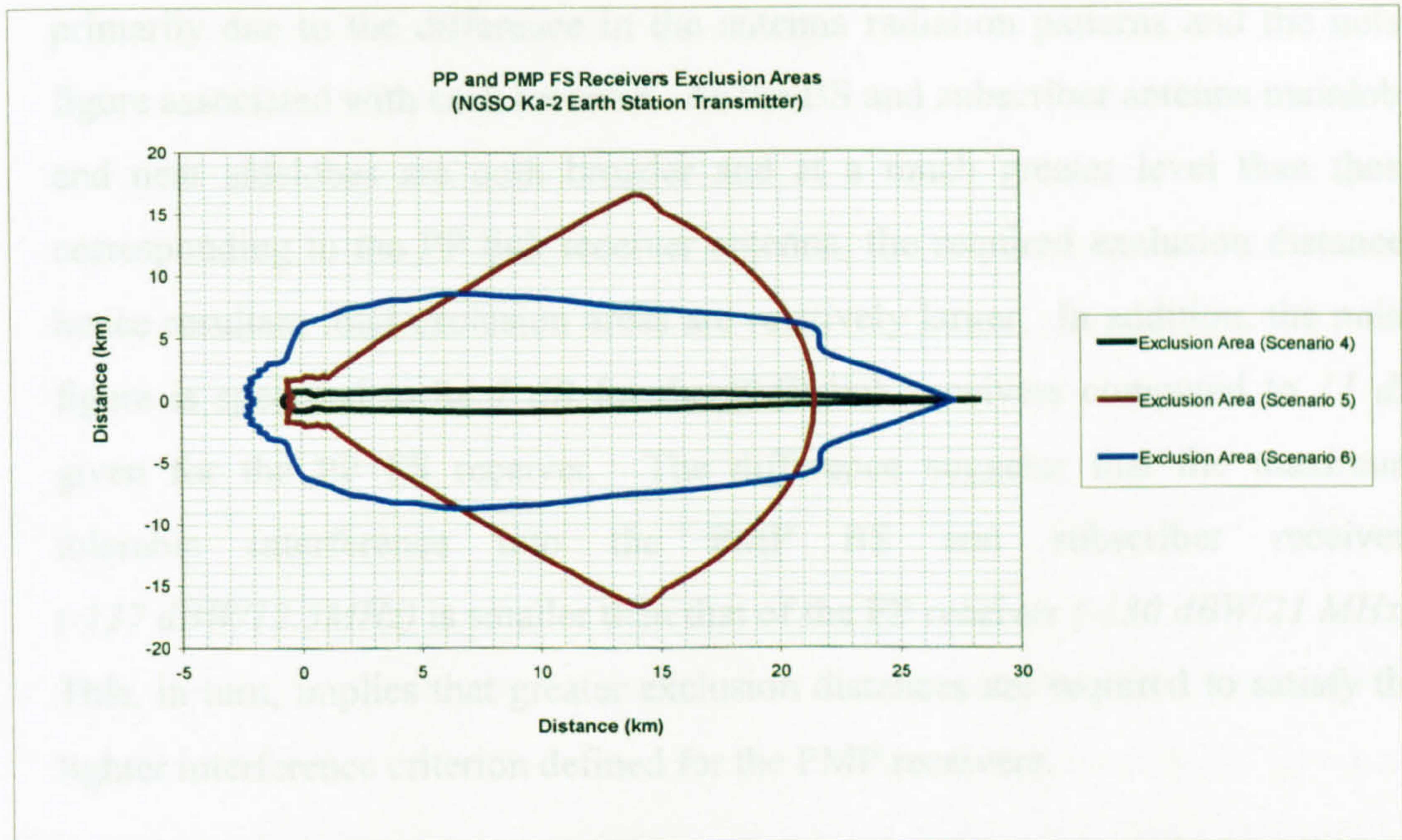


Figure 6.17 : FS Exclusion Areas (from NGSO Ka-2 Earth Station Transmitter)

On the basis of the calculated exclusion distances, the following conclusions can be drawn:

- For all scenarios considered, when the NGSO FSS Earth station operates near the FS receiver antenna boresight (*off-axis angle at FS receiver* $< 5^\circ$) the required exclusion to satisfy the FS receiver interference criterion is significantly large ($> 6\text{km}$). This indicates that, in a typical urban deployment, co-frequency operation may not be possible.
- It is necessary to examine the likelihood of the above mentioned interference alignments occurring for a given sharing scenario. The significant sharing parameters that need to be considered include the NGSO FSS Earth station transmitter density, transmitter antenna height and pointing distributions, building density and height distributions. This is investigated in the aggregate interference analysis section by employing the Monte Carlo simulation technique explained previously.
- For the PMP FS link, the exclusion areas calculated for both BS and subscriber receiver are much greater than those calculated for the PP FS receiver. This is

primarily due to the difference in the antenna radiation patterns and the noise figure associated with each receiver. As the BS and subscriber antenna mainlobe and near sidelobes are both broader and at a much greater level than those corresponding to the PP link receiver antenna, the required exclusion distances hence resultant total exclusion areas are relatively larger. In addition, the noise figure is specified to be 7 dB for the PMP link receivers compared to 11 dB given for the PP FS receiver. The difference suggests that the maximum tolerable interference into the PMP BS and subscriber receivers ($-137\text{ dBW}/12.5\text{ MHz}$) is smaller than that of the PP receiver ($-130\text{ dBW}/21\text{ MHz}$). This, in turn, implies that greater exclusion distances are required to satisfy the tighter interference criterion defined for the PMP receivers.

- The use of free space propagation model for calculating the exclusion distance corresponding to the FS receiver antenna near boresight alignment is unrealistically pessimistic, leading to the distances in order of 100 kilometres. In these circumstances, the inclusion of the additional spherical diffraction loss results in more realistic figures. If the details of the deployment scenario are known in advance, the propagation loss that would be introduced by the irregular terrain and man-made obstructions is likely to give rise to even smaller distances.
- The exclusion areas resulting from the NGSO Ka-2 interference are greater than those calculated for the NGSO Ka-1 interference. This is the result of relatively higher NGSO Ka-2 *EIRP* radiated towards the FS receiver. The NGSO FSS Earth station transmitter characteristics given in Table 6.10 indicates that the NGSO Ka-1 *EIRP* is $-8.6\text{ dBW}/3.1\text{ MHz}$ while the NGSO Ka-2 *EIRP* is $-4.4\text{ dBW}/1.43\text{ MHz}$.
- It should be noted that as the exclusion distances are based on satisfying the FS receiver long term interference criterion, the effective Earth radius of $8,500\text{ km}$ which corresponds to 50% propagation percentage time (i.e. the calculated loss caused by the propagation medium at a given distance is to be exceeded for 50% of time) has been assumed (see Figure 6.14) when applying the spherical

diffraction model. For the higher percentages (e.g. $>99.99\%$), the FS receiver short term criterion (defined in Rec. IS.847 [173]) would tolerate more interference which would give rise to closer exclusion distances. However, the higher propagation percentage time would dictate much greater distances for which the Rec. P.452 [88] transhorizon model including troposcatter, diffraction and ducting/layer reflection would be applicable.

6.2.3.2 FS Base Station Receiver Operating Within NGSO FSS Antenna Boresight

Propagation conditions in the 30GHz band necessitate line-of-sight wanted links. The PMP base stations are, therefore, placed at elevated locations to provide good line-of-sight visibility to the maximum number of subscriber antennas within a sector coverage area. This may, potentially, give rise to the interference alignment illustrated in Figure 6.18.

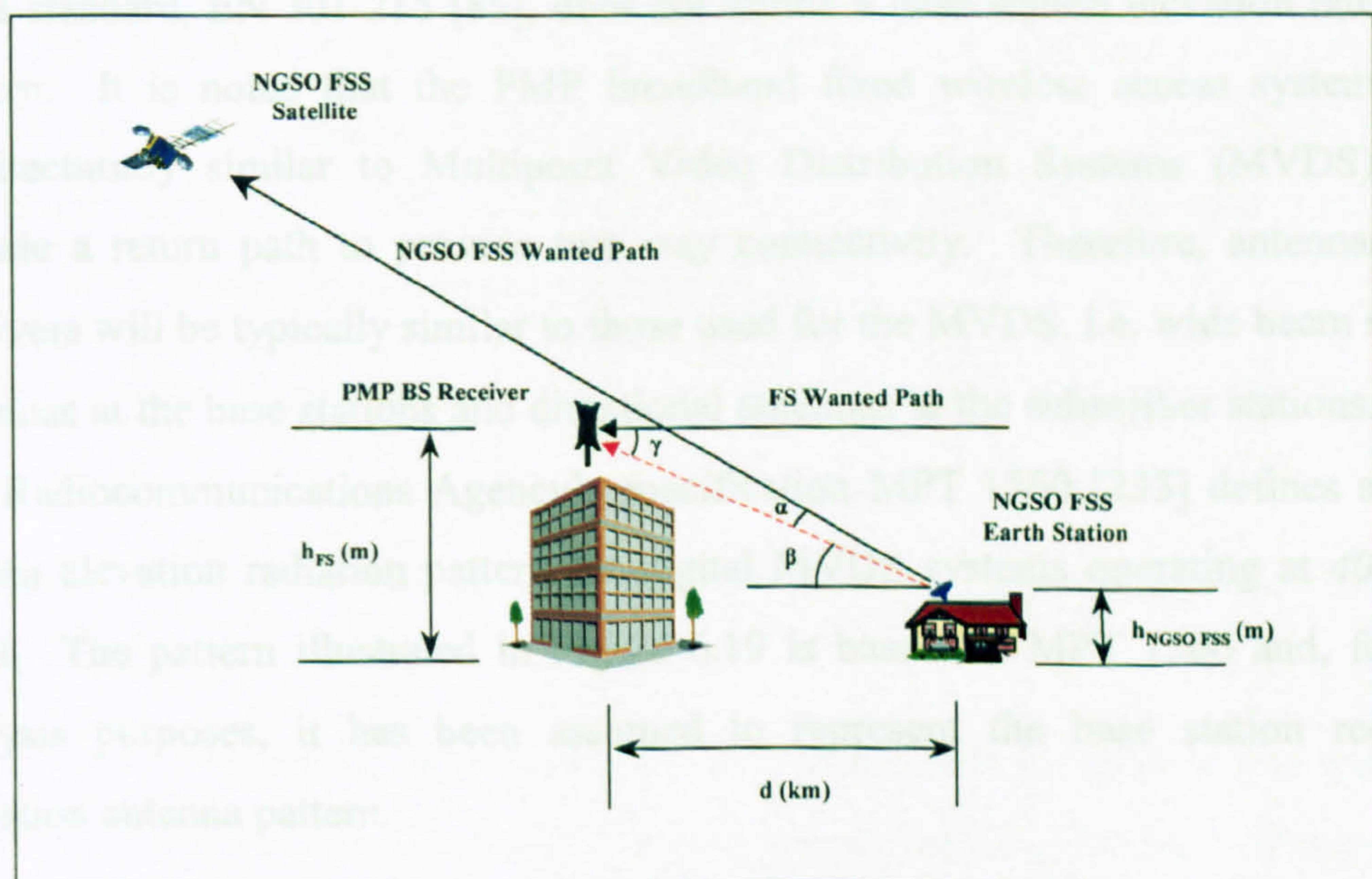


Figure 6.18 : Interference Geometry

As can be seen, the interference geometry comprises an NGSO FSS Earth station, constrained by the height of a subscriber premise, is located very close to the base station receiver, positioned at a top of a high building. As before, the base station

receiver antenna is assumed to be operating at 0° elevation. In some specific cases, the base station antennas may be down-tilted to reduce the impact of intra-system interference into neighbouring cell sites. In these situations, the NGSO FSS interference is likely to increase as the antenna discrimination at the base station receiver (γ) will be smaller.

It should be noted that the interference level is maximum when the transmitter off-axis angle (α) is 0° and the receiver antenna discrimination (γ) is minimum. As γ is equal to β , the worst case interference is obtained when the transmitter is operating at a minimum elevation allowed which is $\gamma=40^\circ$ for the NGSO Ka-1 and $\gamma=20^\circ$ for the NGSO Ka-2 systems.

As mentioned earlier, the base station receiver antenna pattern (given in Figure 6.13) is defined for the azimuth plane. However, Figure 6.18 indicates that the base station receiver antenna elevation radiation pattern also needs to be considered. The ETSI standard, EN 301 215 [85], does not define a base station elevation radiation pattern. It is noted that the PMP broadband fixed wireless access systems are architecturally similar to Multipoint Video Distribution Systems (MVDS), but include a return path to provide two way connectivity. Therefore, antennas and receivers will be typically similar to those used for the MVDS, i.e. wide beam sector antennas at the base stations and directional antennas at the subscriber stations. The UK Radiocommunications Agency's specification MPT 1560 [233] defines a base station elevation radiation pattern for digital MVDS systems operating at 40 GHz band. The pattern illustrated in Figure 6.19 is based on MPT 1560 and, for the analysis purposes, it has been assumed to represent the base station receiver elevation antenna pattern.

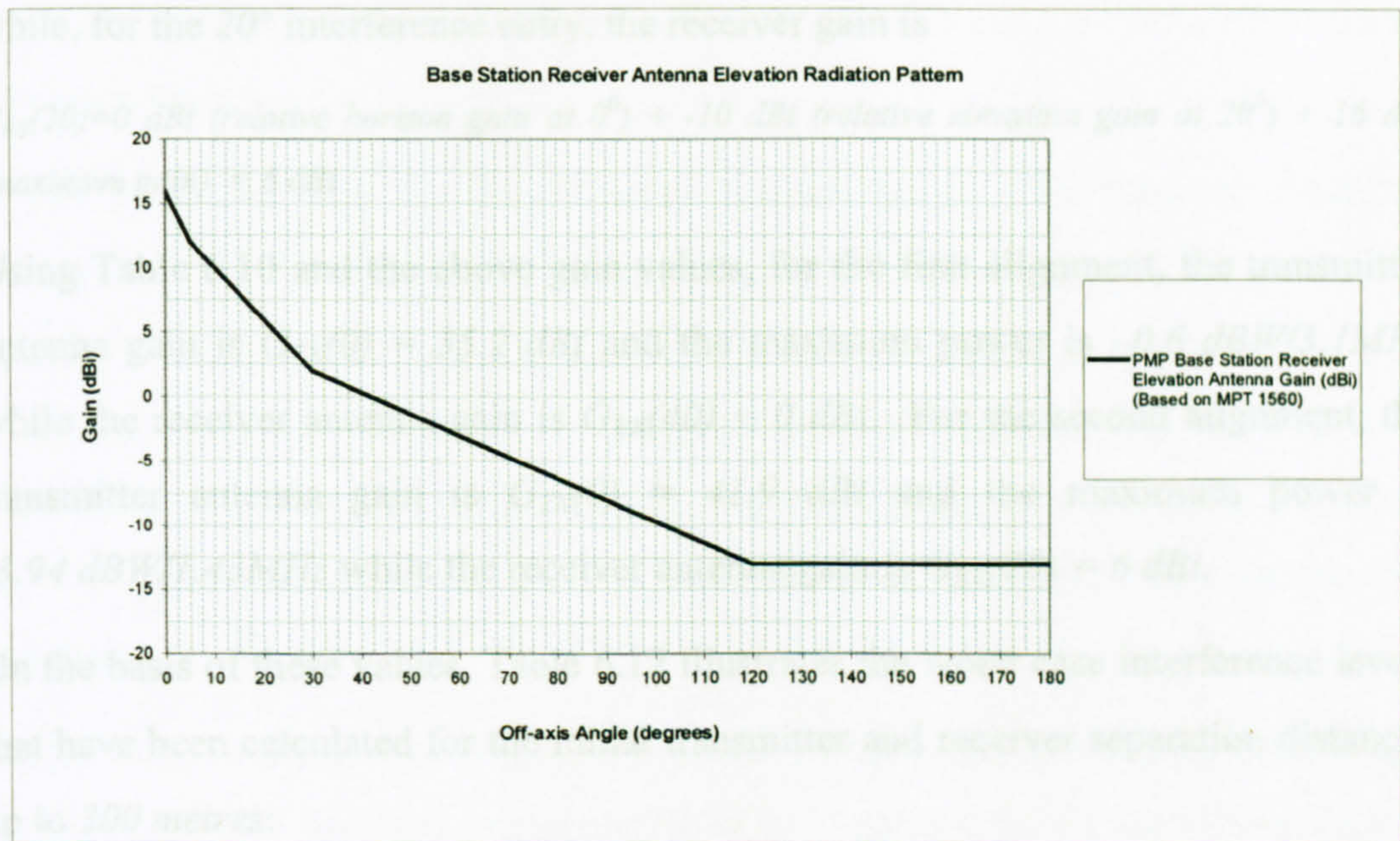


Figure 6.19 : Base Station Receiver Elevation Antenna Pattern

The aim of the analysis presented here is to evaluate the possibility of co-frequency operation within the same area by calculating and comparing the received interference power against the long term criteria for a number of relative height differences between the NGSO FSS Earth station and PMP base station receiver. Two worst case alignments have been considered:

1. NGSO Ka-1 Earth station antenna (at 40° elevation) boresight into PMP BS receiver,
2. NGSO Ka-2 Earth station antenna (at 20° elevation) boresight into PMP BS receiver.

For the geometry shown in Figure 6.18, it is reasonable to assume that the base station receiver antenna gain values for interference entries at 20° and 40° elevation are calculated by adding the corresponding horizon and elevation gain values (relative to the maximum gain). Therefore, for the 40° interference entry, the receiver gain is

$$G_{RX}(40) = 0 \text{ dBi (relative horizon gain at } 0^\circ) + -16 \text{ dBi (relative elevation gain at } 40^\circ) + 16 \text{ dBi (maximum gain)} = 0 \text{ dBi}$$

while, for the 20° interference entry, the receiver gain is

$$G_{RX}(20)=0\text{ dBi (relative horizon gain at }0^0)+ -10\text{ dBi (relative elevation gain at }20^0)+ 16\text{ dBi (maximum gain)} = 6\text{ dBi}$$

Using Table 6.10 and the above gain values, for the first alignment, the transmitter antenna gain is $G_{TX}(0) = 35.2\text{ dBi}$ and the maximum power is $-0.6\text{ dBW}/3.1\text{MHz}$ while the receiver antenna gain is $G_{RX}(40) = 0\text{ dBi}$. For the second alignment, the transmitter antenna gain is $G_{TX}(0) = 41.9\text{ dBi}$ and the maximum power is $-3.94\text{ dBW}/1.43\text{MHz}$ while the receiver antenna gain is $G_{RX}(20) = 6\text{ dBi}$.

On the basis of these values, Table 6.12 illustrates the worst case interference levels that have been calculated for the initial transmitter and receiver separation distances up to 300 metres:

Distance (d) (m)	First Worst Case Alignment (NGSO Ka-1)		Second Worst Case Alignment (NGSO Ka-2)	
	Relative Height Difference ($h = h_{FS} - h_{NGSO\ FSS}$) ($h = d \tan(\beta)$) (m)	Interference (dBW/12.5 MHz)	Relative Height Difference ($h = h_{FS} - h_{NGSO\ FSS}$) ($h = d \tan(\beta)$) (m)	Interference (dBW/12.5 MHz)
100	84	-67.4	36	-58
200	168	-73.4	72	-64
300	252	-76.9	108	-67.5

Table 6.12 : Worst Case Interference Power

Comparison of the above calculated interference figures against the base station long term interference criterion of $-137\text{ dBW}/12.5\text{ MHz}$ (based on 10% of the receiver noise power) suggests that the spectrum sharing would not be possible for the worst case alignments considered.

As an example, the required exclusion distance has been calculated in order to satisfy the base station long term interference criterion. It has been assumed that the interference scenario comprises the base station positioned at 84 metres higher than the NGSO FSS Earth station transmitter which is operating at 40° elevation (i.e. the first worst case alignment with a 100 metre initial separation shown in Table 6.12). Calculation is iterative and takes account of the joint effects of the transmitter and

receiver distance, the transmitter off-axis angle and the receiver antenna discrimination.

It can be shown that, for the 84 metre relative height difference, an exclusion distance of 14 km results in: *free space path loss* = 144.9 dB, $G_{TX}(39.6^\circ) = -7.8 \text{ dBi}$, $G_{RX}(0.4^\circ) = 15.6 \text{ dBi}$ ($G_{RxHorizonRelative}(0^\circ) = 0 \text{ dBi}$) + ($G_{RxElevationRelative}(0.4^\circ) = -0.4$) + ($G_{RxMax} = 16 \text{ dBi}$) = 15.6 dBi). Using these figures together with the maximum transmitter power of $-0.6 \text{ dBW}/3.1 \text{ MHz}$, the interference level has been calculated as $-137.7 \text{ dBW}/12.5 \text{ MHz}$ which is just below the base station long term interference criterion.

On the basis of the above analysis, it has been recognised that the worst case single entry interference situation corresponding to an alignment where the FS base station receiver, located at a highly elevated position, operating within the NGSO FSS Earth station boresight gives rise to an interference power level exceeding the FS receiver criterion with a significant margin. Under such circumstances, the required exclusion distances are also large ($>10 \text{ km}$) implying that the co-frequency operation within the same area may not be possible. As mentioned in the preceding section, it is necessary to examine the probability of the above mentioned interference alignments occurring in a typical urban deployment scenario. This is considered in the following section.

6.2.4 Aggregate Interference Analysis

The Monte Carlo simulation module, part of the Aegis Systems Spectrum Engineering Toolkit, has been used for assessing the impact of multiple interfering sources. Simulations of a variety of NGSO FSS Earth station interferer / FS victim receiver scenarios have been carried out for different interferer/victim combinations.

As stated earlier, the analysis considers line-of-sight interference paths. Therefore, In order to determine the size of the area over which simulations will be run, a maximum NGSO FSS Earth station transmitter height and an FS receiver antenna height have been used together with a smooth Earth approximation

(see Figure 6.15). Table 6.13 illustrates the calculated radius of the simulation area for a number of antenna height combinations.

FS Receiver Height (m)	NGSO FSS Earth Station Transmitter Maximum Height (m)					
	10	20	30	40	50	60
10	22	27	31	34	37	39
20	27	32	36	39	41	44
30	31	36	39	42	45	47
40	34	39	42	45	48	50
50	37	41	45	48	51	53
60	39	44	47	50	53	55

Table 6.13 : Radius of Simulation Area For Different Transmitter and Receiver Antenna Combinations

For the building blockage, Rec. P.1410 [232] specifies the following parameter values obtained from averaging over the main town region of a typical sub-urban location in the UK:

α (the ratio of land covered by buildings to total land area) = 0.11

β (the mean number of buildings per unit area) = 750 buildings/km²

γ (the most probable building height for Rayleigh distribution) = 7.63 metre

For the purposes of building blockage modelling, these parameter values have been assumed in the analysis.

In order to prevent situations where co-located transmitter and receiver antennas operate simultaneously at the same frequency, an artificial exclusion area of a radius of 50 metres has been introduced around an FS receiver when locating NGSO FSS Earth station transmitters randomly in each Monte Carlo trial.

Initially, two scenarios have been simulated. In the first scenario, interference into the PP FS has been investigated while the second scenario has examined interference into the PMP subscriber receiver terminal. For both cases, it has been assumed that the receiver is located at a 10 metre height at the centre of the simulation area. This area has been randomly populated by the NGSO Ka-1 Earth station transmitters

whose heights are assumed to be uniformly distributed between *10* and *30 metre*. On the basis of figures given in Table 6.13, these assumptions imply that the maximum, smooth Earth, line-of-sight interference path length will be *31 km* which has been assumed to be the radius of the simulation area.

The geographical density of the transmitters has been calculated taking the NGSO Ka-1 system filing data into account. The NGSO Ka-1 system filing states that the *500 MHz* spectrum allocated to uplink is divided among 7 cells forming a supercell of $160 \times 160 \text{ km}^2$. Each cell is assigned an uplink beam satisfying the minimum elevation angle requirement of 40° . Within a cell, an available spectrum ($500 \div 7 \approx 72 \text{ MHz}$) is subdivided into carriers each of which has an approximate bandwidth of *3.1 MHz*, and is shared among multiple users by employing Time Division Multiple Access (TDMA). FS receiver characteristics given in Table 6.9 suggest that the receiver carrier bandwidth is *21 MHz* for the PP FS receiver and *12.5 MHz* for the PMP subscriber receiver. It is, therefore, reasonable to assume that, at a given instant, there may be $21 \div 3.1 \approx 7$ NGSO Ka-1 Earth station transmitters within the PP FS receiver carrier bandwidth in a given NGSO Ka-1 cell area of $(160 \times 160) / 7 = 3657 \text{ km}^2$. Similarly, $12.5 \div 3.1 \approx 4$ NGSO Ka-1 Earth station transmitters may be sharing the same band as the PMP subscriber receiver in an area of 3657 km^2 .

Using the above calculated figures, the average geographical density of NGSO Ka-1 interferers has been calculated, assuming a uniform distribution of cells, to be $0.002 / \text{km}^2$ for the PP FS receiver and $0.001 / \text{km}^2$ for the PMP subscriber receiver.

On the basis of the simulation area radius of *31 km* and the calculated density figures of $0.002 / \text{km}^2$ and $0.001 / \text{km}^2$, it can be shown that there are 6 and 3 NGSO Ka-1 Earth stations operating within the simulated areas of the PP FS and PMP subscriber models, respectively. Figure 6.20 shows the interference statistics for both models obtained from *1,000,000* Monte Carlo trials.

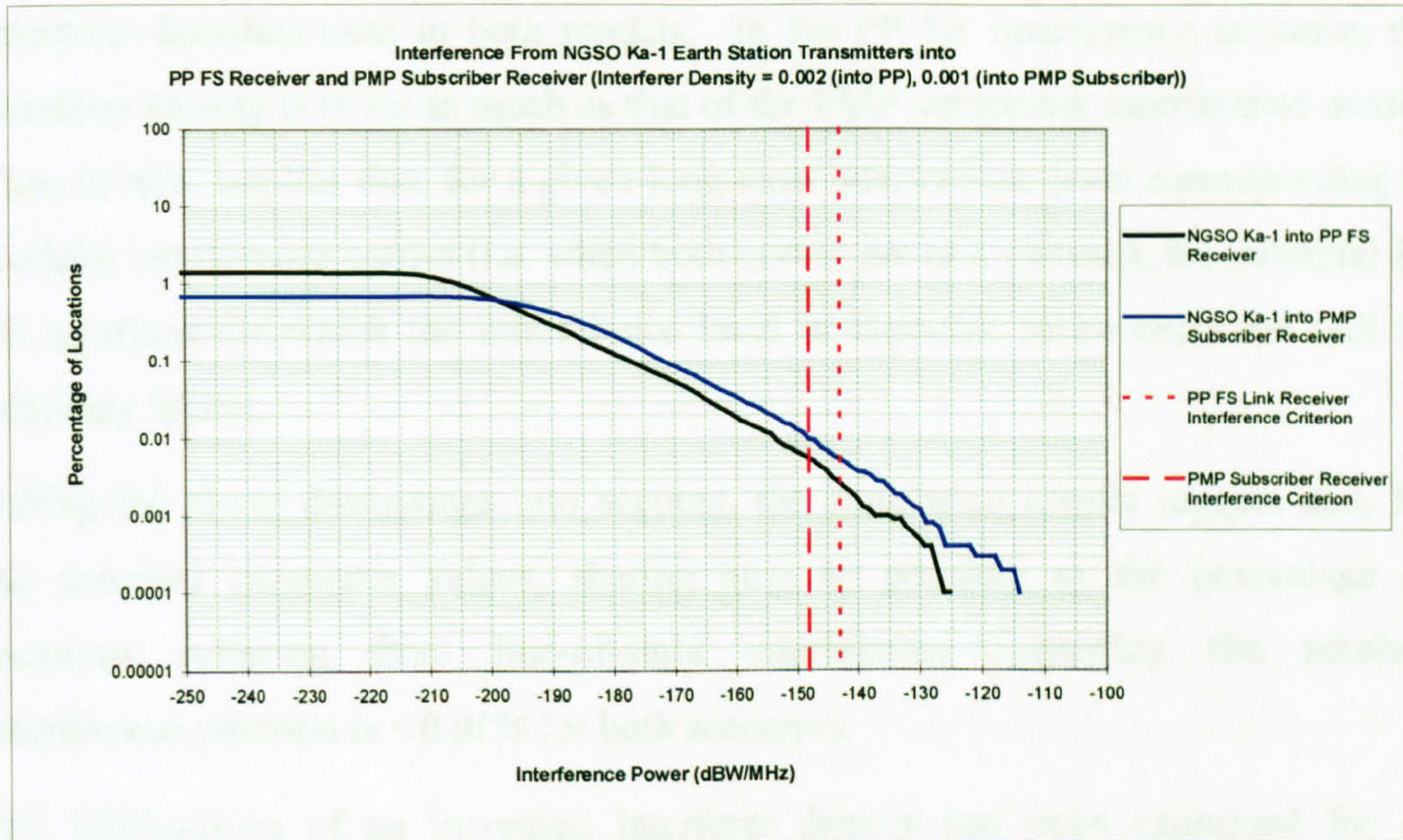


Figure 6.20 : Interference Statistics

For the assumed building blockage parameters, the results suggest that the PP FS link receiver interference criterion would be exceeded for 0.003% of the potential receiver locations for an NGSO Ka-1 transmitter density of 0.002 transmitters/km². The percentage of PMP subscriber locations likely to suffer interference from NGSO Ka-1 transmitters is 0.01% for a transmitter density of 0.001 transmitters/km².

It is worth noting that although the density of interferers is relatively lower in the PMP subscriber model, the expected interference level is relatively higher for a given percentage of locations, when interference is > -200 dBW/1MHz. This is the result of the PMP subscriber receiver antenna sidelobe levels being significantly greater than those of the PP FS link receiver (for example, there is a 20 dB difference at 50 degrees off-axis as shown in Figure 6.13).

For the interference values < -200 dBW/1MHz (representing rearlobe interference entries), the plots indicate that there is no line-of-sight interference path to the victim PP FS link receiver for 98.5% of the simulated locations. In the case of interference into the PMP subscriber receiver, the percentage is 99.4% . It should be noted that the difference between these two percentages is mainly due to the difference in the

interferer densities used in both models. In the PP FS interference scenario, the interferer density is twice as much as that of the PMP subscriber interference model. This, in turn, implies that, for a given long term interference level corresponding to rearlobe interference entries (i.e. when both curves are at a plateau), the potential PP FS locations for which the interference level is expected to be exceeded will be relatively higher.

Taking the above discussions into account, the simulation results suggest that, for the assumed parameter values, sharing may be possible as the percentage of locations suffering from line-of-sight interference exceeding the receiver interference criterion is $<0.01\%$ for both scenarios.

The implications of an increased interferer density has been examined for an assumed NGSO Ka-1 transmitter density of $0.02 / \text{km}^2$ and $0.2 / \text{km}^2$ by re-calculating the aggregate interference statistics at the PP FS receiver. The resultant cumulative distribution functions corresponding to 1,000,000 trials are illustrated in the following figure.

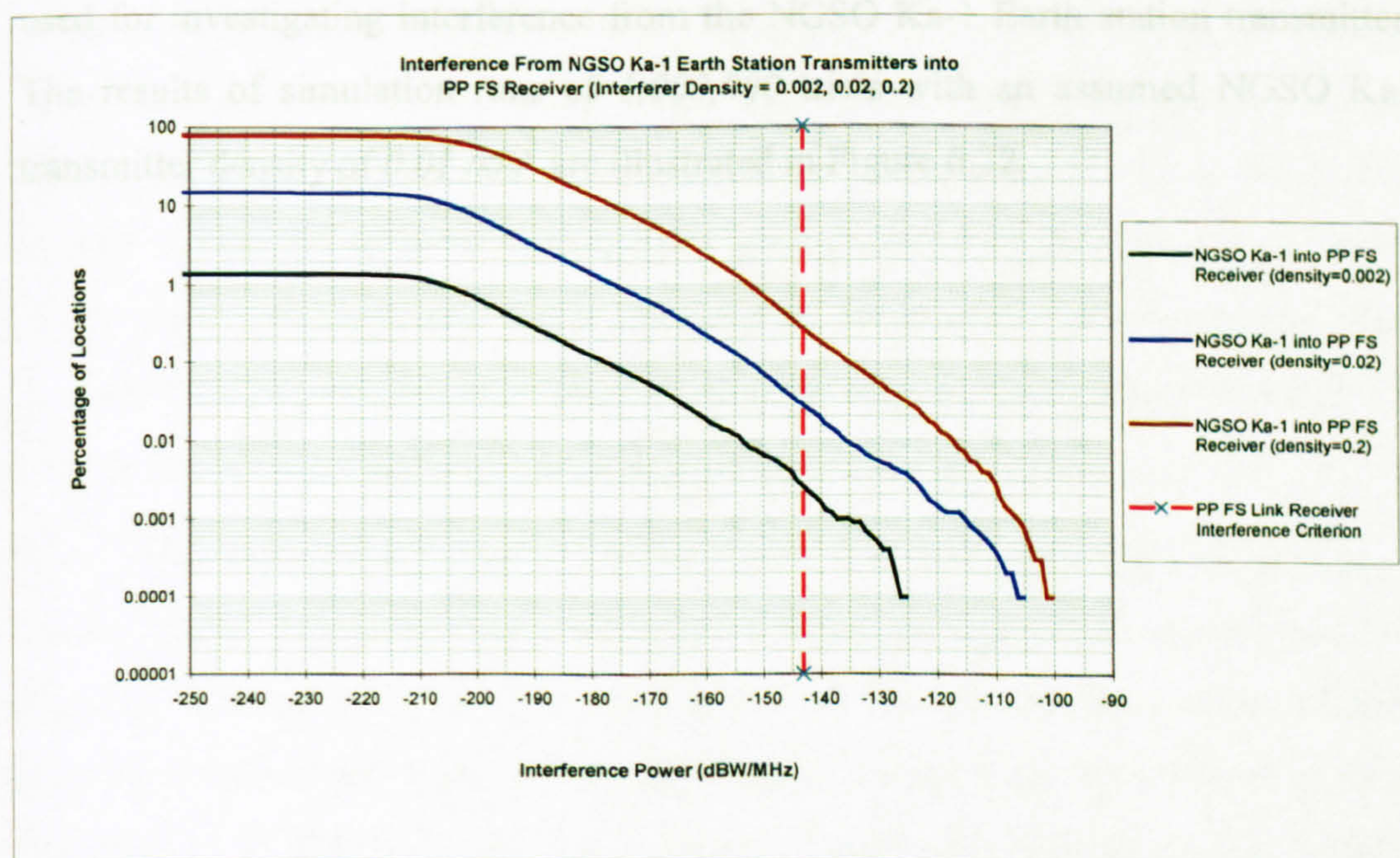


Figure 6.21 : Interference Statistics vs. NGSO FSS Earth Station Density

The results show that the percentage of locations, for which the aggregate interference is likely to exceed the receiver interference criterion, increases with an increasing interferer density. For a given set of transmitter and receiver antenna heights and building blockage parameters, the probability of having line-of-sight paths between the interferers and the receiver increases with an increasing interferer density. This, in turn, implies that the percentage of receiver locations likely to exceed a given interference level increases.

Figure 6.21 illustrates that the aggregate interference from NGSO Ka-1 Earth stations is likely to exceed the receiver interference threshold at 0.003% to 0.25% of the receiver locations when the interferer density is increased from $0.002 / km^2$ to $0.2 / km^2$.

The variation of the aggregate interference statistics with an interferer and receiver antenna height has been examined by considering the NGSO Ka-2 Earth station transmitter and PMP base station receiver characteristics (given in Table 6.9 and Table 6.10 in the preceding sections). The simulation models are similar to those used for investigating interference from the NGSO Ka-1 Earth station transmitters. The results of simulation runs of 1,000,000 trials with an assumed NGSO Ka-2 transmitter density of $0.01 / km^2$ are illustrated in Figure 6.22.

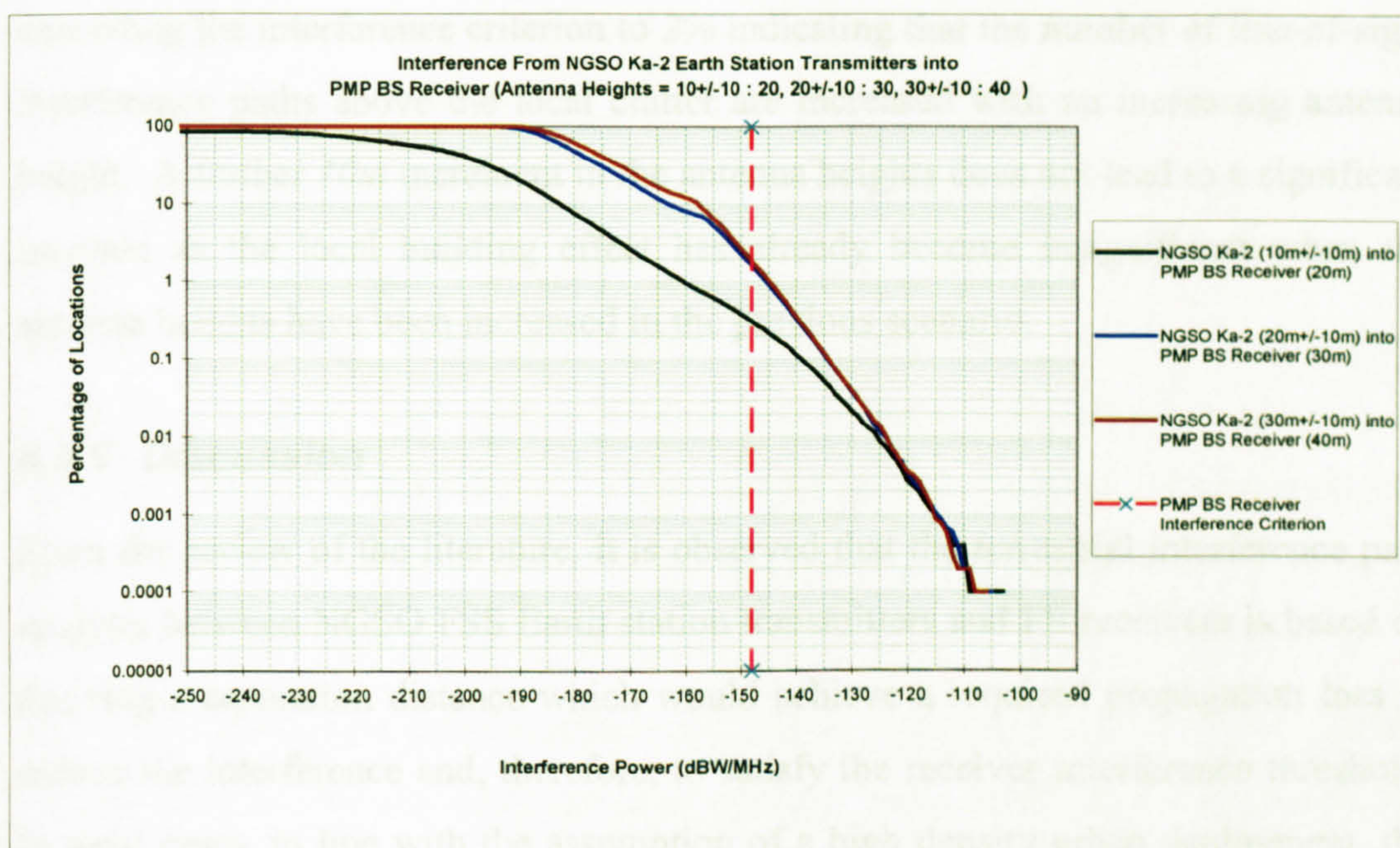


Figure 6.22 : Interference Statistics vs. Interferer and Receiver Antenna Height

Interference statistics suggest that, for the assumed building blockage parameters and the interferer density, the number of line-of-sight paths (therefore, percentage of locations at which interference is likely to exceed interference threshold) become significant when the NGSO Ka-2 Earth station and PMP base station receiver heights are above the local clutter. When the average NGSO Ka-2 transmitter antenna and the BS receiver antenna heights are greater than *20 metres*, all possible FS receiver locations are likely to receive interference power greater than *-190 dBW/1MHz*. For the same range of antenna heights, the aggregate interference exceeds the criterion at 2% of the likely receiver locations.

The comparison of the curves shown in Figure 6.22 illustrates the implications of relative height difference between the local buildings and the transmitter/receiver antennas. For the interference scenario where the average interferer antenna height is *10m* and the receiver is located at a *20m* height, the aggregate interference exceeds the criterion at 0.35% of the likely receiver locations. For the same building blockage model parameters and the interferer density, an increment of *10m* in the transmitter and receiver antenna heights increases the percentage of locations

exceeding the interference criterion to 2% indicating that the number of line-of-sight interference paths above the local clutter are increased with an increasing antenna height. A further 10m increment in the antenna heights does not lead to a significant increase as the local building effect has already become insignificant when the antenna heights have been increased in the previous scenario.

6.2.5 Discussion

From the review of the literature, it is observed that the terrestrial interference path analysis between NGSO FSS Earth station transmitters and FS receivers is based on deriving a separation distance which would achieve a required propagation loss to reduce the interference and, therefore, to satisfy the receiver interference threshold. In most cases, in line with the assumption of a high density urban deployment, the free space model has been employed for calculating the propagation loss values.

In this research, the implications of the NGSO FSS terrestrial interference paths have been examined by considering both the single entry and aggregate interference effects. The single entry and aggregate interference analysis methods have been developed and applied for investigating the sharing feasibility between the representative NGSO FSS and FS systems, including both point-to-point and point-to-multipoint radio stations.

For the purposes of single entry interference analysis, the propagation model combining the free space and diffraction over spherical Earth mechanisms has been developed. The model employs an iterative process in deriving the required exclusion distance at which the required transmission loss (based on satisfying the receiver long term interference criterion) becomes equal to the loss contributed by the propagation medium. Using the relative transmitter and the receiver antenna heights, in the iterative calculations, the model employs free space propagation to calculate distances where there is a line-of-sight path between the transmitter and receiver (assuming a smooth Earth surface), and takes account of the additional spherical Earth diffraction loss for distances beyond the line-of-sight. The exclusion distances are derived for each receiver azimuth interval. The area of sector wedges

are summed to arrive at an exclusion area in which an NGSO FSS transmitter can not operate without risk of causing interference into an FS receiver.

In practice, the implications of the terrain irregularities should also be taken into account in calculating the exclusion areas when the deployment area is known in advance. The clutter loss due to terrain structure is likely to reduce the required exclusion distances. However, it is worth noting that although the use of a smooth Earth assumption is a conservative approach, it provides a good initial insight into the feasibility of co-existence, in that satisfactory protection requirements are derived for the existing FS systems in generic co-frequency sharing scenarios.

The use of the single entry interference analysis model for examining the sharing possibilities among the representative systems has shown that large exclusion distances are required when the NGSO FSS Earth station is operating within/near the FS receiver antenna boresight or when the FS receiver (typically PMP base station) is located at a sufficiently elevated position is operating within/near the NGSO FSS Earth station transmitter antenna boresight.

In this study, a statistical analysis approach has been applied in order to evaluate the likelihood of these alignments occurring in a given sharing scenario and to assess the implications of aggregating interference paths. The approach taken combines the Monte Carlo simulation analysis technique with the generic building blockage prediction method which is based on the findings of EC funded CRABS project [231]. The building blockage prediction method is used to determine if a line-of-sight path exists between a transmitter and receiver for an assumed set of parameters characterising the simulation area.

The Monte Carlo simulator distributes the NGSO FSS Earth station interferers randomly, assigns a random antenna height for each interferer using an antenna height distribution specified by the user, points each interferer randomly and determines line-of-sight paths to the receiver by applying the building blockage model. Interference is then aggregated at each Monte Carlo trial by applying the free space propagation model to each line-of-sight path.

As, in each trial, the aggregate interference power is determined by the relative positions of interferers and the victim receiver, the simulation results are reported in the form of a cumulative distribution function where “the percentage of receiver locations for which a given aggregate interference level is exceeded” is specified.

The use of the aggregate interference analysis model for examining the feasibility of spectrum sharing for the representative systems has shown that the percentage of locations for which the receiver interference criterion is not satisfied increases when

- the NGSO FSS transmitter density is increased for a given set of blockage model parameters and transmitter/receiver characteristics,
- the FS receiver and NGSO FSS transmitter antenna heights are increased for a given set of blockage model parameters and a transmitter density.

It is reasonable to assume that the aggregate interference statistics obtained from the Monte Carlo simulator is not pessimistic as the analysis considers the impact of line-of-sight interfering paths only and does not take into account likely interference arising from scattering and diffraction mechanisms.

6.3 Conclusions

One of the key areas that needs to be examined when considering the implications of NGSO FSS systems is the analysis of interference into the existing and planned terrestrial radio stations operating in the fixed service. Therefore, in this chapter, interference analysis methods have been developed and applied for examining the possibility of spectrum sharing at the Ku and Ka band between the representative NGSO FSS and FS systems.

Initially, the analysis approach has been defined to investigate the downlink interference originating from the NGSO FSS satellite transmitters into the terrestrial radio links. This approach primarily considers the joint effects of the NGSO FSS interference statistics and the FS link fading mechanisms. The NGSO FSS downlink interference statistics are derived from the dynamic simulation analysis where the NGSO FSS and FS systems are modelled fully taking account of actual system

parameters. The FS link fading statistics are obtained from the propagation estimation models described for designing terrestrial line-of-sight links. Assuming that the interference and fading statistics are uncorrelated, the convolution process is applied to derive the FS link carrier-to-noise ratio statistics which are then compared against the FS link performance criteria to determine if performance degradation due to interference is within the tolerable limits.

For the analysis of interference paths originating from the NGSO FSS Earth station transmitters into the FS receivers, the single entry and aggregate interference analysis methods have been described.

The single entry interference analysis approach employs the propagation model combining the free space and spherical diffraction mechanisms. The propagation model is used in the iterative exclusion distance calculation process for the interference alignments where the NGSO FSS Earth station is assumed to be transmitting towards the FS station at each receiver azimuth considered. The calculated exclusion distances are then used to determine the exclusion area where the NGSO FSS transmitter could not operate without causing an unacceptable interference into the FS receiver.

The aggregate interference analysis is based on a statistical approach combining the Monte Carlo simulation technique with the generic building blockage prediction method defined in ITU-R Recommendation P.1410. In the application of the analysis method, the aggregate interference is calculated, at each Monte Carlo trial, using the relative random position and pointing of the interferer antenna together with the probability of having a line-of-sight path to the victim FS receiver which is mainly determined by the parameter values assumed for the building blockage prediction method. The resultant statistics are expressed in the form of a cumulative distribution function indicating the proportion of the FS victim receiver locations that are likely to suffer a given level of interference from multiple NGSO FSS Earth station transmitters operating at the same frequency band.

CHAPTER 7

CONCLUSIONS

In the preceding chapters, research into the development and application of radio frequency spectrum sharing methodologies has been presented. These methods are proposed for the investigation of interference from NGSO FSS systems into GSO FSS systems and FS terrestrial radio systems operating (or planned for operation) at Ku and Ka band frequencies. This chapter provides a summary of the work provided in each chapter and identifies the key conclusions.

7.1 Chapter 1

Chapter 1 introduced the concept of radio spectrum management and investigated technical characteristics of fixed satellite and terrestrial service networks, with a view to obtaining an initial insight into the system design parameters related to use of the radio frequency spectrum.

In this chapter, the need for spectrum management was described together with an introduction to international organisations responsible for regulations concerning use of the radio spectrum. The requirement for spectrum sharing among different radio communication services was then explained and the implications of sharing constraints were outlined. This was followed by a review of fixed satellite and terrestrial service system characteristics from the frequency management point of view.

For the fixed satellite service systems, a general description of technologies used in designing transponders, power amplifiers, Earth stations and satellite orbits was provided. Based on the literature review, the Ku and Ka band GSO FSS and NGSO FSS system characteristics were summarised, taking account of constellation parameters, beam characteristics and Earth station design parameters. Typical network configurations were also described together with potential system applications.

For the fixed service systems, the benefits of the use of wireless technology for terrestrial communication networks were outlined. A brief consideration was given to the technical characteristics of the fixed point-to-point links and the fixed wireless access networks designed for the Ku and Ka band applications. Parameters used in the fixed point-to-point link design were identified and typical values were provided. The need for an effective local access network was explained. Different fixed wireless access network technologies and architectures were summarised. In this context, a review of point-to-multipoint and mesh network topologies was carried out taking typical system deployment scenarios into account. Issues related to standardisation and system applications were also briefly considered.

From these investigations, it was noted that spectrum sharing is a powerful mechanism allowing major frequency allocations to be made to new services whilst maintaining the existing allocations in the same part of the radio spectrum. It was further noted that spectrum sharing analysis methodologies need to be developed to examine technical and operational compatibility among networks operating in the fixed satellite and terrestrial service at Ku and Ka band frequencies.

The investigations also suggested that propagation characteristics together with location and terrain conditions play a significant role in determining the feasibility of sharing. A range of system parameters are required to be considered to investigate the possibility of frequency sharing. From the fixed satellite service point of view, these include antenna characteristics, coverage, power and bandwidth requirements, beam characteristics (i.e. single/multiple, spot/global and fixed/dynamic), resource sharing mechanisms (i.e. multiple access and duplexing techniques) and constellation parameters (i.e. number of satellites, orbital height, satellite spacing etc.). In fixed terrestrial service applications, the implications of link length, power, bandwidth and antenna requirements, availability objectives, modulation techniques and network topologies should primarily be taken into account.

7.2 Chapter 2

Chapter 2 investigated the key propagation impairments that would be experienced by radio transmissions operating at the frequencies of interest to this research. For these purposes, the implications of the use of ITU-R Recommendations developed for modelling terrestrial and space path propagation effects were examined in detail taking both wanted and interference paths into consideration.

In general, it was noted that the prediction of the propagation behaviour at Ku and Ka band frequencies with reasonable accuracy is one of the key issues in the investigation of frequency sharing. Propagation statistics are derived from empirical models based on the results of long term measurements, and these models have limited validity range in terms of frequency, path length and time percentages.

Atmospheric gas attenuation is primarily determined by frequency, path length and meteorological parameters including pressure, temperature and humidity. ITU-R Rec.676 describes line summation and simplified prediction methods for the calculation of total terrestrial and space (i.e slant) path atmospheric attenuation.

In this study, both methods were implemented to assess the impact of atmospheric gas attenuation at Ku and Ka band frequencies. It was noted that the simplified method was recently modified in the new version of the recommendation and, therefore, both simplified prediction methods were also used to examine the implications of the modifications in the context of NGSO / GSO FSS and NGSO FSS / FS spectrum sharing. The modelling results showed that the attenuation values obtained from simplified methods are very close to each other at Ku and Ka band frequencies while the comparison of line summation and simplified model indicated that the latter estimates higher attenuation for elevation angles less than 3°.

From the Ku and Ka band spectrum sharing point of view, the results obtained from the line summation method indicated that, at Ku band, space paths are subject to atmospheric loss of less than 2 dB for all elevation angles while a terrestrial link loss for a 10 km path length is about 1 dB. At Ka band, space path loss remains below 7 dB and a 10 km terrestrial path loss is approximately 1 dB. These figures suggest

that atmospheric absorption is not a dominant factor but does have a limited impact at these frequencies when it is compared against other fading mechanisms including rain and multipath fading.

Terrestrial path propagation is influenced by troposphere and terrain effects which result in refraction, reflection and scattering of radiowaves. The impact of absorption and scattering caused by rain also play a significant role at Ku and, in particular, Ka band frequencies. In this study, the implications of terrestrial wanted and interference path propagation mechanisms were considered. The wanted path mechanisms were examined from a fixed terrestrial link planning point of view while the interference path propagation effects were investigated from an NGSO FSS / FS spectrum sharing point of view (i.e. when considering interference paths from NGSO FSS Earth stations into FS radio links).

At the frequencies considered here, wanted path fading due to multipath and rain mechanisms needs to be taken into account in sharing studies. The prediction models for both mechanisms are defined in ITU-R Rec.530 which was also modified recently.

As far as Ku and Ka band FS link planning is concerned, the results obtained from the implementation of the multipath and rain fading prediction methods defined in the previous and modified Rec.530 suggested that the modification to the interpolation algorithm defined for the small multipath fades does not have a significant impact on the overall multipath fading statistics at Ku and Ka band frequencies. However, it was noted that the additional expression introduced to the new rain fading prediction model for use at locations less than 30° in latitude does have not an impact on the overall rain statistics for percentages between 0.01% and 0.1%. The modification implies that according to the new model, the FS links located at latitudes less than 30° and designed for availability objectives greater than 99.99% and less than 99.9% will require a relatively smaller fade margin.

Finally, the exceedence percentages for a given fading value corresponding to multipath and rain fading are added together to derive combined fading statistics.

From the modelling, it was observed that, at Ku band, combined fading statistics are influenced by both multipath and rain fading effects. At Ka band, on the other hand, rain fading dominates combined fading statistics.

Propagation effects causing short and long term interference should be taken into account when addressing terrestrial interference paths from NGSO FSS ground terminals into FS radio links. The long term mechanisms include line-of-sight propagation, diffraction, tropospheric scatter and clutter loss. The short term interference is primarily due to ducting and layer reflection, and hydrometeor scatter. In sharing studies, the empirical methods defined in ITU-R Rec.452 are employed for the prediction of these effects.

The modelling carried out using the interference propagation methods suggested that the recent modification in the ducting and layer reflection method does not give rise to a significant difference in interference path loss statistics at Ku and Ka band frequencies. It was noted that the combined effects of individual propagation mechanisms need to be considered depending on the type of interference path. When interference paths are line-of-sight, the free space path loss together with the local clutter loss is applied for the calculation of total path loss. In the case of transhorizon interference paths, the effects of troposcatter, diffraction, ducting and layer reflection and local clutter are combined to derive overall loss statistics. Furthermore, it was also noted that the scattering of radiowaves occurring when transmitter and receiver beams form a common volume within the part of atmosphere where a rain cell exist may also be significant for short periods of time.

Space path propagation is influenced by rain, atmospheric absorption and tropospheric effects. The operating frequency, geographic location and path elevation angle determine the degree to which these mechanisms are effective. In this study, the implications of space wanted and interference path propagation mechanisms were taken into consideration.

Wanted space paths are designed to be line-of-sight. This implies that clear-air propagation should be modelled by free space path loss and atmospheric gas

attenuation. The most significant Ku and Ka band space path propagation impairment is rain fading. To reduce the impact of rain fading, the links are generally designed to operate at elevation angles greater than 10° . The space path rain fading estimation method is defined in ITU-R Rec.618 which was modified to extend its validity range in terms of frequency and percentage time.

From the results obtained from the modelling, it was recognised that the fading values obtained from the modified method are significantly lower than those derived from the previous method which, in turn, implies relatively lower margin to compensate for rain fading and, therefore, a relatively lower EIRP requirement to achieve given link performance objectives. In addition, the modelling confirms that a decreasing path elevation angle increases the slant path rain fading as the path length becomes longer. Therefore, for a given required link availability, the minimum path elevation angle will be constrained by the rain attenuation and the power available.

It is generally true to say that, space interference paths are line-of-sight. Therefore, free space propagation is used to calculate interference at victim receivers. It was noted that additional loss may also result from the atmospheric absorption when a path elevation angle is very small.

7.3 Chapter 3

Chapter 3 reviewed the key aspects of Ku and Ka band interference paths originating from NGSO FSS transmitters into GSO FSS receivers. In this chapter, an overview of the current regulations was followed by identification of key sharing topics. A revision of sharing methodologies applied to address these topics was then presented. The chapter also provides representative system characteristics to be used in sharing analysis applications carried out in the succeeding chapters.

From the literature review presented in Chapter 3, it was observed that the ITU-R Radio Regulations Article S.22 defines power flux density limits for a number of receiver antenna diameters to protect GSO FSS Earth stations and satellites from

NGSO FSS interference. These limits are applicable to a single NGSO FSS system. In addition, ITU-R Rec.1323 provides minimum protection requirements for the GSO FSS systems sharing the same bands with NGSO FSS systems. The key requirement is an allocation of at most 10% of the total GSO FSS link unavailability objective to NGSO FSS interference. The recommendation also defines a number of methodologies to be used in deriving maximum tolerable power flux density levels for given GSO FSS link characteristics.

It was noted that the key issues considered to be significant in determining co-existence of NGSO FSS and GSO FSS include implications of interference mitigation techniques, modification to power flux density definitions, revision of power flux density limits, refinement of reference antenna patterns, examination of aggregate interference from multiple NGSO FSS systems, development of conversion algorithms from the aggregate to single entry power flux density limits, protection of large GSO FSS Earth station antennas and implications of short term NGSO FSS interference peaks.

Finally, the literature review suggested that the common approach used to examine the feasibility of NGSO/GSO FSS spectrum sharing is to develop simulation methodologies. In addition, analytic methods defined in Rec.1323 are implemented to investigate whether Article S.22 limits provide adequate protection for the GSO FSS links.

7.4 Chapter 4

Chapter 4 described the author's work concerning spectrum sharing methodologies employed to investigate the NGSO FSS and GSO FSS system co-existence at Ku and Ka band frequencies. Investigations were primarily directed towards the development of analytic and simulation methods to address different topics that are significant in determining the feasibility of NGSO/GSO FSS spectrum sharing.

Firstly, analysis methods for examining the NGSO FSS interference mitigation techniques were described, including GSO arc avoidance, latitude avoidance and

improved NGSO FSS satellite antenna patterns. The analysis method required that simulation scenarios be designed by identifying key system parameters which include constellation parameters (number of satellites, altitude, inclination and satellite phasing), beam frequency re-use pattern, operational characteristics (mitigation techniques, power control and minimum elevation angle), transmitter and receiver power and antenna characteristics and beam coverage area size.

The simulation approach taken to examine the implications of the mitigation techniques was based on the comparison of the resultant statistics obtained from the scenarios where NGSO FSS systems were modelled with and without the mitigation techniques. For these purposes, deterministic simulation analysis was applied to the scenarios. In the analysis, the satellite positions in a given NGSO FSS system are calculated at regular time intervals over the simulated time period and from this data interference alignments are determined. The calculated interference levels are then analysed statistically and the results are presented in the form of graphs showing interference level against the percentage of time over the simulated period for which that level was exceeded. In addition, the significant points that need to be considered when interpreting the resultant statistics were outlined in this chapter.

Mathematical models for the investigation of the single entry interference entries corresponding to mainbeam-to-mainbeam and rearlobe-to-rearlobe interference alignments were developed. These models were used to verify the simulation results. Additionally, the analysis method was developed to calculate and compare the GSO FSS link overall performance degradation in the presence of interference from the NGSO FSS system modelled with and without GSO arc and latitude avoidance mitigation techniques.

It was observed from the sharing analysis carried out using the representative system characteristics that the near on-beam interference entries leading to relatively higher interference power at GSO FSS Earth stations are not prevented when the GSO arc avoidance is applied. This technique allows interference alignments where the NGSO FSS satellite is in the GSO FSS receive Earth station antenna boresight and

transmitting towards the NGSO FSS user terminal, satisfying the geostationary arc avoidance requirement, placed at some distance from the GSO FSS Earth station receiver.

On the other hand, the latitude avoidance technique where all transmissions are suppressed when the NGSO FSS satellites are within the volume defined by $\pm\theta^\circ$ in latitude proved to be more efficient in that near on-beam interference coupling is prevented. It was noted that the off-axis angle at the GSO FSS receiver antenna between the wanted and the interfering path is dependent on the NGSO FSS system orbit height, the latitude of the co-located Earth stations and the value of the latitude avoidance angle. A larger off-axis gives rise to an improved antenna discrimination and avoids single entry boresight hits.

Finally, the analysis indicated that the use of the NGSO FSS space station antennas with improved sidelobe performance reduces the amount of aggregate interference into the GSO FSS Earth station receivers which, in turn, increases the efficient use of the spectrum.

The development and application of methods for the revision of the *epfd* limits constituted the next step in the NGSO /GSO FSS sharing analysis. The implications of two methods were examined. The first method, simulation approach, is based on determining aggregate interference statistics from the simulation modelling, application of the analytical method to the interference distributions to derive *epfd* statistics and comparison of the *epfd* statistics against the Article S.22 limits to determine whether the protection is adequate or any revision to the limits is required. The second method, analytic approach, comprised the implementation of the Methodology A', defined in Rec.1323. This methodology takes account of the joint effects of the rain fades and interference events. The implementation includes a convolution process, involving simplified interference and fading probability density functions, to derive the *epfd* levels which are then compared against the Article S.22 limits.

In the application of the simulation approach, initially, the expression to be used in translating interference statistics into *epfd* statistics was derived. It was noted that the operating frequency, the GSO FSS receiver antenna maximum gain and the bandwidth are required to convert the aggregate interference statistics obtained from the simulation analysis into the *epfd* statistics which are then compared against the Article S.22 limits for verifying the compliance.

The mechanisms by which interference from multiple NGSO FSS systems aggregate were then examined. It was shown that, in the interference scenarios including multiple inhomogeneous NGSO FSS systems, the *epfd* statistics are largely driven by the dominant NGSO FSS constellation. In the case of several homogeneous NGSO FSS systems, it was noted that the long term *epfd* aggregates in power while the short term *epfd* aggregates in time.

The implications of conversion from the aggregate *epfd* statistics based on several NGSO FSS systems to the single entry *epfd* statistics based on a single NGSO FSS system formed the next step in the analysis. It was recognised that the conversion is required in order to achieve a meaningful comparison against the Article S.22 limits which are defined for a single NGSO FSS system. The accuracy of the conversion algorithm defined by the ITU-R is determined by the assumption related to the effective number of NGSO FSS systems. The results suggested that when the actual number of NGSO FSS systems is less than the assumed value, the single entry statistics obtained from the conversion method are further away from the Article S.22 *epfd* limits than the actual single entry statistics obtained from the simulation analysis.

The use of the discontinuous *epfd* limits to check the compliance with the Article S.22 limits was also analysed. It was shown that this approach gives rise to pessimistic conclusions for the NGSO FSS systems. The comparison against the continuous *epfd* limits based on the linear interpolation between the breakpoints was implemented and noted to be more appropriate as, in practice, the NGSO FSS interference statistics would be in the continuous form.

Finally, the empirical approach defined by the ITU-R for the use of deriving $epfd_{down}$ limits for the GSO FSS receiver antenna diameters not included in the Article S.22 was taken into consideration. It was observed from the analysis that the $epfd_{down}$ limits derived from the empirical method are stringent than those specified in Article S.22 which, in turn, suggests that the GSO FSS protection provided by Article S.22 is preserved.

The application of the simulation approach was followed by the implementation of Methodology A'. It was shown that the method is based on the calculation of the maximum tolerable interference $epfd$ levels on the basis of the stated GSO FSS link performance requirements. The calculated values are compared against the Article S.22 limits to determine whether the GSO FSS link examined will be sufficiently protected from the NGSO FSS interference. It was pointed out that Article S.22 limits are defined for limiting interference from a single NGSO FSS system while the $epfd$ limits derived from the application of Methodology A' are attributed to the aggregate NGSO FSS interference.

In this phase of the analysis, investigations were primarily directed towards determining the implications of the modification to the rain fading prediction model defined in Rec.618. The analytical models including both versions of this recommendations were implemented and applied to the representative GSO FSS link to calculate the $epfd_{down}$ values. In addition, Methodology A' was improved by taking novel approaches related to convolution of uplink and downlink rain statistics, assumption on rain fading on interference paths, use of the bisection method, implications of stated and achieved unavailability, assumption on percentage time representing no rain fading and use of overall effective noise temperature.

It was recognised that the end-to-end GSO FSS link rain fading distribution needs to be obtained by convolving the uplink and downlink rain fading statistics assuming they are uncorrelated. The convolution process requires two complete (defined up to 100% of the time) probability density functions but the Rec.618 prediction model

defines empirical algorithms to derive partial rain statistics which, in turn, suggests that the rain statistics have to be extrapolated. It was noted that the convolution of two extrapolated distributions may introduce inaccuracies to the total fading statistics and the *epfd* values derived from the application of the Methodology A' may not be representative.

The analysis presented in this research was, therefore, based on the assumption that the rain fading occurs on the uplink and downlink separately, but not simultaneously. This assumption eliminated the ambiguity that would be introduced when deriving complete rain fading statistics. In addition, in this study, it was assumed in the derivation of *epfd* limits that the rain fading occurs on the wanted path but not on the interfering paths which provides interference protection for such interference situations.

The complexity of the empirical formula defined for calculating the rain fading for a given percentage time meant that the bisection method had to be applied to derive percentage times for which given rain fading values are exceeded. This method is based on the iterative bisection of the rain fading distribution.

It was shown that when the rain fades occur very short periods of time, the total stated GSO FSS link unavailability time attributed to the rain fading is not entirely taken up by rain. Therefore, the unavailability due to the NGSO FSS interference takes up the greatest share of the total stated unavailability which is generally greater than the 10% limit stated in Rec.1323. In this study, findings indicated that in order to comply with the 10% criterion, the total unavailability target should be equal to the sum of the *"total achieved unavailability"* (derived from the Rec.618 rain models) and 10% of the *"total stated unavailability"*.

It was noted that the methodology does not specify any value with regard to the parameter representing the percentage time for which no rain fading occurs (β_0). Therefore, during the analysis, two criteria were considered in assigning a value to this parameter:

- 1) $\beta_o \leq 100$ - *unavailability percentage time associated with the second GSO FSS link short term performance criteria,*
- 2) $\beta_o \geq 99\%$ *in the previous Rec.618 model and $\beta_o \geq 95\%$ in the revised Rec.618 model.*

Finally, with regard to the application of the Methodology A', it was proposed in this research that the use of the effective overall link noise temperature as the system noise temperature is required in the process of translating the GSO FSS link degradation to the *epfd* statistics since all degradations in the GSO FSS link budget need to be taken into consideration.

The application of the methodologies used in the revision of the *epfd* limits was followed by an examination of the modifications to the GSO FSS Earth station reference antenna radiation patterns. Within ITU-R, it has been argued that the reference radiation pattern defined in Rec.1323 represents an envelope of the side-lobe peaks which is required for interference analysis involving a single fixed transmitter and receiver to ensure that the worst case scenario is accommodated. With the introduction of the NGSO FSS systems, sharing scenarios will no longer be static. Therefore, the new reference pattern (defined in Rec.1428) based on averaging the troughs and peaks in the gain pattern has been developed to model more closely interference variations with time due to the dynamic nature of the sharing environment.

For the analysis implemented in this research, a Monte Carlo simulator was designed to simulate the interference scenarios developed for the preliminary analysis of the use of both antenna patterns in a typical NGSO/GSO FSS sharing scenario. It was observed that use of the probabilistic approach developed in this study reduces the computational complexity encountered in the deterministic simulation modelling of large constellations.

The Monte Carlo simulator design is based on the calculation of aggregate interference from a number of interference entries each of which originates from satellites randomly positioned at the NGSO FSS orbit. The total interference levels

obtained at each Monte Carlo trial are stored in 1 dB wide bins. After the simulation run of a given number of trials, the simulator analyses the interference levels to derive the interference probability density function which is then converted to the cumulative distribution function of the percentage time for which a particular level of interference is exceeded vs. the total interference level (dB).

The simulation model employs a novel random pointing algorithm together with vector analysis. The random pointing algorithm is based on mapping a uniform random variable to a random variable representing probability density function of an NGSO satellite orbital location. This approach ensures that a higher probability of an interference entry originating from an NGSO FSS satellite at a lower elevation angle as seen from a GSO FSS receiver is taken into account in simulation analyses.

In the application of the probabilistic analysis, it was noted that the Rec.1323 pattern is partial and this results in discontinuity at the angle breakpoints when $D/\lambda < 100$. It was found out that this pattern originated from the APS8 Annex III pattern and it was obtained by suppressing the sidelobe envelopes, defined for $D/\lambda \geq 100$ by 3 dB . Therefore, by applying the same 3 dB reduction approach, the Rec.1323 pattern was modified to obtain continuous envelope for the smaller antenna diameters used in the analysis.

The Monte Carlo analysis based on the representative system characteristics suggested that the relative interference statistics are dependent on the receiver antenna diameter and elevation. At 10° elevation, the reductions introduced in the new radiation pattern's sidelobe and far lobe envelopes give rise to a decreased long term interference at the small receive antennas ($D/\lambda < 100$). In the case of large receive antennas ($D/\lambda \geq 100$), although the new pattern sidelobe and far lobe envelopes are decreased, the inclusion of a spillover lobe reduces the impact of this modification on the mid-term and long term interference. Therefore, very similar interference statistics were calculated for both antennas. It was noted that when the elevation angle is 90° , the resultant statistics no longer include interference entries coming through the modified far sidelobes.

From the analysis, it is reasonable to conclude that the use of the Rec.1428 radiation pattern instead of the Rec.1323 radiation pattern does not have a significant impact on the feasibility of the spectrum sharing with regard to the calculation of $epfd_{down}$ limits as the short term interference statistics for both patterns do not differ significantly.

In Chapter 4, final consideration was given to the analysis of the NGSO FSS interference peaks. For this purpose, the analytical approach aiming to determine the degradation at the GSO FSS link $C/(N+I)$ ratio resulting from the NGSO FSS interference peaks, and to relate this to the calculation of the $epfd_{down}$ limits was implemented. In the application of the method, the GSO FSS $C/(N+I)$ was calculated assuming that the NGSO FSS interference corresponds to the maximum tolerable $epfd$ level. The results were compared against the synchronisation loss criterion which is dependent on the modulation and coding used in the GSO FSS link.

The analysis showed that the near on-beam interference entries at the GSO FSS receive antennas may reduce the $C/(N+I)$ ratio to a level where the modem may lose synchronisation. The degree of severity is largely determined by the type of modulation and coding employed in the GSO FSS link. In particular, it was noted that the protection of the large GSO FSS receive antennas with the use of $epfd$ limits may not be feasible without an excessive burden on the NGSO FSS systems.

7.5 Chapter 5

Chapter 5 provided a review of key issues related to NGSO FSS and FS spectrum sharing. Initially, a summary of the regulatory requirements and the relevant ITU-R recommendations was presented. This was followed by a brief outline of sharing methodologies employed in the previous studies.

The findings of the literature review suggested that ITU-R Radio Regulations Article S.21 defines maximum EIRP and minimum elevation angle limits applicable to Earth stations of fixed satellite service to protect FS links from ground path

interference. In addition, power flux density limits are specified to limit interference from satellites. These limits are defined for a single satellite as a function of an interference path angle of arrival at the Earth's surface.

It was noted that a number of recommendations are in use defining performance and availability objectives of FS links. These objectives specify the total allowable degradation of the FS links attributable to the combined effects of thermal noise, interference within the system and interference from other systems. In order to determine the allowable degradation levels due to interference from other systems as a permissible fraction of the total allowable degradation in performance and availability of the FS links, further recommendations have been developed. One of the key issues is how to partition the allowable degradation due to interference from all other systems into the allowance attributable a single NGSO FSS system.

It was observed from previous studies concerned with interference from NGSO FSS satellites into FS links that investigations primarily addressed the suitability of Article S.21 power flux density limits. In general, simulation methodologies were applied to derive interference statistics at FS receivers pointing at an azimuth resulting worst case interference levels. The worst case approach was used to ensure protection for all possible interference alignments. In addition, FS link parameters were either based on representative characteristics taken from ITU-R Recommendations or real system values provided by the operators. Various methodologies were proposed to derive interference criteria for the protection of FS receivers.

The review of previous studies investigating terrestrial interference paths from NGSO FSS Earth station transmitters into FS receivers suggested that a minimum required separation distance approach was employed to avoid harmful interference. In these studies, using transmitter and receiver characteristics, minimum required distance calculations were carried out assuming clear line-of-sight propagation conditions which represents the worst case conditions. By repeating separation distance calculations for all azimuths, a two dimensional exclusion zone was

calculated which represented a region around FS receiver where the operation of an NGSO FSS Earth station transmitter would not be possible without a risk of causing unacceptable interference. Interference mitigation techniques including high performance antennas, power control, dynamic channel assignment and relatively higher minimum elevation angle were proposed to improve the sharing conditions.

It was noted that, at Ka band frequencies, point-to-multipoint and mesh fixed wireless access networks are planned for operation. Previous studies argued that the co-existence of NGSO FSS Earth stations and fixed wireless access networks in the same geographical area may not be feasible due to the potential for the high density deployment. Therefore, various interference mitigation techniques and a band segmentation scheme were proposed to accommodate both systems.

7.6 Chapter 6

Chapter 6 presented the author's work into the development of spectrum sharing methodologies to assess the feasibility of NGSO FSS and FS system co-existence at Ku and Ka band frequencies.

It was observed from the literature that the analysis of interference from NGSO FSS satellites into FS links (i.e. downlink interference) is generally based on calculating and comparing aggregate interference statistics (primarily derived from simulation analysis) against the FS link interference criteria which are defined relative to the FS receiver noise power. This approach gives an initial insight into the NGSO FSS / FS downlink sharing environment.

In Chapter 6, a more precise analysis method combining analytic worst case interference modelling, dynamic deterministic simulation analysis and terrestrial link propagation fading statistics was developed for examining the impact of interference from NGSO FSS satellites into FS links. The method is based on modelling joint effects of aggregate NGSO FSS interference and FS link received power statistics. Aggregate interference statistics are derived from simulation modelling comprising an NGSO FSS constellation (modelled fully by taking individual beam patterns and

transmission characteristics into account) and an FS receiver (pointing at its worst-case azimuth). In the simulation analysis, propagation effects are modelled using free space and atmospheric loss mechanisms as the interference paths are assumed to be line-of-sight. The FS link received power statistics are calculated from multipath and rain fading prediction methods defined in Rec.530. The analysis method is completed by convolving the aggregate interference and the FS link received power probability density functions. The result of the convolution is the FS receiver C/N+I probability density function which is then converted to a cumulative distribution function and compared against the FS link C/N+I objectives to determine if the degradation due to joint effects of interference and wanted path fading is at an acceptable level.

The application of the analysis method was demonstrated using the representative systems. In this process, initially, the simplified FS link design procedure was developed to derive representative link parameters. The FS link interference criteria derivation method was then described. This method takes account of new definitions of error performance objectives and relates them to conventional bit error rate performance requirements which are then used to derive the interference criteria.

The analytic approach was applied for the calculation of potential single entry interference values to be used to validate the aggregate interference statistics obtained from the simulation modelling. The simulation scenario was developed to derive aggregate interference statistics. The key simulation design parameters were identified (including the maximum number of visible satellites, the service area covered by each beam, the maximum number of co-frequency beams per satellite and receiver elevation angle and azimuth pointing) and incorporated into the model.

Linear interpolation was applied to remove the discontinuity resulting from the addition of rain and multipath fading statistics of the FS link and to obtain a complete distribution (i.e. up to 100%) which is required by the convolution process. In addition, a similar approach was taken to make the interference and FS link fading probability density function bin size equal which is also required by the convolution

process. After convolution, the resultant probability density function was normalised and validated.

In addition to the above defined downlink interference analysis procedure, sharing analysis methods were developed in order to investigate the implications of single entry and aggregate interference from NGSO FSS Earth station transmitters into FS receivers (i.e. terrestrial interference paths).

The review of the previous studies suggested that the terrestrial interference path analysis primarily considered the single entry interference path and was based on deriving a separation distance which would achieve a required propagation loss to reduce interference and, therefore, to satisfy a receiver interference limit. In most cases, in line with the assumption of a high density urban deployment, the free space model was employed for calculating propagation loss values.

In this study, the implications of both single entry and aggregate interference were examined. For the purposes of single entry interference analysis, the combined effects of the free space and diffraction over spherical Earth mechanisms were incorporated into the propagation model developed during the course of this research.

The model is based on an iterative process where a calculation of a required exclusion distance at which a required transmission loss (based on satisfying a receiver long term interference criterion) becomes equal to a loss contributed by the propagation medium is implemented. In the iterative calculations, the model applies free space propagation for line-of-sight distances (assuming a smooth Earth surface) and introduces the additional spherical Earth diffraction loss for distances beyond the line-of-sight. This approach results in more realistic exclusion distances between an FS receiver and an NGSO FSS transmitter than those would be obtained by applying only the free space propagation loss model to the distances beyond the line-of-sight which are related to an NGSO FSS Earth station transmitter being located on or very near to an FS receiver main lobe. The calculation of exclusion distances are implemented for each receiver azimuth interval and the area of sector wedges are

summed to arrive at an exclusion area in which an NGSO FSS transmitter can not operate without risk of causing interference into an FS receiver.

Although the use of the smooth Earth assumption is still a pessimistic approach as the additional loss due to local clutter is not taken into account, this method provides a good initial insight into the feasibility of spectrum sharing in that the calculated exclusion areas ensure satisfactory protection generic co-existence scenarios.

The use of the single entry interference analysis method was demonstrated by investigating interference between representative systems comprising NGSO FSS Earth station transmitters (operating at 20° and 40° elevation), point-to-point FS receiver and fixed wireless access point-to-multipoint base station and subscriber receivers. The analysis involved

- Development of the worst case interference alignments where the FS receivers were assumed to be operating at the same azimuth plane as the NGSO FSS transmitters.
- Determination of the maximum line-of-sight range (using a smooth Earth assumption) as a function of the transmitter and the receiver antenna heights.
- Examination of the implications of the FS receiver antenna radiation patterns and noise figures as well as the NGSO FSS transmitter elevation angles on the required exclusion areas.
- Evaluation of the introduction of the additional spherical diffraction loss for beyond line-of-sight distances.
- Investigation of the interference alignments where an NGSO FSS Earth station transmitter was located very close to a point-to-multipoint base station receiver which was positioned at a top of a high building and operating within the NGSO FSS transmitter boresight.
- Incorporation of the point-to-multipoint base station receiver antenna azimuth and elevation radiation patterns into the separation distance calculations.

The single entry interference analysis indicated that when the NGSO FSS Earth station transmitter operates near the FS receiver antenna boresight or the highly elevated FS base station receiver is within the NGSO FSS transmitter boresight, co-frequency operation within the same urban area may not be possible. The likelihood of these interference alignments occurring within a given sharing environment was investigated by developing a novel aggregate interference analysis methodology employing a Monte Carlo simulation technique combined with a generic building blockage prediction procedure.

The Monte Carlo simulation approach employed in this study takes the implications of multiple interfering sources into consideration. The simulations comprise a large number of trials and, at each trial, a population of potential interferers is randomly located, at a specified geographic density, within an area of a specified radius. Interference is then aggregated at a victim receiver (positioned at the centre of the simulation area.) considering the significant propagation mechanisms. The simulation results are in the form of a cumulative distribution function, indicating the proportion of the receiver locations that are likely to suffer a particular level of interference from multiple interferers.

In order to take account of the probability of line-of-sight interference path between potential interferers and a victim receiver in a generic urban sharing scenario, the Monte Carlo simulator was combined with a building blockage statistical model defined in ITU-R Rec.1410. The model considers the ratio of land covered by buildings to total land, the density of buildings (buildings/km²) and the distribution of building height in calculating the line-of-sight probability which is determined from the combination of the probabilities that each building lying in the propagation path is below the height of the propagation path joining the transmitter and receiver.

The Monte Carlo simulator combined with the building blockage statistical model was used to calculate the aggregate interference at each trial by applying the free space propagation model to each line-of-sight interfering path.

In the application of the above described model to examine interference between representative systems, the size of the areas over which the trials are implemented was calculated as a function of the antenna heights using a smooth Earth approximation. The transmitter antenna heights were assumed to be uniformly distributed between the two values specified.

The method taking account of the interfering system carrier bandwidth, frequency reuse pattern, multiple access technique and the receiver bandwidth was described to calculate the geographical density of the NGSO FSS Earth station transmitters. An artificial exclusion area of a radius of *50 metres* was introduced around an FS receiver when locating NGSO FSS Earth station transmitters randomly at each Monte Carlo trial to prevent situations where the co-located transmitter and receiver antennas operate simultaneously at the same frequency. Finally, sensitivity analysis was carried out to examine the implications of the use of different interferer density and the transmitter and receiver antenna heights.

The use of the aggregate interference analysis model to examine the feasibility of spectrum sharing for the representative systems suggested that the percentage of locations likely to suffer from NGSO FSS interference increases when the NGSO FSS transmitter density is increased for a given set of blockage model parameters and transmitter/receiver characteristics and the FS receiver and NGSO FSS transmitter antenna heights are increased for a given set of blockage model parameters and a transmitter density.

7.7 Further work

Ever greater demand for bandwidth has led to a growing interest in the use of frequencies above Ka-band. Known variously as V-band, the 37-52 GHz region is now being targeted for future systems operating in both FS and FSS allocations. The FSS systems have been primarily filed in the US are a mixture of GSO and NGSO systems. One of their main characteristics is the high level of frequency re-use they achieve through the use of very small spot beams. This will enable the various systems to offer cost effective broadband services to a relatively large number of

users equipped with transceiver terminals. FS systems to be deployed at these high frequencies are also able to operate with high levels of frequency re-use.

Further study might usefully be directed towards an investigation of the FS and FSS co-existence at V-band frequencies. Perhaps the most important factor needs to be examined is the propagation impairment, in particular atmospheric gas absorption and degradations due to rain. In addition, a study of the implications of system design technologies employed at these frequencies might also be an interesting research activity.

Another potential research area might be the development of measurement procedures to be applied for the identification of NGSO FSS systems causing harmful interference when they are operational. The measurement procedures might comprise computer controlled steerable antennas and spectrum analysers. The repeatability of the interference measurements might probably be the most important parameter. In addition, the capability of measuring level, time duration and frequency of interference together with the transmission characteristics (i.e. modulation and bit rate) might be required in identifying the interfering NGSO FSS system.

REFERENCES

- [1] Struzak R. : 'Spectrum Management', ITU News Journal, pp. 27-31, March 1999
- [2] Withers D.J. : 'Radio Spectrum Management', Peter Peregrinus, 1991
- [3] Matos F. : 'Spectrum Management and Engineering', IEEE Publications, 1985
- [4] 'ITU History', www.itu.org
- [5] Webb, W. : 'Role of Economic Techniques in Spectrum Management', IEEE Communications Magazine, Vol:36, No:3, pp. 102-107, March 1998
- [6] Kobb B.Z. : 'Wireless Spectrum Finder: Telecommunications, Government and Scientific Radio Frequency Allocations in the US from 30 MHz to 300 GHz', McGraw Hill, 2000
- [7] Bazelon D., Moore D. and Beider P. : 'FCC Auctions and the Future of Radio Spectrum Management', Diane Publications, 1997
- [8] Abramovitz, A. : 'Cultivating Spectrum Business', International Telecommunications Journal, Horizon House Publications, Vol:33, No:2, pp. 69-71, February 1999
- [9] ITU Radio Regulations, Articles, 'Terms and Definitions', Geneva 1998
- [10] ITU Radio Regulations, Articles, 'Frequency Allocations', Geneva 1998
- [11] Peha, J.M. : 'Wireless Communications and Coexistence for Smart Environments', IEEE Personal Communications, Vol:7, No:5, pp. 66-68, October 2000
- [12] Lewis, S.A. : 'Radio Frequency Spectrum Management from the Perspective of a Major Network Operator', Proceedings of the 4th IEEE Africon Conference, pp. 322-325, September 1996

- [13] Song X. T. : 'Spectrum Management and Electromagnetic Compatibility for Today's Communication', Proceedings of the IEEE International Symposium on Electromagnetic Compatibility, pp. 421-425, May 1997
- [14] Evans B.G. : 'Satellite Communication Systems', Peter Peregrinus, 1991
- [15] Maral G. and Bousquet M. : 'Satellite Communications Systems', John Wiley, 1993
- [16] Boucheret M., Mortensen I. and Favaro H. : 'Fast Convolution Filter Banks for Satellite Payloads with On-Board Processing', IEEE Journal on Selected Areas in Communications, Vol:17, No:2, pp. 238-249, February 1999
- [17] 'Summary Characteristics of Eutelsat Atlantic Bird, Sesat, Hot Bird and W Satellites', www.eutelsat.com
- [18] 'Summary Characteristics of Astra 1A, 1B, 1C, 1D, 1E, 1F, 1G, 1H, 1K, 2A, 2B Satellites', www.ses-astra.com
- [19] 'Summary Characteristics of Intelsat 511, 601, 602, 603, 604, 605, 701, 702, 704, 705, 706, 707, 709, 801, 802, 804, 805, 901, 902, 903, 904, 905, 906, 907, 10-01, 10-02 Satellites', www.intelsat.com
- [20] 'Summary Characteristics of Panamsat PAS-1R, PAS-2, PAS-3, PAS-4, PAS-5, PAS-6, PAS-6B, PAS-7, PAS-8, PAS-9, PAS-10, Galaxy IIR, Galaxy IIIC, Galaxy IVR, Galaxy XR, Galaxy XI, SBS-6 Satellites', www.panamsat.com
- [21] 'Astrolink-Phase II Satellite Communication System', FCC Filing, December 1997
- [22] Aghvami A.H. and Robertson I.D. : 'Power Limitation and High-Power Amplifier Nonlinearities in On-board Satellite Communications Systems', IEE Electronics and Communication Engineering Journal, pp. 65-70, April 1993
- [23] Phillips, K.P. : 'An overview of Propagation Factors Influencing the Design of Mobile Satellite Communication Systems', IEE Electronics and Communication Engineering Journal, Vol:9, No:6, pp. 281-288, December 1997

- [24] Martin J. : 'Communications Satellite Systems', Prentice Hall, 1978
- [25] Azaran D., Courtney W. and Freitag J. : 'The Multimedia Migration: Transponder vs. Processing Payload VSAT Networks', Proceedings of the IEE Colloquium on Broadband Satellite: The Critical Success Factors, Technology, Services and Markets, pp. 22/1-22/10, October 2000
- [26] Bate R.R., Mueller D.D. and White J.E. : 'Fundamentals of Astrodynamics', Dover Publications, 1971
- [27] Jansky D.M. and Jeruchim M.C. : 'Communication Satellites in the Geostationary Orbit', Artech House, 1987
- [28] ITU-R Recommendation S.743, 'The Coordination Between Satellite Networks Using Slightly Inclined Geostationary Satellite Orbits and Between Such Networks and Satellite Networks Using Non-inclined Geostationary Satellites', 1994
- [29] Rose J.L. : 'Broadband Satellites: Solutions Looking for Problems', Proceedings of the IEE Colloquium on Broadband Satellite: The Critical Success Factors, Technology, Services and Markets, pp. 2/1-2/5, October 2000
- [30] Colcy J.N. and Fenech H. : 'Eutelsat Advanced Multimedia Satellite and New Wideband Demand Assigned Multiple Access Service', Proceedings of the IEE Colloquium on Broadband Satellite: The Critical Success Factors, Technology, Services and Markets, pp. 14/1-14/6, October 2000
- [31] Gerakoulis D., Chan W. and Geraniotis E. : 'Throughput Evaluation of a Satellite Switched CDMA Demand Assignment System', IEEE Journal on Selected Areas in Communications, Vol:17, No:2, pp. 286-303, February 1999
- [32] Koraitim H. and Tohme S. : 'Resource Allocation and Connection Admission Control in Satellite Networks', IEEE Journal on Selected Areas in Communications, Vol:17, No:2, pp. 345-360, February 1999
- [33] Williamson M. : 'Settling New Territory', Satellite Today Journal, Philips Business Information Publications, pp. 16-21, March 1999

- [34] Gargione F., Brandon W.T. : 'Ka-band Update', Satellite Communications Journal, Intertec/Primedia Publications, pp. 48-53, March 1999
- [35] Acosta R., Bauer R., Krawczyk J, and Reinhart C. : 'Advanced Communications Technology Satellite (ACTS)', IEEE Journal on Selected Areas in Communications, Vol:17, No:2, pp. 193-203, February 1999
- [36] 'Spaceway EXP Satellite Communication System', www.hns.com/spaceway
- [37] Sarraf J. : 'The Spaceway System', Proceedings of the IEE Colloquium on Broadband Satellite: The Critical Success Factors, Technology, Services and Markets, pp. 15/1-15/6, October 2000
- [38] Evans J.V. : 'Ka-band Network Design Considerations', Satellite Communications Journal, Intertec/Primedia Publications, pp. 44-50, November 1999
- [39] Evans J.V. : 'U.S. Filings for Multimedia Satellites: A Review', International Journal of Satellite Communications, John Wiley & Sons Ltd, Vol:18, No:3, pp. 121-160, May 2000
- [40] Bulloch C. : 'For High Flying Satellite Systems', International Telecommunications Journal, Horizon House Publications, Vol:33, No:6, pp. 27-31, June 1999
- [41] 'KaStar Satellite Communication System', www.wildblue.com
- [42] 'Euroskyway Satellite Communication System', www.alespazio.it
- [43] Williamson M. : 'Can Satellites Unblock the Internet?', IEE Review, pp. 107-111, May 1999
- [44] 'Wideband European Satellite Telecommunications (WEST) Satellite System', www.matra-marconi-space.com
- [45] Vasseur H. : 'Degradation of Availability Performance in Dual-polarised Satellite Communications Systems', IEEE Transactions on Communications, Vol:48, No:3, pp.464-472, March 2000

- [46] Weil C. and Jakoby R. : 'Availability and Bit Error Performance of Dual Polarised Digital PSK-Satellite Systems in Ka-band', *Electronics Letters*, Vol:35, No:16, pp. 1302-1303, December 2000
- [47] Lothian J. and Ashford E. : 'Critical Success Factors for the Introduction of Broadband Multimedia in Europe', *Proceedings of the IEE Colloquium on Broadband Satellite: The Critical Success Factors, Technology, Services and Markets*, pp. 20/1-20/8, October 2000
- [48] King G. : 'Where does Broadband Fit in the Market Place', *Proceedings of the IEE Colloquium on Broadband Satellite: The Critical Success Factors, Technology, Services and Markets*, pp. 5/1-5/5, October 2000
- [49] Abramson N. : 'Internet Access Using VSATs', *IEEE Communications Magazine*, Vol:38, No:7, pp.60-68, July 2000
- [50] Losquado G. and Marziale V. : 'The Euroskyway Network with On Board Processing to Support Fast Internet and Interactive TV Services for Residential Users', *Proceedings of the IEE Colloquium on Broadband Satellite: The Critical Success Factors, Technology, Services and Markets*, pp. 8/1-8/7, October 2000
- [51] Cruickshank H., Iyengar S. and Sun Z. : 'Securing IP Multicast over GEO Satellites', *Proceedings of the IEE Colloquium on Broadband Satellite: The Critical Success Factors, Technology, Services and Markets*, pp. 10/1-10/5, October 2000
- [52] Evans A.L., Rose J. and Venkataraman R. : 'The future of Satellite Communications', *Communicate Journal*, Dmg World Media Publications, pp. 34-37, May 1999
- [53] 'Skybridge Satellite Communication System', FCC Filing, February 1997
- [54] 'Teledesic Satellite Communication System', FCC Filing, March 1994
- [55] '@Contact Satellite Communication System', FCC Filing, December 1997
- [56] 'Spaceway NGSO Satellite Communication System', FCC Filing, December 1997

- [57] 'Technical Characteristics of the Rostelesat Satellite System in the Bands 11/13 GHz and 20/30 GHz', ITU-R Document 4-9-11/TEMP/61, January 1999
- [58] ITU-R Recommendation S.1328, 'Satellite System Characteristics to be Considered in Frequency Sharing Analyses Between Geostationary-Satellite Orbit (GSO) and Non-GSO Satellite Systems in the Fixed-Satellite Service (FSS) including Feeder Links for the Mobile-Satellite Service (MSS)', 2000
- [59] Kiernan V. : 'Clash of the Titan Technologies', Satellite Communications Journal, Intertec/Primedia Publications, pp. 26-28, April 1999
- [60] Gavish B. and Kalvenes J. : 'The Impact of Satellite Altitude on the Performance of LEO Satellite Based Communications Systems', Wireless Networks Journal, Baltzer Science Publishers, Vol:4, No:2, pp. 199-213, February 1998
- [61] Chang Y. and Geraniotis E. : 'Optimal Policies for Handoff and Channel Assignment in Networks of LEO Satellites Using CDMA', Wireless Networks Journal, Baltzer Science Publishers, Vol:4, No:2, pp. 181-187, February 1998
- [62] Uzunalioglu H., Akyildiz F. and Bender M. : 'A routing algorithm for Connection Oriented LEO Satellite Networks With Dynamic Connectivity', Wireless Networks Journal, Baltzer Science Publishers, Vol:4, No:2, pp. 214-225, February 1998
- [63] Ephremides A. and Vatalaro F. : 'Hybrid Satellite Communication Networks', Wireless Networks Journal, Baltzer Science Publishers, Vol:4, No:2, pp. 99-100, February 1998
- [64] Ephremides A., Vatalaro F. and Gargione F. : 'Direct-to-user Satellite Systems and Technologies at Ka-band and Beyond', IEEE Journal on Selected Areas in Communications, Vol:17, No:2, pp. 129-133, February 1999
- [65] Lida T., Valdoni F. and Vatalaro F. : 'Services, Technologies and Systems at Ka-band and Beyond', IEEE Journal on Selected Areas in Communications, Vol:17, No:2, pp. 134-145, February 1999

- [66] Golding L. : 'Satellite Communications Systems Move into the Twenty-first Century', Wireless Networks Journal, Baltzer Science Publishers, Vol:4, No:2, pp. 101-107, February 1998
- [67] ITU Radio Regulations, Articles, 'Space Services (Article S.22)', Geneva 1998
- [68] McGann J. : 'Caring and Sharing', International Telecommunications Journal, Horizon House Publications, Vol:33, No:12, pp. 58-62, December 1999
- [69] Krauss J. : 'NGSO Satellites – Creating New Spectrum Capacity', Communications and Engineering Design Magazine, Cahners Business Information Publications, pp. 25-27, March 1999
- [70] ITU Digital Radio Relay Systems Handbook, Geneva 1996
- [71] 'UK Radio Interface Requirement 2000 Point-to-Point Radio Relay Systems Operating in Fixed Service Frequency Bands Administered by the Radiocommunications Agency', The UK Radiocommunications Agency Fixed Terrestrial and Satellite Links Unit, Technical Regulations, www.radio.gov.uk
- [72] 'Frequency Assignment Criteria', The UK Radiocommunications Agency Fixed Terrestrial and Satellite Links Unit, www.radio.gov.uk
- [73] ITU Wireless Access Local Loop Handbook, Geneva 1996
- [74] 'Fixed Radio Systems; Point-to-Point Antennas; Antennas for Point-to-Point Fixed Radio Systems Operating in the Frequency Bands 3 GHz to 60 GHz', ETS 300 833, June 1999
- [75] ITU-R Recommendation F.699, 'Reference Radiation Patterns For Line-Of-Sight Radio Relay System Antennas for use in Coordination Studies and Interference Assessment in the frequency Range From 1 GHz to about 70 GHz', 2000
- [76] ITU-R Recommendation F.1245, 'Mathematical Model of Average and Related Radiation Patterns for Line-of-sight Point-to-point Radio Relay System Antennas for use in Certain Coordination Studies and Interference Assessment in the Frequency Range from 1 GHz to about 70 GHz', 2000

- [77] 'Transmission and Multiplexing; Digital Radio Relay Systems; Plesiochronous Digital Hierarchy; Low and Medium Capacity Digital Radio Relay Systems Operating in the 13, 15 and 18 GHz Frequency Bands ', EN 301 128, October 1996
- [78] 'Transmission and Multiplexing; Sub-STM1 Digital Radio Relay Systems Operating in the 13, 15 and 18 GHz Frequency Bands with about 28 MHz Co-polar and 14 MHz Cross-polar Channel Spacing ', ETS 300 639, October 1996
- [79] 'Fixed Radio Systems; Point-to-Point Equipment; Parameters for Radio System for the Transmission of Digital Signals Operating in the Frequency Range 24.5 GHz to 29.5 GHz', EN 300 431, October 1999
- [80] 'AIReach Broadband Fixed Wireless Access System', Hughes Network Systems, www.hns.com
- [81] 'Reunion Broadband Fixed Wireless Access System', Nortel Networks, www.nortelnetworks.com
- [82] 'Mini Link Broadband Fixed Wireless Access System', Ericsson, www.ericsson.com
- [83] 'Radiant Broadband Fixed Wireless Access System', Radiant Networks, www.radiantnetworks.co.uk
- [84] 'Point-to-multipoint Digital Radio Relay Systems in Frequency Bands in the Range 24.25 GHz to 29.5 GHz Using Different Access Methods', EN 301 213, July 1998
- [85] 'Antennas for Use in Point-to-Multipoint Digital Radio Relay Systems in the 11 GHz to 60 GHz Band', EN 301 215, July 1998
- [86] ITU-R Recommendation P.676-4, 'Attenuation by Atmospheric Gases', 1999
- [87] ITU-R Recommendation P.530-8, 'Propagation Data and Prediction Methods Required for the Design of Terrestrial Line-of-Sight Systems', 1999

- [88] ITU-R Recommendation P.452-9, 'Prediction Procedure for the Evaluation of Microwave Interference Between Stations on the Surface of the Earth at Frequencies above about 0.7 GHz ', 1999
- [89] ITU-R Recommendation P.618-6, 'Propagation Data and Prediction Methods Required for the Design of Earth-Space Telecommunication Systems', 1999
- [90] ITU-R Recommendation P.619-1, 'Propagation Data Required for the Evaluation of Interference Between Stations in Space and Those on the Surface of the Earth', 1992
- [91] Hall, M.P.M., Barclay, L.W., and Hewitt, M.T.: 'Propagation of Radiowaves', The Institution of Electrical Engineers, 1996
- [92] ITU-R Recommendation F.1395-1, 'Minimum Propagation Attenuation due to Atmospheric Gases for Use in Frequency Sharing Studies Between the Fixed Satellite Service and the Fixed Service', 1999
- [93] ITU-R Recommendation P.835-3, 'Reference Standard Atmospheres', 1999
- [94] ITU Radio Regulations, Articles, 'Terrestrial and Space Services Sharing Frequency Bands Above 1 GHz (Article S.21)', Geneva 1998
- [95] Doble J. : 'Introduction to Radio Propagation for Fixed and Mobile Communications', Artech House, 1996
- [96] Crane, R.K. : 'Electromagnetic Wave Propagation Through Rain', John Wiley & Sons, 1996
- [97] ITU-R Recommendation P.837-2, 'Characteristics of Precipitation for Propagation Modelling', 1999
- [98] ITU-R Recommendation P.838-1, 'Specific Attenuation Model For Rain for Use in Prediction Methods', 1999
- [99] Ballabio E. : 'Influence of the Atmosphere on Interference Between Radio Communications Systems at Frequencies Above 1 GHz', COST 210 Final Report, Commission of the European Communities, 1991

- [100] ITU-R Recommendation P.526-6, 'Propagation by Diffraction', 1999
- [101] 'The COST 210 Hydrometeor Scatter Prediction Procedure', www.itu.org
- [102] ITU-R Recommendation F.758-2, 'Considerations in the Development of Criteria for Sharing Between the Terrestrial Fixed Service and Other Services', 1999
- [103] Allnut, J.E. : 'Satellite-to-Ground Radiowave Propagation', The Institution of Electrical Engineers, 1989
- [104] Feldhake G. : 'Estimating the Attenuation due to Combined Atmospheric Effects on Modern Earth-space Paths', IEEE Antennas and Propagation, Vol:39, No: 4, pp. 26-34, August 1997
- [105] Dissanayake A., Allnutt J. and Haidara F. : 'Prediction Model that Combines Rain Attenuation and Other Propagation Impairments Along Earth-space Paths', IEEE Transactions on Antennas and Propagation, Vol: 45, No:10, pp. 1546-1558, October 1997
- [106] Crane R., and Rogers D. : 'Review of the Advanced Communications Technology Satellite Propagation Campaign in North America', IEEE Antennas and Propagation, Vol:40, No:6, pp. 23-27, December 1998
- [107] Arbesser R., Bertram R. and Paraboni A. : 'European Research on Ka-band Slant Path Propagation', Proceedings of the IEEE, Vol: 85, No:6, pp. 843-852, June 1997
- [108] Pinder J., Ippolito L., Horan S. and Feil J. : 'Four Years of Experimental Results from the New Mexico Advanced Communications Technology Satellite Propagation Terminal at 20.185 and 27.505 GHz', IEEE Journal on Selected Areas in Communications, Vol:17, No:2, pp. 153-163, February 1999
- [109] ITU-R Recommendation S.1323-1, 'Maximum Permissible Levels of Interference in a Satellite Network (GSO/FSS, NGSO FSS, NGSO/MSS Feeder Links) for a Hypothetical Reference Digital Path in the Fixed Satellite Service Caused by Other Codirectional Networks Below 30GHz', 2000

- [110] ITU Radio Regulations, Resolutions and Recommendations, 'Use of Nongeostationary Systems in the Fixed satellite Service in Certain Frequency Bands (Resolution 130)', Geneva 1998
- [111] 'Suitability of the Concept of "Aggregate pfd" (apfd) as Defined in Article S.22 for the Bands 27.5-28.6 GHz and 29.5-30.0 GHz', ITU JTG 4-9-11, Document 141, June 1998
- [112] 'Introduction of GSO Satellite Antenna Characteristics in the Definition of apfd in the 12.75-13.25 GHz and 14.0-14.5 GHz Bands', ITU JTG 4-9-11, Document 120, June 1998
- [113] 'Impact of Inclusion of Satellite Receive Antenna Pattern in apfd Definition of Article S.22 for the 30 GHz Bands', ITU JTG 4-9-11, Document 294, January 1999
- [114] 'Review of the apfd Definition', ITU JTG 4-9-11, Document 257, January 1999
- [115] Report of the Fourth Meeting of ITU-R JTG 4-9-11, June 1999
- [116] Modifications to ITU Radio Regulations Articles, 'Space Services (Article S22)', Istanbul 2000
- [117] Report of the Meeting of ITU-R WP-4A, May 1999
- [118] 'Methods for NGSO FSS Systems to Enhance Sharing with GSO FSS Systems in the Frequency Bands Between 10 and 30 GHz', ITU WP-4A, Document 327, April 1999
- [119] 'Reference Angles Used in the GSO Arc Avoidance Technique ', ITU WP-4A, Document 251, April 1999
- [120] 'Satellite Based Reference for NGSO Sharing', ITU WP-4A, Document 370, April 1999
- [121] 'Continuous Curves for Article S.22 epfd Limits', ITU JTG 4-9-11, Document 313, January 1999

- [122] 'Methodology to Describe Continuous Curves of Long-term epfd Limits as a Function of Antenna Size', ITU WP-4A, Document 254, April 1999
- [123] 'Proposed Revision to Resolution 130 Provisional epfd and apfd Limits in the 14/11 GHz Bands', ITU JTG 4-9-11, Document 342, January 1999
- [124] 'Study to Evaluate Sharing Between NGSO and GSO FSS Systems in the 10-14 GHz Bands and to Demonstrate the Effectiveness of Simulation in Verifying Sharing Feasibility', ITU WP-4A, Document 27, February 1998
- [125] 'Simulation Results on the epfd Calculation for NGSO FSS System Operating in the 12 GHz Frequency Range', ITU JTG 4-9-11, Document 28, February 1998
- [126] 'Results of the Application of the Proposed Methodology A' of Rec.1323 in Determining epfd Limits for NGSO FSS Transmissions Interfering with Intelsat Typical Carriers ', ITU JTG 4-9-11, Document 73, June 1998
- [127] 'Information on Canada's Ku Band GSO FSS Links and Calculation of epfd Levels due to Interference from NGSO FSS Networks, ITU JTG 4-9-11, Document 138, June 1998
- [128] 'Use of Procedure D of Rec.1323 to Evaluate the Impact of epfd Limits on GSO FSS Carriers', ITU JTG 4-9-11, Document 154, June 1998
- [129] 'An Investigation into the Behaviour of Methodology A' for Assessing Permitted Levels of Interference Between GSO FSS and NGSO FSS Systems', ITU JTG 4-9-11, Document 177, June 1998
- [130] 'Applicability of Methodology A' in the Establishment of epfd Limits', ITU JTG 4-9-11, Document 305, January 1999
- [131] 'Simulation of Equivalent Power Flux Densities from NGSO Systems Using Exclusion Zone Mitigation Technique', ITU JTG 4-9-11, Document 282, January 1999
- [132] 'Simulation Analysis of the Short Term Interference Effects from NGSO FSS Satellites into GSO Earth Stations', ITU JTG 4-9-11, Document 359, January 1999

- [133] ITU-R Recommendation S.580-5, 'Radiation Diagrams for Use as Design Objectives for Antennas of Earth Stations Operating with Geostationary Satellites', 1994
- [134] ITU-R Recommendation S.465-5, 'Reference Earth Station Radiation Pattern for Use in Coordination and Interference Assessment in the Frequency Range from 2 to about 30 GHz', 1993
- [135] 'Reference GSO FSS Earth Station Radiation Patterns for Use in Interference Assessment Involving NGSO Satellites in Frequency Bands below 30 GHz', ITU WP-4A, Liaison Statement Document 214, October 1998
- [136] 'Use of Bessel Functions for the Representation of Earth Station Reference Antenna Patterns', ITU JTG 4-9-11, Document 320, January 1999
- [137] 'Reference GSO Receiving Earth Station Radiation Patterns for Use in Interference Assessment from NGSO Satellites', ITU JTG 4-9-11, Document 351, January 1999
- [138] 'Measured Direct to Home Antenna Diagrams for Evaluation of NGSO Interference into GSO Networks', ITU JTG 4-9-11, Document 360, January 1999
- [139] 'Analysis of Sample Earth Station Radiation Patterns of Small Receive only Antennas in the Context of Suitable Reference Patterns for Use in Cases of Interference from NGSO Satellites', ITU JTG 4-9-11, Document 362, January 1999
- [140] ITU-R Recommendation S.1428-1, 'Reference FSS Earth Station Radiation Patterns for Use in Interference Assessment Involving NGSO Satellite in Frequency Bands Between 10.7 GHz and 30 GHz', 2000
- [141] 'Study of the Sharing of the Same Frequency Band by Several NGSO FSS Systems', ITU WP-4A, Document 122, September 1998
- [142] 'Simulation Results Giving the Minimum Required Separation Angle Between NGSO Satellites to Enable Co-directional Co-frequency Sharing Between NGSO FSS Systems Operating in the 18.8-19.3 GHz and 28.6-29.1 GHz Bands', ITU WP-4A, Document 132, September 1998

- [143] 'Impact of the Need to Avoid Main Beam to Main Beam Interference Between NGSO FSS Systems', ITU WP-4A, Document 145, September 1998
- [144] 'Interference Between Multiple NGSO FSS Systems Operating in the 10-14 GHz Frequency band', ITU JTG 4-9-11, Document 278, January 1999
- [145] 'Simulation Results on Sharing Between Multiple Inhomogeneous NGSO FSS Systems in the 19.7-20.2/29.5-30.0 GHz Bands ', ITU JTG 4-9-11, Document 279, January 1999
- [146] 'Assessing the Potential Benefits of Having Two NGSO FSS Systems Simultaneously Implementing In-line Avoidance ', ITU JTG 4-9-11, Document 288, January 1999
- [147] 'Downlink Interference Between NGSO FSS Systems Operating in the 19.7-20.2 GHz Band ', ITU JTG 4-9-11, Document 310, January 1999
- [148] ITU Radio Regulations, Articles, 'Procedure for Effecting Coordination with or Obtaining Agreement of Other Administrations (Article S9.12)', Geneva 1998
- [149] ITU-R Recommendation S.1431-1, 'Methods to Enhance Sharing Between NGSO FSS Systems in the Frequency Bands Between 10-30 GHz', 2000
- [150] 'Derivation of Alternative *epfd* Limits in the 10-12 GHz Band', ITU JTG 4-9-11, Document 255, January 1999
- [151] 'Impact of Multiple NGSO Systems on a GSO System', ITU JTG 4-9-11, Document TEMP/59, January 1999
- [152] 'Aggregation of Interference from Multiple NGSO FSS Systems into GSO FSS Systems in the FSS Bands Between 10 and 30 GHz', ITU JTG 4-9-11, Document 286, January 1999
- [153] 'Aggregation of Interference from Multiple NGSO FSS Systems into GSO FSS Systems Operating in the 10.7 and 12.75 GHz Band', ITU WP-4A, Document 362, April 1999

- [154] 'Derivation of Number of NGSO FSS Networks to be Used in Sharing Studies', ITU WP-4A, Document 217, February 1999
- [155] 'Determination of the Number of NGSO Systems to be used in Derivation of Single Entry and Aggregate epfd Masks', ITU WP-4A, Document TEMP/187, April 1999
- [156] 'Methodology Used in the Derivation of Single Entry epfd Limits from an Aggregate', ITU WP-4A, Document TEMP/176, April 1999
- [157] Report of the Third Meeting of ITU-R JTG 4-9-11, January 1999
- [158] 'System Characteristics of a GSO FSS Network with large Earth Station Antennas and epfd Limits', ITU WP-4A, Document 161, September 1998
- [159] 'Operating Parameters, Link Budgets and Protection Criteria for a GSO FSS Network with Large Earth Station Antennas', ITU JTG 4-9-11, Document 281, January 1999
- [160] 'Protection Criteria for GSO Network with Large Earth Station Antennas in the band 12.5-12.75 GHz', ITU WP-4A, Document 261, April 1999
- [161] 'A Comparison of Required and Provisional epfd Limits for a Ku-band GSO FSS Network with Large Earth Station Antennas', ITU JTG 4-9-11, Document 324, January 1999
- [162] 'Protection of Very Large Antennas', ITU WP-4A, Document TEMP/137, April 1999
- [163] WRC-2000 Provisional Final Acts, Articles, 'Procedure for Effecting Coordination with or Obtaining Agreement of Other Administrations (Article S9.7A and S9.7B)', Istanbul 2000
- [164] 'Thresholds for Coordination of Frequency Assignments Between Systems in NGSO Orbit and Networks in GSO Orbit with Very Large Earth Station Antennas in the Fixed Satellite Service in the Frequency Bands 10.7-12.75 GHz, 17.8-18.6 GHz and 19.7-20.2 GHz', ITU WP-4A, Document 486, January 2000

- [165] 'epfd Coordination Thresholds for the Protection of GSO Earth Stations with very large Antennas Against Interference From NGSO FSS Systems', ITU WP-4A, Document 518, February 2000
- [166] 'Synchronisation Loss', ITU JTG 4-9-11, Document TEMP/50, January 1999
- [167] 'Measurement Results on the Synchronisation Losses Caused by Short Term Interference into GSO Earth Station Demodulators', ITU JTG 4-9-11, Document 248, January 1999
- [168] 'Results of Further Measurements of Worst Case NGSO Interference Peaks on Demodulators Used for High Data Rate Carriers in Typical Large Dish GSO Earth Station Receivers', ITU JTG 4-9-11, Document 315, January 1999
- [169] 'Analysis by Simulation and Measurement of the Short term Interference Effects from NGSO Satellites into GSO Earth Stations', ITU JTG 4-9-11, Document 359, January 1999
- [170] 'Analysis of the Impact of the epfd Limits on the Potential for Synchronisation Losses in FSS Transmissions in the 11-12/13-14 GHz Bands' ITU WP-4A, Document 276, April 1999
- [171] 'Impact of Loss of Synchronisation on GSO Transmissions', ITU WP-4A, Document 371, April 1999
- [172] 'Assumed Level of Synchronisation Loss for the Development of $\text{epfd}_{\text{down}}$ Limits', ITU WP-4A, Document TEMP/181, April 1999
- [173] ITU-R Recommendation IS.847-1, 'Determination of the Coordination Area of an Earth Station Operating with a Geostationary Space Station and Using the Same Frequency Band as a System in a Terrestrial Service', 1993
- [174] ITU-R Recommendation S.672-4, 'Satellite Antenna Radiation Pattern for Use as a Design Objective in the Fixed Satellite Service Employing Geostationary Satellites', 1997

- [175] ITU Radio Regulations, Appendices, 'Radiation Patterns for Earth Station Antennae to be Used When They are not Published (Appendix 28/29)', Geneva 1994
- [176] 'Study to Evaluate Sharing Between NGSO and GSO FSS Systems in the 10-14 GHz Bands, and to Demonstrate the Effectiveness of Simulation in Verifying Sharing Feasibility ', ITU WP-4A, Document 27, February 1998
- [177] 'NGSO Interference into GSO Earth Stations in the Ku Band Fixed Satellite Service', ITU JTG 4-9-11, Document 134, June 1998
- [178] 'Minimum Achievable epfd for Some NGSO Systems During In-line Events', ITU JTG 4-9-11, Document 339, January 1999
- [179] 'A Preliminary Analysis on GSO Interference Mitigation Technique for NGSO Satellites ', ITU JTG 4-9-11, Document 150, June 1998
- [180] 'Development of epfd Limits for NGSO Systems Operating in the 10.7-12.75 GHz Band', ITU WP-4A, Document 280, April 1999
- [181] 'Recommended Antenna Patterns for NGSO Satellite Multiple Beam Antennas Operating in the Fixed Satellite Service Below 30 GHz', ITU WP-4A, Document TEMP/138, April 1999
- [182] ITU Radio Regulations, Resolutions and Recommendations, 'Use of the Bands 18.8-19.3 GHz and 28.6-29.1 GHz by Nongeostationary Fixed Satellite Service Systems (Resolution 118)', Geneva 1996
- [183] ITU Radio Regulations, Resolutions and Recommendations, 'Power Flux Density Limits Applicable to Nongeostationary Fixed satellite Service Systems for Protection of Terrestrial Services in the Bands 10.7-12.75 GHz and 17.7-19.3 GHz (Resolution 131)', Geneva 1998
- [184] ITU-T Recommendation G.821, 'Error Performance of an International Digital Connection Forming Part of an Integrated Services Digital Network', 1996

- [185] ITU-R Recommendation F.557, 'Availability Objective for Radio Relay Systems Over a Hypothetical Reference Circuit and a Hypothetical Reference Digital Path', 1997
- [186] ITU-R Recommendation F.594, 'Error Performance Objectives of the Hypothetical Reference Digital Path for Radio Relay Systems Providing Connections at a Bit Rate Below the Primary Rate and Forming Part or All of the High Grade Portion of an Integrated Services Digital Network', 1997
- [187] ITU-R Recommendation F.1092, 'Error Performance Objectives for Constant Bit Rate Digital Path at or Above the Primary Rate Carried by Digital Radio Relay Systems which may Form Part of the International Portion of a 27 500 km Hypothetical Reference Path', 1997
- [188] ITU-R Recommendation F.1189, 'Error Performance Objectives for Constant Bit Rate Digital Paths at or Above the Primary Rate Carried by Digital Radio Relay Systems which may Form Part or All of the National Portion of a 27 500 km Hypothetical Reference Path', 1997
- [189] ITU-T Recommendation G.826, 'Error Performance Parameters and Objectives for International, Constant Bit Rate Digital Paths at or Above the Primary Rate', 1999
- [190] ITU-T Recommendation G.212, 'Hypothetical Reference Circuits for Analogue Systems', 1984
- [191] ITU-R Recommendation F.391, 'Hypothetical Reference Circuit for Radio Relay Systems for Telephony Using Frequency Division Multiplex with a Capacity of 12 to 60 Telephone Channels', 1963
- [192] ITU-R Recommendation F.392, 'Hypothetical Reference Circuit for Radio Relay Systems for Telephony Using Frequency Division Multiplex with a Capacity of more than 60 Telephone Channels', 1963
- [193] ITU-R Recommendation S.352, 'Hypothetical Reference Circuit for Systems Using Analogue Transmission in the Fixed Satellite Service', 1982

- [194] ITU-R Recommendation F.396, 'Hypothetical Reference Circuit for Transhorizon Radio Relay Systems for Telephony Using Frequency Division Multiplex', 1966
- [195] ITU-R Recommendation F.697, 'Error Performance and Availability Objectives for the Local Grade Portion at Each End of an Integrated Services Digital Network Connection at a Bit Rate Below the Primary Rate Utilising Digital Radio Relay Systems', 1997
- [196] ITU-R Recommendation F.593, 'Noise in Real Circuits of Multi Channel Transhorizon FM Radio Relay Systems of Less than 2500 km', 1982
- [197] ITU-R Recommendation SF.357, 'Maximum Allowable Values of Interference in a Telephone Channel of an Analogue Angle Modulated Radio Relay System Sharing the Same Frequency Bands as Systems in the Fixed Satellite Service', 1997
- [198] ITU-R Recommendation SF.615, 'Maximum Allowable Values of Interference From the Fixed Satellite Service into Terrestrial Radio Relay Systems which may Form Part of an ISDN and Share the Same Frequency Band Below 15 GHz', 1997
- [199] ITU-R Recommendation F.1241, 'Performance Degradation due to Interference from Other Services Sharing the Same Frequency Bands on a Primary Basis with Digital Radio Relay Systems Operating at or Above the Primary Rate and which may Form Part of the International Portion of a 27 500 km Hypothetical Reference Path', 1997
- [200] ITU-R Recommendation F.1398, 'Performance Degradation due to Interference from Other Services Sharing the Same Frequency Bands on a Primary Basis with Digital Radio Relay Systems Operating at or Above the Primary Rate and which may Form Part of the National Portion of a 27 500 km Hypothetical Reference Path', 1999

- [201] ITU-R Recommendation IS.849, 'Determination of the Coordination Area for Earth Stations Operating with Nongeostationary Spacecraft in Bands Shared with Terrestrial Services', 1993
- [202] ITU-R Recommendation P.620, 'Propagation Data Required for the Evaluation of Coordination Distances in the Frequency Range 100 MHz to 105 GHz', 1999
- [203] ITU-R Recommendation F.1494, 'Interference Criteria to Protect the Fixed Service from Time Varying Aggregate Interference from Other Services Sharing the 10.7-12.75 GHz Band on a Co-primary Basis', 2000
- [204] ITU-R Recommendation F.1495, 'Interference Criteria to Protect the Fixed Service from Time Varying Aggregate Interference from Other Services Sharing the 17.7-19.3 GHz Band on a Co-primary Basis', 2000
- [205] ITU-R Recommendation F.1108, 'Determination of the Criteria to Protect Fixed Service Receivers from the Emissions of Space Stations Operating in Nongeostationary Orbits in Shared Frequency Bands', 1997
- [206] 'Sharing Between the FS and NGSO FSS Downlinks in the Bands 10.7-11.7 GHz and 17.7-19.3 GHz ', ITU WP 4-9S, Document 18, February 1998
- [207] 'Sharing Between NGSO FSS Satellites and FS in the 10-12 GHz Frequency Range', ITU WP 4-9S, Document 19, February 1998
- [208] 'Typical Characteristics and Short Term Interference Criteria for UK FS Stations in the 17.7-19.7 GHz Band', ITU WP 9A, Document 43, September 1998
- [209] 'Downlink PFD Limits for NGSO Fixed Satellite Service Systems in the 18.9-19.3 GHz Band', ITU WP 4-9S, Document 43, December 1996
- [210] 'Evaluation of PFD Levels Required to Protect Fixed Service Receivers from Interference from satellites of NGSO FSS Networks Operating in the 18.8-19.3 GHz Band', ITU WP 4-9S, Document 57, September 1998
- [211] 'Simulation of FS Systems Subject to Interference from NGSO FSS Systems', ITU WP 4-9S, Document 68, September 1998

- [212] 'Consideration of Sensitive FS Links in the Establishment of FS Protection Criteria in the 18.8-19.3 GHz band', ITU WP 4-9S, Document 113, April 1999
- [213] 'An Analysis of the Interference into FS Receivers from NGSO FSS Satellites Operating in the 18.8-19.3 GHz band', ITU WP 4-9S, Document 140, April 1999
- [214] 'Evaluation of Power Flux Density Limits Required to Protect the Fixed Service Operating in the 17.7-19.3 GHz Band from NGSO FSS Interference with Different Constellation Sizes', ITU WP 4-9S, Document 160, April 1999
- [215] ITU-R Recommendation S.1257, 'Analytical Method to Calculate Short-term Visibility and Interference Statistics for Nongeostationary Satellite Orbit Satellites as Seen from a Point on the Earth's Surface', 2000
- [216] ITU-R Recommendation F.1190, 'Protection Criteria for Digital Radio Relay Systems to Ensure Compatibility with Radar Systems in the Radiodetermination Service', 1995
- [217] 'Frequency Coordination Between NGSO FSS Earth Stations and Fixed Service Stations', ITU WP 4-9S, Document 9, March 1996
- [218] 'Coordination Area for Earth Stations Operating with NGSO Space Stations in the Fixed Satellite Service in Bands Shared With the Terrestrial Services', ITU WP 4-9S, Document 71, September 1998
- [219] 'Methodologies for Determination of the Coordination Area for Earth Stations Operating to NGSO FSS Space Stations', ITU WP 4-9S, Document 156, April 1999
- [220] 'An Analysis of Potential Techniques Proposed to Facilitate Sharing Between FS Transmitters and NGSO FSS User Terminals Operating in the 18.8-19.3 GHz Band ', ITU WP 4-9S, Document 147, April 1999
- [221] 'Analysis of Site Shielding as a Possible Mitigation Technique to Facilitate FSS and FS Coexistence in the 18.8-19.3 GHz Band', ITU WP 4-9S, Document 166, April 1999
- [222] 'Current Status of Sharing Studies Between FSS User Terminals and FS Stations in the 17.7-19.7 GHz Band', ITU WP 4-9S, Document 45, October 2000

- [223] 'Use of the Band 28.6-29.1 GHz by the FS and NGSO FSS in the Earth-to-space Direction', ITU WP 4-9S, Document 139, April 1999
- [224] 'Identification of High Density Fixed Satellite Service Bands Above 17.3 GHz', ITU WP 4-9S, Document 24, September 2000
- [225] 'Current Status of Working Party 4-9S Sharing Studies Between FSS User Terminals and FS Stations in the Bands 17.7-19.7 GHz and 27.5-29.5 GHz and European Regulatory Framework for the Shared Use of Both Bands', ITU WP 4-9S, Document 22, September 2000
- [226] 'The Feasibility of Proposed Mitigation Techniques Intended to Facilitate Sharing Between FSS User Terminals and FS Stations in the 27.5-29.5 GHz Band', ITU WP 4-9S, Document 46, October 2000
- [227] Aghvami, A.H. : 'Lecturing Notes, Digital Modulation Schemes', King's College London, September 1999
- [228] ITU-R Recommendation F.1491, 'Error Performance Objectives for Real Digital Radio Links Used in the National Portion of a 27500 km Hypothetical Reference Path at or Above the Primary Rate', 2000
- [229] ITU-R Recommendation F.634, 'Error Performance Objectives for Real Digital Radio Relay Links Forming Part of the High Grade Portion of International Digital Connections at a Bit Rate Below the Primary Rate within an Integrated Services Digital Network', 1997
- [230] Shafi M. and Smith P.: 'The Impact of ITU-T Recommendation G.826', IEEE Communications Magazine, September 1993
- [231] Report on ACTS Project 215: Cellular Radio Access for Broadband Services (CRABS), European Commission, January 1999
- [232] ITU-R Recommendation P.1410, 'Propagation Data and Prediction Methods Required for the Design of Terrestrial Broadband Millimetric Radio Access Systems Operating in a Frequency Range of About 20-50 GHz', 1999

[233] MPT 1560, 'Performance Specification for Digital Multipoint Video Distribution Systems (MVDS) Transmitters and Transmit Antennas Operating in the Frequency Band 40.5-42.5 GHz', UK Radiocommunications Agency, June 1996